

Surgical and Perioperative Management of Patients with Anatomic Anomalies

Deepak Narayan
Shanta E. Kapadia
Gopal Kodumudi
Nalini Vadivelu
Editors

 Springer

Surgical and Perioperative Management of Patients with Anatomic Anomalies

Deepak Narayan • Shanta E. Kapadia
Gopal Kodumudi • Nalini Vadivelu
Editors

Surgical and Perioperative Management of Patients with Anatomic Anomalies

 Springer

Editors

Deepak Narayan (Deceased)
Section of Plastic and
Reconstructive Surgery
Yale New Haven Hospital
New Haven, CT
USA

Shanta E. Kapadia
Department of Surgery
Yale School of Medicine
New Haven, CT
USA

Gopal Kodumudi
Department of Anesthesiology
Louisiana State University School
of Medicine, New Orleans Health
New Orleans, LA
USA

Nalini Vadivelu
Department of Anesthesiology
Yale University
New Haven, CT
USA

ISBN 978-3-030-55658-7 ISBN 978-3-030-55660-0 (eBook)
<https://doi.org/10.1007/978-3-030-55660-0>

© Springer Nature Switzerland AG 2021

This work is subject to copyright. All rights are reserved by the Publisher, whether the whole or part of the material is concerned, specifically the rights of translation, reprinting, reuse of illustrations, recitation, broadcasting, reproduction on microfilms or in any other physical way, and transmission or information storage and retrieval, electronic adaptation, computer software, or by similar or dissimilar methodology now known or hereafter developed.

The use of general descriptive names, registered names, trademarks, service marks, etc. in this publication does not imply, even in the absence of a specific statement, that such names are exempt from the relevant protective laws and regulations and therefore free for general use.

The publisher, the authors and the editors are safe to assume that the advice and information in this book are believed to be true and accurate at the date of publication. Neither the publisher nor the authors or the editors give a warranty, expressed or implied, with respect to the material contained herein or for any errors or omissions that may have been made. The publisher remains neutral with regard to jurisdictional claims in published maps and institutional affiliations.

This Springer imprint is published by the registered company Springer Nature Switzerland AG
The registered company address is: Gewerbestrasse 11, 6330 Cham, Switzerland

After completion of the work on this book but prior to its publication, our dear friend and Co-editor Dr. Deepak Narayan sadly passed away. His diligence, mentorship, encouragement, and attention to detail were exemplary and something that those of us who partnered with him will never forget. This book therefore, in all humility, is dedicated to his memory.

*Shanta E. Kapadia
Gopal Kodumudi
Nalini Vadivelu*

Preface

Since ancient times, it has been well recognized that variations of the normal human anatomy exist. Most anatomical variants were identified after the discovery of X-rays. The understanding of normal human anatomy over the centuries was slow since the deliberate opening of a human body to study its contents was strictly forbidden until the twelfth century when human dissections were first performed. Advances in imaging and technology in recent times including magnetic resonance imaging, computerized tomography, and ultrasonography have revolutionized the understanding of anatomical anomalies immensely.

Surgical and perioperative management of patients with anatomic anomalies is truly a challenge. Versatility and excellence in the understanding of anatomical anomalies is essential. Creative and innovative management of these anatomical anomalies is vital. Sadly, there is sparse reference to the perioperative management of anatomical anomalies in the literature.

An important strategy in the creation of this book has been the challenge posed to clinicians involved in the perioperative management of patients with anatomical anomalies in light of the ever-evolving technology in the present era. How does one make it practical for clinicians managing such patients? To achieve that goal we have recruited anatomists, surgeons, and anesthesiologists caring for patients with an array of anatomical anomalies as well as anatomists and other basic scientists.

This book is the first of its kind to outline the perioperative management of patients with anatomical anomalies. Every attempt has been made to present information with conciseness and clarity. The book will also provide optimism and hope to future generations of patients afflicted with anatomical anomalies.

We thank each one of our contributors for their lucent discussion of cutting-edge research and providing the reader with modern-day treatment options. Finally, we thank all our colleagues, teachers, and trainees for their inspiration and our families for their support and patience.

New Haven, CT, USA
New Haven, CT, USA
New Orleans, LA, USA
New Haven, CT, USA

Deepak Narayan (Deceased)
Shanta E. Kapadia
Gopal Kodumudi
Nalini Vadivelu

Contents

Part I Head and Neck

- 1 Anatomy of the Head and Neck** 3
Walter Guillory II, Caroline Miller, Gopal Kodumudi, and
Rajuno Ettarh
- 2 Challenges of Dental Surgery and Oral and Maxillofacial
Surgery in Patients with Anatomical Anomalies** 33
Yoonah Danskin, Jessie Reisig, and Thomas G. Duplinsky
- 3 Airway Management** 57
Monica S. Ganatra

Part II Thorax and Its Contents

- 4 Head and Neck Variations: Vessels** 81
Amanda Norwich-Cavanaugh and Deepak Narayan
- 5 Head and Neck Variations: Soft Tissue, Nerves, and Bones** 93
Amanda Norwich-Cavanaugh and Deepak Narayan
- 6 Common Congenital Syndromes and Disease States
Impacting Regional Anesthesiology Techniques** 111
Donna-Ann Thomas, Omotoke Missih, Richard Zhu, Thomas Suchy,
and Nalini Vadivelu
- 7 Thoracic Aorta and Its Variants** 123
Isidore Dinga Madou, Bulat A. Ziganshin, John A. Elefteriades, and
Young Erben

Part III Abdominal Cavity

- 8 Anatomy of the Gastrointestinal System** 145
Glenn Geesman, Quinto J. Gesiotto, Zain Lalani, and Nizar Tejani

9	Anomalies of the Gastrointestinal Tract	179
	Jill C. Rubinstein, James S. Farrelly, David Stitelman, and Emily Christison-Lagay	
10	Surgical Anatomy of the Hepatobiliary System	205
	Charles Cha and Whitney S. Brandt	
11	Surgical Anatomy, Anomalies, and Normal Variants of the Pancreas . . .	235
	Charles Cha and Lindsay Hollander	
12	Anatomy of the Genitourinary System	251
	Kara Smith, Ty Spillman, Adrienne Cashio, Gopal Kodumudi, and Rajuno Ettarh	
13	Urologic Anomalies and Surgical Implications	267
	Jeannie Jiwon Su, José Murillo B. Netto, and Adam B. Hittelman	
14	Duodenal Fossae	343
	Samuel Kim and Deepak Narayan	
15	Anatomy of Acquired Spinal Disorders	349
	Amberly Reynolds, Brittany Bozzell, Sarah Alturkustani, and Rajuno Ettarh	
16	Neuraxial and Peripheral Nerve Block Placement in Patients with Anatomical Anomalies	359
	Donna-Ann Thomas, Sible Antony, David Sum, and Abbas Asgerally	
Part IV Upper and Lower Extremities		
17	Upper Extremity Variations	375
	Samuel Kim, Xiaolu Xu, James E. Clune, and Deepak Narayan	
18	Anatomical Anomalies of the Foot and Ankle	419
	Beau Vesely, Melissa Gulosh, Gabriel V. Gambardella, and Peter A. Blume	
19	Upper and Lower Extremity Vascular Variations	437
	Xiaolu Xu, Samuel Kim, James E. Clune, and Deepak Narayan	
Part V Vascular Access and Anesthesia		
20	Vascular Access and Anesthesia for Patients with Cardiac Anatomic Anomalies.	469
	Nat Dumrongmongcolgul, Robert J. Searles, Michael D. Casimir, and Qingbing Zhu	
	Index	507

Contributors

Sarah Alturkustani, MS Tulane University School of Medicine, New Orleans, LA, USA

Sible Antony, MD Department of Anesthesiology, Yale University School of Medicine, New Haven, CT, USA

Abbas Asgerally, MD Serendib Pain Care LLC, Vancouver, WA, USA

Peter A. Blume, DPM, FACFAS Department of Podiatry, Diabetes Center, Yale School of Medicine, New Haven, CT, USA

Brittany Bozzell, MS PA-S Louisiana State University Health Sciences Center, School of Allied Health Professions, Shreveport, LA, USA

Whitney S. Brandt, MD Department of Surgery, Yale School of Medicine, New Haven, CT, USA

Adrienne Cashio, MS University of Queensland, La Place, LA, USA

Michael D. Casimir, MD Department of Anesthesiology, NYU Winthrop Hospital, Mineola, NY, USA

Charles Cha, MD Department of Surgery, Yale School of Medicine, New Haven, CT, USA

Emily Christison-Lagay, MD Yale Pediatric Surgery, Yale New Haven Children's Hospital, New Haven, CT, USA

James E. Clune, MD Section of Plastic and Reconstructive Surgery, Yale New Haven Hospital, New Haven, CT, USA

Yoonah Danskin, DDS VA NY Harbor Healthcare Systems, New York, NY, USA

Nat Dumrongmongcolgul, MD Department of Anesthesia, Guam Regional Medical City, Dededo, GU, USA

Thomas G. Duplinsky, DDS Yale University School of Medicine, New Haven, CT, USA

John A. Elefteriades, MD, PhD (hon) Aortic Institute at Yale New Haven, Yale University School of Medicine, New Haven, CT, USA

Young Erben, MD Department of Vascular Surgery, Mayo Clinic, Jacksonville, FL, USA

Rajuno Ettarh, MD, PhD Department of Medical Education/Anatomy, California University of Science and Medicine, Colton, CA, USA

James S. Farrelly, MD, MHS Department of Surgery, Yale New Haven Hospital, New Haven, CT, USA

Gabriel V. Gambardella, DPM, FACFAS Bloomfield Foot Specialists, Bloomfield, CT, USA

Monica S. Ganatra, MD, MPH Department of Anesthesiology, Yale University School of Medicine, New Haven, CT, USA

Glenn Geesman, MD GME General Surgery, Riverside Community Hospital, Riverside, CA, USA

Quinto J. Gesiotto, MD Tampa General Hospital, University of South Florida, Tampa, FL, USA

Walter Guillory II, MD Medical Corps, United States Army, Silver Spring, MD, USA

Melissa Gulosh, DPM, AACFAS Novant Health UVA Culpeper Medical Center, Culpeper, VA, USA

Adam B. Hittelman, MD, PhD Department of Urology and Pediatrics, Yale School of Medicine, New Haven, CT, USA

Lindsay Hollander, MD Department of Surgery, Yale School of Medicine, New Haven, CT, USA

Samuel Kim, MD Section of Plastic and Reconstructive Surgery, Yale New Haven Hospital, New Haven, CT, USA

Gopal Kodumudi, MD, MS Department of Anesthesiology, Louisiana State University School of Medicine, New Orleans Health, New Orleans, LA, USA

Zain Lalani, MD Medical University of South Carolina, Charleston, SC, USA

Isidore Dinga Madou, MD Department of Surgery, Duke University School of Medicine, Durham, NC, USA

Caroline Miller, MS Tulane University School of Medicine, New Orleans, LA, USA

Omotoke Missih, MD Department of Anesthesiology, Susquehanna Anesthesia Affiliates, Johnson City, NY, USA

Deepak Narayan (Deceased), MD Section of Plastic and Reconstructive Surgery, Yale New Haven Hospital, New Haven, CT, USA

José Murillo B. Netto, MD, PhD Department of Urology, Universidade Federal de Juiz de Fora, Juiz de Fora, MG, Brazil

Amanda Norwich-Cavanaugh, MD Department of Reconstructive and Plastic Surgery, Yale School of Medicine, New Haven, CT, USA

Jessie Reisig, DDS Tribeca Endodontics (3D Micro Endo), New York, NY, USA

Amberly Reynolds, MS Tulane University School of Medicine, New Orleans, LA, USA

Jill C. Rubinstein, MD, PhD Department of Surgery, Memorial Sloan Kettering Cancer Center, New York, NY, USA

Robert J. Searles, DO Department of Anesthesiology, Spartanburg Regional Medical Center, Spartanburg, SC, USA

Kara Smith, DO Campbell University School of Osteopathic Medicine, Lillington, NC, USA

Ty Spillman, BS, MSc Creighton University, Omaha, NE, USA

David Stitelman, MD Department of Surgery, Yale School of Medicine, New Haven, CT, USA

Jeannie Jiwon Su, MD Department of Urology, Yale School of Medicine, New Haven, CT, USA

Thomas Suchy, MD Department of Anesthesiology, Yale New Haven Hospital, New Haven, CT, USA

David Sum, MD Town Square Anesthesia, Huntley, IL, USA

Nizar Tejani, MD Ochsner–Louisiana State University Shreveport Health Sciences Center, Shreveport, LA, USA

Donna-Ann Thomas, MD Department of Anesthesiology, Division of Pain Medicine, Yale School of Medicine, New Haven, CT, USA

Nalini Vadivelu, MBBS, MD, D.ABA Department of Anesthesiology, Yale University, New Haven, CT, USA

Beau Vesely, DPM, AACFAS Krohn Clinic, Black River Falls, WI, USA

Xiaolu Xu, MD Yale School of Medicine, New Haven, CT, USA

Qingbing Zhu, MD, PhD Department of Anesthesiology, Yale University School of Medicine, New Haven, CT, USA

Richard Zhu, MD Department of Anesthesiology, Yale New Haven Health, Greenwich Hospital Center for Pain Management, Greenwich, CT, USA

Bulat A. Ziganshin, MD Aortic Institute, Yale New Haven Hospital, New Haven, CT, USA

Part I

Head and Neck



Anatomy of the Head and Neck

1

Walter Guillory II, Caroline Miller, Gopal Kodumudi,
and Rajuno Ettarh

Skull

The skull is comprised of numerous flat bones that encase the brain and provide structural support for the face. The skull consists of two parts:

The **neurocranium** is the bone case surrounding the brain (Fig. 1.1). The bones of the neurocranium are as follows:

- Frontal
- Parietal (2)
- Temporal (2)
- Occipital
- Sphenoid
- Ethmoid

W. Guillory II (✉)

Medical Corps, United States Army, Silver Spring, MD, USA

C. Miller

Tulane University School of Medicine, New Orleans, LA, USA

e-mail: cmille21@tulane.edu

G. Kodumudi

Department of Anesthesiology, Louisiana State University School of Medicine, New Orleans Health, New Orleans, LA, USA

e-mail: gkodum@lsuhsc.edu

R. Ettarh

Department of Anatomy and Medical Education, California University of Science and Medicine, San Bernardino, CA, USA

e-mail: rettarh@tulane.edu

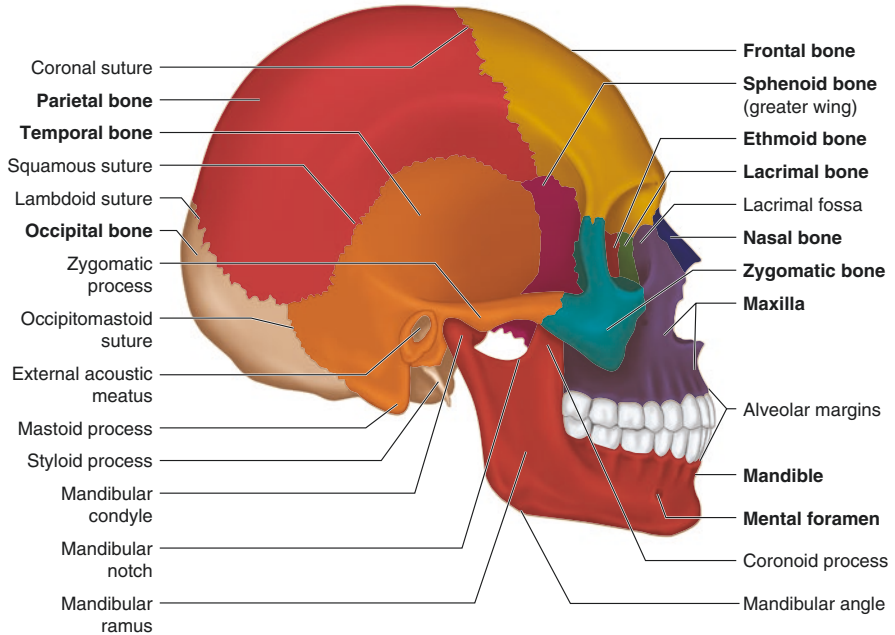


Fig. 1.1 The neurocranium is the bone case surrounding the brain

The bones of the neurocranium join together to form sutures. The major sutures are as follows:

- Coronal: suture between frontal and parietal bones
- Sagittal: suture between parietal bones
- Squamous: suture between parietal and temporal bones
- Lambdoid: suture between the parietal bones and occipital bone

The viscerocranium is the facial component of the cranium and is derived from pharyngeal arches. The bones are as follows.

- Mandible
- Vomer
- Maxilla (2)
- Nasal (2)
- Palatine (2)
- Inferior nasal concha (2)
- Lacrimal (2)
- Zygomatic (2)

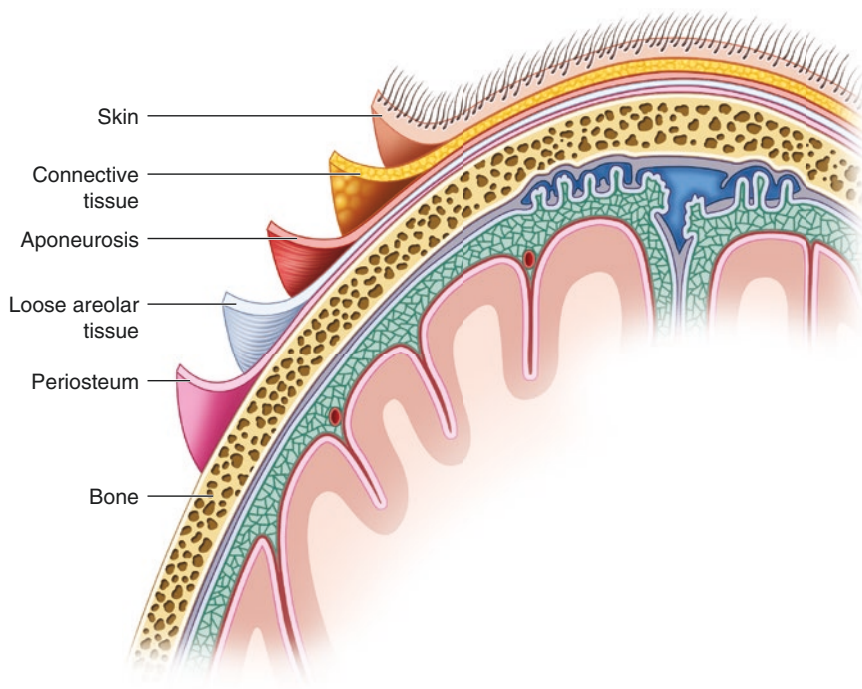


Fig. 1.2 The scalp is made up of five layers: skin, connective tissue, aponeurosis, loose connective tissue, and pericranium

Scalp

The scalp (Fig. 1.2) is made up of five layers:

Skin: contains numerous sebaceous glands, sweat glands, and hair follicles

Connective tissue: contains the vascular and nervous supply of the scalp

Aponeurosis: contains the occipitofrontalis muscle

Loose connective tissue: contains loose areolar tissue and the emissary veins

Pericranium: periosteum covering the external surface of the skull

Meninges

The meninges consist of three connective tissue layers that surround and protect the brain. The meningeal layers include the dura mater, arachnoid mater, and pia mater.

Dura Mater

The dura mater can be divided into two layers:

1. Periosteal: outer layer of dura which lines the internal surface of the skull
2. Meningeal: inner layer of dura which is continuous with the dura of the spinal meninges

The two layers separate to form the dural venous sinuses.

Arachnoid Mater

The arachnoid mater is a thin layer which connects to the pia mater with filaments. The space between the arachnoid mater and pia mater is called the subarachnoid space. The subarachnoid space is where cerebrospinal fluid (CSF) circulates.

Pia Mater

The pia mater is the deepest meningeal layer. Pia mater is adherent to the brain and is the only meningeal layer to dip into the gyri and sulci of the cerebrum (Fig. 1.3).

The middle meningeal artery, which is a branch of the maxillary artery, is the main blood supply of the dura. Middle meningeal artery enters the skull through

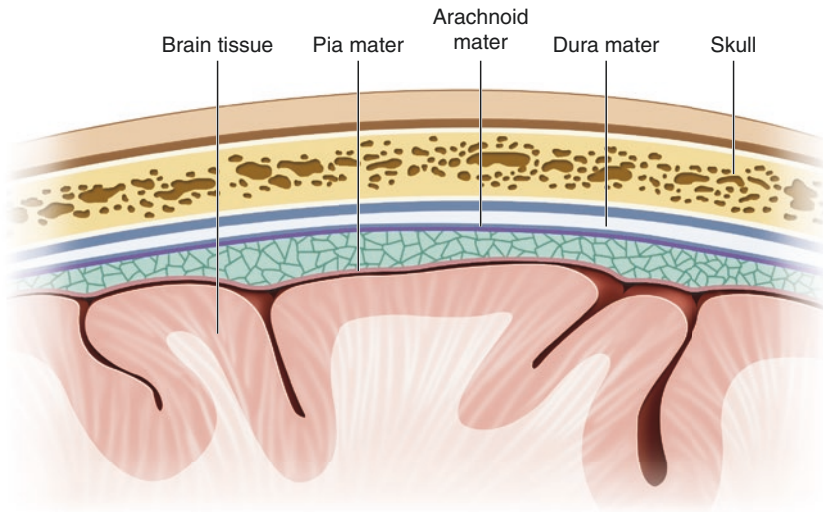


Fig. 1.3 The pia mater is the deepest meningeal layer. Pia mater is adherent to the brain and is the only meningeal layer to dip into the gyri and sulci of the cerebrum

foramen spinosum and courses along the inner surface of the skull superficial to the dura mater.

Brain

The brain can be subdivided into the cerebrum, diencephalon, brainstem, and cerebellum.

Cerebrum

The cerebrum is the control site for the nervous system. There are two hemispheres which are divided by the longitudinal cerebral fissure. Each cerebral hemisphere consists of gyri (ridges) and sulci (depressions) and can be divided into lobes (Fig. 1.4).

- **Frontal lobe:** located in the anterior of the brain and contains the precentral gyrus, which is the primary motor area of the brain

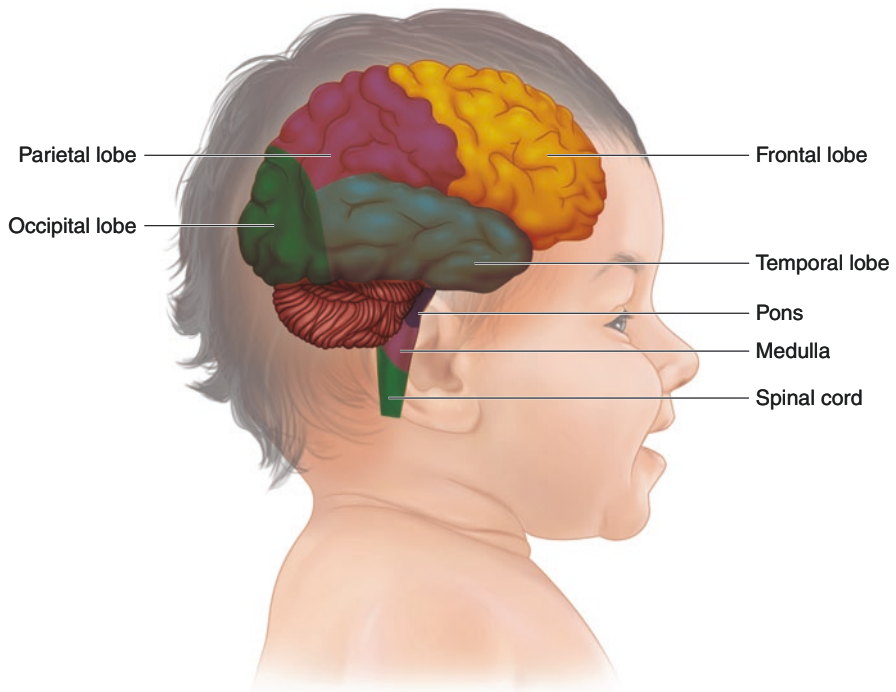


Fig. 1.4 The cerebrum is the control site for the nervous system. There are two hemispheres which are divided by the longitudinal cerebral fissure. Each cerebral hemisphere consists of gyri (ridges) and sulci (depressions) and can be divided into lobes

- **Parietal lobe:** located in the superior middle portions of the cerebrum and contains the postcentral gyrus which is the primary sensory area of the brain
- **Occipital lobe:** located in the posterior portion of the cerebrum and is superior to the cerebellum and is the visual area of the brain
- **Temporal lobe:** located in the inferior middle portions of the cerebrum and is involved with memory and hearing

Diencephalon

The diencephalon is made up of the thalamus, subthalamus, hypothalamus, and epithalamus.

- Thalamus: serves as a relay station of sensory and motor information to and from the cerebral cortex
- Hypothalamus: regulates the autonomic nervous system as well as regulating many metabolic and homeostatic mechanisms

Brainstem

The brainstem is divided into the midbrain, pons, and medulla oblongata. The brainstem plays an important role in the regulation of cardiac and respiratory functions. The brainstem is the location of the cranial nuclei of CN III-XII.

Cerebellum

The cerebellum is located in the posterior cranial fossa. The cerebellum is involved with coordination of skeletal muscles.

Blood Supply

The blood supply of the brain is from the internal carotid artery and the vertebral artery. After these paired arteries enter the skull, they anastomose to form the Circle of Willis.

Ventricular System

The ventricular system within the brain is divided into four chambers and is responsible for the creation and flow of cerebral spinal fluid (CSF). The two lateral ventricles are C-shaped chambers located within each cerebral hemisphere and connect to the third ventricle via the interventricular foramina. The third ventricle is a midline chamber between the diencephalon and communicates with the fourth ventricle through the cerebral aqueduct. CSF is made by

the choroid plexus located on the walls of the ventricles and flows from the ventricles to the subarachnoid space surrounding the brain and spinal cord (Table 1.1, Fig. 1.5).

Table 1.1 Cranial nerves

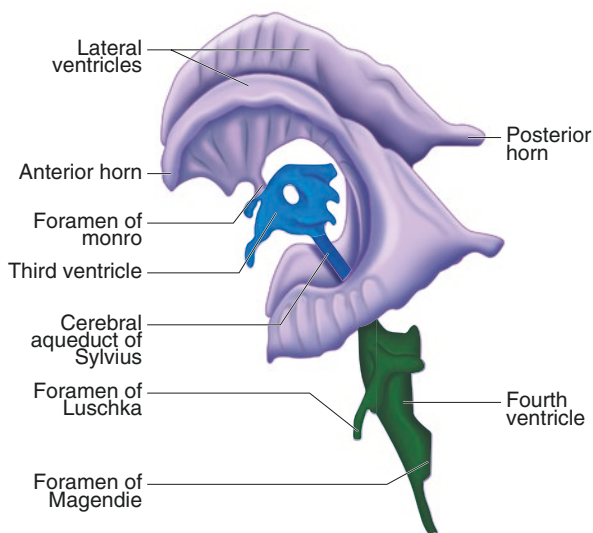
CN #	Name	Components	Function/innervations	Exit from skull
I	Olfactory	SSA	Smell	Cribriform plate
II	Optic	SSA	Sight	Optic canal
III	Oculomotor	GSE	Superior rectus m., inferior rectus, medial rectus m., levator palpebrae superioris m., and inferior oblique m.	Superior orbital fissure
		GVE	Pupillary constriction and lens accommodation	
IV	Trochlear	GSE	Superior oblique m.	Superior orbital fissure
V	Trigeminal Divisions: V-1 ophthalmic V-2 maxillary V-3 mandibular	GSA	V-1: Orbit, cornea & forehead, anterior nasal mucosa V-2: Maxillary region, posterior nasal mucosa, hard palate via greater palatine nerve and anterior part of hard palate by nasopalatine nerve via the incisive fossa. It also supplies the soft palate. V-3: Mandibular region & anterior two-thirds of tongue	V-1: Superior orbital fissure V-2: Foramen rotundum V-3: Foramen ovale
		SVE	V-3: Muscles of mastication, mylohyoid m., anterior digastric m., tensor tympani m., tensor veli palatine m.	
VI	Abducens	GSE	Lateral rectus m.	Superior orbital fissure
VII	Facial	GSA	Concha of the auricle and small area behind the ear	Internal acoustic meatus
		SVE	Muscles of facial expression, posterior digastric m., stylohyoid m., stapedius m.	
		GVE	Parasympathetic innervation to lacrimal, submandibular, sublingual glands, and mucous membranes of nasopharynx, hard and soft palate.	
		SVA	Taste anterior 2/3 of tongue	
VIII	Vestibulocochlear	SSA	Hearing, balance, and equilibrium	Internal acoustic meatus
IX	Glossopharyngeal	GSA	Posterior 1/3 of tongue, oropharynx, tympanic membrane, middle ear and auditory tube	Jugular foramen
		SVE	Stylopharyngeus m.	
		GVE	Parasympathetics to parotid gland	
		SVA	Taste posterior 1/3 of tongue	
		GVA	Carotid sinus (baroreceptor) and carotid body (chemoreceptor)	

(continued)

Table 1.1 (continued)

CN #	Name	Components	Function/innervations	Exit from skull
X	Vagus	GSA	Skin of posterior ear and external acoustic meatus	Jugular foramen
		SVE	Palatal muscles (except tensor tympani), pharyngeal muscles (except stylopharyngeus), and all laryngeal muscles	
		GVE	Parasympathetics to heart, lungs, foregut, and midgut.	
		GVA	Aortic and carotid bodies (chemoreceptors) and aortic arch (baroreceptor), pharynx, larynx, esophagus, thoracic, and abdominal viscera. SVA: From taste receptors in the epiglottis	
XI	Spinal accessory	GSE	Trapezius m. and sternocleidomastoid m.	Jugular foramen
XII	Hypoglossal	GSE	Tongue muscles (except palatoglossus)	Hypoglossal canal

Fig. 1.5 Cerebrospinal fluid (CSF) is made by the choroid plexus located on the walls of the ventricles and flows from the ventricles to the subarachnoid space surrounding the brain and spinal cord



Face

Cutaneous Sensation

The three divisions of the Trigeminal nerve (CN V) provide the cutaneous innervation of the face. V-1 provides general sensation to the forehead, upper eyelid, and the bridge of the nose. V-2 provides sensation to the maxillary region of the face

including the lower eyelid and upper lip. V-3 provides sensation to the mandibular region including the lateral face, lower lip, and chin.

Blood Supply

Branches of the external carotid artery: facial artery and superficial temporal artery supply the face. Terminal branches of the ophthalmic artery also provide blood supply to areas around the orbit.

Muscles

The muscles of the face include the muscles of facial expression and muscles of mastication. The muscles of facial expression are innervated by branches of the Facial nerve (CN VII). These muscles originate on the viscerocranium and insert into the skin allowing them to create facial expressions. The mandibular division of the trigeminal nerve (V-3) innervates the muscles of mastication. These muscles are responsible for chewing (mastication) and all insert onto the mandible. The muscles of mastication include the temporalis, masseter, lateral pterygoid and medial pterygoid muscles (Fig. 1.6).

Parotid Gland

The paired parotid gland is located superficially on the lateral portion of the face. The parotid gland produces and secretes saliva into the oral cavity through a large parotid duct. The parotid duct passes superficially over the masseter muscles to open into the oral cavity. Within the parotid gland reside important structures such as the motor branches of CN VII that supply the muscles of facial expression, the retromandibular vein, and the external carotid artery. The parotid gland receives parasympathetic innervation (GVE) from the lesser petrosal nerve, which is a branch of CN IX. The presynaptic parasympathetic neurons of the lesser petrosal nerve synapse in the otic ganglion. Postsynaptic parasympathetic neurons from the otic ganglion then join with the auriculotemporal nerve to reach the parotid gland.

Oral Cavity

Palate

The palate forms the roof of the oral cavity and is divided into the hard and soft palate. The hard palate is formed by the maxillary bone as well as the palatine bone. The incisive foramen/canal is located anterior midline and transmits branches from CN V-2 as well as arterial branches from the maxillary artery. The soft palate is located posterior to the hard palate. The soft palate acts to move food inferiorly to the esophagus and prevent the food from entering the nasal cavity (Fig. 1.7).

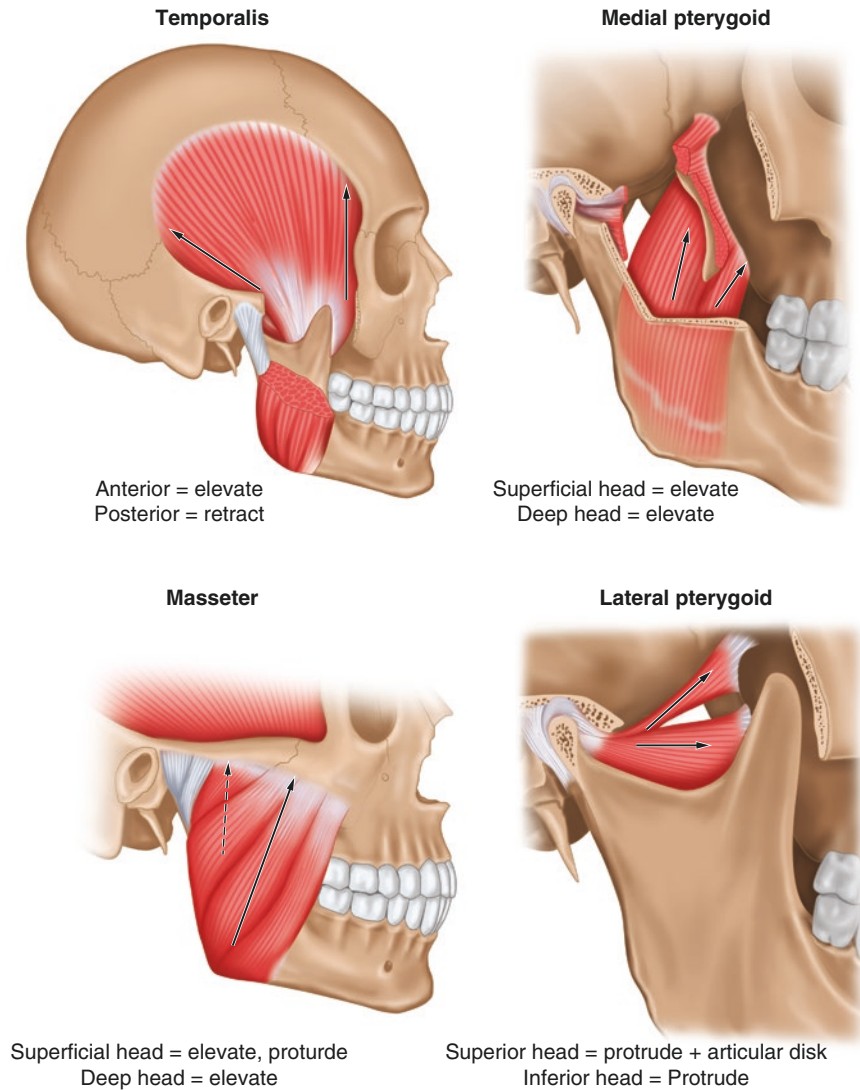


Fig. 1.6 The muscles of mastication include the temporalis, masseter, lateral pterygoid, and medial pterygoid muscles

Tongue

The tongue is made of powerful skeletal muscle with taste buds and general sensory nerve endings within the covering. The muscular component of the tongue is supported through connections to the mandible, hyoid bone, styloid process, the palate, and pharynx. The tongue can be anatomically and embryologically divided into an anterior 2/3 and posterior 1/3. Table 1.2 outlines the innervation of the tongue:

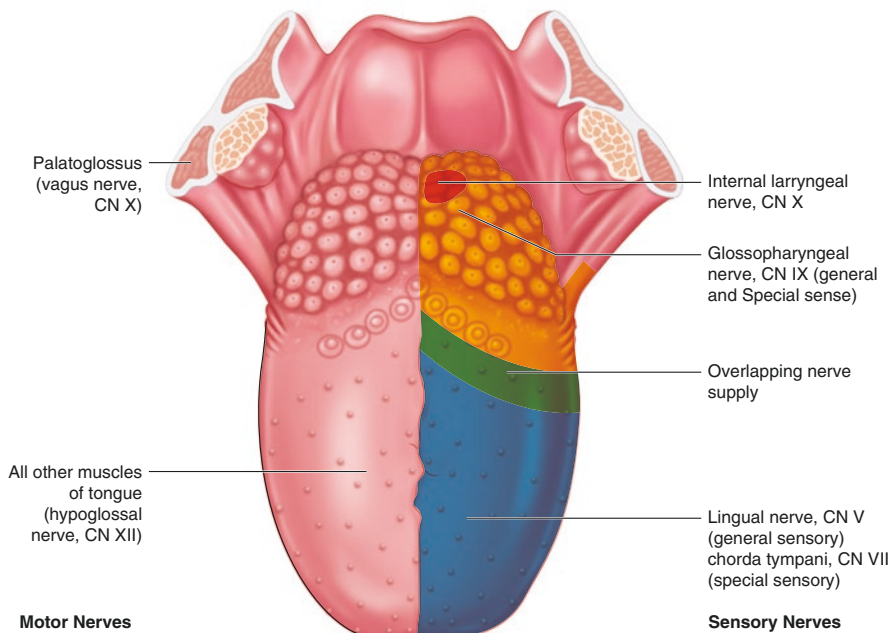


Fig. 1.7 The soft palate acts to move food inferiorly to the esophagus and prevent the food from entering the nasal cavity

Table 1.2 Divisions of the tongue

Divisions of the tongue	Anterior 2/3	Posterior 1/3
Taste – SVA	CN VII – chorda tympani n.	CN IX
General sensation – GSA	CN V-3 – lingual n.	CN IX
Skeletal motor – GSE	CN XII	CN XII *except palatoglossus m. which is innervated by CN X

The blood supply of the tongue is from the lingual artery, which is a branch of the external carotid artery.

Submandibular and Sublingual Glands

The paired submandibular and sublingual glands, as well as the parotid glands, produce and secrete saliva. The submandibular glands are situated superficially inferior to the mandible. The sublingual glands are located just inferior to the tongue. Both the submandibular and sublingual glands receive parasympathetic innervation from the chorda tympani nerve, which is a branch of CN VII. Presynaptic

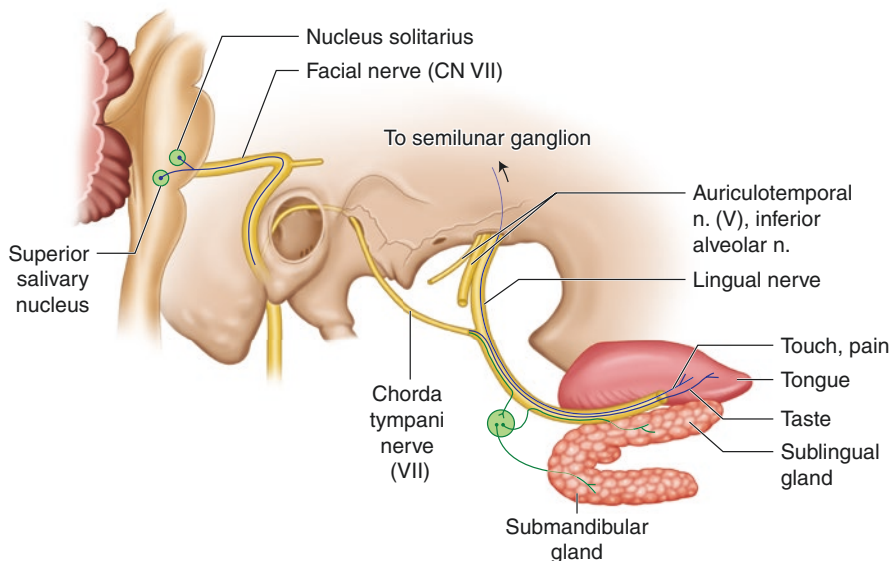


Fig. 1.8 Postsynaptic parasympathetic neurons then travel on lingual nerve to reach the submandibular and sublingual glands

parasympathetic neurons travel on the chorda tympani nerve and then join with the lingual nerve to synapse on the submandibular ganglion. Postsynaptic parasympathetic neurons then travel on lingual nerve to reach the submandibular and sublingual glands (Fig. 1.8).

Neck Anatomy

The neck is comprised of a myriad of structures nutritionally supported by a labyrinth of neurovasculature and lymphatics. It serves as the structural and neural link between the head and remainder of the body, housing a portion of the spinal cord and several major vessels that deliver blood directly to the brain. Due to its relatively narrow width and abundance of anatomical features, the neck is a common site of severe injuries and pathologies. This section will focus on the anatomy of the neck, beginning superficially with the skin and delving deep to the level of the spinal cord, from the body of the mandible anterosuperiorly and the occipital triangle posterosuperiorly to the level of the clavicle anteroinferiorly and to the level of vertebra T4 inferiorly.

Platysma

The following visual perspective is of the cadaver in anatomical position lying supine. The alveolar crest/mental protuberance of the mandible is pushed upward as perpendicularly as possible to the coronal plane, such that the skin covering the

floor of the oral cavity is fully visible and stretched as tightly as possible, exposing the anterior neck fully as well. The platysma muscle and fascial layers will be defined in the following section, down to the level of the trachea and esophagus, both located in the center of the neck. The layers defined are spatially located at the level of vertebrae C7 (vertebra prominens) and T1, to account for the presence of the thyroid gland. The terms “posterior” and “deep” will be used interchangeably, respective to the coronal plane.

Immediately deep to the subcutaneous tissue is a very thin superficial muscle called the platysma which, except for a small gap aligned with the midline of the mental protuberance, follows the contour of the neck, originating on the superficial fascia inferior to the clavicle, traveling superiorly over the clavicle, and inserting near the oblique line/ramus of the mandible and oral muscles. Directly deep to the platysma muscle is the superficial (investing) layer of deep cervical fascia. This layer’s anterior aspect extends from the geniohyoid fascia superiorly to the manubrium of the sternum inferiorly, splitting just before reaching the manubrium to form the suprasternal space of Burns. The layer’s posterior aspect extends from the external occipital protuberance superiorly, down far inferiorly to the termination of the neck and into the back region. Moving toward the posterior of the neck, the investing fascia forms the first structure deep to the subcutaneous layer after passing the lateral boundary of the platysma. This layer is described as “investing” due to its total envelopment of several superficial muscles: the sternocleidomastoid muscles anteriorly, and the trapezius muscles posteriorly. Upon reaching these muscles, the investing fascia splits into two layers (anterior and posterior respective to the invested muscle) in order to fit around the muscle on all sides, converging again into a single fascial layer after completing the investment and continuing its path around the superficial neck. There is a layer of fat in the posterior cervical triangle located between the investing fascia and the prevertebral fascia.

Fascial Layers

Fascial layers become more complex deep to the superficial (investing) fascia. Keep in mind that the neck layers are highly symmetrical on both sides of the midsagittal plane. If we divide the neck along the coronal plane and look upon it from a superior perspective, one intuitive demarcation is between the esophagus anteriorly and the vertebral bodies posteriorly. This results in an unequal “amount of neck” on either side of the demarcation, with the lesser “share of neck space” being on the esophageal side and continuing anteriorly, and the greater “share of neck space” being on the vertebral side and continuing posteriorly. The next paragraph is concerned with the esophageal (anterior) side, and we will begin the description directly deep to the superficial (investing) fascial layer.

The esophageal side of the neck contains the infrahyoid fascia surrounding several muscles; the pretracheal fascia (also known as the visceral fascia and the thyroid capsule), which invests the thyroid gland, the trachea, the esophagus, the left and right recurrent laryngeal nerves; and the carotid sheath, which invests three structures: the common carotid artery, internal jugular vein, and vagus nerve. The

infrahyoid fascia extends from the level of the superior boundary of the investing fascia to the manubrium of the sternum inferiorly. This fascial layer lies directly deep to the superficial (investing) fascia and invests the following muscles individually in a manner similar to the investing action of the superficial fascia: sternohyoid, sternothyroid, and omohyoid muscles. The infrahyoid fascia fuses with the superficial fascia laterally and the carotid sheath more medially. Located directly deep to the infrahyoid fascia is the pretracheal fascia (thyroid capsule) investing the thyroid gland. The pretracheal fascia extends from the level of C6 superiorly to the arch of the aorta and pericardium inferiorly. The thyroid gland itself wraps loosely into a cupping around the trachea and esophagus. In the depression formed by this cup-shaped gland is, of course, the trachea anteriorly, the esophagus directly bordering the trachea posteriorly, and the left and right recurrent laryngeal nerves located on each of the tracheal–esophageal boundary. Directly deep to the esophagus and terminating on the medial thyroid capsule on each side is the buccopharyngeal (visceral) fascia. The carotid sheaths are located laterally to the posterior thyroid capsule bilaterally. The sheath contains the internal jugular vein laterally, the common carotid artery medially, and the vagus nerve between the two blood vessels.

Remembering our neck demarcation described earlier, there is a small space deep to the buccopharyngeal fascia, termed the retropharyngeal space. In this space lie the left and right sympathetic trunks, each bordering the medial aspect of the carotid sheath bilaterally.

Regarding the vertebral side of our neck demarcation, matters become simpler. We are now moving from the coronal midline toward the posterior surface of the neck, so do not allow the term “deep” to confuse you: it still means “posterior” in this context. The entire side is enclosed within the prevertebral layer of deep cervical fascia. Located in the retropharyngeal space, deep to the buccopharyngeal fascia, the prevertebral fascia splits to form an out-pocketing. The fascia overlying this out-pocketing on the anterior side is called alar fascia. The alar fascia projects a very short isthmus that connects to the buccopharyngeal fascia along the midsagittal plane, and extends the length of the neck from the level of C1 to T2. At C7 (vertebra prominens), the alar fascia is briefly interrupted by the long spinous process of this particular vertebra.

The width of the vertebral body borders the prevertebral fascia. Directly lateral to the vertebral body and resting in the anterior pocket formed by the transverse processes are the longus colli muscles on either side. Lateral to the longus colli are the anterior scalene muscles. Directly posterior to the anterior scalene muscles are the left and right spinal nerves. Directly posterior to the spinal nerves are the middle and posterior scalene muscles, so named by their position in the coronal plane relative to each member of the scalene group. Directly posterior to the transverse processes and medial to the posterior scalene muscles are several deep cervical muscles, which will be elaborated later. The levator scapulae muscles are located directly posterior to the middle and posterior scalene muscles. Remember that the muscles discussed in this paragraph are all located within the prevertebral layer of deep cervical fascia (Fig. 1.9).

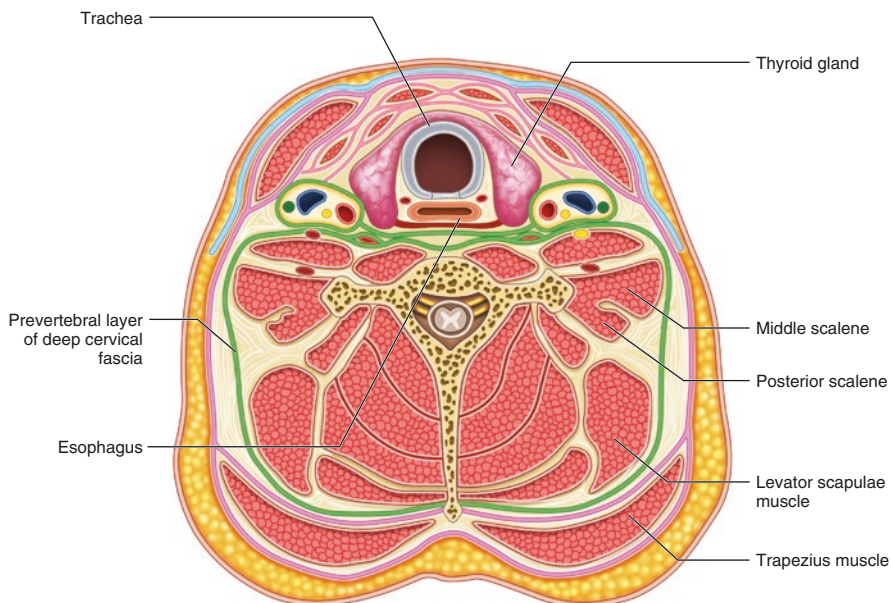


Fig. 1.9 The levator scapulae muscles are located directly posterior to the middle and posterior scalene muscles within the prevertebral layer of deep cervical fascia

Neck Bones and Cartilages

To set reference points for muscular attachments and neurovasculature pathways through the neck, the locations of the intrinsic bones, cartilages, and membranes of the neck will be described in this section, extending from the level of C1 down to the manubrium of the sternum. The most superior bony landmark useful in an examination of the neck is the mandible, a movable bone anchored to the skull by its condylar and coronoid processes. The following visual perspective is of the anterior aspect of the larynx. Inferior and posterior to the angle of the mandible is the hyoid bone, the site of many muscular attachments in the area. It is located spatially at the level of the C3–C4 intervertebral disc. The bone is roughly C-shaped and characterized by the following descriptive terms: the hyoid body is the wide face of the bone located on its anterior aspect; the lesser horn is a small bony projection a small distance posterior to the front of the hyoid body; the greater horn is the long bony projection of the hyoid, traveling posteriorly and overlapping with C3 in the coronal plane. The hyoid bone itself is anchored to the styloid process at the lesser horn by the stylohyoid ligament, to the directly posterior epiglottis by the hyoepiglottic ligament, and to the inferior thyroid cartilage by the thyrohyoid membrane. The triticeal cartilage joins the greater horn of the hyoid bone to the superior horn of the thyroid cartilage. The thyroid cartilage extends from the C4 to C6 level, and is comprised of

the following structural peculiarities: the thyroid cartilage lamina is the main medial aspect of the cartilage located predominately at the C5 level and anchored to the cricoid cartilage inferiorly by the median and lateral cricothyroid ligaments; two superior horns project superiorly from the lateral thyroid cartilage bilaterally to the C4 level and are anchored to the thyrohyoid membrane; one superior thyroid notch is present as a superior–inferior oriented indentation in the thyroid cartilage (termed the laryngeal prominence at its apex) along the cartilage midline and filled in by the thyrohyoid membrane; two inferior horns project inferiorly from the lateral thyroid cartilage bilaterally to the C6 level and are anchored to the cricoid cartilage inferiorly at the thyroid articular surface of the cricothyroid joint. Located on the posterolateral thyroid cartilage lamina is a prominent oblique line that serves as a point of origin for the thyrohyoid muscle. The cricoid cartilage is located at the C6 level and is anchored to the thyroid cartilage above and the trachea directly inferiorly. Unlike the thyroid cartilage, which terminates in its wrap-around of the larynx at points directly aligned with the superiorly located hyoid greater horn, the cricoid cartilage wraps completely around the larynx. The posterior aspect of the cricoid cartilage is termed the arch of the cricoid cartilage.

Viewing the thyroid cartilage from a posterior perspective, the epiglottis is anchored to the posterior aspect of the thyroid cartilage lamina by the thyroepiglottic ligament. Two arytenoid cartilages rest directly posterior to the thyroid cartilage lamina, each anchored to the lamina by a vocal ligament and resting atop the cricoid cartilage lamina on the arytenoid articular surface. The posterior-most extension of the arytenoid cartilages is termed the muscular process. Sitting at the superior apex of each arytenoid cartilage is a small corniculate cartilage.

Neck Musculature

The following initial visual perspective is of the cadaver in anatomical position lying supine. The alveolar crest/mental protuberance of the mandible is pushed upward as perpendicularly as possible to the coronal plane, such that the skin covering the floor of the oral cavity is fully visible and stretched as tightly as possible, exposing the anterior neck fully as well. It will be useful to rotate your mental image around the midsagittal plane when we consider the muscles obscured by superficial structures and located laterally. We will now begin to define the muscle groups of the neck. When a muscle is introduced, its characteristics will be described in the following order: name of muscle, origin, insertion, nerve supply, blood supply, and action.

Sternocleidomastoid

The sternocleidomastoid muscle is located on the superficial lateral neck, just deep to the platysma and investing fascia. It is comprised of two heads that have different origins. The sternal head originates on the anterior surface of the manubrium of the

sternum, while the clavicular head originates on the upper surface of the medial 1/3 of the clavicle. Both heads insert on the lateral surface of the mastoid process and lateral half of the superior nuchal line of the occipital bone. The sternocleidomastoid is innervated by the accessory nerve (CN XI) and receives blood from several sources: sternocleidomastoid branch of the superior thyroid and occipital arteries, the muscular branch of the suprascapular artery, and the occipital branch of the posterior auricular artery. The muscle functions bilaterally to flex the head and raise the thorax. Unilaterally, each sternocleidomastoid functions to turn the face toward the contralateral side (Fig. 1.10).

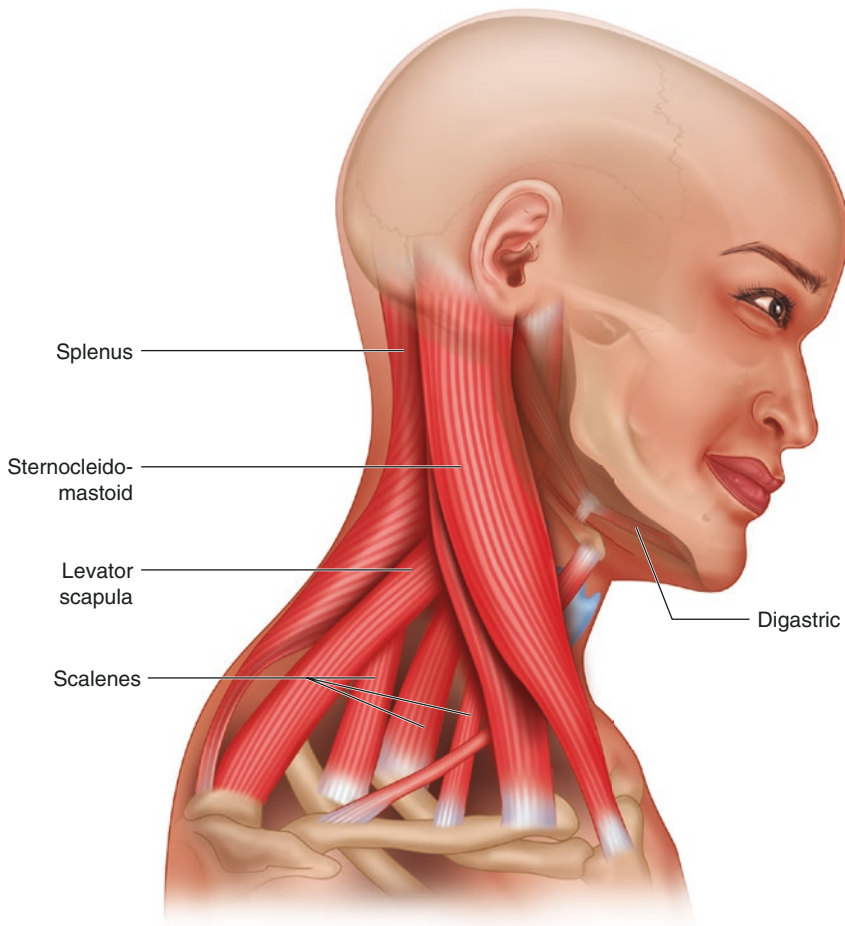


Fig. 1.10 The sternocleidomastoid is innervated by the accessory nerve (CN XI) and receives blood from several sources: sternocleidomastoid branch of the superior thyroid and occipital arteries, the muscular branch of the suprascapular artery, and the occipital branch of the posterior auricular artery. The muscle functions bilaterally to flex the head and raise the thorax. Unilaterally, each sternocleidomastoid function to turn the face toward the contralateral side

Subclavius

The subclavius muscle originates on the upper border of the first rib and its cartilage. It inserts on the inferior surface of the middle third of the clavicle. It is innervated by the nerve to subclavius, and it receives blood from the clavicular branch of the thoraco-acromial artery. It functions to anchor and depress the clavicle.

Beneath the Mandible/Floor of the Oral Cavity/Suprahyoid Muscles (Fig. 1.11)

Geniohyoid

Forming the floor of the oral cavity is a group of muscles involved in moving the mandible. The following muscles are known as suprahyoid muscles due to their

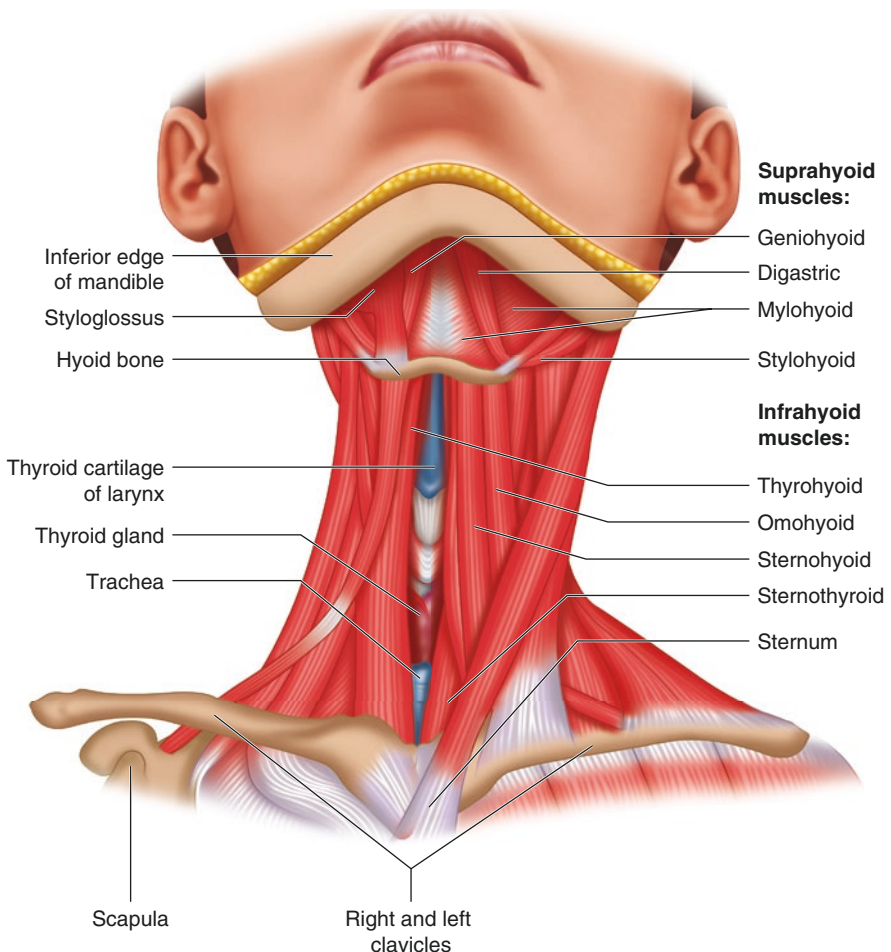


Fig. 1.11 A view of the oral cavity floor, beneath the mandible. Also shown are the suprahyoid and infrahyoid muscles

position superior to the hyoid bone. The geniohyoid muscle originates on the inferior genial tubercle on the back of the mandible symphysis; it inserts on the anterior hyoid body. The geniohyoid is innervated by the hypoglossal (cranial nerve XII) nerve, and it receives blood via the sublingual and submental arteries. The muscle functions to elevate the hyoid bone and depress the mandible.

Mylohyoid

The mylohyoid muscle originates along the mylohyoid line of the mandible and inserts on the median raphe and body of the hyoid bone. The median raphe is a tendon line dividing the mylohyoid into two halves along its sagittal plane. The mylohyoid rests inferior to the geniohyoid muscle. It is innervated by the nerve to mylohyoid, which is a branch of the trigeminal nerve (CN V). It receives the blood via the sublingual branch of the lingual artery and the submental branch of the facial artery. It functions to elevate the hyoid bone, the base of the tongue, and the floor of the mouth, while also functioning to depress the mandible.

Digastric

The digastric muscle is divided into anterior and posterior bellies, joined by an intermediate digastric tendon and held in position by the pulley-like arrangement of a fibrous loop that wraps around the tendon. The fibrous loop is anchored on the body of the hyoid. The bellies have different innervations and blood supplies. The anterior belly of the digastric originates at the digastric fossa of the mandible and inserts on the intermediate tendon. It is innervated by the nerve to mylohyoid and receives blood via submental artery branches. It functions to raise the hyoid and the tongue base, steadies the hyoid bone, and opens the mouth by depressing the mandible. The posterior belly of the digastric originates at the mastoid notch of the temporal bone and inserts on the intermediate tendon. It is innervated by the facial nerve (CN VII) and receives blood via the muscular branches of the posterior auricular artery and muscular branches of the occipital artery. It also functions to raise the hyoid and the tongue base, steadies the hyoid bone, and opens the mouth by depressing the mandible.

Stylohyoid

The stylohyoid muscle originates on the posterior border of the styloid process and inserts at the junction of the hyoid body and greater horn. Just before the insertion point, the stylohyoid tendon splits to straddle the intermediate tendon of the digastric muscle. It is innervated by the facial nerve (CN VII) and receives blood via the muscular branches of the facial artery and muscular branches of the occipital artery. It functions to elevate the hyoid bone and tongue base.

Hyoglossus

The hyoglossus muscle originates on the ipsilateral body and greater horn of the hyoid bone. It inserts on the lateral and inferior aspect of the ipsilateral tongue. It is innervated by the hypoglossal nerve (CN XII), and receives blood via the sublingual and submental arteries. It functions to depress and retract the tongue.

The submandibular gland is located on the lateral aspect of the mylohyoid muscle. A small portion is located superior to the muscle, giving off the duct of Wharton.

The majority of the gland is located inferior to the muscle. The sublingual gland sits superior to the mylohyoid and anterior tip of the geniohyoid.

Anterior Infrahyoid Muscles

Several muscles occupy the infrahyoid space. This section is concerned with superficial muscles located inferior to the hyoid bone, superior to the clavicle, and primarily between the internal jugular veins. These muscles are the sternohyoid, omohyoid, thyrohyoid, and sternothyroid. These muscles have similar functions. The small muscles closely associated with the thyroid cartilage, thyroid gland, cricoid cartilage, and nearby cartilages will be described later in the chapter (Fig. 1.12).

Sternohyoid

The sternohyoid muscle originates on the posterior surface of the manubrium of the sternum, the posterior sternoclavicular ligament, and the medial end of the clavicle. It inserts on the medial portion of the lower border of the hyoid body. It is innervated by the ansa cervicalis, and receives blood via the sternocleidomastoid and hyoid branches of the superior thyroid artery, as well as via the hyoid branch of the lingual artery. It functions to depress the larynx and hyoid bone, as well as to steady the hyoid bone.

Omohyoid

The omohyoid muscle is similar to the digastric muscle in that it is comprised of two bellies. These bellies are the superior and inferior bellies, named according to their spatial relationship to each other and joined together by the intermediate omohyoid tendon located underneath the sternocleidomastoid muscle. The superior belly originates on the omohyoid tendon and inserts on the hyoid body. The inferior belly originates on the upper border of the scapula and suprascapular ligament. It inserts on the intermediate tendon. The omohyoid is innervated by the ansa cervicalis, and it receives blood via the hyoid branch of the lingual artery and the sternocleidomastoid branch of the superior thyroid artery. It functions to steady and depress the hyoid bone.

Thyrohyoid

The thyrohyoid muscle is located deep to the sternohyoid and omohyoid muscles. It originates on the oblique line of the thyroid cartilage lamina, and inserts on the lower border of the body and greater horn of the hyoid bone. It is innervated by the thyrohyoid branch of the C1 nerve, a portion of which travels with the hypoglossal nerve (CN XII). It receives blood from the hyoid branch of the superior thyroid artery. It functions to depress the larynx and hyoid bone, as well as to elevate the thyroid cartilage.

Sternothyroid

The sternothyroid muscle originates on the posterior surface of the manubrium of the sternum inferior and posterior to the sternohyoid origin at the sternal edge of the first costal cartilage. It inserts on the oblique line of the thyroid cartilage lamina. It

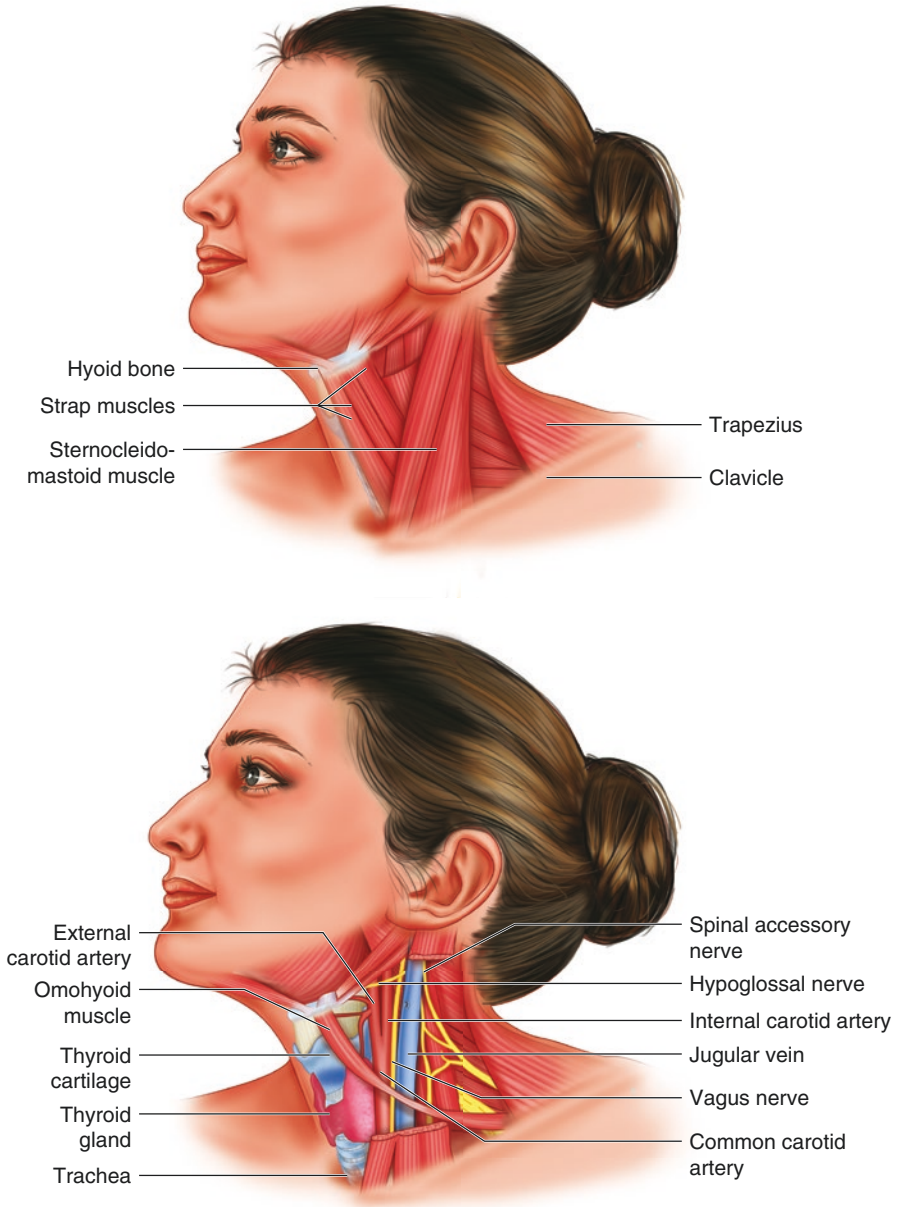


Fig. 1.12 Superficial muscles located inferior to the hyoid bone, superior to the clavicle, and primarily between the internal jugular veins are the sternohyoid, omohyoid, thyrohyoid, and sternothyroid

is innervated by the ansa cervicalis, and receives blood via the cricothyroid branch of the superior thyroid artery. It functions to depress the larynx and thyroid cartilage.

Laryngeal Muscles

The cricothyroid muscle originates on the anterior cricoid cartilage. It inserts on the inferior border of the thyroid cartilage and its inferior horn. It is innervated by the external branch of the superior laryngeal nerve, and receives blood via the superior and inferior thyroid arteries. It functions to lengthen and tense the vocal ligaments.

The lateral cricoarytenoid muscle originates on the arch of the cricoid cartilage. It inserts on the muscular process of the arytenoid cartilage. It is innervated by the recurrent laryngeal nerve, and receives blood from the superior and inferior thyroid arteries. It functions to adduct the vocal cords.

The posterior cricoarytenoid muscle originates on the posterior surface of the lamina of the cricoid cartilage. It inserts on the muscular process of the arytenoid cartilage. It is innervated by the recurrent laryngeal nerve, and receives blood from the superior and inferior thyroid arteries. It functions to abduct the vocal folds.

The thyro-arytenoid muscle originates on the posterior aspect of the thyroid cartilage. It inserts on the muscular process of the arytenoid cartilage. It is innervated by the recurrent laryngeal nerve, and receives blood from superior and inferior thyroid arteries. It functions to shorten and relax the vocal cords and acts as the sphincter of the laryngeal vestibule.

The transverse and oblique arytenoid muscles originate on the arytenoid cartilage and insert opposite the arytenoid cartilage. They are innervated by the recurrent laryngeal nerve, and receive blood from the superior and inferior thyroid arteries. They function to close the intercartilaginous aspect of the rima glottides.

The vocalis muscle originates on the vocal process of the arytenoid cartilage. It inserts on the vocal ligament. It is innervated by the recurrent laryngeal nerve, and it receives blood from the superior and inferior thyroid arteries. It functions to tense the anterior vocal ligament and relax the posterior vocal ligament.

Circular Pharyngeal Muscles

The following muscles are classified as circular pharyngeal muscles, which wrap around and constrict the pharynx.

The superior pharyngeal constrictor muscle originates from three points: the hamulus, the pterygomandibular raphe, and the mylohyoid line of the mandible. The constrictor inserts on the median raphe of the pharynx. It is innervated by the vagus nerve, via the pharyngeal plexus, and it receives blood from several sources: the ascending pharyngeal artery, the ascending palatine and tonsillar branches of the facial artery, and the dorsal branches of the lingual artery. It functions to constrict the wall of the pharynx during swallowing.

The middle pharyngeal constrictor muscle originates on the stylohyoid ligament and the horns of the hyoid bone. It inserts on the median raphe of the pharynx. It is innervated by the vagus nerve via the pharyngeal plexus, and it receives blood from several sources: the ascending pharyngeal artery, the ascending palatine and tonsillar branches of the facial artery, and the dorsal lingual branches of the lingual artery. Its functions to constrict the wall of the pharynx during swallowing.

The inferior pharyngeal constrictor muscle originates on the oblique line of the thyroid cartilage and on the cricoid cartilage. It inserts on the median raphe of the pharynx. It is innervated by the vagus nerve via the pharyngeal plexus, and receives blood from the ascending pharyngeal artery and from branches of the superior thyroid artery. Its functions to constrict the wall of the pharynx during swallowing. The cricopharyngeus muscle is classified as part of the inferior pharyngeal constrictor muscle.

Longitudinal Pharyngeal Muscles

The following muscles are classified as longitudinal pharyngeal muscles.

The palatopharyngeus muscle originates on the hard palate and on the superior palatine aponeurosis. It inserts on the lateral pharyngeal wall. It is innervated by the vagus nerve, via the pharyngeal plexus, and receives blood from the ascending pharyngeal arteries and the palatine branches of the facial and maxillary arteries. Its functions to elevate the posterior tongue and depress the palate.

The salpingopharyngeus muscle originates on the pharyngotympanic tube, also called the auditory/Eustachian tube. It inserts on the side of the pharyngeal wall. It is innervated by the vagus nerve via the pharyngeal plexus and receives blood from the pharyngeal branch of the ascending pharyngeal artery. Its functions to elevate the pharynx during swallowing and speaking.

The stylopharyngeus muscle originates on the medial aspect of the styloid process. It inserts on the pharyngeal wall. It is innervated by the glossopharyngeal nerve (CN IX), and it receives blood from several sources: the ascending pharyngeal artery, ascending palatine and tonsillar branches of the facial artery, and the dorsal branches of the lingual artery. Its functions to elevate the pharynx and larynx during swallowing and speaking.

Prevertebral Muscles

The following muscles are classified as prevertebral muscles. They are primarily involved in moving the head, neck, cervical vertebral column, and first two ribs.

The longus capitis muscle originates on the anterior tubercles of the C3–C6 transverse processes. It inserts on the inferior surface of the basilar aspect of the occipital bone. It is innervated by the ventral rami of cervical nerves C1–C4, and it receives blood from several sources: the ascending cervical branch of the inferior thyroid artery, the ascending pharyngeal artery, and the muscular branches of the

vertebral artery. It functions to flex and assist in rotating the cervical vertebrae and head.

The longus colli muscle has three points of origin and three points of insertion. The vertical portion originates on the C5–T3 vertebrae and inserts into the C2–C4 vertebrae. The inferior oblique portion originates on the T1–T3 vertebrae and inserts on the anterior tubercles of the C5–C6 transverse processes. The superior oblique portion originates on the anterior tubercles of the C3–C5 transverse processes and inserts on the tubercle of the anterior arch of atlas (C1). The longus colli muscle is innervated by the ventral primary rami of cervical nerves C2–C8, and it receives blood from several sources: the prevertebral branches of the ascending pharyngeal artery and the muscular branches of the ascending cervical and vertebral arteries. It functions bilaterally to flex and assist in rotating the cervical vertebrae and head. It functions unilaterally to flex the vertebral column laterally.

The rectus capitis anterior muscle originates on the lateral mass of atlas (C1). It inserts on the base of the occipital bone in front of the foramen magnum. It is innervated by the ventral rami of cervical nerves C1–C2, and it receives blood from the muscular branches of the vertebral artery and from the ascending pharyngeal artery. It functions to flex the head.

The rectus capitis lateralis muscle originates on the upper surface of the transverse process of atlas (C1). It inserts on the interior surface of the jugular process of the occipital bone. It is innervated by the ventral rami of cervical nerves C1–C2, and it receives blood from the muscular branches of the vertebral artery, from the occipital artery, and from the ascending pharyngeal artery. It functions to flex the head laterally to the same side.

The anterior scalene muscle originates on the anterior tubercles of the C3–C6 transverse processes. It inserts on the scalene tubercle on the first rib. It is innervated by the anterior rami of cervical nerves C5–C8, and it receives blood from the ascending cervical branch of the inferior thyroid artery. It functions to elevate the first rib and bend the neck.

The middle (medius) scalene muscle originates on the posterior tubercles of the C2–C7 transverse processes. It inserts on the upper surface of the first rib, behind the subclavian groove. It is innervated by the anterior rami of cervical nerves C3–C7, and it receives blood from the muscular branches of the ascending cervical artery. It functions to elevate the first rib and bend the neck.

The posterior scalene muscle originates on the posterior tubercles of the C4–C6 transverse processes. It inserts on the outer surface of the second rib, behind the attachment of the serratus anterior muscle. It is innervated by the anterior rami of the lower four cervical nerves (C5–C8), and it receives blood from the muscular branches of the ascending cervical division of the inferior thyroid artery and from the superficial branch of the transverse cervical artery. It functions to elevate the second rib and bend the neck.

This concludes the section concerning the major musculature of the neck region.

Neurovasculature

Having described the locations of the major muscles of the neck, we will now describe the pathway of the major nerves and blood vessels of the neck. Locations of the nerves will be made apparent through referencing the major musculature previously described (Fig. 1.13).

Superficial Nerves

The transverse cervical nerves originate from the ventral rami of spinal nerves C2 and C3 deep to the posterior aspect of the sternocleidomastoid and course

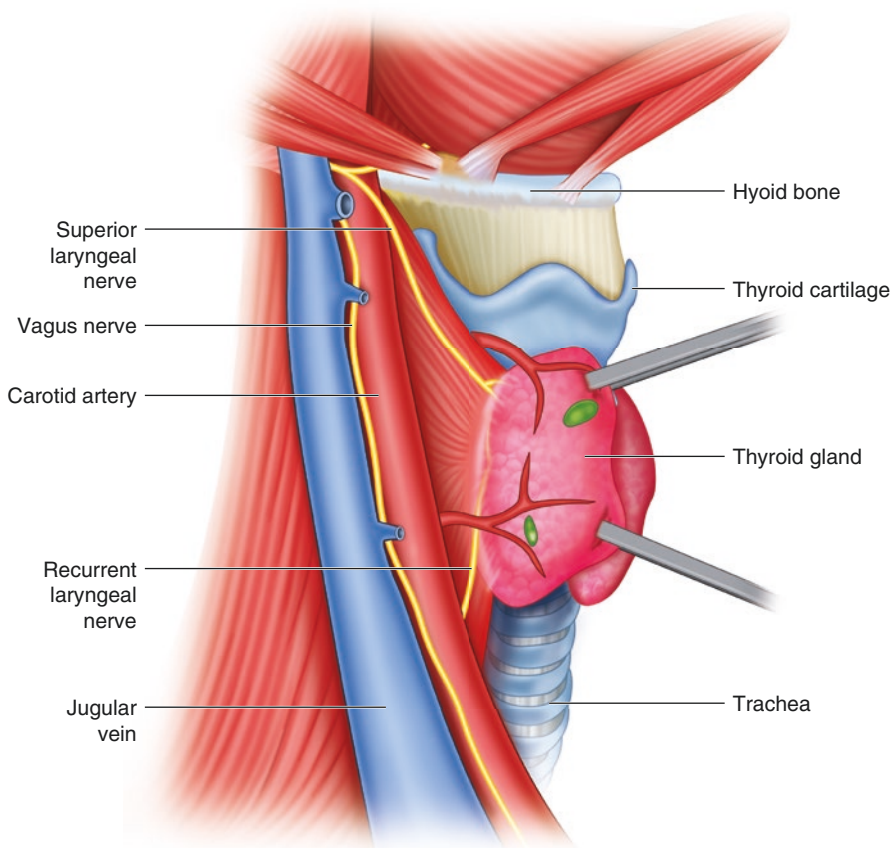


Fig. 1.13 The pathway of the major nerves and blood vessels of the neck

superficially to the sternocleidomastoid muscle and the omohyoid and sternohyoid muscles, from lateral to medial. These nerves branch widely across the sternocleidomastoid and terminate on the sternohyoid.

The great auricular nerve originates from the ventral ramus of spinal nerve C2. It emerges from behind the sternocleidomastoid and travels superiorly toward the head, anterior to the lesser occipital nerve. The lesser occipital nerve also originates from the ventral ramus of spinal nerve C2, and it remains deep to the sternocleidomastoid until emerging near the occipital base of the skull.

The supraclavicular nerves emerge from behind the sternocleidomastoid and divide into several (3) branches, each branch coursing inferiorly toward the clavicle in a different position along the sagittal plane.

The accessory nerve (CN XI) is largely obscured by the sternocleidomastoid; upon reflection of the muscle, the course of XI can be visualized. Having its origins directly from the brain stem, XI receives a nerve branch from the ventral rami of spinal nerves C2, C3, and C4. These ventral rami emerge between the anterior and middle scalene muscles before each contributing a branch to XI (Fig. 1.14).

The ventral rami each receive a gray ramus from the superior cervical sympathetic ganglion, which converges with the ventral ramus very soon following its emergence from the vertebral column.

The ventral ramus of C1 feeds into that of C2. This feeder branch gives off a communicating branch to the vagus nerve and also gives off branches to supply the rectus capitis lateralis, longus capitis, and rectus capitis anterior muscles. C1 also

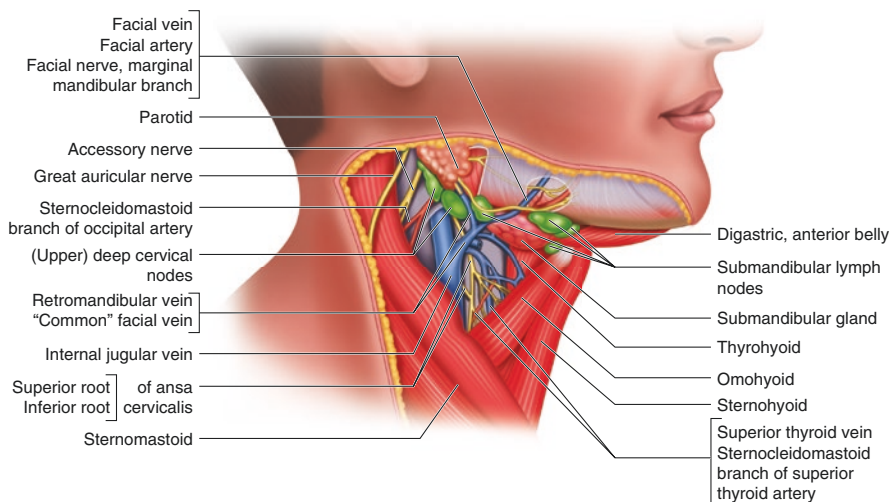


Fig. 1.14 The accessory nerve (CN XI) is largely obscured by the sternocleidomastoid; upon reflection of the muscle, the course of XI can be visualized. Having its origins directly from the brain stem, XI receives a nerve branch from the ventral rami of spinal nerves C2, C3, and C4. These ventral rami emerge between the anterior and middle scalene muscles before each contributing a branch to XI

gives rise to the superior root of the ansa cervicalis loop and continues anteriorly to give off branches to innervate the geniohyoid and thyrohyoid muscles. For much of its course, C1 travels adjacent to the hypoglossal nerve (CN XII). The ventral ramus of C2 gives off early branches to supply the longus capitis and longus colli muscles. C2 then gives off a branch joining to the accessory nerve and continues on to feed into C3. This feeder branch gives off a posteriorly coursing branch from which arise the great auricular nerve and the lesser occipital nerve. This same feeder branch also gives off an anteriorly coursing branch from which arise the three transverse cervical nerves. The main ventral ramus of C2 also serves as the origin of the inferior root of the ansa cervicalis loop. The ventral ramus of C3 gives off early branches to supply the longus capitis and longus colli muscles, and then gives off a branch joining to the accessory nerve. Continuing on, the feeder branch from C2 joins C3. Moving further, C3 contributes a branch to the inferior root of the ansa cervicalis loop, joins a branch of C4 to give off a branch from which the supraclavicular nerves arise, joins another branch of C4 to give off a branch from which the phrenic nerve arises (which also receives a contribution from C5), and gives off branches to the scalene and levator scapulae muscles. The ventral ramus of C4 gives off early branches to supply the longus capitis and longus colli muscles, and then gives off a branch joining to the accessory nerve. Continuing on, C4 joins C3 to give off a branch from which arise the supraclavicular nerves. C4 also contributes with C3 to give rise to the phrenic nerve. Furthermore, C4 gives off branches that supply the scalene and levator scapulae muscles.

Moving anteriorly, the ansa cervicalis is a looping nerve that receives its origins from the ventral rami of spinal nerves C1, C2, and C3. The loop is divided into two roots: the superior root is the anterior aspect of the loop, and the inferior loop is the posterior aspect of the loop. Moving along the loop from the inferior root to the superior root (after the contribution from C3), the ansa cervicalis gives off the following branches: a branch to the omohyoid muscle (inferior belly), a branch to the sternohyoid muscle, a branch to the sternothyroid muscle, a branch to the superior belly of the omohyoid muscle (located on the superior root). Then the loop converges with C1.

The nerve to mylohyoid branches off the mandibular branch of the trigeminal nerve to innervate the mylohyoid muscle. The pharyngeal plexus is located at the level of the mandibular angle and is comprised of branches from the glossopharyngeal nerve (CN IX), the vagus nerve (CN X), and sympathetic nerves.

The hypoglossal nerve (CN XII) courses in the superior neck in a posterior-to-anterior direction before delving deep to the mylohyoid muscle.

The vagus nerve (CN X) courses in a superior-to-inferior direction down the neck, near the internal and common carotid arteries and superficial to the anterior scalene muscle. In its downward course, the vagus nerve gives off branches that contribute to the pharyngeal plexus; it gives off the superior cervical cardiac branch; it also gives off the superior laryngeal nerve, which gives rise in turn to an internal branch (which pierces the foramen in the thyrohyoid membrane) and an external branch (which continues its inferior course toward the pharyngeal constrictors). Continuing inferiorly, the vagus nerve gives off the recurrent laryngeal nerve: on the

right side of the body, the right recurrent laryngeal nerve loops under the right subclavian artery to course superiorly and innervate pharyngeal constrictor muscles; on the left side of the body, the left recurrent laryngeal nerve branches off the vagus nerve under the arch of the aorta and continues its course superiorly to innervate pharyngeal constrictor muscles.

The sympathetic trunk courses in a superior-to-inferior direction anterior and adjacent to the vagus nerve. The trunk also contains notable ganglia such as the middle cervical ganglion located at the level of the superior trachea.

The phrenic nerve (C3, C4, C5) courses in a superior-to-inferior direction posterior to the vagus nerve and superficial to the anterior scalene muscle.

The brachial plexus (superior, middle, and inferior trunks) emerges between the anterior and middle scalene muscles.

The following paragraphs will describe the major vasculature of the neck region (Figs. 1.13, 1.15).

The largest veins in the neck are the internal jugular veins, which course directly deep to the sternocleidomastoid muscle. It receives blood from the superior thyroid vein and the middle thyroid vein. Inferiorly, the internal jugular vein feeds directly

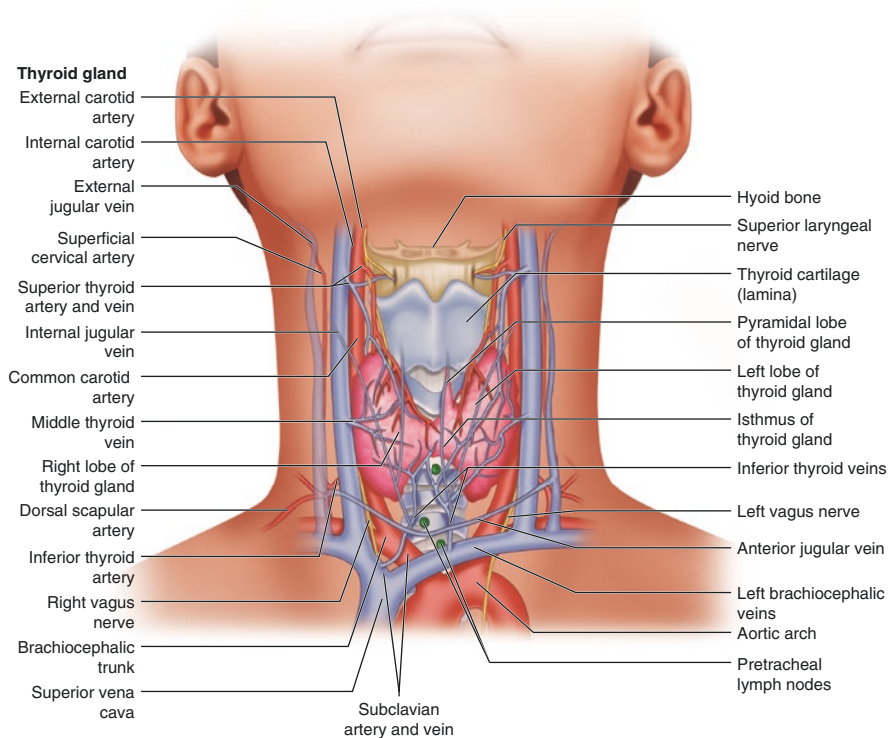


Fig. 1.15 The major vasculature of the neck region

into the subclavian vein at the level of the clavicle. The external jugular veins are smaller in diameter than the internal jugulars, and they course superior to the sternocleidomastoid muscle and the superficial layer of deep cervical fascia. Superiorly, the external jugular veins become the retromandibular vein anteriorly and the posterior auricular vein posteriorly, just below the level of the lower mandible border. Two anterior jugular veins course near the midline of the neck, becoming the submental veins superiorly. A communicating vein runs adjacent to and connects to each external jugular vein.

Coming directly off the subclavian artery is the thyrocervical trunk, which gives rise to the inferior thyroid artery. The main artery in the neck is the common carotid artery. Traveling superiorly, it bifurcates into the internal carotid artery and the external carotid artery inferior to the digastric muscle. The external carotid artery has several branches. Beginning directly after the common carotid bifurcation and traveling superiorly, the external carotid gives off the superior thyroid artery, which in turn gives off the superior laryngeal branch. Next, the ascending pharyngeal artery arises. Then, the lingual artery arises. Next, a branch arises that gives off the sternocleidomastoid branch, then the descending branch, and finally the occipital artery. About the same level but on the contralateral side of the external carotid, the facial artery arises. Next, the posterior auricular artery arises. Next, the maxillary artery is given off. It is about this point that the external carotid artery becomes the superficial temporal artery, which gives off the transverse cervical artery.

Conclusion

As evidenced by the descriptions above, the neck is an area of great complexity, with critically important musculature and neurovasculature. Its dense anatomy testifies to its importance to the body, linking the head and thorax and housing crucial nerves that control vital functions. The neck is a fascinating and highly involved area of anatomical study.

Suggested Reading

1. Hiatt JL, Gartner LP. Chapter 7: Neck. In: Textbook of head and neck anatomy. 4th ed. Philadelphia: Lippincott Williams & Wilkins; 2010. <https://thelivesaversblog.files.wordpress.com/2015/11/textbook-of-head-and-neck-anatomy.pdf>. Accessed 4 August 2019.
2. Moore KL, Dalley AF, Agur AMR. Chapter 8: Neck. In: Clinically oriented anatomy. 7th ed. Baltimore: Lippincott Williams and Wilkins; 2014.
3. Netter FH. Atlas of human anatomy. 6th ed. Philadelphia: Saunders/Elsevier; 2014.



Challenges of Dental Surgery and Oral and Maxillofacial Surgery in Patients with Anatomical Anomalies

2

Yoonah Danskin, Jessie Reisig, and Thomas G. Duplinsky

Introduction

Restricted mouth opening (RMO) in patients with anatomical anomalies is a major challenge in dental and oral surgery. There are many causes of restricted mouth opening. The origin of the anatomic anomaly may be acquired, such as in burn victims and in patients with disorders of the temporomandibular joint, or developmental, such as in Marfan syndrome.

In this chapter, we will discuss some of the most common anatomical anomalies associated with restricted mouth opening. Anatomical anomalies may arise in skeletal bone, muscle, and connective tissue. We will discuss dental management of these challenging cases.

Trismus

Restricted mouth opening (RMO) is an umbrella term for decreased mouth opening that results from various causes. Normal mouth opening is considered between 40 and 60 mm [1]. RMO can lead to difficult surgical access to the oral cavity and complicated esophagogastroduodenoscopy, requiring creative means to intubate the patient safely [2].

One cause of RMO is trismus, defined as restricted mouth opening of muscular cause. Trismus has several different etiologies including infection of the

Y. Danskin
VA NY Harbor Healthcare Systems, New York, NY, USA

J. Reisig
Tribeca Endodontics (3D Micro Endo), New York, NY, USA

T. G. Duplinsky (✉)
Yale University School of Medicine, New Haven, CT, USA
e-mail: Thomas.Duplinsky@yale.edu

Table 2.1 Muscles of mastication and their respective functions

Muscle of mastication	Basic function
Masseter	Elevation of mandible
Temporalis	Elevation and retraction mandible
Medial pterygoid	Elevation of mandible
Lateral pterygoid – superior head	Elevation and retraction of mandible
Lateral pterygoid – inferior head	Protraction of mandible (bilateral), depression of mandible (bilateral), contralateral excursion (unilateral)

masticatory spaces, trauma (especially to the temporomandibular joint or zygomaticomaxillary complex), recent local anesthetic administration, tumors or neoplasms, and radiotherapy. Trismus may also be of congenital origin. The source of the trismus, especially when ruling out neoplasm, is diagnosed through medical history and clinical exam, and appropriate radiographs and laboratory testing. Patients may present with trismus and guarding because of pain; the relief of the pain may resolve the trismus [3, 4]. The muscles of mastication and their respective functions are presented in Table 2.1. Pathology in any of these muscles may be associated with trismus.

Trismus Caused by Head and Neck Radiotherapy

After treatment of head and neck tumors, the incidence of trismus ranges from 5% to 38% [5, 6]. Radiation therapy-induced trismus has been attributed to radiation-induced fibroatrophic activity, a fibrosis of the muscles of mastication because of fibroblast dysregulation. Radiation-induced ischemia and endarteritis obliterans contribute to the fibrosis of the muscles and to subsequent trismus [7]. Trismus may develop as early as 1 month or as late as 12 months after radiation therapy. In general, higher doses of radiation increase the risk of trismus; the masseter and pterygoid muscles are the most sensitive to dose-related trismus [8, 9]. Post-radiation RMO should be further investigated to rule out causes other than trismus; these include osteomyelitis-induced pathologic fractures, presence of tumor, or pathology of the temporomandibular joint.

Management of Post-radiotherapy Trismus

Reported treatments of post-radiation trismus include pain relief with warm compresses, warm saline rinses, anti-inflammatory analgesics, and muscle relaxant administration. Pentoxifylline administration is thought to increase range of motion by influencing cytokine-mediated inflammation. Physical therapy using various intraoral appliances, along with jaw exercises such as chewing gum, may be recommended to increase mouth opening and reduce further restriction [3, 7, 10, 11]. In severe cases, when conservative therapies have been exhausted, surgical intervention to release the musculature may be considered [12].

Infectious Origins of Trismus

Infections can cause inflammation and spasm of the elevator muscles, resulting in trismus and decreased opening ability. Deep fascial plane abscesses of the head and neck are most commonly of odontogenic origin [13]. Infections originating in teeth may spread through the medullary spaces and perforate the cortical plate of the maxilla or mandible to a fascial plane from which there are no natural pathways for drainage [14]. Odontogenic infection may originate in the tooth root canal system (caused by caries or trauma) or in the soft tissue surrounding teeth (including periodontal disease, pericoronitis, and infection of dental surgical sites) [4]. Clues to possible odontogenic infection (besides obvious swelling) include broken-down and carious teeth and erythema of periodontal tissues.

Frequent causes of trismus are infections of fascial spaces of the head and neck, including the submasseteric, pterygomandibular, lateral pharyngeal, temporal, infratemporal, and masticator spaces. Trismus may be the only external sign of pterygomandibular and lateral pharyngeal space infections and should be treated aggressively because of the risk of spread to the retropharyngeal space, with possible resultant airway compromise. Diagnosis of deep fascial space infections often requires CT scans to determine the extent of the infection and possibly the location of the source [14].

Management of Trismus of Infectious Origin

The primary treatment of trismus of infectious origin is intraoral or extraoral surgical drainage followed by antibiotic coverage [14]. Mature or severe odontogenic infections predominately involve anaerobic organisms, some resistant to penicillin [15]. The source of the infection must also be addressed, typically with extraction or endodontic treatment (root canal therapy) of the offending tooth, or infection is likely to recur [14].

Temporomandibular Joint Closed Lock

The temporomandibular joint (TMJ) is a ginglymoarthrodial joint. On normal initial opening, the mandibular condylar head acts in a hinge-like movement and then slides anteriorly to enable maximal opening of the mouth. A biconcave articular disc is present between the mandibular fossa of the temporal bone and the condylar head of the mandible. The articular disc has circumferential soft tissue attachments to help hold the disc in appropriate place while moving in sequence with the mandibular condylar head. It is fairly common for the articular disc to become displaced from the articular head upon opening of the joint and reduced or recaptured by the articular head on closing. If the disc becomes displaced and does not reduce spontaneously, then trismus may result. In these cases, when opening, the articular disc becomes displaced anteriorly, medially, or laterally relative to the condylar head and is not recaptured on closing; opening of the jaw is limited to that allowed by the

hinge movement function only (see Fig. 2.1). The disc may be examined by MRI studies; however, in advanced cases, inflammation of the joint may occur [16, 17].

Management of Temporomandibular Joint Closed Lock

In the acute phase, mobility may be restored by bilateral manipulation of the mandible with the affected side pressed inferiorly and then anteriorly in an effort to recapture the disc. In cases of chronic disc displacement, conservative treatments include exercises and splints [16, 17]. More invasive procedures to treat chronic disc displacement without reduction include arthrocentesis to reduce inflammation in the joint space; arthroscopic surgery to lyse inflammatory adhesions in the joint; and

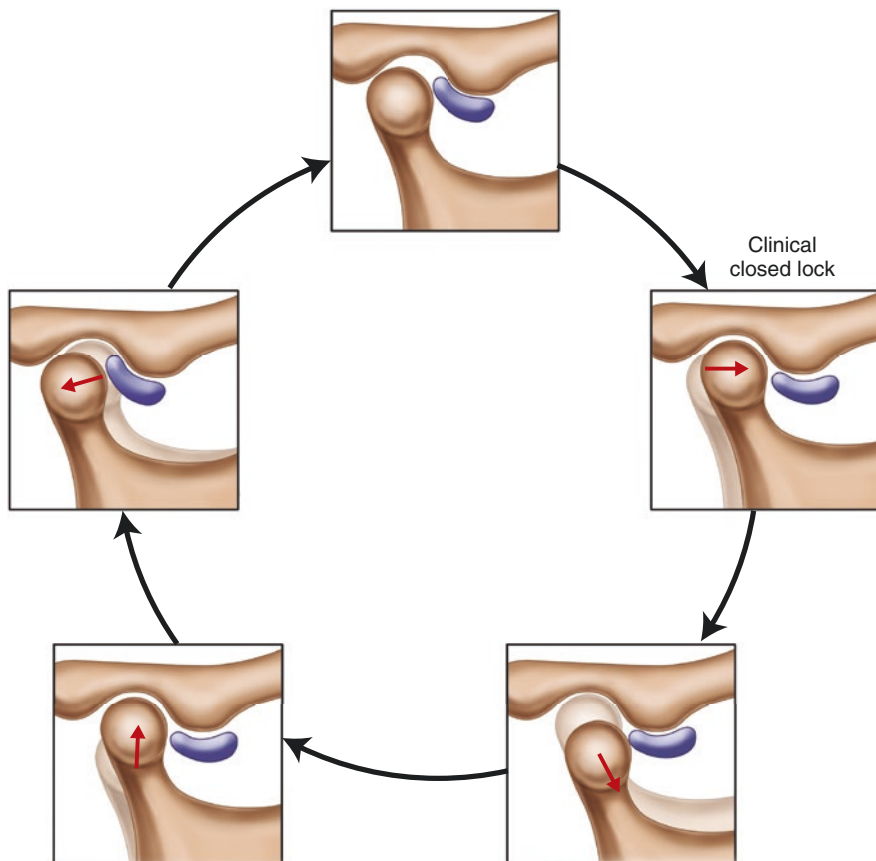


Fig. 2.1 Diagram showing temporomandibular joint mechanics with anteriorly displaced condylar disc blocking normal forward excursion of the condylar head of the mandible during mouth opening. The non-reduced disc in this abnormally forward position prevents normal movement of the condylar head, thus restricting mouth opening (“closed lock”)

arthroplasty, including possible disc repositioning, articular surface recontouring, or disc removal. Conservative treatment is recommended prior to initiation of invasive surgical techniques and following more invasive treatments [17].

Temporomandibular Joint Ankylosis

TMJ ankylosis can result in restricted mouth opening and is most commonly caused by trauma (*see* Fig. 2.2a–c). Traumatic hematomas may result in fusion of the condylar head and/or coronoid process to the base of the skull. Local or systemic infection, systemic autoimmune diseases (ankylosing spondylitis, rheumatoid arthritis, psoriatic arthritis), and congenital deformation are also common causes of TMJ ankylosis. Ankylosis can result in bone growth in juxta-articular tissue, which can limit the range of mouth opening. In the growing pediatric population, TMJ

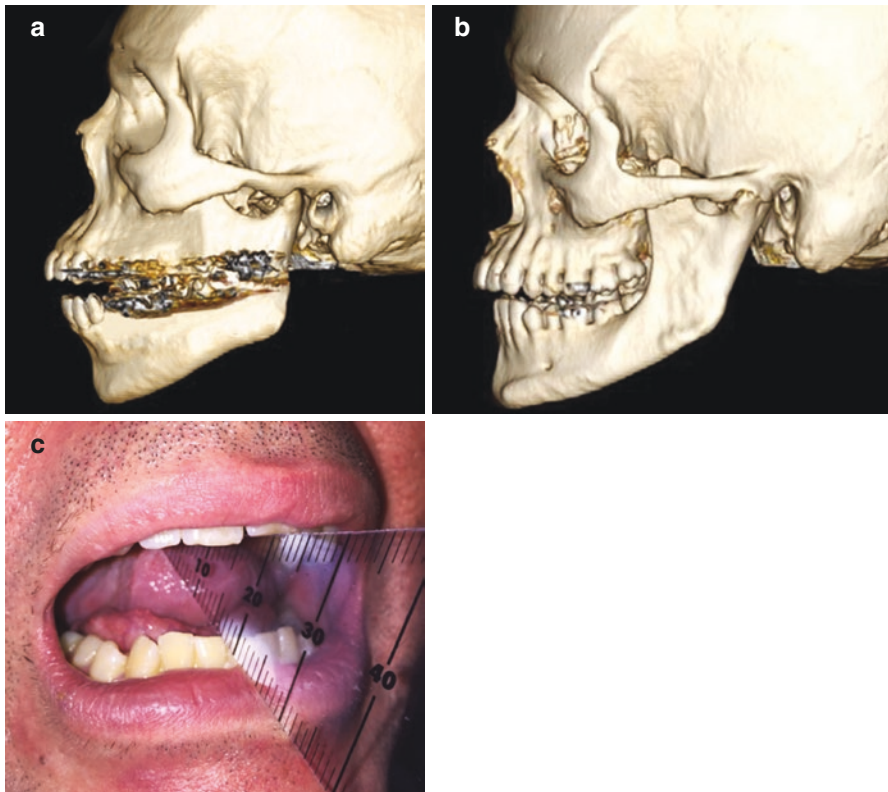


Fig. 2.2 (a) Three-dimensional CT scan reconstruction showing normal temporomandibular joint and coronoid process. (b) Three-dimensional CT scan reconstruction showing coronoid process hyperplasia of the mandible and ankylosis of the temporomandibular joint. (c) Photograph of patient depicted in Fig. 2.2b showing restricted mouth opening of 17 mm

ankylosis may present with micrognathia, retrognathia, and obstructive sleep apnea. The term “complete ankylosis” is used when TMJ ankylosis results in RMO of less than 5 mm [18].

Management of Temporomandibular Joint Ankylosis

Options for surgical correction include gap arthroplasty and interpositional gap arthroplasty; joint reconstruction may be required in severe cases of ankylosis as determined by clinical presentation and radiologic examination [19].

Coronoid Process Hyperplasia

Coronoid process hyperplasia, also known as coronoid impingement syndrome, usually presents as a painless, progressive diminution in maximum mouth opening caused by increased size of the coronoid process of the mandible, medial surface of the zygomatic arch, or temporal aspect of the zygomatic bone [20]. Hyperplasia can be bilateral or unilateral. Unilateral hyperplasia often presents with facial asymmetry [21, 22]. Osteomas and osteochondromas must be considered in cases of unilateral facial asymmetry and restricted mouth opening [23]. Jacob’s disease includes the pathological elongation of the coronoid process including the formation of a new joint (including cartilage and synovial fluid) with the zygomatic process and may present in pediatric patients but is most likely to present in young adult males [22, 24, 25]. Possible causative factors for coronoid process hyperplasia also include previous trauma to the TMJ (*see* Fig. 2.2b), temporal muscle hyperactivity, chronic disc displacement, endocrine anomalies, genetic abnormalities, and previous growth hormone therapy for idiopathic short stature [26]. Open-mouth CT scans are particularly useful for diagnosis because these scans can show direct impingement of the coronoid process on the zygoma [27].

Management of Coronoid Process Hyperplasia

Surgical intervention is indicated if limited mouth opening impedes function. Treatment usually includes coronoidectomy via an intraoral approach followed shortly thereafter by physiotherapy. Early physiotherapy avoids fibrosis of the area and conditions the muscles for a greater opening envelope [28].

Oral Submucous Fibrosis

Oral submucous fibrosis (OSF) is characterized by inflammation of the epithelium of the oral mucosa, followed by fibrosis of the associated lamina propria [29]. The fibrosis progresses by collagen deposition from increased proliferation of

fibroblasts; OSF may include vesicle formation and ulceration [29]. The etiology of OSF is multifactorial, although it is highly correlated with the chewing of areca nut and betel quid, most common in the Indian Subcontinent and South Asia [29, 30, 31]. OSF is more prevalent in males than in females and occurs most commonly between the ages of 40 and 60 [31].

Oral-Facial Manifestations of Oral Submucous Fibrosis

Reported symptoms of OSF are burning sensation and petechiae of the oral mucosa, deafness, and/or referred pain to the ear due to fibrosis of the eustachian tubes, trismus, and restricted mouth opening [29]. The latter two result from fibrosis of the pterygomandibular raphe, muscles, and the overlying intraoral submucous tissue [29]. Fibrosis may extend to the lips, tongue and palate, nasopharynx, and the oropharynx, leading to dysphagia [29]. OSF is also highly correlated with the development of oral cancer, most commonly squamous cell carcinoma [29, 30].

Management of Oral Submucous Fibrosis

Although fibrosis itself cannot be reversed, slowing the progression of the disease through behavioral changes is crucial, involving cessation of betel quid and areca nut usage. Physical therapy aimed to improve restricted mouth opening includes various splints and heat treatment. This may be concomitantly recommended with anti-inflammatory medications such as steroids, anti-ischemic medications such as pentoxifylline, and/or proteolytic agents such as collagenase or hyaluronidase. In most severe cases, surgery may be recommended, involving incision and releasing of fibrous bands and forceful opening of the jaw under general anesthesia [29].

There is a high rate of oral cancer in patients afflicted with OSF. Radiation therapy (RT) is contraindicated in treating these patients with oral cancer because pre-existing fibrosis will lead RT to have even worse ischemic and hypoxic effects on the involved tissue. When RT or chemotherapy is inevitable, hyperbaric oxygen therapy may be considered [30].

Masticatory Muscle Tendon-Aponeurosis Hyperplasia

Masticatory muscle tendon-aponeurosis hyperplasia (MMTAH) was first identified in year 2000, characterized by bilateral hyperplasia of the tendons and aponeurosis associated with masticatory muscles, leading to restricted mouth opening [32–34]. MMTAH progresses slowly from childhood and is more common in females than in males [34]. Magnetic resonance imaging (MRI) study of this condition from the axial view uniquely shows bilateral overhang of masseter muscle from the anterior border of the mandibular ramus, and histological study of the affected tendon and aponeurosis shows evidence of intramembranous ossification [33]. The etiology of

MMTAH is unknown, although current hypotheses include parafunctional habits and genetic tendencies [33]. Currently, the condition is divided into three types depending on cephalometric measurements. In type 1 disease, there is a flattening of both occlusal and mandibular planes. Type 2 describes the flattening of only the mandibular plane, whereas type 3 describes normal occlusal and mandibular planes [33].

Oral-Facial Manifestations of Masticatory Muscle Tendon-Aponeurosis Hyperplasia

Square mandible, palpable dense band at the anterior border of the masseter muscle on maximum opening of the jaw, and restricted mouth opening are all clinical manifestations of MMTAH [34]. The condition appears to have no effect on protrusive and lateral mandibular movements. Difficulty of intubation is a chief concern for patients with MMTAH [33].

Management of Masticatory Muscle Tendon-Aponeurosis Hyperplasia

There is no evidence that physical therapy is effective in increasing the mouth opening of patients with MMTAH. Surgical treatment options include aponeurectomy of the masseter muscle with coronoidectomy, mandibular anglectomy, or masseter muscle myotomy. Postoperative mouth opening exercises are strongly recommended [33].

Scleroderma

Scleroderma is a rare chronic autoimmune disease that involves fibrosis of connective tissue from excessive collagen deposition and involves obliteration of microvasculature [35–37]. Scleroderma can be either systemic or localized. In systemic scleroderma, skin, vessels, and various internal organs such as the gastrointestinal tract, heart, lungs, and kidneys can be affected by the fibrosis [36]. Interstitial lung disease is the most common cause of death in patients with systemic scleroderma [38]. In localized scleroderma, only discrete areas of skin are affected, with or without nearby bone and muscle involvement [39]. Scleroderma is more common in females than in males [39]; the median age of onset is 30–50 years [38]. The cause of scleroderma is unknown [38]; there is no cure and the management of the disease manifestations is crucial to the well-being of the patient.

Oral-Facial Manifestations of Scleroderma

Common oral-facial manifestations of scleroderma include restricted mouth opening [35–41] and movements [36, 38] as well as perioral cutaneous fibrosis resulting in deep rhytids (*see* Fig. 2.3a and b). Xerostomia and decreased lacrimal secretion result from fibrosis of glandular tissues [37, 40]. Other common manifestations include dysphagia caused by fibrosis of the tongue, palate, and larynx [35, 36, 39], gastroesophageal reflux [38], increased risk of periodontal disease and caries [35, 38], widening of periodontal ligaments and thickening of lamina dura [39], and enamel erosion [40]. Additional manifestations may include resorption of borders of the mandible from continuous pressure applied by the taught facial skin [38], trigeminal neuropathy by fibrosis of the perineurium and decreased vascularity [38, 41], telangiectasia of oral mucosa [35, 41], obliteration of taste buds [35], and signs and symptoms of temporomandibular disorder [39]. In addition to oral-facial manifestations, claw-like deformity of the hands from sclerodactyly (fibrosis of fingers) significantly decreases the manual dexterity needed to practice proper oral hygiene [39, 41].

Management of Scleroderma

Seventy percent of patients with scleroderma have microstomia [40], limiting oral access required for routine dental care. Some management recommendations include physical therapy [37, 40], use of sectional flexible dentures [37],

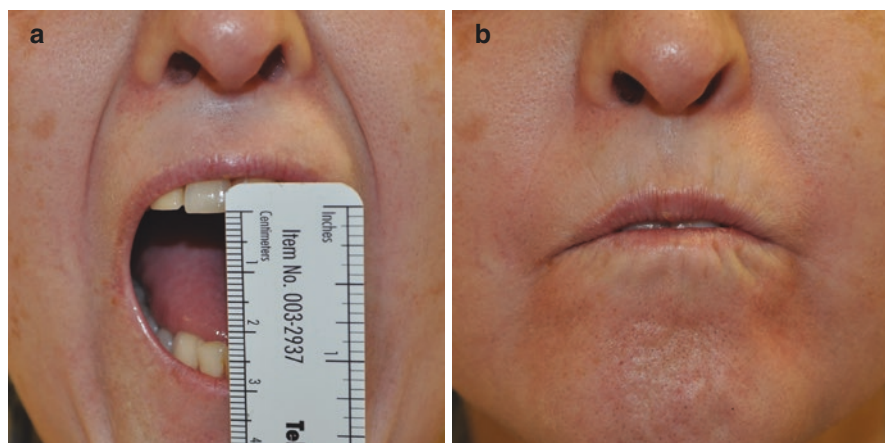


Fig. 2.3 (a) Photograph showing restricted incisal opening in a scleroderma patient. The normal incisal opening (maximal distance between cutting edges of upper and lower incisors) is 35 mm or more. (b) Photograph showing fibrosis of perioral skin causing deep rhytids in a scleroderma patient

mouth-opening exercises using splints [37], or stacked tongue depressors placed between the incisal openings [39]. Additional recommendations for dental professionals include various pharmacological management of Raynaud's phenomenon which can be seen in patients with scleroderma [40], limitation of epinephrine when providing local anesthesia, and quadrant dentistry to avoid prolonged treatment time [37]. Early diagnosis and aggressive preventive measures are crucial [37] and should involve regular hygiene recall and oral hygiene instructions. The clinician should consider recommending fluoride trays, pharmacological agents to stimulate salivary flow, and electric toothbrushes for the patient.

Management of Scleroderma in the Operating Room

Before a patient with scleroderma is brought to the operating room, extensive evaluation by the anesthesiologist and a multidisciplinary approach are required. The anesthesiologist needs to evaluate the extent of the involvement of pulmonary hypertension and cardiac fibrosis. The following should also be assessed: the difficulty in starting an IV line due to fibrosis of the skin, the level of microstomia which will dictate whether oral intubation will be possible, and also whether the patient has gastroesophageal reflux which will increase the risk for aspiration pneumonia after extubation [37]. While the scleroderma patient is intubated, their temperature should be monitored carefully to avoid Raynaud's phenomenon [37, 40, 42]. Any jaw manipulation to increase oral access or the use of bite blocks may lead to commissural disruption, which will require surgical intervention [37]. In the most severe cases, bilateral commissurotomy may be necessary for access [39].

Burn Injuries

Up to 2 million burn injuries are reported every year in the United States [43]. Facial burns involving the perioral region can have life-altering consequences by causing skin contracture, decreasing the size of oral aperture [43, 44]. Deeper burn injuries increase the severity of microstomia [45].

Manifestations of Microstomia from Burn Injuries

Among the many clinical manifestations of microstomia from burn injuries are facial disfiguration [46], reduced function while eating or speaking [47], reduced access for regular oral hygiene [48], difficult airway control during orotracheal intubation for general anesthesia [44, 48], limited range of facial expressions [46], and inability to control spillage of saliva from the mouth [47]. In the pediatric population, clinical manifestations of microstomia are further complicated by the

psychological and developmental challenges of a growing child where the skeletal and dental development is inhibited by the overlying taut skin [43].

Management of Microstomia from Burn Injuries

Any signs of microstomia in burn patients require immediate attention and multidisciplinary care [43]. Clinicians need to investigate what treatments have been rendered since the burn injury. Patients may have already undergone initial surgical care to minimize tissue contracture around the mouth and to optimize healing [44].

Early physical therapy will reduce the contracture of the tissue, increase function, and decrease the likely need for surgical interventions. Physical therapy consists of the use of intraoral or extraoral mouth-stretching devices; use of these devices may increase the opening of the mouth in vertical, horizontal, and/or in circumoral orientations. Use of combination of different types of appliances has shown to provide maximum results. Mouth-stretching devices may facilitate proper oral intake, oral hygiene, facial expression, and intubation in burn patients. Stretching mouth devices are customized and may be fabricated by dentists, occupational therapists, or physical therapists. The fabrication of such device requires assessment of various patient specific factors such as age, compliance, state of current dentition, as well as severity of the burn, as continuous wear of the device is essential for maximum benefit [49].

If a conservative method is not adequate, commisuroplasties under general anesthesia with nasotracheal intubation may be considered. Commisuroplasty is challenging due to the difficulty of reconstructing the vermilion border. The surgery is generally recommended after full scar maturation in order to prevent recurrent scar contracture; however, sometimes early surgery may be necessary in cases of severe microstomia. Commissure reconstructive surgery can be performed with mucosal advancement flaps [44]. Scar excision and skin grafting are generally not recommended because these procedures may deform the oral angles, making mucosa visible in the commissure zone [44, 48]. After surgery, the use of a custom splinting device is recommended for as long as 6 months for best results [44].

Subcutaneous Emphysema

Subcutaneous emphysema (SE) occurs from inadvertent introduction of gas or air into fascial planes [50]. Connective tissue is loose and expandable, and fascial planes are interconnected, all of which accommodates the spread of SE. Fascial planes can be categorized into superficial and deep. Superficial fascia of the face and neck envelopes muscles of facial expression and platysma muscle. Deep fascia

surrounds the temporal, masseteric, and medial pterygoid muscles. SE can affect both levels of fascial planes.

SE has been observed in the head, neck, and thorax. The clinical signs of SE generally include painless localized swelling with crepitus upon palpation [50]. This differentiates SE from other conditions such as allergic reactions, hematoma, cellulitis, or angioedema.

Etiologies of SE can be divided into iatrogenic, traumatic, infectious, and spontaneous [51]. SE can result from mucosal laceration of the trachea during endotracheal intubation [51], damage of the alveoli from increased pressure during mechanical ventilation [51], head and neck surgeries or injuries [51], or dental procedures [50] (*see* Fig. 2.4).

Introduction of gas or air into fascial planes from dental procedures is facilitated when there is unattached gingiva, either from preexisting conditions such as periodontitis or from intentional surgical incisions. Unattached gingiva allows easy access for gas or air to be introduced into the periosteum and fascial planes.

Cases of SE from dental procedures have largely been observed in patients on whom air-driven hand pieces [50, 52] or air-water syringes [53] have been used. SE has been observed in surgical extractions [50], in endodontic treatments [52], in treatments using dental lasers [53], and in restorative procedures [50]. SE during extractions can occur when air-turbine hand pieces instead of high torque surgical drills are used [50]. SE has been reported in endodontic treatment in which the surgeon dried root canals with air syringes [52]. In one report, SE resulted from the release of oxygen when hydrogen peroxide (used as a canal irrigant and disinfectant in root canal therapy) contacted blood [54]. SE has also been observed during dental treatment using laser [53].

The occurrence of SE of the face and neck can be immediate [50], crossing the midline, often extending superiorly and inferiorly. Symptoms of SE usually subside within 7 days [50, 55]; however, the extent of morbidity is still unpredictable and can have life-threatening consequences with the risk of air embolism to the heart or brain, causing ischemic lesions in the brain or pericardial emphysema [50]. Other possible complications of SE of the face and neck include pneumothorax or pneumomediastinum. Clinical symptoms of pneumomediastinum include dyspnea, chest pain, back pain, and Hamman's sign, a crunching sound with heart beat [50].

Management of Subcutaneous Emphysema

A common treatment for SE is antibiotic therapy. This is because SE may introduce bacteria from the oral cavity or from the air. Although there is no consensus, some case reports include treating patients with steroids such as dexamethasone. Exploratory surgery or tracheotomy has also been performed in some cases of SE. In cases of SE, radiographic examination is recommended in order to determine the extent and location of emphysema [50].

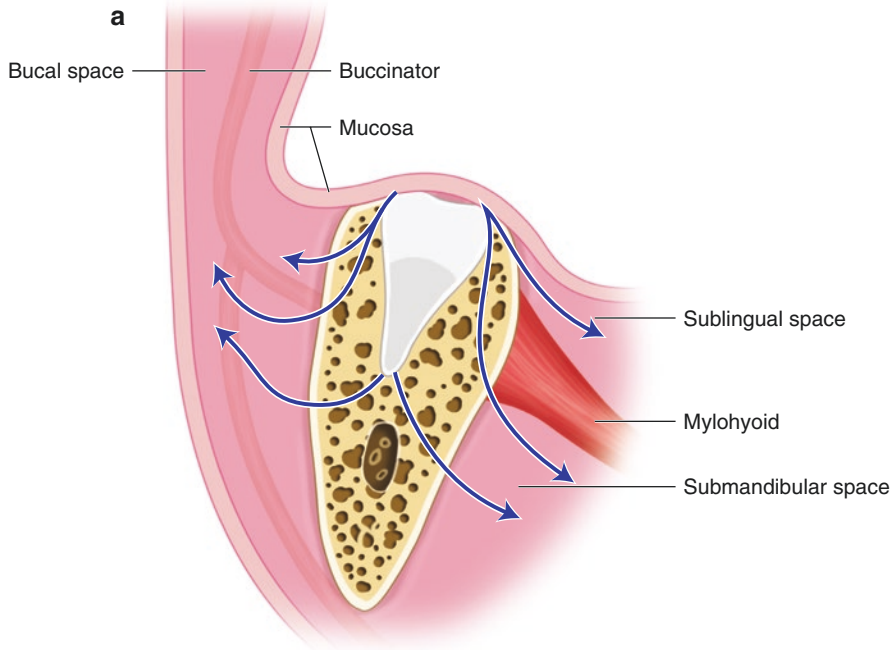


Fig. 2.4 (a) Diagram showing potential spread of air through fascial planes after introduction by an air-driven handpiece used for tooth sectioning. (b) Example of patient with subcutaneous emphysema

SE is best prevented by the careful use or avoidance of directed compressed air in the presence of unattached gingiva, during root canal therapy, open flap procedures, or during extractions. For the latter, high torque surgical drills that rely on an electric motor drive system should be used instead of air driven hand pieces. Lastly, the use of hydrogen peroxide is not recommended during root canal therapy.

Obesity

Obesity is a chronic medical condition that is multifactorial in origin and is characterized by excess adipose tissue [56, 57]. Obesity is defined by excessive body mass index (BMI), calculated as the patient's weight in kilogram divided by the square of their height in meters (kg/m^2). For adults, a BMI of $30 \text{ kg}/\text{m}^2$ or greater is considered obese [56]. Obesity is a major public health concern [56]. According to the Centers for Disease Control, more than one-third of US adults are obese [58]. Many serious systemic and chronic medical conditions are associated with obesity [56]. The most common co-morbidities of obesity include type II diabetes [56], hypertension [57], cardiovascular disease [56, 57], cancer [59], sleep disorder [57, 59], osteoarthritis [56], rheumatoid arthritis [57], and pulmonary complications such as obesity-hypoventilation syndrome [59] and asthma [56]. Studies also suggest that obese patients are more likely to have postoperative complications such as dehiscence of wounds or infection [56].

Fig. 2.5 Photograph of enlarged tongue of obese patient, obstructing access to mouth



Oral-Facial Manifestations of Obesity

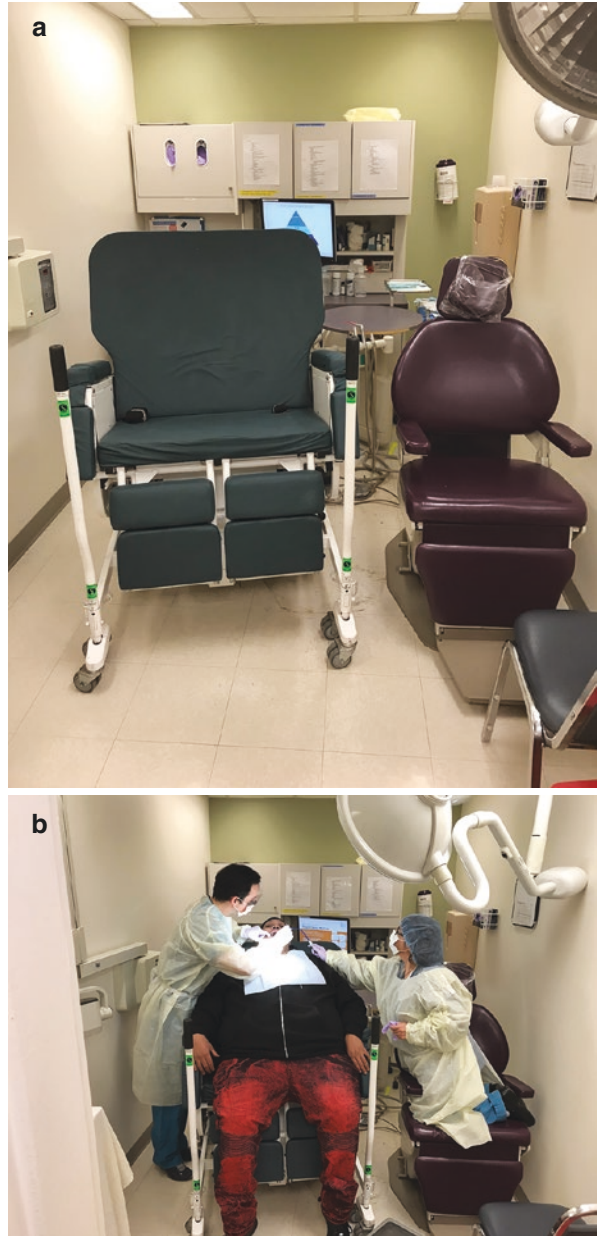
Studies have suggested that obesity is associated with dental decay and periodontal disease [56]. A study by Vasquez-Nava et al. (2010) found a significant association between dental decay and obesity in preschool children in Mexico [60]. Excess adipose tissue of the neck and face may make it difficult for clinicians to determine the extent of fascial space infection from an odontogenic source and also significantly decrease the visibility and access for dentists performing dental procedures [59]. For example, a large tongue can inhibit the view of third molars (*see* Fig. 2.5). Administration of local anesthetics in obese patients can also be difficult if excess fatty tissue inhibits the correct placement of the needle [59]. Routine third molar extractions can become challenging because of restricted mouth opening and also because an obese body can inhibit the ability of the clinician to gain access to the mouth [59].

Management of Patients with Obesity

Dental treatment protocols will need to be modified to treat obese patients. A thorough review of history and systems and a comprehensive physical examination including but not limited to BMI, airway, and range of cervical motion are necessary [59]. Obese patients will require longer time for treatment and transportation of the patient in and out of the operatory [57]. The dental chair may not be wide enough to accommodate extremely obese patients whose weight may also exceed the maximum capability of powered dental chairs [57]. Also needed will be an armless chair [59] as well as perioperative personnel trained in transporting obese patients into the chair [57]. A standard size blood pressure cuff may give inaccurate readings; thus, an oversized blood pressure cuff should be used [56]. In the operatory chair, Trendelenburg and supine positions should be avoided to minimize the risk of airway obstruction by soft tissue during treatment [59]. To maximize pulmonary ventilation, the reverse Trendelenburg position or sitting upright will be the optimal positions [59]. In addition, placing large throat packs should be avoided. Lastly, the surgeon should assure comfortable access to the surgical site before beginning any procedure.

Because of the increased chance of airway obstruction, conscious sedation, deep sedation, or general anesthesia is challenging in obese patients [59, 61]. It is often difficult to initiate intravenous (IV) access in obese patients because of excess fatty tissue; therefore, the level of IV access capability should be determined preoperatively [57]. Co-morbidities of obese patients such as pulmonary and cardiac conditions increase the likelihood of complications, such as pulmonary atelectasis, during general anesthesia [57]. Following general anesthesia, obese patients are also more likely to aspirate gastric content, suffer from deep vein thrombosis, or develop

Fig. 2.6 (a) Comparison of normal and bariatric dental chairs. (b) Bariatric dental chair in use



pulmonary embolism [59]. Because of the challenges in sedating obese patients, dental treatment should be performed under local anesthesia whenever possible [59].

Marfan Syndrome

Several developmental disorders affect the jaw and may result in decreased visibility and access for dentists. These disorders include Marfan syndrome (MFS), Rett syndrome, and tori. A review article by Ghada et al. (2016) provides additional insight into developmental disorders that affect visibility and access by dentists and recommendations on how to manage these limitations [62].

MFS is an inherited autosomal dominant connective tissue disorder that results from a mutation in the gene that encodes the protein fibrillin-1 [63]. The condition affects multiple organ systems [63]. The syndrome is one of the most commonly inherited connective tissue disorders, affecting about 1 in every 5000 individuals [64]. MFS is diagnosed from clinical manifestations, the cardiovascular system being the most significantly affected. Aortic regurgitation or dilation/dissection of the ascending aorta can significantly shorten life [63]. However, the most noticeable characteristic of MFS may be the affected musculoskeletal system manifested by tall stature with long and slim limbs and digits [65], joint hypermobility [63], scoliosis and crowding of ribs [66], and muscle hypotonicity [63]. Other common clinical characteristics of MFS include dislocation of the lens, pulmonary conditions, and learning disability [63].

Oral-Facial Manifestations of Marfan Syndrome

Patients with MFS commonly have distinct oral-facial skeletal characteristics, including a high palatal vault and crowded teeth. Other common features of patients with MFS include convex profile, retrognathia, micrognathia, posterior cross-bite, malocclusion, and open bite. In addition, temporomandibular joint disorder from subluxation and hypermobility is frequently seen [65].

Dentin and enamel defects in patients with Marfan syndrome put them at high risk for tooth decay [64]. In addition, long and narrow individual teeth often have deformed pulp shape and roots, making root canal therapy challenging [63]. MFS patients are also at higher risk for gingivitis [63].

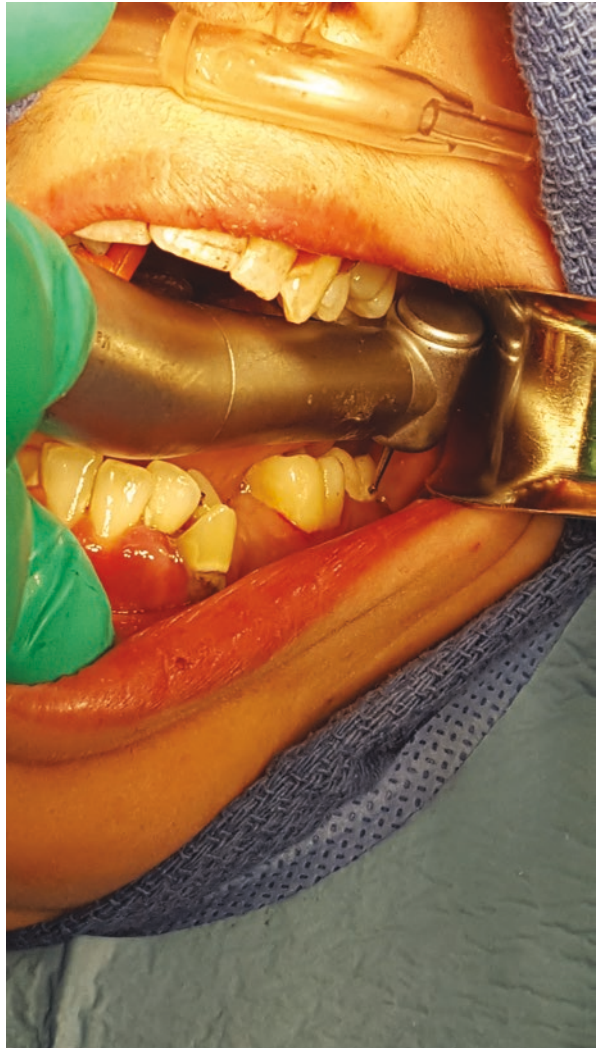
Management of Patients with Marfan Syndrome

A primary concern in providing dental treatment to patients with MFS is preventing bacteremia during dental procedure that may subsequently cause cardiovascular infection because these patients are at high risk of cardiovascular complications [65]. The source of bacteremia may be periodontitis or advanced tooth decay. Prophylactic antibiotic therapy is essential before dental procedures [65]. Use of

epinephrine in local anesthetics should be limited to avoid adverse cardiovascular effects [64, 65]. Vital signs should be monitored during treatment.

Sedation is recommended if extensive and long dental treatment is to be performed [64]. Difficult orotracheal intubation may be expected because many patients with MFS have protruding maxillary teeth and a high palatal vault, which may also result in restricted mouth opening [66] (*see* Fig. 2.6). Comprehensive pre-operative assessment, with emphasis on the cardiopulmonary system, is essential to avoid spontaneous pneumothorax, atelectasis, or cardiac failure during general anesthesia [66]. In the event that dental crowding becomes an issue, extraction or orthodontic treatment may be warranted.

Fig. 2.7 Photograph of patient with Marfan syndrome with restricted mouth opening limiting access of dental drill



Rett Syndrome

Rett syndrome (RTS) is a progressive developmental disorder seen only in girls, resulting from a mutation of a gene within the X chromosome [67]. The chance of a girl being born with the syndrome is 1 in 10,000 to 1 in 15,000 [68]. The first signs of the syndrome are generally seen when the child is between 1 and 2 years of age, with regression in cognitive and psychomotor development [68]. The overall result of RTS is a general failure to thrive with a decrease in life expectancy [67]. Regression in cognitive development is characterized by microcephaly [69], mental retardation [69], autistic behaviors [67], and loss of communication skills [67]; as a result, patients become socially withdrawn [69]. Seizures [69] and EEG abnormalities are also seen [70]. Regression in psychomotor development is characterized by parkinsonism [67], dystonia [67], lack of manual dexterity [69], repetitive hand movements [69], gait apraxia [69], spasticity [67], and joint contraction [67]. Muscle tone and mobility may decrease due to inability to control movement [69]. Scoliosis may also be seen [69]. In addition to displaying regression in psychomotor development, patients with RTS may also have breathing complications. These patients are often mouth breathers [68] with respiratory dysrhythmia [67], have bouts of wakeful apnea [67], or may show evidence of tachypnea [70]. These breathing complications may lead to sudden death [70]. Other significant complications include cardiac arrhythmia [70], gastrointestinal dysfunction [67], and difficulty gaining weight, which all can be life-threatening [68].

Oral-Facial Manifestations of Patients with Rett Syndrome

A common clinical feature of RTS is bruxism [68]. Patients with RTS are highly likely to have bruxism during the day rather than at night [69]. Common signs associated with bruxism include trismus [70], dental wear [68], and bilateral masseteric hypertrophy [69]. Other significant oral habits in patients with RTS include tongue thrusting, and biting and sucking of the hand or fingers [69]. As a result, open bite [69] and narrow maxillary arch are commonly seen [68]. Although tooth decay is infrequently seen in patients with RTS, perhaps due to mineralization of the teeth from hypersalivation, gingivitis is common due to plaque accumulation and lack of manual dexterity that prevents adequate oral hygiene [68]. To prevent plaque accumulation, it is essential to establish an oral hygiene routine with caretakers. Lastly, anterior dental trauma may result from patients falling because of seizures and gait apraxia [68].

Patients with RTS have oral-facial features that make direct laryngoscopy, air management, and treatment by dental surgeons difficult [67]. These features may include lateralization of the mandible [68], micrognathia [70], swollen tonsils and adenoids [68], upper airway infections [68], and restricted mouth opening [70].

Management of Patients with Rett Syndrome

Bruxism may be managed with the use of soft night guards and splints, although clinical effectiveness is unclear. Because patients with RTS are often uncooperative during dental treatment in the chair, nitrous oxide or sublingual midazolam may be considered. It is also helpful to minimize noise and keep visits as brief as possible. Mouth props will be necessary because RTS patients will lack muscle control [69].

If conscious sedation proves inadequate, the patient may need to be treated in the operating room under general anesthesia. Careful preoperative assessment of all systems is crucial, including evaluation of the airway, electrocardiogram, respiratory, gastrointestinal, and musculoskeletal systems. During procedures, fiberoptic-guided nasotracheal or orotracheal intubation may be considered for better visibility [70].

Tori

Tori are benign intraoral protuberances composed primarily of dense cortical bone, often covered by thin mucosa [71]. Tori are named based on their locations: torus palatinus and torus mandibularis. Torus palatinus is located in the palate (*see* Fig. 2.7a and b). Torus mandibularis is located on the lingual aspect of the floor of the mouth (*see* Figs. 2.8a, b and 2.9), generally above the mylohyoid line. Tori are present in various shapes and numbers. Tori may be flat, nodular, sharp, spike-like, or a combination of shapes [72]. It may be singular or multiple, or unilateral or bilateral [71]. Tori increase in size with age and are often seen for the first time by a dentist [72]. The prevalence of tori is reported to be as high as 26.9%, and their cause of origin is unknown [71].

Oral-Facial Manifestations of Tori

Tori are benign and no surgical treatment is recommended unless necessary to accommodate the fabrication of partials or dentures or to serve as an autogenous bone source [71]. More severe cases of mandibular tori can cause difficulty during direct laryngoscopy, larger and more posterior mandibular tori being most challenging [73]. This is because large mandibular tori prevent adequate compression of the tongue and soft tissue into the mandibular space to visualize the vocal cords with the Macintosh blade [74].

Management of Tori

Mental prominence is a common marker in predicting the difficulty for vocal cord exposure during direct laryngoscopy [73]. However, it is important to note that the existence and the size of mandibular tori do not correlate with the degree of

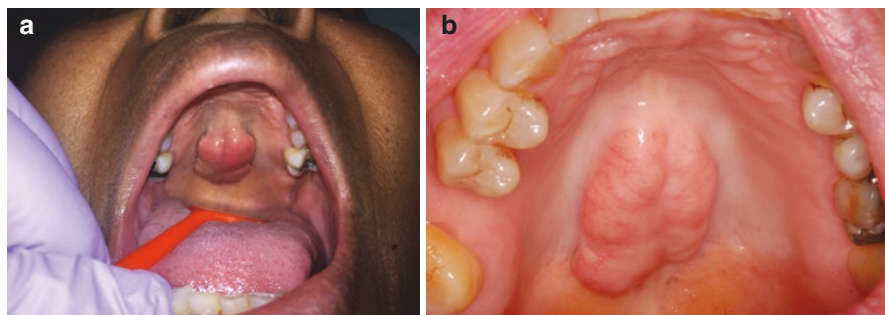


Fig. 2.8 (a) Photograph of palatal torus (courtesy of Ronald Delfini, DDS). (b) Photograph of palatal torus (courtesy of Austin Green, DDS)

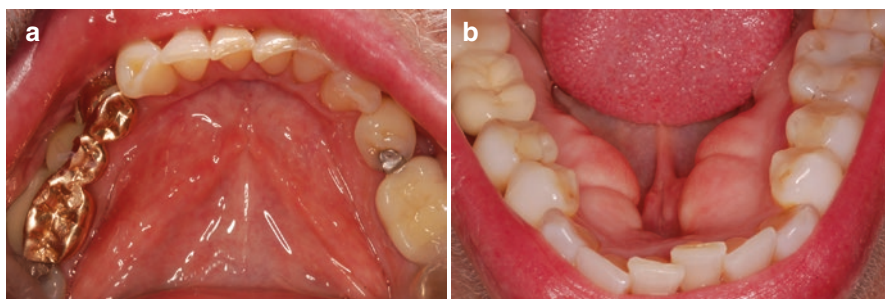


Fig. 2.9 (a) Photograph of normal mandible without tori (courtesy of Ronald Delfini, DDS). (b) Photograph of lingual mandibular tori (courtesy of Ronald Delfini, DDS)

mental prominence and that tori should always be examined separately during pre-admission testing [73]. To check for mandibular tori, the patient should be directed to raise the tongue to the roof of the mouth. In the event that large mandibular tori are observed, the clinician may choose to obtain a preoperative computed tomography to visualize the extent of the protuberance and/or have alternative laryngoscopy instruments prepared in the operating room such as flexible fiberoptic bronchoscope, Miller's blade, or the video laryngoscope [74]. In certain cases, nasotracheal intubation may be recommended over oropharyngeal intubation [75].

In the most severe cases, tori may need to be removed prophylactically before the patient undergoes definitive surgery [71, 73]. Tori removal can be done under local anesthesia and does not require general anesthesia. Double-Y incision design is most common for torus palatinus removal, whereas incision at the ridge is most common for mandibular tori removal [71]. After bony tori are exposed, a bone file or a large bur can be used to reduce the tuberosity of the bone [71]. The surgeon should keep in mind that removal of tori may be associated with various complications, including hematoma, dehiscence, infection, edema, necrosis of hard and soft tissues, nerve damage, and scarring [71].

References

1. Mezitis M, Rallis G, Zachariades N. The normal range of mouth opening. *J Oral Maxillofac Surg.* 1989;47:1028–9.
2. Buckley CE, Achakzai AA, O'Hanlon D. A simple technique for intubating the mouth during OGD in patients with previous neck radiation. *BMJ Case Rep.* 2014;2014:203778. <https://doi.org/10.1136/bcr-2014-203778>.
3. Dijkstra P, Kalk W, Roodenburg J. Trismus in head and neck oncology: a systematic review. *Oral Oncol.* 2004;40:879–89.
4. Zeitoun IM, Dhanrajani PJ. Cervical cellulites and mediastinitis caused by odontogenic infection. Report of two cases and review of literature. *J Oral Maxillofac Surg.* 1995;53:203–8.
5. Thomas F, Ozanne F, Mamelle G, Wibault P, Eschwege F. Radiotherapy alone for oropharyngeal carcinomas: the role of fraction size (2 Gy vs 2.5 Gy) on local control and early and late complications. *Int J Radiat Oncol Biol Phys.* 1988;15:1097–102.
6. Steelman R, Sokol J. Quantification of trismus following irradiation of the temporomandibular joint. *Mo Dent J.* 1986;66:21–3.
7. Dhanrajani PJ, Jonaidel O. Trismus: aetiology, differential diagnosis and treatment. *Dent Update.* 2002;29(2):88–92, 94. <https://doi.org/10.12968/denu.2002.29.2.88>.
8. van der Molen L, Heemsbergen WD, de Jong R, van Rossum MA, Smeele LE, Rasch CRN, Hilgers FJM. Dysphagia and trismus after concomitant chemo-intensity-modulated radiation therapy (chemo-IMRT) in advanced head and neck cancer: dose-effect relationships for swallowing and mastication structures. *Radiother Oncol.* 2013;106:364–9.
9. Watters AL, et al. Prevalence of trismus in patients with head and neck cancer: a systematic review with meta-analysis. *Head Neck.* 2019;41(9):3408–21. <https://doi.org/10.1002/hed.25836>.
10. Lund TW, Cohen JJ. Trismus appliances and indications for their use. *Quintessence Int.* 1993;24:275–9.
11. Marien M. Trismus: causes, differential diagnosis and treatment. *Gen Dent.* 1997;45(4):350–5.
12. Satheshkumar P, Mohan MP, Jacob J. Restricted mouth opening and trismus in oral oncology. *Oral Surg Oral Med Oral Pathol Oral Radiol.* 2014;117:709–15.
13. Biederman GR, Dodson TB. Epidemiologic review of facial infections in hospitalized pediatric patients. *J Oral Maxillofac Surg.* 1994;52:1042–5.
14. Flynn TR. The swollen face: severe odontogenic infections. *Emerg Med Clin North Am.* 2000;18:481–519.
15. Brook I, Frazier EH, Gher ME. Aerobic and anaerobic microbiology of periapical abscess. *Oral Microbiol Immunol.* 1991;6:123–5.
16. Okeson JP, editor. Management of temporomandibular disorders and occlusion. St. Louis: Mosby, Inc; 2003.
17. Young AL. Internal derangements of the temporomandibular joint: a review of the anatomy, diagnosis, and management. *J Indian Prosthodont Soc.* 2015;15:2–7.
18. Goswami D, Singh S, Bhutia O, Baidya D, Sawhney C. Management of young patients with temporomandibular joint ankylosis—a surgical and anesthetic challenge. *Indian J Surg.* 2016;78:482–9.
19. Xiaohan L, Shan P, Zhan S, Yang C, Wang Y. Effectiveness of different surgical modalities in the management of temporomandibular joint ankylosis: a meta-analysis. *Int J Clin Exp Med.* 2015;8:19831–9.
20. McLoughlin PM, Hopper C, Bowley NB. Hyperplasia of the mandibular coronoid process: an analysis of 31 cases and a review of the literature. *J Oral Maxillofac Surg.* 1995;53:250–5.
21. Colquhoun A, Cathro I, Kumara R, Ferguson MM, Doyle TCA. Bilateral coronoid hyperplasia in two brothers. *Dentomaxillofac Radiol.* 2002;31:142–6.
22. Coll-Anglada M, Acero-Sanz J, Vila-Masana I, Navarro-Cuéllar C, Ochandiano-Caycoia S, López De-Atalaya J, Navarro-Vila C. Jacob's disease secondary to coronoid process osteochondroma. A case report. *Med Oral Patol Oral Cir Bucal.* 2011;16:e708–10.
23. Smyth AG, Wake MJC. Recurrent bilateral coronoid hyperplasia: an unusual case. *Br J Oral Maxillofac Surg.* 1994;32:100–4.
24. Lee ST, Chung IK. Severe trismus due to bilateral coronoid process hyperplasia in a growth hormone therapy patient: a case report. *J Korean Assoc Oral Maxillofac Surg.* 2012;38:249–54.

25. Blanchard P, Henry JF, Souchere B, Breton P, Freidel M. Permanent constriction of the jaw due to idiopathic bilateral hyperplasia of the coronoid process. *Rev Stomatol Chir Maxillofac.* 1992;93:46–50.
26. Jaskolka MS, Eppley BL, van Aalst JA. Mandibular coronoid hyperplasia in pediatric patients. *J Craniofac Surg.* 2007;18:849–54.
27. Baik JS, Huh KH, Park KS, Park MS, Heo MS, Lee SS, et al. The diagnosis of coronoid impingement using computer tomography. *Korean J Oral Maxillofac Radiol.* 2005;35:231–4.
28. Gerbino G, Bianchi SD, Berrone BS. Hyperplasia of the mandibular coronoid process: long-term follow-up after coronoidotomy. *J Craniofac Surg.* 1997;25:69–73.
29. Arakeria G, Brennan PA. Oral submucous fibrosis: an overview of the aetiology, pathogenesis, classification, and principles of management. *Br J Oral Maxillofac Surg.* 2013;51:587–93.
30. Sharma M, Radhakrishnan R. Limited mouth opening in oral submucous fibrosis: reasons, ramifications, and remedies. *J Oral Pathol Med.* 2017;46:424–30.
31. Wollina U, Verma SB, Ali FM, Kishor PK. Oral submucous fibrosis: an update. *Clin Cosmet Investig Dermatol.* 2015;8:193–204.
32. Inoue N, Yamaguchi T, Satou J, Satou C, Minowa K, Lizuka T. A case of restricted mandibular movement resulting from hyperplasia of the masseter muscle aponeurosis. *Jpn J Oral Maxillofac Surg.* 2000;46:307–9.
33. Sato T, Yoda T. Masticatory muscle tendon-aponeurosis hyperplasia: a new clinical entity of limited mouth opening. *Jpn Dent Sci Rev.* 2016;52:41–8.
34. Sato T, Hori N, Nakamoto N, Akita M, Yoda T. Masticatory muscle tendon-aponeurosis hyperplasia exhibits heterotopic calcification in tendons. *Oral Dis.* 2014;20:404–8.
35. Dghoughi S, El Wady W, Taleb B. Systemic sclerosis: case report and review of the literature. *N Y State Dent J.* 2010;76:30–5.
36. Crincoli V, Fatone L, Fanelli M, Rotolo RP, Chialà A, Favia G, Giovanni LG. Orofacial manifestations and temporomandibular disorders of systemic scleroderma: an observational study. *Int J Mol Sci.* 2016;17:1189.
37. Alantar A, Cabane J, Hachulla E, Princ G, Ginisty D, Hassin M, Sorel M, Maman L, Pilat A, Mouthon L. Recommendations for the care of oral involvement in patients with systemic sclerosis. *Arthritis Care Res (Hoboken).* 2011;63:1126–33.
38. Tolle SL. Scleroderma: considerations for dental hygienists. *Int J Dent Hyg.* 2008;6:77–83.
39. Fischer DJ, Patton LL. Scleroderma: oral manifestations and treatment challenges. *Spec Care Dentist.* 2000;20:240–4.
40. Albilia JB, Lam DK, Blanas N, Clokie CML, Sándor GKB. Small mouths ... big problems? A review of scleroderma and its oral health implications. *J Can Dent Assoc.* 2007;73:831–6.
41. Chebbi R, Khalifa HB, Dhidah M. Temporomandibular joint disorder in systemic sclerosis: a case report. *Pan Afr Med J.* 2016;25:164.
42. Steen VD, Medsger TA Jr. Epidemiology and natural history of systemic sclerosis. *Rheum Dis Clin N Am.* 1990;16:1–10.
43. Egeland B, More S, Buchman SR, Cederna PS. Management of difficult pediatric facial burns: reconstruction of burn-related lower eyelid ectropion and perioral contractures. *J Craniofac Surg.* 2008;19:960–9.
44. Zweifel CJ, Guggenheim M, Jandali AR, Mehmet A, Altintas MA, Künzi W, Giovanoli P. Management of microstomia in adult burn patients revisited. *J Plast Reconstr Aesthet Surg.* 2010;63:e351–7.
45. Clayton NA, Ward EC, Maitz PKM. Orofacial contracture management outcomes following partial thickness facial burns. *Burns.* 2015;41:1291–7.
46. Koymen R, Gulses A, Karacayli U, Aydintug YS. Treatment of microstomia with commissuroplasties and semidynamic acrylic splints. *Oral Surg Oral Med Oral Pathol Oral Radiol Endod.* 2009;107:503–7.
47. Clayton NA, Ellul G, Ward EC, Scott A, Maitz PK. Orofacial contracture management: current patterns of clinical practice in Australian and New Zealand adult burn units. *J Burn Care Res.* 2017;38:e204–11.
48. Grishkevich VM. Post-burn microstomia: anatomy and elimination with trapeze-flap-plasty. *Burns.* 2011;37:484–9.
49. Dougherty ME, Warden GD. A thirty-year review of oral appliances used to manage microstomia, 1972 to 2002. *J Burn Care Rehabil.* 2003;24:418–31.

50. McKenzie WS, Rosenberg M. Iatrogenic subcutaneous emphysema of dental and surgical origin: a literature review. *J Oral Maxillofac Surg*. 2009;67:1265–8.
51. Aghajanzadeh M, Dehnadi A, Ebrahimi H, Karkan MF, Jahromi SK, Maafi AA, Aghajanzadeh G. Classification and management of subcutaneous emphysema. A 10 year experience. *Indian J Surg*. 2015;77:673–S677.
52. Rickles N, Joshi B. Death from air embolism during root canal therapy. *J Am Dent Assoc*. 1963;67:397–404.
53. Mitsunaga S, Iwai T, Kitajima H, Yajima Y, Ohya T, Hirota M, Mitsudo K, Aoki N, Yamashita Y, Omura S, Tohnai I. Cervicofacial subcutaneous emphysema associated with dental laser treatment. *Aust Dent J*. 2013;58:424–7.
54. Kaufman AY. Facial emphysema caused by hydrogen peroxide irrigation: report of a case. *J Endod*. 1981;7(10):470–2.
55. Mishra L, Patnaik S, Patro S, Debnath N, Mishra S. Iatrogenic subcutaneous emphysema of endodontic origin – case report with literature review. *J Clin Diagn Res*. 2014;8(1):279–81.
56. Yuan JC, Lee DJ, Afshari FS, Galang MTS, Sukotjo C. Dentistry and obesity: a review and current status in U.S. predoctoral dental education. *J Dent Educ*. 2012;76:1129–36.
57. Marciani RD, Raezer BF, Marciani HL. Obesity and the practice of oral and maxillofacial surgery. *Oral Surg Oral Med Oral Pathol Oral Radiol Endod*. 2004;98:10–5.
58. Ogden CL, Carroll MD, Fryar CD, Flegal KM. Prevalence of obesity among adults and youth: United States, 2011–2014. *NCHS Data Brief*. 2015;219:1–8.
59. Krishnan B. Obese oral and maxillofacial surgical patient. *J Craniofac Surg*. 2009;20:53–7.
60. Vazquez-Nava F, Vazquez-Rodriguez EM, Saldivar-Gonzalez AH, Lin-Ochoa D, Martinez-Perales GM, Joffre-Velazquez VM. Association between obesity and dental caries in a group of preschool children in Mexico. *J Public Health Dent*. 2010;70:124–30.
61. Kempers KG, Foote JW, DiFlorio-Brennan T. Obesity: prevalence and considerations in oral and maxillofacial surgery. *J Oral Maxillofac Surg*. 2000;58(2):137–43.
62. Ghada A, Scott O, Mel M. Developmental Disorders Affecting Jaws. *Dent Clin N Am*. 2016;60:39–90.
63. De Coster PJA, Martens LCM, De Paepe A. Oral manifestations of patients with Marfan syndrome: a case-control study. *Oral Surg Oral Med Oral Pathol Oral Radiol Endod*. 2002;93:564–72.
64. Morales-Chávez MC, Rodríguez-López MV. Dental treatment of Marfan syndrome. With regard to a case. *Med Oral Patol Oral Cir Bucal*. 2010;15:e859–62.
65. França EC, Abreu LG, Paiva SM, Drummond AF, Cortes ME. Oral management of Marfan syndrome: an overview and case report. *Gen Dent*. 2016;64:54–9.
66. Kamat S, Travasso B, Borkar D, Dias M. Anaesthetic considerations in a patient with Marfan syndrome for maxillary corrective osteotomy. *Indian J Anaesth*. 2006;50:51–4.
67. Nho JS, Shin DS, Moon JY, Yi JW, Kang JM, Lee BJ, Kim DO, Chung JY. Anesthetic management of an adult patient with Rett syndrome and limited mouth opening—case report. *Korean J Anesthesiol*. 2011;61:428–30.
68. Ribeiro RA, Romano AR, Birman EG, Mayer MPA. Oral manifestations in Rett syndrome: a study of 17 cases. *Pediatr Dent*. 1997;19:349–52.
69. Fuertes-González MC, Silvestre FJ, Almerich-Silla JM. Oral findings in Rett syndrome: a systematic review of the dental literature. *Med Oral Patol Oral Cir Bucal*. 2011;16:e37–41.
70. Kako H, Martin DP, Cartabuke R, Beebe A, Klamar J, Tobias JD. Case report. Perioperative management of a patient with Rett syndrome. *Int J Clin Exp Med*. 2013;6:393–403.
71. García-García AS, Martínez-González JM, Gómez-Font R, Soto-Rivadeneira A, Oviedo-Roldán L. Current status of the torus palatinus and torus mandibularis. *Med Oral Patol Oral Cir Bucal*. 2010;15:e353–60.
72. Nery E, Corn H, Eisenstein IL. Palatal exostosis in the molar region. *J Periodontol*. 1977;48:663–6.
73. Best SR, Kobler JB, Friedman AD, Barbu AM, Zeitels SM, Burns JA. Effect of mandibular tori on glottic exposure during simulated suspension microlaryngoscopy. *Ann Otol Rhinol Laryngol*. 2014;123:188–94.
74. Yoshida H, Sawada M, Takada N, Kushikata T, Hirota K. Rigid videolaryngoscope for difficult intubation caused by mandibular tori. *J Anesth*. 2011;25:473–4.
75. Takasugi Y, Shiba M, Ikamoto S, Hatta K, Koga Y. Difficult laryngoscopy caused by massive mandibular tori. *J Anesth*. 2009;23:278–80.



Airway Management

3

Monica S. Ganatra

Introduction

Proper airway management is vitally important to ensure adequate oxygenation and ventilation in a patient; without it, death, brain injury, and cardiopulmonary compromise can quickly ensue. Whether a patient receives general anesthesia—in which normal airway reflexes are deliberately suppressed in a controlled fashion—or intravenous sedatives that depress normal respirations in a dose-dependent manner, it is paramount to understand the anatomic abnormalities that can affect management of the airway. This chapter will examine features of both the normal and abnormal airway; highlight the nature of airway anomalies found in common pediatric and adult syndromes; discuss components of a comprehensive airway examination; and describe the airway management for these patients. A thorough understanding of proper airway assessment can go a long way in minimizing the morbidity and mortality that can result from inadequate oxygenation and ventilation.

Normal Airway Anatomy

Airway management refers to the ability to maintain adequate oxygenation and ventilation. In spontaneously ventilating patients, the primary goal is to avoid airway obstruction; and in cases of general anesthesia or unconsciousness from underlying pathology, the aim is to support or control these functions via various invasive devices.

There are several key considerations of a normal airway, including: the relative size of the tongue versus the pharynx in the oral cavity; space in the anterior

M. S. Ganatra (✉)

Department of Anesthesiology, Yale University School of Medicine, New Haven, CT, USA

e-mail: Monica.Ganatra@yale.edu

mandible; integrity of the vertebral column; mobility of the temporomandibular joint (TMJ); and development of the maxilla [1, 2].

When the goal is to intubate a patient for a surgical procedure, there must be sufficient space for the laryngoscope/intubating device, endotracheal tube (ETT), and adequate visualization of the larynx in order to successfully and atraumatically intubate. This is why the ratio of tongue size to pharynx is so important. Similarly, mouth opening is also important; the inability to widen the mouth (which could be due to a congenital anomaly, pain, infection, or scar tissue from radiation) can make it difficult to fit in all the necessary equipment [3].

The oral cavity can be considered to be a box that is composed of the bones of the maxilla and the mandible. The partial content of this box, then, is the soft tissue of the tongue. Any enlargement of the tongue or decrease in box size (due to hypoplasia of the maxilla and/or mandible) will alter this ratio and predispose the patient to airway obstruction [2].

The anterior mandibular space refers to the space in the mandible into which the tongue can be displaced during laryngoscopy. Any decrease in this area will make intubation more difficult because there is literally no room to displace the tongue during laryngoscopy. Mandibular hypoplasia can decrease the anterior mandibular space, and an anterior larynx will also create a similar problem during laryngoscopy [2]. Similarly, hypoplasia of the maxilla will alter the framework of the oral cavity and create a smaller space (Fig. 3.1).

When referring to vertebral column integrity, the two most important elements are the cervical vertebral bones and the atlanto-axial joint, as they play a crucial role in neck extension and flexion. This is necessary to get the best view for intubation. The presence of hemivertebrae, arthritic changes, or vertebral fusion can make intubation more difficult. In the presence of loose ligaments (e.g., atlanto-axial joint laxity in Down syndrome), excess force can cause vertebral column instability and damage to the spinal cord from impingement [2].

The temporomandibular joint is an important bilateral joint. There are articular discs interspersed between the mandible and the temporal bones, splitting the

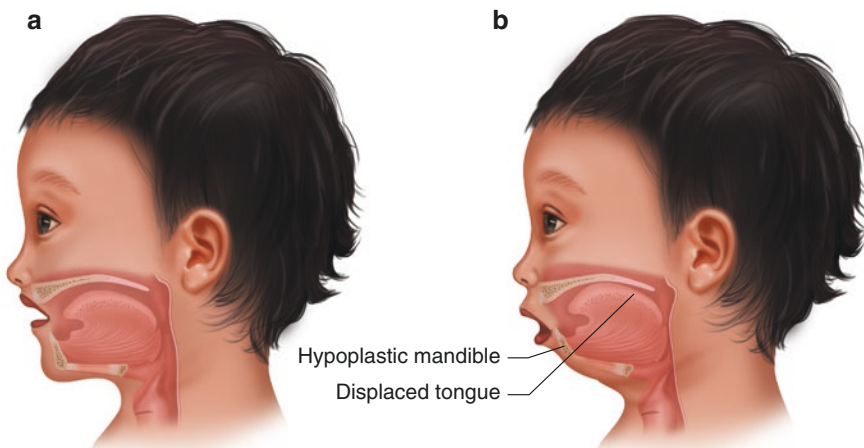


Fig. 3.1 Mandibular hypoplasia and anteriorly displaced tongue

Table 3.1 Pediatric versus Adult Airway

Pediatric Airway	Adult Airway
Long, narrow, and stiff epiglottis	Short and floppy epiglottis
Larynx located at level of C3–C4	Larynx located at level of C4–C5
Larger tongue in proportion to oral cavity	
Narrowest portion at level of cricoid cartilage	Narrowest portion at level of vocal cords
Relatively larger head, especially the occiput	

articular space into upper and lower compartments. The upper compartment is responsible for gliding movements, while the lower compartment serves as a hinge joint. Mouth opening, which is important so that a laryngoscope can safely be inserted with adequate space, relies on two distinct motions. The first is a hinge action that enables the mouth to be opened about halfway. In the second action, the forward gliding of the articular surface on the articular tubercle is necessary [4].

To best visualize the vocal cords, optimal alignment between the oral and pharyngeal long axes is necessary. The “sniffing position” describes head and neck positioning such that the oral and pharyngeal axes are most advantageously aligned to provide the best visualization of the vocal cords, such that the view from the lips to the glottic opening is most nearly a straight line. Typically, the head should be extended by 15 degrees and the neck flexed 35 degrees. The patient’s head is elevated by approximately 8 cm with the use of foam pads or blankets [1, 5].

Previously, it had been thought that the “sniffing position” was required to optimize visualization of the larynx; however, more recent studies have shown that head extension is the more important factor for the majority of patients. Such patients must have normal dentition, adequate submental distance (for tongue decompression), normal glottic structure, and larynx position. For obese patients, the sniffing position is still considered highly beneficial [3].

Table 3.1 highlights the important anatomical differences between the normal pediatric and the adult airway.

Difficult Airway

The definition of a difficult airway, according to the ASA Task Force on Management of the Difficult Airway, is: “the clinical situation in which a conventionally trained anesthesiologist experiences difficulty with facemask ventilation of the upper airway, difficulty with tracheal intubation, or both” [6]. Proper assessment of the airway and knowledge of airway anomalies can help minimize creating a situation where the provider cannot ventilate or intubate a patient.

Congenital Airway Anomalies

There are several characteristics of the pediatric airway that make intubation more difficult. A congenital airway anomaly can make airway management particularly challenging. This section will examine common pediatric syndromes, describe the airway anomaly, and discuss airway management.

Intubation of a pediatric trachea is anatomically more challenging than intubating an adult trachea. First, children have a long, thin, and stiff epiglottis. The infant epiglottis is angled especially posteriorly during laryngoscopy, making it difficult to visualize the vocal cords as the epiglottis blocks direct vision. Straight-tipped blades for intubation (such as the Miller) are more commonly used in neonates and infants because the narrower tip of the Miller (as opposed to the curved tip of the Mac blade) makes it easier to lift the epiglottis, a maneuver known to significantly improve the laryngeal view for intubation.

Because the pediatric larynx is located more cephalad at C3–C4 than the adult C4–C5, the tongue is closer to the palate and causes upper airway obstruction more easily than in adults. Additionally, the pediatric tongue in proportion to the mouth is larger than that of an adult. This also means there is less space to maneuver the laryngoscope to obtain an adequate view for intubation. Additionally, the more cephalad location of the larynx creates a more acute angulation during laryngoscopy, which increases the difficulty of the intubation procedure.

The upper airway obstruction in children (due to the relatively larger tongue) is made worse with sedation, inhalational induction of anesthesia, and emergence from anesthesia [14]. When patients are in a deeper plane of anesthesia, the airway muscles relax and predispose the patient to upper airway obstruction.

A shoulder roll placed under the occiput can help improve views for laryngoscopy.

The narrowest portion of the airway in children is at the level of the cricoid cartilage, which is located below the glottic opening. Therefore, while it may seem that a larger endotracheal tube may be passed through the vocal cords, it will not fit. Diligence must be taken to place correctly sized endotracheal tubes in children so that no damage is incurred from traumatizing the airway by trying to place too large a tube. Such complications can include tracheal stenosis, airway perforation, edema, and scarring.

Historically, cuffed endotracheal tubes were discouraged in children less than 8–10 years of age, out of concern that the inflated cuff would cause subglottic injury. Uncuffed tubes were also thought to be beneficial because a tube with greater internal diameter size could be used. (When cuffed endotracheal tubes are placed, the internal diameter is decreased by 0.5 mm.) However, this belief has been disproven, as modern endotracheal tubes are now equipped with high volume, low pressure cuffs [21]. Nonetheless, uncuffed endotracheal tubes are still preferred in neonates, owing to the use of an endotracheal tube with a larger internal diameter and concern for causing tracheal injury.

Intubated patients are at risk for post-extubation croup and stridor, especially infants and small children. Edema in the upper airway at the narrowest portion (which is the cricoid cartilage in pediatric patients) can cause severe resistance to airflow. Poiseuille's Law states that airflow resistance is dependent on the radius to the fourth power. Consequently, any decrease in radius that occurs from edema will decrease airflow to the fourth power. Infants and small children already have small airways, and any swelling can cause severe restrictions to breathing. The edema is a result of excess pressure on the tracheal submucosa, which can occur with use of too large an endotracheal tube. Venous congestion (and with high enough pressures,

even arterial blood flow compromise) can occur [7]. The edema can be symptomatic, and not surprisingly it is more easily manifest in those with smaller airways (neonates, infants, and small children). It is therefore essential that the proper endotracheal tube size is used. Cuffed tubes are safe to use in infants >30 days of age, provided that a leak is checked so that there is not excessive pressure on the tracheal mucosa.

A simple formula for determining uncuffed endotracheal tube size is:

$$(\text{Age in years} / 4) + 4$$

Note that age is in years and the formula works for patients 1 year and up. To obtain a cuffed endotracheal tube size, subtract the obtained number by 0.5.

To estimate depth of endotracheal tube insertion, one can simply triple the endotracheal tube in size; however, it is important to always auscultate for equal, bilateral breath sounds and to inspect for equal, bilateral chest rise. Table 3.2 summarizes age-appropriate endotracheal tube sizes (both uncuffed and cuffed) along with approximate depth of insertion. Of course, clinical judgment should be used to alter these recommendations based on each individual patient.

Laryngotracheomalacia

Laryngotracheomalacia is the most common laryngeal disease of infancy. In this congenital disease, the supraglottic structures collapse with the inspiratory phase of respiration, resulting in high-pitched stridor. The epiglottis is long and narrow, and the aryepiglottic folds are floppy [8]. Most patients (70–90%) have a mild form of the

Table 3.2 Appropriate Endotracheal Tube Size Selection and Depth Insertion Based on Age of the Patient

Age of Patient	Endotracheal tube size: uncuffed (internal diameter, mm)	Endotracheal tube size: cuffed (internal diameter, mm)	Depth of endotracheal tube at lips, cm
Premature neonate	2.5		8
Term neonate	3.0		9
Infant <6 months	3.5	3.0	10
Infant >6 months	4.0	3.5	11
1 year	4.0	3.5	12
2 years	4.5	4.0	13
4 years	5.0	4.5	14
6 years	5.5	5.0	15
8 yrs	6	5.5	16
10 yrs	6.5	6.0	18
12 yrs	7	6.5	19
Adult female	7–8	7.0–7.5	21
Adult male	8–8.5	7.5–8.0	23

disease, with occasional stridor as their only symptom (which is exacerbated with crying or upper respiratory infections), and resolution usually occurs by 12–24 months of age. Symptoms tend to be worse in the supine position. In more severe cases, the child may demonstrate dyspnea with retractions, obstructive sleep apnea (OSA), dysphagia, failure to thrive (poor weight gain), and episodes of choking while feeding [9]. For the small proportion of patients who have the severe form, associated laryngotracheal lesions (subglottic stenosis, tracheomalacia, vocal cord paralysis, and laryngeal dyskinesia) are more frequently present [9]. Laryngotracheomalacia is commonly associated with gastro-esophageal reflux disease (GERD).

There is serious concern that the child may have total airway obstruction. It is best to maintain spontaneous ventilation, with continuous positive airway pressure (CPAP) as needed. It is best to minimize coughing, and topical lidocaine on the vocal cords can help accomplish this [8]. Prone positioning may have some benefit.

Non-invasive ventilation is useful as it can increase alveolar ventilation and decrease the patient's work of breathing. CPAP, bilevel positive airway pressure (BiPAP), and positive end-expiratory pressure (PEEP) are recommended for improving ventilation in these patients. Maintaining spontaneous ventilation is preferred. More severe cases require surgical evaluation, to assess for other lesions and possible therapeutic interventions. A supraglottoplasty is a procedure designed to remove the excess tissue that contributes to the airway collapse. Severe cases may require tracheostomy [9].

Cleft Lip and Palate

Cleft lip, with or without associated cleft palate, is the most common congenital anomaly of the head and neck. The clefts may be unilateral or bilateral. For complete cleft lips, there is extension through the lip and into the nasal sill, whereas an incomplete cleft lip extends through the orbicularis oris and skin, but intact lip tissue is present [10].

For cleft palates, the most commonly used classification system is the Veau system. In this system, there are four groups. Group 1 defects involve clefts of the soft palate only. Group 2 defects extend into the hard palate. For Group 3 defects, there is unilateral extension into the entire palate and alveolus. And with Group 4 defects, this is bilateral [10].

The greater the severity of the cleft, the greater the chance that there are other associated anomalies, such as those of the limbs, vertebral column, and cardiovascular system. The cleft lip/palate may be associated with other syndromes that have special airway considerations, including, for example, Pierre–Robin, Goldenhar, and Treacher–Collins syndrome. Additionally, children with cleft lip/palate commonly have chronic nasal and sinus infections, which can increase their risk of respiratory complications (such as laryngospasm and bronchospasm) while under general anesthesia [11].

Intubation of patients with clefts may be difficult; therefore, personnel and equipment for managing a difficult airway must be readily available. Packing the cleft with moist gauze can help prevent damage to surrounding tissue. For patients

in whom a difficult airway is anticipated, administering glycopyrrolate prior to airway manipulation can help decrease the amount of secretions and decrease the risk of laryngospasm [38]. Inhalational induction and maintenance of spontaneous ventilation is preferred if there is reason to suspect that laryngoscopy may be difficult. Paralytics should be administered only when it has been ascertained that the patient can be easily mask-ventilated. Care should be taken to select a facemask that fits the patient well and does not place undue pressure on the clefts. While it should be noted that those cleft patients who are less than 6 months old or have associated anomalies are at higher risk of difficult intubation [11], it should be acknowledged that patients with isolated cleft palate tend to become easier to intubate as they get older (Fig. 3.2) [12].

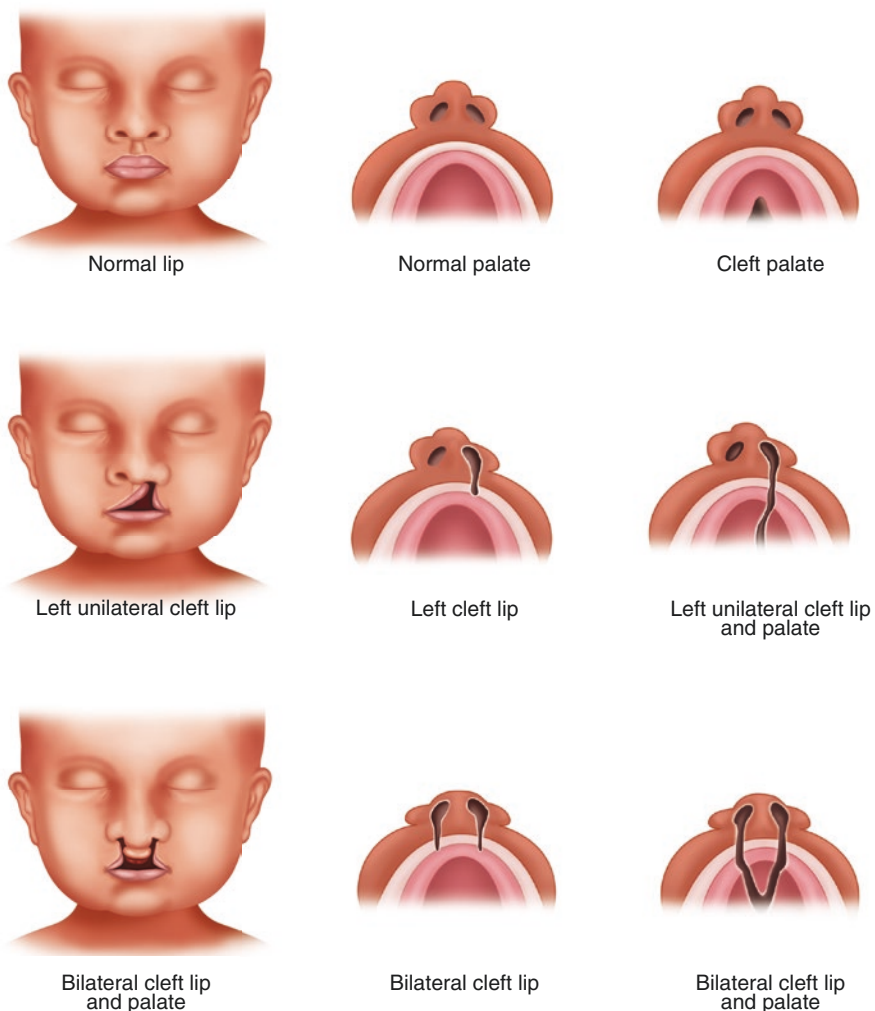


Fig. 3.2 Normal lip and palate and cleft lip and palate

Juvenile RA

In juvenile rheumatoid arthritis, a systemic autoimmune disease, deposits of rheumatoid factor accumulate in the joints and cause damage. The temporomandibular joint may be involved, causing limited opening of the oral aperture. There may also be restricted mobility of the cervical vertebrae, causing limited extension and flexion of the neck. This can make intubation of the trachea challenging and require use of video-assisted laryngoscopy or a fiberoptic scope. Other anatomical anomalies include involvement of the cricoarytenoid joints, narrowing of the glottic opening, and laryngeal deviation caused by chronic fibrotic changes [7].

Mucopolysaccharidoses

The mucopolysaccharidoses refer to a group of genetic disorders known as glyco-gen storage diseases, where absence of key enzymes leads to deposition of glycosaminoglycans [13]. Specifically, there is absent or aberrant function of lysosomal enzymes which are normally required to break down the glycosaminoglycans. The accumulation of these long chain sugar carbohydrates can be seen in bone, skeletal structures, connective tissue, and organs. These deposits increase with time, and it should be expected that airway management will be more difficult as these patients grow older. Bone and joint disease may be present, including instability of the cervical spine. Cervical canal stenosis may also be present, placing the patient at risk for spinal cord compression. Extreme care should be taken when manipulating the airway, and in-line stabilization should be employed. Further work-up with an MRI may be needed if the patient has signs of a cervical myelopathy.

Always assume a patient with a mucopolysaccharidoses is a difficult airway. This is because the patient may have deposits of glycosaminoglycans in the airway, a short and often unstable neck, poor joint mobility affecting not just the c-spine but the temporomandibular joint as well, micrognathia, and macroglossia. Furthermore, OSA may be present. As there is no way for the body to break down these carbohydrates, the airway worsens with time.

Because of the abnormal facies, facemasks may not be a good fit. In such cases, children will often obstruct upon induction of anesthesia. Placement of an oropharyngeal airway may exacerbate the situation by pushing the enlarged epiglottis posteriorly and cause laryngeal obstruction. Due to nasopharyngeal deposits, it may be difficult to place a nasopharyngeal airway. It has been suggested that forward traction of the tongue may be beneficial in relieving obstruction. Laryngeal mask airways (LMAs) have proven to be beneficial as a way to ventilate the patient and as a conduit for intubation. Because of the glycosaminoglycan deposits, endotracheal tubes that are smaller than expected for age should be used [14].

Trisomy 21

Trisomy 21, more commonly known as Down syndrome, has several features that can make airway management more challenging. These patients have macroglossia and hypotonia, placing them at high risk for airway obstruction. Their oral and nasal passages are characteristically narrow [15]. They also have short necks, mid-facial and mandibular hypoplasia, atlanto-axial instability with vertebral ligamentous abnormalities, and a higher incidence of congenital subglottic or tracheal stenosis [13]. Additionally, these patients often have adenotonsillar hypertrophy and obstructive sleep apnea. Use of an oral or nasal airway will help relieve the obstruction. To move the tongue out of the way for intubation, a Macintosh blade is preferable for intubation.

Patients with Down syndrome are at risk of having atlanto-axial instability. Asymptomatic patients with plain cervical flexion and extension radiographs demonstrating an atlanto-dens interval of less than 4.5 mm and a neural canal width of more than 14 mm should be able to proceed to surgery. If the patient has abnormal x-rays and/or symptoms, consultation with a neurosurgeon is advisable in the elective setting. Lateral films may not rule out atlanto-axial instability with any precision, and are often not routinely performed at many centers. Since ongoing mineralization precludes accurate radiological imaging in children under the age of 3 years old, the safest course is to treat all Down syndrome patients as if they *do* have laxity of the atlanto-axial joint. C-spine neutrality should be maintained at all times, using foam pillows and gel-cushioned pads to support the head. During LMA placement and intubation, maintain in-line stabilization by having one provider hold the neck neutral while the other person intubates without placing force on the neck. Any undue flexion or extension of the head can cause damage to the cervical spinal cord. When intubating, endotracheal tubes that are 0.5 to 1 mm smaller than expected are often used because of the known tracheal narrowing and also to avoid subglottic trauma. Intubation is not generally known to be difficult, as the mouth opening is normal and the large tongue is usually easy to displace [13].

Beckwith–Wiedemann Syndrome

Beckwith–Wiedemann Syndrome is characterized by macroglossia, visceral organomegaly, and gigantism. OSA may be present. Maxillary hypoplasia and macroglossia can cause upper airway obstruction and lead to difficult direct laryngoscopy. Abdominal organ visceromegaly may push the diaphragm upward, shortening the distance from the lips to the carina and making endobronchial intubation more likely.

The macroglossia can cause upper airway obstruction. Oral and nasopharyngeal airways can help relieve this obstruction, but if this is not successful, the patient may be placed in a lateral or prone position for relief. Having someone pull the

tongue forward (e.g., with McGill forceps) can help facilitate direct laryngoscopy. The tracheal diameter in these patients tends to be wider than expected for age; cuffed endotracheal tubes are recommended. It is advisable to have a fiberoptic bronchoscope available for intubation [13].

Pierre–Robin Syndrome

Pierre–Robin Syndrome consists of micrognathia, glossoptosis, and cleft palate. The micrognathia (which is also known as mandibular hypoplasia) forces the tongue to be relatively posterior within the oropharynx, such that intubation via direct laryngoscopy is extremely difficult, if not impossible, because the vocal cords cannot be visualized. The symptoms can be so severe that the newborn in a supine position can have complete obstruction. Placing the patient in a prone position can help relieve the obstruction by displacing the tongue. In some cases, a glossolabiopexy may be necessary, in which the tongue is kept anterior and prevented from prolapsing posteriorly by placing a stitch that connects the tongue to the lower lip [7]. During anesthesia, if the tongue has not already been sutured to the lip, use of McGill forceps to pull out the tongue can help relieve airway obstruction. The lateral position can also be beneficial because it moves the tongue out of the way and prevents obstruction of the epiglottis [4]. In addition to maintaining spontaneous ventilation, a flexible fiberoptic scope should be readily available for intubation as direct laryngoscopy is often unsuccessful. An otolaryngologist should also be readily available should fiberoptic intubation be difficult or unsuccessful. The LMA is an important tool for Pierre–Robin patients, because it can move the tongue out of the way and thereby minimize or prevent airway obstruction that will occur from the prolapsing tongue [7]. Fortunately, as infants grow, so do their mandibles, making it easier to manage the airway. Severe cases of Pierre–Robin may require a surgical airway (Fig. 3.3).

Treacher–Collins (Mandibulo-Facial Dysostosis)

In Treacher–Collins Syndrome, there is maxillary, zygomatic, and mandibular hypoplasia. Downward sloping palpebral fissures, notched lower eyelids, small mouth opening, and a high arched palate are characteristic features, with cleft palate and velopharyngeal incompetence as secondary concerns. There may be associated TMJ abnormalities as well. Mask ventilation and intubation is extremely difficult and nearly impossible if there are associated TMJ abnormalities. As these children grow, airway management can become even more challenging as the basilar kyphosis of the cranial base may increase. Therefore, although it may be useful to examine previous anesthetic records for airway management, it is important to recognize that in patients with mandibulo-facial dysostosis, the airway management may subsequently be even more difficult (Fig. 3.4) [2, 16].

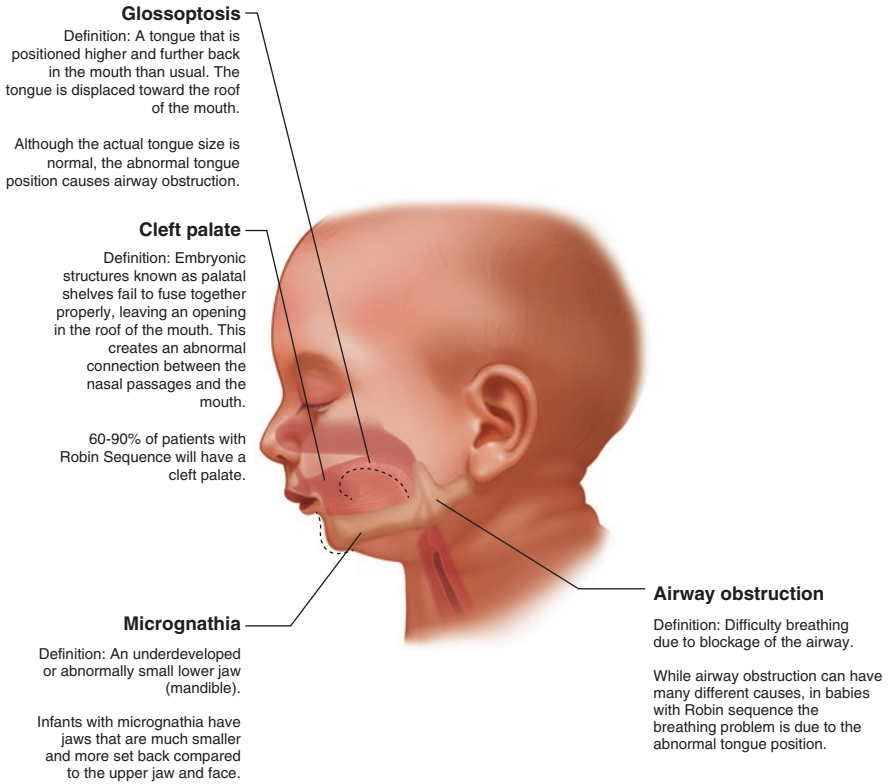


Fig. 3.3 Features of Pierre–Robin syndrome

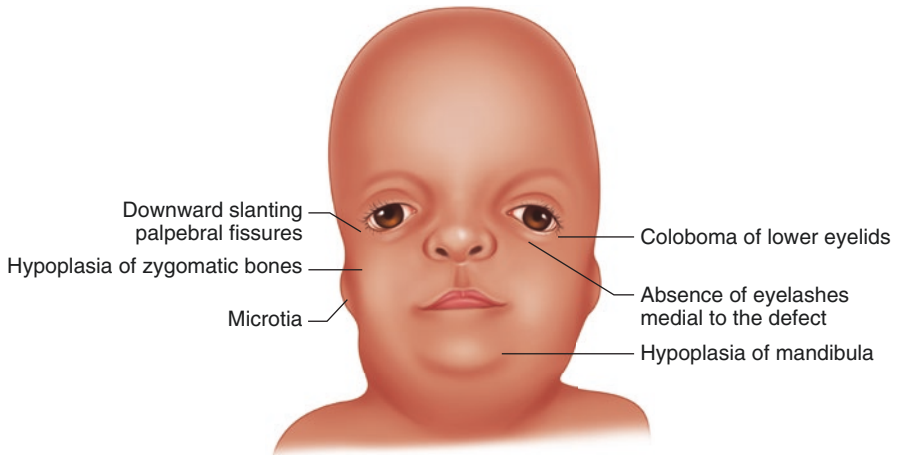


Fig. 3.4 Treacher–Collins syndrome

Goldenhar Syndrome (Hemifacial Microsomia)

The developmental disorder Goldenhar Syndrome, also known as oculo-auriculo-vertebral syndrome, features mandibular hypoplasia, malformations of the external and middle ear, eye abnormalities (microphthalmos and epibulbar dermoids), and vertebral anomalies that include scoliosis and cervical spine malformations. There may be various phenotypic presentations of Goldenhar, ranging from mild facial asymmetry to severe deformities with mandibular hypoplasia [15]. Fiberoptic intubation or video-assisted laryngoscopy is frequently needed for tracheal intubation.

Apert's Syndrome

The disorder known as Apert's Syndrome is characterized by a flat, elongated forehead; obtuse nasofrontal angle; and maxillary retrusion/mandibular prominence. There is also acrocephaly (congenital abnormality of the skull in which the top of the head assumes a conical or pointed shape) due to synostosis of the coronal suture. A cleft soft palate is also featured, with reports of closure causing obvious airway obstruction. Cervical spine fusion is often present, most commonly at the C5–C6 level. Laryngomalacia, bronchomalacia, and a cartilaginous tracheal sleeve may also be seen. Obstructive sleep apnea is also associated with this syndrome. Choanal stenosis or atresia may be present, and a definitive airway (tracheostomy) may be necessary. And finally, it is important to note that midface hypoplasia may make it more difficult to mask ventilate [15].

Crouzon's Syndrome

Crouzon's Syndrome is a type of craniosynostosis characterized by premature fusion of the bicoronal sutures, maxillary hypoplasia, and shallow orbits that lead to ocular proptosis and a characteristic beaked nose. Due to midfacial deformities, nasopharyngeal obstruction is common and can lead to sleep apnea and debilitated nasal breathing [15]. Intervertebral fusion, including that of the c-spine, may be present. A difficult airway should be anticipated.

Obstructive Sleep Apnea

Obstructive sleep apnea (OSA) occurs when there is periodic obstruction of the upper airway, and the obstruction may be partial or complete. This leads to repetitive arousal during sleep, and the child may exhibit signs of aggressive behavior or easy distraction. Additionally, as in adults, children may also have daytime hypersomnolence. Clinically, patients will have oxygen desaturation while sleeping and

exquisite sensitivity to opioids, benzodiazepines, and inhaled anesthetics. They may also have hypercarbia and cardiovascular dysfunction [17]. Even asymptomatic patients will show signs of upper airway obstruction when given sedatives and anesthetics.

In the adult population, obesity is the single most important physical characteristic associated with OSA. Pharyngeal airway tissue enlargement leads to upper airway obstruction. In children, OSA is mostly due to either craniofacial anomalies or tonsillar hypertrophy, although the incidence of obesity in children is rising [18].

Almost half of all patients with craniofacial dysostosis develop OSA and require airway intervention at some point in time. Having a reduced cranial base angle pulls the pharyngeal wall forward and results in anteroposterior shortening of the nasal and oral airway. Furthermore, the temporomandibular joint may be drawn posteriorly, such that the mandible is now positioned retrusively. With a mandible that is small and retrognathic (e.g., patients with Pierre–Robin), the tongue is positioned posteriorly and encroaches on the oropharynx and hypopharynx. Upper airway obstruction may be exacerbated in the presence of other anomalies, such as choanal atresia, septal deviation, and turbinate hypertrophy [15].

Sher and colleagues [19] used flexible fiberoptic nasopharyngoscopy to identify the ways in which pharyngeal obstruction occurs in patients with OSA. The four mechanisms are outlined as follows:

The tongue moves posteriorly against the posterior pharyngeal wall.

The tongue moves posteriorly and compresses the soft palate or cleft palatal tags posteriorly against the back pharyngeal wall. The tongue, velum, and posterior pharyngeal wall meet in the upper oropharynx.

The lateral pharyngeal walls move medially and appose each other.

The pharynx constricts in a circular or sphincteral manner.

Drugs that act centrally affect OSA patients by decreasing the action of the pharyngeal dilator muscles, encouraging pharyngeal collapse. Furthermore, volatile anesthetics and intravenous sedatives cause respiratory depression, which can exacerbate the hypoxemia and hypercarbia seen in patients with OSA [18].

Patients who have OSA will especially benefit from oxygen supplementation prior to administration of any sedative drugs. Continuous positive airway pressure may be required. Placing the patient in the lateral, recumbent, or prone position may increase the functional residual capacity (FRC) and help to relieve the obstruction. Oral or nasopharyngeal airways are beneficial in maintaining airway patency, and are much better tolerated in heavily sedated and anesthetized patients.

OSA patients can be difficult to intubate, whether or not they have an associated craniofacial anomaly. LMAs are useful as they can push the tongue out of the way and help relieve airway obstruction. In some cases, an awake fiberoptic intubation may be needed, although the advent of advanced airway videolaryngoscopy has decreased this need (Fig. 3.5).

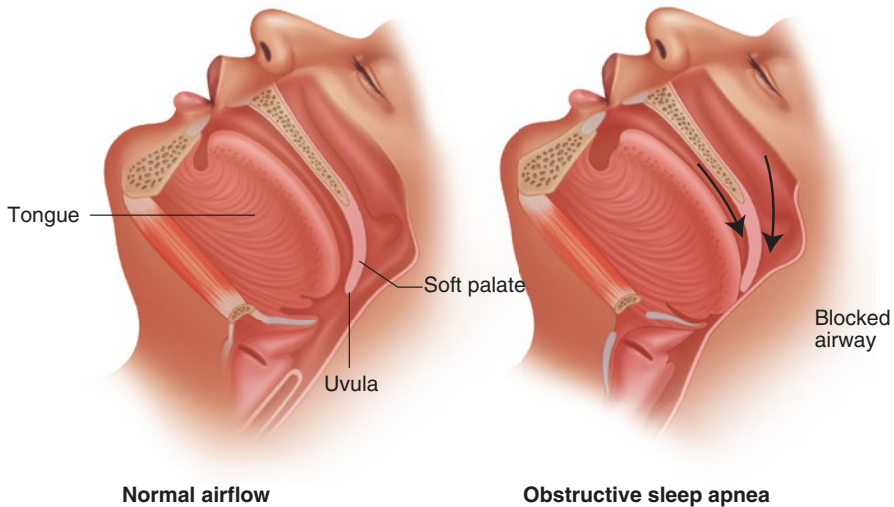


Fig. 3.5 Airflow in a normal patient and in a patient with obstructive sleep apnea

Klippel–Feil Syndrome

Klippel–Feil Syndrome is characterized by congenital fusion of the cervical vertebrae, severe shortness of the neck, and a low posterior hairline. Intubation may be difficult because of limited neck flexion and extension. Intubation may require use of a fiberoptic scope or other advanced airway management device [7].

Subglottic Stenosis

The subglottic area is defined as the area extending from the lower surface of the true vocal cords to the lower surface of the cricoid cartilage [20]. A partial or complete narrowing of the subglottic area may be congenital or acquired. If there is no history of intubation or other acquired causes (such as trauma, infection, foreign body, inflammation, or chemical irritation), then the stenosis is classified as congenital. Severe cases of congenital stenosis are diagnosed in childhood, with misdiagnoses of asthma and bronchitis. Symptoms of subglottic stenosis include dyspnea, stridor, hoarseness, recurrent pneumonitis, cyanosis, and a brassy cough.

Subglottic stenosis involves narrowing of the cricoid cartilage, the only complete cartilage that forms a circumferential ring around the trachea. If the patient requires intubation, care must be taken to not place an endotracheal tube that is larger than the narrowest portion of the airway, as this can cause further inflammation and damage to the surrounding tissue. If the otolaryngologist has already evaluated the patient's airway, sizing of the patient's airway should be documented, and this can

be used as a guide for what size endotracheal tube can be placed. If the patient is coming in for evaluation of the stenosis, then the surgeon and anesthesiologist will work together to evaluate and maintain the patient's airway during the procedure. The surgeon will use a rigid bronchoscope to evaluate movement of the patient's vocal cords, assess the extent of the stenosis, and possibly perform an intervention to decrease the diameter of the stenotic lesion. This may be accomplished by a laser or balloon dilation. More severe cases of airway stenosis may require laryngotracheal reconstruction, where portions of the stenotic airway are removed and replaced with cartilage from the ribs. Initial assessment of the stenosis can occur in the otolaryngologist's office, with the use of a flexible nasal fiberoptic scope. However, children may not cooperate with this procedure, in which case the patient will require anesthesia.

The anesthetic goals during assessment of airway stenosis are challenging. The patient must have enough anesthesia on board to be still during the airway exam and simultaneously be spontaneously breathing so that the surgeon can assess movement of the vocal cords. Two popular techniques are total intravenous anesthesia with propofol and inhalational anesthesia with sevoflurane [21]. In the first case, an IV infusion of propofol is incrementally titrated to achieve the goals of adequate sedation with spontaneous ventilation. Once this is achieved, and the surgeon has a view of the glottis, topical lidocaine is applied to the vocal cords to minimize the risk of laryngospasm. In the second method, the patient's ventilation is intermittently assisted via the use of bag and mask to deliver an inhalational agent. Sevoflurane is most commonly used as it is considered to be the least irritating volatile agent. Occasionally, an endotracheal tube must be placed intra-operatively to help with ventilation. Dexamethasone (up to 1 mg/kg, max 20 mg) is often administered intra-operatively to help decrease airway edema. Table 3.3 summarizes the Meyer–Cotton grading system for classifying the severity of the subglottic stenosis.

Laryngeal Webs

Laryngeal webs account for 5% of congenital anomalies of the larynx. Webs occur when the laryngeal lumen fails to recanalize during embryogenesis. This can result in simply a thin strand of tissue between two areas of the larynx to complete airway infiltration with thick tissue. Seventy-five percent of the webs occur at a glottic level [23]. Patients with only a thin membrane of tissue in the larynx may

Table 3.3 Meyer–Cotton Grading System for Subglottic Stenosis

Stenosis grade	Degree of obstruction
I	0–50% obstruction
II	51–70% obstruction
III	71–99%
IV	Absence of a detectable lumen

Data from Hartnik and Cotton [22]

be asymptomatic or present with a weak cry or mild hoarseness. Those with bulky webs, webs that extend into the posterior glottis, or those that involve the subglottis will have biphasic stridor and either a weak voice or aphonia [22]. Flexible laryngoscopy is usually performed by an otolaryngologist for diagnosis; in the operating room, rigid bronchoscopy is performed and treatment may involve ablation with laser, excision of the web, and/or serial dilations. Shared airway procedures with the surgeon often require use of intravenous anesthesia and spontaneous ventilation.

Pyramiform Aperture Stenosis

Congenital nasal pyramiform aperture stenosis (CNPAS) is a rare disorder where narrowing of the anterior-most nasal process of the maxilla is caused by bony overgrowth in utero. Clinical signs and symptoms are similar to bilateral choanal atresia—tachypnea, feeding difficulties, apnea, or cyanosis—that resolves with crying or mouth-breathing, and difficulty passing a suction catheter through the nose [23]. These patients are often managed with conservative treatment that includes nasal decongestants, frequent suctioning, intranasal steroid drops, humidification, and use of an oral airway. Usually, as the neonate grows and develops, the nasal passage is no longer stenotic enough to cause symptoms. However, surgical repair is warranted if conservative management fails and the child needs persistent ventilation or has failure to thrive. When managing the airway of a patient with CNPAS, care must be taken to not traumatize the nasal passages. Oral airways will help relieve the obstruction. This is a rare neonatal disease, and if surgery is indicated, it usually occurs within the first month of life [24].

Laryngeal Clefts

Another rare pediatric congenital airway anomaly is laryngeal clefts. These are posterior airway defects, where there is an abnormal connection between the larynx and hypopharynx or esophagus, and it is caused by failure of the interarytenoid tissues, cricoid cartilage, or tracheoesophageal septum to fuse [23]. The Benjamin and Inglis classification is often used to describe the laryngeal clefts based on its depth. Type 1 clefts involve the interarytenoid region superior to the level of the vocal cords; Type 2 clefts partially extend into the cricoid lamina; Type III clefts involve the entire cricoid cartilage; and Type IV clefts extend into the intrathoracic aorta [25]. The clinical presentation can vary, depending on type of cleft as well as any co-morbidities the patient may have. The symptoms may range from none to mild feeding difficulties to aspiration, cyanosis, stridor after feeding, and recurrent pneumonia or cough.

The goals of airway management are to maintain spontaneous ventilation and avoid positive pressure ventilation so as to not obscure the signs of airway collapse. Use of a fiberoptic scope can help to assess the airway [26].

Table 3.4 Airway Pathology and Management for Additional Congenital Syndromes

Syndrome	Airway pathology	Airway management
Freedman–Sheldon	Microstomia Micrognathia Microglossia A high arched palate Midfacial hypoplasia characteristically known as whistling mouth syndrome	Abnormal facial features make direct laryngoscopy and intubation extremely challenging maintain spontaneous ventilation and use LMA [27]
Cri Du chat	Microcephaly Micrognathia Long curved, floppy epiglottis Narrow, diamond-shaped vocal cords Laryngomalacia Stridor [28]	
Cretinism	Macroglossia Goiter that may compress trachea Laryngeal or tracheal deviation	Obtain CT imaging to determine extent of tracheal compression Maintain spontaneous ventilation with LMA
Cherubism	Tumorous lesion of mandible and maxillae with intraoral masses	
Meckel syndrome	Microcephaly Micrognathia Cleft epiglottis	
Ankylosing spondylitis	Ankylosis of c-spine Lack of c-spine mobility Ankylosis of temporomandibular joints	
Acromegaly	Macroglossia Prognathism	

Based on data from sources cited and Rosenblatt and Sukhpragar [5]

It is impossible to describe all the anatomical anomalies and implications for airway management. In addition to the anomalies described above in detail, Table 3.4 summarizes other syndromes and describes the airway considerations in bullet form.

Pre-Operative Assessment of the Airway

When assessing a patient’s airway, it is prudent to look at prior anesthetic records to review previous airway management, specifically how easy or difficult it was to mask ventilate the patient and the ease or difficulty with which an LMA or endotracheal tube was placed. However, it is important to note that the airway anatomy changes over time, and it may be easier or more difficult to manage the airway than had been previously shown. Therefore, it is always best to have back up plans/ equipment/personnel in case it is the latter.

Children often do not have formal sleep studies for OSA. Therefore, it is important to ask families if their child snores, and if so, use narcotics judiciously as OSA

Table 3.5 Physical Examination to Predict Ease of Tracheal Intubation

Clinical Feature	How to Assess
Anterior mandibular space	Thyromental distance should be greater than 3 fingerbreadths of the patient
Cervical spine mobility	Assess degree of neck flexion and extension
Tongue versus pharyngeal size	Mallampati classification

Table 3.6 Mallampati Classification

Grade I	Soft palate, anterior and posterior tonsillar pillars, fauces, and uvula visible
Grade II	Tonsillar pillars and base of uvula hidden by posterior tongue
Grade III	Soft palate and base of uvula is visible
Grade IV	Hard palate only visible

may be suspected. Airway obstruction should be anticipated and properly sized oral or nasopharyngeal airways readily available.

Children can often be uncooperative and fail to follow directions. Fortunately, external examination is often sufficient (Table 3.5). The thyromental distance is important as it predicts anterior mandibular space. For children, adequate space is anticipated if it is equal to or greater than the width of the child's three fingerbreadths. Inspect for airway abnormalities such as micrognathia, macroglossia, and mandibular hypoplasia. If the patient's chin is posterior to upper lip, expect a difficult airway; if the chin is neutral with upper lip, it is likely the patient has a normal airway [7]. Assess c-spine mobility by asking the patient to extend and flex the neck.

A cursory dental exam is important. Specifically, inquire about loose teeth, as they can be inadvertently dislodged during airway management and aspirated. The absence of upper incisors allows for better laryngoscopic vector alignment; conversely, the presence of long upper incisors makes laryngoscopy and tracheal intubation more difficult [3].

In predicting the ease of tracheal intubation, the importance of each physical component has already been described in detail at the beginning of this chapter.

The Mallampati Classification system (Table 3.6) is used to visually grade the size of the oral cavity relative to the tongue. The examiner asks the patient to maximally open his/her mouth (normal adult opening is 5–6 cm) and protrude the tongue as far as possible. Based on the pharyngeal structures that are visible, the patient is assigned a Mallampati Score. Grade I and II views are technically easy, whereas a grade III or IV view often predicts a technically difficult or impossible intubation [29]. In children, the Mallampati score has less predictive value (Fig. 3.6).

General Principles of Airway Management

It is beyond the scope of this chapter to describe how to intubate, place a laryngeal mask airway, or use advanced airway management devices such as a fiberoptic scope or videolaryngoscopy. Airway management should be performed in the hands of a skilled provider, an anesthesiologist, or an otolaryngologist who is specially trained to manage airways. Which particular method is used will depend

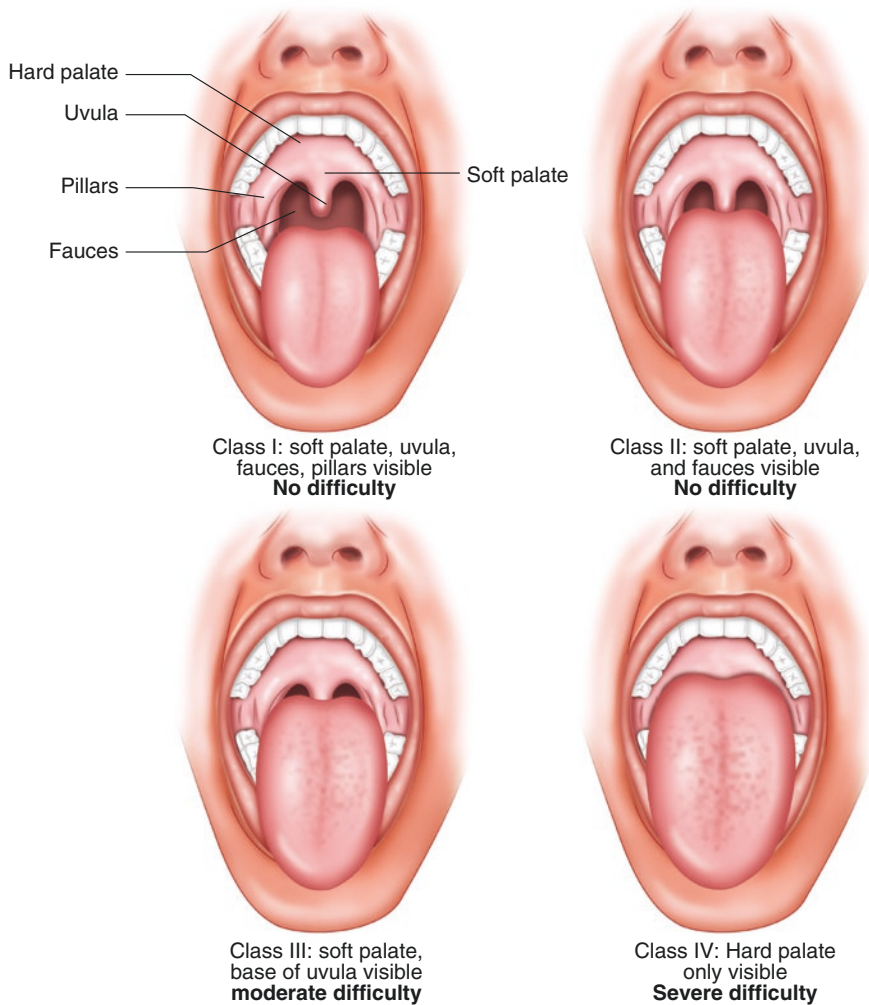


Fig. 3.6 Mallampati Classification

on operator experience, what is available at your institution, and preference of operator. Listed below is a simple explanation of some of the most commonly used airway devices.

Laryngeal Mask Airway (LMA)

The LMA is a supraglottic device that can be rapidly and blindly inserted. Since it is placed above the glottis, there is no risk of placing the LMA in the wrong place (i.e., the esophagus), as there is with intubation. Patients often breathe spontaneously through the LMA, though it is possible to manually ventilate the patient as

well. There are various sizes and types of LMAs (e.g., the LMA Supreme has a port through which an orogastric tube can be placed so that gastric contents and air can be removed). LMAs can also be used as a guiding device for intubation; this requires advanced management skills. The primary disadvantage of the LMA is that it does not protect the patient from aspiration, which can cause severe morbidity, including death.

Endotracheal Tube (ETT)

Intubation is a technique in which an endotracheal tube (with or without a cuff) is placed into the trachea. Direct laryngoscopy is used to visualize the vocal cords and to confirm that the tube is in fact passing through the trachea and not the esophagus. With the advent of modern devices, video laryngoscopy is often used to visualize the vocal cords. There are many anatomical factors that will help determine if the patient is expected to be easy or difficult to intubate, as this chapter has described in detail. The ETT provides a secure, definitive airway, and cuffed tubes minimize the risk of aspiration. However, the process of intubation has several risks, including but not limited to: dental injury; bronchospasm; laryngospasm; mainstem intubation; esophageal intubation; aspiration; trauma to surrounding tissue; and bleeding.

Pre-Oxygenation

Pre-oxygenation is a simple but important task to perform prior to any manipulation of the airway. Prior to the induction of anesthesia, pre-oxygenation by mask maintains higher oxygen saturation values compared with room air controls [30]. Whenever possible, 100% oxygen should be delivered to the patient using an appropriately fitting mask that forms a good seal. The time it takes for a patient to reach desaturation with thresholds of 93–95% oxygen concentration are longer for patients who received 3 minutes of pre-oxygenation compared to those who did not [31–33].

The ability to mask ventilate should not be underestimated—this technique alone can save lives, especially in situations where experts in airway management are not readily available.

In a study involving 53,041 adult patients, Kheterphal et al. reported an incidence of 0.15% for patients that were impossible to mask ventilate [34]. This means that 99.85% of patients were able to be successfully ventilated. Independent risk factors for those that are impossible to mask ventilate included: neck radiation changes, male sex, obstructive sleep apnea, Mallampati score of III or IV, and the presence of a beard [34]. In a study by Langeron et al., “Using a multivariate analysis, five criteria were recognized as independent factors for a difficult mask ventilation (DMV): [age older than 55 yrs., body mass index >26 kg/m², beard, lack of teeth, and history of snoring]; the presence of two indicating high likelihood of DMV (sensitivity, 0.72; specificity, 0.73)” [35].

Summary

Normal airway anatomy, specifically assessment of oral aperture opening, anterior mandibular space, ratio of tongue size to oropharyngeal cavity, and cervical spine mobility are all important features in predicting the ease of airway management. Anatomical abnormalities in one or more of these areas can result in difficulties with ventilating the patient, intubating the patient, or both, all of which can have detrimental effects. The vital organs of the body—namely the brain, heart, and lungs—cannot sustain prolonged periods of hypoxemia, and the resulting damage from cellular hypoxia and organ dysfunction may be irreversible and lead to permanent disability or death. Without proper oxygenation and ventilation at the cellular level, the body's organs will not be able to sustain life. Careful pre-operative evaluation, adequate preparation, and an understanding of how anatomical anomalies can affect airway management and go a long way in ensuring safe airway management.

References

1. Miller RD, Pardo M Jr, Stoelting RK. *Basics of anesthesia*. 6th ed. Philadelphia: Elsevier/Saunders; 2011.
2. Nargoziyan C. The airway in patients with craniofacial abnormalities. *Pediatr Anesth*. 2004;14:53–9.
3. Ramachandran SK, Kheterpal S. The expected difficult airway. In: *The Difficult Airway*.
4. Block C, Brechner V. Unusual problems in airway management II. The influence of the temporomandibular joint, the mandible, and associated structures on endotracheal intubation. *Anesth Analg*. 1971;50(1):114–23.
5. Rosenblatt W, Sukhpragarn W. Airway management. In: Barash P, Cullen B, Stoelting R, Cahalan M, Stock C, Ortega R, editors. *Clinical Anesthesia*. 7th ed. Philadelphia: Lippincott Williams & Wilkins; 2013. p. 762–802.
6. Apfelbaum JL, Hagberg CA, Caplan RA, Blitt CD, Connis RT, Nickinovich DG, et al. Practice guidelines for management of the difficult airway: an updated report by the American Society of Anesthesiologists Task Force on Management of the Difficult Airway. *Anesthesiology*. 2013;118(2):251–70.
7. Infosino A. Pediatric upper airway and congenital anomalies. *Anesthesiol Clin North Am*. 2002;20:747–66.
8. Hagberg C. *Benumof and Hagberg's airway management*. 3rd ed. Philadelphia: Elsevier/Saunders; 2013.
9. Ayari S, Aubertin G, Girschig H, Van Den Abbeele T, Denoyelle F, Couloignier V, et al. Management of laryngomalacia. *Eur Ann Otorhinolaryngol Head Neck Dis*. 2013;130:15–21.
10. Crockett D, Goudy S. Cleft lip and palate. *Facial Plast Surg Clin North Am*. 2014;22(4):573–86.
11. Steward DJ. Anesthesia for patients with cleft lip and palate. *Semin Anesth*. 2007;26(3):126–32.
12. Gunawarda RH. Difficult laryngoscopy in cleft lip and palate surgery. *Br J Anaesth*. 1996;76(6):757–9.
13. Raj D, Luginbuehl I. Managing the difficult airway in the syndromic child. *Contin Educ Anaesth Crit Care Pain*. 2014;15(1):7–13.
14. Stuart G, Ahmad N. Perioperative care of children with inherited metabolic disorders. *Contin Educ Anaesth Crit Care Pain*. 2011;11(2):62–8.
15. Gregory GE, Andripoulos DB. *Gregory's pediatric anesthesia*. 5th ed. Wiley-Blackwell: Chichester, UK; 2012.

16. Inagawa G, Miwa T, Hiroki K. The change of difficult intubation with growth in a patient with Treacher Collins syndrome. *Anesth Analg*. 2004;99:1874.
17. Gross JB, Bachenberg KL, Benumof JL, Caplan RA, Connis RT, Coté CJ, et al. Practice guidelines for the perioperative management of patients with obstructive sleep apnea: A report by the American Society of Anesthesiologists Task Force on Perioperative Management of Patients with Obstructive Sleep Apnea. *Anesthesiology*. 2006;104(5):1081–93. Updated in: American Society of Anesthesiologists Task Force on Perioperative Management of patients with obstructive sleep apnea. Practice guidelines for the perioperative management of patients with obstructive sleep apnea: an updated report by the American Society of Anesthesiologists Task Force on Perioperative Management of patients with obstructive sleep apnea. *Anesthesiology*. 2014;120(2):268–86.
18. Benumof JF. Obstructive sleep apnea in the adult obese patient: implications for airway management. *J Clin Anesth*. 2001;13(2):144–56.
19. Sher AE, Shprintzen RJ, Thorpy MJ. Endoscopic observations of obstructive sleep apnea in children with anomalous upper airways: predictive and therapeutic value. *Int J Pediatr Otorhinolaryngol*. 1986;11(2):135–46.
20. Bath AP, Panarese A, Thevasagayam M, Bull PD. Paediatric subglottic stenosis. *Clin Otolaryngol Allied Sci*. 1999;24:117–21.
21. Eid EA. Anesthesia for subglottic stenosis in pediatrics. *Saudi J Anaesth*. 2009;3(2):77–82. <https://doi.org/10.4103/1658-354X.57882>.
22. Hartnik CJ, Cotton RT. Congenital laryngeal anomalies: laryngeal atresia, stenosis, webs and clefts. *Otolaryngol Clin N Am*. 2000;33:1293–308.
23. Windsor A, Clements C, Jacobs I. Rare upper airway anomalies. *Pedi Respir Rev*. 2016;17:24–8.
24. Al Abri R, Javad H, Kumar S, Bharga D, Koul R, Al Futaisi A, et al. Congenital nasal pyriform aperture stenosis: first case report in Oman. *Oman Med J*. 2008;23(3):192–4.
25. Benjamin B, Inglis A. Minor congenital laryngeal clefts: diagnosis and classification. *Ann Otol Rhinol Laryngol*. 1989;98:417–20.
26. Reza R, Rouillon I, Gilles R, Lin A, Nuss R, Denoyelle F, et al. The presentation and management of laryngeal cleft: a 10-year experience. *Arch Otolaryngol Head Neck Surg*. 2006;132(12):1335–41.
27. Patel K, Gursale A, Chavan D, Sawant P. Anaesthesia challenges in Freeman-Sheldon syndrome. *Indian J Anaesth*. 2013;57(6):632–3.
28. Han I, Kim YS, Kim SW. Anesthetic experience of a patient with cri du chat syndrome. *Korean J Anesthesiol*. 2013;65(5):482–3.
29. Frerk CM. Predicting difficult intubation. *Anaesthesia*. 1991;46(12):1005–8.
30. Haynes SR, Allsop JR, Gillies GW. Arterial oxygen saturation during induction of anesthesia and laryngeal mask insertion: prospective evaluation of four techniques. *Br J Anaesth*. 1992;68:519–22.
31. Baraka AS, Taha SK, Aouad MT, El-Khatib MF, Kawkabani NI. Preoxygenation: comparison of maximal breathing and tidal volume breathing techniques. *Anesthesiology*. 1999;91:612–6.
32. Valentine SJ, Marjot R, Monk CR. Preoxygenation in the elderly: a comparison of the four-maximal-breath and three-minute techniques. *Anesth Analg*. 1990;71:516–9.
33. Gambee AM, Hertzka RE, Fisher DM. Preoxygenation techniques: comparison of three minutes and four breaths. *Anesth Analg*. 1987;66:468–70.
34. Kheterphal S, Martin L, Shanks AM, Tremper KT. Prediction and outcomes of impossible mask ventilation: a review of 50,000 anesthetics. *Anesthesiology*. 2009;110:891–7.
35. Langeron O, Masso E, Huraux C, Guggiari M, Bianchi A, Coriat P, et al. Prediction of difficult mask ventilation. *Anesthesiology*. 2000;92:1229–36.

Part II

Thorax and Its Contents



Head and Neck Variations: Vessels

4

Amanda Norwich-Cavanaugh and Deepak Narayan

Carotid Artery

Normal Course

The carotid artery is located in the medial neck within the carotid triangle, which is defined by the medial border of the sternocleidomastoid laterally, inferior border of the mandible or posterior belly of the digastric superiorly, and superior belly of the omohyoid or the midline medially. The common carotid takeoff is dependent on laterality; however, both sides travel in front of the trachea in the thorax, then laterally on either side of the trachea in the neck. On the left, the common carotid originates directly from the aortic arch, while on the right, it originates at the brachiocephalic (or innominate) trunk, which is a tributary of the aortic arch [1]. From this point on the course of the common carotid is identical on both sides.

The common carotid artery (CCA) usually has no branches in either the thoracic or cervical portions. In two-thirds of the population, the order of takeoff from the aortic arch, proximal to distal, is the brachiocephalic trunk, left CCA, and left subclavian. The brachiocephalic trunk then bifurcates into the right CCA and right subclavian artery as mentioned above. The CCA typically bifurcates into the internal carotid artery (ICA) and external carotid artery (ECA) near the superior margin of the thyroid cartilage, which is where the internal carotid artery (ICA) begins. The ICA is posterolateral to the ECA, which is an important concept in carotid surgery. In addition, the ECA is typically located medial to the digastric and stylohyoid

A. Norwich-Cavanaugh (✉)

Department of Reconstructive and Plastic Surgery, Yale School of Medicine,
New Haven, CT, USA

D. Narayan (Deceased)

Section of Plastic and Reconstructive Surgery, Yale New Haven Hospital,
New Haven, CT, USA

muscles. The ICA has three segments: cervical, petrous, and intracranial. For the purposes of this review, we will discuss only the cervical portion, which exists in the carotid sheath, along with the internal jugular vein, situated laterally, and the vagus nerve (Cranial nerve X), located between the two vessels. The external carotid artery has an extensive branching network that supplies the upper neck and extracranial soft tissue of the head. There are nine branches in total, some of which will be discussed with their variations later [2].

Variations and Pathologies

Variations in carotid anatomy are prevalent in the population. Here we will examine the three portions in the following order: CCA, ECA, ICA. A general principle in these variations is that lack of visualization on imaging, especially of the CCA or vertebral artery, can lead to the improper diagnosis that a vessel is occluded [3]. Additionally, variations in known orientations of these vessels become problematic when performing a carotid endarterectomy, radical neck dissection, or other invasive and non-invasive procedures. Above we discussed the branching pattern of the brachiocephalic trunk, left CCA, and left subclavian arteries. Two-thirds of the population have “normal” anatomy, where the right CCA exists as a branch of the brachiocephalic artery. The remaining one-third have one of two variations. The most common of these variations is when the right CCA originates from the proximal portion of the brachiocephalic trunk. There is little literature on the clinical implications of this anomaly, and it is likely not significant because the right CCA typically branches brachiocephalic artery just distal to this anomaly and in this case, does not cross midline. The location of the bifurcation of the CCA is also quite variable, normally ranging between C2 and C6. The most common location is C4, which exists on the right in 20% and the left in 50% of people. Uncommon locations of the carotid bifurcation are T1–T3 [4]. Additionally, as mentioned above, the classic anatomic location of the bifurcation is the superior border of the thyroid cartilage. However, in one study, the CCA bifurcated at the level of the hyoid bone located cranial to the thyroid cartilage in the same frequency. In this study, there was also a correlation between a high bifurcation and aberrant course of the superior thyroid artery, which typically branches off the ECA, but in these cases originated at the bifurcation itself [5]. The presence of a high CCA bifurcation will typically lead to more injury to the hypoglossal nerve during carotid exposure. One study showed that all hypoglossal nerve injuries in patients undergoing CEA occur in those with a high bifurcation; however, it should be noted the number of patients with this injury is so small in their study that it may be a misrepresentation [6].

Variations in the ECA also exist in varying frequencies. The most clinically relevant is probably a laterally positioned ECA. In this anatomic anomaly, surgeons performing a carotid endarterectomy must carefully bypass the branches of the ECA in order to obtain sufficient exposure of the ICA. Another worrisome variation of the ECA involves its relationship to the digastric and stylohyoid muscles. Normally, the ECA is medial to both muscles. Occasionally, it will be between or

lateral to the two muscles, and more rarely, it will loop around the styloid process [4]. This is clinically important in parotidectomy or any surgery nearby as the facial nerve exits through the stylomastoid foramen, with its five terminal branches passing through the parotid to innervate the facial muscles [7]. Additionally, this is important during exposure in modified radical and radical neck dissection [8].

Branches of the ECA can arise from the ICA in rare instances. Usually, these branches are the ascending pharyngeal artery, occipital artery, superior thyroid artery, and the superficial temporal artery. The ascending pharyngeal artery can also originate from the carotid bifurcation [3]. This is also important for the purposes of planning and performing carotid endarterectomy and endovascular embolization. Interestingly, this abnormality may be protective. Cases of critical ICA stenosis with collateral flow from the ECA have been reported [9].

Kinking is also a reported anomaly. In one study, it was the most common variation of the ICA. Usually bilateral, kinking has clinical significance as it is associated with atheromatous plaques and fibrodysplasia. Failure of the heart to descend and the carotid artery to stretch, thereby eliminating kinks in vitro, is thought to result in vascular loops and kinking [10].

An interesting but exceedingly rare anomaly is the presence of *persistent fetal branches*, *persistent primitive hypoglossal* (Fig. 4.1), and *proatlantal intersegmental arteries*, which have a prevalence of 0.023% each [9]. The proatlantal intersegmental artery is an abnormal connection between the ECA or ICA and the vertebral artery.

Size-related abnormalities are also possible. A hypoplastic ICA is prevalent in <0.2% of the population. The ipsilateral CCA is usually hypoplastic as well, and it is postulated that these patients are more at risk for aneurysm on the contralateral side because of abnormally increased flow. ICA hypoplasia is more common on the left and diagnosed by CTA, MRA, or angiography [3].

Innominate Artery

Normal Course

The innominate artery is the most proximal and largest tributary of the aortic and gives rise to the right subclavian and right common carotid arteries. It is 4–5 cm in length and bifurcates just above the jugular notch. Classically, the innominate ascends anterior to the trachea, then travels to the right. The clinical importance of this location will be discussed below.

Variations and Pathology

By far the most common anomaly of the innominate artery is its location to the left or right of the trachea. In one cadaveric study, 43% were located to the left of the trachea and 5% to the right [4]. This anomaly is particularly important when

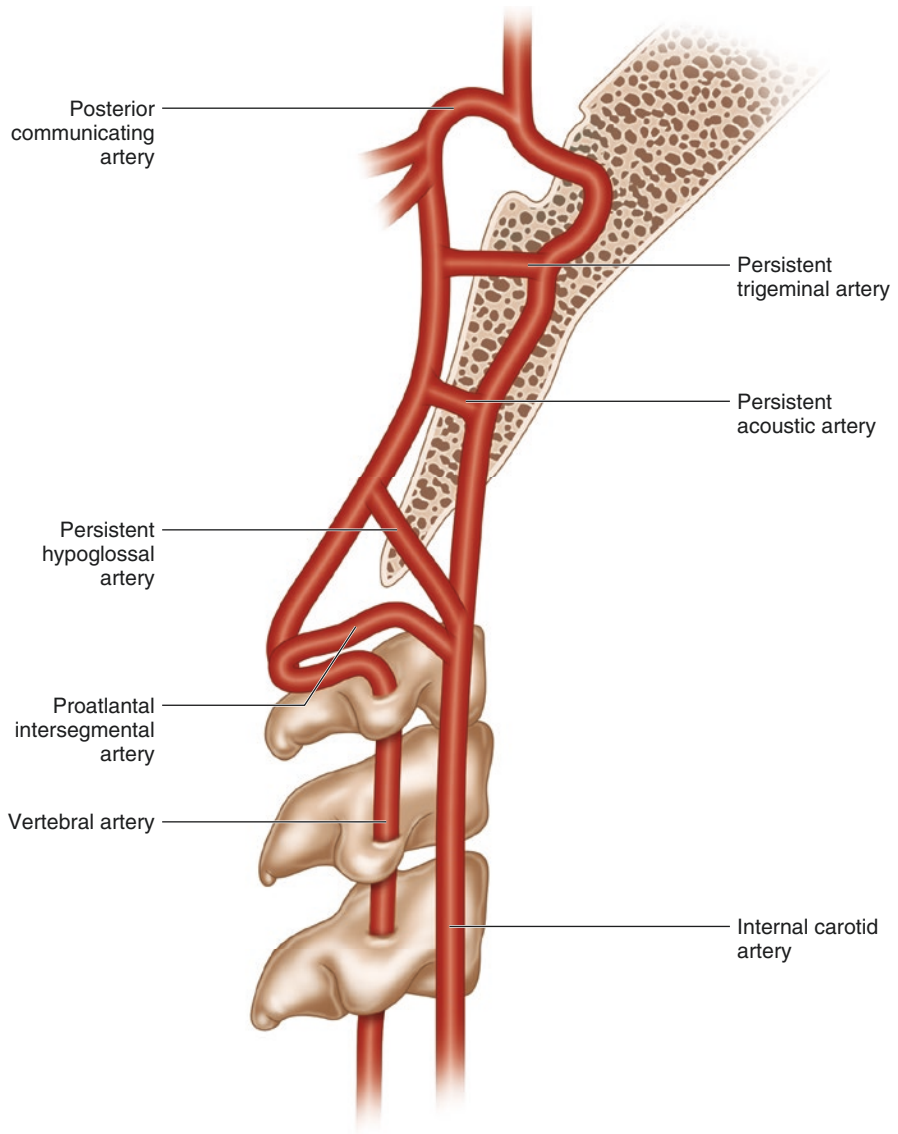


Fig. 4.1 Schematic representation of the different fetal anastomoses between the vertebral arterial system and the carotid arterial system

performing a tracheostomy, as this artery is a common site of injury, and if the surgeon is not aware of its exact location, this may lead to undesirable outcomes. In these cases, surgeons may be aided by radiologic studies [11]. Another variation is a high-riding innominate. This creates a possibly lethal complication in the event of an inferiorly placed tracheostomy with high cuff pressure, as this will erode the trachea and create a tracheo-innominate fistula. The incidence of this complication is 0.1–1%. In the case of a high-riding innominate, the surgeon must ensure the

tracheostomy site is sufficiently superior to this large artery and use moderate cuff pressure. Tracheo-innominate fistula usually presents within the first or second week after surgery [12].

On occasion, the bifurcation of the innominate artery may be close to the thyroid gland. This is an important variation to consider in thyroid and parathyroid surgery [4]. In one study of 110 cadavers, 0.9% demonstrated a brachiocephalic artery surrounding the right hemithyroid less than 1 cm away. As expected, this would make dissection of this gland very difficult [13].

The right-sided innominate artery may also share an origin with the left common carotid artery, with the left subclavian artery arising separately. This is called a “bovine trunk.” The prevalence of this anomaly has been reported anywhere from 3 to 29% based on angiographic and autopsy studies. In one study of over 3000 patients, 40.6% of patients with a common origin had structural heart disease, and the prevalence in the population with structural heart disease was 17.5%, which is not significantly different from 15.1% in the “normal” population. This may have a protective effect in some carotid procedures, such as repair coarctation of the aorta, in which the most distal portion of the arch is clamped. Bilateral perfusion from both carotids will preserve cerebral perfusion. Conversely, cerebral blood flow is compromised during the placement of a Blalock–Taussig shunt between the right subclavian and right pulmonary artery as the base of the innominate is clamped [14].

Subclavian Artery

Normal Course

Paths of the right and left subclavian artery vary significantly. They will therefore be discussed separately in this section. The right subclavian artery originates from the brachiocephalic trunk posterior to the upper border of the sternoclavicular joint. It ascends superomedial to the clavicle and posterior to the scalenus anterior, then descends laterally to the outer border of the first rib. At this point, it becomes the axillary artery [15].

The left subclavian artery originates directly from the aortic arch. It is the most distal branch of the aortic arch and arises posterolaterally. The left subclavian is usually exposed for repair related to trauma. Exposure of the left subclavian is completed by exposing its supraclavicular segment. For more expedient control, a section of the medial clavicle may be excised. This exposure may also be used for a carotid–subclavian bypass. Median sternotomy does not provide adequate visualization, as this artery arises posterolaterally. Third-space thoracotomy also provides immediate exposure for proximal control [1].

Variations and Pathology

Anomalies of the right subclavian artery can be quite unfavorable and sometimes fatal during vascular and non-vascular procedures. The anomaly most commonly cited in the literature is an aberrant right subclavian arising distally to the left

subclavian artery, which runs in a retroesophageal course (Fig. 4.2). This is sometimes referred to as the “arteria lusoria” [16]. If this vessel becomes aneurysmal, it can cause fatal hemorrhage during endoscopy. This is also an important variation to note in the case of aneurysm which will then lead to dysphagia or tracheal compression. These are not the typical signs and symptoms related to an aneurysm of the right subclavian artery. The right subclavian may also form a vascular ring around the esophagus and trachea. This presents in the neonate as an inability to properly feed and failure to thrive [15].

Variations of the left subclavian artery have been described less frequently. The only anomaly found in most literature is a right-sided arch with isolation of the left subclavian artery. In this case, the left subclavian artery is “isolated” from the aortic arch and is attached to the left pulmonary artery by the ductus arteriosus. An isolated left subclavian artery is supplied by retrograde flow from the left vertebral artery, creating a physiologic subclavian steal [17].

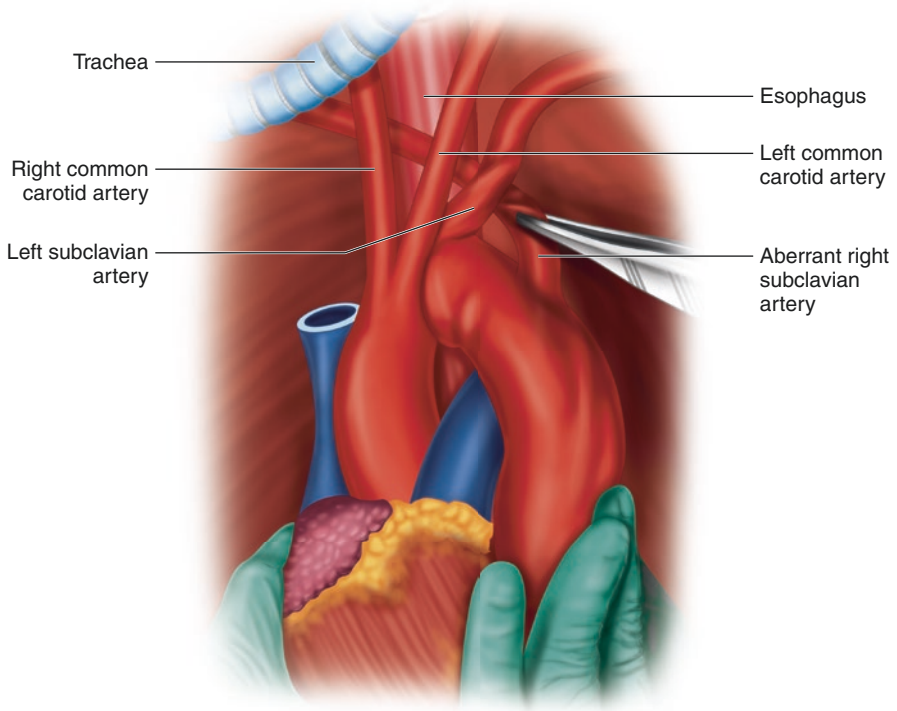


Fig. 4.2 Shows the origin and retrotracheal course of the aberrant right subclavian artery. Trachea has been lifted up and the arch of aorta is slightly twisted forward for clarity. *T* trachea, *E* esophagus, *RCC* right common carotid artery, *LCC* left common carotid artery, *LSA* left subclavian artery, *ARSA* aberrant right subclavian artery

Vertebral Artery

Normal Course

The vertebral arteries exist, as most vessels addressed here, as a pair. In contrast to the arteries described above, they have almost identical origins and paths within the neck. These arteries are the first and largest branches of the subclavian arteries. They then travel through the transverse processes of the upper six cervical vertebrae, pass behind the lateral masses of the atlas, and enter the dura mater behind the occipital condyles. Their path then enters the skull, at which point we will stop our discussion in this chapter. The extracranial vertebral artery is divided into three segments, of which the ostial segment (V1) is most proximal. This branch ascends to C6 and is differentiated from the more distal thyrocervical and costocervical branches of the subclavian artery by its lack of branches. The inferior thyroid artery passes anterior to V1. This section of the vertebral artery is particularly at risk because it is unprotected by bony structures. V2 ascends through the transverse foramina of C3–C6, the axis and atlas. This area deviates just lateral to V1 to reach the more laterally placed transverse foramina of the upper cervical vertebrae. V3 is a short segment that extends from the atlas to the foramen magnum. It takes a complex and circuitous path so as to allow neck rotation without strain on the artery [18].

There are cervicospinal branches from the vertebral artery, including muscular arteries and lateral spinal arteries. The lateral spinal branches enter the intervertebral foramina and divide to pass dorsal and ventral to the spinal cord. This branch also supplies the vertebral body and periosteum [18].

Variations and Pathology

Anatomic variants of the vertebral artery are unusual. In 80% of people, this vessel originates at the upper posterior aspect of the first segment of the subclavian artery [2]. On the left, the most common variation is when the vertebral artery originates directly from the aortic arch between the left common carotid and subclavian arteries, which occurs in 2.4–5.8% of the population [16]. According to a review written in 2007, at that time one case of bilateral origins from the vertebral artery had been reported [16]. The right vertebral artery may also originate from the carotid artery. Occasionally, the left vertebral artery will be the most distal branch of the aortic arch. In this case, it could give rise to the thyroidea ima artery described below [4]. Origin from the common carotid artery is present in <1% of the population and usually occurs on the right in conjunction with an aberrant right subclavian artery [3].

The right and left vertebral arteries are similar in size, but a left dominant vertebral artery is more common. When the left subclavian artery is occluded, there is vertebral artery “steal,” which leads to enlargement of both vertebral arteries and reversal of flow. This in turn depletes posterior cerebral circulation and causes syncope, especially when heavy exercise is performed with the left arm. This phenomenon is less common on the right [2].

Another anomaly associated with clinical outcomes is an abnormal level of entry to the transverse foramen of the dura. In 90% of the population, the V2 segment enters the transverse foramen at C6. In others, the entry can be anywhere from C2 to C7. This is important in the evaluation of trauma where injury to the vertebral artery is closely evaluated and failure to visualize in its typical location may lead to an inappropriate diagnosis of dissection or occlusion [3]. Similarly, hypoplastic vertebral arteries occur in 10–30% of the population. This may cause a similar misdiagnosis of dissection or occlusion and lead to potentially harmful iatrogenic injury if catheter angiography is used. In these cases, multiple imaging studies such as MRA or CTA should be performed before intervention is planned [3]. A third example of an atretic vertebral artery is in conjunction with a fetal remnant, the proatlantal intersegmental artery mentioned in sect. 1.1.1 above. The proatlantal artery is an abnormal connection between the internal or external carotid and the vertebral artery. When present, the proximal segment of the vertebral artery may be atretic [2].

Facial Artery

Normal Anatomy

The facial artery is the fifth branch of the ECA and originates above the greater horn of the hyoid. It courses behind the submandibular gland, then turns downward toward the angle of the mouth through the medial canthus. Due to its location, it is commonly ligated in radical neck dissection. This must be taken into consideration when performing free flaps following ablation procedures for cancer [19].

At the level of the mouth, the facial artery branches to the inferior and superior labial arteries. Near the medial canthus it continues as the angular artery with collateral flow from the transverse facial artery [20]. This is particularly important in cases of facial artery hypoplasia and agenesis.

Variations

The branching pattern of the anterior branches of the ECA is variable. The classic anatomy configuration, as mentioned above, is when it originates as the fifth branch of the ECA. This is present in 80% of cases. Other configurations occur when the facial and lingual arteries have a common origin. This may be present as a more proximal or distal branch. A common origin with the lingual artery means both tributaries may be inadvertently ligated. In such circumstances, the only available vessel for free flap implantation following radical neck dissection would be the superior thyroid artery, leaving the surgeon with unfavorable options if this is not possible [19].

In the event of this inadvertent transection due to aberrant origin of the facial artery, perfusion may not be as robust as it would be otherwise in, for example, facial transplant. According to an article by Rodriguez et al., the majority of facial subunits, with the exception of the lateral forehead, are supplied by the facial artery. The lateral forehead is perfused by the superficial temporal artery [21]. A limitation of this study is the use of cadaveric grafts, which does not account for angiogenesis and reconfiguration of perfusion, as noted in a following discussion paper [22].

In a case report, agenesis of the left facial artery was noted with a concomitant large transverse facial artery and submental artery coursing medially toward the eye, terminating as the angular artery. This may be accompanied by compensation from the contralateral facial artery as well. The agenesis of the facial artery, and thereby presence of an abnormal submental artery, is an important note in submental island flaps and submandibular gland excision through a retro-auricular approach [23].

Thyroidea Ima

The thyroidea ima is an inherently atypical variant that acts as a collateral vessel feeding the thyroid gland. Johann E. Neubauer first described the anomaly in 1772, and occasionally it is referred to as the thyroid artery of Neubauer. Literature reports this vessel occurs in up to 16.9% of the population [16]. Frequently, it is a branch of the brachiocephalic artery, but less commonly it may be branch directly from the aortic arch between the brachiocephalic artery and the left subclavian artery. Even more unlikely is when it originates from the right common carotid artery [16]. The thyroidea ima ascends in front of the trachea to the bottom of the thyroid gland (Fig. 4.3). It may be 3–5 mm in diameter, and as mentioned above, it supplies the thyroid gland and may perfuse the trachea and parathyroid glands as well [24].

According to reports, there is no known standardized method to avoid injury to this abnormal vessel, except for anticipating its presence and undergoing very careful dissection in thyroid and parathyroid surgery. In cases of patients with thyroidea ima who are undergoing percutaneous tracheostomy, life-threatening bleed is usually inevitable. There is no known technique to eliminate the risk of this complication, as there would be no reason to deviate from the standard incision, which is made somewhere between the first and third tracheal rings. In addition, the precautionary use of bronchoscopy only allows for direct internal visualization. Hemorrhage after surgical tracheostomy is also possible with a similar insertion at the second to fourth tracheal rings. In cases where hemodynamic vital signs are compromised, urgent sternotomy is required to gain proximal control [24].

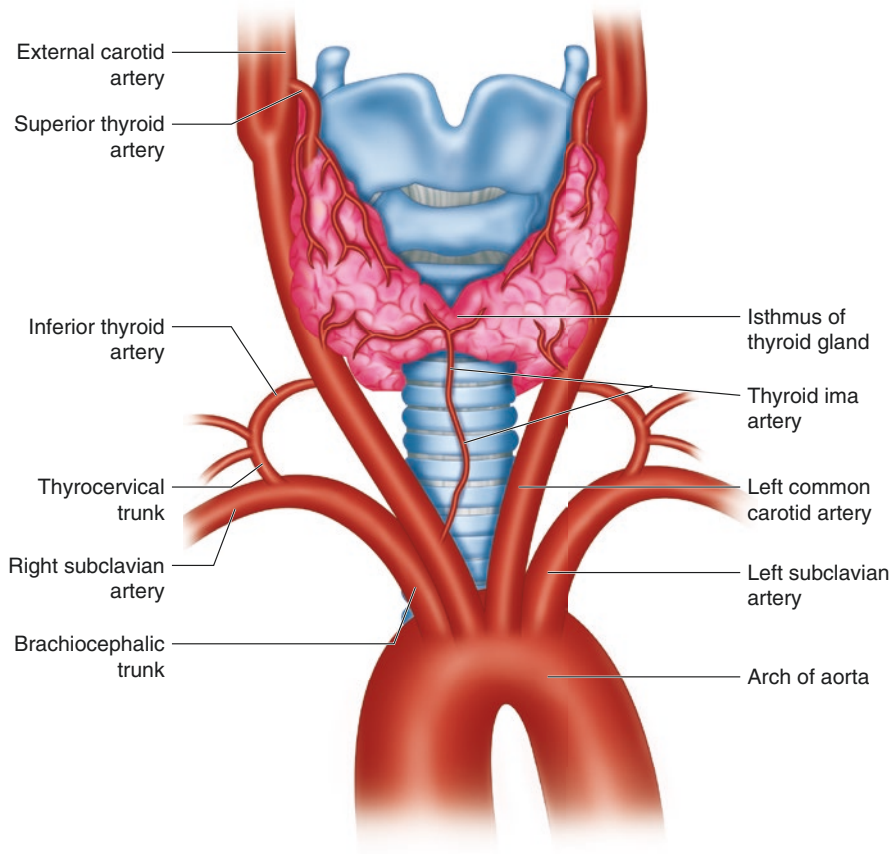


Fig. 4.3 Arterial supply of the thyroid

References

1. Ascher E. Haimovici's vascular surgery, 6th ed: Philadelphia: Blackwell Publishing Ltd.; 2012.
2. Uflacker R. Atlas of vascular anatomy: an angiographic approach. Chapter 2. Philadelphia: Lippincott Williams and Wilkins; 2007.
3. McKinney AM. Cervical carotid and vertebral arterial variants. In: McKinney AM, editor. Atlas of Normal imaging variations of the brain, skull and Craniocervical vasculature. Cham: Springer International Publishing; 2017. p. 971–94.
4. Krmptić-Nemanić J, Draf W, Helms J. The neck and thorax. In: Krmptić-Nemanić J, Draf W, Helms J, editors. Surgical anatomy of head and neck. Berlin: Springer-Verlag; 1988. p. 1–52.
5. Lo A, Oehley M, Bartlett A, Adams D, Blyth P, Al-Ali S. Anatomical variations of the common carotid artery bifurcation. ANZ J Surg. 2006;76(11):970–2.
6. Assadian A, Senekowitsch C, Pfaffelmeyer N, Assadian O, Ptakovsky H, Hagmüller GW. Incidence of cranial nerve injuries after carotid eversion endarterectomy with a transverse skin incision under regional anaesthesia. Eur J Vasc Endovasc Surg. 2004;28(4):421–4.
7. Hansen JT, Koepfen BM, Netter FH. Netter atlas of human physiology. Icon Learning Systems: Teterboro; 2002.

8. Zollinger RM. Atlas of surgical operations. 7th ed. New York: McGraw-Hill; 1993.
9. Small JE, Harrington J, Watkins E. Prevalence of arterial branches arising from the extracranial internal carotid artery on CT angiography. *Surg Radiol Anat.* 2014;36(8):789–93.
10. Cappabianca S, Somma F, Negro A, Rotondo M, Scuotto A, Rotondo A. Extracranial internal carotid artery: anatomic variations in asymptomatic patients. *Surg Radiol Anat.* 2016;38:893–902.
11. Huempfer-Hierl H, Hierl T, Halama D. Rare anatomical variation of the brachiocephalic trunk encountered in tracheostomy. *Br J Oral Maxillofac Surg.* 2017;55(3):312–3.
12. Komatsu T, Sowa T, Fujinaga T, Handa N, Watanabe H. Tracheo-innominate artery fistula: two case reports and a clinical review. *Ann Thorac Cardiovasc Surg.* 2013;19(1):60–2.
13. Iterezote AM, Dantas de Medeiros A, Cesar R. Anatomical variation of the brachiocephalic trunk and common carotid artery in neck dissection. *Int J Morphol.* 2009;27(2):601–3.
14. Katz JC, Chakravarti S, Ko HH, Lytrivi ID, Srivastava S, Lai WW, et al. Common origin of the innominate and carotid arteries: prevalence, nomenclature and surgical implications. *J Am Soc Echocardiogr.* 2006;19(12):1446–8.
15. Standring S. Great Vessels. In: Gray's anatomy: the anatomical basis of clinical practice. vol. 10; 2005:Section 58. <https://doi.org/10.1111/j.1365-2923.1977.tb00635.x>.
16. Kau T, Sinzig M, Gasser J, Lesnik G, Rabitsch E, Celedin S, et al. Aortic development and anomalies. *Semin Intervent Radiol.* 2007;24(2):141–52.
17. Luetmer PH, Miller GM. Right aortic arch with isolation of the left subclavian artery: case report and review of the literature. *Mayo Clin Proc.* 1990;65(3):407–13.
18. Campero A, Rubino PA, Rhoton AL Jr. Anatomy of the vertebral artery. In: Bernard G, Bruneau M, Spetzler RF, editors. Pathology and surgery around the vertebral artery. Paris: Springer-Verlag; 2011. p. 29–40.
19. Tan B-K, Wong C-H, Chen H-C. Anatomic variations in head and neck reconstruction. *Semin Plast Surg.* 2010;24(2):155–70.
20. Prendergast PM. Anatomy of the face and neck. In: Shiffman MA, Di Giuseppe A, editors. Cosmetic surgery: art and techniques. Berlin: Springer-Verlag; 2013. p. 29–45. https://doi.org/10.1007/978-3-642-21837-8_2.
21. Rodriguez-Lorenzo A, Audolfsson T, Wong C, Saiepour D, Nowinski D, Rozen S. Vascular perfusion of the facial skin: implications in Allotransplantation of facial aesthetic subunits. *Plast Reconstr Surg.* 2016;138(5):1073–9.
22. Aycart M, Pomahac B. Discussion: vascular perfusion of the facial skin: implications in Allotransplantation of facial aesthetic subunits. *Plast Reconstr Surg.* 2016;138(5):1080–1.
23. Eid N, Ito Y, Otsuki Y. Anomalous branching pattern of external carotid artery: clinical relevance to cervicofacial surgery. *Clin Anat.* 2011;24(8):953–5.
24. Kamparoudi P, Paliouras D, Gogakos AS, Rallis T, Schizas NC, Lazopoulos A, et al. Percutaneous tracheostomy-beware of the thyroidea-ima artery. *Ann Transl Med.* 2016;4(22):449.



Head and Neck Variations: Soft Tissue, Nerves, and Bones

5

Amanda Norwich-Cavanaugh and Deepak Narayan

Nerves

Hypoglossal Nerve (Cranial Nerve XII)

Normal Course

This vital nerve is a general somatic efferent nerve supplying the intrinsic and extrinsic muscles (all except the palatoglossus muscle) of the ipsilateral tongue. After passing through the hypoglossal canal, the nerve turns sharply downward and travels in the upper carotid sheath between the internal carotid artery (ICA) and internal jugular vein (IJV). At the level of the transverse process of the atlas, it turns forward and travels along the lateral surface of the ICA and external carotid artery (ECA) before entering the digastric triangle, at which point it gives off muscular branches to the intrinsic and extrinsic muscles of the tongue [1, 2]. The hypoglossal nerve crosses over the ECA and ICA about 1 cm above the bifurcation, in most cases, deep to the internal jugular. As it crosses the ICA fibers, the hypoglossal nerve courses downward to form the superior root of the ansa cervicalis (a.k.a. ansa hypoglossis), which then crosses the IJV and curves upward to form the inferior root [2].

Variations and Pathologies

Successful surgery in the neck depends on the knowledge of consistent anatomic relationships of important structures. Lesions of the hypoglossal nerve will produce deviation to the side of the lesion due to an inability of that side to protrude, which

A. Norwich-Cavanaugh (✉)

Department of Reconstructive and Plastic Surgery, Yale School of Medicine,
New Haven, CT, USA

D. Narayan (Deceased)

Section of Plastic and Reconstructive Surgery, Yale New Haven Hospital,
New Haven, CT, USA

is caused mainly by the dysfunction of the genioglossus muscle, while preserving muscle function on the contralateral side. Damage may also cause dysarthria or impaired speech due to abnormal muscle control [2].

A more common abnormality is the distance between where the hypoglossal nerve crosses over the ICA/ECA and the location of the CCA bifurcation. As might be expected, when the bifurcation is more cranial at the level of the hyoid bone, the hypoglossal nerve is closer [3]. In a study of 15 cadavers, the distance from the crossover to the bifurcation ranged from 2.63 to 29.43 mm, which may contribute to the vulnerability of this nerve during carotid endarterectomies (CEA) [4]. The risk of nerve injury is a well-known complication of CEA. One study of over 5000 patients in the New England area showed a 5.6% incidence of cranial nerve injury. The hypoglossal nerve was injured in around 50% of those pathologic cases, with an overall incidence of 2.7%. These lesions, along with facial nerve lesions, were the most persistent in their course. These cases are usually recoverable, but increased hospital stay by an average of 0.5 days. Interestingly, risk factors influencing cranial nerve injury were included procedures, re-exploration, and return to the operating room specifically for stroke or transient ischemic attack (TIA). Surprisingly, reoperation was a risk factor for overall nerve injury, except in the case of the hypoglossal nerve [5].

There have been cases reported in which a direct branch of the hypoglossal nerve was found to stimulate the sternocleidomastoid muscle (SCM). In a cadaveric study, this was found in 2.5% of cadavers. It is known that the C1 branch of the ansa cervicalis innervates the sternocleidomastoid in 24% of cadaveric necks; however, this showed a direct branch from the hypoglossal nerve can innervate this muscle, adding a layer of complexity to neck dissections and clinical presentation of hypoglossal nerve injury [6].

A procedure in which the anatomy and location of the hypoglossal nerve is vital is the hypoglossal/facial nerve jump anastomosis. This is used for reanimation after injury to the facial nerve during, for example, radical parotidectomy or in acoustic neuroma patients. This technique has been described using the remaining facial nerve, the hypoglossal nerve, or a combination of the two [7]. In one particular case report of a hypoglossal/facial nerve anastomosis, a “double” hypoglossal nerve was found with a motor branch directly into the tongue arising from the nerve’s main trunk in the digastric triangle, as opposed to running alongside the IJV as classically described. For an inexperienced surgeon, this would cause some confusion as to which nerve is best for the anastomosis. The only way the main trunk of the hypoglossal nerve was identified was by tracing it proximally [8]. Again, the precise location of the hypoglossal nerve trunk is vital to the success of this procedure.

Recurrent Laryngeal Nerve

Normal Course

The recurrent laryngeal nerve (RLN) and the superior laryngeal nerve (SLN) (discussed below) are branches of Cranial Nerve X, and innervate the larynx. The

recurrent laryngeal nerve supplies all intrinsic muscles of the larynx and carries sensory fibers from the subglottis and trachea [9].

The course of the RLN is determined by its associated arteries and differs depending on laterality. Bilateral recurrent laryngeal nerves arise from the vagus nerve in the superior thorax. The right RLN crosses under the right subclavian artery and ascends to the right tracheoesophageal groove. It may cross superficial or deep to the inferior thyroid artery (ITA). The left RLN hooks around the arch of the aorta and ascends vertically to the left tracheoesophageal groove. During neck dissection, the nerve can usually be found at most 1 cm lateral to or within the tracheoesophageal groove. At this level, the nerve is usually immediately anterior or posterior to the inferior thyroid artery (ITA).

The relationship between the RLN and inferior thyroid artery is particularly important for dissection. According to a review, there are three main relationships between the RLN and the ITA. These are: (1) RLN anterior to the ITA; (2) RLN posterior to the ITA; and (3) RLN between the branches of the ITA. There does not seem to be any defined “normal” variant within these options. For the sake of completeness, the ITA is a branch of the thyrocervical trunk, which ascends deep to the structures in the neck toward the inferior pole of the thyroid gland behind the common carotid artery. There are typically two branches, anterior and posterior, which bifurcate within the larynx [9].

Variations and Pathologies

One of the most important post thyroidectomy complications is recurrent laryngeal nerve injury. Symptoms from RLN injury vary widely from mild-to-severe voice change in unilateral lesions to vocal cord paralysis and airway obstruction in cases of bilateral injury. It may also change the patient’s ability to swallow which leads to aspiration. In contrast to these debilitating injuries, however, many patients with injuries may not have any symptoms. Up to one-third of patients with unilateral vocal cord paralysis are symptom-free. In symptomatic patients, partial lesions usually recover in the first few days after surgery. Beyond that time frame, two-thirds of “transient” palsies will recover within 1 month, and 89% within 1 year. Incidence of injury to RLN in thyroidectomies is up to 11%, and 35.7% of RLN injury are due to thyroidectomies, according to some studies. The three mechanisms of injury are stretch, transection, thermal injury, and ligature. To prevent this complication, the principle of routine identification of the RLN during thyroid surgery was presented in 1938. It is a well-established principle that identification of the RLN prevents most injuries [9].

The RLN is typically more oblique during its ascent from the neck base toward the larynx. When it is more medially placed alongside the trachea below the inferior pole of the thyroid, the RLN can be parallel to inferior thyroid vessels. Branches of the inferior thyroid artery are ligated, leaving the RLN susceptible to transection or stretch injury if it is nearby. Additionally, growth of the tubercle of Zuckerkandl, the pyramidal extension of the thyroid gland at the posterior side of each lobe, may push the RLN anteriorly and give it the appearance of a blood vessel entering the thyroid. Substernal extension of a goiter will also elevate the RLN and cause a

similar presentation. Inflammatory conditions, such as Grave's disease, may lead to adherence of the RLN to the thyroid, causing a difficult dissection [9].

The branching pattern of the RLN may also be aberrant. In some cases, the bifurcation of anterior and posterior branches will occur proximal to the larynx and even before crossing the ITA. Since these branches are thinner and more susceptible to injury, this will increase unwanted surgical outcomes. Identification of a nerve branch that only produces pharyngeal muscle contraction during intraoperative monitoring will alert the surgeon that this is the anterior branch of the RLN. This area proximal to the laryngeal entry point has the highest overall risk of injury [9].

A non-recurrent laryngeal nerve (NRLN) is a rare but dreaded abnormality with an incidence of 0.5–1%. It almost always occurs on the right along with an aberrant right subclavian artery and left-sided arch. A NRLN can branch from the cervical vagus anywhere from the inferior thyroid artery to the superior thyroid pole. There have been two general types described in the literature: Type 1 is a short superior course arising behind the superior pole, and type 2 arises caudally with the ITA (Fig. 5.1). Making this an even more complicated issue is the possibility of a concurrent RLN and NRLN on the same side. In this case, the RLN is usually much smaller than normal [9].

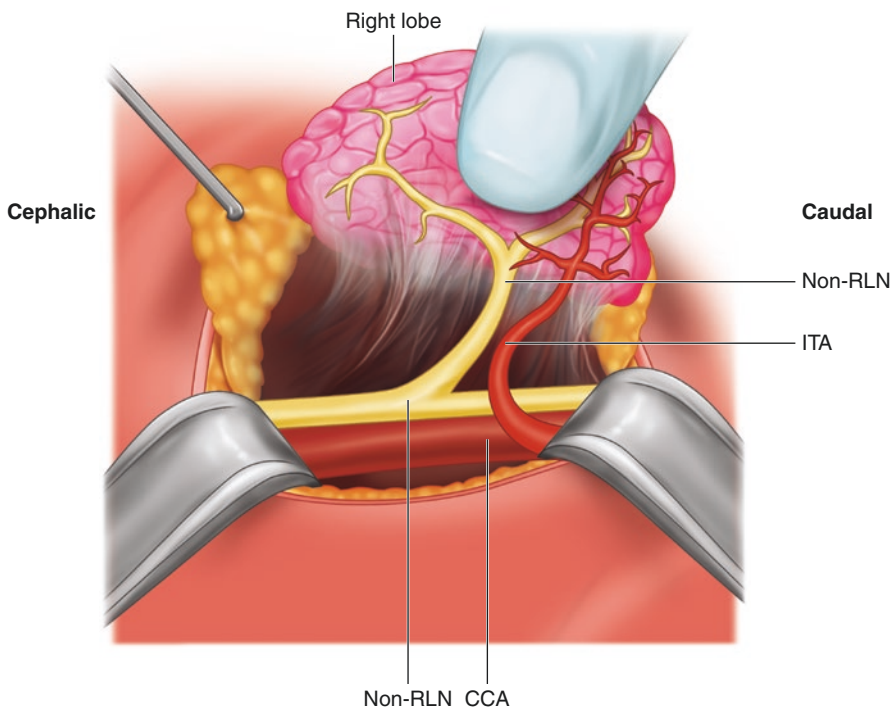


Fig. 5.1 Non-recurrent laryngeal nerve. Full exposure of the right non-RLN has a parallel course with the inferior thyroid artery (ITA) from the posterior to the common carotid artery (CCA) until laryngeal entry

Superior Laryngeal Nerve

Normal Anatomy

The superior laryngeal nerve (SLN) is described as the “neglected nerve in thyroid surgery” despite the fact that injury can cause significant morbidity. The SLN separates from the vagus just below the nodose ganglion, about 4 cm cranial to the carotid bifurcation, then bifurcates to internal and external branches at the level of the cricoid. The internal branch travels medial to the carotid and penetrates the larynx. The external branch travels down toward the superior pole of the thyroid and approaches the larynx within Joll’s triangle, which is bordered by the sternothyroid muscle superiorly, the cricothyroid muscle and inferior constrictor muscles medially, and the superior thyroid pole inferiorly. The internal branch is purely sensory, carrying afferent fibers from the supraglottic larynx and vocal folds. The external branch of the SLN innervates the cricothyroid muscle.

Usually, the external branch of the superior laryngeal nerve (EBSLN) passes above the superior pole of the thyroid, but in some cases, it has caudal extent, which is important in later descriptions of anatomic variations. There are multiple proposed classification systems. The most widely recognized is the Cerna classification based on the potential risk of injury. A Type 1 nerve crosses the superior thyroid vessels more than 1 cm above the upper edge of the thyroid superior pole. A Type 2A nerve crosses the vessels less than 1 cm above the upper edge of the superior pole. A Type 2B nerve crosses the superior thyroid pedicle below the upper border of the superior thyroid pole.

Variations and Pathologies

During thyroid surgery, the EBSLN is at risk due to its close relationship with the superior pole and thyroid vessels. Inadvertent electrothermal damage, ligation, or transection of the nerve is possible when dissecting the superior pole. Incidence of EBSLN injury varies widely, from 0 to 58%; however, this is likely due to imprecise and non-standardized diagnosis methods. Consequences of intraoperative injury to the EBSLN are described less frequently than injury to the RLN described above. It may lead to temporary or permanent voice change. Dysfunction of the cricothyroid muscle will manifest in changes to voice quality and projection. It will also cause hoarseness, breathy voice, the inability to make high-frequency tones, and an increased need for voice clearing. In contrast to the RLN, there is no risk of vocal cord paralysis, asphyxiation, or aspiration. The symptoms described here will likely affect singers and performers the most.

Again, in contrast to the RLN, surgeons typically do not go out of their way to identify the EBSLN. Some studies challenge this dogma and suggest routine neuro-monitoring of the EBSLN. In one study, the rate of symptomatic injury with monitoring was 8% versus 14% without monitoring [10]. Common variations are discussed under Section “[Normal Anatomy](#)” above. These are not inherently aberrant courses but have a great impact on the nerve’s vulnerability. The most prone to injury are Type 2A and Type 2B nerves as they cross near and below the upper border of the superior pole of the thyroid and can be damaged during manipulation.

Therefore, care should be taken when dissecting the superior pole and ligating individual branches of the superior thyroid vessels. Visual or nerve monitoring identification of the EBSLN has been suggested to avoid injury.

Facial Nerve

Normal Course

Cranial nerve VII, also known as the facial nerve, has multiple efferent and afferent functions. It is the motor nerve for muscles of facial expression (including orbicularis oculi/oris, zygomaticus major, levator/depressor anguli oris, risorius, mentalis, buccinator, frontalis, occipitalis, and platysma), as well as the lacrimal gland, oral and nasal mucosa, and submandibular and sublingual glands. The facial nerve also functions as a somatic afferent from the external auditory meatus, auricle, retroauricular area, as well as a special sensory afferent for taste from the anterior two-thirds of the tongue and the hard and soft palates.

The facial nerve is quite complex, as shown by the innervation pattern above, and its anatomic course is no exception. The facial nerve exits the stylomastoid foramen and gives off three branches to the posterior belly of the digastric muscle, the stylohyoid muscle, and the posterior auricular muscles. It then runs lateral to the styloid process, ECA, and posterior facial vein, and anterior to the posterior digastric. It is about 3 mm in diameter during the course described above. The nerve then turns anteriorly about 2 cm before bifurcating to upper (temporofacial) and lower (cervicofacial) divisions in the “pes Ansari” or “goose foot.” Between these two divisions, five branches are given off. Three of these branch from the temporofacial division: temporal, zygomatic, and buccal. The other two branch from the cervicofacial division: marginal mandibular and cervical [11]. There are extensive connections between these branches and consequently many variations in their branching patterns. In practice, it has been noted that there is no distinct separation between the zygomatic and buccal branches in location or the muscles they innervate, so it is therefore sometimes referred to as the zygomaticobuccal branch [12]. Both divisions run within the parotid gland and usually pass over the external jugular vein. The temporofacial division lies between the superficial and deep lobes of the parotid gland above the isthmus. It is imperative to find the main trunk of the facial nerve to avoid injury that leads to ipsilateral loss of facial muscle control. Reliable anatomic landmarks are the tympanomastoid suture, the posterior belly of the digastric, and the styloid process. Some sources recommend the tympanomastoid suture as the most consistent since it is relatively easy to find, has a constant position 2–4 mm deep to the medial end, and leads directly to stylomastoid foramen [11].

Variations and Pathology

Facial nerve injury is a severe complication of parotid surgery because it results in both cosmetic and functional deficits. The incidence of transient facial nerve deficit following parotid surgery is reported between 9.3 and 64.6%. Although there are not many reviews or articles regarding anomalies of facial nerve anatomy, there are

a few that are of interest. In one case report of a large parotid mass abutting the branches of the facial nerve, a pes anserinus was not found. In its place was a single facial nerve trunk [13]. In this case, it did not result in injury, but as mentioned above regarding other cases of anatomic abnormalities, inaccurate identification of structures in head and neck surgery may lead to injury.

In another case report, an 88-year-old female cadaver showed six branches emerging from the facial nerve trunk. Again, this is important in parotid surgery as the supernumerary nerve may be confused for a different structure if a surgeon only anticipates the usual five branches.

Vagus Nerve

Normal Course

The vagus nerve, named with the same Latin root as *vagabond*, is ubiquitous in the body and provides special visceral efferent, general visceral efferent, general sensory efferent, visceral afferent, and special afferent signals. From the brainstem, the vagus nerve leaves the medulla as 8–10 rootlets that exit through the jugular foramen with CN XI (accessory nerve). The jugular ganglion lies with the foramen, where it is joined by the accessory nerve. Traversing through the jugular fossa, the vagus divides at the jugular foramen into the meningeal branch and auricular branch or Arnold's nerve. After exiting the jugular foramen branches from proximal to distal are the pharyngeal nerves, superior laryngeal nerve, and recurrent laryngeal nerves. These were discussed earlier and will not be mentioned in detail in this section. Additionally, the superior cardiac branches arise from the vagus in the neck and follow the internal carotid artery to the aorta to supply the cardiac plexus along with postganglionic sympathetic fibers from the upper four to five segments of the thoracic spinal cord. For anatomic reference, the vagus then enters the thorax to provide inferior cardiac, anterior and posterior bronchial, and esophageal branches [2].

Variations and Pathology

Iatrogenic injury of the vagus nerve typically occurs after thyroid, parathyroid, or cervical disc surgery. Postradiation injury may damage the vagus nerve as well, but this is rare. Another surgery that particularly involves the vagus nerve is, as its name suggests, vagus nerve stimulation. Vagus nerve stimulation, or VNS, is a new treatment for treatment-resistant epilepsy (TRE), which occurs in 20–30% of patients with epilepsy. VNS was approved in 1997 by the FDA for the treatment of intractable partial epilepsy in adults and children over the age of 12. The surgery is performed with the patient supine, neck slightly extended. After incision, the cervical fascia is opened to expose the left vagus nerve in between the common carotid artery and internal jugular vein. The electrode is then wrapped around the vagus nerve in this position under microscope visualization. In a study from 2015, 59 patients underwent VNS device placement in the same institution. The mean reduction of seizure frequency was 31%. VNS therapy was tolerated by most patients, and side effects were mild and caused no permanent injury [14].

In a study of all complications from VNS procedures, multiple causations were found including injury by traction, interruption of blood supply, clamping, or heating. This leads to vocal cord paralysis, which, as in cases of RLN injury in thyroid surgery, is usually transient. Vocal cord paralysis is an expected consequence of injury to the vagus nerve at this position because the RLN branches just distally at the left carotid artery takeoff from the aortic arch. In a longitudinal study of 143 patients between 1994 and 2010, 5.6% experienced vocal cord palsy, which persisted in at least 0.7% for more than 1 year. This was identified as a complication of stimulator insertion as well as lead removal secondary to fibrosis [15].

Although anatomic variations of the vagus nerve are rarely described, there have been some examples in the literature. One paper investigated cervical vagus nerve branching in 35 cadavers. In 29% of cases, abnormal cervical vagus nerve branching was identified, with right-sided branching being more common than left-sided branching. As mentioned above, VNS is used for epilepsy, in which case electrodes are usually placed on the left side. It is also used for cardiac dysfunction, in which case electrodes are placed on the right side. The trouble in these cases becomes improper placement of the electrode, at a site other than the main trunk, which may explain side effects of vocal cord palsy described above. The branches of the vagus extended to the inferior larynx, which also explains the origin of vocal cord dysfunction [16]. This article also referenced a study by Seki et al., showing that the vagus nerve contains a small amount of sympathetic fibers, which may lead to Horner's syndrome in response to VNS therapy. The amount of the sympathetic component of the vagus nerve is variable between cases, but according to this study of 31 cadavers, it is always present. Sympathetic innervation was identified by tyrosine hydroxylase staining [17].

Phrenic Nerve

Normal Anatomy

The phrenic nerve provides motor supply to the ipsilateral hemidiaphragm. Part of the cervical plexus, it receives innervation mostly from C4, but also C3 and C5. It is formed at the upper part of the lateral border of the scalenus anterior and descends almost vertically across its anterior surface. It is posterior to the sternocleidomastoid, internal jugular vein, and, on the left, the thoracic duct. At the root of the neck, it runs posterior to the suprascapular and transverse cervical arteries and anterior to the subclavian artery. It enters the thorax by crossing medially in front of the internal thoracic artery [18].

An accessory phrenic nerve also exists, composed of fibers from C5, and serves as a branch to the subclavius muscle. It is lateral to the phrenic nerve and descends posterior to the subclavian vein. It usually joins the phrenic nerve at the first rib but may not do so until the pulmonary hilum or beyond. The accessory phrenic nerve may also arise from C4, C6, or the ansa cervicalis [18].

Variations and Anomalies

While anatomic variations to the phrenic nerve are quite rare, there are some notable complications that arise and therefore should be discussed. A supraclavicular brachial plexus block is used to anesthetize the ipsilateral arm at times when sedation and paralysis are not possible. It fell out of favor due to the incidence of complications including hemi diaphragm paralysis, RLN block, Horner's syndrome, and pneumothorax [19]. In modern times, the use of ultrasound has made the supraclavicular block accepted practice again. The brachial plexus is located posterior to the anterior scalene muscle and lateral to the subclavian artery. In one study evaluating variations of the brachial plexus, 20% of phrenic nerves and about the same percentage of accessory phrenic nerves originated entirely from the brachial plexus [20]. This may account for the partial hemi diaphragm paralysis seen with supraclavicular blocks. An interscalene block, another technique targeting the upper arm, will often paralyze the phrenic nerve, as this is a more proximal block with close proximity to the cervical plexus. However, in the case of a supraclavicular block, the cervical plexus is unrelated.

In the case of subclavian vein catheterization, a rare but significant complication is injury to the phrenic nerve. This is due to an anomaly where the phrenic nerve passes anterior to the subclavian vein. In one study, this was observed in 2.38% of patients and was always in close proximity to the jugulo-subclavian junction. If penetration is too lateral, damage to the nerve may be done during venipuncture. Therefore, the authors of this article recommend catheter insertion more laterally to avoid this complication. Briefly mentioned was also the extremely rare presence of the phrenic nerve penetrating through the subclavian vein dividing it into two channels seen in 1/900 cadavers [21]. This would obviously have a much higher risk of injury.

Lymphatics

Thoracic Duct

Normal Anatomy

The thoracic duct is a lymphatic structure approximately 2–5 mm diameter and 45 cm long which transports 1–2 L of lymph per day from the lower extremities and abdomen. The thoracic duct carries lymph from the cisterna chyli, where the lower extremity and abdominal lymphatic channels meet, through the aortic hiatus. It crosses anteriorly to the aortic arch and runs posterior to the left subclavian artery, traveling from right to left at the level of the fifth or sixth thoracic vertebra. Finally, it enters the thorax and empties into the juncture of the left subclavian and internal jugular veins [22]. Visual representation of normal anatomy can be seen in Fig. 5.2.

Variations and Anomalies

There are multiple described variations of the thoracic duct as show in Fig. 5.3. The channel can open to the left or right subclavian, or the azygos vein which runs

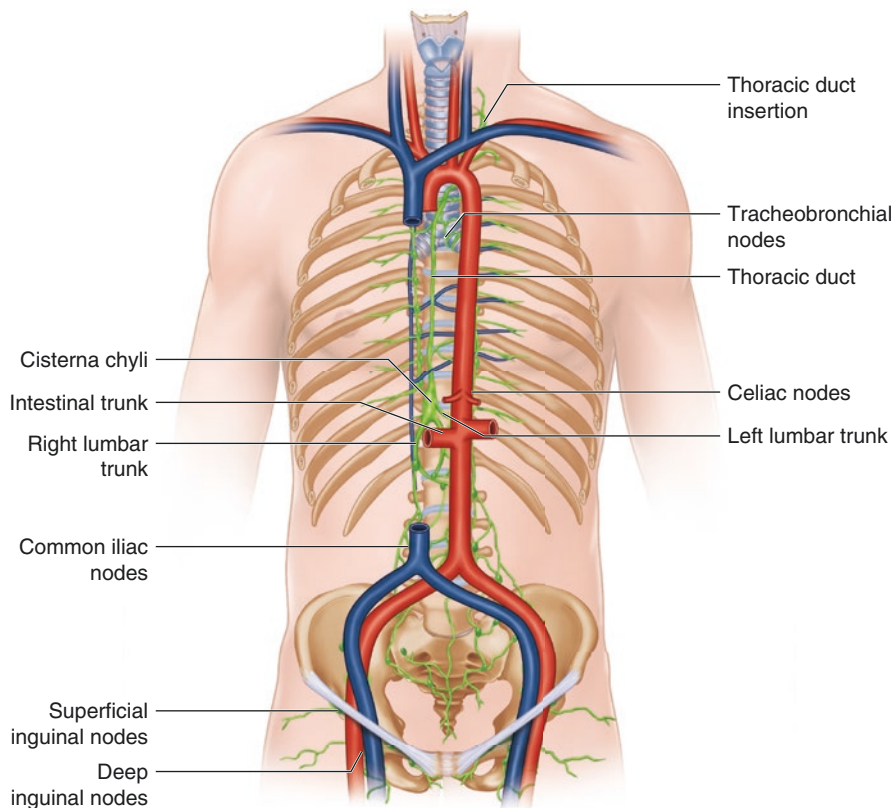


Fig. 5.2 Lymph vessels and nodes of the pelvis, abdomen, and thorax

parallel. It may also be completely or partially duplicated [22]. In a meta-analysis of thoracic duct variations, the most common site of termination was at the IJV (46%), followed by the jugulo-subclavian angle (32%) and the subclavian vein (18%). Fewer than 5% have other termination sites, including the external jugular vein, vertebral vein, brachiocephalic vein, transverse cervical vein, and suprascapular vein. Ostia to the IJV and subclavian vein are usually within 2 cm of the jugulo-subclavian angle. Interestingly, 16–28% of each morphology had multiple entry points, the most common location of multiple channels being T4 (28%) with T3 and T5 close behind. Multiple points of entry may be explained by the formation of two large vessels anterior to the aorta at the seventh and eighth gestational weeks. The two channels then fuse to form the classic formation of the thoracic duct. No matter the entrance of the duct into the venous system, it almost always enters obliquely, initially ascending toward the left and forward before descending back toward the right. In a rare number of cases (6%), the thoracic duct does not cross midline, which is of utmost importance in understanding the anatomic variations critical during surgery [23].

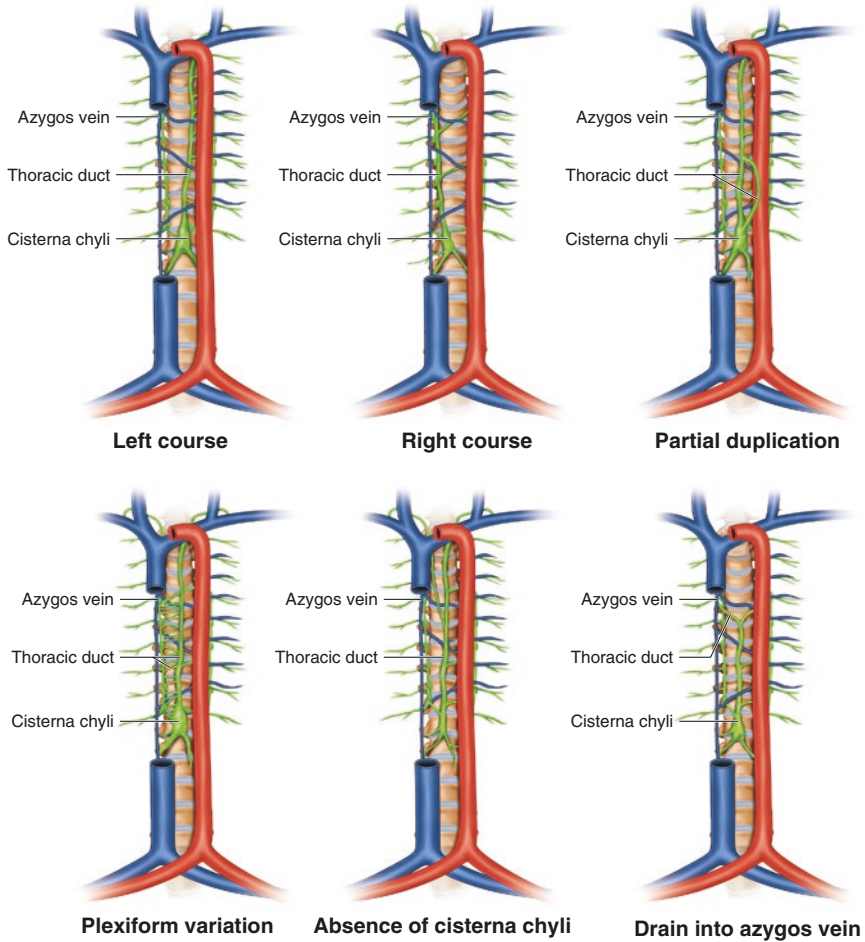


Fig. 5.3 Common variations of the thoracic duct

Multidetector row computed tomography (MDCT) with multiplanar reformation images of 1 mm slice thickness shows “complete” visualization as read by experienced radiologists only 14% of the time. Lower sections had much higher visualization rates at 72%, likely due to increased caliber of the vessel [24]. High-resolution ultrasound with linear probes has a high success rate with 96% visualization of the cervical thoracic duct. This technique, however, is operator-dependent and therefore unreliable [25].

Multiple surgical procedures risk damage to the thoracic duct. Chylothorax due to this complication occurs after various surgeries such as esophagectomy, pneumonectomy, and spine surgery. Prevalence ranges from 0.5 to 2% [24]. Particularly in esophagectomies, chyle leak is a deadly complication, showing up to 50% mortality rate. In a study of 536 patients undergoing esophagectomy for malignant disease

with transthoracic or hiatal approach, 3.7% experienced a chyle leak. The incidence was 7% after transthoracic and 2% after transhiatal approaches [26]. On occasion, surgeons may opt to prophylactically ligate the thoracic duct to prevent this. In the case of thoracic duct laceration and its subsequent management, proper anatomic identification and visualization of both thoracic ducts, if a duplication exists, is paramount to a successful operation.

Soft Tissue

Sternocleidomastoid Muscle

Normal Anatomy

The sternocleidomastoid muscle (SCM), named for its origins and insertions, is the second most superficial muscle of the lateral neck after the platysma. It originates from the manubrium sternum and clavicle, extending posterior and laterally to insert on the ipsilateral mastoid process and lateral portion of the occipital ridge. The clavicular head arises from the anterior superior surfaces of the medial third of the clavicle and is directed vertically upward. The medial head arises from the anterior surface of the manubrium and is directed superolaterally and posteriorly. The muscle functions to flex and turn the neck to the ipsilateral side and elevate the chin. It is an important surface landmark for neck dissection and other procedures, dividing the neck into anterior and posterior triangles. It also allows identification of the spinal accessory nerve at its most exposed location in the posterior triangle [27].

Variations and Pathology

Known as a “classic mammalian feature,” the sternocleidomastoid is considered a symbol of human beauty. It is also referred to as the Pandora’s box of the neck because it provides protection against injury to many vital structures underneath it, such as the accessory nerve, carotid artery, brachial plexus, cervical plexus, and internal jugular vein. Most of its variations are at its origin, especially the clavicular head. Occasionally, there is a more defined separation of the cleidomastoid and sternomastoid bellies, sub-dividing the anterior triangle. This extra triangle may also result in an extra supraclavicular fossa. Some studies have noted an extra belly, which is separate from the SCM, that courses from the clavicle to the occipital ridge. Another more distal variation is fusion of the SCM with the trapezius. This is in line with the theory that two muscles with the same innervation, in this case the accessory nerve, originate from the same muscle mass in development. A clinically relevant variation is extra sternal and clavicular heads which may cause stenosis of the lesser supraclavicular fossa, which aids in proper “blind” central venous access from the anterior approach and changes the clinical approach to a clavicle fracture [28, 29]. Supernumerary heads may also limit access and dissection of level IV and V cervical lymph nodes [29]. All of the variations above may affect the surgeon’s ability to properly identify landmarks in neck dissection, sternocleidomastoid flaps, and other procedures.

Benign fibrosis, hypoplasia, or aplasia of the SCM is the most common cause of congenital torticollis. Abnormal head positioning in utero or a difficult birth can lead to development of the compartment syndrome and the sequelae of torticollis [28]. There have also been a few cases of a unilaterally absent SCM which sometimes leads to herniation of the lung into the neck [30].

Digastric Muscle

Normal Course

The digastric muscle is a suprahyoid muscle that has two bellies, anterior and posterior, joined by an intermediate tendon. It is situated in the anterior region of the neck and divides the region between the hyoid and mandible into the lateral submandibular and medial submental triangle. The anterior belly inserts into the digastric fossa in the lower interior of the mandible. The intermediate tendon attaches to the body of the hyoid. The posterior belly originates on the medial side of the mastoid process in the mastoid notch. Together, the two bellies and adjoining tendon function to anchor the hyoid bone against traction of the infrahyoid muscles. When the hyoid is fixed, the digastric muscles open the mouth by lowering the mandible. In contrast, when the mandible is fixed, it raises the hyoid bone [31].

Many important structures lie in the triangles created by the digastric muscle. The submandibular triangle contains the submandibular gland, submandibular lymph nodes, hypoglossal nerve, facial vein, as well as nerves and veins supplying the mylohyoid muscle and the carotid sheath. The submental triangle contains submental lymph nodes and the anterior jugular vein. The carotid triangle contains the carotid sheath and tributaries of the internal jugular vein [31].

Variations and Pathology

Most of the described variations of the digastric muscle are of the anterior belly. Reported incidence varies widely, from 2.7 to 69.9% [32]. Most descriptions of anomalies of the digastric muscle are in the form of case reports. For example, a man presented with a painless mass in his submental region. A CT scan showed a mass in the submandibular fossa with a possible lymph node, hematoma, or tumor included in the differential. After ultrasound and CT with contrast, it was discovered the mass had the same density as the nearby digastric muscle [33]. Another study showed six variations of the anterior belly. All were accessory muscles or slips. Unilateral anomalies were equal in prevalence to bilateral in this paper; overall, however, there are mixed reviews. In addition, oblique connections between accessory bellies were more common than parallel. Again, the evidence is mixed overall [34].

Variants of the anterior belly of the digastric may cause confusion during procedures such as submental lipectomy, rhytidectomy, surgical alteration of the cervicomentale angle via partial resection of the anterior belly, muscle transfer for reanimation of the mouth, and submental artery flap procedures [32]. This structure is also a landmark for the lingual nerve and submandibular salivary duct [32].

Thyroglossal Duct

Variations and Pathology

The thyroglossal duct is an embryologic structure that is obliterated before maturation of the fetus. At the fourth week of gestation, the thyroid diverticulum forms at the foramen cecum, which will later become the base of the tongue. It then descends, forming the thyroglossal duct, and as the thyroid reaches its permanent location in the neck, the duct becomes a tract that is obliterated. Pathologic remnants may persist anywhere along the tract from the base of the tongue to the thyroid, but occur most commonly midline at the hyoid bone [35]. Twenty-five percent of patients have a supra-hyoid lesion [36]. Persistence of the thyroglossal tract has been detected in 7% of adults and is the most common developmental neck cyst, accounting for 70% of cases [36]. There is a wide age range of diagnosis, and the lesion is common anywhere between birth and 30 years old. There is no discrepancy in gender. Some ducts contain thyroid tissue, which must be identified prior to excision. In children, a thyroid scan, thyroid function tests, or ultrasound may be used for diagnosis. In adults, palpation of the normal thyroid tissue in its anatomic position is adequate, although some surgeons prefer confirmation with the tests mentioned above or CT scan [37]. Presentation is most commonly a 1–3 cm painless well-defined solitary mass in the midline which may fluctuate in size. Figure 5.4 shows an abnormally large thyroglossal duct cyst seen in a 75-year-old patient. It is characterized by change of location when the patient swallows. Patients may complain of pain, drainage secondary to infection, or dysphagia [36]. Differential diagnosis includes branchial cleft cysts, dermoid and epidermoid cysts, thymic cysts, ectopic salivary gland, various thyroid nodules, teratomas, choristomas, cervical bronchogenic cysts, laryngeal squamous cell carcinoma, and ectopic thyroid gland [36].

Treatment of a thyroglossal duct cyst is the Sistrunk procedure, first performed by Walter Ellis Sistrunk in the 1920s, that involves resection of the cyst, tract, midline portion of the hyoid bone, and cuff of the surrounding base of the musculature of the tongue [38]. Surgical excision is the mainstay of treatment for thyroglossal duct cysts due to a high rate of infection, cosmetic deformities, and propensity for malignancy, which is relatively low, but not insignificant, at 1–2% [35, 36]. Eighty percent of malignant transformations are in the form of papillary thyroid cancer [36]. Sudden infant death for lesions at the base of the tongue, which is a rare location to begin with, is a rare occurrence, but is possible [36]. Infected cysts must be treated with a course of antibiotics prior to excision. Surgical excision is commonly curative, and recurrence is uncommon. Incomplete resection secondary to challenging anatomy and other unforeseen intraoperative complications will have a higher recurrence rate [35].

Branchial Complex

Variations and Pathology

Abnormalities of branchial clefts are all fetal remnants. Before describing these, general definitions of these pathologies are helpful. The first general category is a

Fig. 5.4 Clinical picture showing a 6 × 5 cm lobulated mass in the anterior aspect of the neck. From: Sudharsanan S, Vijayakumar C, Dharanya S, Elamurugan TP, Manwar AS. A Rare Case of Carcinoma in the Thyroglossal Duct Cyst of an Elderly Patient. *Cureus*. 2017;9(6):e1365. (Creative Commons CC-BY license at <https://doi.org/10.7759/2Fcureus.1365>)



cyst which is defined as an epithelial-lined structure without an internal opening. It is the most common, accounting for 75% of branchial cleft abnormalities. Next, a sinus is defined as a blind track with an external opening through the skin on the side of the neck or internally into the foregut. Fistula is also possible, defined as a tract communicating with the skin externally or foregut internally [39].

The second branchial cleft develops into the sinus of His, the arch develops into muscles of facial expression, the malleus and incus, and the hyoid bone, and the pouch develops into the palatine tonsils and supratonsillar fossa. A second branchial cleft cyst is the most common of branchial abnormalities, accounting for at least 75% of all abnormalities. It is typically detected between 10 and 40 years old. Signs and symptoms are usually painless, fluctuant masses in the lateral portion of the neck adjacent to the anteromedial border of the sternocleidomastoid muscle at the mandibular angle (Fig. 5.5). They tend to enlarge slowly over time and are painful and tender if infected, which makes them highly possible in the differential of a young patient with recurrent inflammation at the mandibular angle. Abnormalities of the second branchial cleft require surgical excision because of the risk of infection [39].

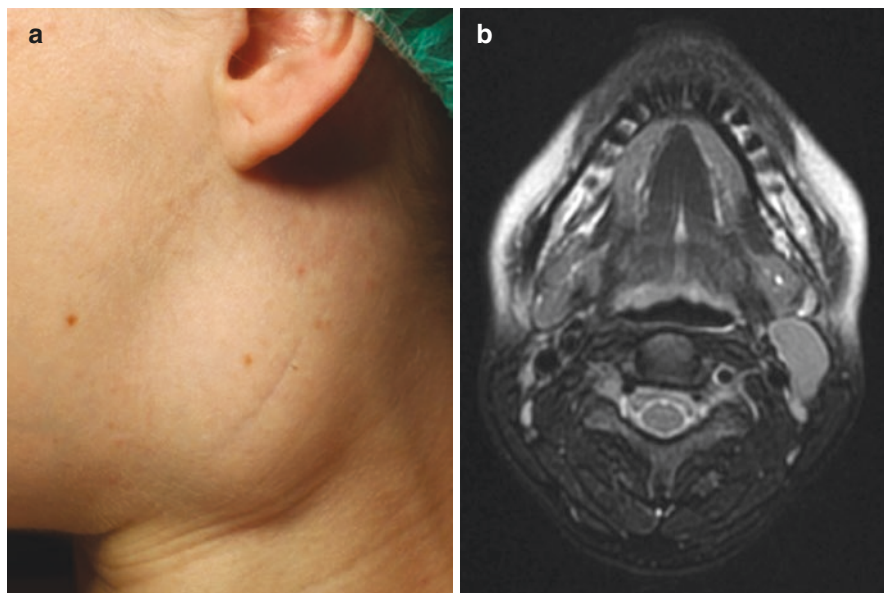


Fig. 5.5 Clinical picture of a pregnant patient with a branchial cleft cyst on the left side of the neck (a) and the corresponding MRI showing the cystic mass in the vessel/nerve sheath (b) by Raguse JD, Anagnostopoulos I, Doll C, Heiland M, Jöhrens K. Possible Estrogen Dependency in the Pathogenesis of Branchial Cleft Cysts. *Biomed Res Int.* 2017;1,807,056. (Creative Commons CC-BY license at <https://doi.org/10.1155%2F2017%2F1807056>)

The first branchial cleft develops into the external auditory canal, the arch develops into the mandible and muscles of mastication, and pouch develops into the Eustachian tubes. Cysts of the first branchial cleft account for 5–8% of all defects and are most commonly seen in middle-aged women. They usually present as recurrent infections around the ear or angle of the mandible associated with refractory parotid abscesses. In addition, they may drain into the external auditory canal causing otitis, cervical skin tags at birth, or auricular swelling. They may also be associated with facial nerve palsy. Fistulas and sinuses of the second branchial cleft are commonly unilateral and present at birth, evidenced by a small opening to the skin. They may go unnoticed for years if there is no drainage. They may also cause recurrent infections of the upper respiratory tract. Probing may produce irritation of the vagus nerve. First branchial cleft cysts require complete surgical excision, which is the only curative therapy [39].

The third branchial cleft develops into the sinus of His, the arch develops into the hyoid bone and stylopharyngeus muscle, and the pouch develops into the inferior thyroid glands and the thymus. Third branchial cleft cysts are extremely rare abnormalities, usually located in the posterior cervical space posterior to the sternocleidomastoid muscle. These are the most congenital lesions of the posterior cervical space following cystic hygromas. They manifest as a painless, fluctuant mass of the posterior triangle. Abnormalities of the third branchial cleft require surgical excision because of the risk of infection [39].

References

1. Prendergast PM. Anatomy of the face and neck. In: Shiffman MA, Di Giuseppe A, editors. *Cosmetic surgery: art and techniques*. Berlin: Springer; 2013. p. 29–45.
2. Binder DK, Sonne DC, Fischbein NJ. *Cranial nerves: anatomy, pathology, imaging*. New York: Thieme Publishing; 2010.
3. Lo A, Oehley M, Bartlett A, Adams D, Blyth P, Al-Ali S. Anatomical variations of the common carotid artery bifurcation. *ANZ J Surg*. 2006;76(11):970–2.
4. Kim T, Chung S, Lanzino G. Carotid artery-hypoglossal nerve relationships in the neck: an anatomical work. *Neurol Res*. 2009;31(9):895–9.
5. Fokkema M, De Borst GJ, Nolan BW, Indes J, Buck DB, Lo RC, et al. Clinical relevance of cranial nerve injury following carotid endarterectomy. *Eur J Vasc Endovasc Surg*. 2014;47:2–7.
6. Brennan PA, Alam P, Ammar M, Tsiroyannis C, Zagkou E, Standring S. Sternocleidomastoid innervation from an aberrant nerve arising from the hypoglossal nerve: a prospective study of 160 neck dissections. *Surg Radiol Anat*. 2017;39(2):205–9.
7. Tomita K, Nishibayashi A, Yano K, Hosokawa K. Differential reanimation of the upper and lower face using 2 interpositional nerve grafts in total facial nerve reconstruction. *Plast Reconstr Surg Glob Open*. 2015;3(10):e544.
8. Islam S, Walton GM, Howe D. Aberrant anatomy of the hypoglossal nerve. *J Laryngol Otol*. 2012;126(5):538–40.
9. Randolph GW. *The recurrent and superior laryngeal nerves*. Cham: Springer International Publishing; 2016.
10. Hurtado-Lopez LM, Pacheco-Alvarez MI, Montes-Castillo Mde L, Zaldivar-Ramirez FR. Importance of the intraoperative identification of the external branch of the superior laryngeal nerve during thyroidectomy: electromyographic evaluation. *Thyroid*. 2005;15(5):449–54.
11. Bagheri SC, Bell RB, Khan HA. *Current therapy in Oral and maxillofacial surgery*. Elsevier Saunders: *Curr Ther Oral Maxillofac Surg*; 2012.
12. Neligan PC. *Plastic surgery*. 2nd ed. New York: Elsevier Saunders; 2006.
13. Wong AS, Teh BM, Safdar A. The absent facial nerve pes anserinus: implications for parotid surgery. *ANZ J Surg*. 2016;86(12):1067–8.
14. Galbarriatu L, Pomposo I, Aurrecochea J, Marinas A, Agúndez M, Gómez JC, et al. Vagus nerve stimulation therapy for treatment-resistant epilepsy: a 15-year experience at a single institution. *Clin Neurol Neurosurg*. 2015;137:89–93.
15. Kahlow H, Olivecrona M. Complications of vagal nerve stimulation for drug-resistant epilepsy: a single center longitudinal study of 143 patients. *Seizure*. 2013;22(10):827–33.
16. Hammer N, Glätzner J, Feja C, Kühne C, Meixensberger J, Planitzer U, et al. Human vagus nerve branching in the cervical region. *PLoS One*. 2015;10(2):e0118006.
17. Seki A, Green HR, Lee TD, Hong L, Tan J, Vinters HV, et al. Sympathetic nerve fibers in human cervical and thoracic vagus nerves. *Heart Rhythm*. 2014;11(8):1411–7.
18. Standring S. *Neck: Phrenic nerve*. In: *Gray's Anatomy*. 41st ed: Elsevier; 2016. <https://doi.org/10.1308/003588406X116873>.
19. Bigeleisen PE. Anatomical variations of the phrenic nerve and its clinical implication for supraclavicular block. *Br J Anaesth*. 2003;91(6):916–7.
20. Sassoli Fazan VP, de Souza AA, Caleffi AL, Rodrigues Filho OA. Brachial plexus variations in its formation and main branches. *Acta Cir Bras*. 2003;18(suppl5)
21. Paraskevas GK, Raikos A, Chouliaras K, Papaziogas B. Variable anatomical relationship of phrenic nerve and subclavian vein: clinical implication for subclavian vein catheterization. *Br J Anaesth*. 2011;106(3):348–51.
22. Toliyat M, Singh K, Sibley RC, Chamarthy M, Kalva SP, Pillai AK. Interventional radiology in the management of thoracic duct injuries: anatomy, techniques and results. *Clin Imaging*. 2017;42:183–92.
23. Phang KL, Bowman M, Phillips A, Windsor J. Review of thoracic duct anatomical variations and clinical implications. *Clin Anat*. 2014;27(4):637–44.

24. Kiyonaga M, Mori H, Matsumoto S, Yamada Y, Sai M, Okada F. Thoracic duct and cisterna chyli: evaluation with multidetector row CT. *Br J Radiol.* 2012;85(1016):1052–8.
25. Seeger M, Bewig B, Günther R, Schafmayer C, Vollnberg B, Rubin D, et al. Terminal part of thoracic duct: high-resolution US imaging. *Radiology.* 2009;252(3):897–904.
26. Lagarde SM, Omloo JM, De Jong K, Busch OR, Obertop H, Van Lanschot JJ. Incidence and management of chyle leakage after esophagectomy. *Ann Thorac Surg.* 2005;80(2):449–54.
27. Robinson JK, Hanke CW, Sengelmann RD, Siegel DM. *Surgery of the skin*: Elsevier Mosby; 2005.
28. Hasan T. Variations of the sternocleidomastoid muscle: a literature review. *Internet J Hum Anat.* 2010;2(1):1–6.
29. Ferreira AH. Muscular variation in the neck region with narrowing of the minor and major supraclavicular Fossa. *Int Arch Med.* 2017;10(208) <https://doi.org/10.3823/2478>. Accessed 15 Mar 2019.
30. Bayne SR, Lehman JA, Crow JP. Lung herniation into the neck associated with congenital absence of the sternocleidomastoid muscle. *J Pediatr Surg.* 1997;32(12):1754–6.
31. De-Ary-Pires B, Ary-Pires R, Pires-Neto MA. The human digastric muscle: patterns and variations with clinical and surgical correlations. *Ann Anat.* 2003;185(5):471–9.
32. Zdilla MJ, Soloninka HJ, Lambert HW. Unilateral duplication of the anterior digastric muscle belly: a case report with implications for surgeries of the submental region. *J Surg Case Rep.* 2014;2014(12):rju131.
33. Bonala N, Kishan T, Pavani B, Murthy P. Accessory belly of digastric muscle presenting as a submandibular space mass. *Med J Armed Forces India.* 2015;71:S506–8.
34. Mangalagiri AS, Razvi MR. Variations in the anterior belly of Diagastric. *Int J Health Sci (Qassim).* 2009;3(2):257–62.
35. Agnoni AA. Thyroglossal duct cyst. In: Coppola CP, Kennedy Jr AP, Scorpio RJ, editors. *Pediatric surgery diagnosis and treatment*. Cham, Switzerland: Springer International Publishing; 2014. p. 237–9.
36. Volvavsek M. Thyroglossal duct cyst. In: *Head and Neck Pathol*; 2016. p. 487–92.
37. Cohen JI. Thyroglossal duct excision (Sistrunk Procedure). In: Cohen JI, Clayman GL, editors. *Atlas of head and neck surgery*: Elsevier Saunders; 2011. p. 121–7.
38. Simon LM, Magit AE. Impact of incision and drainage of infected thyroglossal duct cyst on recurrence after Sistrunk procedure. *Arch Otolaryngol Head Neck Surg.* 2012;138(1):20–4.
39. Chen H. Branchial cleft anomalies. In: Chen H, editor. *Atlas of genetic diagnosis and counseling*. 3rd ed. New York: Springer; 2017. p. 323–7.



Common Congenital Syndromes and Disease States Impacting Regional Anesthesiology Techniques

6

Donna-Ann Thomas, Omotoke Missih, Richard Zhu, Thomas Suchy, and Nalini Vadivelu

Turner Syndrome

Turner Syndrome results from the absence of a sex chromosome, resulting in a female with the 45XO karyotype and major anatomic and physiological changes. Anatomically from head to toe, features may include a short and wide neck which may be webbed, hearing changes, limited neck mobility, high-arched palate, mandibular and maxillary hypoplasia, coarctation of the aorta, bicuspid aortic valve, a smaller than normal trachea, hypothyroidism, and gonadal dysgenesis. Patients have short stature and a higher rate of scoliosis. Physiologically, patients are at higher risk of cognitive impairment. Cardiac anatomic differences result in a higher risk of aortic dissection and intraoperative hypertension. Hypothyroidism often results in delayed gastric emptying and subsequent increased risk of aspiration. There is a higher risk of type 2 diabetes and insulin resistance, as well as liver dysfunction. Kidney abnormalities such as horseshoe kidney may be present; however,

D.-A. Thomas (✉)

Department of Anesthesiology, Division of Pain Medicine, Yale School of Medicine, New Haven, CT, USA

e-mail: donna-ann.thomas@yale.edu

O. Missih

Department of Anesthesiology, Susquehanna Anesthesia Affiliates, Johnson City, NY, USA

R. Zhu

Department of Anesthesiology, Yale New Haven Health, Greenwich Hospital Center for Pain Management, Greenwich, CT, USA

e-mail: richard.zhu@yale.edu

T. Suchy

Department of Anesthesiology, Yale New Haven Hospital, New Haven, CT, USA

e-mail: thomas.suchy@yale.edu

N. Vadivelu

Department of Anesthesiology, Yale University, New Haven, CT, USA

they rarely affect kidney function. There are no contraindications to anesthesia in patients with Turner Syndrome, but the phenotypic changes do demand attention to management (Fig. 6.1).

For regional anesthesia, the main considerations relate to scoliosis, which might pose a challenge to epidural or intrathecal anesthesia (Fig. 6.2). In some cases, the scoliosis has been advanced enough to result in hemivertebrae. Prior radiographic imaging of the back or point-of-care ultrasound, if available, would help to assess the feasibility of neuraxial anesthesia. Due to the shorter stature of Turner syndrome patients, any neuraxial anesthesia will have to be dosed carefully as well. Additionally, depending on the patient's degree of liver dysfunction, coagulopathy and impaired metabolism of amide local anesthetics may be present. Checking an International Normalised Ratio (INR) may be helpful when planning any kind of neuraxial or regional anesthetic.

While not the focus of the chapter, there are also significant considerations for general anesthesia. Briefly, anatomic abnormalities of the head and neck may make securing the airway and tracheal intubation a challenge. Coarctation may result in a higher incidence of intraoperative hypertension; a preoperative echocardiogram

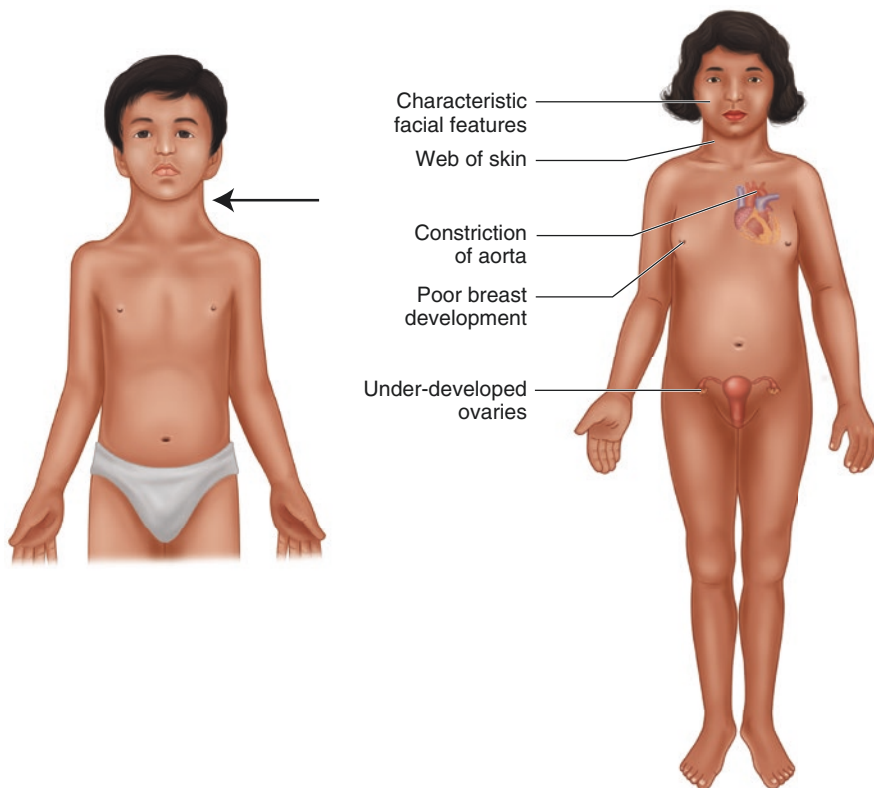
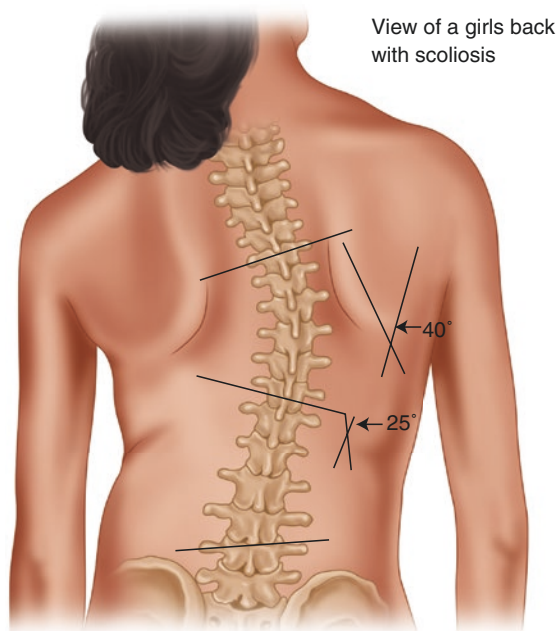


Fig. 6.1 Turner syndrome

Fig. 6.2 Scoliosis

may be helpful to assess the degree of anatomic variation. Patients with decreased gastric emptying may benefit from premedication to prevent aspiration complications, such as an H2 blocker. As with regional anesthesia, dosing of drugs that are metabolized by the liver or excreted by the kidney should be adjusted accordingly [1].

Noonan Syndrome

Noonan Syndrome is an autosomal-dominant disorder found in both sexes, although it is more common in males. It has been called the male version of Turner Syndrome in the past due to some similarities to the Turner phenotype. The incidence is 1 in 1000 to 1 in 2500 live births. The main phenotypic features include musculoskeletal abnormalities such as short stature, a short and webbed neck, widely spaced nipples, pectus deformities (carinatum in the superior chest and excavatum in the inferior chest), and scoliosis in 10–15% of patients. Important systemic manifestations that may impact anesthetic practice are present in the cardiovascular system, central nervous system, and hematologic systems.

Over 80% of Noonan syndrome patients are estimated to have cardiac defect, the most common type being pulmonary stenosis. Hypertrophic cardiomyopathy is also present in about 20% of patients. These conditions pose concerns for management during general anesthesia, and have an impact on the ability to perform neuraxial anesthesia. The sympathectomy created during neuraxial anesthesia

may cause hypotension and decreased preload, which could severely compromise cardiac output in patients with these cardiac defects. From a central nervous system perspective, there is an association between Noonan Syndrome and Arnold Chiari malformation type I and hydrocephalus; such central nervous defects also increase the risk and may be a contraindication to performing neuraxial anesthesia due to the possibility of herniation from increased Intra-cranial pressure (ICP). Additionally, like Turner Syndrome, there is an increased incidence of scoliosis (10–15%), kyphosis, vertebral anomalies, and rib anomalies, which may make the technical aspect of performing neuraxial anesthesia and paravertebral blocks challenging, depending on the particular patient. Preoperative imaging of the back and head may be helpful if there is the possibility of performing neuraxial anesthesia on a patient with Noonan's syndrome.

Hematologically, bleeding disorders are reported in 30–65% of patients with Noonan Syndrome. Factor XI deficiency is the most common bleeding disorder in these patients, though thrombocytopenia and platelet dysfunction have also been described. The thrombocytopenia may be secondary to splenomegaly in some patients with Noonan Syndrome; splenomegaly has been reported in up to 50% of patients with Noonan Syndrome. The most common laboratory abnormality in patients will be an elevated partial thromboplastin time. Due to the coagulation abnormalities, it would be prudent to check coagulation labs before deciding to proceed with any regional or neuraxial anesthesia.

There are several aspects of Noonan Syndrome that are also significant but more relevant to general than regional anesthesia. Like Turner Syndrome, gastroesophageal reflux is common in patients and is an important consideration when also incorporating a general anesthetic. Noonan Syndrome has also been associated with malignant hyperthermia (MH); however, the evidence linking the two is weak, with only one strong case report. It has been suggested that other case reports suggesting a link with MH may have confused Noonan Syndrome with King–Denborough syndrome, which has a similar phenotype (Fig. 6.3) [2, 3].

Aortic Stenosis

Aortic stenosis, the obstruction of the left ventricular outflow tract due to narrowing of the aortic valve, is the most common valvular abnormality and an important consideration in the preoperative anesthetic assessment for all patients undergoing surgery, since it can precipitate heart failure, arrhythmias, and syncope. It is common throughout the elderly population, with estimations of 2% of people over 65, 3% over 75, and 4% over 85 with aortic stenosis. The 2014 ACC/AHA guidelines have identified severe aortic stenosis, with an aortic valve area less than 1.0 cm² or a mean transvalvular gradient of 40 mmHg, as a major predictor of adverse outcomes in surgery. The risks of aortic stenosis in general anesthesia have been described often in other texts, but overall the goal is to avoid hypotension and tachycardia in order to maintain adequate preload, coronary perfusion pressure, and cardiac output. Patients with aortic stenosis may develop left



Fig. 6.3 Noonan syndrome

ventricular hypertrophy due to the chronic outflow obstruction and may be very sensitive to changes in intravascular volume due to subsequent changes in stroke volume and cardiac output.

Regarding regional and neuraxial anesthesia, the main consideration in aortic stenosis is the use of neuraxial anesthesia. Neuraxial anesthesia can cause a sympathectomy and venous blood pooling in the lower extremities that can sharply drop preload and thus coronary perfusion and cardiac output. However, neuraxial anesthesia is not contraindicated if titrated carefully and with adjunctive measures such as the use of vasopressors or fluid-loading prior to administering a neuraxial block. Indeed, general anesthesia agents such as propofol and inhaled gases also can decrease preload and depress myocardial function. In some cases, the sympathectomy of neuraxial anesthesia, if affecting cardiac innervation, may help avoid dangerous tachycardia as well. Because a spinal has a quicker onset and a denser block than an epidural, if aortic stenosis is severe and neuraxial anesthesia is desired, it may be safer to place an epidural catheter than to perform a spinal. Regarding vasopressors, both phenylephrine and ephedrine are effective for counteracting the sympathectomy caused by neuraxial anesthesia. Ephedrine may be slightly superior since with its beta-agonist activity, it does not decrease cardiac output like phenylephrine.

Obese Patient

Obesity, a disorder with excessive body fat, is defined as having a body mass index (BMI) of 30 or greater. The incidence of obesity has multiplied worldwide over the years with about 65% of adult Americans classified as overweight. Medical comorbidities such as hypertension, type 2 diabetes, cardio-pulmonary disease, obstructive sleep apnea, and venous thromboembolism are seen with higher incidence in obese patients compared to normal weight patients of similar ages. The presence of these comorbidities makes regional anesthesia a good option when trying to avoid airway manipulation, cardiopulmonary-depressing anesthetic drugs, and opioids, and trying to reduce postoperative nausea and vomiting (PONV), which is commonly associated with general anesthesia.

The anatomic changes associated with obesity make performing peripheral nerve blockade technically difficult because landmarks are difficult to palpate and long needles may be required. Studies have shown that obesity is an independent risk factor for block failure and the rate of block failure increases with increasing BMI. “Of the failed blocks, paravertebral and continuous epidural, continuous supraclavicular, and superficial cervical plexus blocks had the highest failure rates” [4].

Taivainen et al. [5] and Hodgkinson et al. [6] reported that compared to non-obese patients, obese patients require less local anesthetic to achieve the same level of block with subarachnoid and epidural blocks, respectively.

A retrospective cohort study by Bomberg et al. [7] suggests that obesity is an independent risk factor for peripheral, but not neuraxial, catheter-related infections.

Achondroplasia

Achondroplasia is the most frequent cause of dwarfism, with a prevalence of 1/26,000 live births. Anatomic abnormalities include short status, macrocephaly, protuberant buttocks and abdomen, short limbs, airway and facial abnormalities, thoracic dystrophy, pectus carinatum, spinal stenosis, scoliosis, kyphosis, lordosis, cardiac abnormality, hydrocephalus, mental retardation, seizure disorders, and tracheal compression during head and neck flexion. The presence of spinal stenosis and vertebral misalignment from scoliosis, kyphosis, or lordosis may complicate regional technique. The failure rate of neuraxial anesthesia is high because of thoracolumbar deformity and spinal canal stenosis seen in this patient population. Failure rate is reduced with combined spinal–epidural technique. Due to the presence of spinal stenosis in these patients, correction of 30% reduction in the dose of intrathecal drugs should be carried out in parturient with achondroplasia as proposed by Ravenscroft et al. [8]. Intrathecal local anesthetic dosing should be based on the height of the patient. A comprehensive neurologic exam should be performed to identify preexisting neurologic disorders before performing a regional anesthesia in this patient (Fig. 6.4).

Achondroplasia

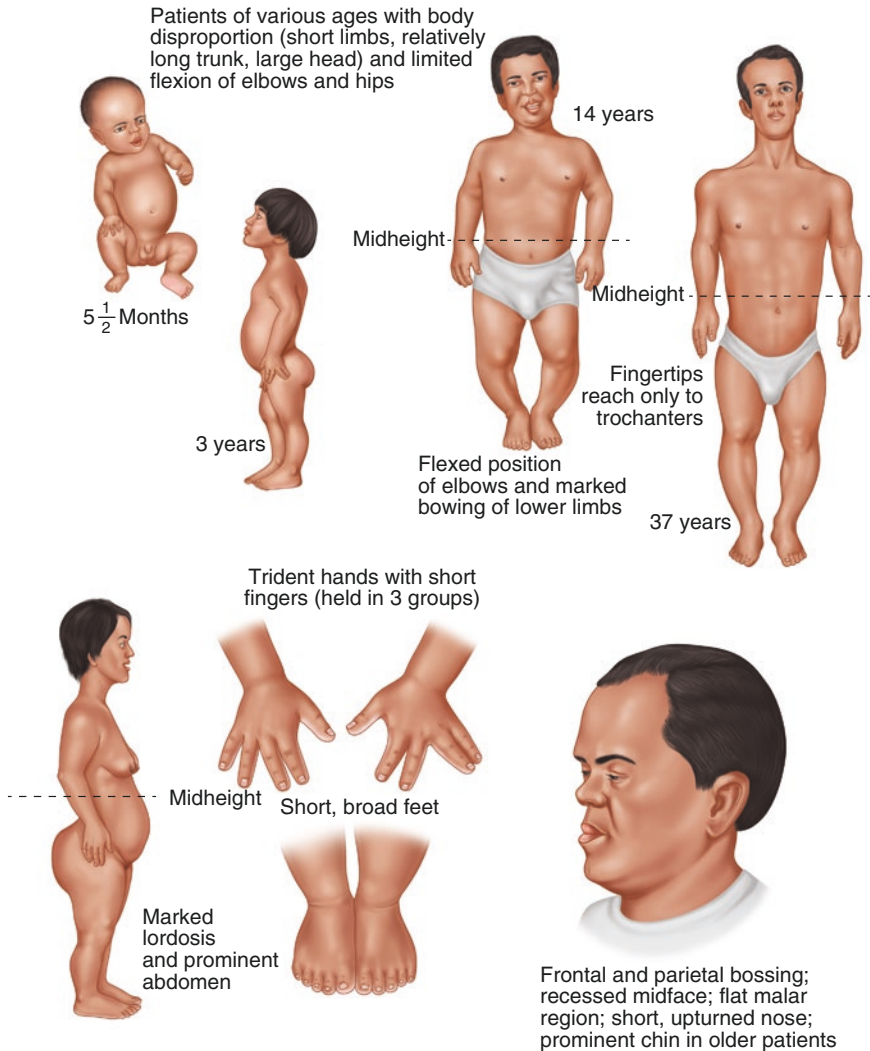


Fig. 6.4 Achondroplasia

Trisomy 21

Based on a thorough literature review, there is no documented evidence of contraindications to the use of regional anesthesia in this patient population.

Ehlers–Danlos

Ehlers–Danlos Syndrome (EDS) describes a spectrum of genetically heterogeneous diseases often grouped together for their similar phenotypic features including joint hypermobility and instability, skin texture abnormalities, and fragility of soft tissue and blood vessels. The overall incidence ranges from 1/10,000 to 1/25,000. There is a paucity of literature regarding anesthetic management of EDS patients, with most recommendations gleaned from case reports and based on theory.

Of the subtypes of EDS, the most risk with neuraxial and regional anesthesia occurs with vascular EDS. Vascular EDS is characterized by thin, easily-bruised, translucent skin, with very fragile blood vessels. There is also fragility of the gastrointestinal tract, uterus, lungs, spleen, and liver, with these organs at an increased likelihood of rupture. Neuraxial anesthesia and, to a lesser extent, regional anesthesia are not recommended due to the bleeding risk from fragile tissues, especially if there is no significant benefit of neuraxial anesthesia over general anesthesia. Inadvertent bleeding during a neuraxial procedure increases the risk of developing an epidural hematoma, a serious complication that requires timely neurosurgical intervention to avoid permanent severe neurologic deficits such as paralysis and bowel/bladder dysfunction. In EDS subtypes with tissue fragility, there are case reports of spontaneous dural rupture and subsequent headache similar to post-dural puncture headache, which further favors avoiding neuraxial anesthesia.

Additionally, other subtypes of EDS, including the classic, hypermobile, and kyphoscoliotic subtype, are characterized by Tarlov cysts, perineural cysts filled with CSF. These cysts are typically located from S1 to S4 so they are not an absolute contraindication to performing neuraxial anesthesia; however, preoperative imaging with MRI, CT, or ultrasound is recommended before attempting a neuraxial block, especially in the kyphoscoliotic type.

It is recommended, in the overall anesthetic management, to contact the patient's EDS specialist to obtain a clear picture of the patient's specific phenotype, as well as to ensure that the surgery is performed in a location that is able to handle EDS patients. Because of the skin fragility and joint hypermobility that characterizes the general syndrome, special care may be required in patient positioning, the use of tape and tourniquets, and airway management to avoid inadvertent trauma. In fact, in the absence of vascular EDS, regional anesthesia may be advantageous by avoiding endotracheal tube placement (risk of mucosal damage and overinflated cuff) and temporomandibular joint dislocation from mask ventilation (Fig. 6.5) [9, 10].

Scoliosis

Scoliosis is present in about 2% of the population and is about twice as prevalent in women as in men. There are different degrees of scoliosis, and it can be treated either conservatively, with bracing, or surgically (which may involve the placement of spinal hardware or a spinal fusion), depending on severity, which is typically assessed by measuring the Cobb's angle. Scoliosis may be idiopathic (70% of cases)

Ehlers Danlos syndrome

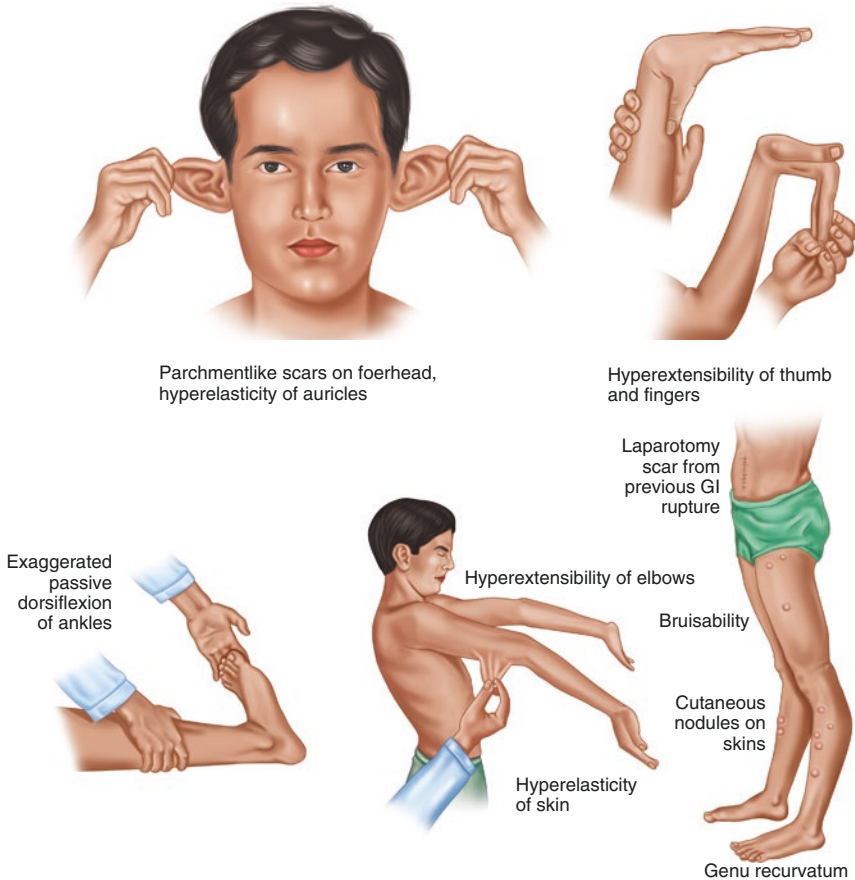


Fig. 6.5 Ehlers–Danlos syndrome

or a secondary process related to trauma or disease processes, including several that are discussed in this chapter.

There are no specific concerns for peripheral nerve blocks in a scoliotic patient, but neuraxial anesthesia does present a challenge. In a scoliotic patient, spinous processes may be distorted, twisted, or in the case of a post-surgical patient, absent. This in turn distorts surface anatomy, making it difficult or impossible to find landmarks, and palpation may not be effective. For a curved spinous process, it is recommended that the needle approach be paramedian with insertion on the convex side of the spinous curve rather than the concave side, due to larger interlaminar processes on the convex side. Patients with prior surgery also present additional challenges. The presence of hardware (e.g., Harrington rods), bone grafts, and scar tissue may hinder the path of the needle. There is also an increased incidence of

spondylolisthesis and retrolisthesis caudal to the surgical site, which may further complicate attempts to reach the target for a block.

One of the recent advances in overcoming these challenges is the use of point-of-care two-dimensional ultrasound. Low-frequency probes can achieve an adequate depth to identify the necessary interspaces for placement of neuraxial anesthesia. Operative and radiographic reports may also be useful in guiding placement, though not as useful as ultrasound. Despite successful placement, a neuraxial block may still not be successful in a scoliotic patient due to alterations in the epidural or subarachnoid space. Several strategies to overcome this problem include rotating the patient with the non-blocked side in the dependent position and using a large volume/low concentration local anesthetic mix to overcome the unilaterality. In the case that the epidural space is difficult to access, running an intrathecal catheter infusion rather than an epidural infusion is also an option (Fig. 6.6) [11, 12].

Cerebral Palsy

Cerebral palsy (CP) describes a syndrome of disorders, classically with movement and cognitive features, caused by damage to the developing fetal brain. While cerebral hypoxia in the perinatal period was historically thought to be a major contributor, with neonatal hypoxia becoming increasingly rare, it has become evident that there are a range of other risk factors. These include low birth weight, prematurity, prenatal infections (especially those in the TORCH category—*toxoplasmosis, rubella, cytomegalovirus, and herpes*), seizures at birth, neonatal hypoglycemia, neonatal respiratory distress syndrome, genetic disorders, and vascular disorders. CP patients are characterized by abnormal movement (spasticity or ataxia, spasticity being more common) and cognitive impairment, which may include learning disabilities, impaired intellectual ability, and impaired speech. Due to abnormalities of muscle function beyond simply those of movement, CP patients often have chronic gastroesophageal reflux, recurrent aspiration pneumonia, and respiratory muscle hypotonia. Chronic muscle contractures, decubitus ulcers, and epilepsy are also features.

Regional and neuraxial anesthesia may be quite beneficial in CP patients. Use of continuous epidural or continuous peripheral nerve block may help prevent postoperative increase in muscle spasms resulting from pain or anxiety more effectively than systemic medications. Such spasms can complicate post-operative healing and be as painful as the surgery itself. It is suggested that the addition of clonidine to the epidural can help especially with suppressing muscle spasms. In addition, use of regional and neuraxial anesthesia can decrease the need for systemic opioids. Over-titration of opioids is especially dangerous in the CP patient due to a preexisting risk of atelectasis and aspiration pneumonia from respiratory muscle hypotonia, reflux, and an impaired cough reflex. Due to the possibility of CP patients taking anti-epileptic drugs, many of which undergo hepatic metabolism, it is important to titrate amide local anesthetics carefully, as patients' metabolism of amides may also be affected. Lastly, relevant to the performance of a nerve block itself is the importance of assessing for a latex allergy. CP patients have often had multiple exposures to

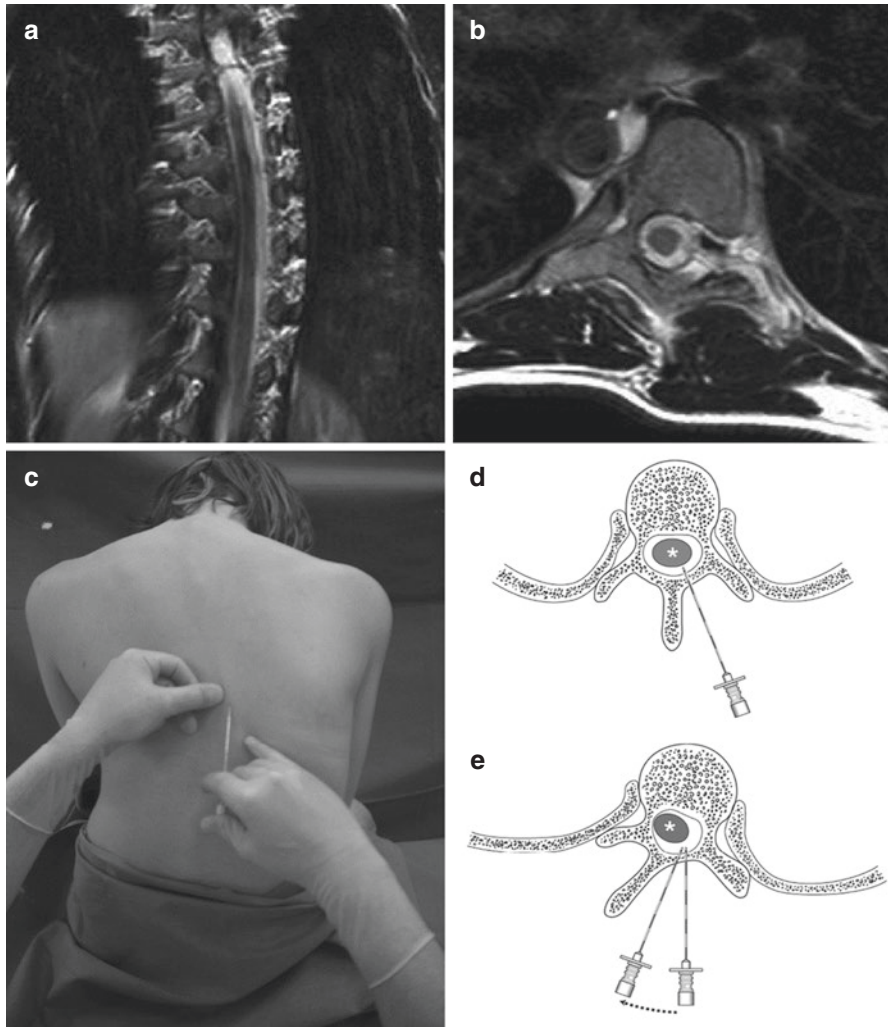


Fig. 6.6 Scoliosis

latex from an early age due to surgical procedures or the presence of indwelling urethral catheters, and this may sensitize their bodies to developing an allergic or anaphylactic response to the latex allergen [13].

Trisomy 18

Trisomy 18, also known as Edwards' Syndrome, is caused by duplication in whole or part of chromosome 18. First described in 1960, It occurs in 1/6000 patients, the majority being female, but the majority die before birth, and as many as 90% may die within the first year of life. This disorder is characterized by microcephaly,

micrognathia, club feet, cardiac defects (including atrial septal defect, ventricular septal defect, patent ductal arteriosus), developmental delays, and esophageal atresia. With the poor prognosis of this disorder, some advocate avoiding surgery altogether in these patients due to the questionable long-term benefit. There are no specific recommendations regarding regional or neuraxial anesthesia [14–16].

References

1. Divekar VM, Kothari MD, Kamdar BM. Anaesthesia in Turner's syndrome. *Can Anaesth Soc J*. 1983;30(4):417–8.
2. Romano AA, Allanson JE, Dahlgren J, Gelb BE, Hall B, Pierpont ME, et al. Noonan syndrome: clinical features, diagnosis, and management guidelines. *Pediatrics*. 2010;126(4):746–59.
3. McLure HA, Yentis SM. General anesthesia for caesarean section in a parturient with Noonan's syndrome. *Br J Anesth*. 1996;77:665–8.
4. Ingrande J, Brodsky JB, Lemmens HJ. Regional anesthesia and obesity. *Curr Opin Anaesthesiol*. 2009;22(5):683–6.
5. Taivainen T, Tuominen M, Rosenber PH. Influence of obesity on the spread of spinal analgesia after injection of plain 0.5% bupivacaine at the L3–4 or L4–5 interspace. *Br J Anaesth*. 1990;64(5):542–6.
6. Hodgkinson R, Husain FJ. Obesity and the cephalad spread of analgesia following epidural administration of bupivacaine for cesarean section. *Anesth Analg*. 1980;59:89–92.
7. Bomberg H, Albert N, Schmitt K, Gräber S, Kessler P, Steinfeldt T, et al. Obesity in regional anesthesia—a risk factor for peripheral catheter-related infections. *Acta Anaesthesiol Scand*. 2015;59(8):1038–48.
8. Ravenscroft A, Govender T, Rout C. Spinal anaesthesia for emergency caesarean in an achondroplastic dwarf. *Anaesthesia*. 1998;53:1236–7.
9. Wiesman T, Castori M, Malfait F, Wulf H. Recommendations for anesthesia and perioperative management in patients with Ehlers-Danlos syndrome(s). *Orphanet J Rare Dis*. 2014;9:109.
10. De Paepe A, Malfait F. The Ehlers–Danlos syndrome, a disorder with many faces. *Clin Genet*. 2012;82(1):1–11.
11. Ko JY, Leffert LR. Clinical implications of Neuraxial anesthesia in the parturient with scoliosis. *Anesth Analg*. 2009;109(6):1930–4.
12. Perlas A. Evidence for the use of ultrasound in Neuraxial blocks. *Reg Anesth Pain Med*. 2010;35(2):S43–6.
13. Wongprasartsuk P, Stevens J. Cerebral palsy and anaesthesia. *Pediatr Anesth*. 2002;12(4):296–303.
14. Van Dyke DC, Allen M. Clinical management considerations in long-term survivors with trisomy 18. *Pediatrics*. 1990;85(5):753–9.
15. Bos AP, Broers CJ, Hazebroek FW, van Hemel JO, Tibboel D, Wesby-van Swaay E, et al. Avoidance of emergency surgery in newborn infants with trisomy 18. *Lancet*. 1992;339:913–5.
16. Tucker ME, Garringer HJ, Weaver DD. Phenotypic spectrum of mosaic trisomy 18: two new patients, a literature review, and counseling issues. *Am J Med Genet A*. 2007;143A(5):505–17.



Thoracic Aorta and Its Variants

7

Isidore Dinga Madou, Bulat A. Ziganshin,
John A. Elefteriades, and Young Erben

Introduction

The cardiovascular system is the first system in the body to reach a functional state, at around the 21st and 22nd day of gestation. As a result, any aortic arch anatomical variant results from the aberrant embryologic migration and/or differentiation of undifferentiated cardiac cell precursors. Initially, six paired aortic channels encircle the embryonic pharynx. They supply the developing pharyngeal arches and arise from the aortic sac. These channels run dorsally, embedded in the mesenchyme of the pharyngeal arches, and terminate in the right and left dorsal aortae [1].

The normal anatomy of the aortic arch and branched vessels is constituted by the ascending aorta, three branches from the arch itself (the brachiocephalic trunk or innominate artery, left carotid artery, and left subclavian artery), and the descending aorta (Fig. 7.1). The objective of this chapter is to provide an overview of aortic arch anatomy and its specific anatomic variants, and when possible, the common clinical presentation of these variants, associated cardiac and/or congenital abnormalities, and clinical relevance.

I. D. Madou

Department of Surgery, Duke University School of Medicine, Durham, NC, USA
e-mail: isidore.dinga@kp.org

B. A. Ziganshin

Aortic Institute, Yale New Haven Hospital, New Haven, CT, USA
e-mail: bulat.ziganshin@yale.edu

J. A. Elefteriades (✉)

Aortic Institute at Yale New Haven, Yale University School of Medicine,
New Haven, CT, USA
e-mail: john.elefteriades@yale.edu

Y. Erben

Department of Vascular Surgery, Mayo Clinic, Jacksonville, FL, USA
e-mail: young.erben@mayo.edu

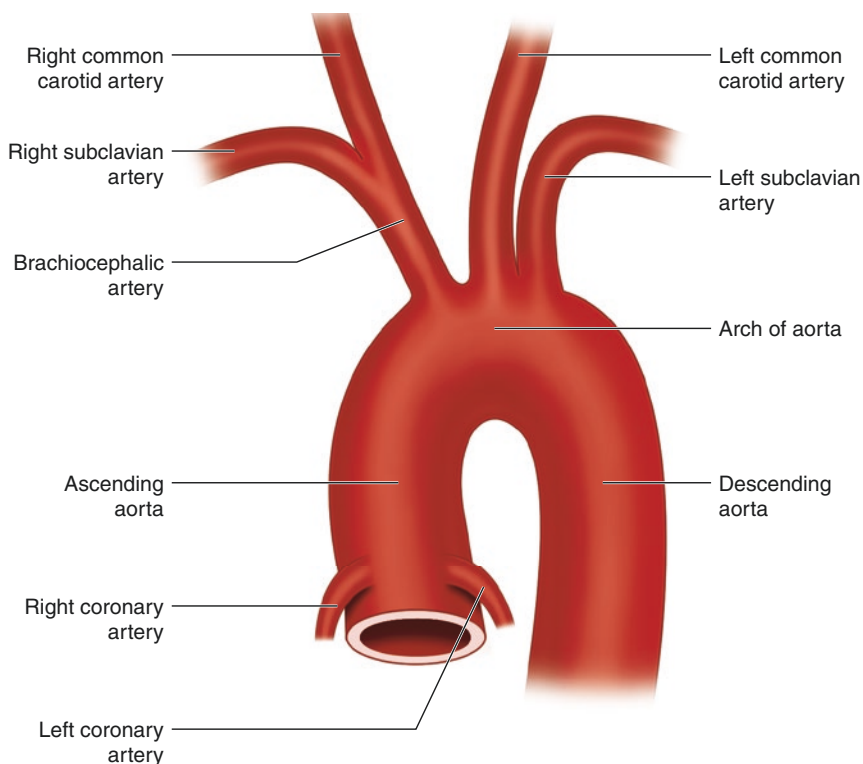


Fig. 7.1 Normal aortic arch

Embryology of the Aortic Arch

The first arch arteries to appear in the embryo are the right and left primitive aorta. Each primitive aorta consists of a portion lying ventral to the foregut (ventral aorta), an arched portion lying in the first pharyngeal arch, and a dorsal portion lying dorsal to the foregut (dorsal aorta). The dorsal aortae fuse caudally during the fourth week of gestation, forming a single median vessel, the descending aorta. The descending aorta gives branches to the median sacral artery (caudate end of the descending aorta), lateral segmental, ventral segmental, and dorsal intersegmental arteries. After fusion of two endocardial heart tubes, the two ventral aortae partially fuse to form the aortic sac, which is the primordial vascular channel from which the aortic arches arise [2, 3].

There are six pairs of aortic arches, but the fifth pair is poorly developed and disappears soon after formation. Not all six pairs develop at the same time, and by the time the sixth aortic arches form, the first and second have disappeared. During the sixth through eighth weeks of gestation, the primitive aortic arch pattern is transformed into the adult arterial arrangement of carotid, subclavian, and pulmonary arteries (Fig. 7.2). The first pair largely disappears; its dorsal part persists as the

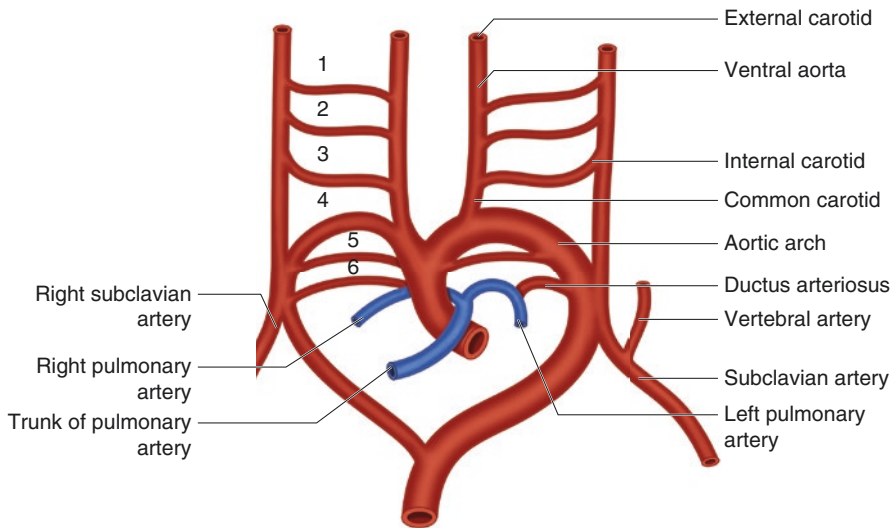


Fig. 7.2 All six paired aortic arches

maxillary arteries, which supply the ear, teeth, and muscles of the eyes and face. It may at times give rise to the external carotid artery. The second pair also largely disappears. The dorsal aspect persists as the hyoid and stapedial arteries. The third pair persists, and its proximal part forms the common carotid arteries; the distal part joins the dorsal aortae to form the internal carotid arteries. The fate of the fourth pair of aortic arches differs according to its laterality: the right becomes the proximal part of the right subclavian artery, and the left forms part of the arch of the aorta. The fifth pair disappears completely, with no vascular derivatives. Finally, the sixth pair's arch embryology depends on its laterality: the right turns into the proximal part of the right pulmonary artery, and the left turns into the left pulmonary artery proximally; distally, it forms the ductus arteriosus, a vital shunt during fetal circulation between the pulmonary artery and the dorsal aorta [2].

Arch Anatomical Variants

Aortic branch anomalies are significant when they cause symptoms; otherwise, they are physiologically tolerated. Being aware of the presence of variations may be crucial when planning radiological or surgical interventions to the chest and neck and for avoiding complications during such procedures. The most common pattern of the aortic arch configuration occurs in approximately 80% of individuals (Fig. 7.1). This pattern includes a left-sided aortic arch with the brachiocephalic artery as the first and largest vessel arising from it and branching into the right subclavian and right common carotid artery, followed by the left common carotid artery and the left subclavian artery [4].

Double Aortic Arch

In normal embryonic development, the right fourth arch becomes the proximal part of the right subclavian artery, and the left fourth arch forms part of the arch of the aorta. In double aortic arch, there is persistence of both the right and left fourth arches, which leads to an ascending aorta that divides into left and right arches, which fuse together to completely encircle the trachea and esophagus before forming the descending aorta. Both arches can be patent, or one (usually the left) can be hypoplastic/atretic. If both are patent, they usually form a symmetric origin of four arch vessels (Fig. 7.3). Double aortic arch is characterized by a complete vascular ring encircling the trachea and esophagus, causing compression of both structures [5]. Vascular rings comprise 1% of surgically managed cardiovascular malformations, of which about half are double arches. The degree of compression varies. The right arch is usually larger and passes posterior to the esophagus.

The right common carotid and subclavian arteries arise separately from the right arch. Most commonly, the right arch is dominant, with a more superior apex and descending aorta on the left. This variant is rarely associated with other congenital heart diseases; when present, tetralogy of Fallot is the most common association with a double aortic arch, and 20% have chromosome band 22q11 deletion. There is no gender or race predilection. The patient usually presents with respiratory

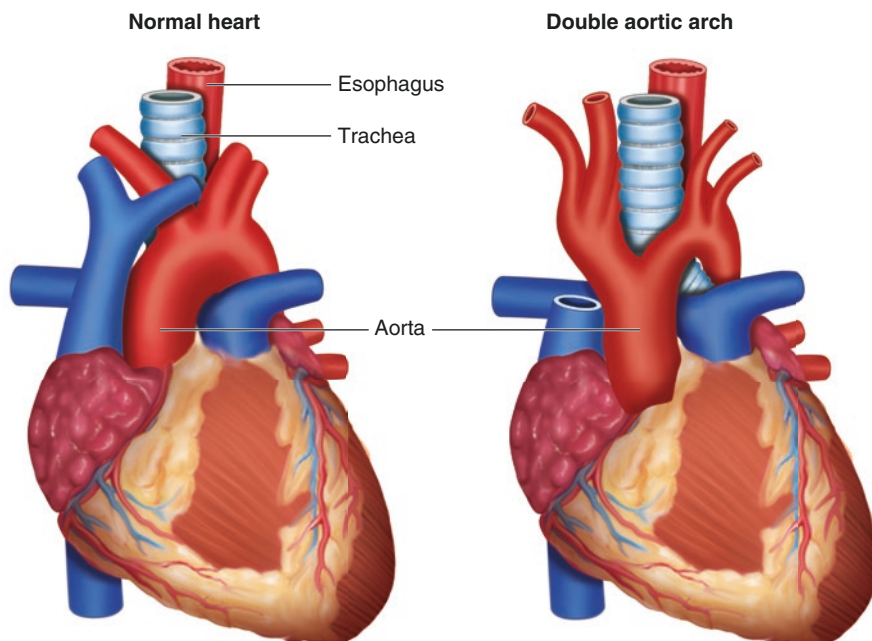


Fig. 7.3 Double aortic arch

difficulties like stridor, but apparent life-threatening events like dysphagia, vomiting, and choking sometimes occur.

Multiple imaging modalities exist to diagnose a double aortic arch. A chest radiograph may show indentation of the trachea or indeterminate arch sidedness, and an esophagram may reveal a bilateral and posterior indentation of the esophagus. CT scan and MRI of the chest will define the anatomy, determine the dominant arch for surgical planning (contralateral thoracotomy), and evaluate airway compression (Fig. 7.4) [3].

Right-Sided Aortic Arch

This phenomenon occurs when the entire right aortic arch persists and the distal segment of the left dorsal artery distal to the seventh intersegmental artery involutes. There are a few variations of this right-sided aortic arch:

- *Right-sided aortic arch with aberrant left subclavian artery*: This is the most common variant of a right-sided aortic arch, representing at least 39.5% of all right-sided arches. It is associated with a Kommerell's diverticulum [6]. It evolves from the interruption of the dorsal segment of the left arch between the

Fig. 7.4 Magnetic resonance angiography (MRA) showing a double arch



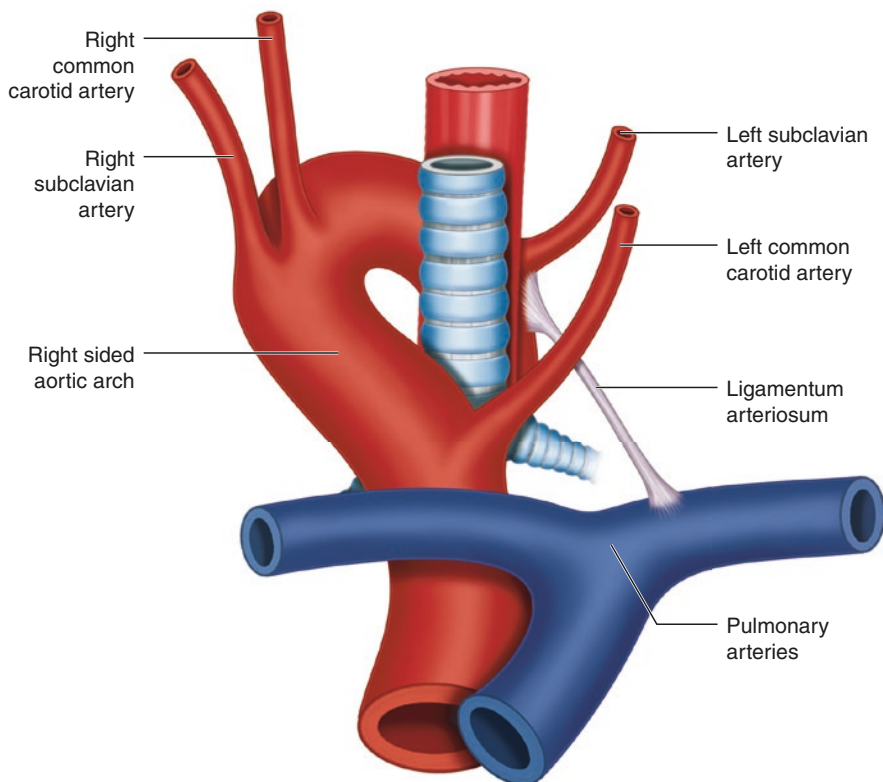


Fig. 7.5 Right-sided aortic arch with aberrant left subclavian artery

left common carotid and left subclavian arteries, with regression of the right ductus arteriosus in the hypothetical double aortic arch (Fig. 7.5). Although esophageal and tracheal compression have been reported, this anomaly is usually asymptomatic, and associations with other cardiovascular abnormalities are rare [2, 3, 7].

- *Right-sided aortic arch without a retropharyngeal component:* The ductus arteriosus passes from the right pulmonary artery to the right arch of the aorta. There are no effects on the trachea and esophagus.
- *Right-sided aortic arch with a retropharyngeal component:* In this case, the arch lies posterior to the esophagus. The left ligamentum arteriosum can form a vascular ring. The Kommerell's diverticulum is a remnant of the left dorsal aortic root and can be associated with a midline descending aorta. The vascular ring forms around the trachea and esophagus, which may lead to compression. There are two regions of potential airway compression: at the level of the arch and subclavian artery, and at the level of the carina [2, 3, 8].

Hypoplastic Ascending Aorta

Hypoplasia of the ascending aorta occurs in conjunction with a hypoplastic left heart syndrome, which is characterized by marked hypoplasia of the left ventricle and ascending aorta (Fig. 7.6). The hypoplasia of the left heart results in atretic, hypoplastic, or stenotic aortic and mitral valves, severely reducing blood flow to the body. The exact cause of the hypoplastic left heart syndrome is unknown; it comprises 1.2–1.5% of all congenital heart defects. It is more common in males than in females, with a 55–70% male predominance [2, 9]. The newborn usually presents with symptoms within the first 24 to 48 hours of life. If the infant has a concomitant patent ductus arteriosus, he or she may have few initial symptoms, but as the ductus arteriosus begins to close, symptoms of cyanosis, tachypnea, respiratory distress, metabolic acidosis, and oliguria will develop. The infant will develop profound shock, and without treatment or an attempt to keep the ductus arteriosus open, the infant will generally die within a few weeks after birth [2, 10].

Coarctation of the Aorta

Coarctation of the aorta is characterized by narrowing of the aorta caused by a defect in the vessel media—with posterior in-folding that may be circumferential. It is located near the ductus arteriosus and can cause a tubular hypoplasia of the arch with poststenotic dilatation (Fig. 7.7). It is more common in males (2,1) and

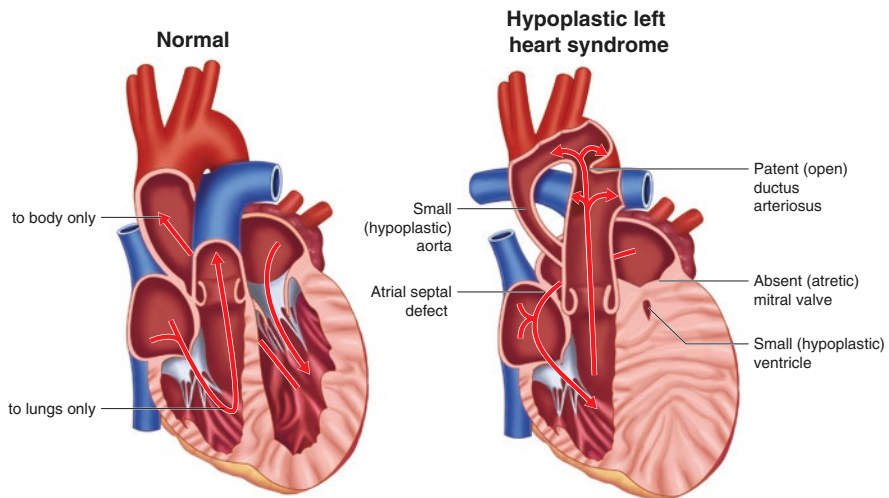


Fig. 7.6 Hypoplastic ascending aorta

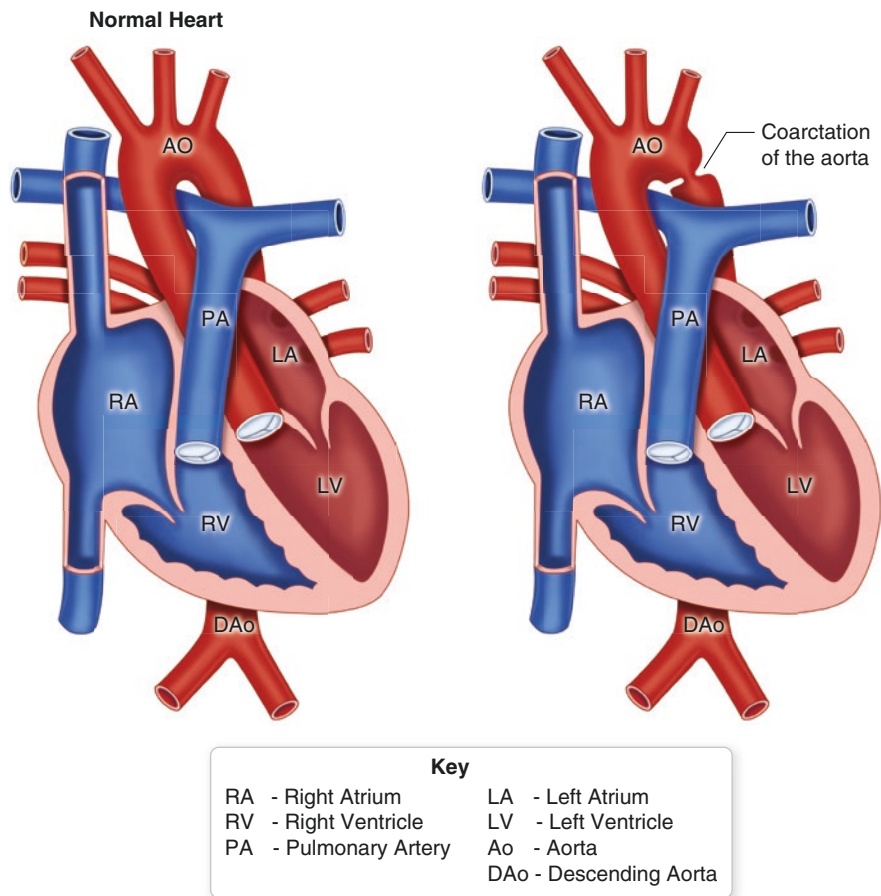


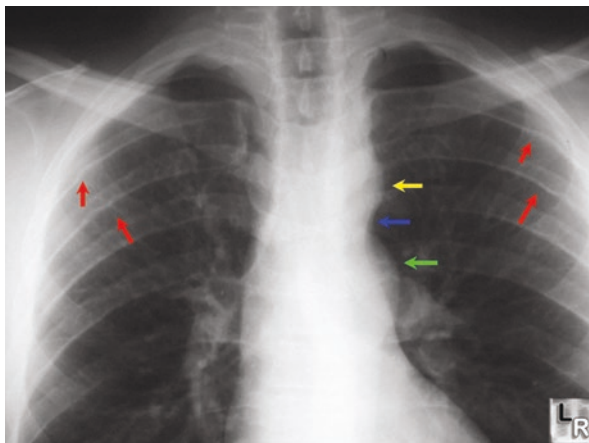
Fig. 7.7 Coarctation of the aorta

represents about 5–10% of all congenital cardiac lesions. If left untreated, fewer than 20% survive to 50 years of age.

The clinical presentation depends on severity. In infancy, patients present with congestive heart failure, acidosis, and claudication. After infancy, they are usually asymptomatic, but could present with a murmur, hypertension, headache, leg cramps, and cold feet. Coarctation often accompanies Turner's syndrome (XO), bicuspid aortic valve, ventricular septal defect, patent ductus arteriosus, and aneurysms of the circle of Willis. Coarctation can be identified on chest radiographs by rib notching, pulmonary edema, and cardiomegaly. Usually classified as preductal or postductal, the constriction generally lies distal to the origin of the left subclavian artery [2].

- *Preductal type*: This is the less common type of coarctation of the aorta. The narrowing is proximal to the ductus arteriosus. If severe, blood flow to the aorta distal to the narrowing depends on a patent ductus arteriosus, so its closure can be life-threatening [2].

Fig. 7.8 Rib notching in coarctation of the aorta (red arrows). See also apparent constriction of the descending aorta (blue arrow) between the upper and lower segments



- *Postductal type*: This is the most common type of coarctation. The narrowing is distal to the ductus arteriosus. The ductus usually remains patent to communicate the pulmonary artery with the descending aorta, which will allow development of collateral circulation during the fetal period. The collateral circulation will develop mainly from branches of both subclavian arteries, scapular, internal thoracic, and intercostal arteries. Although the ductus remains patent after birth, the blood flow to the lower extremities can be impaired. During infancy, it may be associated with notching of the ribs (Fig. 7.8), hypertension in the upper extremities, and weak pulses in the lower extremities [2, 3].

Interrupted Aortic Arch

Interrupted aortic arch (IAA) is defined as complete separation of ascending and descending aorta. This is a rare anomaly that represents about 1.5% of congenital heart disease. An isolated IAA is extremely rare; IAA is most often associated with ventricular septal defect or with patent ductus arteriosus, truncus arteriosum, transposition of great arteries, or double-outlet right ventricle. Twenty-five percent of patients have DiGeorge syndrome [2, 11]. IAA represents developmental variations that arise from the failure of the proximal arch (which spans from the innominate artery to the left common carotid, which is derived from the aortic sac) and the distal arch (which spans from the left common carotid artery to the left subclavian artery, which is derived from the fourth embryonic arch), to join with the isthmus (which is derived from the junction of the sixth embryonic arch with the dorsal aorta, and the fourth arch).

Figure 7.9 illustrates the three types of IAA, according to the Celoria and Patton classification [10]: Type A (33–42%), interruption located at the level of the isthmus; Type B (53–65%, the most common), interruption between second carotid and ipsilateral subclavian; and Type C (1–4%, rare), interruption between the innominate artery takeoff and the left common carotid (in other words, between the carotids). An additional three subcategories exist for each of the types: without retroesophageal or isolated subclavian artery, with retroesophageal subclavian artery, and with isolated subclavian artery [2, 11].

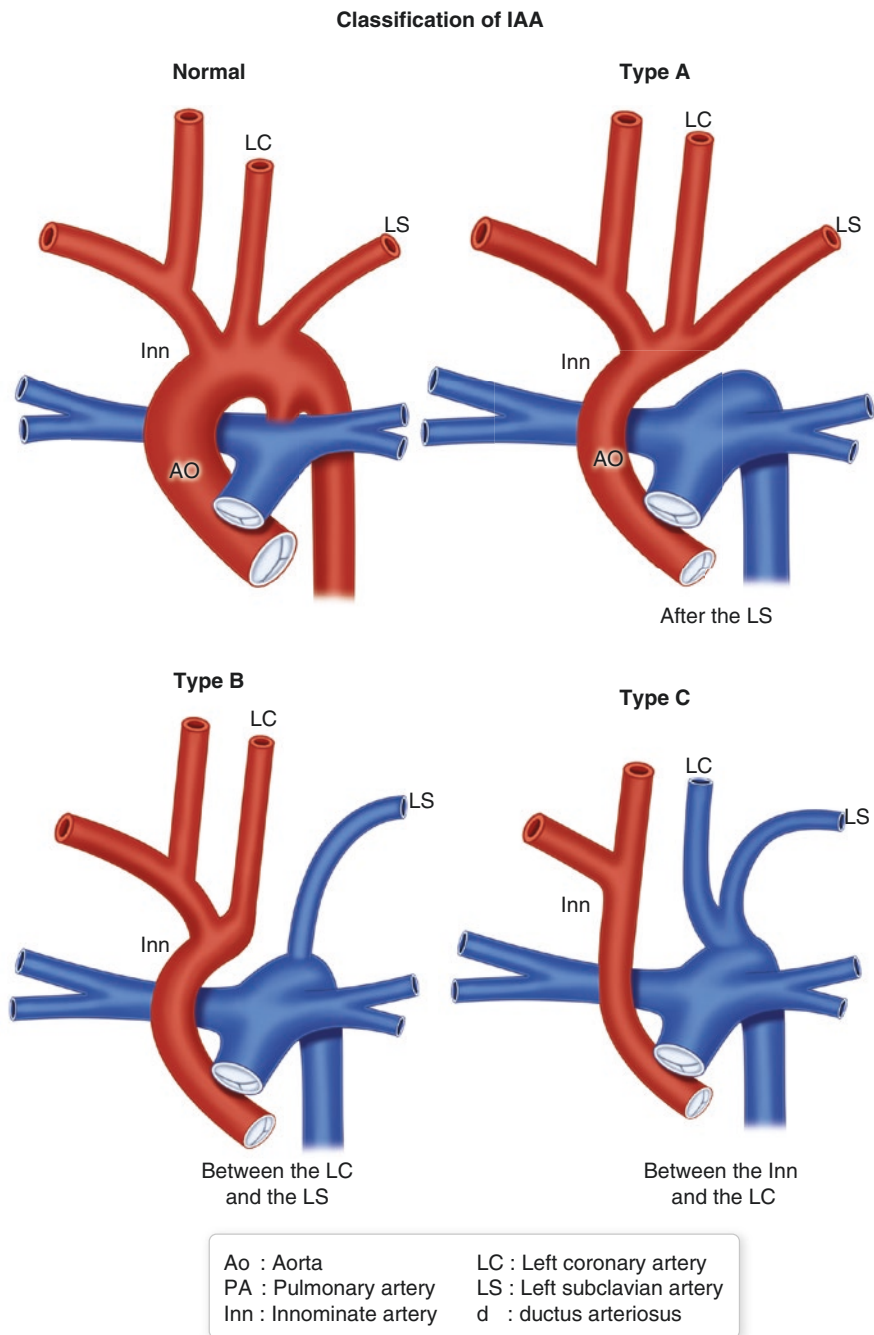


Fig. 7.9 Classification of interrupted aortic arch (IAA)

Most patients present with acute cardiovascular collapse after closure of the ductus arteriosus. They are found to be acidotic, cyanotic, and anuric, and have poor peripheral pulses. Absence of all limb pulses, despite strong carotid pulses, suggests type B with anomalous subclavian. On chest radiographs, the classic findings will be cardiomegaly with increased pulmonary vascularity and pulmonary edema in a critically ill newborn, with midline trachea and an inconspicuous aortic knob. CT scan will define the anatomy and determine the type. Prenatal diagnosis can be made with ultrasound. If the anomaly is diagnosed prenatally, prostaglandin E1 (PGE1) is started immediately after birth in cases associated with a patent ductus arteriosus. Most patients require medical resuscitation for a day or two prior to surgical intervention based on the type of the variation.

Patent Ductus Arteriosus

During gestation, the aorta and the pulmonary artery are normally connected by a blood vessel called the ductus arteriosus, which is an essential part of the fetal circulation. After birth, this vessel is supposed to close within a few days. The obliterated vessel forms the ligamentum arteriosum. In some infants, the ductus arteriosus remains patent, which allows blood to flow directly from the aorta into the pulmonary artery, thus straining the right heart and increasing the pressure in the pulmonary circulation (Fig. 7.10).

Cervical Aortic Arch

This rare aortic arch variant is defined as a supraclavicular position of the aortic arch, which is more predominant on the right side [12] (Fig. 7.11). Two categories exist: normal branching pattern or anomalous subclavian artery with vascular ring. The second group is divided according to the origin of the carotid artery. Cervical aortic arch results from a failure of the normal descent of the aortic arch system, persistence of the ductus caroticus, and involution of the fourth and third arches. Although a rare anomaly, 20% are complicated by aneurysm. This anomaly is often asymptomatic, but patients can have vascular ring-like symptoms (dysphagia, dyspnea, stridor, respiratory infections) or a supraclavicular pulsatile mass [3, 12, 13].

Ductus Diverticulum

Ductus diverticulum is a developmental outpouching forming a large bulge on the lesser curvature of the thoracic aortic isthmus. It is usually divided into the classic and the atypical presentation. The classic presentation is characterized by a smooth, gentle curve of the isthmus found in about 33% of newborns and 9% of adults. The atypical presentation is characterized by a sharper contour, with a shorter and

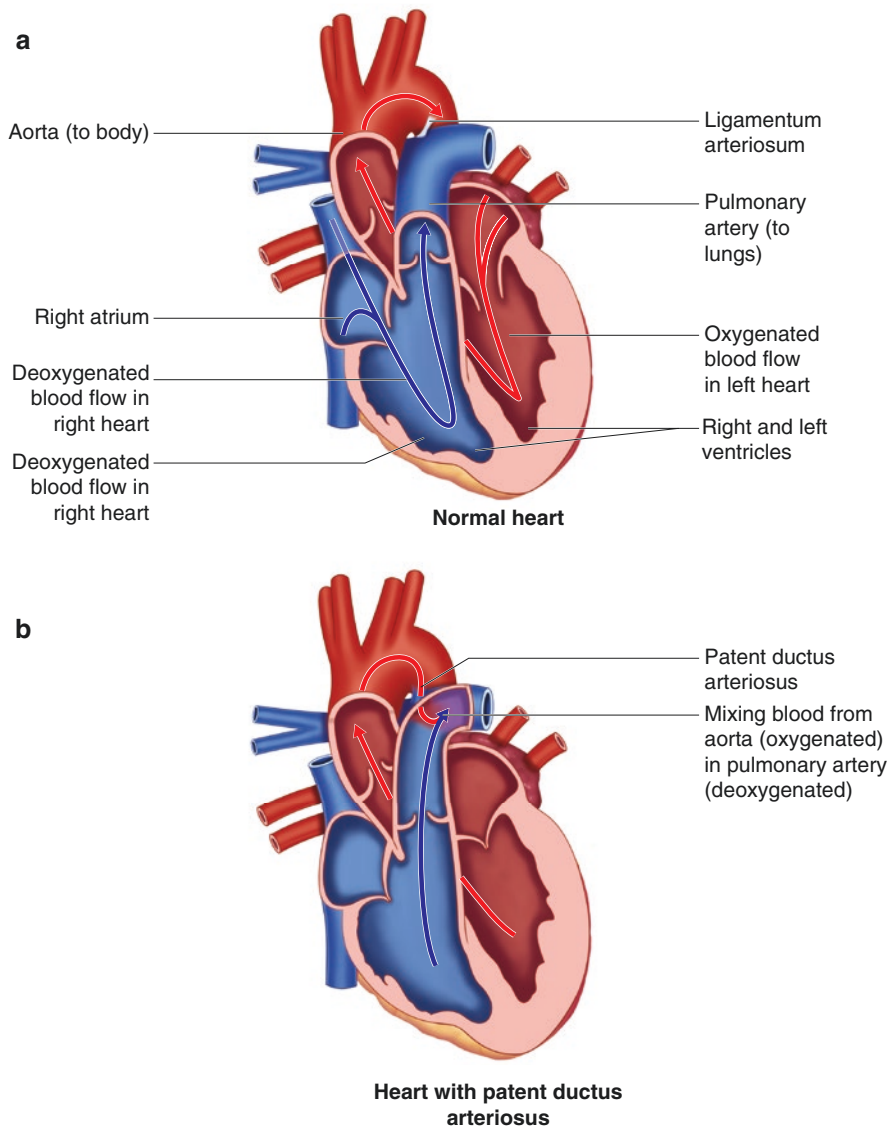


Fig. 7.10 Patent ductus arteriosus

steeper superior slope. The aortic isthmus is the most common location of the ductus diverticulum (Fig. 7.12). It is located in the anteromedial aspect of the aorta at the site of the previous ductus arteriosus. This is also the site of 90% of traumatic pseudoaneurysms. One way to differentiate between the two is that an aortic pseudoaneurysm usually forms sharp margins with the aorta, whereas a ductus

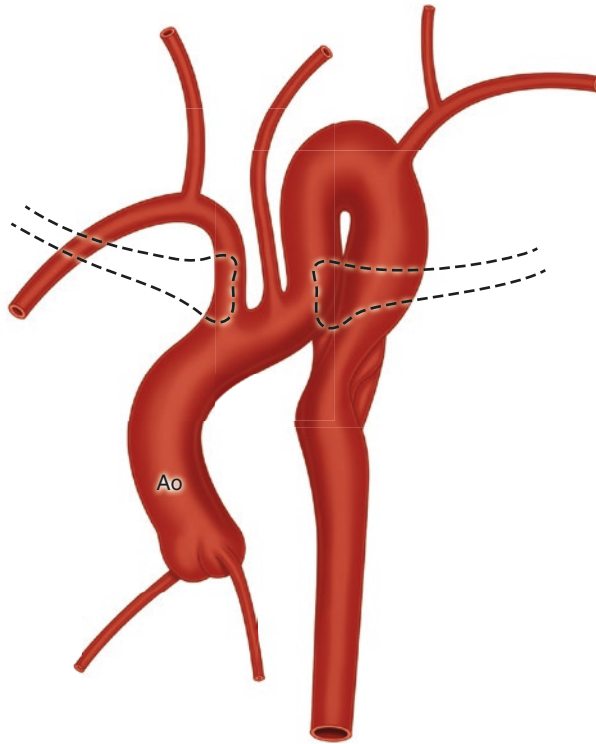


Fig. 7.11 Cervical aortic arch

diverticulum usually appears as a smooth focal bulge with less steep angles with the aortic wall [14, 15].

Branch Vessel Variants

Bovine Arch

A bovine arch develops when the brachiocephalic or innominate artery and the left common carotid artery share a common origin from the aortic arch (Fig. 7.13). This is one of the most common anatomic variants, reported to occur in about 15% of the population, with a predominance among people of African descent. It is asymptomatic, but in combination with other anatomical variants such as arteria lusoria (aberrant right subclavian artery), dysphagia lusoria has been reported [2, 16]. Furthermore, the presence of a bovine arch is associated with higher growth rates of the thoracic aorta and a higher prevalence of thoracic aortic aneurysm [17, 18].

Fig. 7.12 Ductus diverticulum (*arrows*)



Aberrant Right Subclavian Artery

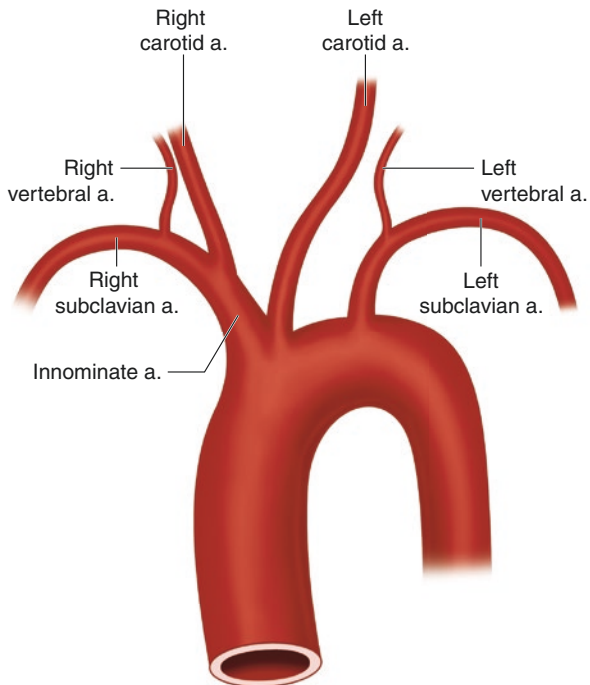


Fig. 7.13 Bovine arch

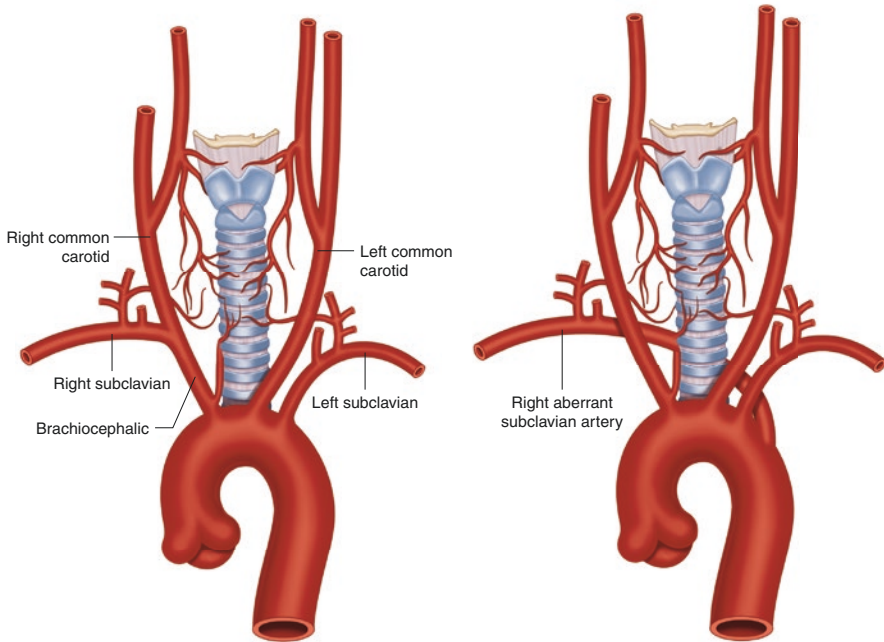


Fig. 7.14 Aberrant right subclavian artery

This artery may arise from the distal part of the arch of the aorta, with an incidence reported at around 0.5–2%. In some cases, the right subclavian artery arises from the descending aorta and runs behind the trachea and the esophagus to supply the right upper limb (Fig. 7.14). Its relationship to the esophagus is variable: 80% run posterior to the esophagus, 15% between the esophagus and trachea, and 5% anterior to the trachea. This anomaly is most often asymptomatic, but dysphagia lusoria has been reported, especially in association with a bovine arch. Associations with trisomy 21, 18 and other chromosomal defects have been reported [16].

Thyroidea Ima Artery

The thyroidea ima artery is present in about 8% of the population. It is an uncommon variant of the blood supply to the inferior aspect of the thyroid gland and the trachea. It can arise from the brachiocephalic trunk (Fig. 7.15), right common carotid artery, aortic arch, or internal thoracic artery. It is usually present when there is no inferior thyroid artery. If unrecognized, the thyroidea ima artery can be a source of brisk, potentially fatal bleeding that can be difficult to control during head and neck surgery [2, 19].

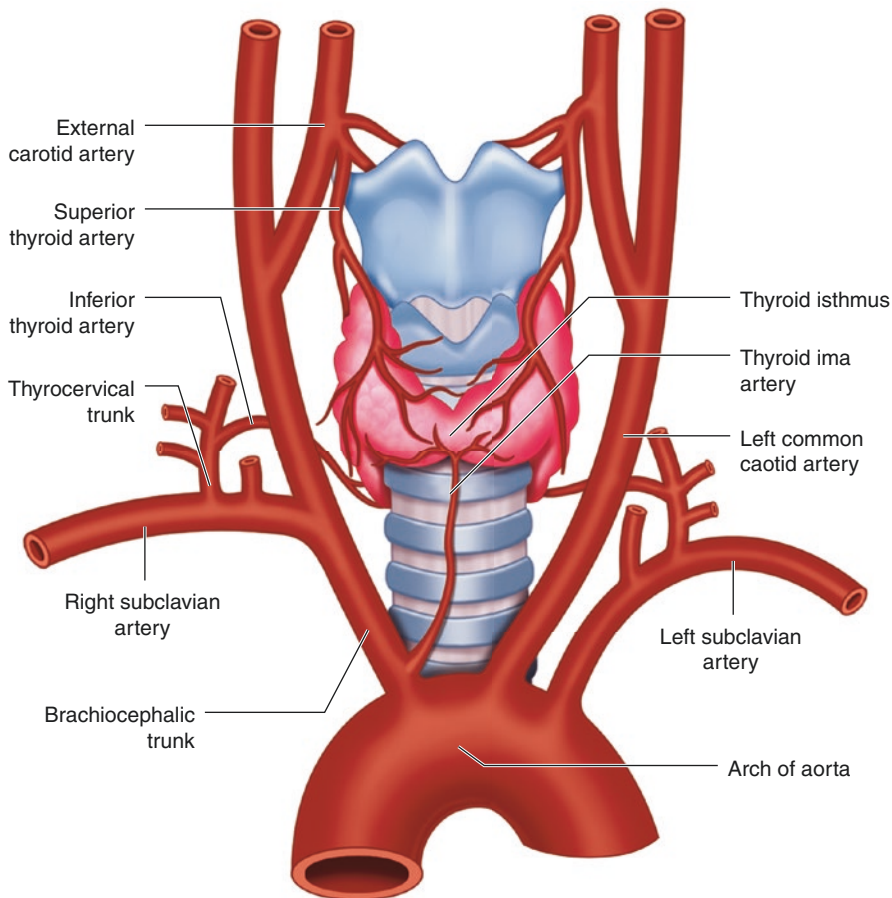


Fig. 7.15 Thyroidea ima artery

Common Brachiocephalic Trunk

A common brachiocephalic trunk is an anatomic variant in which both common carotid arteries and the right subclavian artery arise from the aortic arch via a single trunk (Fig. 7.16). This is a rare variant, with an incidence less than 5%, but when it is present, other congenital malformations can be found in 98% of cases. Also, it is linked to genetic syndromes [20].

Anomalous Origin of the Pulmonary Artery

An anomalous pulmonary artery forms when a pulmonary artery branch arises separately from the main pulmonary artery. These are the main variations [2]:

- *Anomalous right pulmonary artery (RPA)*: The embryonic branch of the pulmonary artery joins the right side of the thoracic aorta sac, but fails to join the main

Fig. 7.16 Common brachiocephalic trunk

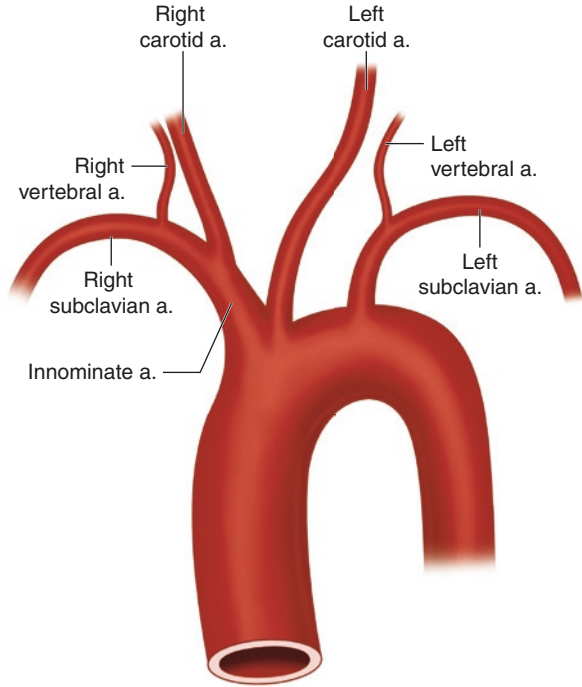
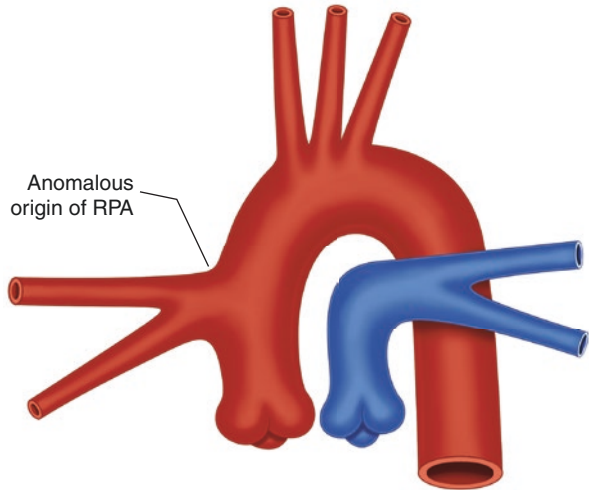


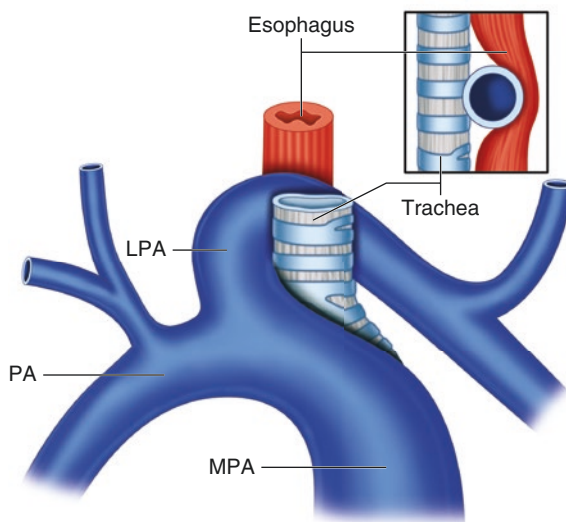
Fig. 7.17 Anomalous right pulmonary artery (RPA)



pulmonary artery before septation (Fig. 7.17). There is a high incidence of associated aorticopulmonary septal defect.

- *Anomalous left pulmonary artery (LPA)*: This less common anomaly is associated with tetralogy of Fallot in 74% of cases. The embryonic branch pulmonary artery fails to join the truncus arteriosus sac. This anomaly usually presents as congestive cardiac failure in infancy, followed by early development of pulmonary vascular disease.

Fig. 7.18 Anomalous origin of LPA from RPA



- *Anomalous origin of LPA from RPA*: The LPA arises from the RPA and passes between the trachea and the esophagus, forming a pulmonary artery sling (Fig. 7.18). Tracheal compression can lead to severe respiratory distress and stridor. This is usually an isolated anomaly, rarely associated with tetralogy of Fallot. The LPA passes behind the trachea before joining the truncus arteriosum sac. This variant can be identified anteriorly on barium swallow.

Conclusion

Aortic arch anatomic variants can be easily interpreted on the basis of embryology. Understanding normal aortic arch embryology and anatomy provides an excellent basis for better understanding and interpretation of its anatomic variants. Intervention is required only when variants are symptomatic or are associated with other cardiovascular anomalies.

References

1. Murillo H, Lane MJ, Punn R, Fleischmann D, Restrepo CS. Imaging of the aorta: embryology and anatomy. *Semin Ultrasound CT MR*. 2012;33:169–90.
2. Mavroudis C, Backer CL. *Pediatric cardiac surgery*. 4th ed. Hoboken: Wiley-Blackwell; 2013.
3. Knipe H, D'Souza D, et al. Variant anatomy of the aortic arch. <https://radiopaedia.org/articles/variant-anatomy-of-the-aortic-arch>. Accessed 22 Jan 2019.
4. Celikyay ZR, Koner AE, Celikyay F, Deniz C, Acu B, Firat MM. Frequency and imaging findings of variations in human aortic arch anatomy based on multidetector computed tomography data. *Clin Imaging*. 2013;37:1011–9.

5. Ryu C, Puchalski J, Perkins M, Honiden S. Management of an elderly patient with respiratory failure due to double aortic arch. *Respir Med Case Rep*. 2015;17:37–9.
6. Ka-Tak W, Lam WW, Yu SC. MDCT of an aberrant right subclavian artery and of bilateral vertebral arteries with anomalous origins. *AJR Am J Roentgenol*. 2007;188:W274–5.
7. Chai OH, Han EH, Kim HT, Song CH. Right-sided aortic arch with the retroesophageal left subclavian artery as the fourth branch. *Anat Cell Biol*. 2013;46:167–70.
8. Grillo HC, Wright CD. Tracheal compression with “hairpin” right aortic arch: management by aortic division and aortopexy by right thoracotomy guided by intraoperative bronchoscopy. *Ann Thorac Surg*. 2007;83:1152–7.
9. Norwood WI Jr. Hypoplastic left heart syndrome. *Ann Thorac Surg*. 1991;52:688–95.
10. Celoria GC, Patton RB. Congenital absence of the aortic arch. *Am Heart J*. 1959;58:407–13.
11. Collins-Nakai RL, Dick M, Parisi-Buckley L, Fyler DC, Castaneda AR. Interrupted aortic arch in infancy. *J Pediatr*. 1976;88:959–62.
12. Farsak B, Yilmaz M, Kaplan S, Böke E. Cervical aortic arch with aneurysm formation. *Eur J Cardiothorac Surg*. 1998;14:437–9.
13. Edwards JE. Anomalies of the derivatives of the aortic arch system. *Med Clin North Am*. 1948;32:925–49.
14. Grollman JH. The aortic diverticulum: a remnant of the partially involuted dorsal aortic root. *Cardiovasc Intervent Radiol*. 1989;12:14–7.
15. Goodman PC, Jeffrey RB, Minagi H, Federle MP, Thomas AN. Angiographic evaluation of the ductus diverticulum. *Cardiovasc Intervent Radiol*. 1982;5:1–4.
16. Donnelly LF, Fleck RJ, Pacharn P, Ziegler MA, Fricke BL, Cotton RT. Aberrant subclavian arteries: cross-sectional imaging findings in infants and children referred for evaluation of extrinsic airway compression. *AJR Am J Roentgenol*. 2002;178:1269–74.
17. Dumfarth J, Chou AS, Ziganshin BA, Bhandari R, Peterss S, Tranquilli M, et al. Atypical aortic arch branching variants: a novel marker for thoracic aortic disease. *J Thorac Cardiovasc Surg*. 2015;149:1586–92.
18. Becker C, Csatai Z, Pfeiffer J. Truncus bicaroticus: an underestimated anatomic variation. *Laryngoscope*. 2014;124:1141–2.
19. Krudy AG, Doppman JL, Brennan MF. The significance of the thyroidea ima artery in arteriographic localization of parathyroid adenomas. *Radiology*. 1980;136:45–51.
20. Moskowitz WB, Topaz O. The implications of common brachiocephalic trunk on associated congenital cardiovascular defects and their management. *Cardiol Young*. 2003;13:537–43.

Part III

Abdominal Cavity



Anatomy of the Gastrointestinal System

8

Glenn Geesman, Quinto J. Gesiotto, Zain Lalani,
and Nizar Tejani

Surface Anatomy

Landmarks

The palpable landmarks of the abdomen are the linea alba, which divides left from right and crosses the umbilicus along the midline of the abdomen, and the linea semilunaris, which defines the lateral border of the rectus abdominis muscle in the midclavicular line. Also of note is the pubic crest at the midline and most inferior point of the anterior abdominal wall. Moving laterally, one can identify the superficial inguinal ring, the inguinal ligament, and the anterior superior iliac spine (ASIS). Continuing superiorly along the skeletal border of the abdomen, one palpates the costal margin and finally the xiphoid process of the sternum at the midline most superior point on the anterior abdomen.

The muscular anatomy of the anterior abdominal wall can also be partially appreciated upon gentle palpation. Medial to the linea semilunaris and on either side of the linea alba run the rectus abdominis between the pubic symphysis, pubic crest, and pubic tubercle and the xiphoid process and costal cartilages of ribs 5, 6, and 7. Palpable within these muscle bodies and visible in individuals with a lean body habitus are the horizontal tendinous insertions that divide the “six-pack” of a well-defined abdominal muscle wall. Laterally to the linea semilunaris, and wrapping the

G. Geesman

GME General Surgery, Riverside Community Hospital, Riverside, CA, USA

Q. J. Gesiotto

Tampa General Hospital, University of South Florida, Tampa, FL, USA

Z. Lalani

Medical University of South Carolina, Charleston, SC, USA

N. Tejani (✉)

Ochsner–Louisiana State University Shreveport Health Sciences Center,
Shreveport, LA, USA

abdomen toward either flank bilaterally, is the external oblique muscle of the abdomen. The aponeurosis of the external oblique forms the inguinal ligament inferiorly; medially, fibers at the linea semilunaris wrap around the rectus abdominis before decussating at the linea alba. The external oblique originates at the outer surfaces of ribs 5–12, and inserts at the linea alba, the pubic symphysis and tubercle, and the anterior superior iliac spine and the iliac crest. The external oblique may not be easily visualized in more obese patients due to the common accumulation of subcutaneous fat overlying the external oblique, colloquially referred to as “love handles.”

Regions

Two methods exist for dividing the abdomen into regions. The preferred method designates four quadrants separated vertically by the linea alba at the sagittal midline and horizontally by the transverse umbilical plane. The less common (yet still useful) method divides the abdomen into nine regions, with three columns and three rows. The most superior row includes the right hypochondriac, epigastric, and left hypochondriac regions. The middle row consists of the right lumbar, umbilical, and left lumbar regions. The most inferior row contains the right iliac (inguinal), pubic (hypogastric), and left iliac (inguinal) regions.

Esophagus

Overview

The esophagus, in a general sense, connects the alimentary canal between the oropharynx and stomach, and is separated into three divisions: cervical, thoracic, and abdominal. The cervical division is between the upper esophageal sphincter (usually around C6) down to T1. The thoracic division lies between T1 and the diaphragm (the esophageal hiatus where the esophagus penetrates the diaphragm is around the level of T10). And the abdominal division lies between the diaphragm and the lower esophageal sphincter at the cardiac orifice of the stomach. As the alimentary tract descends via the esophagus, it moves along the right side of the thoracic aorta before crossing it anteriorly to penetrate the diaphragm. The upper esophagus runs down the posterior mediastinum, neighbored anteriorly by the trachea and posteriorly by the vertebral column. Inferior to the bifurcation of the trachea, the esophagus travels posterior to the right pulmonary artery, left main bronchus, and left atrium. The lower esophagus is posterior to the heart and anterior to the thoracic aorta. The thoracic duct passes posteriorly to the esophagus, lying posteriorly and to the right of the inferior portion of the esophagus, and posterior and to the left of the superior portion. Other noteworthy structures neighboring the esophagus are the hemiazygos veins and right intercostal veins posteriorly, as well as the vagus nerve, which divides left and right (anteriorly and posteriorly, respectively), and wraps the esophagus in its esophageal plexus.

Structure

The structure of the esophagus can be visualized as a long, muscular tube that connects the pharynx and stomach. Beginning at the cricothyroid cartilage at the C6 level, the esophagus spans 25 cm long and has an average diameter of about 2 cm. It is divided into three parts: cervical (C6-T1), thoracic (T1-esophageal hiatus of the diaphragm), and abdominal (esophageal hiatus-gastric cardia). The esophagus penetrates the diaphragm at T10. The route of the esophagus is both anatomically and clinically significant, as it lies to the right of the thoracic aorta and sits posterior to several important structures including the trachea, tracheal bifurcation, and the left atrium of the heart.

The esophageal wall is comprised of four layers: mucosa, submucosa, muscularis propria, and adventitia. It is important to note that the esophagus is the only portion of the gastrointestinal tract that does not contain a serosal layer. There are multiple layers of muscle that surround the esophagus and contribute to the waves of peristalsis along its length. These include the longitudinal muscle and circular muscle. The muscularis propria is an additional layer of muscle found deep to the mucosal lamina propria. Esophageal musculature is primarily composed of skeletal and smooth muscle. The proximal 5% contains solely skeletal muscle, while the middle 45% contains a mix of skeletal muscle and smooth muscle. The distal 50% is smooth muscle. Two sphincters are located in the proximal and distal portions of the esophagus. The upper esophageal sphincter is composed of skeletal muscle, while the lower esophageal sphincter is composed of smooth muscle.

Clinical Correlates

Achalasia is a disorder of esophageal dysmotility characterized by an inability to relax the lower esophageal sphincter and by lack of peristalsis. The disease is caused by damaged ganglion cells in Auerbach's plexus.

Tracheoesophageal fistulas (TEs) are congenital mesodermal defects that create a connection between the esophagus and trachea. The most common variant of TE is esophageal atresia with a distal tracheoesophageal fistula; this defect occurs in 85% of TE cases.

Embryology

Early in embryological development, the epiblast gives rise to ectoderm, mesoderm, and endoderm. This endoderm in turn becomes the whole gut tube, including the foregut, midgut, and hindgut. The foregut includes everything from the pharynx to the Ligament of Treitz.

The esophagus arises from the foregut and continues to grow in length until about the seventh week of gestation. Recanalization of the esophagus is complete by the end of week 8. Mesenchymes from pharyngeal arches four and six give rise to the striated muscles of the upper and middle thirds of the esophagus. Smooth

muscles in the middle and lower thirds of the esophagus are derived from splanchnic mesenchyme.

Clinical Correlates

Esophageal atresia occurs due to formation of the tracheoesophageal septum in a posterior direction, allowing patency between the trachea and upper esophagus. Isolated esophageal atresia is rare (5–7% of cases) and is caused by failure to recanalize the esophagus during week 8.

Innervation

The vagus nerve (cranial nerve X) provides parasympathetic innervation to the esophagus, initiating peristalsis and stimulating glandular contraction. This is executed via two sets of vagus nerve fibers. The upper striated muscle and the upper esophageal sphincter are supplied by neurons with cell bodies in the nucleus ambiguus, while neurons supplying the smooth muscle and lower esophageal sphincter are supplied by neurons with cell bodies in the dorsal motor nucleus. Sympathetic innervation of the esophagus is supplied by the sympathetic trunk, which may enhance the effects of the vagus nerve or relax the muscle wall and cause blood vessel constriction. Both nerves are involved in sensation—the vagus nerve receives general sensation and the sympathetic nerve receives pain signals.

Blood Supply

The cervical part of the esophagus is supplied bilaterally by the inferior thyroid artery, and rarely by branches directly from the thyrocervical trunk or common carotid artery. The cervical part is drained by the inferior thyroid vein and by the left brachiocephalic vein. The thoracic part of the esophagus is typically supplied by four to five esophageal arteries branching off the aorta. These are drained superiorly and to the left by the accessory hemiazygos vein or the left brachiocephalic vein, on the inferior left by the hemiazygos vein, and on the right side by the azygos vein. The abdominal part of the esophagus is supplied by the left gastric artery, which branches off the celiac trunk, and is drained by the left gastric vein, which drains into the portal vein (Fig. 8.1).

Lymphatic

The esophagus is lined with paraesophageal lymph nodes. The lymphatic drainage of these nodes is divided into three parts, based on the structural divisions described above. The cervical part drains cranially to the deep cervical lymph nodes, with subsequent drainage into the jugular trunk. The upper half of the thoracic part also drains cranially, while the lower half drains into the superior phrenic lymph nodes.

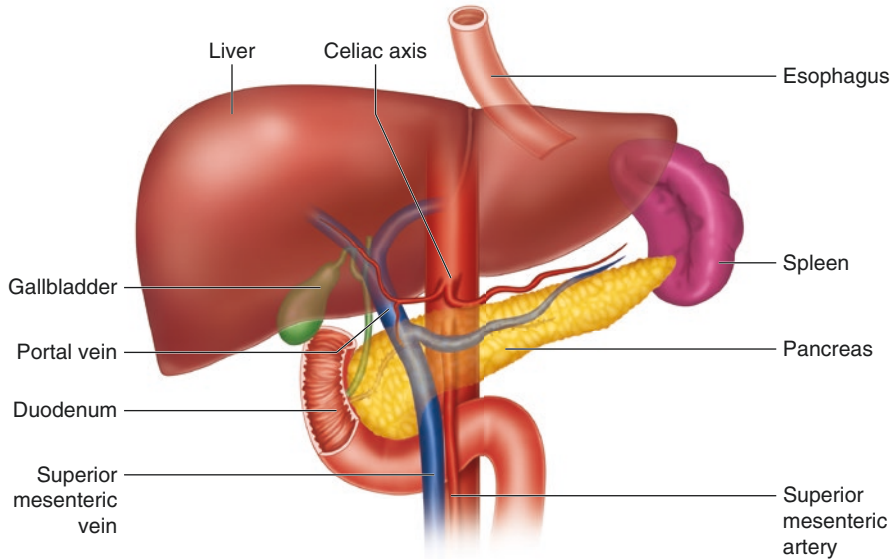


Fig. 8.1 Foregut structures

The lymph nodes of the abdominal part of the esophagus continue alongside the left gastric artery and drain into the gastric and celiac lymph nodes.

Histology

The alimentary canal surrounding the lumen is divided histologically into four sections. From the lumen outward, these are: mucosa, submucosa, muscularis externa, and serosa/adventitia. While the structure and composition of these layers vary slightly between divisions of the digestive tract, the overall architecture of the gastrointestinal wall remains constant.

The mucosa is divided into the inner epithelium, lamina propria, and muscularis mucosae. The epithelium aids in protection, secretion, digestion, and absorption, and its structure changes regionally to reflect these processes. The lamina propria is a loose connective tissue layer and is less fibrous than the underlying submucosal connective tissue (dense irregular). Here, absorption products from certain areas of the digestive tract enter blood and lymphatic vessels. The muscularis mucosae, a layer of smooth muscle fibers oriented in different directions, separates the lamina propria from the submucosa. Its contraction facilitates absorption and secretion by forming ridges and depressions in the intestinal wall.

The submucosa is a dense irregular connective tissue layer containing lymphatics and blood vessels that branch into smaller vessels to supply the mucosa, muscularis propria, and serosa. The submucosa also contains a network of nerves

composed of visceral sensory fibers (sympathetic), terminal ganglia (parasympathetic), and pre- and post-ganglionic parasympathetic nerve fibers. Here, small unmyelinated parasympathetic ganglia form the submucosal plexus (Meissner's plexus).

The muscularis externa (muscular layer) typically contains two sheets of smooth muscle: a circular inner layer and a longitudinal outer layer. There are exceptions to this structure in some areas of the digestive tube, which will be discussed in detail later. Between the two main layers of the muscularis externa lies a thin connective tissue layer containing blood vessels, lymphatics, and nerves. These parasympathetic nerve cells constitute the myenteric plexus (Auerbach's plexus). *Note: The inner circular muscular layer thickens in several points along the digestive tract to form structurally significant sphincters and valves. These will be discussed in each subsection.*

The alimentary canal is enclosed in a serosa or adventitia, constituting the outermost layer. Serosa consists of mesothelium (single squamous epithelium) and an underlying thin connective tissue layer. Serosa is continuous with the mesentery and the abdominal cavity lining, and therefore borders areas of the digestive tract that are suspended within the peritoneum. The serosa contains large blood vessels, lymphatics, and nerves, and sometimes adipose tissue. Areas without serosa (i.e., those in the abdominal and pelvic areas that are fixed to the cavity wall) instead contain adventitia, a connective tissue layer continuous with the connective tissue of the body wall.

These four main layers constitute the general structure of the digestive tract wall. The following sections describe the unique histological features of each main division.

The lumen of the collapsed esophagus has an irregular, folded appearance histologically. The mucosal layer is characterized by nonkeratinized stratified squamous epithelium that serves a protective function against the physical distress of food. Cells of the esophageal epithelium have a high turnover rate, and pathologic metaplasia is seen in Barrett's esophagus (stratified squamous epithelium to simple columnar epithelium with goblet cells).

There are two main types of glands in the esophagus, and these differ in location and structure. Esophageal glands proper are visible in the submucosa along the entire length of the esophagus but are more concentrated in the upper half. These tubuloalveolar glands are characterized by an exocrine duct lined with stratified squamous epithelium, and they produce a slightly acidic mucus that lubricates the lumen. Esophageal cardiac glands are located in the lamina propria of the mucosa and are more concentrated in the terminal part of the esophagus. Glands near the stomach serve a protective function against acidic stomach contents, and their dysfunction may lead to reflux.

The upper two-thirds of the esophagus notably contains a striated muscularis externa, distinguishing this section from the smooth muscle found in the remaining third and the rest of the digestive tract. This striated muscle is innervated by the vagus nerve (cranial nerve X).

The esophagus is surrounded by adventitia.

Physiology

The esophagus' specific muscle types and their distribution were discussed earlier in this chapter. For physiological purposes, the esophagus is split into thirds. The upper third of the esophagus is comprised mostly of striated skeletal muscle, with smooth muscle becoming more prevalent distally. The remainder of the esophagus (and the whole gastrointestinal tract) is composed primarily of smooth muscle. This unitary smooth muscle is made up of cells coupled together via gap junctions to coordinate contractions.

The esophageal muscle is further subdivided by function, determined mainly by the fiber direction. Circular muscle forms rings that contract to decrease lumen diameter and increase pressure, usually behind (proximal to) a food bolus. Longitudinal muscles contract to shorten the length of a segment of the gastrointestinal tract.

Peristalsis is achieved in part by phasic contractions followed by relaxation. Tonic contractions are also present to maintain tone throughout the esophagus. Swallowing is initiated by the swallow reflex, also called the primary peristaltic wave. It propels food boluses distally, along with secondary peristaltic waves that help clear any remaining food.

Along with muscle contractions to propel food boluses, sphincters are present in strategic locations to counter the differences in relative pressure throughout the gastrointestinal tract. Intrathoracic esophageal pressure is equal to the pressure within the thorax, and both are less than atmospheric pressure. The abdomen creates a different pressure environment. Pressure within the abdomen is greater than the pressure within the abdominal esophagus. The upper esophageal sphincter functions to prevent air from entering the esophagus, while the lower esophageal sphincter functions to keep acidic stomach contents out of the esophagus.

Abdominal Cavity

Muscle Layers

The anterior abdominal wall has layers of vertical, transverse, and oblique muscles, with aponeuroses at the linea alba, linea semilunaris, and inferior border of the abdomen. From superficial to deep, the anterior abdominal wall consists of skin, superficial subcutaneous fatty tissue (Camper's fascia), superficial subcutaneous membranous tissue (Scarpa's fascia), external oblique muscle and aponeurosis, internal oblique muscle and aponeurosis, rectus abdominis muscle, transversus abdominis muscle and aponeurosis, transversalis fascia, and parietal peritoneum. There is some variability such that this order is not constant across the abdominal wall. Chiefly, the rectus abdominis is enveloped by a rectus sheath, a continuation and division of the aponeurosis of the internal oblique. The rectus sheath is bordered superiorly by the xiphoid process and inferiorly by the arcuate line (linea semicircularis) about half way between the umbilicus and the pubic crest, superior to which

the rectus abdominis lies anterior to continuations from the aponeurosis of the internal oblique and the transversus abdominis muscles, and inferior to which the rectus abdominis lies directly anterior to the transversalis fascia. The arcuate line also constitutes the height at which the inferior epigastric vessels penetrate the rectus abdominis.

The external oblique muscle originates from the outer surface of the fifth to the twelfth ribs, and inserts along the linea alba, the pubic crest and tubercle, the anterior superior iliac spine, and the iliac crest. It rotates the trunk toward the contralateral side and bends the trunk toward the ipsilateral side, squeezes and depresses the lower thoracic cavity to aid in expiration, weakly aids in trunk flexion, and contributes to abdominal muscle tone. It is innervated by the intercostal nerves, the iliohypogastric nerve, and the ilioinguinal nerve. It is supplied by the musculophrenic artery, the superior epigastric artery, the lumbar arteries, the superficial circumflex iliac artery, the deep circumflex iliac artery, the superficial epigastric artery, and the inferior epigastric artery.

The internal oblique muscle originates from the deep layer of the thoracolumbar fascia, the anterior two-thirds of the iliac crest, the lateral two-thirds of the inguinal ligament, and the iliopsoas fascia. It inserts on the lower margins of the ninth through the twelfth ribs, the pubic crest, and the anterior and posterior layers of the linea alba. The internal oblique acts in ipsilateral rotation and flexion of the trunk, compression of the abdomen, and antagonism of the diaphragm. It is innervated by the intercostal nerves from T7 to T12, the iliohypogastric nerve, and the ilioinguinal nerve. It is supplied by the musculophrenic artery, the superior epigastric artery, the anterior intercostal arteries, the lumbar arteries, the superficial circumflex iliac artery, the superficial epigastric artery, and the inferior epigastric artery.

The rectus abdominis muscle is a vertical muscle divided three to five times with horizontal tendinous intersections. It originates from the pubis and the pubic symphysis and inserts on the xiphoid process of the sternum and the costal cartilages of ribs five, six, and seven. It acts to compress the abdomen, flex the trunk, and stabilize the pelvis. It is innervated by anterior cutaneous intercostal nerves from T7 to T11. It is supplied by the superior epigastric artery, the anterior intercostal arteries, and the inferior epigastric artery.

Transversus abdominis muscle is a transverse muscle originating at the inner surface of the seventh to twelfth rib cartilages, the deep layer of the thoracolumbar fascia the anterior two-thirds of the iliac crest, and the lateral one-third of the inguinal ligament. It inserts on the linea alba, the pubic crest, and the pecten pubis. It acts to ipsilaterally flex and rotate as well as to flatten the abdomen. The transversus abdominis is innervated by the intercostal nerves from T7 to T12, the iliohypogastric nerve, and the ilioinguinal nerve. It is supplied by the musculophrenic artery, the superior epigastric artery, the superficial circumflex iliac artery, and the lumbar arteries.

The diaphragm internally divides the thorax from the abdomen and constitutes the superior border of the abdominal cavity. The diaphragm has two bilateral domes and three openings for the aorta, the vena cava, and the esophagus. The caval opening is most anterior of the three and slightly right of midline. The esophageal hiatus

is slightly left of midline and directly anterior to the aortic hiatus, which lies at the posterior border of the diaphragm against the vertebral column. The diaphragm has three parts, each defined by its origin: the costal part, the lumbar part, and the sternal part. The costal part originates on the inferior inner surface of the seventh through twelfth costal arches. The lumbar part originates medially on the L1, L2, and L3 vertebral bodies, intervertebral disks, and anterior longitudinal ligament as bilateral crura. The lumbar part originates laterally on the lateral and medial arcuate ligaments. The sternal part originates at the posterior surface of the xiphoid process of the sternum. The insertion of the diaphragm is at the central tendon, which fuses with the fibrous pericardium in the pericardiophrenic ligament. The diaphragm acts to increase intrathoracic volume, serving as the primary muscle of respiration during inhalation, and it also compresses the abdominal viscera inferiorly. The diaphragm is innervated by the phrenic nerve via contributions from C3, C4, C5, and the cervical plexus. It is supplied by the musculophrenic artery, the superior phrenic artery, and the inferior phrenic artery.

The posterior abdominal wall muscles, namely the quadratus lumborum, psoas minor, psoas major, and iliacus muscles are functionally muscles of the hip, and will be explored elsewhere.

Abdominal Structures

The abdominal cavity contains both intraperitoneal and retroperitoneal structures. Intraperitoneal structures are contained within the parietal peritoneum and include the stomach, superior duodenum, jejunum, ileum, cecum, transverse colon, and sigmoid colon. Other intraperitoneal organs are the liver, tail of the pancreas, gallbladder, and spleen. Retroperitoneal structures include the suprarenal glands, abdominal aorta, inferior vena cava, horizontal and ascending duodenum, pancreas (head, uncinate process, neck, and body), ureters, ascending and descending colon, kidneys, and rectum.

The abdomen has an abundance of extensions and folds that serve various purposes including containment of neurovascular and lymphatic vessels and tethering of local structures. The omentum is one such extension that connects the lesser and greater curvatures of the stomach with adjacent viscera. The lesser omentum is a double-layered peritoneal fold that joins the lesser curvature of the stomach and initial segment of the duodenum to the liver. Within the lesser omentum are the hepatogastric and hepatoduodenal ligaments. The membranous hepatogastric ligament contains the left and right gastric arteries. The thicker and more peripheral hepatoduodenal ligament contains the portal triad: portal vein, hepatic artery, and bile duct. The greater omentum is derived from the dorsal mesentery and is a quadruple-layered peritoneal fold that drapes over the bowels. It is bound to the greater curvature of the stomach and attaches to the transverse colon and its mesentery. The greater omentum functions to not only contain the left and right gastro-omental vessels, but also to restrict diffuse peritoneal inflammation by encasing inflamed organs. The greater omentum contains the gastrolial, lienorenal, gastrophrenic, and gastrocolic ligaments.

The peritoneal cavity can be subdivided into two sacs: the greater sac and the lesser sac (omental bursa). The greater sac is an anterior space that spans the entire abdomen, bounded by the diaphragm and the pelvic floor. There are important recesses formed by the greater sac that may collect fluid, including blood, pus, and serous fluid. The hepatorenal recess, commonly known as Morrison's pouch, is a deep recess located between the liver and right kidney. The splenorenal recess is located between the spleen and left kidney. Paracolic gutters (recesses) are located lateral to the ascending and descending colon. The omental bursa is a smaller cavity that lies posteriorly to the lesser omentum. The lesser sac is situated between the pancreas and the stomach and extends superiorly to the diaphragm, posterior to the liver. The omental bursa also extends inferiorly, lying between the transverse mesocolon and greater omentum. The foramen of Winslow, or epiploic foramen, is an opening that allows for communication between the greater and lesser sacs.

Another double-layered peritoneal fold is the mesentery. Mesentery contains neurovascular and lymphatic structures, suspends intraperitoneal organs, and attaches organs to the abdominal wall. The mesentery proper holds the jejunum and ileum and roots the bowels to the posterior abdominal wall. This root travels inferiorly from the duodenojejunal flexure to the right iliac fossa. The transverse mesocolon is fused with the greater omentum and attaches the transverse colon to the posterior abdominal wall. This fusion creates the gastrocolic ligament and contains nerves, lymphatics, and vessels of the middle colic artery and vein. The sigmoid mesocolon tethers the sigmoid colon to the pelvic wall. The appendix is bound to the ileal mesentery by the mesoappendix.

The last set of peritoneal folds are the umbilical folds. These include the median fold and paired medial and lateral folds. The median umbilical fold contains remnants of the urachus. The medial umbilical ligaments contain remnants of the fetal umbilical arteries. The lateral umbilical folds contain the inferior epigastric arteries and veins.

Inguinal Canal

The inguinal canal is an important anatomical landmark. Its most inferior border is made up of the lacunar and the inguinal lacunar ligaments. The aponeuroses of both the external and internal oblique muscles comprise the anterior border. Posteriorly, the inguinal canal is bordered by the aponeurosis of the transverse abdominal muscle and fascia. The superior border is made up of muscle fibers from the transverse abdominal muscle and internal oblique muscle.

Clinically, the inguinal canal is a common surgical site for hernia repair. Normally, the canal contains the ilioinguinal nerve (L1), blood and lymphatic vessels, and the spermatic cord (in males) or the round ligament of the uterus (in females). The entrance to the inguinal canal is demarcated by the deep inguinal ring, formed by evagination of the transversalis fascia. It is located lateral to the inferior

(deep) epigastric artery at the midpoint between the anterior superior iliac spine and pubic tubercle. The inguinal canal ends at the superficial ring, formed by the aponeurosis of the external oblique. The superficial inguinal ring is located lateral to the pubic tubercle, superior to the pubic crest.

Stomach

Overview

The stomach lies between the esophagus and the duodenum, participates in the mechanical and enzymatic digestion of food, and some absorptive and gastrointestinal hormone-regulating roles. Many surgeries involve the stomach, from gastrectomy for stomach cancers to pyloromyotomy to treat infantile hypertrophic pyloric stenosis; not to mention the increasingly popular bariatric surgeries, in which the stomach is often functionally modified or bypassed in some way to aid in the treatment goal for weight loss.

The stomach is positioned left of midline with the fundus of the stomach immediately inferior to the left dome of the diaphragm. On its right side, the lesser curvature, the stomach is attached to the liver via the hepatogastric ligament within the lesser omentum. The left lobe of the liver partially overlaps the stomach anteriorly, but the stomach otherwise makes unobstructed contact with the anterior parietal peritoneum. Adjacent to the stomach posteriorly, from medial to lateral, is the pancreas, the omental bursa, and the spleen. The greater curvature of the stomach is attached inferiorly to the transverse colon via the greater omentum, which hangs inferiorly to the level of the small intestines before doubling back on its way to enclose the transverse colon.

Structure

The stomach is a sac-like pouch that connects the esophagus and duodenum (small intestine). The function of the stomach is to store and digest food both mechanically and chemically. It has a superior lesser curvature, an inferior greater curvature, and anterior and posterior walls. The stomach musculature is composed of three layers from superficial to deep: longitudinal, circular, and oblique. The oblique muscular layer is unique to the stomach (Fig. 8.2).

The stomach has four regions. The cardia is the entrance to the stomach at the gastroesophageal (GE) junction. The fundus is the superior pouch of the stomach located inferior to the apex of the heart at the level of the fifth rib; this region participates in receptive relaxation, which is discussed further in the physiology section. The body is the central region of the stomach. The pylorus is the most distal region. This houses the pyloric sphincter, thickened smooth muscle that controls the flow of contents between the stomach and superior duodenum.

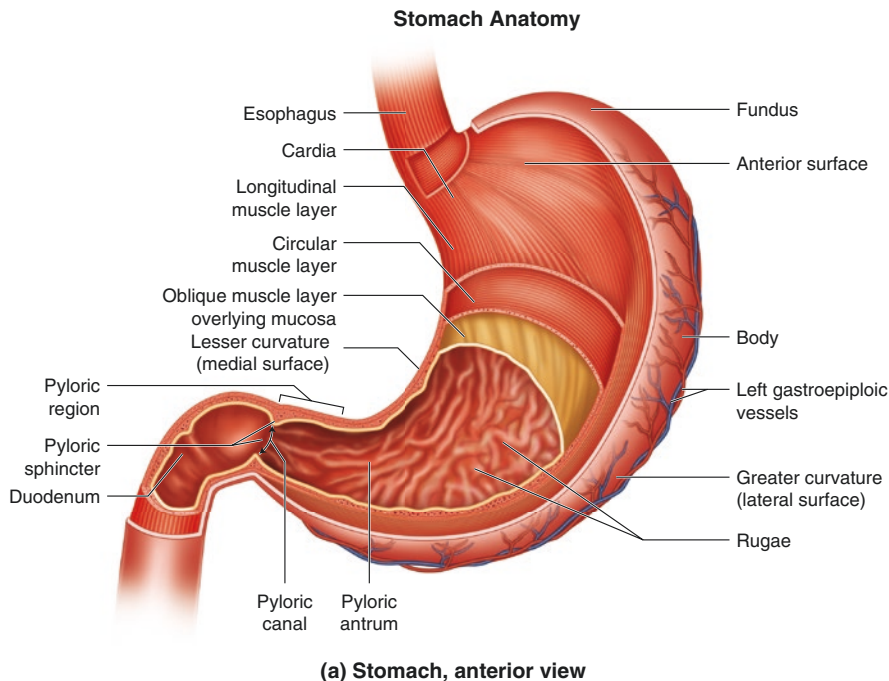


Fig. 8.2 Stomach anatomy

Embryology

Dilation at the distal foregut in week 4 signifies the formation of the early stomach. The next two weeks feature increased growth at the dorsal border of the stomach relative to the ventral border, leading to the greater curvature and lesser curvature of the stomach, respectively.

As the stomach grows, it begins to rotate 90° clockwise (from a cranial perspective), placing the greater curvature (initially dorsal) on the left and the lesser curvature (initially ventral) on the right. This rotation is evidenced by the left vagus nerve's innervation of the anterior wall of the stomach, whereas the right vagus nerve innervates the posterior wall.

Innervation

Innervation of the stomach is provided from several sources. Sympathetic fibers from the splanchnic nerves and celiac ganglion supply muscle and blood vessels. Parasympathetic innervation is provided by the gastric branches of the vagus nerves—acid secretion is mediated by acetylcholine and gastrin-releasing peptide (indirect). Sensory innervation is also received by the vagus nerve.

The stomach has many endocrine functions and is involved in the hormonal control of digestion. Ghrelin, secreted by P/D1 cells in the fundus of the stomach, is a neuropeptide which stimulates hunger through activation of the arcuate nucleus and vagus nerve. Gastrin is produced by G cells in the antrum of the stomach and stimulates gastric acid secretion, gastric mucosa growth, and motility. Histamine also stimulates acid secretion. Somatostatin, produced in the pancreas and hypothalamus, and secretin, produced in duodenal S cells, are inhibitors of gastric acid production. Cholecystokinin (CCK) is synthesized by I cells in the duodenum and jejunum and acts to decrease gastric emptying.

Blood Supply

The stomach is supplied by vessels that follow the borders of the lesser and greater curvatures. Along the lesser curvature runs the anastomosis of the left and right gastric arteries. The left gastric artery arises from the celiac trunk; supplies the lower esophagus, cardia, fundus, and body; and travels inferiorly along the lesser curvature to anastomose with the right gastric artery traveling superiorly along the lesser curvature from the proper hepatic artery (less commonly the common hepatic artery) while it supplies the pylorus and body. Along the greater curvature, within the greater omentum, moving from right to left, the right gastroepiploic (gastro-omental artery) branches off the gastroduodenal artery and supplies the pylorus and body on its way to anastomose with the left gastroepiploic (gastro-omental) artery. The left gastroepiploic artery branches inferiorly off the splenic artery, where it travels left to right through the greater omentum along the greater curvature supplying the body. Finally, the supply to the fundus is supplemented by the short gastric arteries, which branch superiorly off the splenic artery. The arteries supplying the stomach each have corresponding veins that shadow each other's path along the surface of the stomach. The left gastric vein drains the lower esophagus, cardia, fundus, and body into the hepatic portal vein. The right gastric vein drains the pylorus and body into the hepatic portal vein. The right gastroepiploic vein drains the pylorus and body into the superior mesenteric vein. The short gastric veins and the left gastroepiploic veins drain the body and fundus into the splenic vein.

Lymphatic

Lymphatic drainage of the stomach closely follows arterial vessels lining the greater and lesser curvatures. As such, lymph from the stomach initially drains into clusters of nodes including the gastric, gastro-omental, pancreaticosplenic, and pancreaticoduodenal lymph nodes. These nodes drain into the celiac lymph nodes and ascend superiorly.

Histology

The esophagogastric junction marks the division between the esophagus and the stomach. This junction is characterized by an abrupt transition from the nonkeratinized stratified squamous epithelium of the esophagus to the simple columnar epithelium of the gastric mucosa.

The stomach mucosa and gastric pits are lined with a simple columnar epithelium. The inner surface of the collapsed stomach contains longitudinal folds called rugae, which are far less visible upon distention. Gastric glands are visible at higher magnification—these open into the bottom of gastric pits.

The gastric muscularis externa is unique from other gastrointestinal organs and contains three muscular layers: inner oblique, middle circular, and outer longitudinal. Auerbach's plexus is located between the middle circular and outer longitudinal layers.

Physiology

As food continues its journey and leaves the esophagus, it must pass through the lower esophageal sphincter to enter the stomach. Upon relaxation of the sphincter, the orad region of the stomach undergoes receptive relaxation via the vagovagal reflex to increase volume and lower pressure to accept the food. The caudad region of the stomach contracts to break down and mix food with gastric juices, which are highly acidic in order to digest food into chyme. Contractions increase in strength as they approach the pylorus. In the presence of contractile waves, the pylorus closes to allow further mixing of contents via retropulsion. When empty, the stomach lumen is comparable in caliber to that of the large intestine. However, it can expand to accommodate up to 2–3 liters.

Small Intestine

Overview

The small intestine begins after the pyloric sphincter and ends at the ileocecal junction. Spanning 22 feet, the small intestine is the principal site of absorption of water, nutrients, and electrolytes in the human body. The small intestine is divided into three parts: the duodenum, jejunum, and ileum (Fig. 8.3).

Structure

The small intestine ranges from the pylorus of the stomach to the ileocecal junction, including the duodenum, jejunum, and ileum. The C-shaped duodenum is the first part of the small intestine and is also the shortest (25 cm in length) but widest and least mobile part. The organ is mostly retroperitoneal, except for the superior (first)

Fig. 8.3 Human gastrointestinal tract



part. It ranges from the pylorus of the stomach (anterolateral to L1) to the duodenojejunal flexure, which is usually an acute angle approximately at the level of the L2 vertebra, 2–3 cm left of the midline. The descending (second) part is retroperitoneal, travels from the level of L1 to L3, and includes the major and minor papillae, where the main pancreatic duct and accessory pancreatic duct empty, respectively. The transverse (third, and longest) part courses anterior to the IVC, aorta, and L3 of the vertebral column, posterior to the superior mesenteric vessels. The ascending (fourth) part is short and begins left of L3, rises up to the superior part of L2, and ends at the duodenojejunal junction, which is fixed via the suspensory ligament of Treitz to the right crus of the diaphragm posterior to the stomach and pancreas.

The second part of the small intestine is the jejunum, beginning at the duodenojejunal flexure. It makes up two-fifths of the intraperitoneal portion of the small intestine, lying mostly in the left upper quadrant (LUQ) of the abdomen.

The last part of the small intestine is the ileum, which ends at the ileocecal junction. It makes up three-fifths of the intraperitoneal portion of the small intestine, lying mostly in the right lower quadrant (RLQ) of the abdomen.

There is no clear delineation between the jejunum and ileum, but important distinctions exist. The jejunum with its thick and heavy walls is a deeper red color, whereas the thin and light ileal walls are a paler pink. The jejunum is surrounded by less mesenteric fat than the ileum. The vasculature of the small intestine also serves to distinguish jejunum from ileum. Jejunal vasculature is much greater, with few large loops of arcades and long vasa recta. Vasculature supplying the ileum is much more sparse, including many short loops of arcades and short vasa recta.

Embryology

The embryology of the small intestines is complicated by the partitioning of the small intestine into the foregut, the midgut, and the hindgut. In the fourth week of gestation, the duodenum begins to develop from the caudal portion of the foregut and the cranial portion of the midgut.

The quickly growing duodenum projects ventrally as it forms its characteristic C-shaped loop while the stomach rotates it to the right and presses it against the posterior abdominal wall. The duodenum is derived from the foregut and midgut divided at the opening of the bile duct, which explains why it is supplied by branches of the celiac trunk and superior mesenteric arteries, each associated with their respective parts of the primordial digestive tract. Problems in duodenal development can contribute to duodenal stenosis or duodenal atresia.

The midgut develops further into the rest of the small intestine, the cecum, appendix, ascending colon, and right portion of the transverse colon, all supplied by the superior mesenteric artery (SMA). During the elongation of the midgut in development, the midgut loop forms as a ventral U-shaped loop of intestine that undergoes physiologic umbilical herniation by projecting into the remains of the extraembryonic coelom at the proximal end of the umbilical cord, where it communicates with the umbilical vesicle (yolk sac) until the tenth week via the omphaloenteric duct. While in the umbilical cord, the midgut loop rotates counterclockwise 90° around the ventrally projecting superior mesenteric artery. This rotation moves the cranial end of the loop (what will become the small intestine) to the right, and the caudal end of the loop (what will become the large intestine) to the left. It is during this time that the intestinal loops elongate and begin to form the primordial jejunum and ileum.

In the tenth week, the intestine retracts back into the abdomen as the midgut hernia is reduced. The small intestine retracts first, moving superior to the superior mesenteric artery and occupying the central abdomen. The large intestine then retracts, meanwhile undergoing a counterclockwise rotation of 180°. The persistence of the herniation and the failure of the intestine to retract result in congenital omphalocele, which occurs in 1 in 5000 births and requires surgical repair. Problems with the hernia reduction are associated with an imperfectly closed umbilicus, which can result in umbilical hernia, another surgically treatable problem. The mesentery is at first attached to the posterior abdominal wall at the midline, but after the mesentery of the ascending colon disappears, the attachment of the mesentery of the small intestine moves to pass from the duodenojejunal junction inferolaterally to the ileocecal junction.

Innervation

Sympathetic stimulation of the small intestine induces vasoconstriction and halts digestion by inhibiting peristalsis and secretory activity. This frees up blood and energy for “fight or flight” activity. Presynaptic sympathetic nerve fibers originate

in the spinal cord (T8/T9–T10/T11) and travel through the sympathetic trunk and greater and lesser splanchnic nerves, eventually synapsing in the celiac plexus. Postsynaptic fibers follow the superior mesenteric artery and its branches to the intestine.

Parasympathetic stimulation of the small intestine stimulates digestion by increasing peristalsis and intestinal secretion. Presynaptic parasympathetic nerves originate in the medulla oblongata and travel to the intestine via the posterior vagal trunk, synapsing with postsynaptic neurons located in the intestinal wall.

Sensory (afferent) fibers receive distention information from the small intestine and travel via spinal nerves.

Blood Supply

The duodenum is supplied by anastomoses of the anterior and posterior branches of the superior pancreaticoduodenal artery from the celiac trunk (feeding the duodenum proximal to the major papilla) with the anterior and posterior branches of the inferior pancreaticoduodenal artery from the superior mesenteric artery (feeding the duodenum distal to the entry of the bile duct). This anastomosis demarcates the transition from the foregut to the midgut.

The duodenal blood supply drains into the hepatic portal vein, with some of the veins directly emptying into the hepatic portal vein and others indirectly via the superior mesenteric and splenic veins.

The superior mesenteric artery (SMA), arising at the level of L1 from the abdominal aorta, supplies the jejunum and ileum via the jejunal and ileal arteries. The many branches unite to form loops called arcades, which further branch into straight arteries called vasa recta.

Both the jejunum and ileum are drained by the superior mesenteric vein (SMV), coursing anteriorly and to the right of the SMA. The SMV ends at the neck of the pancreas and combines with the splenic vein to become the hepatic portal vein.

Lymphatic

The lymphatic vessels of the duodenum differ in anterior and posterior drainage. The pancreaticoduodenal and pyloric lymph nodes drain the anterior lymphatic vessels. The superior mesenteric lymph nodes drain the posterior lymphatic vessels. While the lymphatic vessels in the duodenum follow major arteries, the lymphatic vessels in the jejunum and ileum run through the mesentery. Lymph follows three major levels of drainage. Lymph initially drains to juxta-intestinal lymph nodes, which are located near the intestinal wall. Next, efferent lymph vessels transport lymph to the mesenteric lymph nodes, which are dispersed among arterial arcades. Lastly, the superior central nodes near the root of the superior mesenteric artery drain into the superior mesenteric lymph nodes. Lymph from the terminal ileum is transported to the ileocolic lymph nodes.

The villi within the jejunum and ileum contain lacteals that aid in the absorption of fat and the fat-soluble vitamins A, D, E, and K. These unique lymphatic vessels drain into lymphatic plexuses found in the jejunal and ileal walls. The plexuses subsequently drain into lymphatic vessels traveling through the mesentery.

Histology

The three sections of the small intestine are lined by a similar simple columnar epithelium containing goblet cells and Paneth cells. However, there are important histological differences between the duodenum, jejunum, and ileum. Peyer's patches are located in the ileal lamina propria and aid in immune surveillance. Brunner's glands, which secrete an alkaline-rich solution, are found exclusively in the duodenal submucosa and are not seen in the jejunum or ileum. The exterior duodenum is lined by serosa (first part) and adventitia (second, third, and fourth parts).

Physiology

The small intestine moves chyme and absorbs nutrients. The movements of the small intestine generally combine mixing and propulsion via serial or isolated contractions. Mixing contractions cause segmentation of the small intestine between areas of localized concentric contraction like links of sausage, and each contraction lasts for less than a minute. These contractions are triggered by the stretching of the intestinal wall. The frequency of electrical slow waves in the intestine defines the frequency of mixing contractions, usually no more than one every 5 seconds, from the duodenum to the proximal jejunum. The basic electrical rhythm of the ileum is slower, where the maximal contraction frequency does not exceed eight or nine in a minute. These contractions function by way of the slow waves in the smooth muscle itself but are dependent upon background excitation from the myenteric nerve plexus.

The propulsive movements of the small intestine consist of peristaltic waves occurring anywhere in the small intestine, which propel the intestinal contents down the alimentary canal at 1 cm/min. These waves move toward the anus at 0.5–2.0 cm/sec, traveling from 3 to 5 centimeters per wave, slowing as the chyme approaches the large intestine. All in all, the transportation of chyme from the pylorus to the ileocecal valve takes from 3 to 5 hours.

Every day, the small intestine is capable of absorbing several kilograms of carbohydrates, 500 grams of fat, 500–700 grams of amino acids, and more than 20 liters of water, though it seldom operates at capacity. Water diffuses through the intestinal membrane, along an osmotic gradient into the blood of the intestinal villi. Water can also diffuse out of the plasma into the chyme in cases where hyperosmotic solutions enter the duodenum. Sodium is actively transported out of the lumen via antiporters with hydrogen atoms or via symporters with amino acids or glucose, and this process of moving cations out of the lumen draws chloride anions out of the lumen as

well. The sodium is pumped out of the epithelial cells and into the plasma via the sodium-potassium ATPase enzyme.

The proximal small intestine secretes a large amount of bicarbonate ions to neutralize acid in the lumen. When hydrogen ions combine with those bicarbonate ions, they form carbonic acid, which dissociates into carbon dioxide and water. The carbon dioxide is then readily absorbed into the blood vessels to be expelled via the lungs. This process represents the indirect absorption of bicarbonate ions by the small intestine. The distal small intestine secretes bicarbonate ions by way of a bicarbonate–chloride ion exchanger. This bicarbonate in the distal small intestine, and large intestine is responsible for neutralizing any acid byproducts of the bacterial flora therein. Calcium, iron, potassium, magnesium, and phosphate are all actively absorbed by the small intestine.

Carbohydrates are primarily absorbed as monosaccharides in the small intestine after digestion by di- and polysaccharide-ase enzymes. Glucose is transported by a sodium co-transporter. Galactose is transported via a similar mechanism. Fructose does not use a sodium co-transporter, but instead is absorbed via facilitated diffusion through the intestinal epithelium, though much of the fructose is phosphorylated prior to being metabolized to glucose while still within the intestinal epithelium.

Proteins are absorbed as amino acids, dipeptides, or tripeptides through the luminal membranes of the intestinal epithelial cells. This transport is powered by a sodium co-transport mechanism in the same way that governs glucose absorption. Most peptides and amino acids bind specific transport proteins, which also require coincident binding of a sodium ion before transport can occur. Some amino acids are transported by facilitated diffusion via special membrane transport proteins in a way similar to fructose transport.

Fats are absorbed as monoglycerides and fatty acids secondary to digestion and emulsification by lipase and bile salts, respectively. Among the microvilli of the intestinal cell brush border, the micelles of emulsified lipids release their nutrients to freely diffuse into the epithelial cells due to the lipophilic nature of the cell membrane. The micelles are key to exposing the dietary fats to the intestinal epithelium, as 97% of the fat is absorbed this way, whereas only 40–50% of fat is absorbed in the absence of bile micelles. Within the epithelial cells the fatty acids and monoglycerides enter the smooth endoplasmic reticulum, where they primarily form new triglycerides that then exit the cell across the basolateral membrane into chylomicrons.

Large Intestine

Overview

The large intestine is the last site of water reabsorption, solidifying stool throughout the length of the organ. It begins at the cecum and ends at the rectum, including the appendix; ascending, transverse, descending, and sigmoid colon; and anal canal.

Omental appendices, teniae coli, and haustra differentiate large intestine from small intestine. The large intestine also has a much larger diameter.

Structure

The large intestine is made up of the cecum; the appendix; the ascending, transverse, descending, and sigmoid colon; the rectum; and the anal canal. The large intestine is distinguishable from the small intestine by the presence of omental appendices, teniae coli, haustra, and a much larger luminal diameter. The teniae coli, thickened smooth muscle, consist of three distinct longitudinal bands: the mesocolic tenia, which attaches to the transverse and sigmoid mesocolon; the omental tenia, which attaches to the omental appendices; and the free tenia, which is free of attachments to either mesocolon or omental appendix. The teniae coli begins at the base of the appendix, each running along the length of the large intestine before merging and encircling the rectum at the rectosigmoid junction. Distal to this point the omental appendices disappear. The teniae shorten the large intestine during contraction, causing the colon to become sacculated and thus forming the haustra.

Embryology

The large intestine is derived from both the midgut and hindgut. The distal part of the midgut loop develops into the distal ileum, cecum, appendix, ascending colon, and proximal two-thirds of the transverse colon. In the sixth week of development, the midgut loop begins to protrude into the extraembryonic coelom. By the eighth week of development, the midgut has fully herniated through the primitive umbilical ring. Around this time, the midgut begins its initial 90° counterclockwise rotation around the superior mesenteric artery, which serves as the axis of the midgut loop. The caudal portion of the midgut loop develops a bulge, commonly referred to as the cecal diverticulum. The appendix begins as a pouch at the apex of the cecum and grows rapidly to become a long tube. As the fetus grows, the abdominal cavity enlarges and allows for the retraction of the midgut. By the 11th week, the midgut rotates an additional 180° counterclockwise.

The hindgut develops into the distal one-third of the transverse colon, descending colon, and sigmoid colon.

It is important to note that the ascending and descending colon are secondary retroperitoneal structures. This is due to the fusion of each section's mesentery with the parietal peritoneum. The cecum, appendix, transverse colon, and sigmoid colon are all intraperitoneal structures.

Clinical Correlates

Omphalocele is a congenital anomaly due to the persistence of the physiological herniation of the midgut. During development, the midgut fails to retract back into the abdomen. As such, on presentation, the intestines will protrude through the umbilicus and will be covered by peritoneum. Infants with an omphalocele will

typically have normal gastrointestinal function. Omphalocele is often associated with Trisomy 21, 18, and 13 and may be accompanied by congenital heart defects, orofacial clefts, and neural tube defects.

Hirschsprung's disease—megacolon is a congenital neurocristopathy that causes massive dilatation of the colon. The failure of neural crest cell migration into the Meissner and Auerbach plexuses causes abnormalities in peristalsis and a failure to relax the distal sigmoid colon and rectum. This functional obstruction will manifest in the infant as failure to pass meconium, empty rectal vault on digital exam, and dilation of large intestine proximal to the diseased segment. Megacolon may also be caused by Chagas disease and may be associated with RET gene mutations and Trisomy 21.

Innervation

The superior mesenteric plexus supplies both sympathetic and parasympathetic innervation to the appendix and cecum. Lower thoracic spinal nerves provide sympathetic innervation, whereas the vagus nerve is responsible for parasympathetic innervation. The appendix sends its own afferent nerves to travel alongside sympathetic fibers to T10.

The ascending colon derives its innervation from the superior mesenteric plexus via the peri-arterial plexuses of the right colic artery. The transverse colon is innervated by way of the peri-arterial plexuses of the right and middle colic arteries from the superior mesenteric plexus. This superior mesenteric plexus supplies visceral afferents, sympathetic, and parasympathetic innervation via the vagus nerve.

The left colic flexure between the transverse and descending colon is a point of distinction for the direction of sympathetic and parasympathetic fibers. Proximal to the splenic flexure, both sympathetic and parasympathetic fibers travel to the peri-arterial nerve plexuses of the abdominal aorta. Distal to the splenic flexure, the descending and sigmoid colon derive their sympathetic innervation from the lumbar sympathetic trunk via abdominopelvic splanchnic nerves, the superior mesenteric plexus, and the peri-arterial plexuses of the inferior mesenteric artery (IMA) and its branches. Parasympathetic innervation distal to the splenic flexure is supplied by pelvic splanchnic nerves via the inferior hypogastric plexus independently of the arterial supply.

Proximal to the middle of the sigmoid colon, sympathetic visceral afferent fibers carrying pain sensation travel to the thoracolumbar spinal sensory ganglia. Parasympathetic fibers conveying reflex information travel to vagal sensory ganglia. Distal to the middle sigmoid colon, all visceral afferent fibers travel with the parasympathetic fibers to the sensory ganglia of S2–S4.

Blood Supply

The blood supply of the large intestine is intimately linked to its embryological origin. As mentioned above, the large intestine is derived from the midgut and hindgut. The midgut develops into the cecum, appendix, ascending colon, and proximal

two-thirds of the transverse colon. These structures are supplied by the superior mesenteric artery (SMA), which stems off the abdominal aorta at the level of L1. The SMA has three main branches that supply the large intestine: right colic, middle colic, and ileocolic arteries. The right colic artery supplies the ascending colon and passes retroperitoneally. The middle colic artery ascends retroperitoneally and courses through the transverse mesocolon to supply the transverse colon. The ileocolic artery is the terminal branch of the SMA and supplies the ileum, cecum, and ascending colon. The appendicular artery is a branch of the ileocolic artery that supplies the appendix.

Structures from the hindgut include the distal one-third of the transverse colon, descending colon, and sigmoid colon. These structures are supplied by the inferior mesenteric artery (IMA), which arises at the level of L3 and descends retroperitoneally to the left of the abdominal aorta. The left colic artery is the first to branch off the IMA and supplies the distal one-third of the transverse colon and descending colon. The sigmoid artery branches into three or four arteries to supply distal parts of the descending colon and the sigmoid colon. The SMA and IMA anastomose through arcades and the marginal artery of Drummond, which runs parallel to the colon between the ileocecal and rectosigmoid junctions.

The large intestine venous system drains into the portal vein. Venous blood from the ascending and transverse colon drains into the superior mesenteric vein. Venous blood from the descending and sigmoid colon drains into the inferior mesenteric vein. The superior mesenteric vein has a direct connection with the portal vein. In contrast, the inferior mesenteric vein joins the splenic vein before draining into the portal vein. Venous blood from the portal vein travels through the liver and into the caval (systemic) system via the hepatic veins.

Clinical Correlate

Acute *mesenteric ischemia* occurs when there is diminished blood supply to the bowels due to an obstruction to flow. This may be due to atherosclerosis, thrombi, emboli, aneurysms, tumors, or hypovolemia most notably at watershed areas. Pain may occur post-prandially in response to increased bowel energy demands. Findings include abdominal pain, red currant jelly stools, nausea, vomiting, and electrolyte imbalances.

Lymphatic

Lymph from the large intestine flows from epicolic lymph nodes on the intestinal wall to paracolic nodes along the mesenteric border, then to intermediate colic nodes along the colic arteries, then to superior and inferior mesenteric nodes and the intestinal trunks. The cecum and appendix are drained by lymph nodes in the mesoappendix and ileocolic lymph nodes located along the ileocolic artery.

Histology

The large intestine is lined with a simple columnar epithelium and contains many colonic crypts (intestinal glands), which are also located in the small intestine. These glands are found in the epithelium and contain many specialized cells including enterocytes, goblet cells, enteroendocrine cells, Paneth cells, and stem cells.

Physiology

The two major functions of the large intestine are absorption of water and electrolytes from chyme, and storage of fecal matter. The proximal half of the colon is more responsible for absorption, while the distal half is more responsible for storage. The movements of the colon are slower, but share the characteristic elements—mixing and propulsion—of the movements of the small intestine. Poor motility increases absorption, thus leading to harder feces more proximal than appropriate and contributing to constipation. Increased motility decreases absorption, contributing to diarrhea.

The mixing movements of the large intestine are termed Haustrations. They normally exhibit a pattern of 30 seconds of contraction, which can nearly occlude the lumen at peak contraction, followed by 60 seconds of relaxation, then minutes of rest. These mixing movements combine contraction of circular and longitudinal strips of smooth muscle, and each Haustration tends to move slightly toward the anus with each contraction, giving gentle propulsion to the contents while digging into and rolling them, thus exposing all the fecal matter to the mucosa of the large intestine to aid in absorption.

Most of the propulsion in the proximal half of the large intestine results from the haustral contractions, requiring as many as 8–15 hours to transport chyme from the ileocecal valve to anal canal. Mass movements take over the propulsion for minutes at a time as many as a few times a day, especially within the first half-hour after eating breakfast. A mass movement exists when a constrictive ring forms from circular muscle contraction secondary to distention or irritation, usually in the transverse colon. Then the 20 cm of colon distal to the ring rapidly relax the haustrations and longitudinally constrict as a unit. The contractile force builds over 30 seconds, then relaxes over the following 2 minutes. This mass movement can be followed by further mass movements distally. Mass movements are initiated by gastrocolic and duodenocolic reflexes (triggered by distention of the stomach or duodenum, respectively). These reflexes are transmitted via the autonomic nervous system, and are either absent or at best extremely weak when the extrinsic autonomic nerves to the colon have been removed.

Most of the water and essentially all the ions are absorbed from the chyme on the way to becoming feces, going from 1500 milliliters of volume when leaving the small intestine to less than 100 milliliters of fluid being excreted with the feces. The mucosa of the large intestine has a high capacity for active sodium absorption,

which generates an electrochemical gradient to drive chloride absorption as well. The large intestine is distinct from the small in that the epithelial tight junctions of the colon are much tighter, discouraging backflow of ions, and allowing for more complete sodium absorption. Additionally, the large intestine mucosa exchanges secreted bicarbonate ions for adsorbed chloride ions. The bicarbonate neutralizes acidic bacterial byproducts, and the osmotic gradient generated by the absorption of sodium and chloride ions drives water out of the lumen.

Rectum

Overview

The rectum is the terminal portion of the large intestine and connects the sigmoid colon and anal canal. Lying retroperitoneally, the rectum functions to store fecal matter until defecation is initiated.

Structure

The rectum is primarily retroperitoneal. The most superior third of the rectum is covered by peritoneum both anteriorly and laterally, the middle third is covered only on its anterior surface, and the most inferior third lies below the peritoneum (subperitoneal).

The junction between the sigmoid colon and rectum is located at the level of S3, at the inferior part of the sigmoid colon mesentery. The rectosigmoid junction can be identified macroscopically by the changes in the teniae coli and the disappearance of the omental appendages. Upon approaching the rectum, the teniae coli begin to spread and widen to become a continuous outer layer of longitudinal smooth muscle.

Multiple flexures exist in the rectum as it curves to meet the anal canal. The sacral flexure of the rectum is the point where the rectum turns as it follows the sacrum and coccyx. The anorectal flexure of the anal canal is a sharper angle where the rectum ends anterior and inferior to the coccyx. The sharp (approximately 80°) angle is maintained by the tonal and active contraction of the puborectalis muscle to prevent incontinence. These two flexures contribute to the “S” shape of the rectum as seen from a lateral perspective. Three lateral flexures are also present in the rectum and can be seen when viewed anteriorly. The transverse rectal folds are formed by three internal folds (two on the left and one on the right). These folds are present at points where the circular muscle layer is thickened. The ampulla of the rectum, the dilated part of the terminal rectum, serves to maintain continence and to store fecal matter until defecation is initiated.

Embryology

The rectum, along with the colon and the anal canal above the dentate line, is derived from the hindgut and is therefore supplied by the inferior mesenteric artery and its associated venous and lymphatic drainage. The division between the endodermal and ectodermal tubes is marked by the dentate line—this is where the terminal portion of the hindgut (cloaca) fuses with the proctodeum.

Innervation

The sympathetic and parasympathetic nervous systems innervate the rectum. From the sympathetic nervous system, branches of the spinal cord at the level of the lumbar spine form the lumbar splanchnic nerves and the hypogastric (pelvic) plexuses, and the sympathetic nervous system also supplies periarterial plexuses from the inferior mesenteric artery and superior rectal arteries. The parasympathetic nervous system innervates the rectum at the S2, S3, and S4 levels of the spinal cord via the rectal (pelvic) plexus by way of the pelvic splanchnic nerves and the bilateral inferior hypogastric plexuses. The rectum is located inferior to the pelvic pain line; therefore, all visceral afferent fibers travel retrograde to the S2–S4 spinal sensory ganglia along the rectal parasympathetic fibers.

Blood Supply

The rectum is supplied by the superior, middle, and inferior rectal arteries. The superior rectal artery is the terminal branch of the internal mesenteric artery (IMA) and supplies the proximal part of the rectum. The paired middle rectal arteries are branches of the internal iliac arteries and supply the middle, inferior, and posterior parts of the rectum. The paired inferior rectal arteries branch off of the internal pudendal arteries and primarily supply the anal canal and anorectal junction. It is important to note that the superior and inferior rectal arteries anastomose, whereas the middle rectal arteries do not.

The superior, middle, and inferior rectal veins drain blood from the rectum. The superior rectal vein drains into the portal venous system. The middle and inferior rectal veins drain into the systemic venous system. Differences in venous drainage become important in pathologic states such as portal hypertension.

The rectal venous plexuses are circumferential networks of vessels located superiorly and inferiorly in the anal canal. The internal rectal venous plexus sits deep to the mucosa at the anorectal junction, while the external rectal venous plexus lies in the subcutaneous tissue outside the rectal muscular wall.

Lymphatics

In the anal canal superior to the pectinate line, the lymphatic vessels drain into the internal iliac lymph nodes, and then into the common iliac and lumbar lymph nodes.

Histology

The mucosa of the rectum is similar to that of the large intestine up until the anal transitional zone (ATZ), which marks a transition from rectal simple columnar epithelium to the stratified squamous epithelium of the perianal area. Anal glands are seen extending into the submucosa and muscularis externa.

Physiology

When fecal matter begins to accumulate in the rectum, the smooth muscle walls contract, and the internal anal sphincter (also composed of smooth muscle) relaxes. This relaxation in response to filling of the rectum is called the rectosphincteric reflex. The external anal sphincter is responsible for preventing defecation, as it is composed of striated muscle and is under voluntary control. Upon filling of the rectum to 25% of its capacity, the urge to defecate presents. Defecation is accomplished via voluntary relaxation of the external anal sphincter, in coordination with contraction of the smooth muscle walls of the rectum to increase pressure and force out feces.

Gallbladder

Overview

Bile is produced in the liver, concentrated and stored in the gallbladder, then released into the biliary ducts where it is conveyed to the duodenum to aid in fat emulsification. The gallbladder is one of the most commonly removed organs in the body, demonstrating the therapeutic significance of a command of the cholecystic system and associated anatomy.

Structure

The gallbladder is a pear-shaped structure that sits on the posterior surface of the liver between the right and quadrate lobes. The gallbladder has three parts: fundus, body, and neck. The fundus is the rounded tip of the gallbladder that extends beyond the liver to the tip of the right ninth costal cartilage in the mid-clavicular line. The body of the gallbladder is the major portion in direct contact with the superior part

of the duodenum, anteriorly, and the transverse colon, inferiorly. The neck of the gallbladder is the narrow, superior portion of the gallbladder that connects to the cystic duct. Spiral folds line the mucosal surface of the neck and maintain patency of the lumen to allow for storage and secretion of bile. The cystic duct joins the common hepatic duct to form the common bile duct. Bile is secreted into the duodenum via the Ampulla of Vater.

Embryology

The liver and biliary system (hepatic ducts, gallbladder, bile duct) are all derived from the endodermal epithelium of the distal foregut, arising from the distal hepatic diverticulum in week four. The smaller, caudal part of the hepatic diverticulum gives rise to the gallbladder, with endodermal proliferation of hepatocytes contributing to the epithelial lining of the intrahepatic portion. The extrahepatic part of the biliary apparatus is canalized by degeneration of the epithelial cells lining the biliary tree. Along the stalk of the hepatic diverticulum, the cystic duct forms. Further along in gestation, the hepatic and cystic ducts connect to the duodenum via the stalk of the hepatic diverticulum. These in turn become the bile duct. Although the bile duct starts in a position ventral to the duodenum, duodenal growth and rotation move the bile duct's entrance to the dorsal side of the duodenum. Bile production in the liver begins in week 12, with bile making its way into the duodenum to produce meconium after the 13th week.

Innervation

Nerve supply to the gallbladder is provided primarily by the celiac plexus (sympathetic) and vagus nerve (parasympathetic). Sensory innervation is provided by the right phrenic nerve (C3,4,5), which is responsible for referred pain to the right shoulder.

Blood Supply

The bile duct is supplied by different arteries along its path from the gallbladder to the duodenum. At the most proximal part, the cystic artery provides arterial oxygenated blood to the bile duct. The middle part of the bile duct is fed by the right hepatic artery. The retroduodenal part of the bile duct is supplied by two arteries: the posterior superior pancreaticoduodenal artery and the gastroduodenal artery. Venous drainage of the proximal bile duct enters the liver directly, while venous drainage of the distal bile duct is accomplished by the posterior superior pancreaticoduodenal vein, which then drains into the hepatic portal vein system.

The cystic artery also supplies the gallbladder and cystic duct. In the majority of cases (75.5%), the cystic artery arises from the right hepatic artery in the

cystohepatic triangle of Calot. Other variations include the cystic artery arising from the right hepatic artery but coursing anterior to the common hepatic duct (13.1%), the left hepatic artery (6.2%), the gastroduodenal artery (2.6%), or the proper hepatic artery (2.1%).

The cystic veins provide the route for venous drainage from the gallbladder neck and cystic duct. After joining the veins draining the proximal bile duct and hepatic ducts, the cystic veins either drain directly into the liver or join with the hepatic portal vein. The fundus and body of the gallbladder send veins directly into the visceral surface of the liver to drain directly into the sinusoids.

Lymphatic

Lymph in the gallbladder is initially drained into cystic lymph nodes located around the neck of the gallbladder. Efferent vessels carry lymph to the node of the omental foramen and hepatic lymph nodes. Lymph from these nodes is then drained into the celiac lymph nodes.

Histology

The mucosa of the gallbladder is lined with a simple columnar epithelium and contains many deep mucosal folds. The tall columnar epithelial cells are lined by microvilli and contain large concentrations of mitochondria both apically and basally. The gallbladder wall beneath the mucosa contains a thick muscularis externa with randomly oriented smooth muscle bundles. Rokitansky–Aschoff sinuses, deep diverticula of the mucosa, may be visible due to hyperplasia and herniation of epithelial cells through the muscularis externa. The gallbladder is attached to the liver by serosa, which also lines the portions of the gallbladder unattached to the liver.

Physiology

Bile plays an important role in both fat digestion and absorption by properties of the bile acids that help emulsify the larger fat particles, which increases the surface area exposed to lipase and aids in the absorption of the digested fatty end products. Bile also allows for the excretion of excess cholesterol and bilirubin from the blood. Bile is continuously generated by hepatocytes in the liver and is conducted down the common bile duct, where it can either directly enter the duodenum or be diverted for minutes to hours to the gallbladder via the cystic duct. En route to the gallbladder, when stimulated by secretin, the liver adds to the bile a watery solution of bicarbonate ions and sodium via the epithelial cells that line the ducts. The capacity of the gallbladder is between 30 and 60 milliliters, but it can accommodate as much as 12 hours worth of freshly produced bile (about 450 milliliters), which is condensed

because the gallbladder mucosa is constantly absorbing water, sodium, chloride, and other small electrolytes, thus concentrating the bile salts, cholesterol, bilirubin, and lecithin. The bile in the gallbladder can be concentrated 5 to 20 times, primarily on account of the active transport of sodium through the gallbladder epithelium and the secondary absorption of water and other diffusible components.

Gallbladder emptying is stimulated by cholecystokinin (CCK). Fatty acids in the duodenum stimulate the release of CCK from the duodenal mucosa. Secondly, the gallbladder is stimulated by cholinergic nerve fibers from the vagus nerve as well as the enteric nervous system. The gallbladder contracts via rhythmic contractions of the gallbladder wall, and effective gallbladder emptying requires concomitant relaxation of the sphincter of Oddi as the bile enters the duodenum. Gallbladder emptying typically begins as soon as food enters the upper GI tract, especially at the duodenum, about 30 minutes after a meal. The gallbladder normally continues its process of emptying via rhythmic contraction for about 1 hour.

Pancreas

Overview

The pancreas is the only organ in the human body that has both exocrine and endocrine functions. It is a retroperitoneal gland, lying at the vertebral levels of L1 and L2. It is bordered by the stomach anteriorly, the duodenum on the right, and the spleen on the left. The pancreas is made up of four parts: the head, neck, body, and tail.

Structure

The pancreas is an accessory digestive organ with both exocrine and endocrine functions found in the epigastric and left hypochondriac region of the abdomen. The pancreas is mostly retroperitoneal, with the exception of a small portion of its tail located within the splenorenal ligament.

Anatomically, the pancreas is subdivided into a head, uncinete process, body, and tail. The pancreatic head is located within the C-shaped concavity of the duodenum and is traversed by the bile duct. The uncinete process is a projection at the lower left lateral border of the head. The body travels across the midline, overlying the aorta, superior mesenteric artery, left renal vein, splenic vein, and inferior mesenteric vein. The tail travels within the splenorenal ligament and terminates at the hilum of the spleen.

The main pancreatic duct originates in the tail and travels through the length of the organ before joining with the common bile duct to form the ampulla of Vater. The duct then enters the second part of the duodenum via the greater papilla. An accessory duct is sometimes present, originating in the upper part of the head and draining into the second part of the duodenum via either the minor duodenal papilla (70%) or the main pancreatic duct (30%) (Fig. 8.4).

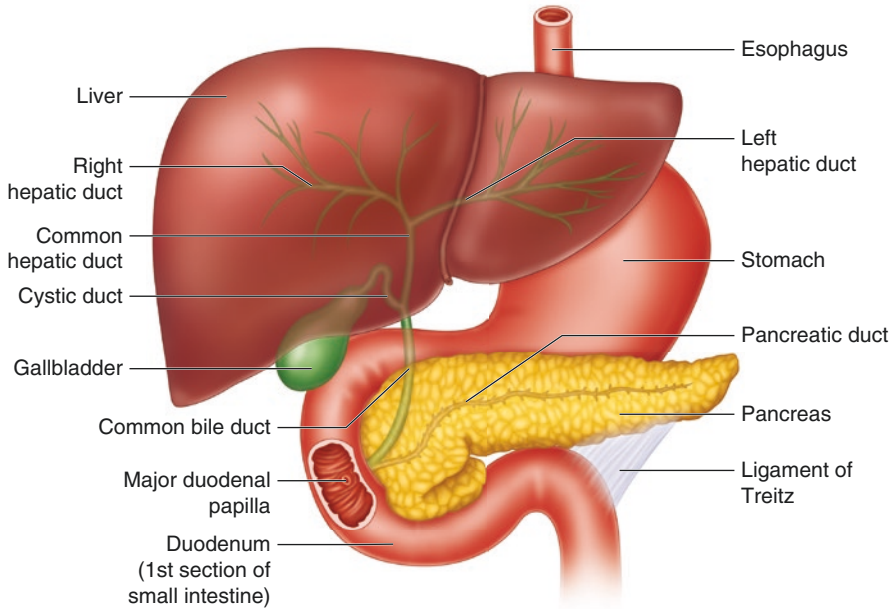


Fig. 8.4 Pancreaticobiliary System

The functional units of the endocrine pancreas are the islets of Langerhans. The islets are spherical formations of cells distributed throughout the parenchyma consisting of α cells, β cells, and δ cells. Capillaries enter the islets and branch to the periphery.

Embryology

Pancreatic development occurs between the fifth and eighth weeks after fertilization with the induction of two different regions of the caudal foregut endoderm. The notochord induces the formation of the dorsal pancreatic bud, and the hepatic mesoderm induces the formation of the ventral pancreatic bud. The ventral pancreatic bud grows from the primordial bile duct. As the duodenum rotates 90° clockwise, the ventral bud rotates dorsally and fuses with the dorsal pancreatic bud. The ventral bud gives rise to the uncinata process and the inferior portion of the head; the pancreatic bud gives rise to the superior portion of the head, body, and tail. The fusion of the ventral and dorsal pancreatic buds allows for an anastomosis of their main ducts. As such, the main pancreatic duct is an anastomosis of the entire ventral duct and the distal two-thirds of the dorsal duct. The main pancreatic duct and bile duct fuse to form the Ampulla of Vater, a dilated opening into the duodenum located at the major duodenal papilla. Often, the proximal one-third of the dorsal duct will form the accessory pancreatic duct, opening into the minor duodenal papilla.

Within the pancreatic buds, endodermal cells proliferate as tubules and branch to form acinar cells and ductal epithelium. Islands of endodermal cells embedded in the mesoderm form the islet cells, including and pancreatic polypeptide cells. Mesoderm forms the pancreatic connective and vascular tissue.

Clinical Correlates

Annular pancreas is a developmental malformation characterized by improper rotation of the ventral pancreatic bud, causing a ring of tissue to form around the descending part of the duodenum. This band of tissue may cause duodenal obstruction. Symptoms may include polyhydramnios, recurrent vomiting, low birth weight, and impaired feeding.

Pancreas divisum is a developmental malformation of the main pancreatic duct where a defect in fusion of the ventral and dorsal ducts leads to two separate ductal systems. The superior portion of the head, body, and tail drain into the larger dorsal duct and open into the minor duodenal papilla. The inferior portion of the head and the uncinuate process drain into the ventral duct and open into the major duodenal papilla. This occurs in 4% of the population and is usually asymptomatic. However, impaired drainage may lead to recurrent pancreatitis.

Innervation

The pancreatic nerves branch off the vagus and abdominopelvic splanchnic nerves, which pass through the diaphragm. Both parasympathetic and sympathetic fibers approach the pancreas by skirting the arteries of the celiac and superior mesenteric plexuses. The sympathetic fibers innervate blood vessels, while both sympathetic and parasympathetic fibers innervate the pancreatic acinar cells and islets. The parasympathetic secretomotor function of the acinar cells and islets is secondary to primary stimulation via hormones. Secretin and cholecystokinin from the epithelium of the duodenum and intestinal mucosa are the primary drivers of pancreatic secretion.

Blood Supply

The main blood supply to the pancreas is the splenic artery, which produces multiple (up to ten) pancreatic arteries that form arcades with branches of the gastroduodenal artery as well as the superior mesenteric arteries. The head of the pancreas is supplied by arcades from the anterior and posterior superior pancreaticoduodenal arteries (branches of the gastroduodenal artery) and the anterior and posterior inferior pancreaticoduodenal arteries (branches of the superior mesenteric artery).

The pancreatic arteries have corresponding pancreatic veins that provide venous drainage from the pancreas. The lion's share of the drainage enters the splenic vein via splenic vein tributaries, while some pancreatic blood is drained via the superior mesenteric parts of the hepatic portal vein.

Lymphatic

The lymphatic channels of the pancreas follow their respective blood vessels. Pancreaticosplenic lymph nodes follow the splenic artery. Along with the pyloric lymph nodes, they empty into the hepatic lymph nodes before draining into the celiac and superior mesenteric lymph nodes.

Histology

The exocrine and endocrine pancreas can be differentiated histologically. Pancreatic islets of Langerhans (endocrine) consist of clusters of pale-staining cells. It is difficult to identify the individual cell types within the islets upon H&E staining. Mallory-Azan staining, however, will reveal α cells (red), β cells (brownish orange), and δ cells (blue). The secretory exocrine units of the pancreas are tubuloacinar in shape and are characterized by a simple epithelium of serous cells with a narrow apical surface and broad basal surface. These serous cells contain basophilic basal cytoplasm and acidophilic apical cytoplasm (due to zymogen granules).

Physiology

The physiology of the pancreas can be understood by examining endocrine functions and exocrine functions separately.

The exocrine pancreas predominantly secretes bicarbonate and enzymes. Bicarbonate neutralizes the acidic chyme in the duodenum, and the enzymes work to digest the ingested nutrients. Pancreatic secretions are produced by centroacinar cells. While all pancreatic secretions are isotonic, the concentrations of electrolytes vary with flow rate. At low flow rates, pancreatic secretions have high concentrations of sodium and chloride and low concentrations of potassium and bicarbonate. At high flow rates, pancreatic secretions have high concentrations of sodium and bicarbonate and low concentrations of potassium and chloride. Ductal cells are responsible for altering the concentrations of electrolytes and contain three key transporters. The basolateral membrane contains a Na^+/K^+ ATPase and a Na^+/H^+ exchanger. The apical membrane contains a $\text{Cl}^-/\text{HCO}_3^-$ exchanger.

Pancreatic enzymes are synthesized on the rough endoplasmic reticulum and are secreted by acinar cells. These enzymes (amylase, trypsin, chymotrypsin, carboxypeptidase, elastase, lipase, colipase, phospholipase A₂, and cholesterol ester hydrolase) are responsible for the digestion of carbohydrates, proteins, and lipids.

Pancreatic exocrine secretions are responsive to many stimuli. Enzymatic secretion is stimulated by smell, taste, conditioning, and distension of the stomach. In addition, enzymatic secretion is stimulated by certain nutrients in ingested food. Fatty acids, small peptides, and amino acids including phenylalanine, methionine, and tryptophan stimulate I cells in the duodenum to secrete cholecystokinin. This gastrointestinal hormone acts on acinar cells to increase the secretion of enzymes.

The acidity of chyme in the duodenum is the chief agonist of bicarbonate secretion. Protons activate S cells in the duodenum, which secrete the gastrointestinal hormone secretin. Acting on the pancreatic ductal cells, secretin causes bicarbonate to be secreted as a buffer.

Pancreatic secretions drain into the pancreatic ducts and flow through the Ampulla of Vater and into the descending part of the duodenum.

The endocrine pancreas functions to regulate metabolism through the secretion of hormones including insulin, glucagon, and somatostatin. The cells that secrete these hormones can be found in groups throughout the pancreas called islets of Langerhans. Insulin is secreted by beta cells in the islets and has a plethora of actions, including decreasing blood glucose concentration, increasing glycogen formation, decreasing glycogenolysis and gluconeogenesis, and increasing protein synthesis. Glucagon is secreted by alpha cells in the pancreatic islets and functions to increase the availability of glucose in the body by stimulating glycogenolysis, gluconeogenesis, and lipolysis. Lastly, somatostatin is secreted by delta cells in the islets. This hormone is not unique to the pancreas and is stimulated by all three nutrient groups. Somatostatin inhibits the secretion of insulin and glucagon.

Suggested Reading

1. Costanzo LS. *Physiology*. 4th ed. Philadelphia: Saunders/Elsevier; 2010.
2. Dudek RW. *Embryology*. Philadelphia: Wolters Kluwer; 2014.
3. Hall JE, Guyton AC. *Guyton and Hall textbook of medical physiology*. Philadelphia: Saunders Elsevier; 2011.
4. Halliday NL. *BRS Gross Anatomy*. Philadelphia: Wolters Kluwer; 2019.
5. Kuo B, Urma D. Esophagus—anatomy and development. *GI Motility Online*. 2006. <https://doi.org/10.1038/gimo6>.
6. Moore KL, Agur AMR, Dalley AF. *Clinically oriented anatomy*. 8th ed. Philadelphia: Wolters Kluwer; 2018.
7. Moore KL, Persaud TVN. *The developing human: clinically oriented embryology*. 5th ed. Philadelphia: Saunders; 1993.



Anomalies of the Gastrointestinal Tract

9

Jill C. Rubinstein, James S. Farrelly, David Stitelman,
and Emily Christison-Lagay

Anomalies encountered during gastrointestinal (GI) tract surgery can be subcategorized based upon the result of aberrant embryogenesis of the foregut (esophagus, stomach, duodenum), midgut (jejunum thru transverse colon), or hindgut (transverse colon through anus). Most embryonic abnormalities present during infancy, although some present later in childhood, and a minority may be asymptomatic through adulthood. In addition to restoring appropriate GI tract function, in treating anatomic variants, it is important to recognize and search for associated anomalies in other systems. Surgical considerations for anatomic variants of the gastrointestinal tract may be specific to the repair of the abnormality itself and may even require the creation of a novel anatomic variant, or may be secondary to frequently associated abnormalities which dictate the surgical approach to repair.

J. C. Rubinstein (✉)

Department of Surgery, Memorial Sloan Kettering Cancer Center, New York, NY, USA
e-mail: rubinstj@mskcc.org

J. S. Farrelly

Department of Surgery, Yale New Haven Hospital, New Haven, CT, USA
e-mail: james.farrelly@yale.edu

D. Stitelman

Department of Surgery, Yale School of Medicine, New Haven, CT, USA
e-mail: david.stitelman@yale.edu

E. Christison-Lagay

Yale Pediatric Surgery, Yale New Haven Children's Hospital, New Haven, CT, USA
e-mail: emily.christison-lagay@yale.edu

Esophagus

Congenital Esophageal Stenosis

Esophageal stenoses are intrinsic narrowings of the wall that are classified into three groups based on their histology (tracheobronchial rests, membranous diaphragm, and fibromuscular stenoses) (Fig. 9.1). Presentation is most common at approximately 6 months of age with introduction of solid foods, but severe cases may present earlier and resemble esophageal atresia (EA). The goals of intervention are resolution of symptoms as well as management of reflux. Treatment options include mechanical bougie dilation, hydrostatic dilation, surgical excision, and myotomy [1–3]. When symptoms cannot be controlled with dilation, early resection with primary anastomosis should be considered. Pre-operative localization and assessment of severity is achieved with barium esophagram and endoscopy. For lesions in the proximal and middle-third of the esophagus, operative approach is via right thoracotomy, whereas more distal lesions require left thoracotomy with the potential addition of a laparotomy to access the abdominal esophagus. The exact extent of stenosis can be assessed intraoperatively either by passage of a balloon catheter or by advancing an esophageal dilator to the point of resistance. Almost all stenoses can be managed via segmental resection and end-to-end anastomosis, with

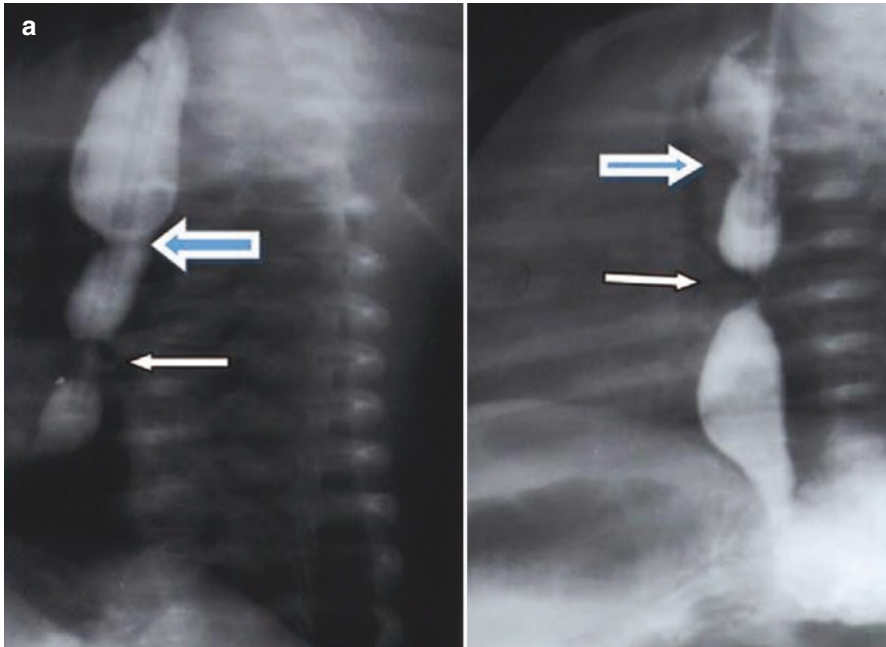


Fig. 9.1 (a) Barium esophagram of a patient with esophageal stenosis (small arrow) discovered after repair of esophageal atresia with tracheoesophageal fistula (large arrow). (b) Hydrostatic dilation of stenosis

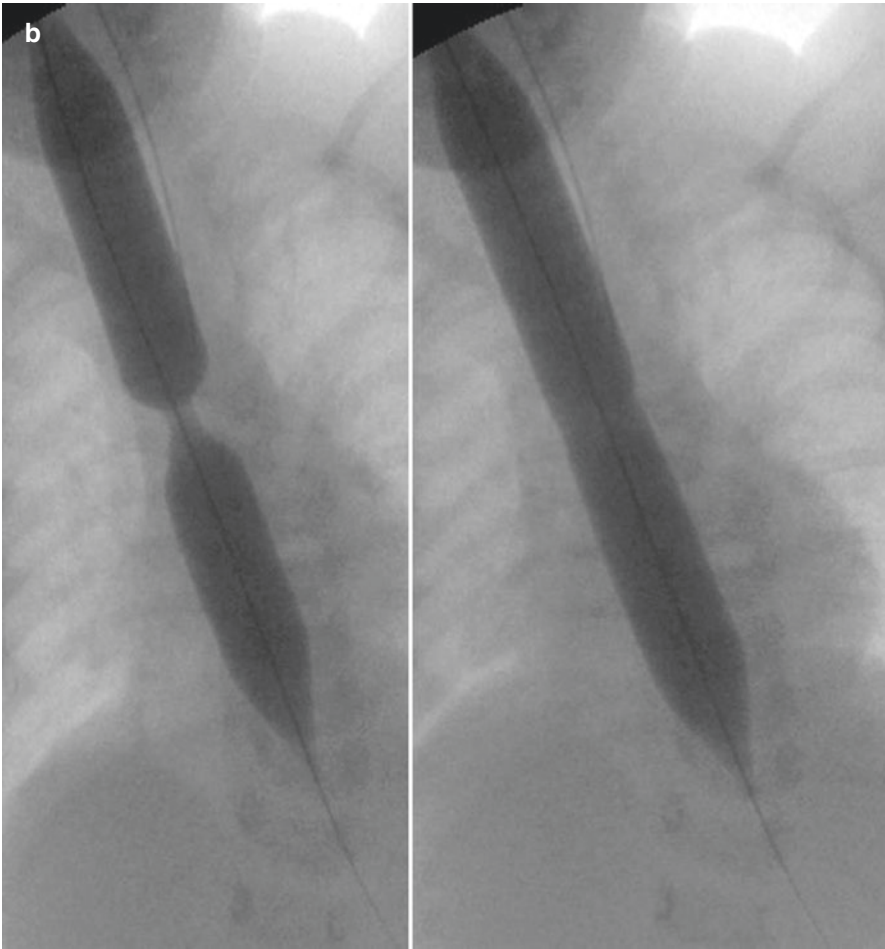


Fig. 9.1 (continued)

preservation of the vagus nerves. For long stenoses that have failed dilation, an interposition graft may be necessary. Resections near the gastroesophageal junction (GE) junction should prompt concomitant anti-reflux procedure.

Esophageal Webs and Rings

The most common structural abnormalities of the esophagus are rings and webs, most of which are asymptomatic. Rings are divided into three subtypes, denoted as A, B, and C. A rings are rare, muscular rings found just proximal to the squamocolumnar junction and are most common in the pediatric population. B rings are located at the junction and are mucosal structures. B rings with a luminal caliber

less than 12.5 mm are referred to as Schatzki rings. C rings are formed by diaphragmatic crural pressure. Lower esophageal rings have been found in up to 15% of routine barium esophagrams [4]. In contrast, esophageal webs are less commonly discovered as an incidental finding but are reported in 5–15% of patients undergoing esophagram specifically to evaluate for causes of dysphagia [5].

The pathogenesis of esophageal rings and webs is unclear. Proposed etiologic contributors include congenital factors (e.g., failure to completely recanalize during embryological development, persistence of tracheobronchial remnants) and chronic inflammation (e.g., from reflux disease, caustic ingestion, radiation, or trauma) [6, 7]. Web formation has been associated with iron deficiency anemia and autoimmune processes, but data to support a causative relationship are conflicting [8–10].

Treatment for esophageal rings includes diet modification, anti-reflux therapy for those with GERD, mechanical bougie dilation, endoscopic sphincterotomy or laser division, and very rarely, surgical resection. Specific anatomic conditions associated with the finding of esophageal ring or webs include the presence of hiatal hernia in the former, and a Zenker's diverticulum in the latter [11, 12].

Duplication Cysts

Esophageal cysts, known as duplications, occur anywhere along length of the esophagus (Fig. 9.2). They can be either intramural or completely separate from the esophagus, but they rarely communicate with the lumen. Large distal duplications may have a subdiaphragmatic communication with a hollow viscus, most commonly the stomach [13]. There is a propensity for duplications to occur on the right side, a trend thought to be related to intestinal rotation during development [13, 14]. Most duplications are solitary, but posterior location is associated with a higher chance of multiple lesions [15]. These posterior, or dorsal enteric, cysts are also commonly fixed to the anterior vertebrae and a subset attached to the dura through a vertebral defect. The presence of a posterior cyst should prompt evaluation for associated vertebral body abnormalities, the presence of intraspinal



Fig. 9.2 Large esophageal duplication in the right posterior thorax

cysts, or intra-abdominal intestinal duplication. Greater than one-third of esophageal duplications are discovered as incidental findings on chest radiograph. Symptomatic presentation can take the form of dysphagia or pain from hemorrhage, ulceration, or perforation. Alternatively, patients may present with varying degrees of respiratory compromise ranging from a persistent cough to severe respiratory distress [16]. Those with neurenteric cysts may develop weakness or even paralysis [17].

Once discovered, surgical excision should be considered for all duplication cysts, given the possibility of infection, hemorrhage, or malignant transformation. Preoperative planning should include thorough review of all imaging, to include CT or MRI in order to define boundaries and assess for the presence of multiple cysts and associated abnormalities.

The essential operative goal is removal of all mucosa contained within the duplication, as the presence of gastric mucosa can lead to hemorrhage, ulceration, and perforation. Such can be achieved through either enucleation with repair of the primary defect, or complete excision. Most duplications are retropleural and located in the posterior mediastinum. Small duplications can potentially be approached by Video-assisted thoracoscopic surgery (VATS) or endoscopy, with larger lesions requiring posterolateral thoracotomy [14, 18–20]. Large distal duplications may require an additional incision via the abdomen. If the duplication contains a spinal component, this should be resected first, to avoid traction on the spinal cord and potential injury during subsequent dissection. Any communication with the lumen of the GI tract should be primarily closed. In this instance, or in case of violation of the mucosa during enucleation or excision, consideration should be given to protective gastrostomy.

Fistula

Tracheoesophageal fistula (TEF), or esophageal atresia (EA) with or without tracheoesophageal fistula, is posited to arise from the failure of the complete division of the primordial foregut. Five principle varieties of TEF/EA are described, with proximal EA and distal TEF comprising 85% of those clinically encountered, followed by pure EA (6%), and TEF without EA (4%) (Fig. 9.3). Over half of infants with TEF/EA have associated anatomic abnormalities, the most common of these being cardiac malformations, particularly ventricular septal defects and tetralogy of Fallot. These cardiac defects are responsible for the majority of deaths in patients with TEF. All patients with TEF/EA should be screened for VACTERL associations (V, vertebral; A, anorectal; C, cardiac; T, trachea; E, esophageal; R, renal; L, limb). Moreover, anomalies of aortic arch anatomy should be defined by echocardiography prior to any attempt at repair. The standard surgical approach to TEF is through the right chest, either via a posterior lateral thoracotomy, or, more recently, a thoracoscopic approach (Fig. 9.4). A right-sided aortic arch is present in up to 2.5% of cases, and most experts recommend approaching repair from the left chest in this event. A double aortic arch can also be found and may significantly complicate the approach to the upper pouch.

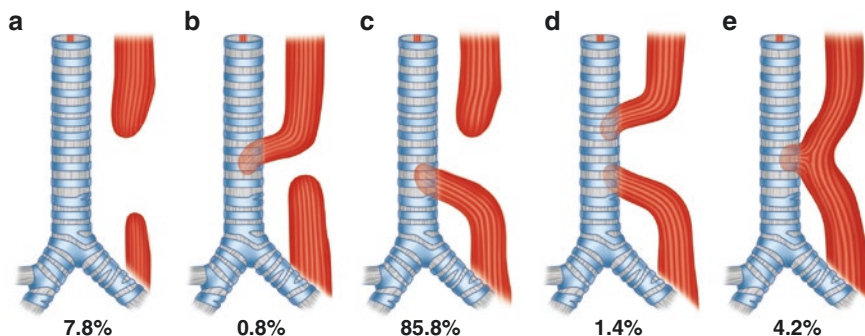
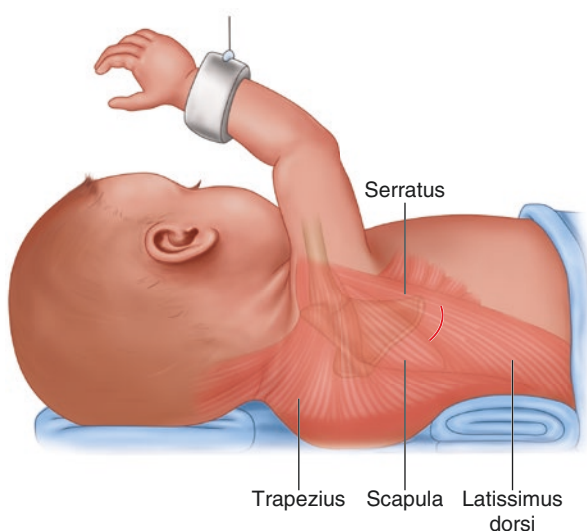


Fig. 9.3 Types of esophageal atresia and tracheoesophageal fistula. (a) Pure esophageal atresia without fistula; (b) proximal tracheoesophageal fistula, blind distal pouch; (c) distal tracheoesophageal fistula, blind proximal pouch; (d) proximal and distal tracheoesophageal fistula; (e), intact continuous esophagus with H-type tracheoesophageal fistula

Fig. 9.4 Muscle sparing approach to posterior lateral thoracotomy, the standard technique of repair of an EA-TEF with a left sided aortic arch



Pure EA without TEF is often associated with a “long gap” between the proximal and distal esophageal ends. Although no consensus exists on the precise definition of a distance that constitutes a “long gap,” a distance larger than 3 cm or 2 vertebral bodies is often cited. Most experts agree that a primary esophageal anastomosis provides the best long-term results [21, 22]. This can often be accomplished by placing a gastrostomy tube to allow distal feeding and waiting for 12 weeks while the esophagus undergoes lengthening. This lengthening is often disproportionately greater than the gain in length of the infant’s torso over the same length of time and is associated with a relative shortening of the distance between the esophageal ends (Fig. 9.5). Other authors advocate placing traction sutures in the proximal and distal pouches and gradually increasing the tension on them to facilitate more rapid

Fig. 9.5 Measurement of distance between proximal and distal pouches in long gap EA. A bougie (such as an Amato dilator) is placed in the mouth and a second one in the stomach through the gastrostomy tube site. The gap between the two ends is measured when gentle traction is applied to each

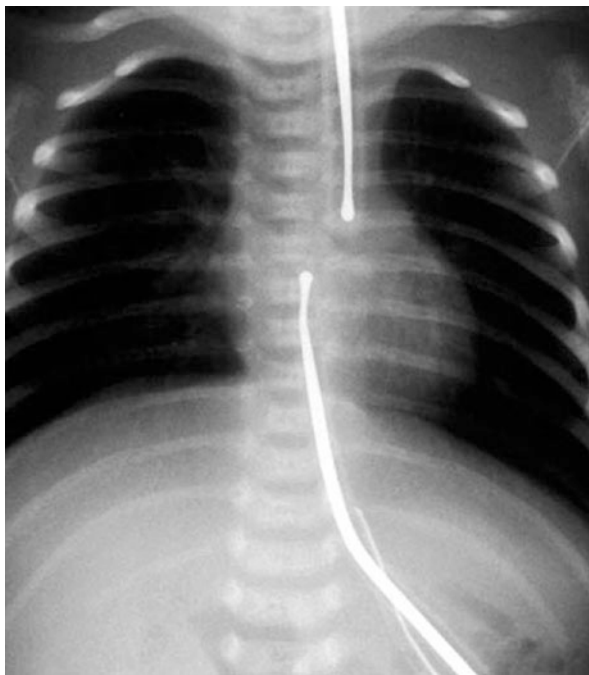
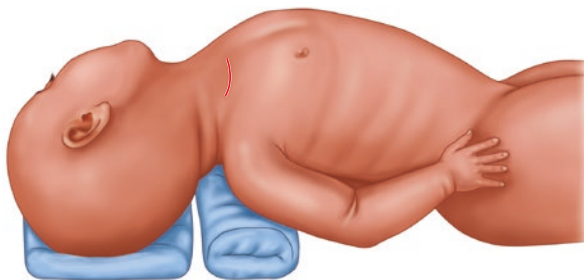


Fig. 9.6 Cervical approach to H-type fistula



approximation of the esophageal ends [23–26]. Finally, in cases in which the esophageal ends cannot be brought into proximity, an esophageal substitution can be performed either by a gastric pull up or a colonic or jejunal interposition graft [27, 28]. One disadvantage of a colonic interposition graft is that the colon also grows disproportionately longer than the long axis of the skeleton and can become very redundant with passing years. This contributes to stasis and dysmotility. Any attempt to plicate or reduce colonic length must be approached with the knowledge that the colon is supplied by a single vascular pedicle arising from the abdomen.

The approach to Type E or H-type TEFs is commonly made through a cervical incision. In this approach, the recurrent laryngeal nerve is placed in jeopardy (Fig. 9.6.). Up to 28% of patients undergoing a cervical approach to fistula division are complicated by nerve injury. A smaller percentage of patients presenting with

Type C anomaly (proximal EA with distal TEF) exhibit transient paresis or permanent nerve paralysis. This injury likely results from aggressive mobilization of the proximal pouch.

Stomach

Microgastria

Congenital microgastria is a rare condition, with fewer than 100 described cases, thought to arise from the early arrest of the fusiform dilation of the mesogastrum during the fourth and fifth weeks of gestation. Affected infants present with vomiting, failure to thrive, and, often, severe gastroesophageal reflux. Moreover, because the total mass of parietal cells is reduced, infants are at further risk of pernicious anemia [29].

Associated anomalies are frequent and include splenic agenesis or splenogonadal fusion, Pierre–Robin sequence, megaduodenum, paraesophageal hernia, intralobar sequestration, and DiGeorge syndrome [30–33]. Long-term outcomes are often dependent upon the severity of these associated abnormalities.

Frequent small volume or continuous nasogastric feeds (sometimes supplemented by total parenteral nutrition (TPN)) may be successful in the initial management of these patients. Surgical options include: Hunt–Lawrence pouch, Roux-en-Y, and total gastric dissociation.

Gastric Atresia

While cases of gastric atresia have been described, the incidence is far less than that in lower portions of the gastrointestinal tract. Most commonly, the obstruction is produced by a membranous diaphragm involving only the mucosa; less often, complete aplasia has been reported. Thin membranes may perforate with gastric pressure and cause difficulties later in life with symptoms referable to annular stenosis at the level of the previous membrane. Symptoms of gastric atresia include persistent non-bilious emesis and a distended upper abdomen with scaphoid lower abdomen (visible on abdominal radiograph as a gastric bubble without distal gas) (Fig. 9.7). An antenatal history of polyhydramnios can be found in at least 50% of infants. Isolated congenital pyloric atresia may be an inherited autosomal-recessive disorder. In over half of cases, however, there are other associated syndromes, the most common of which are epidermolysis bullosa and multiple intestinal atresia (Fig. 9.8) [34, 35]. Older children and adults with annular webs present with epigastric pain, weight loss, nausea, and vomiting.

Treatment of gastric atresia includes excision of the membrane (with or without pyloroplasty) or gastroduodenostomy.

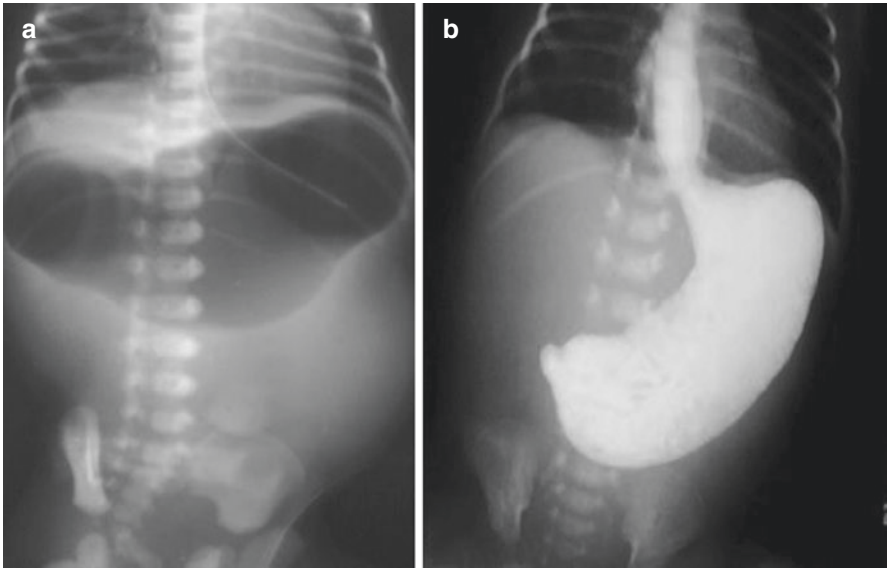


Fig. 9.7 (a and b) Plain abdominal radiograph showing a single large gastric bubble with no distal gas in a patient with congenital pyloric atresia

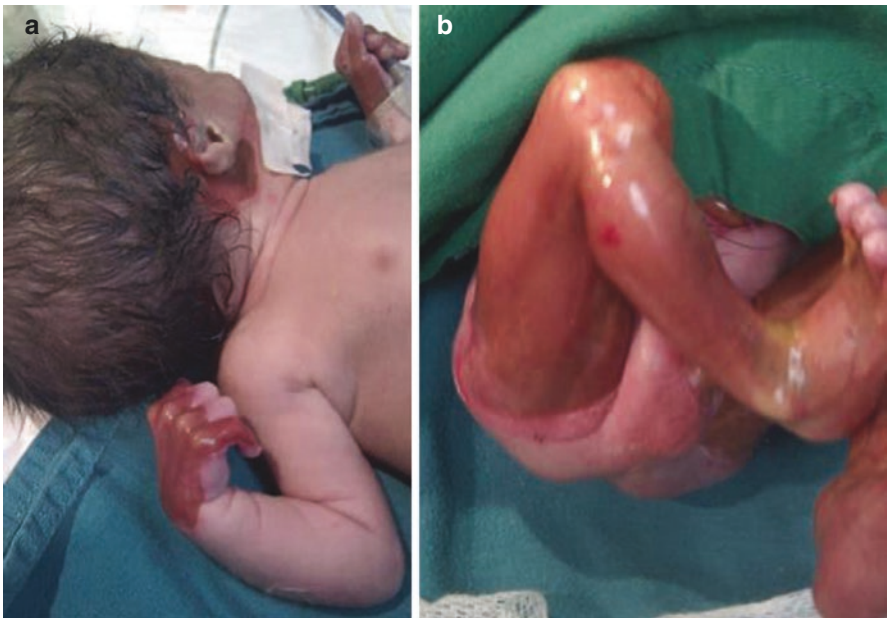
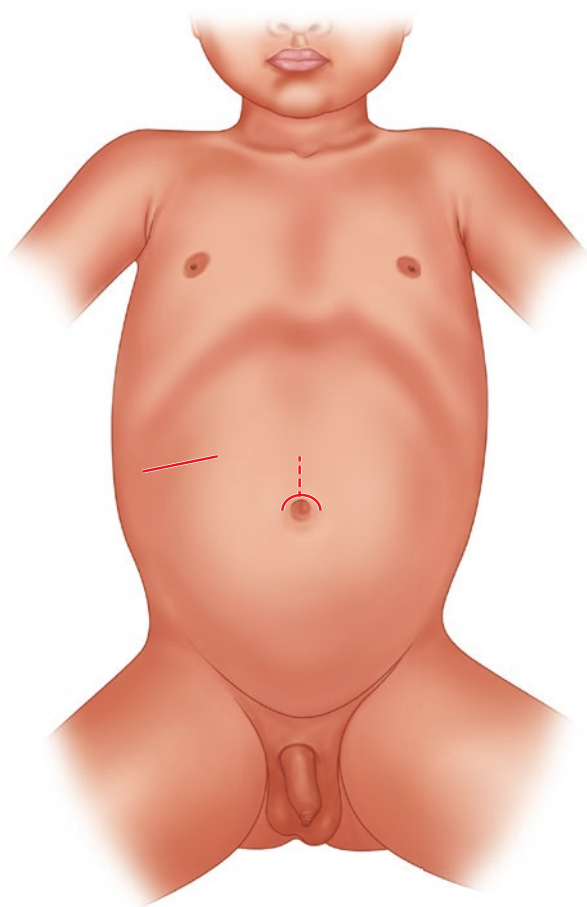


Fig. 9.8 (a and b) Aplasia cutis congenital and epidermolysis bullosa in a patient with congenital pyloric atresia

Pyloric Stenosis

By far the most common cause of gastric outlet obstruction in infants is hypertrophic pyloric stenosis (HPS), which presents as projectile non-bilious emesis most commonly in 2–6-week-old infants. HPS clusters in families suggesting a likely complex genetic contribution to the disorder, with a suggested role for nitric oxide synthase [36–38]. Additional environmental exposures, including erythromycin, have also been linked epidemiologically. Diagnosis is made on the basis of clinical exam with palpation of a palpable pyloric “olive” or, more commonly, ultrasonographic findings of a thickened pyloric wall >3 mm and a pyloric channel longer than 1.4 cm with no passage fluid across the pylorus. Treatment is rehydration and stabilization of electrolytes followed by open or laparoscopic pyloromyotomy (Fig. 9.9). A small body of literature describes the supportive medical treatment of HPS with atropine and TPN, but this results in a greatly extended length of hospitalization and is not recommended.

Fig. 9.9 Open incisional approaches to hypertrophic pyloric stenosis



Hourglass Stomach

Annular constrictions of the stomach may arise from local muscular hypertrophy in response to corrosive substances, ulcer disease, neoplastic, or syphilitic lesions. Compression from the rib cage in rare cases can cause positional changes in gastric anatomy leading to nausea, borborygmi, and abdominal discomfort [39]. Gastric emptying may be impaired in an hourglass stomach, and some authors suggest that the healing of a gastric ulcer may be further impaired by gastric stasis, thus contributing to the perpetuation of a cycle of ulcer disease [40].

Duodenum

Rotational Abnormalities

Variations in the sequence of herniation, rotation, and fixation during the fourth through eleventh weeks of gestation are responsible for the full spectrum of intestinal rotation abnormalities and internal hernias. If the cecocolic loop returns to the abdomen prior to the return of the proximal foregut, the duodenum and jejunum are not pushed superior-laterally and undergo only 180 degrees of rotation. In this scenario, the colon remains on the left side of the abdomen, while the midgut fills in the right abdomen and duodenum descends directly along the course of the SMA. This condition is classically termed “nonrotation,” and because it is associated with a wide-based mesentery, non-rotation does not put the patient at risk for midgut volvulus. Classic “malrotation” occurs as a result of failed extracoelomic rotation. It is also most commonly associated with the duodenal-jejunal juncture in the right upper quadrant and a midabdominal cecum fixed in place by adhesive bands to the gallbladder, liver, duodenum, and right-sided abdominal wall (“Ladd’s bands”). Most important, classic malrotation results in a narrowed mesenteric base, which predisposes the patient to midgut volvulus. If the bowel makes a 90 degree turn clockwise, rather than counterclockwise, reverse rotation results. In reverse rotation, the colon typically returns to the abdomen prior to the duodenum. As a result, the duodenum lies anterior to the SMA and the colon lies posteriorly, producing a retroarterial tunnel which may be associated with partial mesenteric arterial, venous, and lymphatic obstruction. If the mesoderm does not fuse to the retroperitoneum over the fourth and fifth months of gestation, paraduodenal or paracolic hernias may form. Because of the complexity of intestinal rotation, the variations in rotational anomalies are seemingly endless. While not all variations are associated with a narrowed mesenteric base (and are thereby not all at risk for volvulus), attempts to fix the bowel to the retroperitoneum in each case can create focally obstructing bands which require surgical division.

Depending on the source, the reported incidence of rotational abnormalities varies widely from as frequent as 1:200 in autopsy series to 1:6–10,000 diagnosed by symptoms. While the Ladd procedure (detorsion of involved midgut, division of Ladd’s bands, widening of the mesentery, placement of bowel in non-rotation, and

appendectomy) remains the mainstay of management of symptomatic malrotation, the treatment of asymptomatic malrotation remains controversial (Fig. 9.10). Using malrotation data from the Nationwide Inpatient Sample to derive a model of quality-adjusted life expectancy with and without a Ladd procedure in asymptomatic patients, it was estimated that the greatest benefit of a Ladd procedure occurred within the first year of life and declined thereafter. By 20 years of age, a Ladd procedure conferred more risk than non-operative observation. Thus, adults with incidentally detected malrotation need not be offered an operative intervention, while children discovered with malrotation still benefit from an approach which places them in non-rotation.

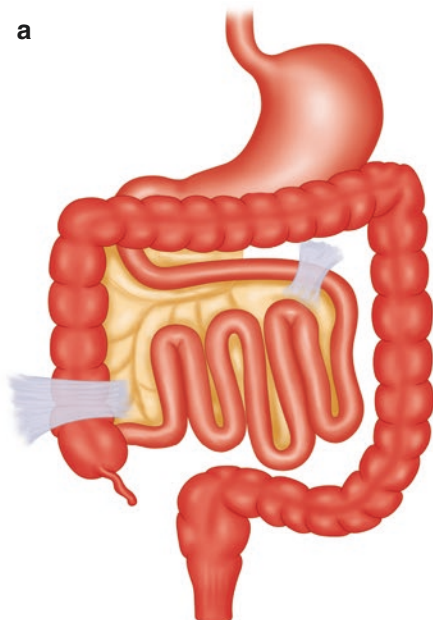
Patients with heterotaxia syndromes (HS), defined as any arrangement of organs that is neither situs solitus nor situs inversus, are estimated to have up to an 80% rate of rotational abnormalities. The frequent coexistence of congenital heart disease in many patients places them at increased risk for operative intervention. While consensus on the management of these patients has not yet been achieved, emerging data suggest that the risks of Ladd procedure both perioperatively and on long-term follow-up are far greater than the risk of volvulus in asymptomatic patients regardless of age.

Duodenal Atresia and Stenosis

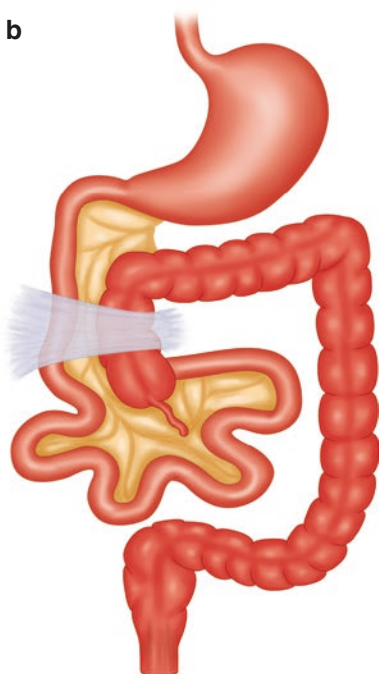
Duodenal atresia and stenosis is a proximal bowel obstruction that occurs in 1–2 cases per 10,000 live births. Approximately 1 in 3 infants with duodenal atresia are affected with Trisomy 21, and 1 in 3 are affected by some degree of congenital heart disease [41]. In contrast to more distal intestinal atresia, which is due to vascular accidents in utero, duodenal atresia is a developmental disorder. In early development, at around 8 weeks of gestation, the duodenum is a tubular structure that is proliferated by the epithelium to occlude the duodenal lumen. Subsequent recanalization and vacuolization are a complex series of apoptotic events that re-establish the duodenal lumen. Failure of this recanalization results in duodenal atresia [42]. Related anatomic abnormalities include annular pancreas, where the head of the pancreas wraps around the duodenum and pre-duodenal portal vein (see sections “[Duodenum](#)” and “[Preduodenal Portal Vein](#)”).

Fig. 9.10 Malrotation and midgut volvulus. **(a)** In normal development, the midgut is fixed to the retro-peritoneum and the mesentery has a wide base. **(b)** In malrotation, the narrow base of mesentery can undergo volvulus **(c)** and requires repair with the Ladd’s procedure **(d)** in which Ladd’s band are divided, the mesentery is widened by the division of constricting fibrous bands which traverse it, and the bowel is placed in non-rotation with the small bowel lying to the right and the large bowel on the left. An appendectomy is performed, as the left-sided placement of the cecum would result in an atypical presentation of appendicitis later in life

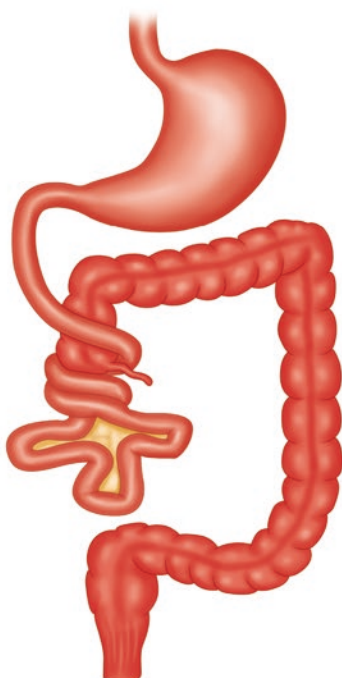
a



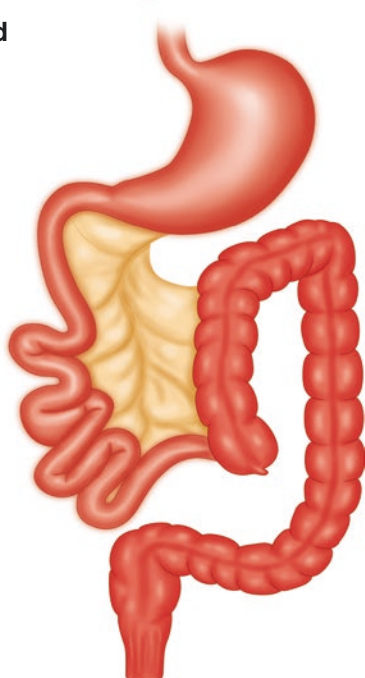
b



c



d



Prenatal diagnosis of duodenal atresia is frequently made. Cases are often associated with polyhydramnios, and the dilated stomach and duodenum can be appreciated as a “double bubble” on prenatal ultrasound (US) [43]. This “double bubble” can be appreciated on postnatal plain film as well (Fig. 9.11). In patients who present prenatally with polyhydramnios and a double bubble, duodenal atresia is the leading diagnosis, but in utero volvulus and midgut loss as well as very proximal jejunal atresia are possible. In infants who present with bilious emesis and a proximal bowel obstruction or double bubble, but in whom there has been no prenatal diagnosis of duodenal atresia, malrotation with volvulus must be strongly considered. Long-standing obstruction in utero generally results in a more dilated stomach than postnatal volvulus.

There are several types of duodenal atresia. In Type I duodenal atresia, there is a web or membrane between the proximal and distal duodenum; this is sometimes called a “wind-sock” deformity (Fig. 9.12). In type II duodenal atresia, there is a fibrous cord between the proximal and distal duodenum, while in type III duodenal atresia, there is nothing connecting the proximal and distal duodenum. About 80% of the atresia is past the ampulla of Vater, and therefore, in those cases, gastric aspirate and emesis should be bilious. These anomalies can be corrected through an open or laparoscopic approach depending on surgeon comfort and experience. The first step upon entering the abdominal cavity is to assess the rotational state of the bowel; a Ladd’s procedure is performed in cases of malrotation. In cases of normal rotation, the colon is mobilized medially to fully expose the duodenum. The duodenum is mobilized from the retroperitoneum. An incision is made transversely in the proximal dilated end about 1 cm proximal to the extent of the atresia; if a web is

Fig. 9.11 “Double bubble” on abdominal radiograph associated with duodenal atresia



Fig. 9.12 Diagram of duodenal web illustrating dilation of proximal duodenum beyond the origin of a windssock-type web

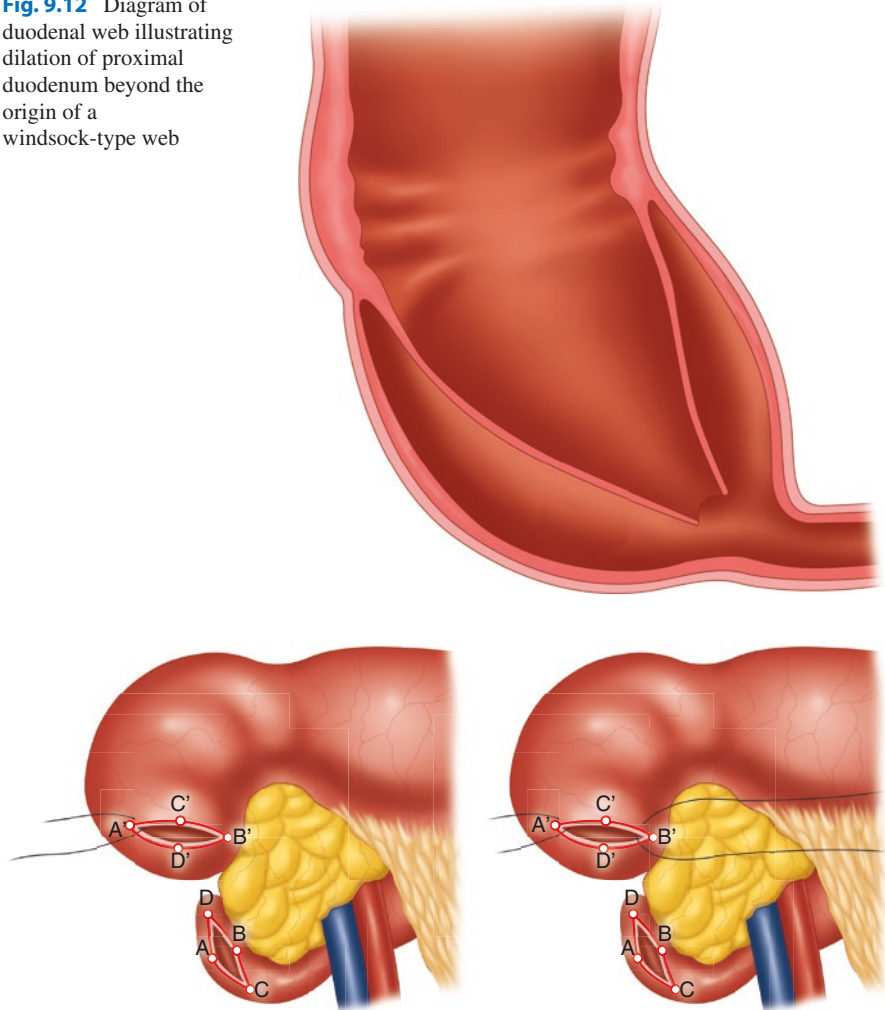


Fig. 9.13 The Kimura technique of a “diamond-shaped” anastomosis between proximal dilated duodenum and distal collapse duodenum

encountered, the gallbladder can be squeezed to look for bile in the lumen to identify the ampulla of Vater. Duodenoduodenostomy can be performed for all three types of duodenal atresia. Excision of the web away from the ampulla may be undertaken, but it is also safe and effective to leave the web and complete a duodenoduodenostomy between the bowel proximal and distal to the web. To complete a duodenoduodenostomy, a longitudinal incision is made in the distal collapsed segment of bowel; a nasogastric tube can be passed from the stomach to the distal duodenum to rule out a missed web and assure anastomotic patency. The Kimura technique of diamond-shaped anastomosis is generally used for the anastomosis (Fig. 9.13). A gastrostomy tube may be considered for patients with congenital heart disease, who may not be able to keep up with caloric need by oral feeds; some

surgeons perform gastrostomy tubes for all duodenal atresia cases in the context of trisomy 21, but this may not be necessary. Bowel function may take up to 3 weeks to commence.

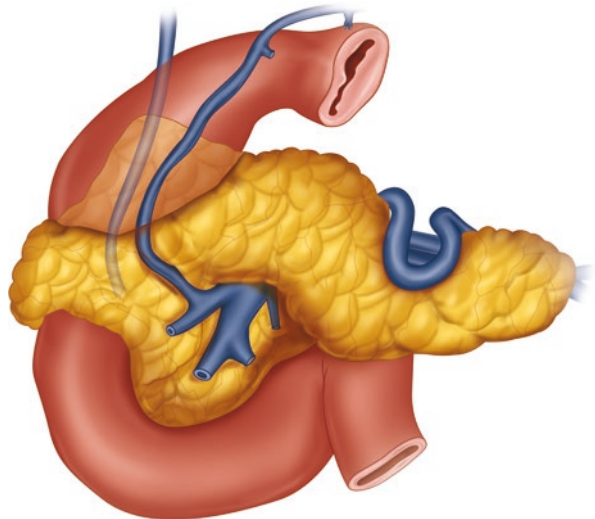
Annular Pancreas

Annular pancreas arises as a failed result of normal rotation of the ventral bud of the pancreas, causing it to elongate and encircle the second portion of the duodenum. Commonly, annular pancreas presents in the neonatal period and is manifest as duodenal atresia (Fig. 9.14). Later in life, annular pancreas can present as persistent failure to thrive, cyclic vomiting, peptic ulcer disease, and duodenal obstruction. Upper endoscopy, upper GI series, and CT scans can be used in the workup, but almost half of cases are definitively diagnosed at the time of operation. Treatment does not involve resection of the pancreas, but bypassing the point of obstruction, most commonly through a duodenoduodenostomy [44].

Preduodenal Portal Vein

Preduodenal portal vein is a rare cause of foregut obstruction. It is most frequently diagnosed at the time of operative approach. As with other causes of duodenal obstruction, treatment is duodenoduodenostomy.

Fig. 9.14 Anatomy of annular pancreas



Jejuno-Ileal Atresia

Jejuno-ileal atresia carries an incidence of approximately 1:1000 live births. In contrast to duodenal atresia, which is an early developmental event, where the lumen fails to recanalize, atresias of the jejunum and ileum are the result of vascular occlusion in development that results in reabsorption and loss of the devascularized segments of bowel. These vascular insults may take the form of thrombo-embolisms, intussusception or volvulus. Proximal atresias may present during prenatal imaging with bowel dilation and polyhydramnios; however, most cases are not detected before birth. After birth, these babies present with feeding intolerance, emesis, abdominal distention, and a plain film with picture of bowel obstruction. The babies are hydrated and will often undergo contrast enema to assess the colon. These babies are then brought for an operation to repair the atresia. There are several variants of jejunal and ileal atresias (Fig. 9.15). The type of atresia depends on the vessel that is occluded and the gestational timing of the vascular accident. In type I, the serosae

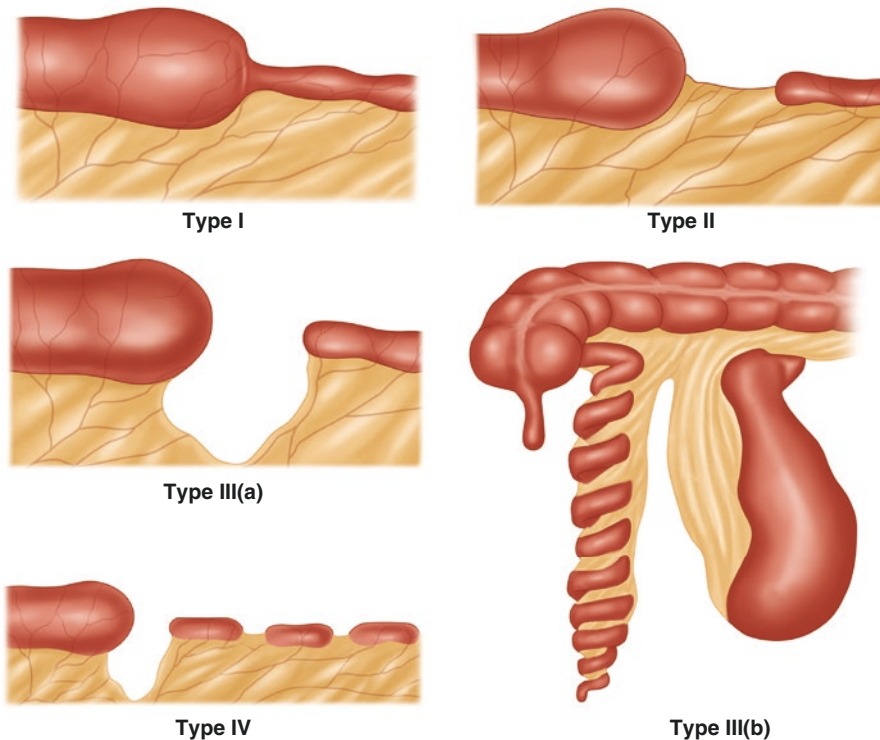


Fig. 9.15 Types of jejunal atresia

of the bowel before and after the atresia are in continuity. In type 2 and 3a, the proximal and distal bowel are clearly separated. For type 4 atresias where there are multiple segments of bowel that are not connected, catheters or fluid is passed through the intestine to confirm the lumen is patent distal to the first atresia. Type 3b atresia is a special case, in which the superior mesenteric artery has been obliterated and the remaining distal bowel is supplied by the ileocolic artery; in this case, the bowel swirls around the supplying vessel. Up to 20 cm proximal to the atresia have abnormal histology and nerve development. This bulbous proximal bowel is often resected for this reason, but in cases of short bowel, this portion is left, recognizing that commencement of bowel function may take several weeks. Upon repair, multiple atresias are ruled out, the bowel length is measured, and the proximal and distal ends are anastomosed with a single layer of sutures.

Omphalomesenteric Duct Abnormalities

The omphalomesenteric duct (OMD) connects the alimentary tract to the embryonic yolk sac during the early stages of gestation. The OMD usually involutes between the fifth and ninth weeks of gestation, and failure of involution can lead to multiple OMD anomalies. Similar to urachal remnant anomalies, an omphalomesenteric remnant might exist as a fistulous tract, a cyst, a fibrous band, or a diverticulum (Meckel's diverticulum) of the small bowel (Fig. 9.16). The Meckel's diverticulum (MD) variant is by far the most common form of omphalomesenteric duct anomaly (approximately 90%).

Meckel's Diverticulum

The anomaly is typically seen as an outpouching of the intestine located in the distal or terminal ileum. The incidence of Meckel's diverticulum is estimated from 1 to

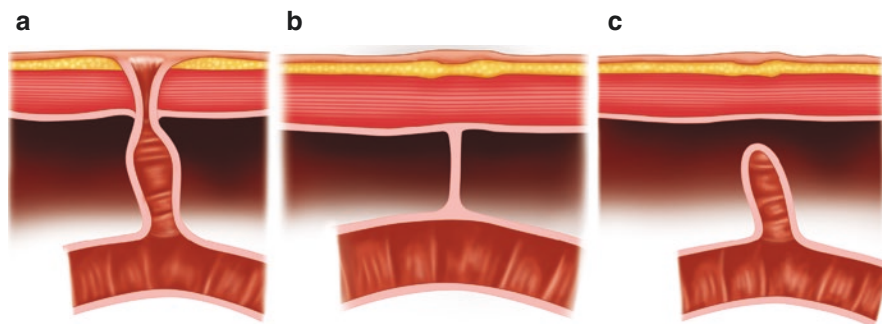


Fig. 9.16 Omphalomesenteric remnants can persist as a fistula between the bowel and the umbilicus (**a**). They can persist as a fibrous band between the bowel and the abdominal wall (**b**). They can present as a diverticulum (with or without a band) in the form of a Meckel's diverticulum

4% in the general population, but the true incidence is unknown and based largely on historical autopsy studies because only 4–6% of patients become symptomatic over the course of a lifetime [45–48]. The incidence of MD is increased in patients with other major anomalies of umbilicus, GI tract, nervous system, or cardiovascular system [49]. The risk of developing symptoms related to MD decreases with age. Pathological analysis of resected specimens has proven that symptomatic diverticula often contain heterotopic gastric, pancreatic, carcinoid, duodenal, colonic, endometrial, or neoplastic tissue. As seen with intestinal duplications, the two most common heterotopic tissues found are gastric and pancreatic tissue, with gastric mucosa being present in up to 75% of symptomatic MD [47, 50].

The most common variant of MD is a free blind-ending pouch on the antimesenteric border of the small bowel (Fig. 9.17). The diverticulum is sometimes attached to the umbilicus via a fibrous band, and it might also have blood supply from an aberrant vitelline vessel originating from the mesenteric circulation. As the name implies, MD is a “true” diverticulum, which means that it contains all three layers of the intestinal wall (serosa, muscularis, and mucosa). There is an unofficial “rule of 2s” that serves as a helpful mnemonic for MD: 2% prevalence; 2:1 male-to-female ratio; presents by 2 years of age; location 2 feet from ileocecal junction; 2 cm diameter; 2 inches in length; 2 common types of heterotopic tissue.

The classic presentation of symptomatic MD is intermittent painless rectal bleeding, but intestinal obstruction and inflammation (diverticulitis) are similarly common presentations. Bleeding associated with MD is usually due to intestinal mucosal ulceration caused by ectopic gastric mucosa within the diverticulum, and up to 75–80% of MD associated with bleeding will contain ectopic gastric mucosa on pathological analysis [47, 51]. The ulceration is located most often at the transition from heterotopic to normal mucosa, but it can also be located at the base of the diverticulum or on the mesenteric side opposite the diverticulum. The majority of bleeding MD cases are hemodynamically stable with variable degrees of anemia

Fig. 9.17 A Meckel’s diverticulum can be appreciated on the antimesenteric side of the small bowel



and heme-positive stools. Though very rare, life-threatening hemorrhage from MD might require transfusion and emergent angioembolization [52, 53].

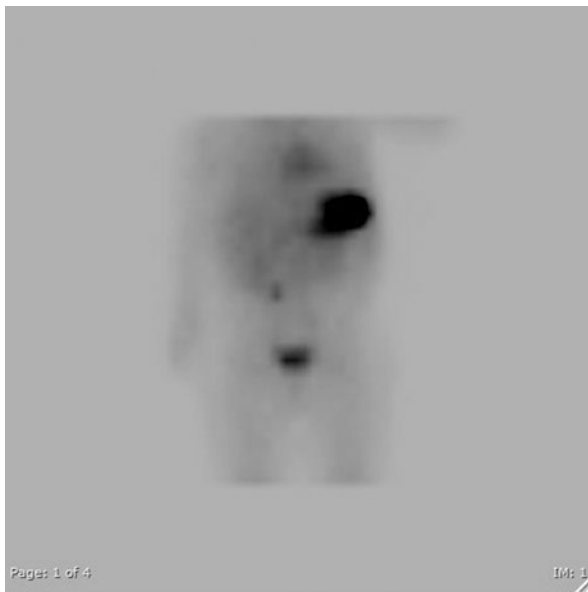
Despite the classic teaching about painless rectal bleeding, multiple reports have shown that intestinal obstruction might actually be more common than bleeding at presentation, especially in the younger pediatric population. According to a review of 217 patients with MD, obstruction was more common for patients aged less than 1 month, while patients aged 1 month to 4 years were more likely to experience painless rectal bleeding [54]. In a larger series of 1476 patients of all ages, children under the age of 11 years with symptomatic MD presented most often with obstruction (40%) followed by bleeding (31%) and diverticulitis (29%) [47]. In this same study, symptomatic adults were only slightly more likely to present with bleeding (38%) compared to obstruction (34%) and diverticulitis (28%). The two main etiologies of obstruction in MD are intussusception and volvulus, but internal hernias are sometimes seen as well. If not diagnosed in a timely fashion, obstruction from MD can progress to bowel strangulation, perforation, and death.

Meckel's diverticulitis is the third most common presentation of MD. Inflammation can be secondary to heterotopic tissue or be attributed to an obstructing enterolith or foreign body (e.g., chicken bone). Cases of inflammation progressing to perforation and peritonitis have been reported with rates of acute perforation reported as high as 8–12% in both adult and pediatric populations [47, 50].

Although a thorough history and physical should raise suspicion for MD in certain symptomatic patients, the low incidence of symptomatic MD contributes to a relatively high rate of incidental diagnosis. The differential diagnosis for rectal bleeding is large and includes anal fissure, (juvenile) intestinal polyps, inflammatory bowel disease, intestinal duplications, and vascular malformations. Patients with acutely inflamed MD are often misdiagnosed with acute appendicitis prior to operation, and so a normal-appearing appendix in a patient with signs and symptoms of appendicitis should prompt examination of the distal ileum for a diverticulum. Imaging modalities used to diagnose MD include upper and lower GI contrast studies (small bowel follow-through, enteroclysis), ultrasound (US), computed tomography (CT), magnetic resonance imaging (MRI), and technetium-99 m pertechnetate scintigraphy (TPS), with the latter being the most commonly used test specifically for MD.

Technetium-99 m pertechnetate scintigraphy, also referred to as a “Meckel's scan,” is a nuclear medicine scan that employs an intravenous injection of the radioactive compound 99 m-technetium pertechnetate (Fig. 9.18). Pertechnetate is taken up by the mucin-producing cells of gastric tissue and secreted into the gut lumen, and therefore, this scan visualizes ectopic gastric mucosa that might be located within the diverticulum (or anywhere else in the body). Problems with TPS include significant false-negative and false-positive rates, especially when the scan is used without proper preparation or clinical findings. False negatives can occur when the MD does not contain ectopic gastric tissue or if bladder tracer activity obscures the diverticulum. False negatives can occur with duplication cysts, inflammatory bowel disease, intussusception, small bowel obstruction (from a different cause), peptic ulcer, vascular lesions (e.g., arteriovenous malformation), and certain neoplasms. In

Fig. 9.18 Meckel's scan of a 9-month-old female who presented with painless bleeding per rectum. There is a focus of persistent increased pertechnetate radiotracer in the right mid to lower abdomen consistent with ectopic gastric mucosa and a Meckel's diverticulum



a predominantly pediatric population, a Meckel scan has an overall sensitivity of 85%, specificity of 95%, and accuracy of 90% for diagnosing MD with ectopic gastric mucosa [55]. In a strictly adult population, however, the sensitivity and specificity fall to 60% and 75%, respectively [51, 56]. The sensitivity of the scan is significantly increased by pre-conditioning with an H₂-blocker (cimetidine, ranitidine, famotidine) or proton-pump inhibitor, pentagastrin, fasting, emptying the bladder, or intravenous glucagon [57].

The treatment for symptomatic MD is surgical excision. The surgeon can perform a simple diverticulectomy, wedge resection of the bowel, or segmental resection of the associated bowel. The procedure can be performed via an open or a laparoscopic approach, and indications for resection of the diverticulum include bleeding, diverticulitis, intussusception, and obstruction. Several authors have investigated parameters that might help when deciding whether to perform a simple diverticulectomy, a wedge resection, or a segmental bowel resection. A study of 77 patients revealed that shorter MD (< 2 cm) contain ectopic gastric mucosa more often at the base, and for these, segmental resection is indicated.

While most pediatric surgeons agree that there is no need to perform surgery on an asymptomatic MD identified incidentally with an imaging study, routine resection of MD found incidentally *during an operation* remains controversial. Some groups have suggested that incidental MD identified during an operation should be removed in younger patients to reduce the risk of future complications and malignancies [47, 58, 59]. Opponents to resection of incidental MD quote the significant complications that can occur after diverticulectomy, the extremely low lifetime risk of death from MD, and the relatively high number needed to treat 758–800 to prevent 1 death from MD [60–64].

Umbilical Polyps

Umbilical polyps are rare OMD remnant anomalies. These polyps are usually diagnosed in the neonatal period as tufts of moist reddish-pink tissue located at the umbilicus. Despite the rather straightforward visual diagnosis, there are reports of initial diagnosis of umbilical polyps in older children and even adults [65]. Umbilical polyps are often confused with granulation tissue, as both entities exist as nodules of pink-red tissue associated with intermittent serous drainage from the umbilicus. A much broader differential diagnosis includes superficial infection (omphalitis), urachal sinus, urachal cyst, urachal diverticulum, patent urachus, herniated MD, and umbilical-enteric fistula [66]. Failure of granulation tissue to resolve with multiple silver nitrate treatments should raise the suspicion for an umbilical polyp. As with other OMD remnants, an umbilical polyp might contain intestinal, gastric, pancreatic, or other heterotopic tissue. When present, a polyp might be associated with another OMD anomaly such as a sinus, cyst, fistula, band, or diverticulum, but the true frequency of the association is currently unknown. The treatment for a simple pedunculated umbilical polyp is ligation of the base with absorbable suture.

Umbilical Enteric Fistula

Polyps associated with complex OMD remnants (e.g., umbilical-enteric fistula) within the abdomen may require further investigation and surgical excision via mini laparotomy or laparoscopy to prevent complications such as bowel obstruction and perforation [67]. If there is concern for a complex OMD anomaly associated with a known polyp, then the polyp should be investigated first with ultrasound and, if patent, a contrast sinogram (fistulogram) to rule out any intra-abdominal sinus or fistula tracts. In this way, one can avoid unnecessary exploration of the abdominal cavity in patients with simple umbilical polyps [68, 69]. If there is frank bilious or fecal drainage from the umbilicus, then a diagnosis of umbilical-enteric fistula is most likely and can be both confirmed and mapped using a contrast fistulogram. An umbilical-enteric fistula will need to be excised via open surgical repair of the umbilicus, resection of the fistula, and primary closure of the enterotomy.

Umbilical Band

If the OMD remnant undergoes partial involution, then it might exist as a fibrous band between the umbilicus and the intestine. The fibrous band might have cystic lesions located at any point along its length, or a band might lead into a blind-ending sinus tract that opens at the umbilicus and results in chronic serous discharge. These entities are relatively rare compared to MD. Like MD, these less common OMD remnants might contain gastric, pancreatic, or other heterotopic tissue [70]. Because these OMD variants tether the small bowel to the umbilicus, they also predispose patients to intestinal volvulus, obstruction, and possible bowel perforation [71]. In

patients who present with a bowel obstruction picture, where there is no history or prior surgery or obvious hernia, OMD bands should be suspected. There are no evidence-based guidelines for the management of asymptomatic OMD remnant fibrous bands and cysts, but there is general consensus that symptomatic OMD remnants should be resected to prevent serious complications. Surgical excision can be performed via open or laparoscopic approach, and there are multiple reports of successful laparoscopic excision of OMD remnant bands and cysts [72–75].

References

1. Michaud L, Coutenier F, Podevin G, Bonnard A, Becmeur F, Khen-Dunlop N, et al. Characteristics and management of congenital esophageal stenosis: findings from a multicenter study. *Orphanet J Rare Dis*. 2013;8:186.
2. Rebelo PG, Ormonde JV, Ormonde Filho JB. Congenital esophageal stenosis owing to tracheobronchial remnants. *Rev Paul Pediatr*. 2013;31(3):406–10.
3. Romeo E, Foschia F, de Angelis P, Caldaro T, Federici di Abriola G, Gambitta R, et al. Endoscopic management of congenital esophageal stenosis. *J Pediatr Surg*. 2011;46(5):838–41.
4. Schatzki R. The lower esophageal ring. Long term follow-up of symptomatic and asymptomatic rings. *Am J Roentgenol Radium Therapy, Nucl Med*. 1963;90:805–10.
5. Kahrilas PJ, Kim HC, Pandolfino JE. Approaches to the diagnosis and grading of hiatal hernia. *Best Pract Res Clin Gastroenterol*. 2008;22(4):601–16.
6. Heyman MB, Berquist WE, Fonkalsrud EW, Lewin KJ, Ament ME. Esophageal muscular ring and the VACTERL association: a case report. *Pediatrics*. 1981;67(5):683–6.
7. Klein MD, Waltner J, Ball W, Kosloske AM. Schatzki ring in a newborn. *Pediatrics*. 1981;68(6):884–5.
8. Okamura H, Tsutsumi S, Inaki S, Mori T. Esophageal web in Plummer-Vinson syndrome. *Laryngoscope*. 1988;98(9):994–8.
9. Chisholm M, Ardran GM, Callender ST, Wright R. Iron deficiency and autoimmunity in post-cricoid webs. *Q J Med*. 1971;40(159):421–33.
10. Elwood PC, Jacobs A, Pitman RG. Entwistle CC epidemiology of the Paterson-Kelly syndrome. *Lancet*. 1964;2(7362):716–20.
11. Müller M, Gockel I, Hedwig P, Eckardt AJ, Kuhr K, König J, et al. Is the Schatzki ring a unique esophageal entity? *World J Gastroenterol*. 2011;17(23):2838–43.
12. Low DE, Hill LD. Cervical esophageal web associated with Zenker's diverticulum. *Am J Surg*. 1988;156(1):34–7.
13. Grosfeld JL, O'Neill JA, Clatworthy HW Jr. Enteric duplications in infancy and childhood: an 18-year review. *Ann Surg*. 1970;172(1):83–90.
14. Liu R, Adler DG. Duplication cysts: diagnosis, management, and the role of endoscopic ultrasound. *Endosc Ultrasound*. 2014;3(3):152–60.
15. Superina RA, Ein SH, Humphreys RP. Cystic duplications of the esophagus and neurenteric cysts. *J Pediatr Surg*. 1984;19(5):527–30.
16. Sethi GK, Marsden J, Johnson D. Duplication cysts of the esophagus. *South Med J*. 1974;67(5):616–8.
17. Holmes GL, Trader S, Ignatiadis P. Intraspinal enterogenous cysts. A case report and review of pediatric cases in the literature. *Am J Dis Child*. 1978;132(9):906–8.
18. Hirose S, Clifton MS, Bratton B, Harrison MR, Farmer DL, Nobuhara KK, et al. Thoracoscopic resection of foregut duplication cysts. *J Laparoendosc Adv Surg Tech A*. 2006;16(5):526–9.
19. Ivekovic H, Jouret-Mourin A, Deprez PH. Endoscopic fenestration of esophageal duplication cysts. *Endoscopy*. 2012;44 Suppl 2 UCTN:E404–5.
20. McMaster WG Jr, Mukherjee K, Parikh AA. Surgical management of a symptomatic foregut duplication cyst. *Am Surg*. 2012;78(6):E306–7.

21. Zani A, Cobellis G, Wolinska J, Chiu PP, Pierro A. Preservation of native esophagus in infants with pure esophageal atresia has good long-term outcomes despite significant postoperative morbidity. *Pediatr Surg Int.* 2016;32(2):113–7.
22. Lee HQ, Hawley A, Doak J, Nightingale MG, Hutson JM. Long-gap oesophageal atresia: comparison of delayed primary anastomosis and oesophageal replacement with gastric tube. *J Pediatr Surg.* 2014;49(12):1762–6.
23. Bairdain S, Hamilton TE, Smithers CJ, Manfredi M, Ngo P, Gallagher D, et al. Foker process for the correction of long gap esophageal atresia: primary treatment versus secondary treatment after prior esophageal surgery. *J Pediatr Surg.* 2015;50(6):933–7.
24. Bobanga ID, Barksdale EM. Foker technique for the management of pure esophageal atresia: long-term outcomes at a single institution. *Eur J Pediatr Surg.* 2016;26(2):215–8.
25. Nasr A, Langer JC. Mechanical traction techniques for long-gap esophageal atresia: a critical appraisal. *Eur J Pediatr Surg.* 2013;23(3):191–7.
26. Sroka M, Wachowiak R, Losin M, Szlagatys-Sidorkiewicz A, Landowski P, Czauderna P, et al. The Foker technique (FT) and Kimura advancement (KA) for the treatment of children with long-gap esophageal atresia (LGEA): lessons learned at two European centers. *Eur J Pediatr Surg.* 2013;23(1):3–7.
27. Gallo G, Zwaveling S, Groen H, Van der Zee D, Hulscher J. Long-gap esophageal atresia: a meta-analysis of jejunal interposition, colon interposition, and gastric pull-up. *Eur J Pediatr Surg.* 2012;22(6):420–5.
28. Gallo G, Zwaveling S, Van der Zee DC, Bax KN, de Langen ZJ, Hulscher JB. A two-center comparative study of gastric pull-up and jejunal interposition for long gap esophageal atresia. *J Pediatr Surg.* 2015;50(4):535–9.
29. Kunisaki SM, Dakhoub A, Jarboe MD, Geiger JD. Gastric dissociation for the treatment of congenital microgastria with paraesophageal hiatal hernia. *J Pediatr Surg.* 2011;46(6):e1–4.
30. Vasas P, Mudan SS, Akle CA. Congenital microgastria with limb defect combined with mega-duodenum: case report and review of literature. *Indian J Surg.* 2011;73(2):122–4.
31. Nagendran S, Johal N, Set P, Brain J, Aslam A, Samuel M. Bilateral communicating intralobar sequestration and microgastria. *Ann Thorac Surg.* 2009;88(6):2040.
32. Filippi L, Serafini L, Fiorini P, Agostini E, Giovannucci Uzielli ML. Congenital microgastria and primary ciliary dyskinesia in a newborn with DiGeorge syndrome and 22q11.2 deletion. *Eur J Pediatr Surg.* 2008;18(3):195–7.
33. Laurie DE, Wakeling EL. Congenital microgastria in association with Pierre-Robin sequence. *Clin Dysmorphol.* 2008;17(2):143–4.
34. Al-Salem AH, Abdulla MR, Kothari MR, Naga MI. Congenital pyloric atresia, presentation, management, and outcome: a report of 20 cases. *J Pediatr Surg.* 2014;49(7):1078–82.
35. Farmakis SG, Herman TE, Siegel MJ. Congenital pyloric atresia, type B; with junctional epidermolysis bullosa. *J Perinatol.* 2014;34(7):572–3.
36. Vanderwinden JM, Mailleux P, Schiffmann SN, Vanderhaeghen JJ, De Laet MH. Nitric oxide synthase activity in infantile hypertrophic pyloric stenosis. *N Engl J Med.* 1992;327(8):511–5.
37. Serra A, Schuchardt K, Genuneit J, Leriche C, Fitze G. Genomic variants in the coding region of neuronal nitric oxide synthase (NOS1) in infantile hypertrophic pyloric stenosis. *J Pediatr Surg.* 2011;46(10):1903–8.
38. Svenningsson A, Söderhäll C, Persson S, Lundberg F, Luthman H, Chung E, et al. Genome-wide linkage analysis in families with infantile hypertrophic pyloric stenosis indicates novel susceptibility loci. *J Hum Genet.* 2012;57(2):115–21.
39. Sharma A, Moriarty K, Burnett H, Paraoan M, Thompson D. Intractable positional boboryngmi – an unusual cause diagnosed by barium contrast study. *BMJ Case Rep.* 2010;2010:bcr0120102637.
40. Fukumoto S, Amano Y, Fukuda R, Gobaru Y, Adachi K, Ashizawa N, et al. Gastric emptying in deformed stomach. *Gastroenterol Jpn.* 1987;22(1):1–6.
41. Freeman SB, Torfs CP, Romitti PA, Royle MH, Druschel C, Hobbs CA, et al. Congenital gastrointestinal defects in down syndrome: a report from the Atlanta and National down Syndrome Projects. *Clin Genet.* 2009;75(2):180–4.

42. Ando H, Kaneko K, Ito F, Seo T, Harada T, Watanabe Y. Embryogenesis of pancreaticobiliary maljunction inferred from development of duodenal atresia. *J Hepato-Biliary-Pancreat Surg.* 1999;6(1):50–4.
43. Escobar MA, Ladd AP, Grosfeld JL, West KW, Rescorla FJ, Scherer LR 3rd, et al. Duodenal atresia and stenosis: long-term follow-up over 30 years. *J Pediatr Surg.* 2004;39(6):867–71; discussion 867–71.
44. Alahmadi R, Almuhammadi S. Annular pancreas: a cause of gastric outlet obstruction in a 20-year-old patient. *Am J Case Rep.* 2014;15:437–40.
45. Holcomb GW, Murphy JP, Ostlie DJ, St Peter SD, Ashcraft KW. *Ashcraft's pediatric surgery.* Saunders Elsevier: London, New York; 2014.
46. Lüdtkke FE, Mende V, Köhler H, Lepsien G. Incidence and frequency or complications and management of Meckel's diverticulum. *Surg Gynecol Obstet.* 1989;169(6):537–42.
47. Park JJ, Wolff BG, Tollefson MK, Walsh EE, Larson DR. Meckel diverticulum: the Mayo Clinic experience with 1476 patients (1950–2002). *Ann Surg.* 2005;241(3):529–33.
48. Ruscher KA, Fisher JN, Hughes CD, Neff S, Lerer TJ, Hight DW, et al. National trends in the surgical management of Meckel's diverticulum. *J Pediatr Surg.* 2011;46(5):893–6.
49. Simms MH, Corkery JJ. Meckel's diverticulum: its association with congenital malformation and the significance of atypical morphology. *Br J Surg.* 1980;67(3):216–9.
50. Menezes M, Tareen F, Saeed A, Khan N, Puri P. Symptomatic Meckel's diverticulum in children: a 16-year review. *Pediatr Surg Int.* 2008;24(5):575–7.
51. Swaniker F, Soldes O, Hirschl RB. The utility of technetium 99m pertechnetate scintigraphy in the evaluation of patients with Meckel's diverticulum. *J Pediatr Surg.* 1999;34(5):760–4; discussion 765.
52. Bevernage C, Maleux G, De Hertogh G, Miserez M. Life-threatening lower gastrointestinal bleeding in a 2-year-old boy treated by transcatheter embolization: uncommon features of a complicated Meckel diverticulum. *Pediatr Radiol.* 2010;40(10):1702–5.
53. Leijonmarck CE, Sundien E, Ahlberg J. Massive intestinal hemorrhage from Meckel's diverticulum. *Lakartidningen.* 1985;82(12):1061–2.
54. Vane DW, West KW, Grosfeld JL. Vitelline duct anomalies. Experience with 217 childhood cases. *Arch Surg.* 1987;122(5):542–7.
55. Sfakianakis GN, Conway JJ. Detection of ectopic gastric mucosa in Meckel's diverticulum and in other aberrations by scintigraphy: I. Pathophysiology and 10-year clinical experience. *J Nucl Med.* 1981;22(7):647–54.
56. Schwartz MJ, Lewis JH. Meckel's diverticulum: pitfalls in scintigraphic detection in the adult. *Am J Gastroenterol.* 1984;79(8):611–8.
57. Spottswood SE, Pfluger T, Bartold SP, Brandon D, Burchell N, Delbeke D, et al. SNMMI and EANM practice guideline for meckel diverticulum scintigraphy 2.0. *J Nucl Med Technol.* 2014;42(3):16–9.
58. Thirunavukarasu P, Sathaiah M, Sukumar S, Bartels CJ, Zeh H 3rd, Lee KK, et al. Meckel's diverticulum—a high-risk region for malignancy in the ileum. Insights from a population-based epidemiological study and implications in surgical management. *Ann Surg.* 2011;253(2):223–30.
59. Cullen JJ, Kelly KA, Moir CR, Hodge DO, Zinsmeister AR, Melton LJ 3rd. Surgical management of Meckel's diverticulum. An epidemiologic, population-based study. *Ann Surg.* 1994;220(4):564–8; discussion 568–9.
60. Pomeranz A. Anomalies, abnormalities, and care of the umbilicus. *Pediatr Clin N Am.* 2004;51(13):819–27, xii.
61. Stone PA, Hofeldt MJ, Campbell JE, Campbell JE, Vedula G, DeLuca JA, et al. Meckel diverticulum: ten-year experience in adults. *South Med J.* 2004;97(11):1038–41.
62. Zani A, Eaton S, Rees CM, Pierro A. Incidentally detected Meckel diverticulum: to resect or not to resect? *Ann Surg.* 2008;247(2):276–81.
63. Leijonmarck CE, Bonman-Sandelin K, Frisell J, Räf L. Meckel's diverticulum in the adult. *Br J Surg.* 1986;73(2):146–9.

64. Soltero MJ, Bill AH. The natural history of Meckel's Diverticulum and its relation to incidental removal. A study of 202 cases of diseased Meckel's Diverticulum found in King County, Washington, over a fifteen year period. *Am J Surg.* 1976;132(2):168–73.
65. Kondoh S, Taniki T, Umemoto A, Kajikawa A, Sogame M, Tanaka K, et al. A case of umbilical polyp with aberrant pancreas and small intestinal mucosa – analysis of cases of umbilical polyp reported in Japan. *Nihon Geka Gakkai Zasshi.* 1994;95(10):786–9.
66. You Y, Yang X, Hao F, Zhong B. The umbilical polyp: a report of two cases and literature review. *Int J Dermatol.* 2009;48(6):630–2.
67. Kutin ND, Allen JE, Jewett TC. The umbilical polyp. *J Pediatr Surg.* 1979;14(6):741–4.
68. Pacilli M, Sebire NJ, Maritsi D, Kiely EM, Drake DP, Curry JJ, et al. Umbilical polyp in infants and children. *Eur J Pediatr Surg.* 2007;17(6):397–9.
69. Taranath A, Lam A. Ultrasonographic demonstration of a type 1 omphalomesenteric duct remnant. *Acta Radiol.* 2006;47(1):100–2.
70. Iwasaki M, Taira K, Kobayashi H, Saiga T. Umbilical cyst containing ectopic gastric mucosa originating from an omphalomesenteric duct remnant. *J Pediatr Surg.* 2009;44(12):2399–401.
71. Grosfeld JL, Franken EA. Intestinal obstruction in the neonate due to vitelline duct cysts. *Surg Gynecol Obstet.* 1974;138(4):527–32.
72. Lassen PM, Harris MJ, Kearsse WS Jr, Argueso LR. Laparoscopic management of incidentally noted omphalomesenteric duct remnant. *J Endourol.* 1994;8(1):49–51.
73. Annaberdyev S, Capizzani T, Plesec T, Moorman M. A rare case presentation of a symptomatic omphalomesenteric cyst in an adult, 24-year-old patient, treated with laparoscopic resection. *J Gastrointest Surg.* 2013;17(8):1503–6.
74. Sawada F, Yoshimura R, Ito K, Nakamura K, Nawata H, Mizumoto K, et al. Adult case of an omphalomesenteric cyst resected by laparoscopic-assisted surgery. *World J Gastroenterol.* 2006;12(5):825–7.
75. Morita K, Haga Y, Miyanari N, Sawayama H, Matsumoto K, Mizumoto T, et al. A case of an omphalomesenteric duct remnant in an adult treated with laparoscopic surgery. *Int J Surg Case Rep.* 2015;8C:179–81.



Surgical Anatomy of the Hepatobiliary System

10

Charles Cha and Whitney S. Brandt

Introduction

Hepatobiliary disease affects many people worldwide. From primary hepatocellular carcinoma and metastatic neoplasms to cholangiocarcinoma, an essential part of management is surgical. A strong knowledge of surgical anatomy is an essential part of managing these patients.

A strong foundation in hepatobiliary anatomy aids in the understanding the risks and potential pitfalls of hepatic resection. Appropriate resection of liver segments and their corresponding arterial, venous, and biliary supply helps minimize blood loss, preserve liver parenchyma, and avoid post-operative complications. In addition, resection of appropriate portions of the liver helps take conservative portions of tissue. Conservation of tissue is especially important in patients with synthetic liver dysfunction or for patients who undergo treatment with hepatotoxic medications (i.e., chemotherapy). Transplantation of livers provides its own difficulties, and knowing the anatomy aids in the delivery of appropriately sized segments for both pediatric patients and living donors [1].

Overview of Hepatic Anatomy

The Hepatocyte

The base of hepatic anatomy is the hepatocyte. Hepatocytes lie in plates of cells (Fig. 10.1a). Between adjacent cells lie bile canaliculi, which form tracts to drain bile into larger ducts. The hepatocytes are surrounded by fenestrated endothelial cells, which allow synthesized proteins to drain directly into the bloodstream.

C. Cha (✉) · W. S. Brandt

Department of Surgery, Yale School of Medicine, New Haven, CT, USA

e-mail: charles.cha@yale.edu; whitney.brandt@yale.edu

© Springer Nature Switzerland AG 2021

D. Narayan et al. (eds.), *Surgical and Perioperative Management of Patients with Anatomic Anomalies*, https://doi.org/10.1007/978-3-030-55660-0_10

205

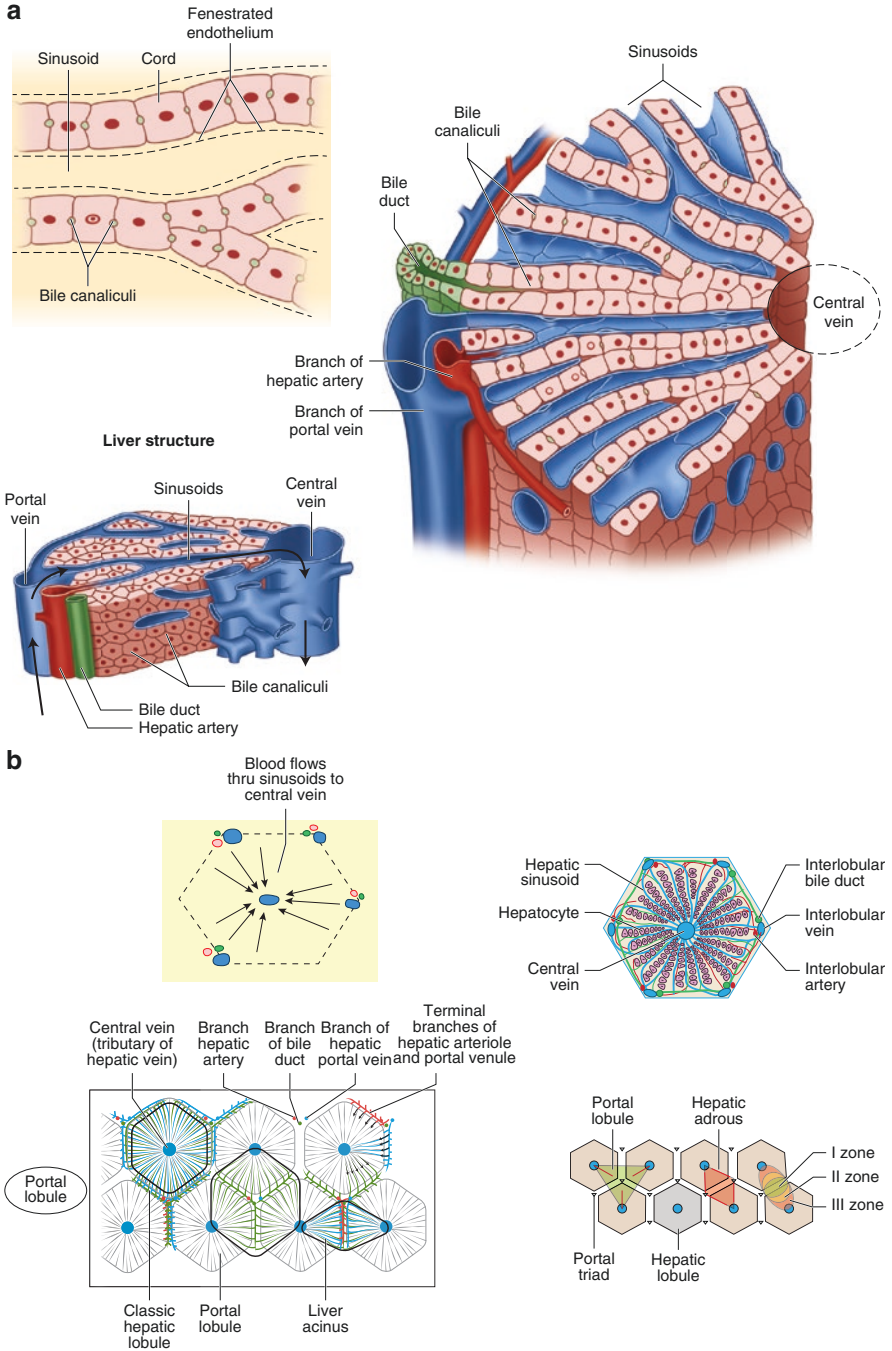


Fig. 10.1 (a) Plate of hepatocytes. (b) Classical versus portal lobule, acinus

Histologically, the functional unit of the liver is the liver lobule. There are two types of liver lobules: classical and portal (Fig. 10.1b). The classical lobule is a hexagonal shape, with the center being the central vein and the corners each holding a mini portal triad: a portal vein branch, a systemic arterial branch, and a bile duct branch. In this model, blood flows toward the central vein and bile flows away toward the corners. Alternatively, the portal lobule is shaped in a triangle, with the center being the portal triad and the central veins at the corners.

The acinus of the liver is a diamond-shaped zone, which has the portal triads at opposing ends and central veins at the other opposing ends. The periportal area is zone 1, which is closest to the blood supply and least likely to undergo ischemic injury but more likely to be affected by toxins, whereas zone 3 is closest to the central veins, making it more susceptible to ischemic injury. The fundamental understanding of the histology of the hepatocyte is important in understanding the complex vascular supply and biliary system of the liver.

Surface Anatomy

The majority of the liver lies in the right upper quadrant with the left lobe which extends in a wedge-like shape toward the left upper quadrant. The superior aspect of the liver lies directly underneath the diaphragm, as far superior as the fourth costal margin. The liver is protected by the ribs as it extends inferiorly. In patients with hepatomegaly, the inferior margin of the liver may extend a fair distance beyond the costal margin, whereas normally the inferior edge rests just a few centimeters below the costal margin.

The liver itself is almost entirely surrounded by peritoneum, with the exception of a small portion on the posterior surface that lies directly along the diaphragm and around the inferior vena cava (IVC), called the “bare area.” Outside of the bare area, multiple ligaments anchor the organ in place. The coronary ligament is an extension of the peritoneum, which holds the liver to the inferior surface of the diaphragm. The falciform ligament extends from the anterior ventral surface of the liver and runs toward the dome of the liver and the inferior vena cava. The round ligament (ligamentum teres) extends from the falciform ligament up to the anterior abdominal wall. It contains the obliterated umbilical vein. The right and left triangular ligaments extend from the superior surface of the diaphragm both laterally and medially (respectively). The left triangular ligament connects to the posterior superior surface of the left hepatic lobe and is continuous with the left layer of the falciform ligament. The right triangular ligament is formed from the upper and lower layers of the coronary ligament and extends laterally from the superior portion of the liver.

The inferior surface of the liver lies adjacent to the visceral organs, which make impressions along the surface of the liver. The renal impression, gastric impression, duodenal impression, and suprarenal impression are marked in Fig. 10.2. On the visceral surface, there is also an H-shaped fissure that separates lobes of the liver as outlined in Fig. 10.2. Another important landmark includes Cantlie’s line, which is an imaginary line along the gallbladder fossa and the IVC groove, which separates the right and left hemilivers (Fig. 10.2c).

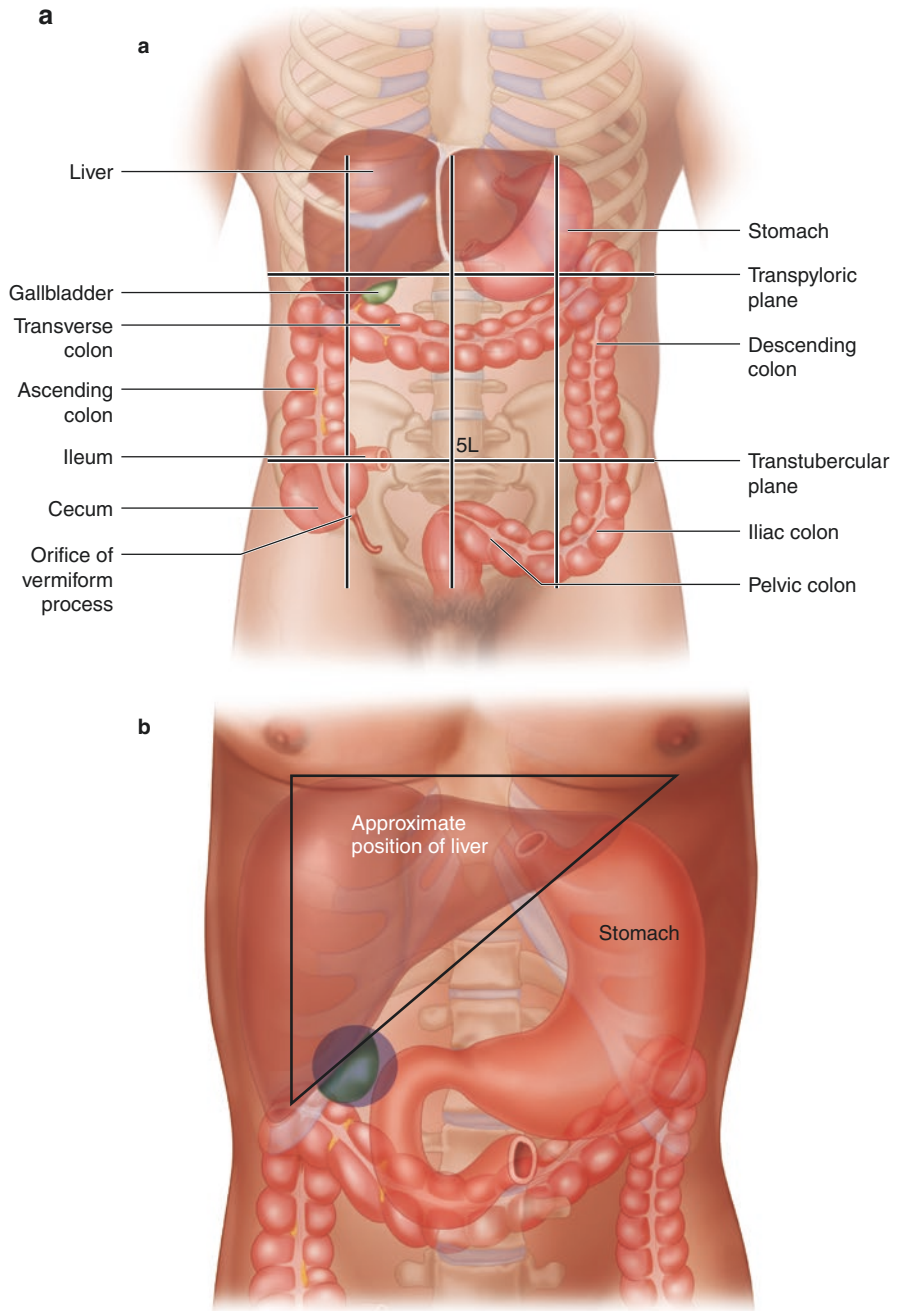


Fig. 10.2 (a) Surface anatomy. (b) Ligaments and surface anatomy of the liver. (c) H-shaped fissure and Cantlie's line

b

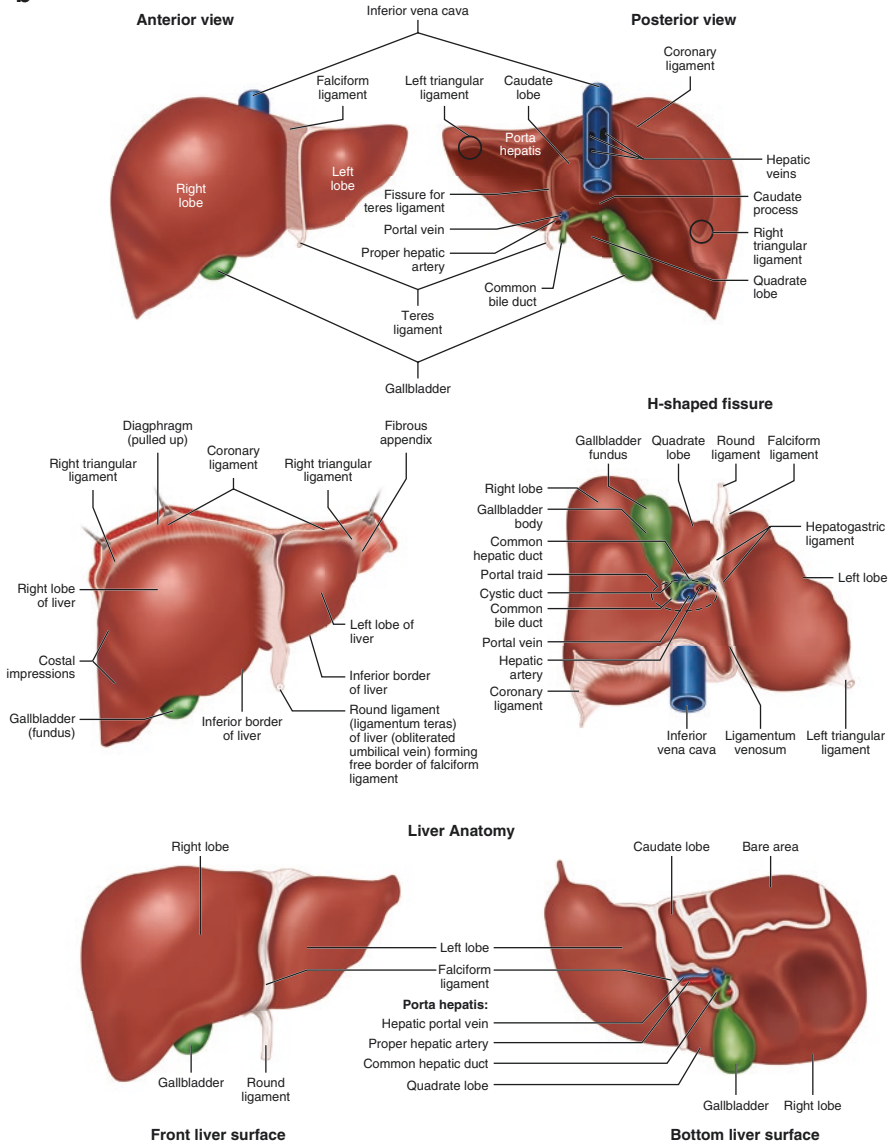


Fig. 10.2 (continued)

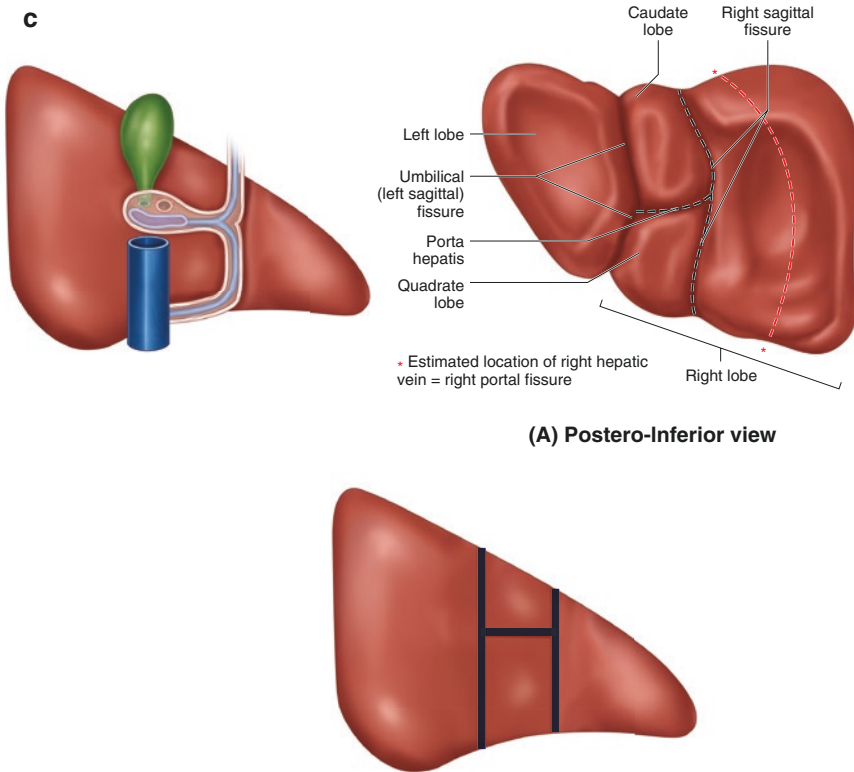


Fig. 10.2 (continued)

Liver Segments

The liver is one of the largest organs in the body and has a very complex blood supply, venous drainage, and an extra component of a biliary drainage system. In order to describe locations of masses and procedures in this complex organ, common terminology is necessary. The most widely accepted segment naming scheme was developed by Couinaud in 1957 and is based on the vascular inflow, outflow, and biliary drainage [2, 3].

According to Couinaud, segment I is formed by the liver tissue between the posterior aspect of the portal bifurcation and the vena cava in between the line of Cantlie and the falciform ligament. Segment I is also known as the caudate lobe.

The second segment is located anteriorly and laterally to the left hepatic vein. From there, segments II through VIII are named by moving clockwise from segment II. Segments II and III are lateral to the left hepatic vein and superior (segment II) and inferior (segment III). Segment IV lies between the middle and the left hepatic veins, with subsegment IVa and IVb located superiorly and inferiorly respectively. In between the middle and right hepatic veins (RHV) lie segments V and VIII (inferior and superior respectively). Segments VI and VII are the two most lateral and most posterior liver segments. Segment VI is located inferiorly, and segment VIII is located superiorly. Cantlie's line, as described above, separates the right (segments V–VIII) and left (segments II–IV) liver (Fig. 10.3).

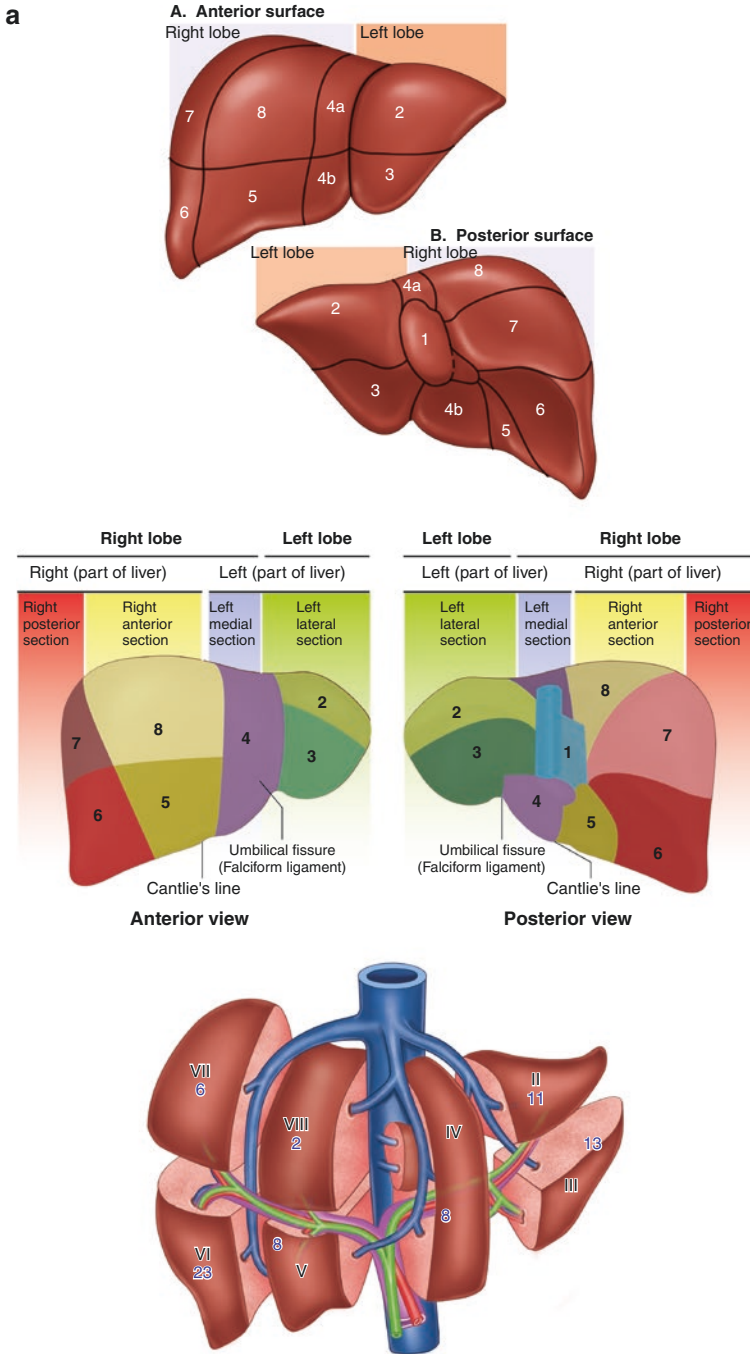


Fig. 10.3 (a and b) Couinaud segments, caudate lobe

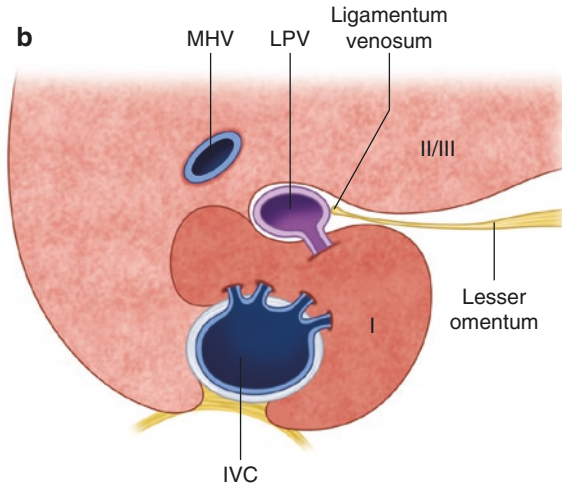


Fig. 10.3 (continued)

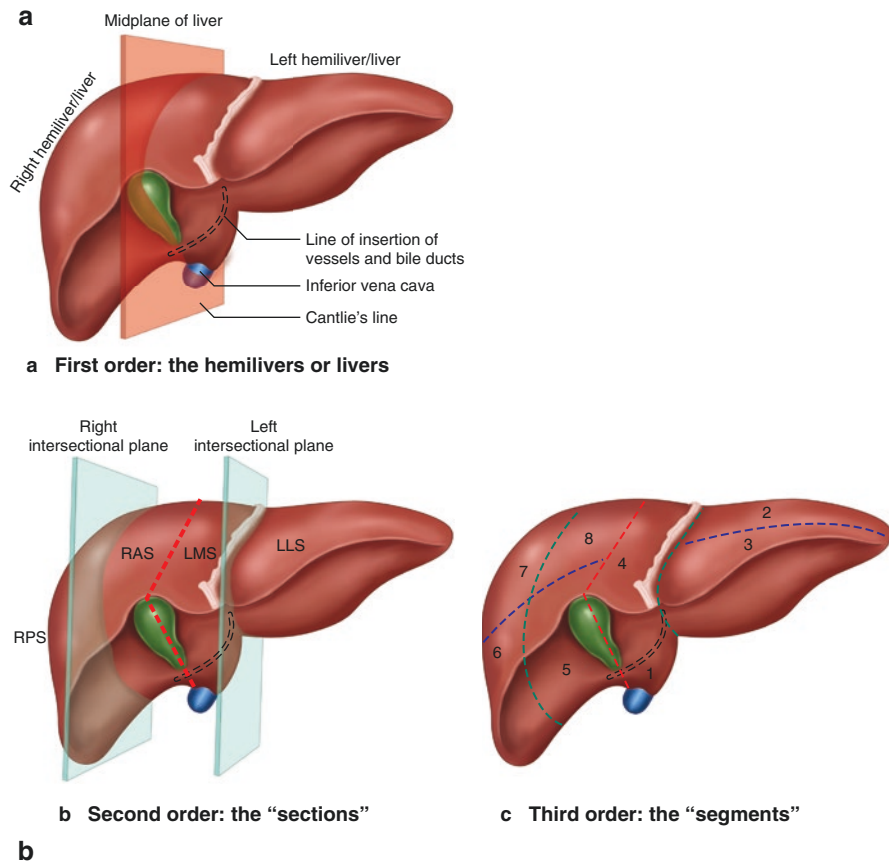
Nomenclature

Although the liver segments according to Couinaud are widely accepted, a discrepancy exists on terminology used to describe hepatic resections. We will describe the Brisbane nomenclature below, as it is the most commonly adopted way to characterize liver resections (Fig. 10.4) [4].

In order to correctly name liver resections, it is first necessary to define portions of the liver. The liver is divided into the left and right liver based on Cantlie's line. Once in halves, the liver is further divided into sectors and segments. A sector of the liver is a region bounded by two hepatic veins or a hepatic vein and the edge of the liver. A segment of the liver is a region of its own inflow, outflow, and biliary drainage, and is synonymous with Couinaud's segments [4].

According to the Brisbane nomenclature, a hemihepatectomy resects all segments on one side of Cantlie's line. This can either be a left or right hepatectomy (segments II–IV or V–VIII respectively). A sectionectomy would include two contiguous segments within the same distal-most portal supply. Sections can also be thought of as the four sections between fissures. A right anterior sectionectomy includes segments V and VIII, while a right posterior sectionectomy includes segments VI and VII. The left lateral and medial sectionectomies are for segments II and III or segment IV respectively. When any of the segments are resected alone, these are called segmentectomies. If any two contiguous segments are resected, this is termed a bisegmentectomy.

When three sections are removed, it is called a trisectionectomy, previously called a trisegmentectomy. Resection of segments IV through VIII is termed a right trisectionectomy, but can also be called an extended right hepatectomy. Similarly, a left trisectionectomy or extended left hepatectomy involves resection of segments II through IV along with segments V and VIII [4].



Anatomical Term	Couinaud Segments	Term for Surgical Resection	Diagram (pertinent area is shaded)
Right Liver OR Hemiliver	Sg 5-8	Right Hepatectomy OR Right Hemihepatectomy	
Left Liver OR Hemiliver	Sg 2-4	Left Hepatectomy OR Left Hemihepatectomy	

Fig. 10.4 (a–d) Segment nomenclature

c

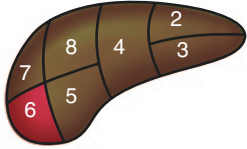
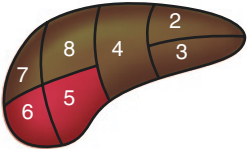
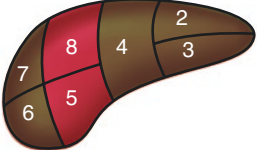
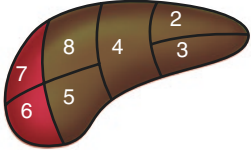
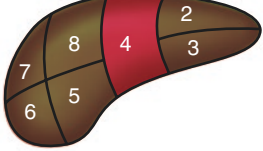
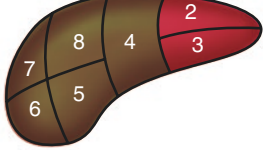
Anatomical Term	Couinaud Segments	Term for Surgical Resection	Diagram (pertinent area is shaded)
Segments 1-8	Any one of Sg 1-8	Segmentectomy (e.g. segmentectomy 6)	
2 contiguous segments	Any two of Sg 1-8 in continuity	Bisegmentectomy (e.g. bisegmentectomy 5,6)	
Anatomical Term	Couinaud Segments	Term for Surgical Resection Add (-ectomy) to any of the anatomical terms	Diagram (pertinent area is shaded)
Right anterior section	Sg 5,8	Right anterior sectionectomy	
Right posterior section	Sg 6,7	Right posterior sectionectomy	
Left medial section	Sg 4	Left medial sectionectomy	
Left lateral section	Sg 2,3	Left lateral sectionectomy	

Fig. 10.4 (continued)

d **Extended resections**
(trisectionectomy)

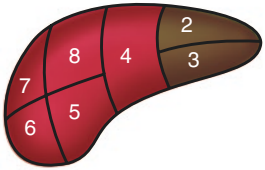
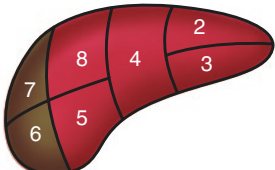
Couinaud Segments	Term for Surgical Resection	Diagram (pertinent area is shaded)
Sg 4-8	Right trisectionectomy (preferred term) or Extended right Hepatectomy or Extended right Hemihepatectomy	
Sg 2,3,4,5,8	Left Trisectionectomy (preferred term) or Extended left Hepatectomy or Extended left Hemihepatectomy	

Fig. 10.4 (continued)

Vascular and Biliary Anatomy

In order to truly understand the anatomy of the liver, thorough understanding of the arterial supply and venous drainage is necessary (Fig. 10.5).

The liver has a dual blood supply via the hepatic arterial system and the portal venous system. The portal system supplies oxygenated, nutrient-rich, and sometimes toxic blood from the gut, while the hepatic arterial system supplies oxygenated blood from the aorta. Normally, the portal vein supplies about 75% of the blood supply by volume and 50% of the oxygenated blood to the liver.

The drainage of the liver is through the hepatic veins, which drain directly into the inferior vena cava. There are three hepatic veins: the left, middle, and right. The right and left portal veins enter the liver between the three hepatic veins and then branch to supply each sector.

Systemic Arterial Supply

The systemic supply to the liver arises from the hepatic artery. The “textbook” hepatic artery arises from the celiac artery as the common hepatic artery. The common hepatic starts its course toward the liver and then divides into the gastroduodenal artery and the proper hepatic artery. The proper hepatic artery continues and then splits into the left and right hepatic arteries. Two studies, one by Löschner and one by Saba et al. [5, 6], reviewed CT angiograms in order to classify hepatic

arterial supply. Both found that 61.4–72.2% of hepatic arteries had the course as described above.

There are numerous variants of hepatic arterial supply, and knowing the major variants is important in hepatobiliary surgery (Fig. 10.6). The most common variants of hepatic arterial supply have been classified by Michels [7]. According to Michels, type I is the classically described textbook arterial anatomy (61.4–72.2%).

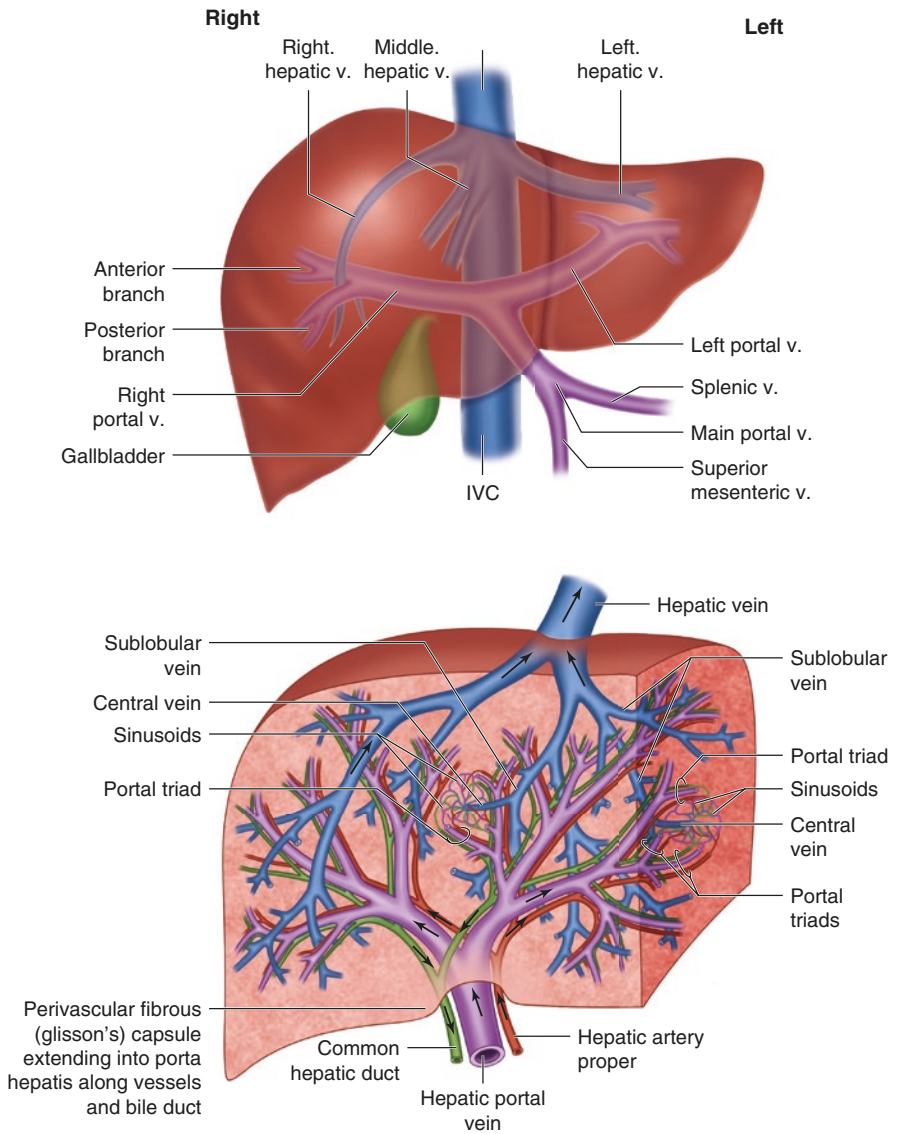


Fig. 10.5 Portal vein/hepatic vein relationship

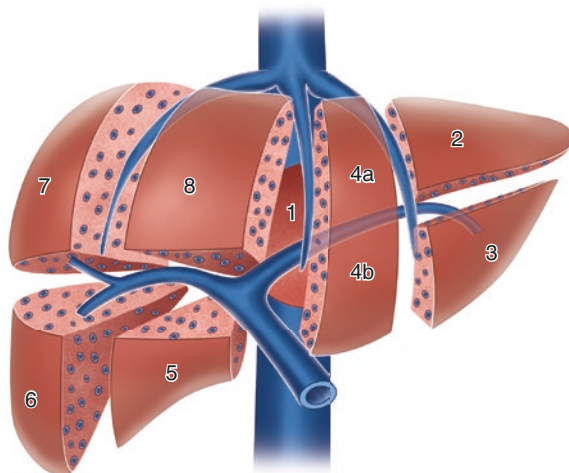


Fig. 10.5 (continued)

A type II variant artery has a replaced left hepatic artery, which arises from the left gastric artery (4.2–7.5%). Type III variants have a replaced right hepatic artery, which arises from the superior mesenteric artery (SMA) (6.4–10.6%). Type IV variants have a replaced right hepatic off the SMA and a replaced left hepatic from the left gastric, but also have a hepatic artery that arises from the celiac in the usual fashion (1.3–1.5%). Type V variants have type I anatomy with an accessory left hepatic artery from the left gastric artery (6.7–8.8%). Type VI variants have an accessory right hepatic artery that arises from the SMA (1.5–6.9%). Type VII lesions have both a right accessory lesion from the SMA and an accessory left hepatic artery from the left gastric artery (0.5–0.7%). A type VIIIa lesion has a replaced right hepatic from the SMA and an accessory left hepatic from the left gastric artery (0.8–1.9%). In type IX lesions, all flow to the liver arises from the gastroduodenal artery, which arises entirely from the SMA without tributaries from the celiac axis (1.6–2.0%). Type X variants have the opposite of type IX; all flow arises from the celiac and the SMA has no connection to the gastroduodenal (0–0.3%) (Fig. 10.6b) [5, 6].

Hepatic Vein Anatomy

There are three hepatic veins that drain the entire liver (right, middle, and left). Each vein drains its respective portion of the liver and then empties into the inferior vena cava at an oblique angle at the superior aspect of the liver. Each hepatic vein interdigitates between liver sectors. Their locations can be approximated by three imaginary fissures along the surface of the liver (Fig. 10.7a). Intraoperatively, it is helpful to use an ultrasound to delineate the approximate location of the veins.

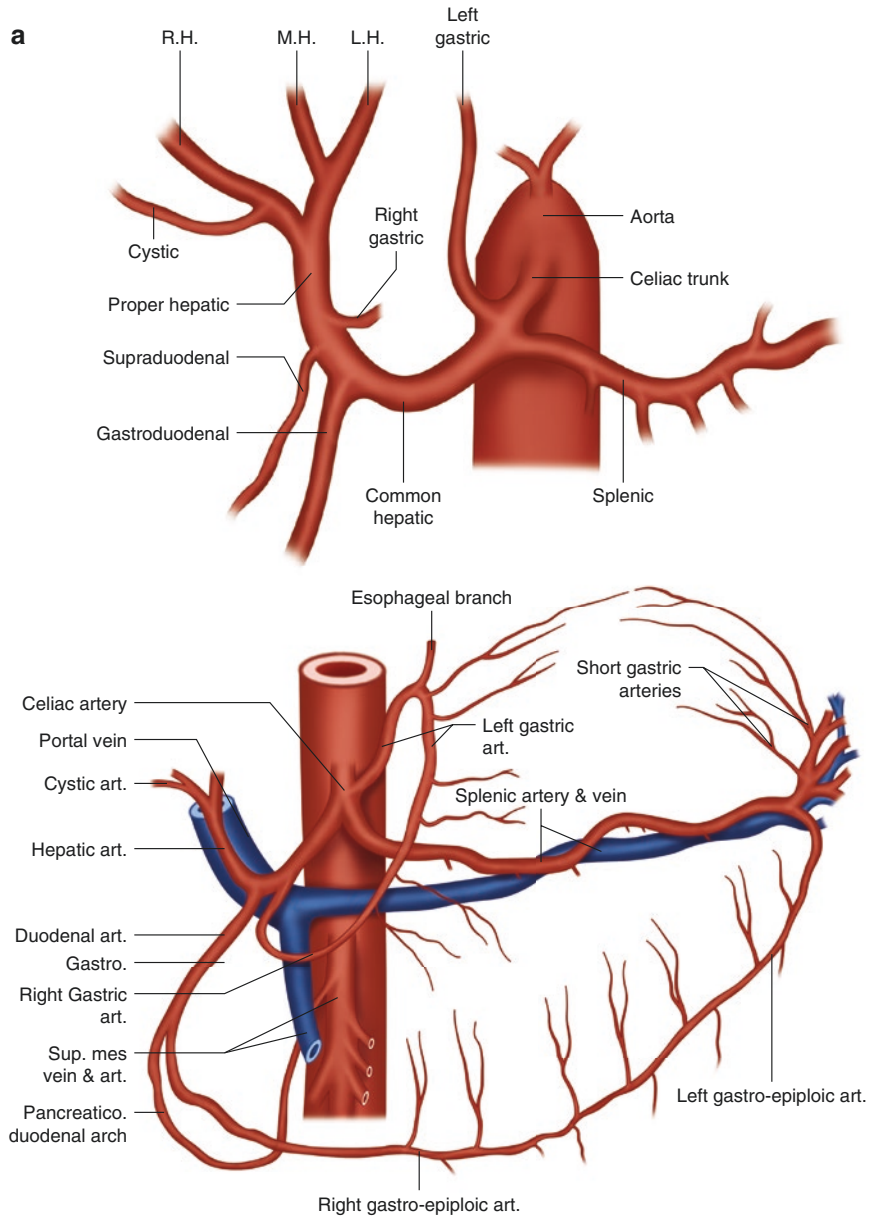


Fig. 10.6 (a) Systemic arterial anatomy. (b) Arterial anatomy variants

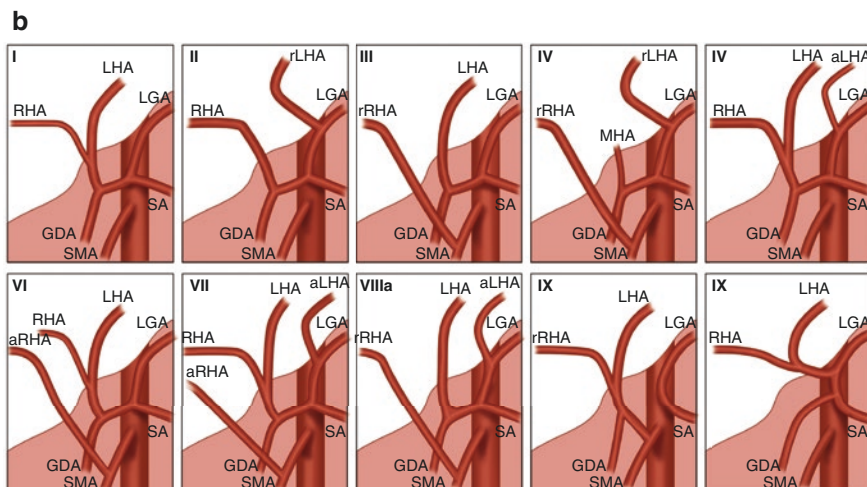


Fig. 10.6 (continued)

The left hepatic vein drains segments II, III, and part of segment IV. It is located in the left fissure, just to the left of the attachment of the falciform ligament. This fissure also divides the left lateral and left medial segments [8]. The middle hepatic vein lies in the median fissure and drains segments IV and V. The median fissure, known as Cantlie's line, is located between the bed of the gallbladder and just to the left of the margin of the IVC. At times, the middle and left hepatic veins join together extrahepatically prior to entering the IVC.

The right hepatic vein is the largest of the three veins and drains the remaining segments: V through VIII. The right hepatic vein lies under the right fissure, which is located on the right margin of the IVC about 3–4 cm from the right inferior layer of the right coronary ligament. The fissure then curves anteriorly midway between the gallbladder fossa and right margin of the liver.

The right hepatic vein has multiple patterns of drainage, which is especially variable for the posterior segment of the right lobe (Fig. 10.7b). According to a study of multiple human livers by Shilal and Tuli [9], the drainage pattern of the right hepatic vein (RHV) can be classified into four types. Type I right hepatic veins drain directly into the IVC the without any tributaries within 1 cm of entrance into the inferior vena cava (58.0%). Type II right hepatic veins have either the right anterosuperior or right posterosuperior vein, which join the RHV within 1 cm of the IVC (23.2%). Type III hepatic veins have both the right anterosuperior and right posterosuperior, which join the RHV within 1 cm confluence to the IVC (6.6%). Finally, type IV right hepatic veins have either the right anterosuperior or posterosuperior, which drain directly into the IVC, with the remaining branch that drains into the right hepatic vein within 1 cm of the RHV and IVC confluence (11.6%) [9].

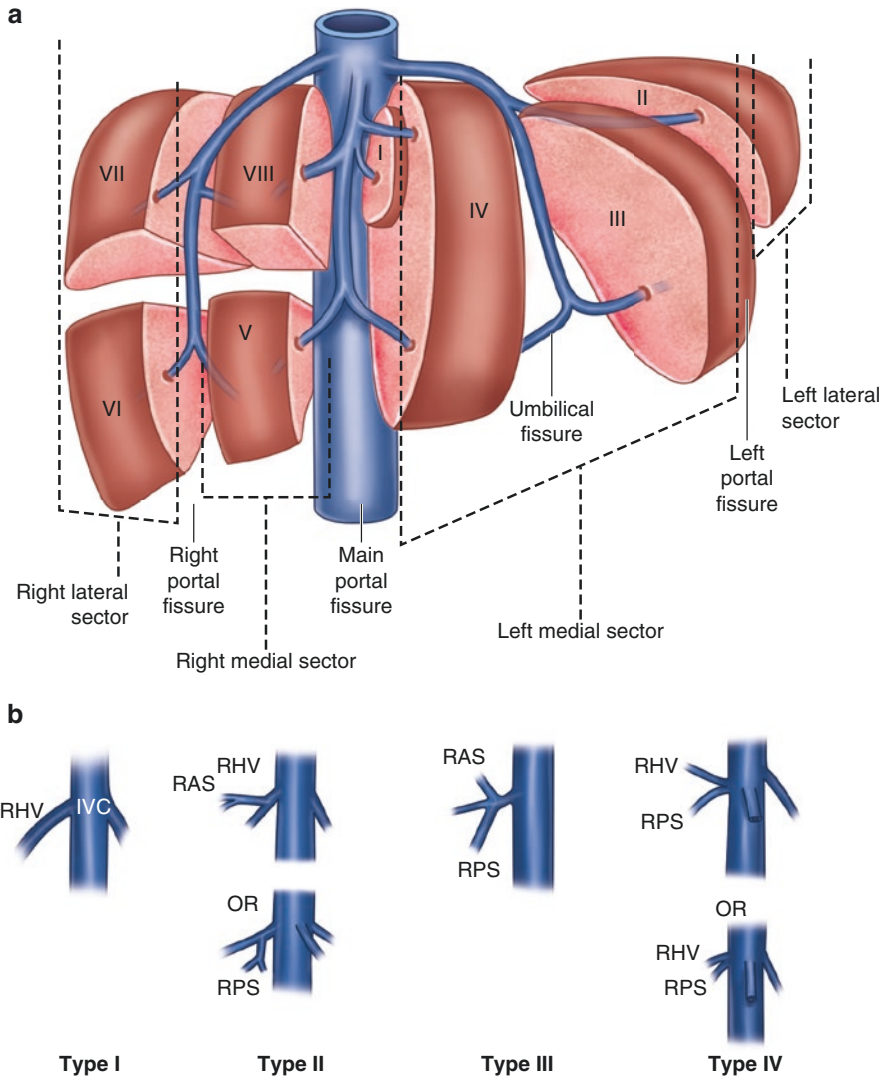


Fig. 10.7 (a) Hepatic veins and fissures. (b) Right hepatic vein variants

The remainder of the drainage of the liver is via accessory veins that mainly drain the caudate lobe. There are numerous accessory hepatic veins, which can drain into the right hepatic vein or directly into the IVC and at times can be quite large.

Portal Vein

The portal system is a network that drains the gastrointestinal system and spleen into the liver. It allows for delivery of nutrients to the liver and allows the liver to filter toxins prior to circulating the bloodstream. The portal vein forms when the

splenic vein and inferior mesenteric vein join the superior mesenteric vein behind the neck of the pancreas. Once formed, the portal vein courses toward the liver in the portal triad and splits into the right and left portal vein, which supply the right and left hepatic lobes, respectively.

The portal vein branches and supplies various segments of the liver. One theory is that the portal vein follows a 1:2:20 pattern in that it starts as one branch, divides into the left and right portal veins, and then the next divides into approximately 20 branches [1]. When looked at more carefully, the general course of the portal tributaries supplies the various liver segments.

Once the left portal vein is formed, it arches toward the round ligament. The concavity of the arch gives rise to the recurrent portal branches to segments IVa and IVb (cranially and caudally, respectively). The convexity of the arch gives two forward branches, the first toward segment II and then a distal branch to segment III [1].

The course of the right portal vein also divides and supplies segments V–VIII. There are two second-order branches of the right portal vein, which divide along the right fissure. One branch heads toward the anterior sector and the other toward the right posterior sector. The third-order branches of each of these tributaries give rise to each individual segment of V–VIII (Fig. 10.8a, b) [1].

Variants of the right portal vein anatomy have been studied by Bageacu et al. [10] and categorized into different types. Type A is considered a right portal vein from the main portal vein, with right anterior and posterior branches. Type B right portal veins have a trifurcation with left, right anterior, and right posterior branches. Type C right portal veins have a right posterior vein that comes directly from the main portal vein. Type D right portal veins originate from the left portal vein. These variants are important to consider when performing a right hepatectomy (Fig. 10.8c) [10].

Biliary Anatomy

Anatomy of the Gallbladder

Knowledge of gallbladder anatomy is extremely important. Not only is a laparoscopic cholecystectomy one of the most frequently performed operations in the United States, but cholecystectomy is also a portion of many other hepatobiliary procedures.

The gallbladder is a small sac that lies between the right hepatic lobe and the quadrate lobe of the liver. It plays a role in storage and concentration of bile. The gallbladder has a fundus, body, and neck. The fundus is the rounded blind end, which extends slightly anterior to the liver edge. The body is the major part of the gallbladder and rests in the upper part of the duodenum and the transverse colon. The neck of the gallbladder is the narrow portion of the gallbladder that gives rise to the cystic duct. The spiral valves (also known as Heister's valves) are located in the neck of the gallbladder. These are thought to keep the gallbladder continuously open and allow bile into the gallbladder when the common bile duct is closed (Fig. 10.9a).

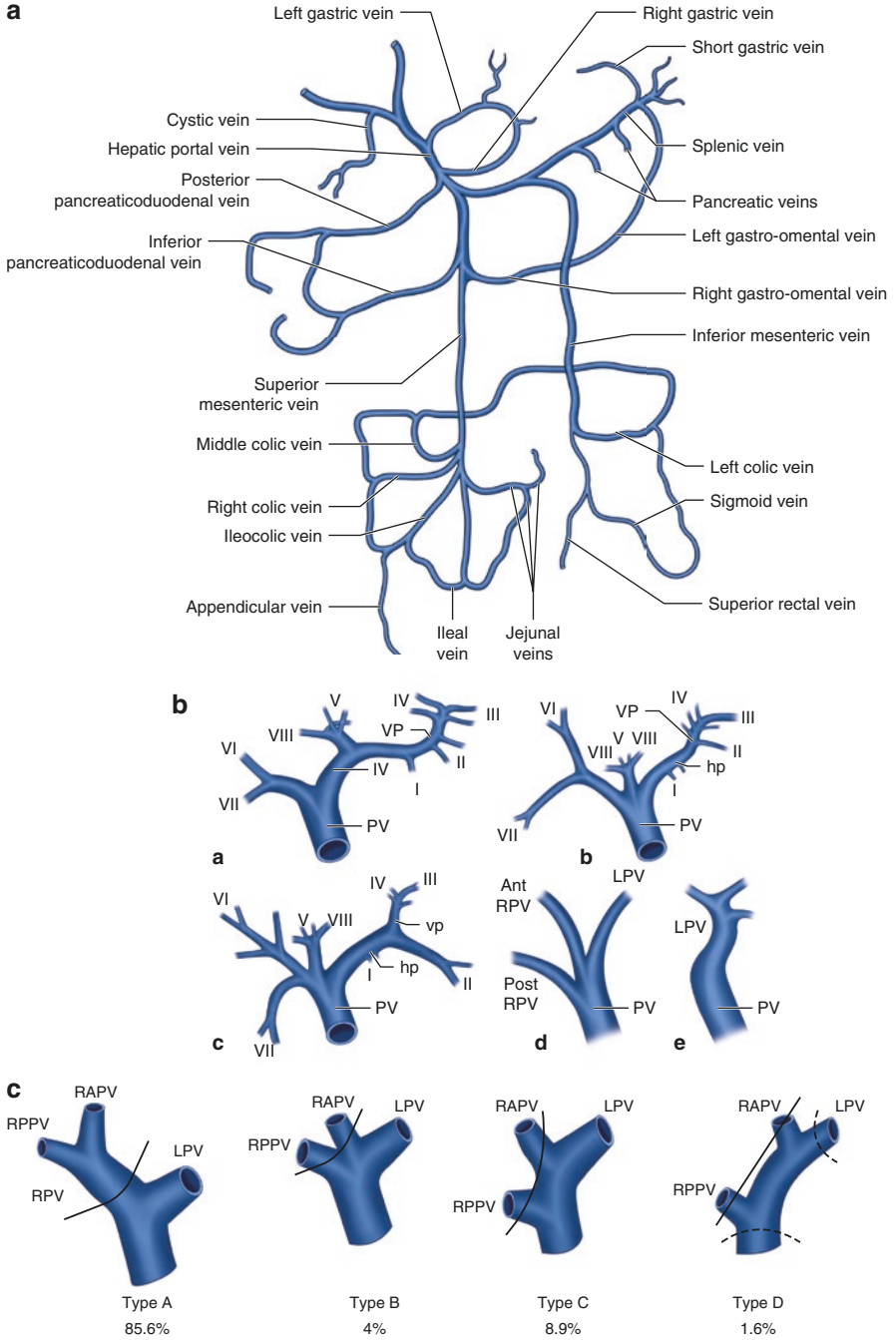


Fig. 10.8 (a) Portal vein formation, (b) Left and right portal vein typical course. (c) Right portal vein variants

There are multiple variations in the gallbladder anatomy. For one, the gallbladder can be duplicated and have two sacs. If this is the case, the sacs can either be drained by a single cystic duct into the common hepatic duct, two ducts (one into the common hepatic and the other into the right hepatic), or both into the common hepatic duct [11].

In non-duplicated gallbladders, there are additional variations. The gallbladder can have a septum creating a bifid gallbladder, multiple septa that all empty into one cystic duct, or diverticula which extend off the gallbladder [11].

The drainage of the gallbladder via the cystic duct can also have variations (Fig. 10.9b). The cystic duct can split and drain via two cystic ducts, it can drain into

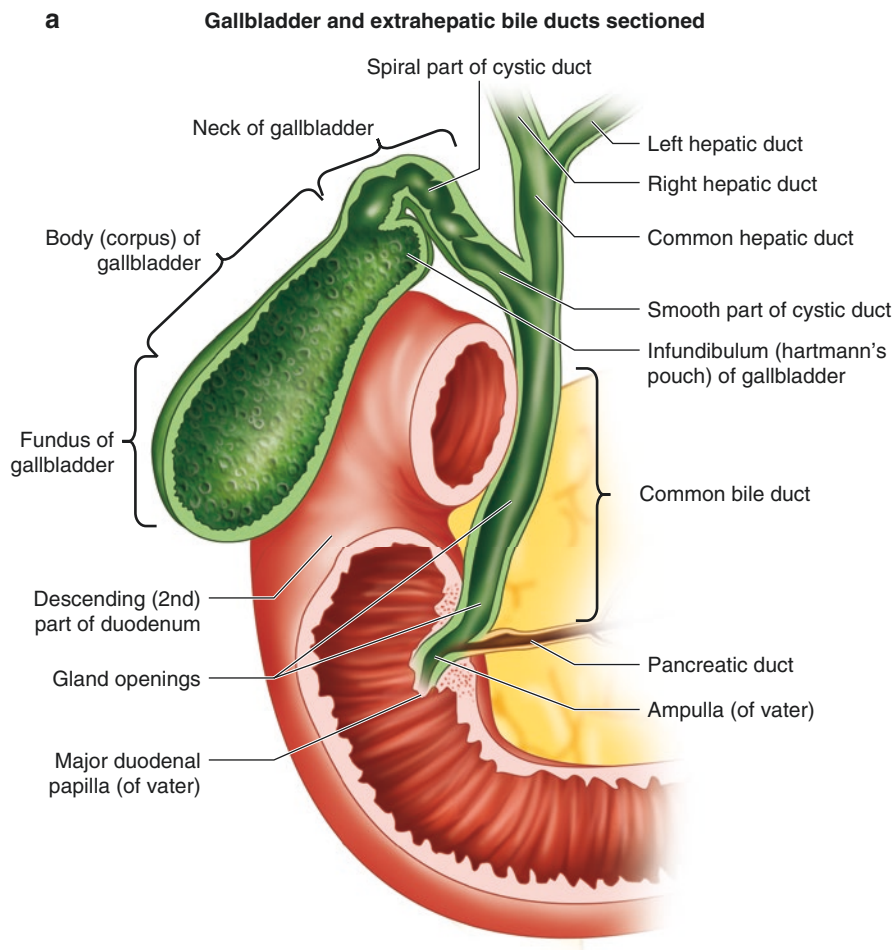


Fig. 10.9 (a) Normal gallbladder anatomy. (b) Gallbladder, cystic duct anatomy, and cystic artery variations. (c) Critical view

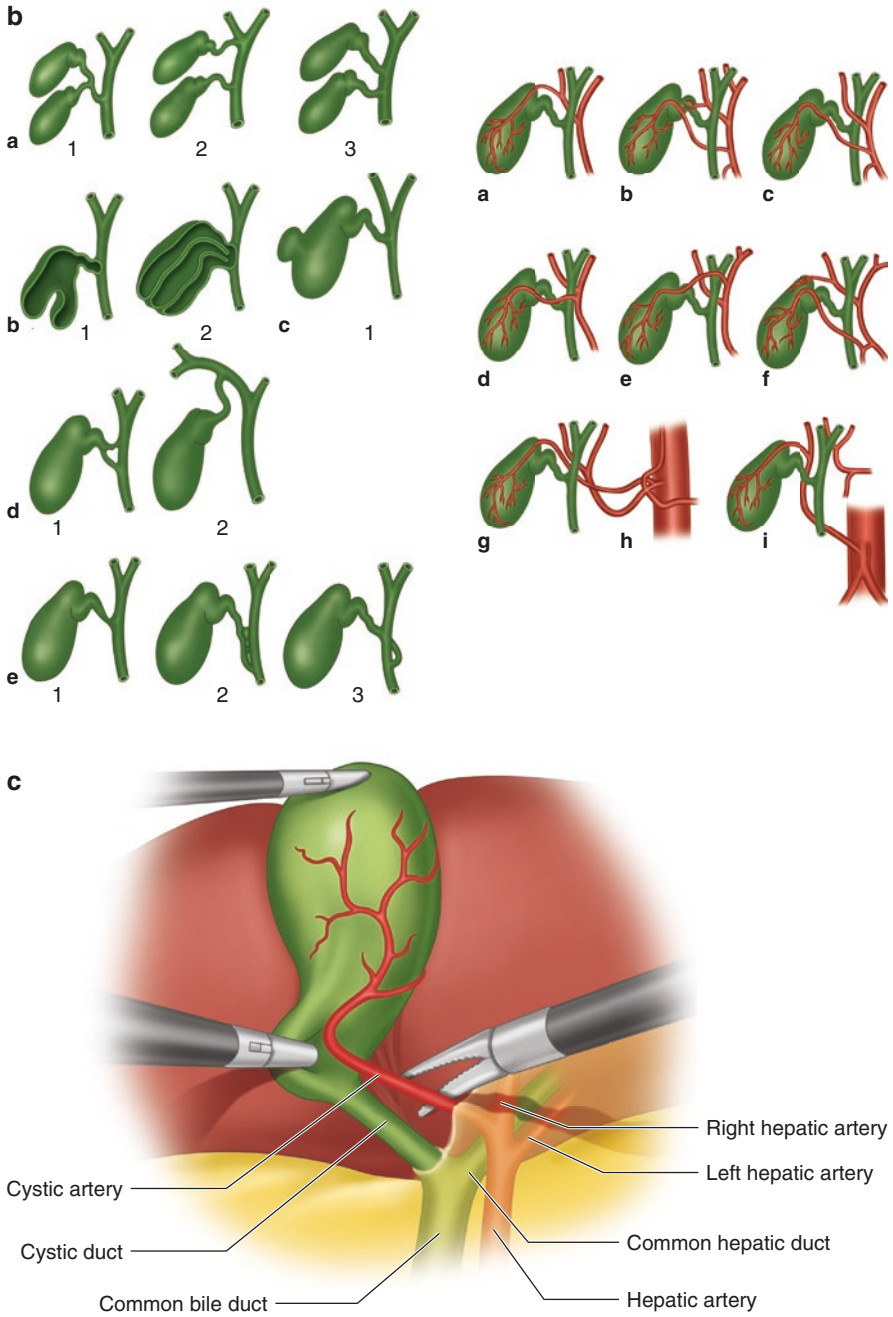


Fig. 10.9 (continued)

the right hepatic duct, or it can join the hepatic duct. If the cystic duct drains into the hepatic duct, it can join with the hepatic duct in a few ways. It can join at an angle (75%), parallel to (20%), or wrap posteriorly around the hepatic duct and join on the left side of the duct (5%) [11].

The gallbladder is supplied by the cystic artery, which is a branch off the right hepatic artery. The triangle of Calot is an important anatomic relationship and includes the visceral surface of the liver, the cystic duct inferiorly, and the common hepatic duct medially.

When performing a cholecystectomy, it is extremely important to visualize the cystic duct and artery well. Upon lateral retraction of the gallbladder fundus and dissection of the peritoneum surrounding the fundus of the gallbladder, the surgeon can view the cystic duct origin from the gallbladder, the cystic artery directly supplying the gallbladder, and the liver bed behind the two. Obtaining this critical view is important to help prevent injuries to the common or hepatic bile duct (Fig. 10.9c).

Intrahepatic Biliary Anatomy

One of the liver's main functions is the creation and excretion of bile. Bile, once made in cells, is transported into bile canaliculi. The bile canaliculi merge and form intrahepatic ductules. Eventually, these intrahepatic ductules merge to form the right and left hepatic duct.

The intrahepatic biliary ductal system follows a course similar to the intrahepatic portal veins. The right and left hepatic ducts drain the right and left hepatic lobes respectively, whereas the caudate lobe is drained by several independent ducts that drain into both the right and left hepatic ducts [11].

The caudate lobe has a biliary drainage system that is separate from that of the rest of the liver. The caudate lobe can be thought of as having its own right lobe, left lobe, and caudate process. According to Healey and Schroy [12], 44% of individuals have three ducts, each of which separately drains one of the sections of the caudate lobe into the main hepatic duct. In about 26%, the right caudate lobe and caudate process have a joint biliary drainage, and the left caudate lobe drains independently. In most people, the caudate lobe ducts described above drain into both the right and left hepatic ducts (78%), although at times the entire drainage is via the left hepatic duct (15%) or right hepatic duct (7%) [12].

The right and left lobes of the liver are drained by the right and left hepatic ducts, respectively. The left hepatic duct drains segments II, III, and IV. The left lateral segment is drained by a superior and inferior branch. The inferior branch is generally longer and larger than the superior. The left lateral duct forms once the superior and inferior ducts join, which is usually under the left lateral segmental fissure or just right of the fissure. In some cases, the two branches join leftward of the fissure (Fig. 10.10c).

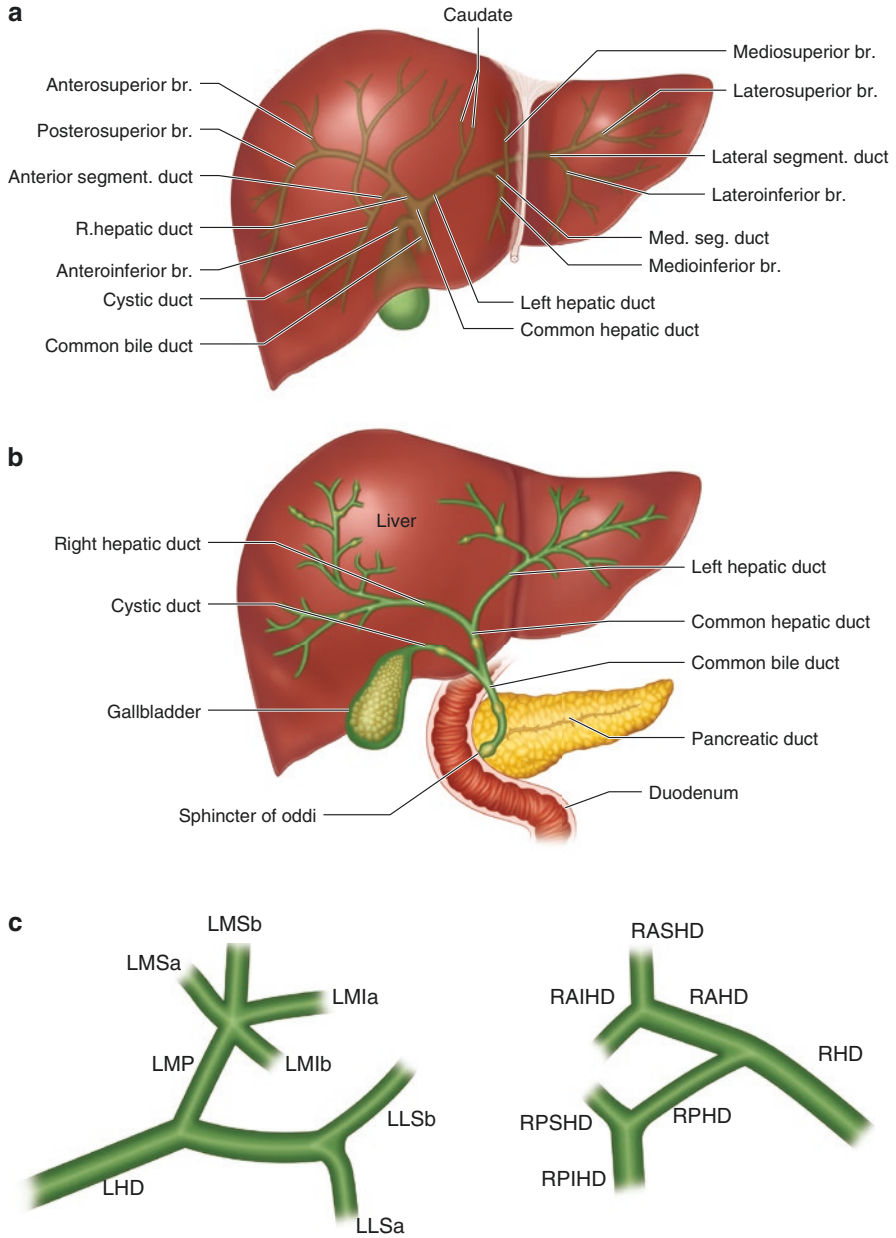


Fig. 10.10 (a) Overview of intrahepatic biliary anatomy. (b) Left hepatic duct. (c) Right hepatic duct. (d) Confluence of the right/left hepatic duct. (e) Alternate drainages into the cystic duct

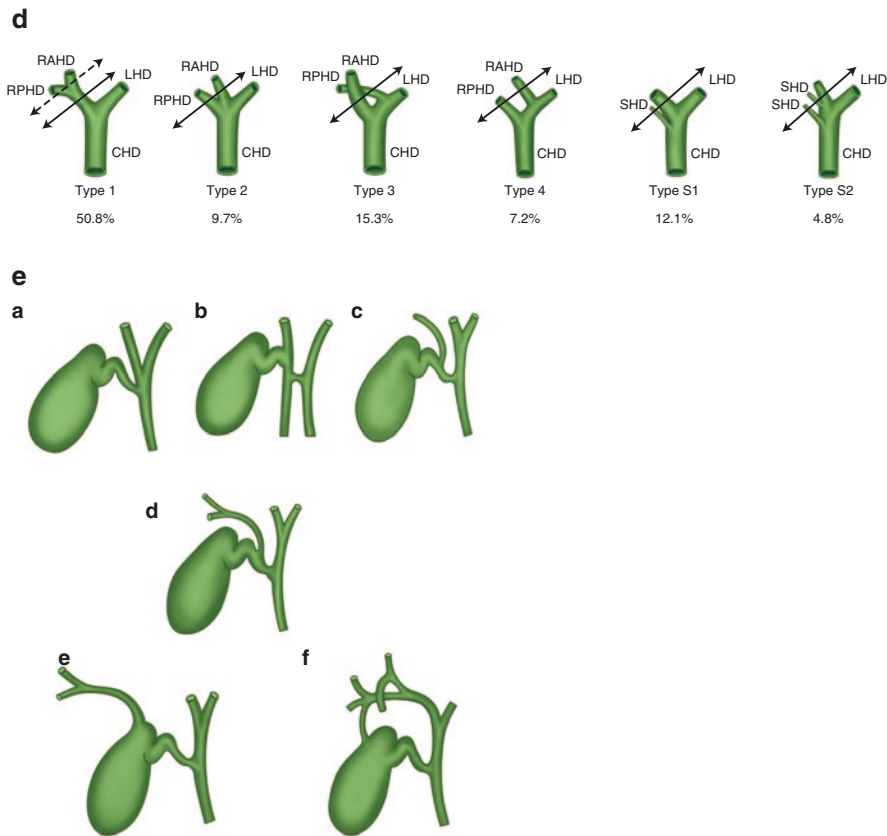


Fig. 10.10 (continued)

The left medial duct is formed by ducts which drain the superior and inferior medial segment (segment IV of the liver). The drainage here of the left medial liver is much more complex than that of the left lateral segment. The left medial segment usually has two ducts that drain the superior portion of the segment, and two other ducts that drain the inferior segment. These individual ducts can join to form the left medial duct in many ways. The ducts can either converge together all at once (type I, 60%); three of them can join together with one separately (type II, 24%); each can join completely separately (type III, 10%); or the two ducts from the superior and inferior portion can join together prior to draining into the main left medial segment duct (Type IV, 6%) [12].

Once all the branches join, the left hepatic duct transverses near the base of segment IV, behind the left portal vein, and joins the right hepatic duct [11].

The right liver, segments V–VIII, is drained by the right hepatic duct. There are two main ducts which drain the right lobe, the posterior and anterior right hepatic ducts, which drain the posterior and anterior sectors, respectively.

The right posterior duct is slightly superior and longer than the anterior duct. It has two branches, which drain the superior and inferior portions of the posterior segment to drain segments VI and VII. The posterior inferior bile duct either drains directly into the anterior biliary duct, directly into the right hepatic duct, or directly into the common hepatic duct [12].

The right anterior biliary duct is also split into superior and inferior ducts to drain segments V and VIII. In most cases, segment VIII drains into the right anterior duct (80%), and segment V drains into the anterior segment duct (91%). According to Healey and Schroy, in 20% of the cases, the right anterior superior duct drains directly into the posterior segment duct. The right anterior inferior duct more consistently would drain directly into the right anterior duct, but can aberrantly drain into the right hepatic duct or into the right posterior duct at times [12].

There are multiple different ways the right and left ducts can join to form the common hepatic duct. In a study by Bageacu et al., the anatomy of 124 right liver donors was analyzed. The variations in the hepatic ductal anatomy were reviewed, and the percent prevalence was reported. Type 1 hepatic ductal anatomy includes a right anterior and posterior duct, which merge to become the right hepatic duct and then merge with the left to form the common hepatic duct. This is present in 50.8% of those analyzed. Type 2 ducts include those ducts in which the right anterior, right posterior, and left hepatic duct all join together at once (9.7% prevalence). Type 3 ductal anatomy is classified as a duplicated right hepatic duct with a right posterior hepatic duct that opens into the left hepatic duct (15.3%). Type 4 is similar to type 3, except the right anterior hepatic duct empties into the left hepatic duct (7.2%). Type S1 and type S2 have a left hepatic and then either one or two, respectively, segmental ducts emptying into the common hepatic duct. The prevalence of S1 and S2 ductal anatomy is 12.1% and 4.8%, respectively (Fig. 10.10d) [10].

The right and left hepatic ducts merge to form the common hepatic duct, which is accompanied by the proper hepatic artery and the portal vein. Once the cystic duct joins with the common hepatic duct, the common bile duct is formed. The common bile duct then courses down behind the first portion of the duodenum and then into the head of the pancreas. Here it joins the main pancreatic duct to form the hepatopancreatic duct and enters into the second portion of the duodenum at the greater papilla (Fig. 10.10).

Portal Triad and the Pringle Maneuver

The portal triad is an important landmark in hepatobiliary surgery. The triad includes the proper hepatic artery, the portal vein, and the common bile duct. The portal triad lies inside the hepatoduodenal ligament at the free edge of the lesser omentum. The duct is anterolateral, the artery is anteromedial, and the vein lies posterior. Although

not included in the triad by name, the hepatic branch of the vagus nerve and lymphatic tissue also course with these three structures.

The Pringle Maneuver is an important maneuver to know when performing liver surgery (Fig. 10.11). It involves using an atraumatic clamp over the portal triad in order to decrease blood flow to the liver and thus reduce blood loss during both traumatic and elective hepatic procedures. Because the portal triad contains the major blood supply to the liver, clamping the area helps prevent blood loss from the

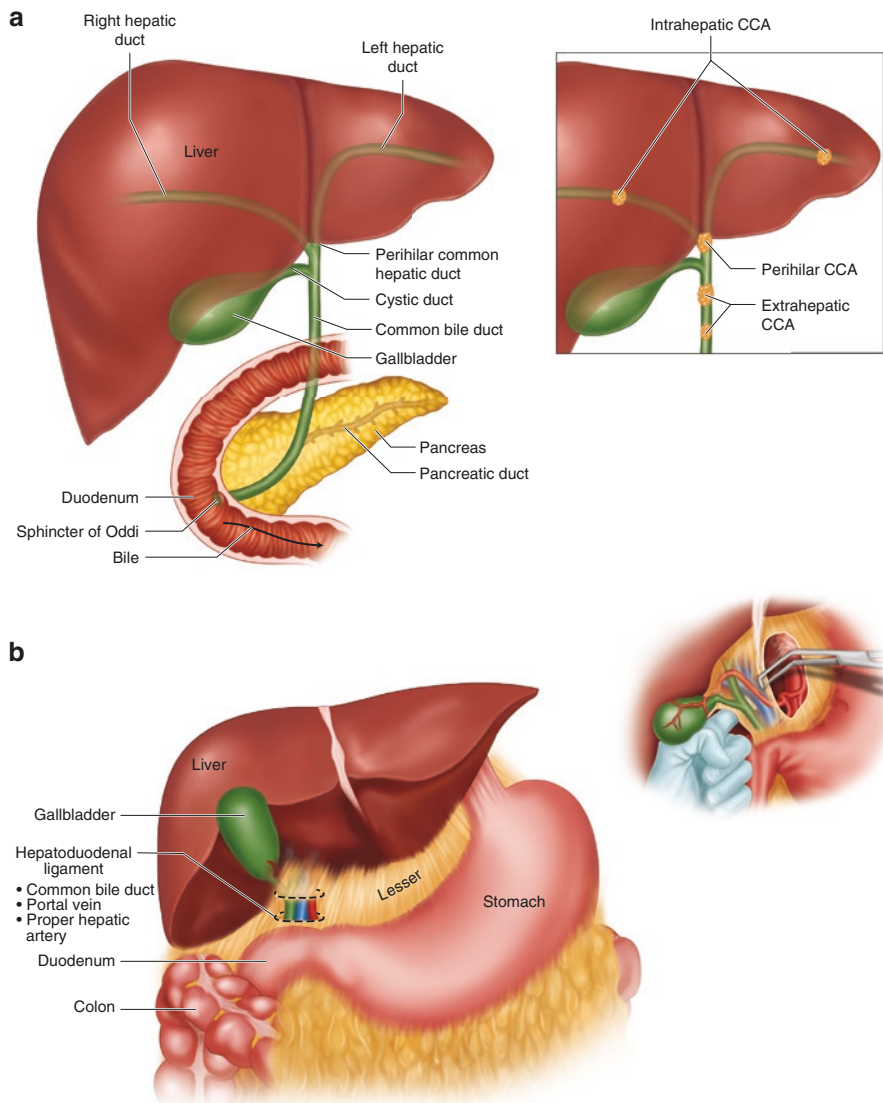


Fig. 10.11 Pringle maneuver

liver parenchyma due to compression of both the portal and systemic arterial supply. Because the hepatic veins are left alone, this method does not slow hepatic vein bleeding.

Overall, the Pringle Maneuver has been shown to be beneficial in elective hepatic transections. Yet, while the maneuver helps decrease blood loss, it produces ischemic and intestinal congestion from compression of the portal vein [13]. Nonetheless, prospective studies continue to show benefit of the maneuver on patient outcomes. In 2005, Lesurtel et al. demonstrated a decreased resection time and decreased transfusion requirement in patients who underwent portal triad clamping over alternative techniques for liver transection without clamping [14].

Numerous researchers have studied the ideal interval for clamping to provide maximum benefit while limiting the ischemic injury and gastrointestinal congestion from clamping. One study evaluated outcomes in patients who underwent intermittent clamping versus “ischemic preconditioning.” The intermittent clamping group would have 15 minutes clamped followed by five minutes unclamped, for a total of 30 minutes clamped during the entire resection. The ischemic preconditioning group patients had a pre-resection 10-minute clamp followed by 10 minutes unclamped to “precondition” the liver tissue. Then, the portal triad would remain clamped for no greater than 75 minutes during resection. The results demonstrated that intermittent clamping was associated with lower blood loss and faster operation [15]. Multiple groups have shown similar results, suggesting that intermittent clamping is well tolerated in patients undergoing liver resection [16–18].

Choledochal Cysts: Anatomy and Classification

Choledochal cysts are congenital cystic dilations of the biliary tract, which can produce cholangitis, sepsis, pancreatitis, abscesses, and in some cases, can progress to malignancy [19].

The most widely accepted classification of these cysts was provided by Todani et al. in 1977 [20]. According to Todani, type I choledochal cysts compromise 80–90% of all the choledochal cysts and consists of fusiform dilation of the extrahepatic biliary system [21]. Type I choledochal cysts are further classified into subtypes: 1A, 1B, and 1C. Type 1A cysts occur when the gallbladder arises from a choledochal cyst, there is a dilated extrahepatic biliary tree with normal intrahepatic ducts. Type 1B cysts have isolated distal CBD dilation without pancreaticobiliary malunion and normal extrahepatic ducts. Type 1C cysts have fusiform dilation to the common hepatic duct with pancreaticobiliary malunion [21].

Type II choledochal cysts compromise 2% of all choledochal cysts and are true diverticula of the common bile duct. Type II choledochal cysts have an anechoic cyst alongside the CBD with a normal common duct and gallbladder.

Type III choledochal cysts are also termed choledochoceoles. These comprise 1–4% of all choledochal cyst disease and are entirely intraduodenal [21].

Type IV choledochal cysts are the second most common type of choledochal cyst (15–20%). These involve both intrahepatic and extrahepatic bile ducts. There are

two sub-classifications of type IV choledochal cysts. Type IV-A cysts have dilation from the common bile duct to the common hepatic duct. Bilateral hepatic lobes are usually involved, but at times there could be isolated left or right hepatic ductal dilation. More commonly, the left hepatic bile duct is involved. Isolated right hepatic ductal dilation is rare [21]. Type IV-B choledochal cysts have multiple dilations of the extrahepatic tree that appear as though the duct is a “string of beads” without intrahepatic involvement [21].

Patients with type V cysts have isolated intrahepatic disease. There is saccular or fusiform dilation of the ducts without overlying obstruction. There are two types of type V choledochal cysts: simple and fibrotic [21]. Patients with fibrotic type V choledochal cysts have associated liver cirrhosis, portal hypertension, and periportal fibrosis [22].

Choledochal Cyst Management

The management of choledochal cysts depends on the type of choledochal cyst according to the Todani classification (Fig. 10.12) [20]. Historical management of choledochal cysts involved internal or external drainage with cholecystectomy, but high rates of infection, pancreatitis, cholangitis, as well as the associated risk of malignancy caused a shift in management [20].

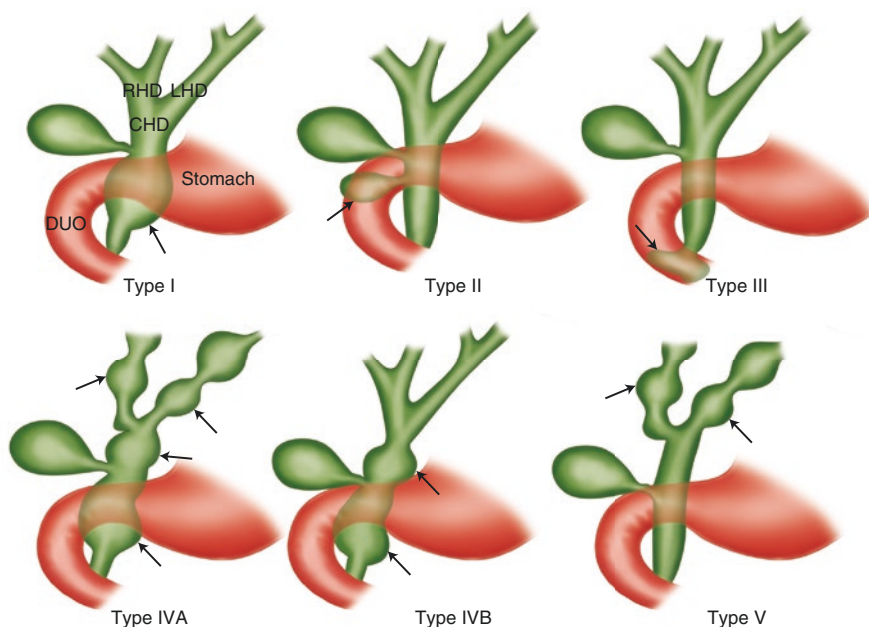


Fig. 10.12 Todani classification of choledochal cysts

The management of type I and type IV cysts is similar. These two types of cysts need complete extrahepatic excision of the bile duct, cholecystectomy, and restoration of biliary-enteric continuity. In patients with Type IV-A cysts, the patients likely need to undergo intrahepatic excision [23].

Type II and type III cysts have a low malignant potential and therefore need less extensive management. Usually, these patients are managed with isolated cyst excision [23].

Patients with type V cysts have isolated intrahepatic disease. If only a portion of the liver is involved, resection may be an option. More extensive involvement requires orthotopic liver transplant for definitive management [23].

Today, more cases of choledochal cysts are diagnosed prenatally. In certain patient populations, early excision can be associated with less hepatic fibrosis and more normal liver function [24].

Novel Techniques for Liver Masses

Surgery provides the best chance at survival in many hepatobiliary diseases. For patients who aren't surgical candidates, a few therapies exist that either improve the disease burden or allow patients who previously were not candidates to become candidates for resection. In performing any of these novel techniques, knowledge of the liver segments as well as the blood supply to various portions of the liver is essential.

Portal Vein Embolization

Portal vein embolization (PVE) is a method used to embolize portal branches that feed hepatic tumors [25]. The theory of PVE is that after embolization of the portal branch that feeds a mass, the remainder blood flow is directed toward the remaining liver remnant. Hypertrophy of the remnant then ensues, allowing for the remaining liver to become stronger and "prepare" the remaining liver for resection.

Portal vein embolization has been shown to reduce complications and lead to shorter hospital stays after hepatic resection [25]. In addition, PVE increases the number of patients who are eligible for surgical resection of their disease due to increased size of the liver remnant [26].

The indications for PVE have been discussed widely in the literature. In patients without hepatic fibrosis or cirrhosis, patients with a predicted resection of >70–75% of their total liver volume are eligible. In patients with fibrosis or cirrhosis, the predicted resection of 60–65% is an indication for PVE [27].

References

1. Majno P, Mentha G, Toso C, Morel P, Peitgen HO, Fasel JH. Anatomy of the liver: an outline with three levels of complexity – a further step towards tailored territorial liver resections. *J Hepatol.* 2014;60(3):654–62.

2. Couinaud C. The liver. Anatomical and surgical investigations. Paris: Masson; 1957. Le foie. Etudes anatomiques et chirurgicales.
3. Couinaud C. Liver anatomy: portal (and suprahepatic) or biliary segmentation. *Dig Surg.* 1999;16(6):459–67.
4. Terminology Committee of the International Hepato-Pancreato-Biliary Association. The Brisbane 2000 Nomenclature of Liver Anatomy and Resections. *HPB.* 2000;2(3):333–9.
5. Löschner C, Nagel SN, Kausche S, Teichgräber U. Hepatic Arterial Supply in 1297 CT-Angiographies. *Rofo.* 2015;187(4):276–82.
6. Saba L, Mallarini G. Anatomic variations of arterial liver vascularization: an analysis by using MDCTA. *Surg Radiol Anat.* 2011;33(7):559–68.
7. Michels NA. Blood supply and anatomy of the upper abdominal organs with a descriptive atlas. Philadelphia: J.B. Lippincott Company; 1955. p. 3–137.
8. Skandalakis JE, et al. Hepatic surgical anatomy. *Surg Clin N Am.* 2004;84(2):413–35.
9. Shilal P, Tuli A. Anatomical variations in the patten of the right hepatic veins draining the posterior segment of the right lobe of the liver. *J Clin Diagn Res.* 2015;9(3):AC08–12.
10. Bageacu S, Abdelaal A, Ficarel S, Elmeteni M, Boilot O. Anatomy of the right liver lobe: a surgical analysis in 124 consecutive living donors. *Clin Transpl.* 2011;25(4):E447–54.
11. Blumgart LH. Surgical and radiographic anatomy of the liver, biliary tract, and pancreas. Blumgart's surgery of the liver, biliary tract, and pancreas. Philadelphia: Elsevier; 2017. p. 32–59e1.
12. Healey JE, Schroy PC. Anatomy of the biliary ducts within the human liver; analysis of the prevailing pattern of branchings and the major variations of the biliary ducts. *AMA Arch Surg.* 1953;66(5):599–616.
13. Figueras J, Llado L, Ruiz D, Ramos E, Busquets J, Rafecas A, et al. Complete versus selective portal triad clamping for minor liver resections. *Ann Surg.* 2005;241(4):582–90.
14. Lesurtel M, Selzner M, Petrowsky H, McCormack L, Clavien PA. How should transection of the liver be performed?: a prospective randomized study in 100 consecutive patients: comparing four different transection strategies. *Ann Surg.* 2005;242(6):814–22.
15. Petrowsky H, McCormack L, Trujillo M, Selzner M, Jochum W, Clavien PA. A prospective, randomized, controlled trial comparing intermittent portal triad clamping versus ischemic preconditioning with continuous clamping for major liver resection. *Ann Surg.* 2006;244(6):921–30.
16. Belghiti J, Noun R, Malafossee R, Jagot P, Sauvanet A, Pierangeli F, et al. Continuous versus intermittent portal triad clamping for liver resection: a controlled study. *Ann Surg.* 1999;229(3):369–75.
17. Kang KJ, Jang JG, Lim TJ, Kang Y, Park KK, Lee IS, et al. Optimal cycle of intermittent portal triad clamping during liver resection in the murine liver. *Liver Transpl.* 2004;10(6):795–801.
18. Rüdiger HA, Kang KJ, Sindram D, Riehle HM, Clavien PA. Comparison of ischemic preconditioning and intermittent and continuous inflow occlusion in the murine liver. *Ann Surg.* 2002;235(3):400–7.
19. Hung MH, Lin LH, Chen DF, Huang CS. Choledocal cysts in infants and children: experience over a 20-year period at a single institution. *Eur J Pediatr.* 2011;170(9):1179–85.
20. Todani T, Watanabe Y, Narusue M, Tabuchi K, Okajima K. Congenital bile duct cysts: classification, operative procedures, and review of thirty-seven cases including cancer arising from choledochal cyst. *Am J Surg.* 1977;134(2):263–9.
21. Soares KC, Arnaoutakis DJ, Kamel I, Rastegar N, Anders R, Maithel S, et al. Choledochal cysts: presentation, clinical differentiation, and management. *J Am Coll Surg.* 2014;219(6):1167–80.
22. Parada LA, Hallén M, Hägerstrand I, Tranberg KG, Johansson B. Clonal chromosomal abnormalities in congenital bile duct dilation. *Gut.* 1999;45(5):780–2.
23. Singham J, Yoshida EM, Scudamore CH. Choledochal cysts: part 3 of 3: management. *Can J Surg.* 2010;53(1):51–6.
24. Diao M, Li L, Cheng W. Timing of surgery for prenatally diagnosed asymptomatic choledochal cysts: a prospective randomized study. *J Pediatr Surg.* 2012;47(3):506–12.
25. May BJ, Talenfeld AD, Madoff DC. Update on portal vein embolization: evidence-based outcomes, controversies, and novel strategies. *J Vasc Interv Radiol.* 2013;24(2):241–54.

26. Azoulay D, Castaing D, Smail A, Adam R, Cailliez V, Laurent A, et al. Resection of nonresectable liver metastases from colorectal cancer after percutaneous portal vein embolization. *Ann Surg.* 2000;231(4):480–6.
27. Van Lienden KP, van den Esschert JW, de Graaf W, Bipat S, Lameris JS, van Gulik TM, et al. Portal vein embolization before liver resection: a systematic review. *Cardiovasc Intervent Radiol.* 2013;36(1):25–34.



Surgical Anatomy, Anomalies, and Normal Variants of the Pancreas

11

Charles Cha and Lindsay Hollander

Introduction

The pancreas is a digestive organ with both exocrine and endocrine functions that sits in the retroperitoneum at the level of the second lumbar vertebra. It has an extremely close spatial relationship with multiple organs (i.e., the duodenum, stomach, transverse colon, and bile duct) and multiple major blood vessels, including the celiac axis, superior mesenteric artery and vein, portal vein, and vena cava [1, 2]. Acknowledgment and understanding of these close proximities is vital when performing surgical procedures involving the pancreas. Knowledge of pancreatic embryology is also key for the identification of congenital anomalies and their relevance for patients. An in-depth understanding of overall pancreatic anatomy and normal variants is also critical for the proper diagnosis and treatment of any potential resulting pancreatic pathology. Anatomic anomalies and variations of the pancreas include pancreas divisum, annular pancreas, ectopic pancreas, pancreatic agenesis and hypoplasia, pancreatic cysts, and variations of the course and configuration of the duct.

Embryologic Development

During the fourth-to-fifth week of gestation, the pancreas begins to develop as dorsal and ventral buds at the junction of the foregut and midgut. The foregut then elongates and rotates. The ventral bud rotates clockwise with the duodenum and fuses with the dorsal bud at approximately the seventh week of gestation. The dorsal bud is the larger of the two and eventually forms most of the head, body, and tail of the pancreas, while the ventral bud develops into the uncinate process and inferior

C. Cha (✉) · L. Hollander
Department of Surgery, Yale School of Medicine, New Haven, CT, USA
e-mail: charles.cha@yale.edu

portion of the pancreatic head. Most commonly, the ventral pancreatic duct will then fuse with the distal portion of the dorsal duct to become the main pancreatic duct (duct of Wirsung), and the proximal portion of the dorsal bud duct will form the minor or accessory pancreatic duct (duct of Santorini) [1, 3, 4]. A schematic representation of the development can be seen in Fig. 11.1.

The same ventral outpouching that produces the ventral pancreatic bud also produces the remaining hepatobiliary system. At about the eighth week of gestation, the remaining ventral outpouching will separate into the pars cystica and the pars hepatica. The pars cystica develops into the cystic duct and gallbladder, while the two major lobes of the liver arise from the pars hepatica [3, 5].

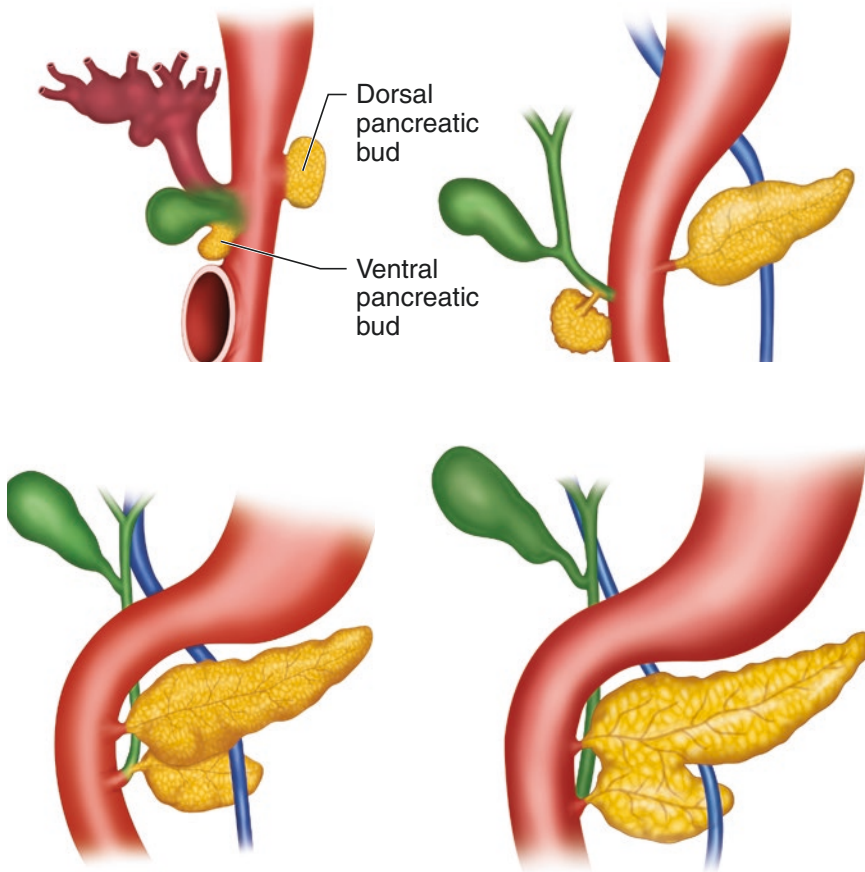


Fig. 11.1 Pancreatic and ductal development during weeks 5 through 8. As the duodenum grows and rotates, the ventral pancreatic bud is normally rotated clockwise to meet and fuse with the dorsal bud. The ventral pancreatic duct and the distal part of the dorsal duct then fuse to form the main pancreatic duct

Pancreatic Anatomy

Spatial Orientation

The pancreas consists of four parts: the head (including the uncinata process), neck, body, and tail. The head lies within the C-loop of the duodenum and includes all the parenchyma that extends to the right of the superior mesenteric artery and vein. It is attached to the medial and superior aspects of the second and third portions of the duodenum, respectively. The uncinata process is the inferior portion of the head that passes posterior to the superior mesenteric vessels, while the pancreatic neck lies anterior to the vessels, directly over the area where the superior mesenteric and the splenic veins join to form the portal vein and immediately posterior to the pylorus of the stomach.

The body is the pancreatic segment to the left of the neck. It directly overlies the aorta, left adrenal gland, left kidney, left renal artery and vein, and the second lumbar vertebra. The anterior surface is covered with peritoneum and forms the floor of the omental bursa within the lesser sac.

The tail of the pancreas begins anterior to the left kidney and continues to the splenic hilum within the layers of the splenorenal ligament. The splenic artery and vein run immediately posterior to the tail (Fig. 11.2) [1, 2, 6].

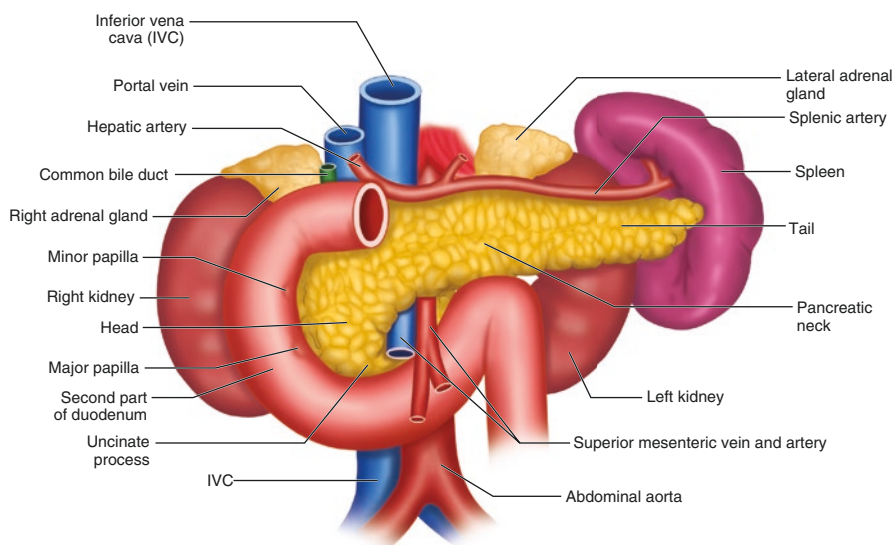


Fig. 11.2 In vivo orientation of the pancreas. The head lies within the C-loop of the duodenum, with the uncinata process portion passing posterior to the superior mesenteric vessels. The pancreatic neck is anterior to the vessels, and the tail runs laterally toward the splenic hilum through the layers of the splenorenal ligament

Ductal Anatomy

The main pancreatic duct, or duct of Wirsung, is about 2–4 mm in diameter. It begins in the tail of the pancreas, runs midway through the parenchyma, toward the head, where it turns inferiorly to join the common bile duct (CBD) and empty into the duodenum. The common channel drains via the ampulla of Vater 7–10 cm distal to the pylorus at the major duodenal papilla. The sphincter of Oddi lies at the opening of the ampulla and prevents reflux of duodenal contents into the bile and pancreatic ducts.

The smaller accessory pancreatic duct, or duct of Santorini, drains into the duodenum via the minor papilla, which lies proximal to the ampulla of Vater. The minor duct drains the uncinete process and the inferior portion of the pancreatic head (Fig. 11.3) [6–8].

Blood Supply

The pancreas receives its blood supply from both the celiac axis and the superior mesenteric artery. The celiac axis arises directly from the abdominal aorta and divides into the splenic artery, the left gastric artery, and the common hepatic artery. The splenic artery travels along the posterior-superior border of the pancreas, giving rise to several branches as it courses toward the splenic hilum. The three most

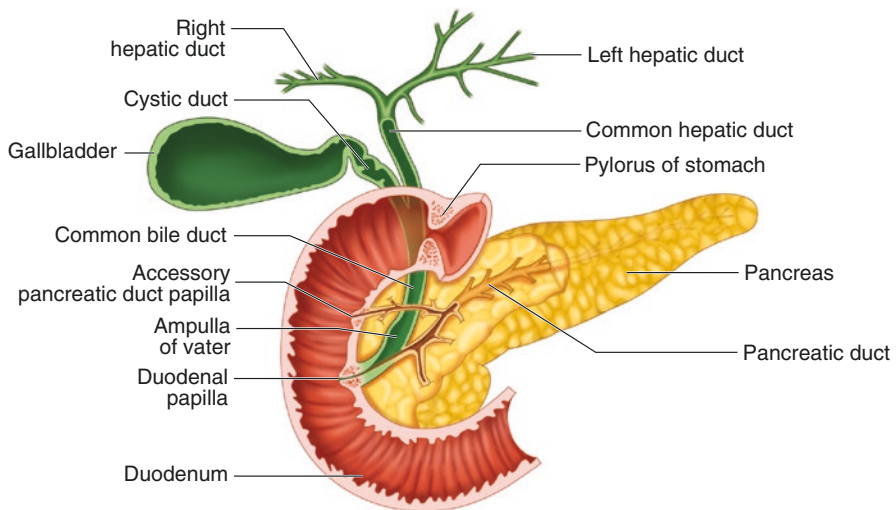


Fig. 11.3 Normal pancreatic ductal configuration. The pancreatic duct begins in the tail and courses through the body, into the head of the pancreas, where it turns inferiorly to meet with the bile duct. This common channel (ampulla of Vater) is drained into the duodenum via the major duodenal papilla. The minor duodenal papilla empties the accessory pancreatic duct into the duodenum just above the major papilla

notable branches include the dorsal pancreatic artery, the great pancreatic artery, and the caudal pancreatic artery, supplying the proximal body, mid-portion of the body, and the tail of the pancreas, respectively.

The common hepatic artery normally gives rise to the gastroduodenal artery. This artery turns into the superior pancreaticoduodenal artery once it passes the first portion of the duodenum, and then it divides into anterior and posterior branches. The inferior pancreaticoduodenal artery originates from the superior mesenteric artery and also divides to form anterior and posterior branches. The inferior and superior pancreaticoduodenal branches form extensive collaterals that supply both the duodenum and the head of the pancreas [1, 6].

Twenty to thirty percent of people have variations in the blood supply. Most commonly, there is a replaced right hepatic artery that arises from the superior mesenteric artery instead of the common hepatic artery. Less commonly, the right hepatic artery may originate from the right gastric or the gastroduodenal artery. The common hepatic artery may also aberrantly arise from the superior mesenteric artery. The left hepatic artery may be found to originate from the left gastric artery instead of the common hepatic artery in about 10% of the population.

The venous drainage of the pancreas follows the arterial blood supply. It is eventually collected in the portal vein and delivered to the liver [1, 6, 8]. Figure 11.4 demonstrates the vascular supply of the pancreas.

Lymphatic Drainage

Five major nodal groups drain the lymphatic network of the pancreas. The superior portion of the head drains into the superior nodal group that lies at the superior border of the pancreas and celiac trunk. The inferior group that lies along the inferior border of the head and body drains the inferior portion of the pancreatic head and the uncinate process. The anterior lymphatics empty into the prepyloric and infrapyloric nodes, while the posterior group empties with the distal common bile duct and ampullary lymphatics into the para-aortic nodes. The splenic nodal group drains the body and tail of the pancreas into the interceliomesenteric nodes [1, 2, 6]. All these major nodal basins draining the pancreas can be seen in Fig. 11.5.

Innervation

The vagus and thoracic splanchnic nerves, as well as the peptidergic neurons that secrete amines and peptides, all innervate the pancreas. As demonstrated in Fig. 11.6, the nerve fibers travel along the celiac axis and the superior mesenteric arteries in order to reach the pancreas. Both endocrine and exocrine secretion are stimulated by the parasympathetics and mostly inhibited by the sympathetics. The peptidergic neurons secrete hormones such as somatostatin, vasoactive intestinal peptide (VIP), calcitonin gene-related peptide (CGRP), and galanin to influence both exocrine and endocrine functions [1, 6].

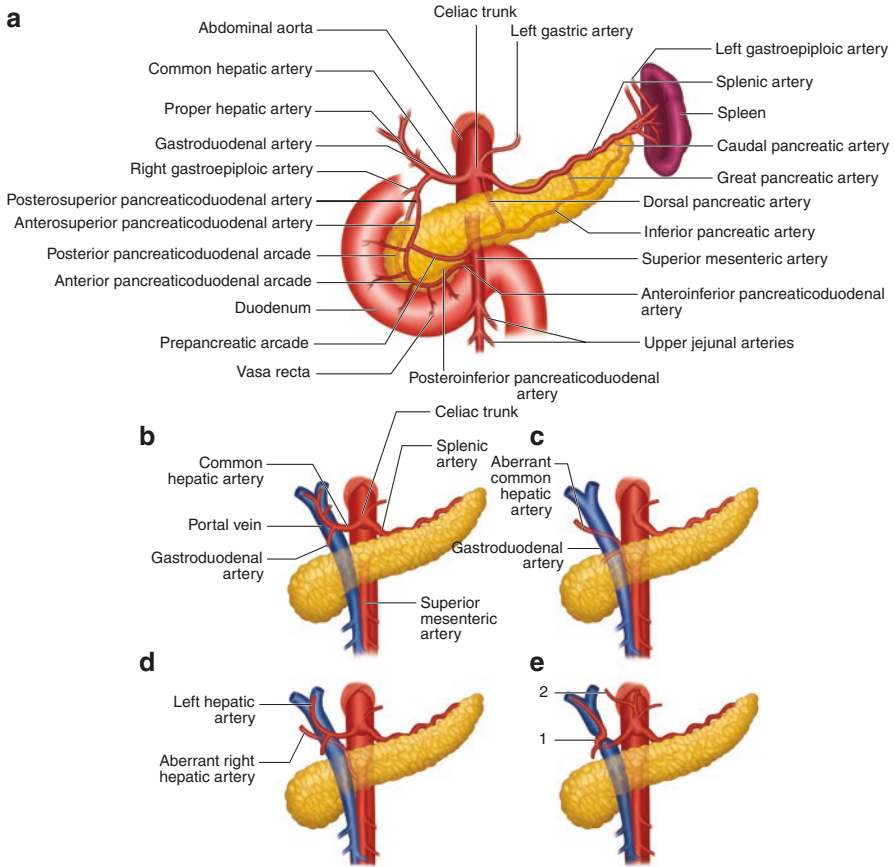


Fig. 11.4 Normal and common variations of the pancreatic arterial supply. (a) Pancreatic arterial supply. (b) Normal arterial supply configuration. (c) Aberrant common hepatic artery. (d) Aberrant right hepatic artery. (e) Either the common hepatic artery looping around the portal vein from behind (1) or an aberrant left hepatic artery arising from the left gastric artery (2)

Congenital Anomalies and Normal Variants of the Pancreas and Pancreatic Duct

Developmental rotation and fusion of the pancreas occur correctly 60% of the time. Abnormalities of these actions lead to congenital anomalies and normal variants of the pancreas that can have surgical significance.

Pancreas Divisum

Pancreas divisum is the most common congenital ductal anomaly, occurring in 4–14% of the population. It develops from an incomplete fusion of the ventral and

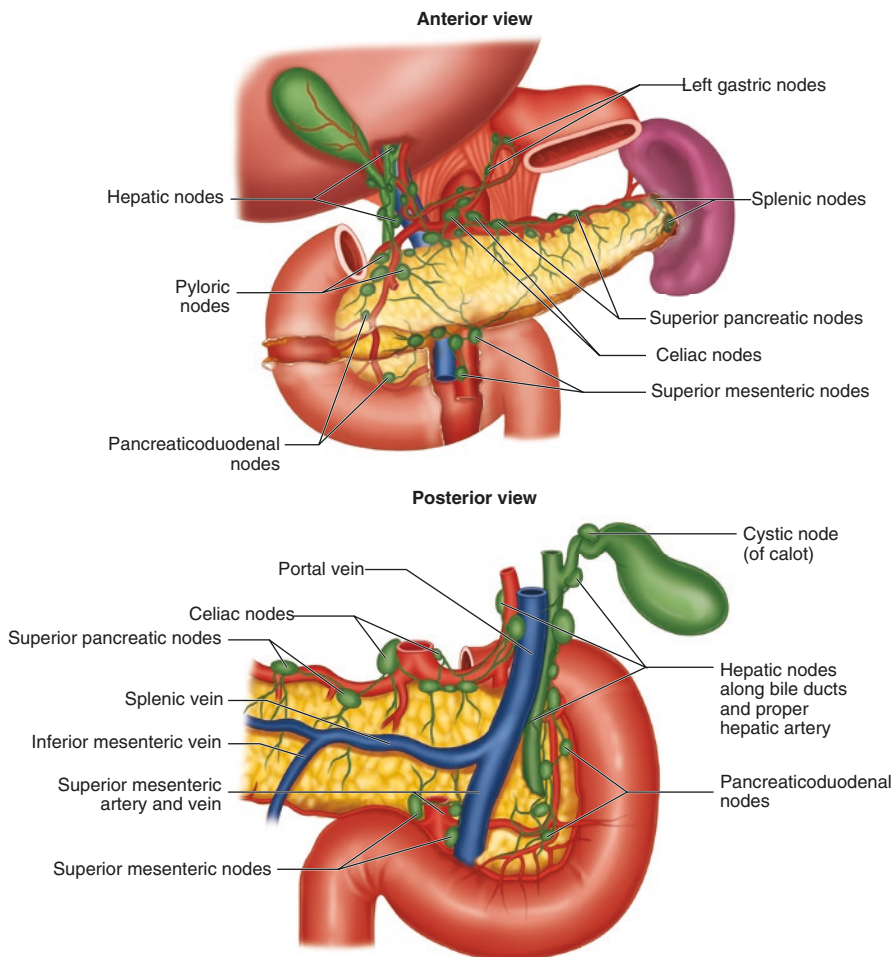
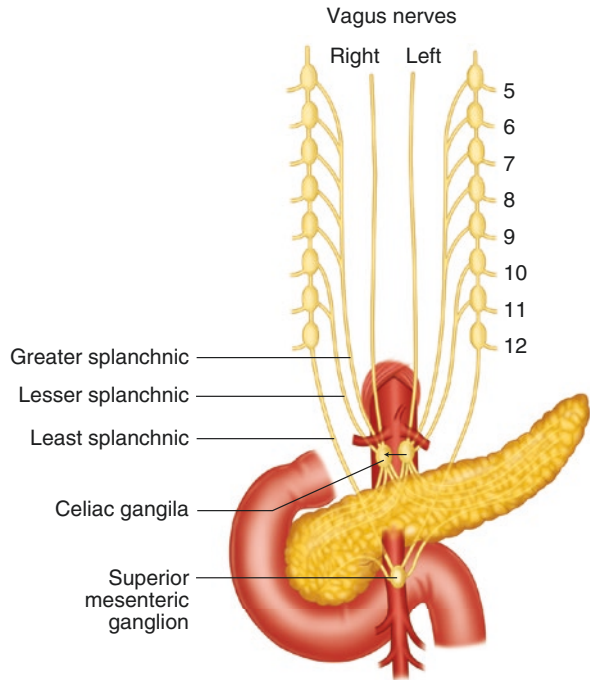


Fig. 11.5 Pancreatic lymph drainage. The five main nodal groups draining any pancreatic lymph include the superior, inferior, anterior, posterior, and splenic groups. The Japanese Pancreas Society has further classified these groups into 18 lymph node stations, which are commonly referenced in the description of pancreatic surgery

dorsal ducts, resulting in the lesser duct draining the majority of the pancreas via the minor papilla. A small remnant duct of the ventral bud drains the uncinate process and the posterior head into the duodenum via the major papilla. Most patients with pancreas divisum are asymptomatic; however, a few will experience recurrent acute pancreatitis due to inadequate drainage of pancreatic secretions through the minor papilla [3, 9–11].

For many years, endoscopic retrograde cholangiopancreatography (ERCP) has been the standard tool utilized to diagnose pancreas divisum. Alternatively, magnetic resonance cholangiopancreatography (MRCP), especially secretin-enhanced

Fig. 11.6 Autonomic nerve supply to the pancreas. The vagus and thoracic splanchnic nerves supply the innervation of the pancreas. The nerves travel along the arteries of the celiac axis and the superior mesenteric arteries to reach the gland



MRCP, provides the means for an accurate diagnosis of the anomaly without the use of contrast material and the risk of ERCP-induced pancreatitis (Fig. 11.7a). Imaging seen from multidetector computed tomography (MDCT) is also sensitive enough to demonstrate divisum, when present (Fig. 11.7b) [12–15].

When patients with pancreas divisum are symptomatic from their disease, endoscopic or operative papillotomy of the minor papilla and accessory duct should be considered for disease treatment [9, 11].

Annular Pancreas

Annular pancreas is a rare congenital anomaly thought to occur in about 1 of every 1000 people. It results from failure of the ventral bud to rotate with the duodenum. Instead, the pancreatic tissue surrounds the descending duodenum, either completely or incompletely, and it is in continuity with the pancreatic head (Fig. 11.8a) [11, 16]. Many patients may be asymptomatic with the anomaly; however, the encircling pancreas can cause compression and stenosis of the duodenum. This may lead to severe duodenal obstruction and feeding intolerance in neonates or usually less severe gastric outlet obstruction and vomiting in symptomatic adults. In children, annular pancreas is more commonly associated with other congenital anomalies, such as Down syndrome and cardiac anomalies, whereas in adults, it is more commonly associated with pancreas divisum and pancreatic neoplasia [5, 8, 17, 18].

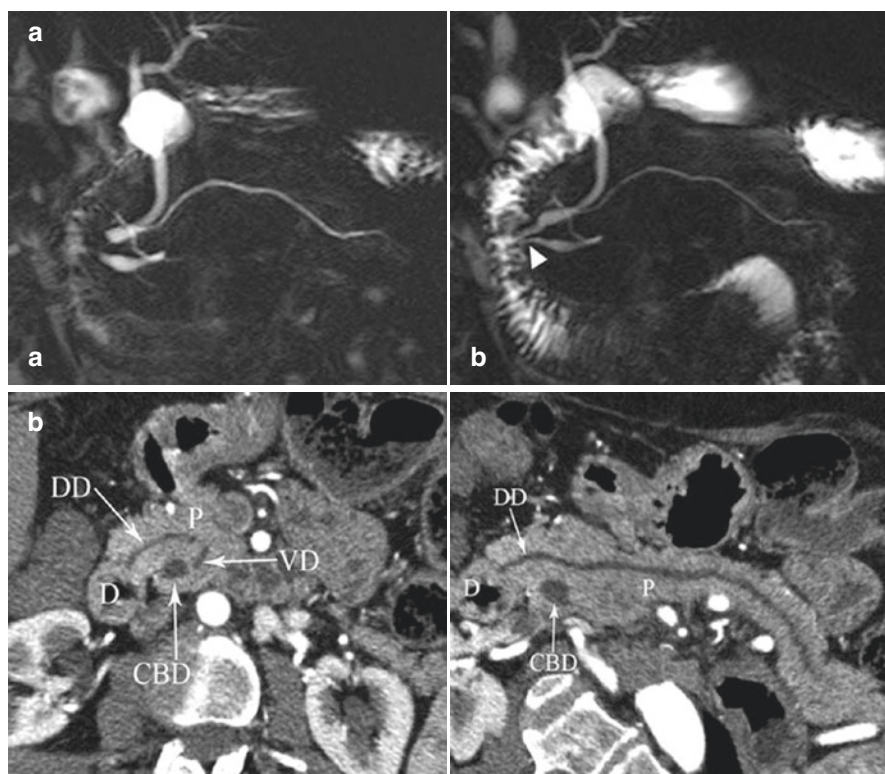


Fig. 11.7 Pancreas divisum. **(a)** Magnetic resonance cholangiopancreatography (MRCP) image showing the dorsal duct crossing anterior to the common bile duct (CBD) and emptying separately into the minor duodenal papilla and the CBD joining the ventral duct and both entering the major duodenal papilla in a patient with pancreas divisum. **(b)** Axial and planar MDCT images demonstrating the dorsal duct crossing anterior to the CBD and emptying separately into the minor papilla

As with pancreas divisum, annular pancreas used to be primarily diagnosed with ERCP. Now, CT, MRI, and MRCP are all potential imaging modalities that can reliably demonstrate annular pancreas as either an aberrant pancreatic duct encircling and extending to the right of the duodenum or simply any pancreatic tissue that extends either postero- or anterolateral to or completely around the second part of the duodenum and is in continuity with the pancreatic head (Fig. 11.8b, c) [19, 20].

If symptomatic of the anomaly, patients may require either some form of duodenal bypass or surgical resection.

Ectopic Pancreas

Ectopic, or heterotopic, pancreas is any pancreatic tissue that lies outside the bounds of the normal pancreas and lacks any anatomic or vascular connection to the normal pancreas. It is present in 1–15% of the population and can be found in many

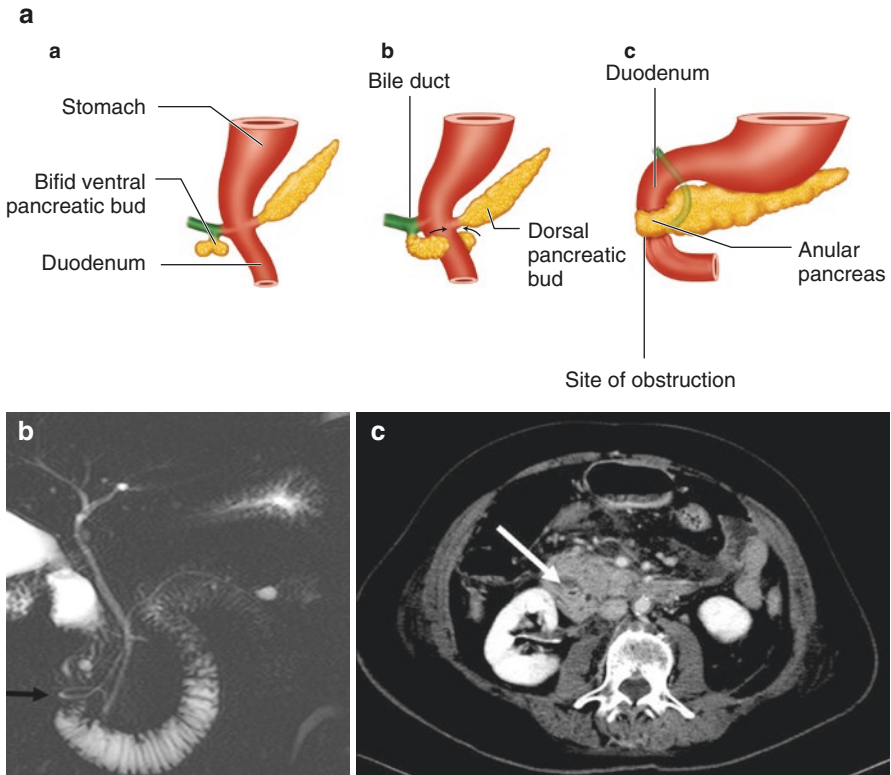


Fig. 11.8 Annular pancreas. (a) The annular pancreas anomaly develops either from failure of the ventral bud to rotate with the duodenum or an early split of the ventral bud into two anlagen, resulting in envelopment of the duodenum with pancreatic tissue and the potential for duodenal obstruction. (b) MRCP image showing the pancreatic duct making a loop in the proximal portion, encircling the second portion of the duodenum. (c) MDCT image shows pancreatic tissue surrounding the descending portion of the duodenum

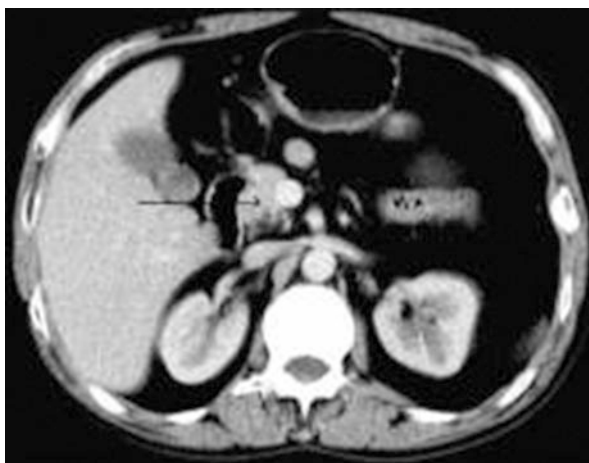
different locations. Seventy percent of the time, it is located within the submucosa of the gastric antrum, but it can also be found in the ileum, colon, appendix, mesentery, gallbladder, or even in a Meckel diverticulum. The existence of ectopic tissue is usually asymptomatic, but it can lead to problems such as bleeding, ulceration, intussusception, obstruction, or neoplastic disease [7, 21, 22].

At times, ectopic pancreas may be diagnosed with barium studies. As highlighted in the ERCP image shown in Fig. 11.9, the tissue may appear as a small, broad-based submucosal lesion with a central umbilication that represents the rudimentary pancreatic duct. Without these findings via barium study, there are no additional diagnostic features that will differentiate it from other submucosal masses [7, 18, 23].

Fig. 11.9 Ectopic pancreas. Endoscopic image of ectopic pancreatic tissue, commonly seen as a small submucosal lesion with a central umbilication that represents a rudimentary pancreatic duct



Fig. 11.10 Pancreatic hypoplasia. Axial CT image demonstrating partial dorsal agenesis of the pancreas



Ectopic pancreatic tissue is usually asymptomatic and an incidental finding requiring no treatment. It is functional and thus susceptible to the same pathology as the normal pancreas. If disease develops, treatment is directed at the presenting symptoms. In rare instances, resection of the tissue may be required [24].

Agnesis and Hypoplasia of the Pancreas

Complete pancreatic agnesis is extremely rare and incompatible with life. Pancreatic hypoplasia may result from the absence of either ventral or dorsal bud. Partial dorsal agenesis is the most common form of pancreatic hypoplasia and is associated with an increased risk of diabetes mellitus, pancreatitis, and polysplenia syndrome. It will appear as a short, rounded pancreatic head lacking the neck, body, and tail on imaging (Fig. 11.10) [25–27].

Pancreatic Cysts

Congenital pancreatic cysts are very rare and develop from the sequestration of primitive pancreatic ducts. They are usually asymptomatic but occasionally can lead to vomiting, jaundice, or pancreatitis. On imaging, they appear as simple, thin-walled cysts within the body or tail of the pancreas (Fig. 11.11). They can be idiopathic or occur in association with other diseases such as Von Hippel-Landau disease, Beckwith-Wiedemann syndrome, or polycystic disease of the pancreas and kidneys [16, 28–30].

Ductal Variants

The pancreatic ductal system develops within a wide spectrum of anatomic variations in both the configuration of the ducts and the manner in which the ducts enter the duodenum. Most commonly, the pancreatic duct travels through the gland in a descending course, but it may also display a sigmoid, vertical, or loop configuration [11, 18]. The ducts are also usually in a bifid configuration with a dominant duct of Wirsung. Other potential configurations include an absent duct of Santorini, a dominant duct of Santorini without pancreas divisum, and a reverse S-shaped duct of Santorini that connects with a duct of Wirsung side branch (ansa pancreatica) [4, 18].

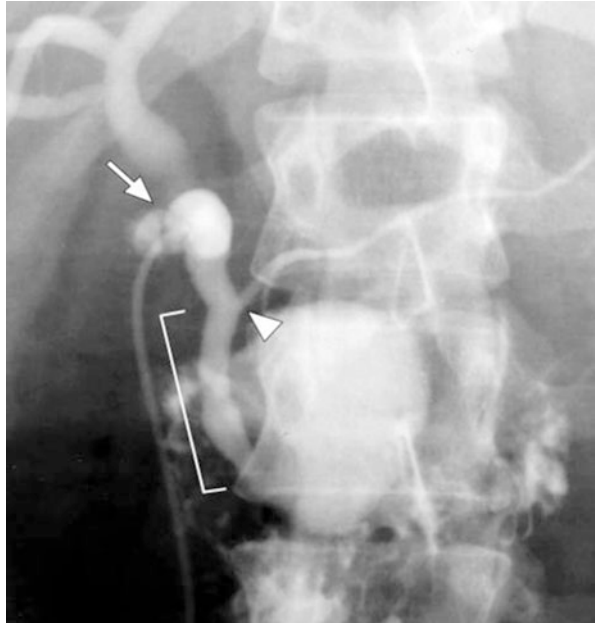
Duplication anomalies of the main pancreatic duct can be present. Cystic dilations of the distal portion of the ducts can also be seen, termed Wirsungoceles and Santoriniceles.

The pancreatic duct and common bile duct normally fuse within the duodenal wall; however, anomalous pancreaticobiliary junction (APBJ) is a congenital ductal anomaly in which the ducts fuse outside of the wall and form an elongated common channel (fused duct >15 mm in length) as seen in Fig. 11.12. This anomaly has been noted in 1.5–3.0% of patients undergoing ERCP and is frequently associated with

Fig. 11.11 Congenital pancreatic cyst. A well-defined cystic mass present in the pancreatic head of a three-year-old boy



Fig. 11.12 Anomalous pancreaticobiliary junction. ERCP spot image showing an abnormal proximal joining of the pancreatic duct with the CBD, resulting in a long common channel



choledochal cysts and carcinoma of the biliary tract. A couple of potential explanations for the etiology of this anomaly includes arrest of the migration of the fused ducts into the duodenal wall or misalignment of the pancreatic buds during their fusion together (oblique fusion of the buds and ducts instead of the normal side-by-side bud fusion) [3, 31–34].

References

1. Riall TS. Pancreas anatomy and physiology. In: Mulholland MW, Lillemoe KD, Doherty GM, Maier RV, Simeone DM, Upchurch Jr GR, editors. *Greenfield's surgery: scientific principles and practice*. Philadelphia: Lippincott Williams & Wilkins; 2011. p. 799–818.
2. Blumgart LH, Hann LE. Surgical and radiologic anatomy of the liver, biliary tract, and pancreas. In: Blumgart LH, editor. *Surgery of the liver, biliary tract, and pancreas*. Philadelphia: Saunders Elsevier; 2007. p. 3–29.
3. Tadokoro H, Takase M, Nobukawa B. Development and congenital anomalies of the pancreas. *Anat Res Int*. 2011;2011:351217.
4. Mortelé KJ, Rocha TC, Streeter JL, Taylor AJ. Multimodality imaging of pancreatic and biliary congenital anomalies. *Radiographics*. 2006;26(3):715–31.
5. Rizzo RJ, Szucs RA, Turner MA. Congenital abnormalities of the pancreas and biliary tree in adults. *Radiographics*. 1995;15(1):49–68; quiz 147–8.
6. Drake RL, Vogl W, Mitchell AWM. *Abdomen: regional anatomy*. In: Drake RL, Vogl W, Mitchell AWM, editors. *Gray's anatomy for students*. Philadelphia: Saunders Elsevier; 2005. p. 242–343.
7. Borghei P, Sokhandon F, Shirkhoda A, Morgan DE. Anomalies, anatomic variants, and sources of diagnostic pitfalls in pancreatic imaging. *Radiology*. 2013;266(1):28–36.

8. Schulte SJ. Embryology, normal variation, and congenital anomalies of the pancreas. In: Stevenson GW, Freeny PC, Margulis AR, Burhenne AR, editors. *Margulis' and Burhenne's alimentary tract radiology*. St. Louis: Mosby; 1994. p. 1039–51.
9. Howard TJ. Pancreas divisum and other variants of dominant dorsal duct anatomy. In: Cameron JL, Cameron AM, editors. *Current surgical therapy*. Philadelphia: Elsevier; 2011. p. 393–8.
10. Agha FP, Williams KD. Pancreas divisum: incidence, detection, and clinical significance. *Am J Gastroenterol*. 1987;82(4):315–20.
11. Kozu T, Suda K, Toki F. Pancreatic development and anatomical variation. *Gastrointest Endosc Clin N Am*. 1995;5(1):1–30.
12. Lehman GA, Sherman S. Diagnosis and therapy of pancreas divisum. *Gastrointest Endosc Clin N Am*. 1998;8(1):55–77.
13. Soto JA, Lucey BC, Stuhlfaut JW. Pancreas divisum: depiction with multi-detector row CT. *Radiology*. 2005;235(2):503–8.
14. Bret PM, Reinhold C, Taourel P, Guibaud L, Atri M, Barkun AN. Pancreas divisum: evaluation with MR cholangiopancreatography. *Radiology*. 1996;199(1):99–103.
15. Morgan DE, Logan K, Baron TH, Koehler RE, Smith JK. Pancreas divisum: implications for diagnostic and therapeutic pancreatography. *AJR Am J Roentgenol*. 1999;173(1):193–8.
16. Yu J, Turner MA, Fulcher AS, Halvorsen RA. Congenital anomalies and normal variants of the pancreaticobiliary tract and the pancreas in adults: part 2, Pancreatic duct and pancreas. *AJR Am J Roentgenol*. 2006;187(6):1544–53.
17. Sandrasegaran K, Patel A, Fogel EL, Zyromski NJ, Pitt HA. Annular pancreas in adults. *AJR Am J Roentgenol*. 2009;193(2):455–60.
18. Türkvtan A, Erden A, Türkoğlu MA, Yener Ö. Congenital variants and anomalies of the pancreas and pancreatic duct: imaging by magnetic resonance cholangiopancreatography and multidetector computed tomography. *Korean J Radiol*. 2013;14(6):905–13.
19. Lecesne R, Stein L, Reinhold C, Bret PM. MR cholangiopancreatography of annular pancreas. *J Comput Assist Tomogr*. 1998;22(1):85–6.
20. Nijs EL, Callahan MJ. Congenital and developmental pancreatic anomalies: ultrasound, computed tomography, and magnetic resonance imaging features. *Semin Ultrasound CT MR*. 2007;28(5):395–401.
21. Thoeni RF, Gedgaudas RK. Ectopic pancreas: usual and unusual features. *Gastrointest Radiol*. 1980;5(1):37–42.
22. Eisenberger CF, Gocht A, Knoefel WT, Busch CB, Peiper M, Kutup A, et al. Heterotopic pancreas – clinical presentation and pathology with review of the literature. *Hepatogastroenterology*. 2004;51(57):854–8.
23. Cho JS, Shin KS, Kwon ST, Kim JW, Song CJ, Noh SM, et al. Heterotopic pancreas in the stomach: CT findings. *Radiology*. 2000;217(1):139–44.
24. Emerson L, Layfield LJ, Rohr LR, Dayton MT. Adenocarcinoma arising in association with gastric heterotopic pancreas: a case report and review of the literature. *J Surg Oncol*. 2004;87(1):53–7.
25. Schnedl WJ, Piswanger-Soelkner C, Wallner SJ, Reittner P, Krause R, Lipp RW, et al. Agenesis of the dorsal pancreas and associated diseases. *Dig Dis Sci*. 2009;54(3):481–7.
26. Alexander LF. Congenital pancreatic anomalies, variants, and conditions. *Radiol Clin N Am*. 2012;50(3):487–98.
27. Low JP, Williams D, Chaganti JR. Polysplenia syndrome with agenesis of the dorsal pancreas and preduodenal portal vein presenting with obstructive jaundice – a case report and literature review. *Br J Radiol*. 2011;84(1007):e217–20.
28. Agarwala S, Lal A, Bhatnagar V, Dinda AK, Mitra DK. Congenital true pancreatic cyst: presentation and management. *Trop Gastroenterol*. 1999;20(2):87–8.
29. Auringer ST, Ulmer JL, Sumner TE, Turner CS. Congenital cyst of the pancreas. *J Pediatr Surg*. 1993;28(12):1570–1.
30. Boulanger SC, Borowitz DS, Fisher JF, Brisseau GF. Congenital pancreatic cysts in children. *J Pediatr Surg*. 2003;38(7):1080–2.

31. Matsumoto Y, Fujii H, Itakura J, Matsuda M, Nobukawa B, Suda K. Recent advances in pancreaticobiliary maljunction. *J Hepato-Biliary-Pancreat Surg.* 2002;9(1):45–54.
32. Kato O, Hattori K, Suzuki T, Tachino F, Yuasa T. Clinical significance of anomalous pancreaticobiliary union. *Gastrointest Endosc.* 1983;29(2):94–8.
33. Misra SP, Dwivedi M. Pancreaticobiliary ductal union. *Gut.* 1990;31(10):1144–9.
34. Cha SW, Park MS, Kim KW, Byun JH, Yu JS, Kim MJ, et al. Choledochal cyst and anomalous pancreaticobiliary ductal union in adults: radiological spectrum and complications. *J Comput Assist Tomogr.* 2008;32(1):17–22.



Anatomy of the Genitourinary System

12

Kara Smith, Ty Spillman, Adrienne Cashio,
Gopal Kodumudi, and Rajuno Ettarh

Introduction

The urinary system is comprised of paired kidneys and ureters, the urinary bladder, and the urethra. Plasma and waste collected in the *lymphatics* and *bloodstream* are carried through the kidneys and filtered through the nephrons. Waste is centrally collected, then flows through the ureters to the urinary bladder where it is collected over an extended period. Once the bladder fills to capacity, the waste is *processed* through the urethra and expelled.

Kidneys

Overview

The kidneys serve a variety of physiologic purposes. Primarily, the kidneys filter blood and begin the process of excretion of the waste. They also regulate the body's

K. Smith
Campbell University School of Osteopathic Medicine, Lillington, NC, USA

T. Spillman
Creighton University, Omaha, NE, USA

A. Cashio
University of Queensland, La Place, LA, USA

G. Kodumudi
Department of Anesthesiology, Louisiana State University School of Medicine, New Orleans
Health, New Orleans, LA, USA
e-mail: gkodum@lsuhsc.edu

R. Ettarh (✉)
Department of Medical Education/Anatomy, California University of Science and Medicine,
Colton, CA, USA
e-mail: EttarhR@cusm.org

© Springer Nature Switzerland AG 2021

D. Narayan et al. (eds.), *Surgical and Perioperative Management of Patients with
Anatomic Anomalies*, https://doi.org/10.1007/978-3-030-55660-0_12

electrolyte balance, blood pressure, and acid–base balance. In addition, the kidneys have endocrine functions that include the production of renin and erythropoietin, and the activation of vitamin D.

Structure

The kidneys are paired bean-shaped organs found in the retroperitoneum between vertebral levels T12–L3 (Fig. 12.1). The right kidney typically sits slightly caudal to the left kidney in compensation for the presence of the large right lobe of the liver. Each kidney is covered by a fibrous renal capsule and surrounded by renal fascia, which is then surrounded by retroperitoneal fat. The perirenal fat layer lies between the renal capsule and the posterior layer of renal fascia, while the pararenal (retroperitoneal) fat lies between the posterior layer of renal fascia and the transversalis fascia lining the abdominal wall. The indentation on the medial aspect of the kidney is called the hilum where the renal vessels, nerves, and ureter enter and leave the kidney. Internally, the kidney is comprised of a cortex that surrounds medullary pyramids that are separated by columns of tissue known as renal columns (Fig. 12.2). A coronal section of a kidney reveals a central collecting duct (renal pelvis) with radiating medullary pyramids. The medulla and renal cortex are the location of the

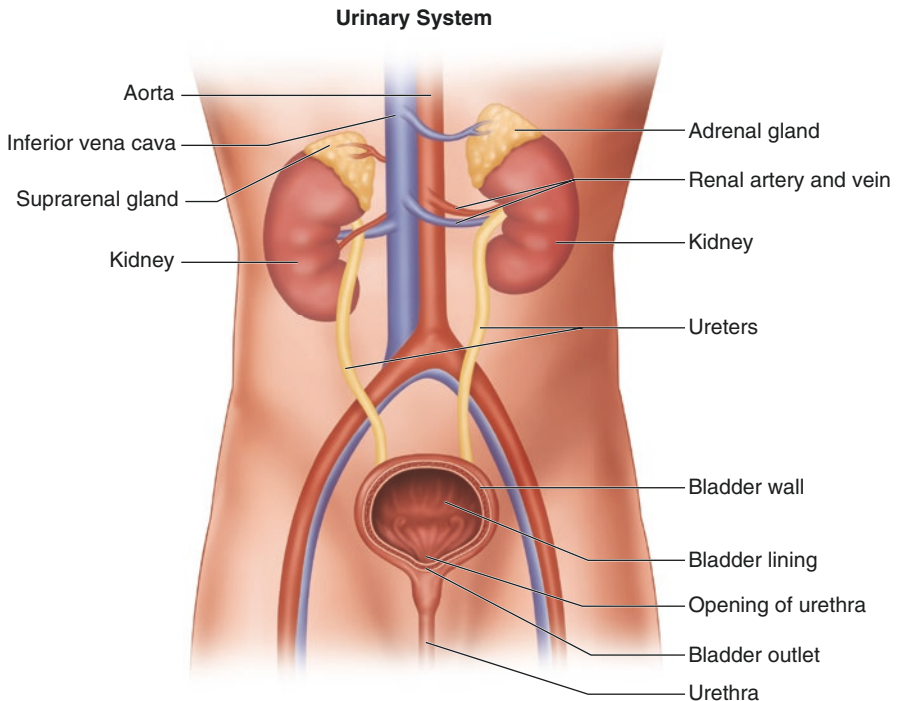


Fig. 12.1 The kidneys in the abdominal cavity. The renal vessels enter and exit the kidneys through the hilum

Fig. 12.2 Sagittal section through kidney showing the renal artery and ureter. The renal calyces converge toward the renal pelvis

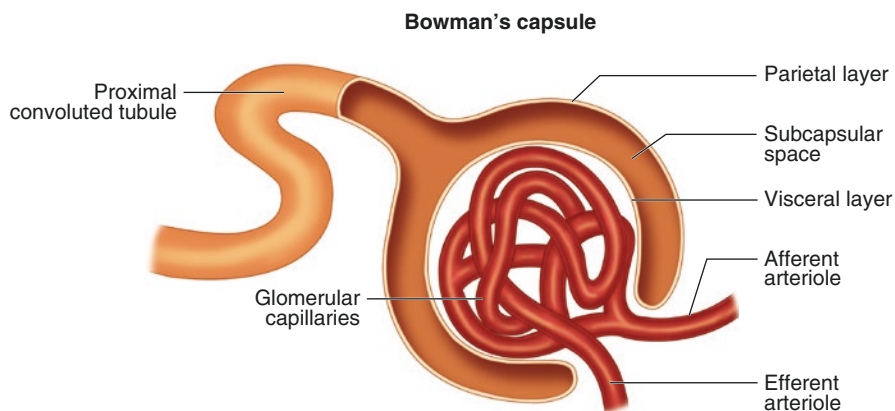
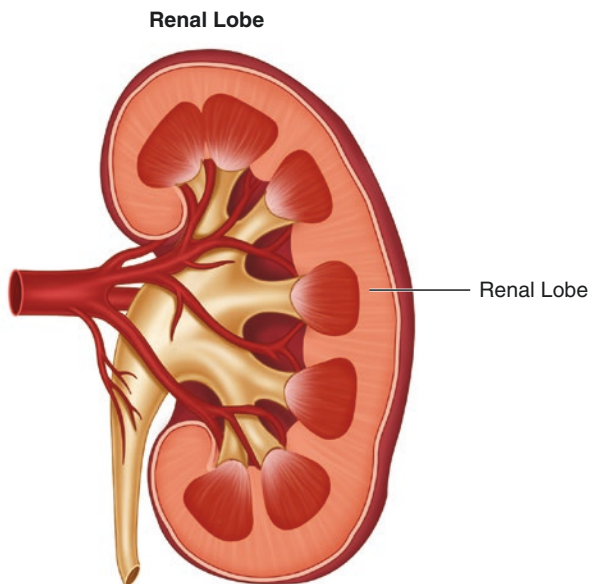


Fig. 12.3 Renal corpuscle with Bowman's capsule sectioned to reveal the subcapsular space. The glomerulus is surrounded by Bowman's capsule into which blood is filtered to form filtrate

glomeruli, called either medullary, cortical, or corticomedullary glomeruli depending on relative location.

Spanning both the cortex and medulla are nephrons, the basic functional unit of the kidney. *Each kidney houses between 1 and 2 million nephrons.* Anatomically, each nephron consists of a renal corpuscle, proximal convoluted tubule, Henle's loop, and distal convoluted tubule. The renal corpuscle contains the glomerulus and Bowman's Capsule (Fig. 12.3). The capsule surrounds the glomerulus and provides a space for filtrate following the filtration of blood through the glomerulus. The

filtrate contains fluid and waste from the blood that travels from the glomerulus, through the proximal convoluted tubule, down into the medulla through the descending limb of Henle's loop, and then travels back to the cortex through the ascending limb. From Henle's loop, remaining waste travels through the distal convoluted tubule and into a collecting duct. The collecting duct extends from just below the subcapsular zone of the cortex, down through the medullary pyramids, to converge with other collecting ducts to form papillary ducts that end at a renal papilla. Waste enters into minor calyces that in turn empty into major calyces, which converge to form the renal pelvis. As the renal pelvis exits the hilum of the kidney, it becomes the proximal ureter.

Embryology

The urinary system develops from the intermediate mesoderm through a three-stage process called nephrogenesis. During the first stage, the pronephros develops through differentiation of the mesoderm into pronephric tubules and the pronephric duct. This transition is temporary and is completed by week 5 of gestation. At the next stage, renewed differentiation of mesoderm results in the formation of the mesonephros which forms mesonephric tubules and the mesonephric duct (Wolffian duct). The third stage kidney is the metanephros and begins with the development of ureteric buds bilaterally from the caudal (pelvic) end of the mesonephric duct. Each ureteric bud and the adjacent mesodermal tissue grow into a definitive adult kidney. Relative to the spinal column, the fetal metanephros initially forms at vertebral levels S1–S2. As the fetal body lengthens, the kidneys seem to ascend to their final relative location of T12–L3. During the “ascent,” the kidneys rotate 90 degrees, causing the hilum to shift from ventral-facing to medial-facing. As the kidney matures, it develops from a lobulated state in the infant, to the more solid bean shape seen in the adult.

Innervation

The kidney is controlled by the autonomic nervous system; we do not think about making our bodies filter our blood (thankfully). The sympathetic component of the autonomic nervous system is mediated by nerve fibers that originate from the spinal cord between the levels of T1–L2. The kidneys are directly innervated by postganglionic nerves that project from the prevertebral renal ganglia that contain nerves from T12. The parasympathetic component is contributed by general visceral motor nerves that travel with the vagus nerve (CN X).

Blood Supply

From the abdominal aorta, near the beginning of the superior mesenteric artery, one renal artery branches off to supply a kidney. The renal arteries each give off the respective inferior suprarenal artery to supply the adjoining adrenal gland. Just prior

to the hilum, the renal arteries also each give off a ureteric branch, which supplies the superior segment of their respective ureter. After entering the hilum, the renal artery branches into a series of segmental arteries, each associated with separate medullary pyramids and renal columns (Fig. 12.4). Each segmental artery and the section of kidney it supplies forms a surgically independent unit known as a renal segment. The five primary segmental arteries are the superior, anterosuperior, anteroinferior, inferior, and posterior segmental arteries. Those segmental arteries then branch into interlobar arteries, which are renamed as arcuate arteries as they curve along the top of a renal pyramid. Small cortical radiate and perforating radiate arteries provide diffuse blood distribution to all aspects of the kidney (including passing through the renal capsule) in the form of the glomerulus. Blood enters the glomerulus through an afferent arteriole. However, unlike most other capillary beds where products are exchanged and filtered, filtered blood leaving the glomerulus exits through an efferent arteriole, rather than a venule (Fig. 12.5). Efferent arterioles descend into the medulla and form the vasa recta spuria. Vasa recta vera form from branches of the arcuate and cortical radiate arteries. All vasa recta eventually form the venulae rectae. Both vasa and venulae rectae form the medullary capillary plexus.

From the venulae rectae, blood flows into arcuate veins and back through interlobar and segmental veins until they all converge to form the renal vein. Due to the presence of abdominal viscera, the inferior vena cava and abdominal aorta sit adjacent to each other, rather than overlapping. Because of this, the inferior vena cava is further from the left kidney than the right, and the left renal vein must cross anterior to the abdominal aorta before joining with the inferior vena cava (Fig. 12.6). It passes posterior to the superior mesenteric artery, and as a result, the left renal vein is susceptible to compression by an aneurysm of either artery. Additionally, the left

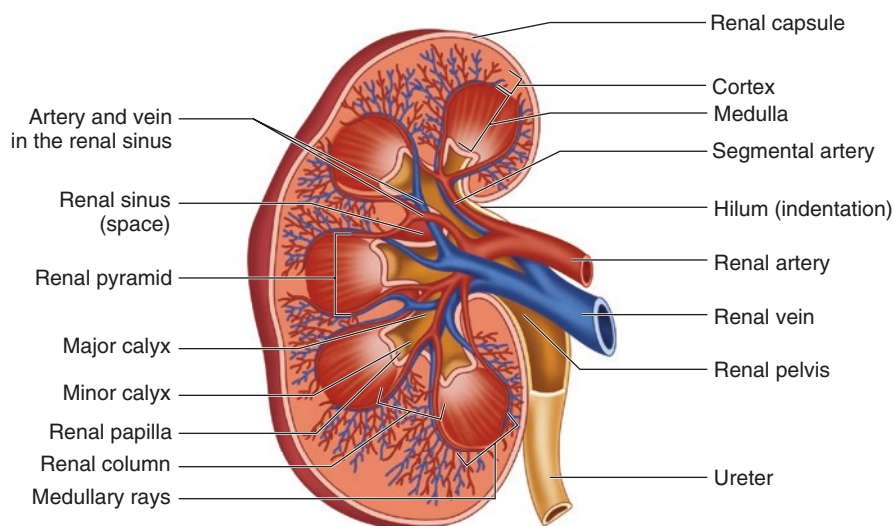


Fig. 12.4 Sagittal section through kidney. The renal artery and vein are connected to their segmental branches through the hilum

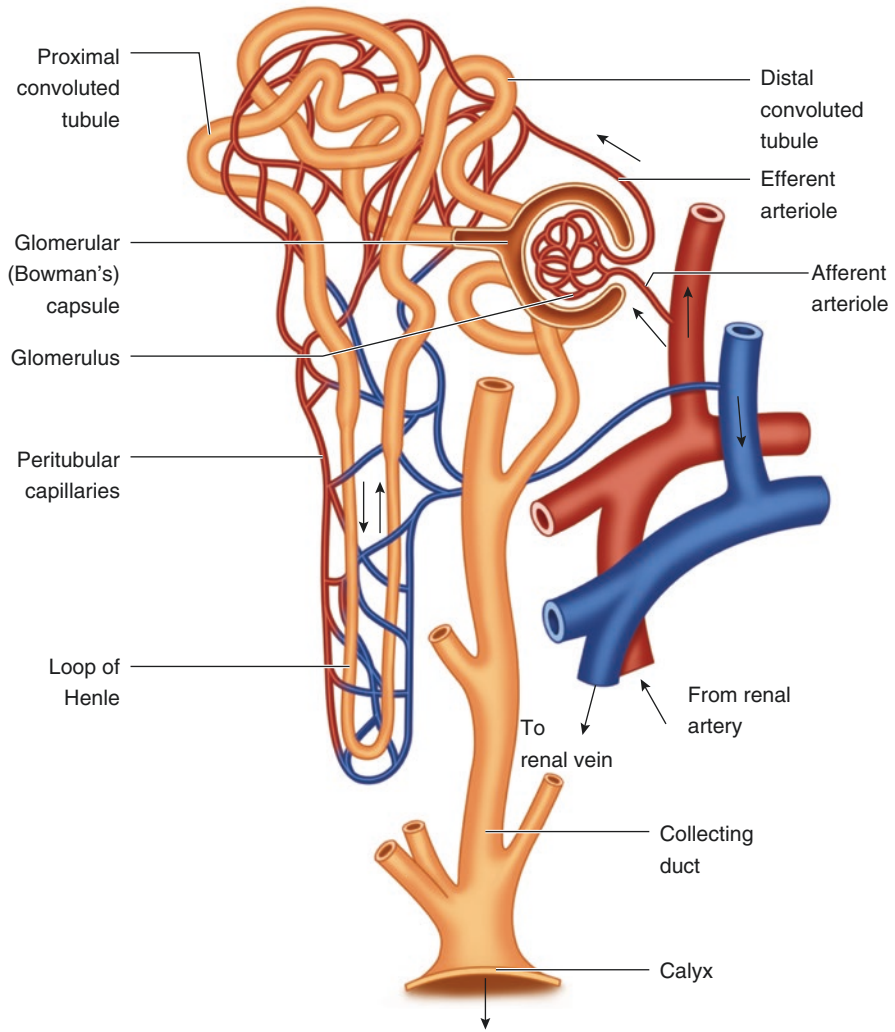


Fig. 12.5 A nephron, collecting duct, and capillary network. The efferent arteriole exits the glomerulus to form the capillary plexus around the nephron

renal vein serves as the common drainage point for other abdominal organs. Deoxygenated blood from the adrenal gland joins the renal vein via the inferior suprarenal vein, and the left gonads drain into the renal vein via the ovarian/testicular vein. Unlike its left counterpart, the right renal vein only drains blood from the kidney. The ovarian/testicular vein and suprarenal veins drain directly into the inferior vena cava.

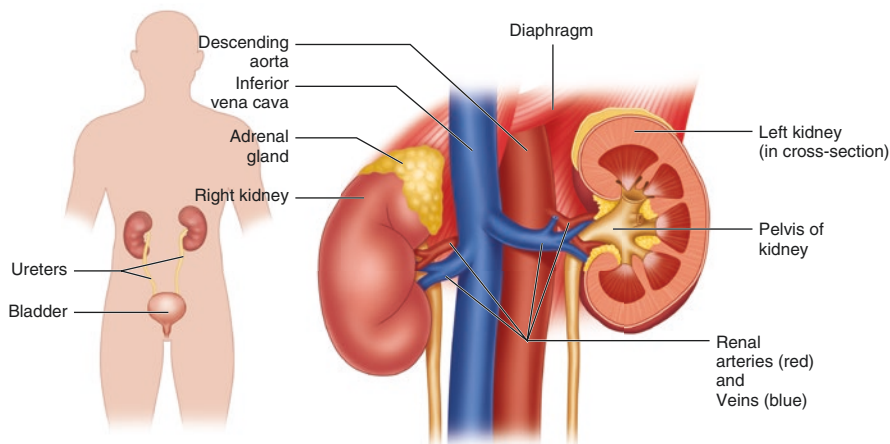


Fig. 12.6 The renal arteries and veins. The left renal vein runs across and anterior to the abdominal aorta to drain into the inferior vena cava

Lymphatics

Lymph vessels drain outward from the medullary pyramids into the cortex and along the path of the arcuate arteries. As the vessels exit the hilum, regional drainage proceeds to the cisterna chyli and thoracic duct via lumbar lymph trunks or to the lateral (lumbar) aortic nodes.

Histology and Physiology

Macroscopically, the inside of a kidney is easily distinguishable through the presence of medullary pyramids bordered with cortex that seem to radiate from the renal pelvis. Microscopically, each layer of the kidney also has easily distinguishable features.

Starting from the outside and moving inward, the renal capsule has two layers. The outermost layer is comprised of fibroblasts and collagen, while the inner layer is comprised of myofibroblasts. Deep to the inner layer lies the renal cortex that is distinguished by the presence of renal corpuscles and medullary rays. When looking at the cortex and medulla, two units need to be defined. A renal lobe is a medullary pyramid and associated cortex tissue. However, in the cortex alone, renal lobules are a medullary ray and the corpuscles associated on either side (*see* Fig. 12.4). Renal lobules are divided by the interlobar arteries running parallel to collecting tubules. All of the nephrons found in a renal lobule drain into the associated collecting ducts. The medullary rays appear as a series of directional tubes that radiate from the renal pelvis toward the cortex. These tubes are descending

and ascending thick limbs of Henle's loop as well as cortical collecting ducts for the associated nephrons. Proceeding inward, the outer medulla is composed of descending and ascending thick as well as thin limbs of Henle's loop and medullary collecting ducts. The inner medulla is composed of thin loops of Henle and papillary collecting ducts. The cell types found in the kidney's connective tissue include fibroblasts and mononuclear cells, as well as pericytes, found along the blood vessels that supply the loops of Henle, and interstitial cells that line medullary blood vessels.

In a microscopic cross section of Bowman's capsule, the capsular space is lined by a parietal layer of simple squamous cells. One afferent arteriole and one efferent arteriole enter and exit the capsule at the vascular pole of the renal corpuscle (*see* Fig. 12.3). Adjacent to the afferent arteriole, epithelial cells of the distal tubule of that nephron show a unique arrangement called the macula densa. The macula densa is made up of cuboidal cells that respond to changes in the sodium chloride levels. Together with juxtaglomerular cells found on the wall of the afferent arteriole, the macula densa forms a unit called the juxtaglomerular (JG) apparatus that is active in the renin–angiotensin–aldosterone system.

Within the glomerulus, the capillaries are fenestrated, similar to a mesh, and surrounded by cells called podocytes that are individually comprised of a cell body, primary processes, and secondary processes or pedicels. The podocytes interlace secondary pedicels like a zipper and are connected to one another through thin diaphragms. This diaphragm, in conjunction with the basal lamina of the fenestrated capillary, makes up the filtration barrier. There are mesangial cells among the capillaries that phagocytose debris, and they can affect surface area available for filtration through expansion and contraction. Surrounding the glomerular capillaries and podocytes is a visually empty space called the urinary or Bowman's space. Filtered waste passes through this space to the urinary pole and into the lumen of the proximal convoluted tubule which is connected to Bowman's space. The proximal convoluted tubule is lined by cuboidal (and sometimes columnar) epithelial cells with a microvillus brush border.

Renal blood flow (RBF) accounts for 25% of cardiac output, and flow rates are controlled by the renin–angiotensin–aldosterone system. Vasoconstriction of the renal arteries, induced by angiotensin II and the activation of the sympathetic nervous system, leads to a decrease in RBF while vasodilation leads to an increase. Angiotensin II primarily constricts efferent arterioles, therefore increasing RBF. In patients with diabetic neuropathy, Angiotensin-Converting Enzyme (ACE) inhibitors counteract the constriction of arterioles by angiotensin II, effectively decreasing RBF and excessive strain on the renal glomeruli. Vasodilation of renal arterioles is accomplished through the presence of prostaglandins E₂, I₂, and bradykinin, or the use of nitric oxide and dopamine.

The physiology of the kidney is defined by the function of the nephron. Beginning with the proximal convoluted tubule, the nephron participates in protein absorption and selective resorption of sodium, chloride, water, glucose, amino acids, ascorbic acid, and bicarbonate. Approximately 75% of water and sodium chloride at the proximal convoluted tubule is returned to the capillary system to continue

circulation. In the process of resorbing bicarbonate, H⁺ ions are exchanged with the interstitium. Creatinine and other organic substances are secreted into the filtrate.

Beyond the proximal convoluted tubule, fluid passes into the descending thick limb of the Loop of Henle, where additional resorption and secretion occur. As the thick limb, characterized by simple cuboidal epithelium with a brush border, extends toward the medulla, it transforms into the thin limb of the loop of Henle which is characterized by simple squamous epithelium. The descending thin limb is very permeable to water, and moderately permeable to sodium chloride. As the limb makes its loop, it becomes less permeable to water and, as it returns toward the cortex as the ascending thin limb, it becomes almost completely impermeable to water. The ascending limb, however, increases its permeability to sodium and chloride for additional resorption.

The ascending thin limb transforms into the ascending thick limb and is characterized by cuboidal epithelial cells with only some microvilli. Once the ascending thick limb reaches the level of the glomerulus, a segment of the epithelial lining becomes the macula densa and helps to monitor the osmolarity and volume of the fluid in the distal tubule. The macula densa in combination with the juxtaglomerular cells on the afferent arteriole make up the juxtaglomerular (JG) apparatus. Beyond the JG apparatus, the ascending thick loop becomes the distal convoluted tubule. This segment has a much wider lumen than its proximal convoluted tubule. The distal convoluted tubule can be distinguished by its lack of brush border. The primary function of the distal convoluted tubule is the resorption of sodium from the filtrate. Resorption is stimulated by aldosterone. Other transported ions include potassium, ammonium, and hydrogen.

At the end of the distal convoluted tubule, a short segment of connecting tubule drains to the collecting tubule (*see* Fig. 12.5). Histologically, the connecting tubule has two distinct types of epithelial cells: principal and intercalated cells. Principal cells remove sodium from the filtrate and replace it with potassium. Intercalated cells remove potassium from the filtrate and replace it with hydrogen ions.

Once the filtrate passes through the connecting tubule, it enters the collecting tubule. Similar to nephrons, collecting tubules can be divided into both cortical and medullary collecting tubules, as well as papillary tubules. Cortical collecting tubes are located within the medullary rays and are lined with two types of simple cuboidal cells: intercalated and principal cells. Medullary collecting tubules are structurally similar to cortical tubules in the outer medulla; however, inner medullary collecting tubules are only lined by principal cells, which can be identified by a round nucleus and single primary cilium. Papillary collecting tubules are large tubules that are formed from the converging of cortical and medullary tubules. They are identifiable by their simple columnar cells with a primary cilium.

Ureters

The ureters are muscular tubes along which urine waste filtered in the kidney passes to the urinary bladder for storage before excretion.

Structure

The ureters join the kidneys to the urinary bladder (Fig. 12.7). Superiorly, they are connected to the kidney at the renal pelvis, part of the renal sinus. As they descend retroperitoneally, the ureters run along the medial aspect of the psoas major muscle. At the brim of the pelvis, the ureters enter the pelvic cavity by crossing anterior to either the common iliac artery or the external iliac artery. In the female, the ureter passes from retroperitoneal space into the pelvis, posterior to the uterine artery. As a result of this placement, a common complication following a hysterectomy is the severing of the ureter leading to an accumulation of urine in the abdomen. En route to the bladder, the ureters are constricted at three locations: the ureteropelvic junction, the crossing of the iliac artery, and the entrance into the urinary bladder. Kidney stones can easily become lodged at these locations.

Innervation

The lumbar splanchnic nerves provide sympathetic innervation, while the parasympathetic innervation is provided by the pelvic splanchnic nerves.

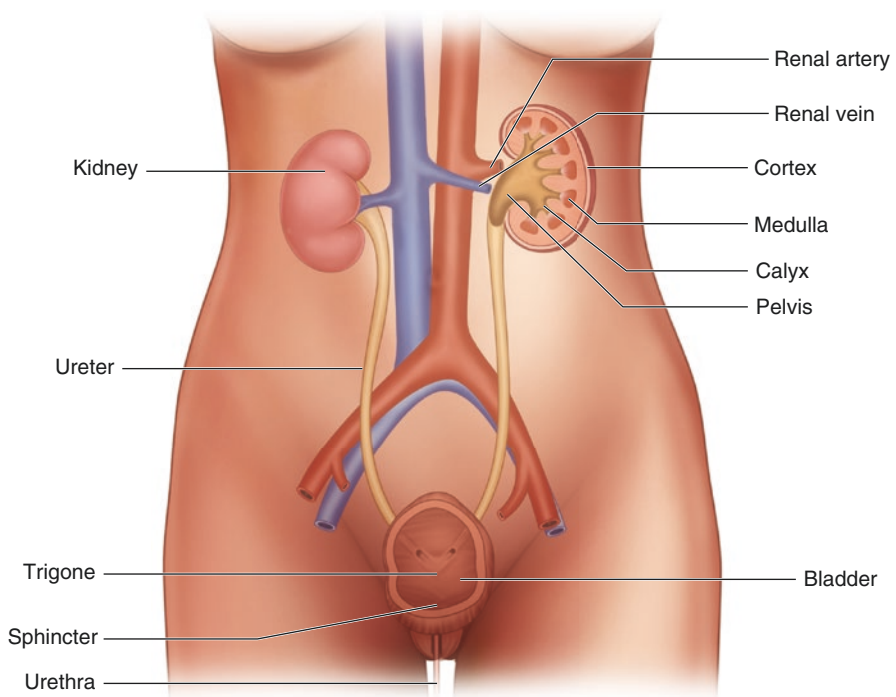


Fig. 12.7 Ureters connecting the kidneys to the urinary bladder

Blood Supply

The ureters receive blood supply through minor branches of major vessels that run adjacent to their course. The superior portion is supplied by the ureteric branches from the renal artery. The middle portion has a varying arterial supply from either the aorta, testicular/ovarian arteries, or the common iliac artery. The inferior third is typically supplied by branches from the internal iliac artery, including ureteric branches of the inferior and superior vesical arteries.

Lymphatics

Lymph from the ureters drains to nodes located along the aorta and common iliac arteries. These include precaval and postcaval nodes along the aorta, common iliac nodes, internal iliac nodes, and external iliac nodes. External iliac nodes also receive lymph drainage from the trigone and dorsal aspect of the urinary bladder.

Urinary Bladder

The urinary bladder is a hollow organ with muscular walls, known for its great elasticity. The position of the bladder can vary depending on the amount of urine it is holding. An empty bladder sits in the lesser pelvis, lying partially superior to and partially posterior to the pubic bones (Fig. 12.8). The space anterior to the bladder

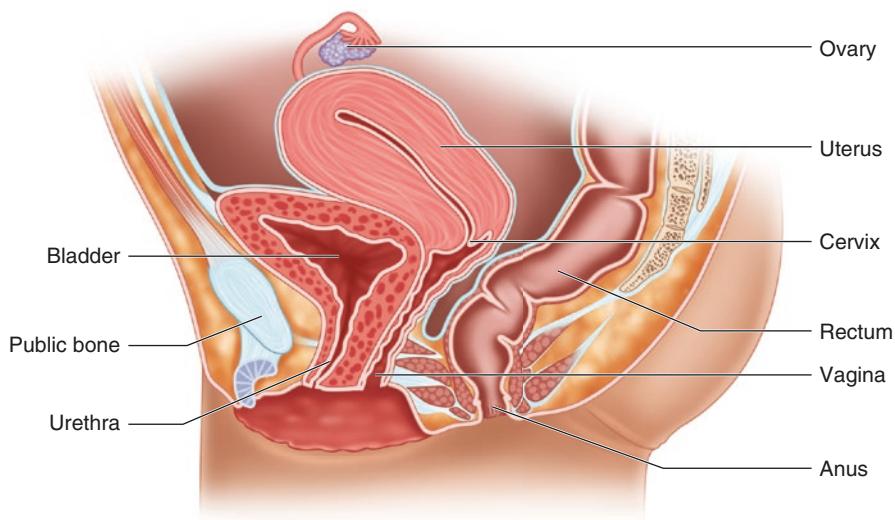


Fig. 12.8 Sagittal section through the female pelvis showing the relationship of the urinary bladder to the pubic symphysis, uterus, and vagina

and posterior to the pubic symphysis is known as the retropubic space, or “Cave of Retzius.” The bladder lies anterior to the prostate in males and anterior to the vagina in females. In children, the bladder actually sits in the abdomen, and does not sit in the lesser pelvis until after puberty. When the bladder fills, it ascends to the greater pelvis.

The bladder can be divided into four sections: the apex, body, fundus, and neck. The apex is the most anterior portion of the bladder, and it is closest to the pubic symphysis. The body lies between the apex and the fundus. The fundus is the most posterior portion of the bladder. The neck sits inferior and connects to the urethra; it is not as distensible as the body of the bladder. The neck of the bladder is instead secured in place by various ligaments. The bladder wall is made up of the detrusor muscle, which is lined by up to six layers of epithelial cells that make up the urothelium (Fig. 12.9). Near the neck of the bladder, there is an internal urethral sphincter in males that is responsible for closing off the bladder to prevent retrograde ejaculation of semen into the urinary bladder. The bladder has three orifices; the ureters deliver urine into the bladder through two ureteric orifices, and the internal urethral orifice allows urine to exit through the urethra. In males, the uvula of the bladder is a small protrusion behind the internal urethral orifice.

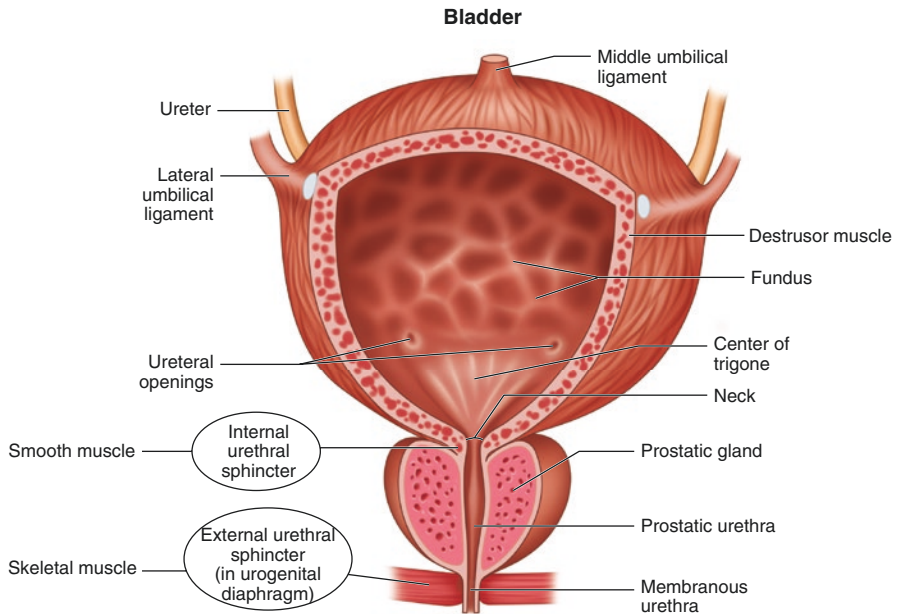


Fig. 12.9 Urinary bladder in the male. The anterior wall of the urinary bladder and the anterior portion of the prostate gland have been cut to show the trigone of the urinary bladder and the prostatic part of the urethra

Blood Supply/Innervation

The branches of the internal iliac arteries supply the bladder. Their exact positions vary from person to person, but they do follow a predictable pattern. The anterosuperior bladder (mainly the body) is supplied by the superior vesical arteries and veins. In males, the fundus and neck of the bladder are supplied by the inferior vesical arteries and drained by the vesical venous plexus; females do not have inferior vesical arteries and instead have vaginal arteries that branch to supply the postero-inferior bladder. (Note: Textbooks differ on this detail.) The bladder is innervated by the hypogastric plexus (sympathetic fibers) and the pelvic splanchnic nerves and the inferior hypogastric plexus (parasympathetic fibers).

Urethra

Male Urethra

The male urethra allows urine to flow from the internal urethral orifice of the bladder to the external urethral orifice at the tip of the glans penis through a tube that varies in length between 18 and 22 cm. This muscular tube has the dual purpose of also allowing semen to flow out of the penis. The urethra can be divided into three parts: prostatic, membranous, and spongy. The prostatic urethra is the widest part of the urethra, and it is where urinary and reproductive tracts meet by way of the ejaculatory ducts. This part of the urethra is surrounded by the prostate gland and the prostatic sinuses (*see* Fig. 12.9). Another important feature of the prostatic urethra is the urethral crest, which is a fold in the posterior wall of the urethra, located near the internal urethral orifice; it is present in both males and females. The narrowest part of the urethra is the membranous urethra, and it passes through the deep perineal pouch, ending at the bulb of the penis. Surrounding this part of the urethra is the external urethral sphincter. On either side of the membranous urethra are bulbourethral glands. The longest part of the urethra is the spongy urethra, and this is where secretions of the bulbourethral glands and urethral glands are deposited. In relation to the penis, the spongy urethra travels through the corpus spongiosum and ends at the external urethral orifice, the narrowest part of the urethra. In the glans of the penis, before the external urethral orifice, the urethra widens into what is called the navicular fossa.

Blood Supply/Innervation

Arterial blood to the prostatic urethra is supplied by the prostatic branches of the middle rectal arteries and the inferior vesical arteries. Branches of the dorsal artery of the penis supply the membranous and spongy parts of the urethra. Autonomic innervation of the prostatic, membranous, and spongy urethra is by way of the prostatic plexus that branches from the inferior hypogastric plexus. Sympathetic fibers

travel from the lumbar splanchnic nerves. Parasympathetic fibers travel from the pelvic splanchnic nerves. Somatic innervation of the spongy urethra travels from a branch of the pudendal nerve called the dorsal nerve of the penis.

Female Urethra

The female urethra is shorter than the male urethra at approximately 4 cm long, traveling from the internal urethral orifice, behind the pubic symphysis, and ending at the external urethral orifice (*see* Fig. 12.8). The external urethral orifice ends between the labia minora, in the vestibule. The urethra is parallel to the vagina, and it passes through the pelvic diaphragm, external urethral sphincter, and perineal membrane. There are paraurethral glands around the urethra that empty near the external urethral orifice.

Blood Supply/Innervation

Arterial blood to the female urethra is supplied by the vaginal arteries and internal pudendal arteries. Innervation is from the vesical plexus and pudendal nerve.

Clinical

Unlike the male urethra, the female urethra is distensible; this is why it is easier to pass instruments like catheters through the female urethra.

Urination

Urination, or micturition, begins when stretch receptors in the detrusor muscle of the bladder are stimulated. Sympathetic fibers cause the bladder wall to relax and the internal sphincter to constrict. General visceral afferent fibers send information from the stretch receptors to the spinal cord. Parasympathetic fibers cause the bladder wall to relax even more and also cause the internal sphincter to relax. General somatic efferent fibers in the pudendal nerve cause the external urethral sphincter to relax, allowing urine to flow out of the urethra.

Suggested Reading

1. Cheuck L. Kidney Anatomy. Medscape. 2013. <http://emedicine.medscape.com/article/1948775-overview>. Accessed 20 Feb 2017.
2. Chung KW, Chung HM. BRS gross anatomy. 7th ed. Baltimore: Lippincott Williams & Wilkins; 2012, 213–7, 228, 258–82, 263.
3. Department of Urology, University of California, San Francisco. Urachal Abnormalities. Undated. <https://urology.ucsf.edu/patient-care/children/urachal-abnormalities>. Accessed 20 Feb 2017.

4. Free Dictionary by Farlex. Congenital Bladder Anomalies. Undated. <http://medical-dictionary.thefreedictionary.com/Congenital+Bladder+Anomalies>. Accessed 20 Feb 2017.
5. Gartner LP, Hiatt JL. BRS Cell Biology and Histology. 7th ed. Philadelphia: Wolters Kluwer Health; 2015. p. 309–26.
6. Mayo Clinic. Addison's Disease. Undated. <http://www.mayoclinic.org/diseases-conditions/addisons-disease/home/ovc-20155636>. Accessed 20 Feb 2017.
7. Mayo Clinic. Hypospadias. Undated. <http://www.mayoclinic.org/diseases-conditions/hypospadias/basics/definition/con-20031354>. Accessed 20 Feb 2017.
8. Moore KL, Dalley AF, Agur AMR. Clinically oriented anatomy. 6th ed. Baltimore: Wolters Kluwer/Lippincott Williams & Wilkins; 2010. p. 368–418.
9. National Institutes of Health, National Institute of Diabetes and Digestive and Kidney Diseases. Cushing's Syndrome. 2012. <http://www.niddk.nih.gov/health-information/health-topics/endocrine/cushings-syndrome/Pages/fact-sheet.aspx>. Accessed 20 Feb 2017.
10. NetDoctor. Conn's Syndrome. 2011. <http://www.netdoctor.co.uk/conditions/heart-and-blood/al1162/conns-syndrome/>. Accessed 20 Feb 2017.
11. Schenkman NS. Male Urethra Anatomy. Medscape, 2016. <http://emedicine.medscape.com/article/1972482-overview>. Accessed 20 Feb 2017.
12. WebMD. Hirsutism. Undated. <http://www.webmd.com/women/guide/hirsutism-hair-women>. Accessed 20 Feb 2017.



Urologic Anomalies and Surgical Implications

13

Jeannie Jiwon Su, José Murillo B. Netto,
and Adam B. Hittelman

Kidney

Anatomy

The kidneys are located in the retroperitoneum. They measure approximately 10–12 cm (longitudinal) and weigh approximately 125–170 g. The kidneys are relatively larger in infants and children, and temporary prominent lobations can be present. The lateral border can have a focal parenchymal bulge, a dromedary hump, which can be a normal variant. Because of displacement by the liver, the right kidney lies 1–2 cm lower than the left kidney. The upper limit of the right kidney reaches the upper border of the 12th rib and lies between the first to third lumbar vertebrae. The left kidney reaches the lower border of the 11th rib and lies between the 12th thoracic to 3rd lumbar vertebrae. Inspiration can cause the kidney to descend about 3–5 cm.

The renal parenchyma is encased a fibrous membrane known as the renal capsule. Perinephric fat and the renal fascia, Gerota's fascia, surround it. Gerota's fascia encompasses the kidney, the adrenal gland, and the perinephric fat, separating it from the outer pararenal fat.

The anatomic relations of the kidney to its adjacent organs are described in Table 13.1.

J. J. Su

Department of Urology, Yale School of Medicine, New Haven, CT, USA

J. M. B. Netto

Department of Urology, Universidade Federal de Juiz de Fora, Juiz de Fora, MG, Brazil

A. B. Hittelman (✉)

Department of Urology and Pediatrics, Yale School of Medicine, New Haven, CT, USA

e-mail: adam.hittelman@yale.edu

Table 13.1 Anatomic relations of the kidney to adjacent organs

	Right	Left
<i>Anterior</i>		
Cranial	Liver (attached by hepatorenal ligament) Right adrenal gland	Spleen (attached by splenorenal ligament) Left adrenal gland
Medial	Descending duodenum	Stomach Tail of pancreas Splenic vessels Jejunum
Caudal	Hepatic flexure	Splenic flexure
<i>Posterior</i>	<i>Superior:</i> Diaphragm, pleura <i>Inferior:</i> Psoas (medial), quadratus lumborum (middle), transversus abdominus (lateral)	
<i>Medial</i>	Inferior vena cava Right ureter	Duodenojejunal flexure Inferior mesenteric vein Left adrenal Left ureter
<i>Lateral</i>	Liver (cranial) Ascending colon (caudal)	Spleen (cranial) Descending colon (caudal)

Renal blood supply and drainage typically consists of one renal artery and one renal vein, which enter and exit medially at the renal hilum. The renal artery branches from the aorta and the renal vein drains to the inferior vena cava (IVC) just below the superior mesenteric artery, at the level of the second lumbar vertebra. The renal vein is anterior to the renal artery. The renal artery splits into the posterior and anterior segmental branches. The four anterior segmental branches—apical, upper, middle, and lower—supply the anterior kidney, whereas the posterior segmental artery supplies the posterior kidney. The renal arteries are end arteries, and thus injury or ligation to a specific segment will cause ischemia in the distribution of its perfusion. Veins drain the entire kidney and thus can be individually ligated without impacting vascular drainage of the kidney. There is an avascular plane, “Brodel’s white line,” which is in the watershed area between the anterior and posterior segmental branches, located approximately one-third of the way posterior from the lateral margin of the kidney. This avascular plane has been utilized historically in open kidney stone surgery to incise the parenchyma and extract the stone. The renal pelvis and ureter are posterior to the vasculature.

Anatomical variations are not uncommon (25–40%), and two or more arteries and/or veins are frequently seen. Multiple renal arteries are more common than multiple veins and disproportionately will occur in the left kidney, but multiple renal veins can also occur. The left renal vein can also course behind the aorta or divide, sending one limb anterior and one limb posterior to the aorta. Lower pole arteries on the right generally cross anterior to the IVC. These lower pole vessels can cross anterior to the collecting system, kinking the ureter, and obstructing drainage, causing an obstruction at the level of the ureteropelvic junction.

Embryology

Embryologically, the development of the kidney has been described in three phases, all of which arise from the mesoderm. The first two phases, the pronephros and mesonephros, regress in utero. It is the third phase, the metanephros, that ultimately becomes the mature kidney.

The kidneys ascend from the pelvis to the lumbar region just caudal to the adrenal glands around the 6th to 9th week of gestation. During ascent, the kidney rotates internally 90°. The kidney is supplied by a series of arteries from the aorta, which form and degenerate until the final pair of arteries in the lumbar region forms to become the definite renal arteries. A more inferior artery sometimes can persist as an accessory lower pole renal artery.

Congenital Anomalies of the Kidney

Multicystic Dysplastic Kidney

Multicystic dysplastic kidney (MCDK) is a congenital condition that is benign in most affected patients. It is usually discovered on prenatal ultrasound, which finds the presence of multiple noncommunicating cysts with minimal or no renal parenchyma (Fig. 13.1). It is usually unilateral as bilateral MCDK is incompatible with life. It can be caused by early ureteric atresia after ureteric ingrowth into the metanephros. Renal nuclear scan, MRI, or other functional imaging confirms a lack of renal function in the dysplastic kidney. Overall kidney function remains normal, as compensatory growth typically occurs in the contralateral, normal kidney [1]. MCDK is associated with contralateral vesicoureteral reflux in approximately 10–20% of patients [2]. Historically, there was concern that MCKD was associated with urinary tract infection (UTI), hypertension, and progression to kidney tumor, though more recent data have shown that this progression rarely occurs [3].

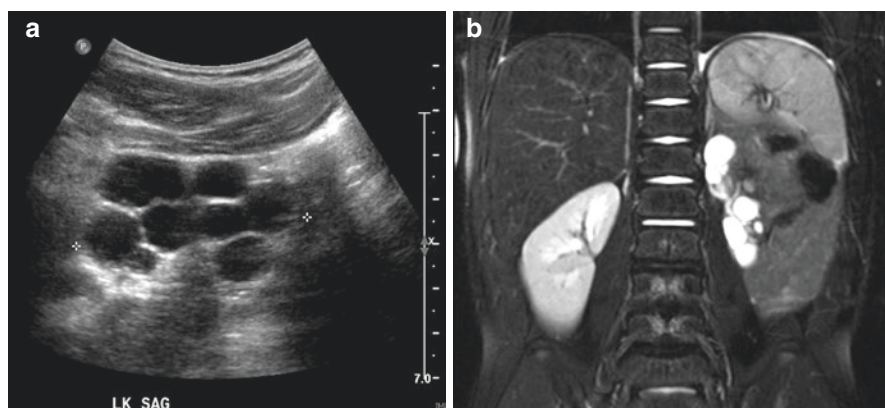


Fig. 13.1 Left multicystic dysplastic kidney (MCDK). (a) Ultrasound and (b) MRI

Observation is the mainstay of care for MCDK, as it remains a benign process in most cases and often will completely involute over time. In cases when hypertension or growth occurs, nephrectomy can be indicated [3]. Segmental dysplasia can occur in a duplicated collecting system (see duplication anomalies below), in which one moiety, often the upper pole, of a duplicated collecting system is impacted.

Polycystic Kidney Disease

Polycystic kidney disease (PKD) can be of the infantile (recessive) or adult (dominant) variant. The kidneys are usually enlarged, with multiple small cysts (Fig. 13.2). Unlike MCDK, PKD affects both kidneys and commonly progresses to renal failure.

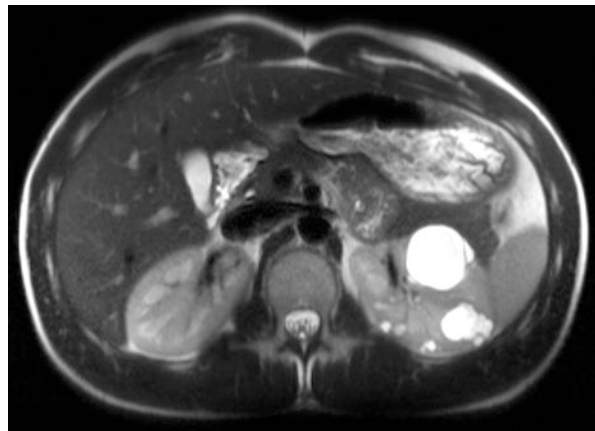
Autosomal recessive PKD (ARPKD) occurs in about 1 in 10,000–20,000 births. It often presents in utero with enlarged, echogenic kidneys, though less severe variants can present postnatally. If present in utero, it is often fatal postnatal, though surviving individuals will often require renal replacement therapy by 3–4 years of age. The earlier the diagnosis, the more severe the disease. There is associated hepatic fibrosis, progressing to portal hypertension in surviving affected individuals [4].

Autosomal dominant PKD (ADPKD) is the most common inherited cystic kidney disease, affecting about 1 in 1000 people. It is a progressive disorder in which kidney dysfunction commonly presents in the fourth to fifth decade of life. It can also affect the liver, pancreas, seminal vesicles, and arachnoid membrane. The majority of patients will progress to renal failure and will need dialysis or kidney transplantation.

Renal Duplication

The term *renal duplication* refers to a kidney with more than one collecting system. This occurs when the ureteric bud divides prematurely, before reaching the metanephric mesenchyme. It can present in varying degrees: The incomplete form affects only the renal pelvis and proximal ureter (having a bifid appearance), whereas in the complete type, two independent ureters insert into the bladder.

Fig. 13.2 Polycystic kidney disease: MRI demonstrating multiple noncommunicating cysts in left kidney



This can be a variant of normal and is usually asymptomatic and carries no clinical impact [5, 6], though it can also lead to vesicoureteral reflux (VUR) or ureteral obstruction [7].

When complete renal duplication occurs, the ureter of the lower pole inserts cranially and laterally in the bladder and, because there is a small submucosal tunnel, it is more susceptible to present with VUR. The upper pole ureter inserts more medially and distally into the bladder and can also insert ectopically, outside of the bladder, making it more susceptible to obstruction and poor drainage. Obstructed, ectopic ureters can lead to hydroureteronephrosis and decreased function of the upper pole moiety [7] (see Section “[Congenital Anomalies of the Ureter](#)” below).

Fusion Anomalies

In these anomalies, the kidneys are fused to each other by their parenchyma and assume an ectopic position.

Horseshoe kidneys, the most common fusion anomaly, affect 1 in 400–800 people (more often in men). A band of tissue, the isthmus, connects the lower poles of the two kidneys, forming a “U” shape positioned in the lower abdomen (L3–L4) (Fig. 13.3). As the kidney ascends during development, the isthmus becomes trapped under the inferior mesenteric artery, preventing further ascension. The renal pelvis is rotated anteriorly, and the lower poles are deviated medially [8]. The ureters usually have a higher insertion, which impacts drainage, often leading to hydronephrosis. This increases risk for kidney stone formation [9] and thus should be followed conservatively with serial ultrasound if hydronephrosis is observed. Horseshoe kidneys can also be associated with other urologic anomalies, such as ureteropelvic junction obstruction or VUR in over 50% of cases [10, 11]. One-third of patients with horseshoe kidneys remain asymptomatic and are only identified incidentally on imaging.

Treatment is indicated only when patients are symptomatic, develop kidney stones, or if progressive loss of function is observed. There is no reason to divide the isthmus to separate the kidneys from each other, unless there is an indication to remove one of the moieties (such as in the setting of renal malignancy).

Crossed fused renal ectopia is a fusion anomaly affecting 1 in 2000 people [12]. It is characterized by two kidneys that are fused and located on the ipsilateral side of midline, while maintaining their own ureters and vessels (Fig. 13.4). The ectopic kidney ureter crosses the midline and implants into the bladder on the contralateral side. Malrotation of bowel into the empty space on the contralateral side can be observed.

Types of crossed fused renal ectopia (Fig. 13.5):

- *Inferior ectopia* is the most common type of crossed fused ectopia. The upper pole of the crossed kidney is inferior and attached to the lower pole of the normally positioned kidney. Both renal pelvises are anterior.
- *Sigmoid or S-shaped kidney* is the second most common type of crossed fused renal ectopia. The crossed kidney is inferior and attached to the other kidney by the adjacent pole (inferior to inferior pole or superior to superior pole).

Fig. 13.3 Horseshoe kidney. **(a)** Intravenous pyelogram. **(b)** CT scan demonstrating a horseshoe kidney with midline fusion, the isthmus

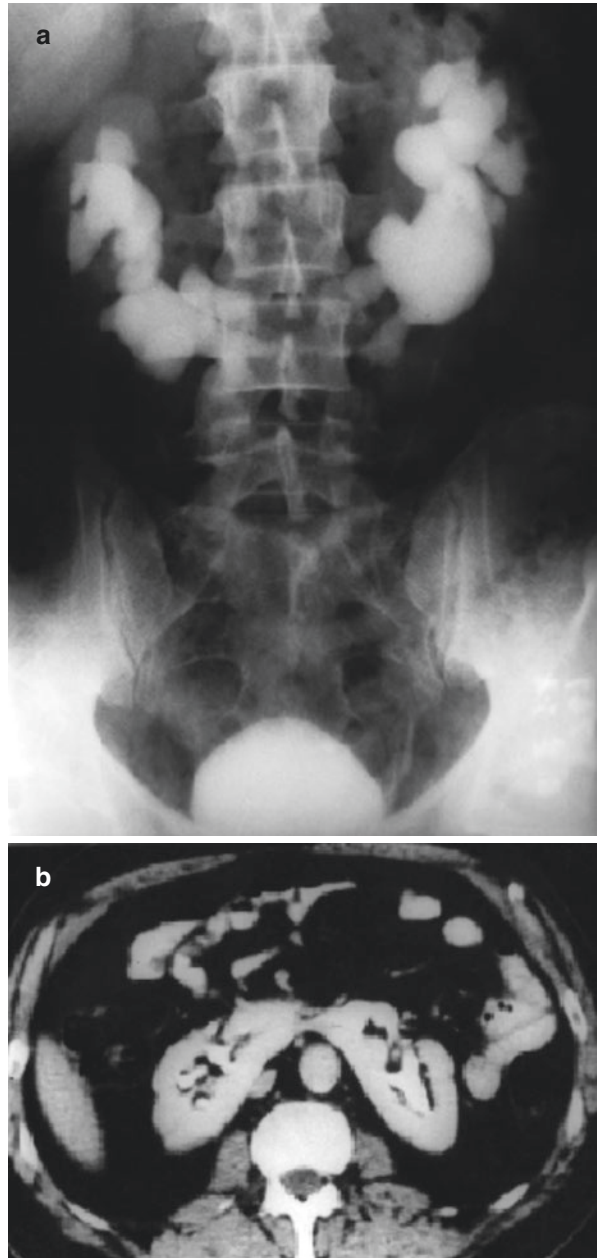


Fig. 13.4 Renal ultrasound demonstrating left-to-right crossed fused renal ectopia

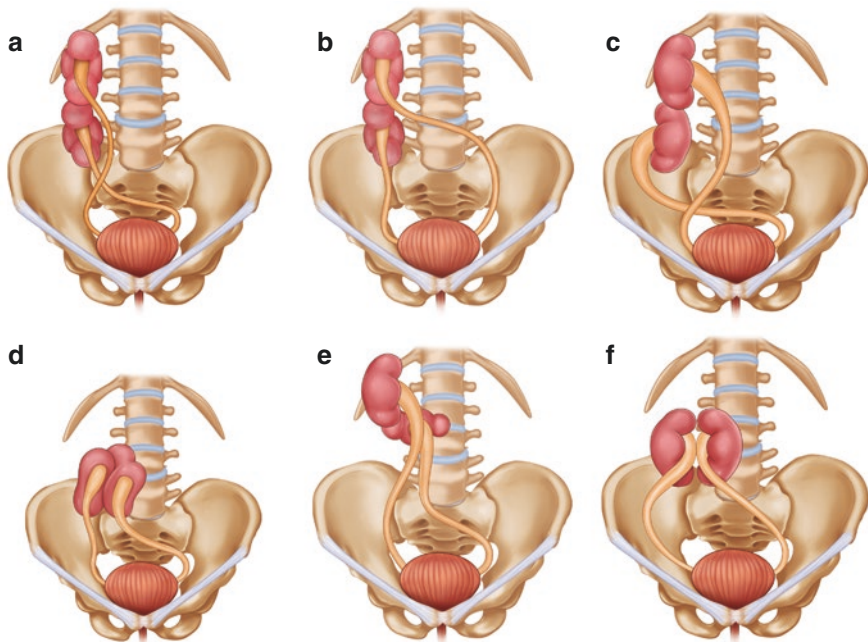


Fig. 13.5 Types of renal crossed fused anomalies. (a) Inferior ectopia. (b) Sigmoid kidney. (c) Cake kidney. (d) L-shaped kidney. (e) Disc kidney. (f) Superior ectopic kidney

- *Lump kidney (cake kidney)* is a relatively rare form of fusion in which extensive joining of both kidneys generates an irregular and lobulated mass. Both pelvises are anterior and drain different areas of the parenchyma. The ureters do not cross.
- *L-shaped kidney (tandem kidney)* is a form of fusion in which the crossed kidney assumes a transverse position at the time of attachment to the inferior pole of the normal kidney. The ureters of each kidney enter the bladder on their respective side.
- *Disc kidney (doughnut, shield, pancake kidney)* fuses at both poles, producing a ring-shaped mass. The reniform shape is better preserved than in the lump kidney, and the lateral aspect of each kidney retains its normal contour. The pelvises are anteriorly placed and the ureters do not cross.
- *Superior ectopic kidney* is the least common variety of renal fusion. In this kind of fusion, the lower pole of the crossed kidney is fused to the upper pole of the uncrossed kidney. Each unit remains with its fetal orientation, with both pelvises lying anterior.

The majority of patients with crossed renal ectopia anomalies, with or without fusion, remain asymptomatic, and the diagnosis is often made incidentally during fetal ultrasound or routine examination for other diseases. In some cases, an abdominal mass can be detected. The presence of hydronephrosis, calculi, and pain are usually secondary to the abnormal position of the kidney and its anomalous blood supply, which can impact urinary drainage. Treatment is required only if symptoms are present; it should be focused on preventing renal damage [13].

Rotation Anomalies

Renal malrotation occurs in approximately 1 in 2000 people and is almost always an incidental finding. Patients can have incomplete rotation, hyper-rotation, or reversed rotation. The result can be partial ureteropelvic junction obstruction and hydronephrosis, leading to urinary stasis and increasing the risk of urolithiasis and infections. In these cases, treatment of the underlying conditions is indicated [13].

Anomalies of Number

Renal agenesis is a condition in which one (unilateral) or both (bilateral) kidneys fail to develop. Bilateral renal agenesis is associated with Potter's syndrome, which is characterized by oligohydramnios, pulmonary hypoplasia, and various physical anomalies, and is fatal [14]. Unilateral renal agenesis occurs in 1 to 1100 to 1500 people and can be associated with agenesis of the ipsilateral vas deferens or uterine anomalies [15]. Diagnosis is usually made during prenatal ultrasound or routine abdominal evaluation later in life. Unilateral agenesis can represent involution of a MCDK, which may not have been identified in utero. Most patients are asymptomatic, but some reports have shown an associated increased risk of hypertension, compromised renal function, and glomerulosclerosis, potentially due to hyperfiltration in the contralateral kidney [15–17]. Routine follow-up of renal function is advised.

Supernumerary kidneys, more than two kidneys, is exceedingly rare, and few cases have been documented in the literature.

Renal Ectopia

Renal ectopia, an abnormal renal location, usually occurs when the kidney fails to ascend to its normal position at the lumbar region. The most common site of renal ectopia is the pelvic region, where a palpable mass may be identified. A pelvic kidney will often be smaller than the orthotopically placed contralateral kidney, though it will typically function normally relative to its size. In the setting of obstruction, hydronephrosis and kidney stones can develop. Treatment is necessary only in the setting of abdominal pain or renal colic, hematuria, or kidney stone formation [18]. Rarely, a kidney can be ectopically located in the thorax. A thoracic kidney is caused by incomplete closure of the posterior diaphragm and ascension of the kidney into the chest through Bochdalek's foramen.

Ureter

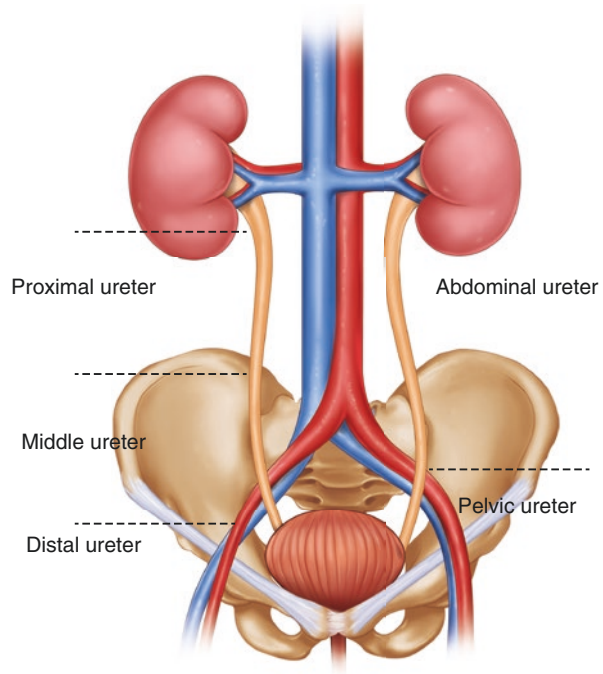
Anatomy

The ureters are tubular structures that transport urine from the renal pelvis to the bladder via peristalsis. They range from 22 to 30 cm in length, depending on the height of the person. The layers of the ureter include the inner mucosal lining, muscle, and outer adventitia. The adventitia encompasses the vasculature and lymphatics that supply and travel along the ureter.

The ureter can be subdivided by its anatomic location (Fig. 13.6). In one classification, the abdominal ureter extends from the renal pelvis to the iliac vessels and the pelvic ureter extends from the iliac vessels to the bladder. In another classification, the ureter is divided into proximal, middle, and distal segments. The proximal ureter extends from the renal pelvis to the upper border of the sacrum. The middle ureter extends from the upper to the lower border of the sacrum. The distal ureter extends from the lower border of the sacrum to the bladder.

The ureter arises from the ureteropelvic junction, which sits posterior to the vasculature at the renal hilum. It travels caudally along the anterior edge of the psoas muscle. Approximately two thirds of the course down to the bladder, the gonadal vessels cross anterior to the ureter and become more lateral. The ureter crosses anterior to the iliac vessels, commonly at the bifurcation of the common iliac artery into the external and internal iliac arteries. In women, the uterine arteries cross anterior to the ureter approximately 2 cm lateral to the cervix. The ureter is closely related to the cervix and anterior vagina prior to entering the bladder. This puts the ureters at risk for injury or involvement during gynecologic surgery or with a gynecologic inflammatory or mass-producing process. In men, the vas deferens crosses anterior to the ureter after leaving the internal inguinal ring laterally and before joining with the seminal vesicles medially to form the ejaculatory ducts.

Fig. 13.6 Ureteric anatomy



Branches from various arteries—renal, gonadal, common and internal iliac arteries, and the aorta—supply blood to the ureter as they run along its course. It is important to note that the arterial branches approach the proximal ureter medially and the distal ureter laterally. The middle ureter is at greatest risk for injury, as it is thought to be the most poorly vascularized. The ureteral venous and lymphatic drainage follow that of the arteries.

Ureteral peristalsis is independent from autonomic input and it is thought to be controlled by intrinsic smooth muscle pacemaker sites located in the minor calyces of the collecting system. The ureter receives preganglionic sympathetic input from the 10th thoracic through 2nd lumbar spinal segments, with postganglionic fibers arising the aortic, superior, and inferior hypogastric autonomic plexuses. Parasympathetic input is received from the second through fourth sacral spinal segments.

Embryology

Embryologically, the ureter arises from the ureteric bud, which originates from the distal posterior medial mesonephric duct as it joins the cloaca. The ureteric bud grows into the mesonephros and bifurcates repeatedly to form the collecting system. The mesonephros, in turn, differentiates into nephrons.

Congenital Anomalies of the Ureter

Ureteropelvic Junction Obstruction

Unilateral ureteropelvic junction obstruction (UPJO) is the most common cause of prenatal and postnatal obstructive uropathy [19]. It is characterized by an obstruction at the level where the ureter meets the renal pelvis, typically resulting in hydronephrosis without hydroureter (Fig. 13.7). Fetal hydronephrosis is the most common anomaly identified on antenatal ultrasound. UPJO most often is initially detected with fetal ultrasound, but it can present later with abdominal pain or can be incidentally identified during imaging for other reasons. The most common cause is an intrinsic obstruction caused by late ureteric atresia following ureteric ingrowth into the mesonephros, fibroepithelial polyps, or an adynamic, non-peristalsing ureteric segment, caused by abnormal distribution of smooth muscle, collagen fibers, and innervation. External compression can result from a crossing vessel, such as an aberrant accessory renal artery, or from ureteral kinks or adhesions [20].

Most patients identified with fetal ultrasound are asymptomatic, and many cases spontaneously resolve with time. Symptomatic patients can present with flank pain, nausea, and vomiting that increases with a high fluid intake, which is called Dietl's crisis. In some instances, patients will present with UTI/pyelonephritis. The degree of renal damage is related to the severity and duration of obstruction, which can lead to progressive deterioration of renal function and atrophy of the renal parenchyma in severe cases.

Radiologic evaluation of UPJO with ultrasound [21] and diuretic radionuclide scan (MAG3 or DTPA) or MR urography (MRU) is necessary to define the degree of obstruction and assess renal drainage and function [22]. Treatment can be conservative if the patient remains asymptomatic and renal function is preserved. In symptomatic patients or when renal function is compromised, pyeloplasty is the intervention of choice. It can be performed with laparoscopic or open approaches, with robotic-assisted laparoscopic approaches used in most older children, adolescents, and adults. In infants, open surgery is still the method chosen by most

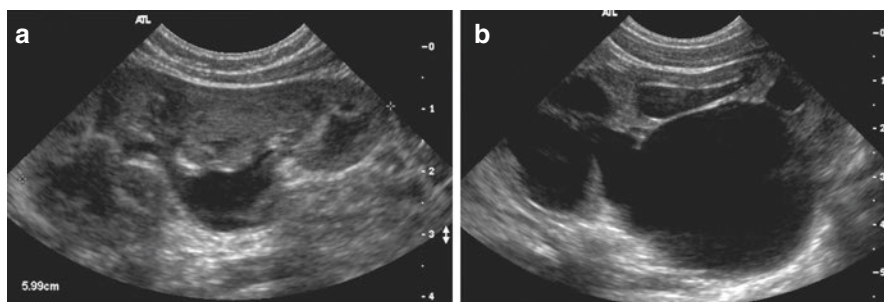


Fig. 13.7 Renal ultrasound demonstrating (a) mild right hydronephrosis and (b) severe left hydronephrosis, consistent with a left ureteropelvic junction obstruction (UPJO)

pediatric urologists [23], though robot-assisted approaches are becoming more common in younger babies.

Ureteral Duplication

Duplication of the ureter, the most common ureteral anomaly (affecting 1% of the population), is associated with renal duplication, described above. It is more common in women than in men. The Weigert-Meyer law describes the relationship of the upper and lower pole moieties and their drainage patterns [24]. The lower pole moiety ureter inserts orthotopically into the bladder at a more lateral and superior location than the upper pole moiety ureter. The upper pole moiety ureter inserts in a more medial and inferior location. The lower pole ureter can be associated with ureteropelvic obstruction and, more commonly, can also present with VUR [25] (Fig. 13.8). The upper pole ureter can more commonly present with obstruction from ectopic insertion (Figs. 13.9 and 13.10a) as well as from a ureterocele (*see below*) [6, 25].

In incomplete ureteral duplications, the upper and lower pole ureters join together somewhere in their course through the retroperitoneum, implanting in the bladder in a normal position as a single ureter (Fig. 13.10b).

Ectopic Ureters

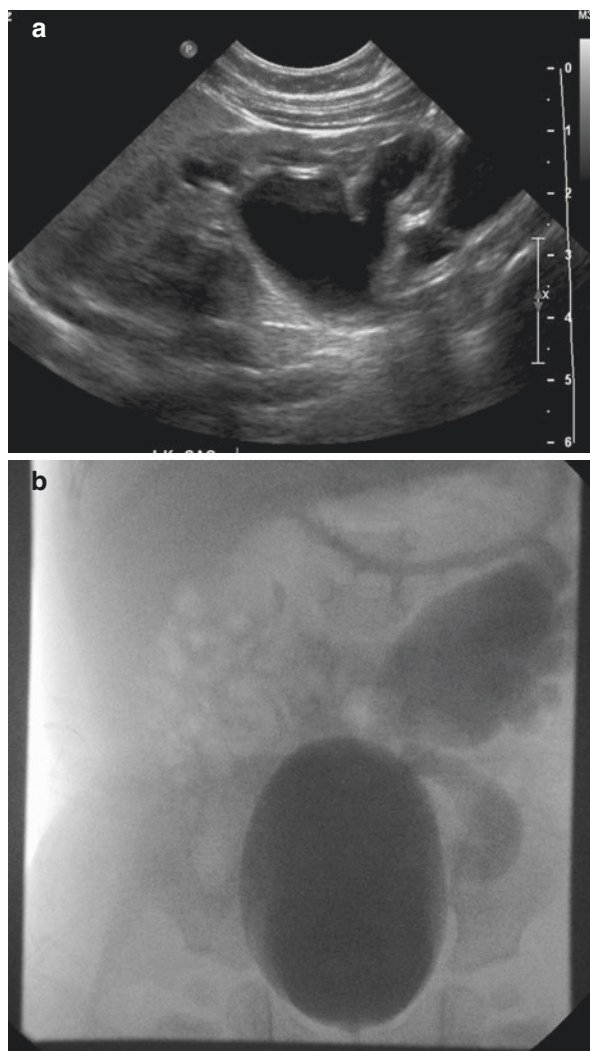
Ectopic ureters are usually associated with the upper pole moiety of a duplicated system, though they can also be associated with a single system. The ureters can be implanted into the bladder in an ectopic location close to the bladder neck or outside of the bladder [6]. In males, the ectopic ureter insertion is suprasphincteric; the ureter may implant in the lower trigone, the prostatic urethra, the ejaculatory duct, or the seminal vesicle [25]. In females, the ectopic ureter insertion occurs distal to the external urethral sphincter, potentially inserting into the urethra, vagina, uterus, or fallopian tubes; thus, it can present with urinary dribbling or primary incontinence [25].

Treatment of ectopic ureters depends on the ectopic location of its implantation, maintenance of upper function, and symptoms. Management options include upper pole heminephrectomy in a setting of poor upper pole function or infections, but upper-to-lower-pole pyeloureterostomy or ureteroureterostomy or vesicoureteral reimplantation can also be performed to preserve upper pole function.

Ureterocele

A ureterocele is a cystic dilatation at the distal end of the ureter. It is proposed to be caused by an incomplete or delayed dissolution of the thin membrane (called *Chwalla's membrane*) that separates the ureteral bud from the urogenital sinus, leading to obstruction between the ureteric bud and the urogenital sinus. It is associated with the upper pole of duplicated ureters, though it can present in single systems. Depending on the degree of obstruction, it can lead to

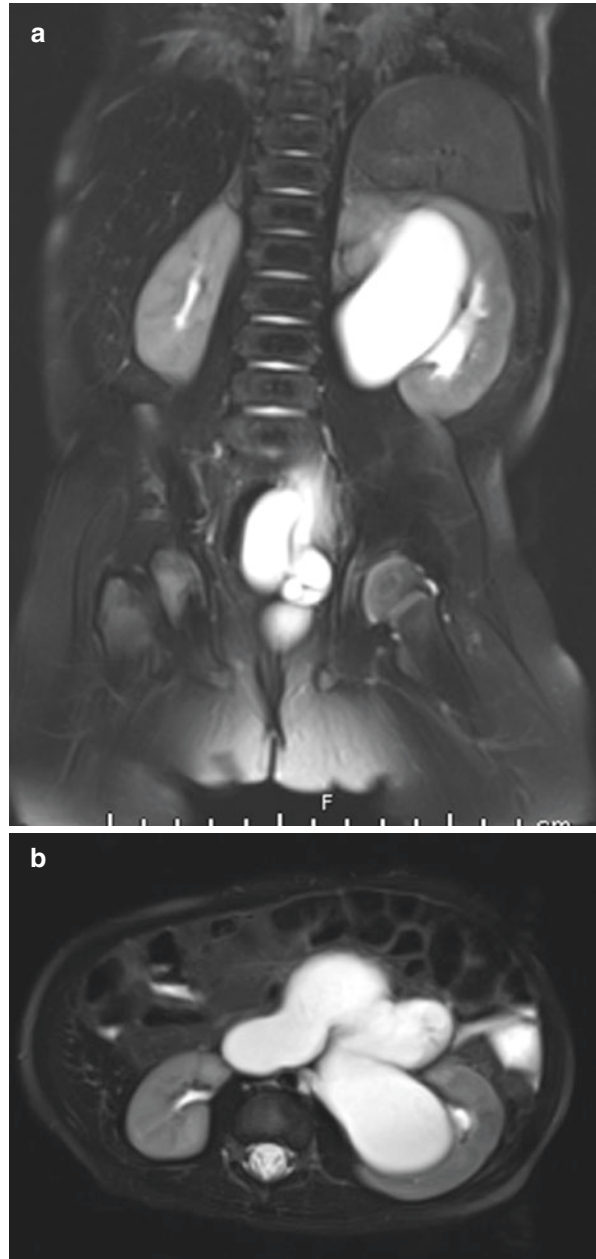
Fig. 13.8 Left vesicoureteral reflux (VUR) into lower pole moiety of a duplicated collecting system. **(a)** Renal ultrasound demonstrating a duplicated collecting system with normal upper moiety and lower pole hydronephrosis. **(b)** Voiding cystourethrogram demonstrating VUR into the left lower pole collecting system



significant hydroureteronephrosis with parenchymal loss in the associated upper renal pole (Fig. 13.11). Depending on the size and location of the ureterocele, it can prolapse through the bladder neck and cause bladder outlet obstruction (Fig. 13.12).

Ureteroceles are often identified on antenatal ultrasound, presenting as hydroureteronephrosis. Postnatal diagnosis is confirmed with renal ultrasound, though historically it has been identified with voiding cystourethrography (VCUG), with the ureterocele displacing the intravesical contrast.

Fig. 13.9 T2-weighted MR images demonstrating a duplicated left collecting system with an ectopic, obstructed left upper pole moiety and associated hydronephrosis, and a nondilated left lower pole collecting system. **(a)** Coronal view; **(b)** axial view



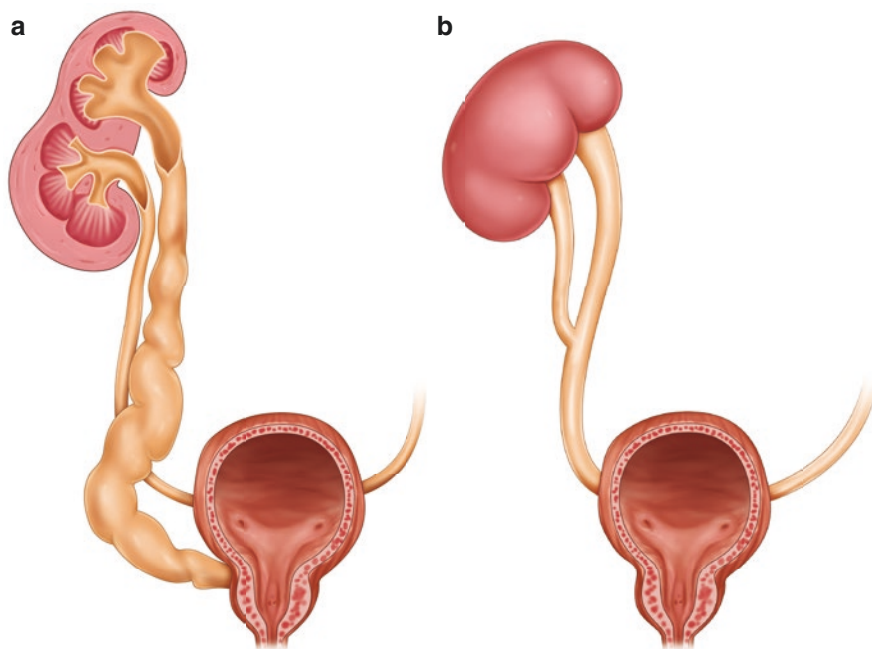


Fig. 13.10 (a) Complete ureteral duplication with hydronephrosis of the upper pole and ectopic implantation of the ureter into the bladder neck. (b) Incomplete ureteral duplication

Although patients with ureterocele are often clinically asymptomatic, the ureteral obstruction can lead to severe hydronephrosis, with associated parenchymal thinning and potential functional loss of the upper moiety. UTIs can ascend to the upper tract and present with pyelonephritis and/or sepsis. Initial management is based on relieving the obstruction with an endoscopic puncture of the ureterocele, utilizing cautery or laser, though endoscopic puncture can potentially introduce secondary VUR into the punctured ureter and collecting system. Definitive management is similar to that for ectopic ureter, with upper pole heminephrectomy in symptomatic, poorly functioning systems, or vesicoureteral reimplantation with the goal of renal preservation. Excision of the ureterocele and bladder neck reconstruction are often required to remove the residual ureterocele. If surgical intervention is performed prior to endoscopic puncture, the ureterocele may be left in place and the upper ureter anastomosed to the lower ureter (ureteroureterostomy) to divert the obstructed upper ureter.

Fig. 13.11 Renal ultrasound demonstrating upper pole hydroureteronephrosis from an obstructing ureterocele in a duplicated collecting system. **(a)** Upper pole hydroureteronephrosis. **(b)** Ureterocele within bladder

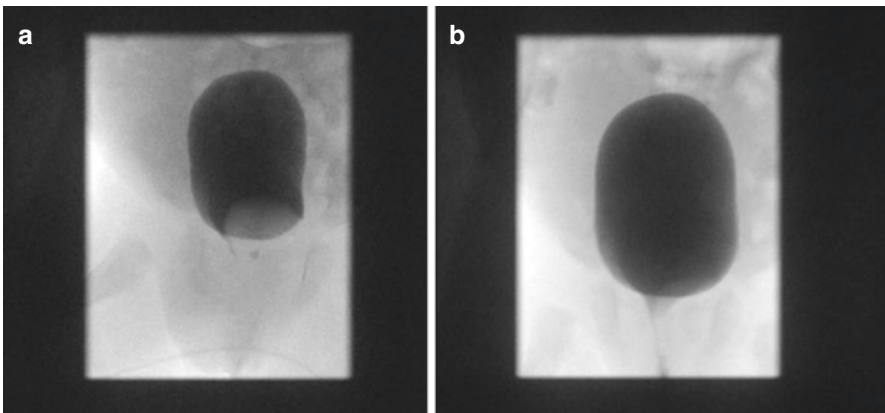
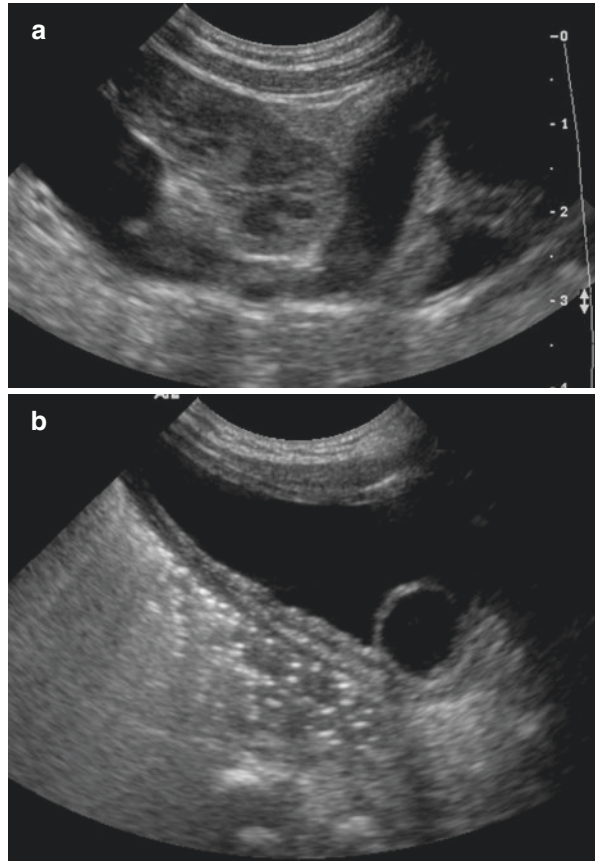


Fig. 13.12 Voiding cystourethrogram (VCUG) demonstrating a filling defect in the bladder, consistent with a large left ureterocele **(a)**, which can prolapse into the bladder neck during urination **(b)**

Retrocaval Ureter

When the ureter descends in a posterior position and circumvents the IVC, it is called *retrocaval ureter*. It generally occurs on the right side, owing to persistence of the posterior cardinal vein during development of the IVC. Left-sided retrocaval ureters occur only with persistence of the left cardinal vein system or with complete situs inversus.

Most people with retrocaval ureter are asymptomatic in the first decades of life. Symptoms usually present in the third or fourth decade as urinary tract obstruction and consequent hydronephrosis, causing lumbar pain. Recurrent UTI and hematuria may occur. The classic imaging sign is a fish-hook-shaped pyeloureteral segment [26]. Treatment is indicated in symptomatic cases and consists of dividing the ureter and performing a ureteroureterostomy in a position anterior-lateral to the vena cava, carried out via an open or laparoscopic approach [27].

Ureteral Stenosis

The ureteral caliber is not uniform throughout its course; it is physiologically narrower in three sites: the ureteropelvic junction, the crossing of the iliac vessels, and the ureterovesical junction. Pathological stenosis of the ureter can occur at any location and can be idiopathic or caused by intrinsic inflammation from a ureteral stone, retroperitoneal masses, or malignancy; it also can be iatrogenic, after ureteral manipulation [28]. Iatrogenic causes of ureteral stricture account for 35% of cases, with gynecologic operations responsible for 74% and urological manipulation of the ureter for 8–13% [28]. Ureteral stenosis increases the risk for infection, hematuria, stones, and hydronephrosis because of the associated obstruction. Treatment is required when the patient is symptomatic or presents with associated renal damage from the obstruction. Surgical intervention consists of resection of the stricture followed by ureteroureteral anastomosis, or endoscopic incision or balloon dilation [28].

Megaureter

The term *megaureter* describes an increase in diameter or dilatation of the ureter. A ureter is considered to be a megaureter when its diameter measures 0.7 cm or more [29, 30]. Megaureter represents about 23% of all children with urinary tract obstruction referred to the pediatric urologist. It is more common on the left side, and is bilateral in 25% of cases [31]. The most accepted classification divides megaureters into those that are obstructed, refluxing, obstructed and refluxing, or neither obstructing nor refluxing [32]. The pathogenesis of *primary obstructive megaureter* is thought to be related to an increased amount of collagen fibers in the distal portion of the ureter, associated with an abnormal response to neurotransmitters, which reduces peristalsis [33, 34].

Prenatal ultrasound currently diagnoses 73% of cases of megaureter [35], but no evidence has been found that a prenatal diagnosis will influence the postnatal outcome [21]. In some instances, older children may present with abdominal pain, though more severe presentations may be related to UTIs that progress to upper tract infection and urinary sepsis.

All children with a megaureter should be evaluated independent of whether the diagnosis was made prenatally [30] or postnatally. Investigation starts with a kidney and bladder ultrasound. VCUG should be performed to exclude the presence of VUR and also evaluate the bladder and urethra. When obstruction is suspected, a diuretic renogram (MAG3 or DTPA) [31] or MRU is indicated.

In up to 87% of cases, no surgical intervention will be necessary, as hydronephrosis will reduce and no damage to the kidney will be found [36]. In those children with worsening of hydronephrosis and progressive renal compromise, recurrent UTI, or obstructive symptoms such as abdominal pain, surgical intervention is indicated [30], with ureteral reimplantation. If the diameter of the ureter is greater than 1.0 cm, the distal portion of the ureter may need to be tapered during the reimplantation to reduce its caliber [30].

Vesicoureteral Reflux

Vesicoureteral reflux (VUR) is the abnormal back flow of urine into the ureter or the kidney during bladder filling and/or emptying (Fig. 13.13). It is one of the most frequent pediatric urologic problems, especially in children who present with febrile UTI, and is twice as frequent in girls than in boys. VUR is also often identified based on prenatal hydronephrosis, prompting VCUG; these cases are more common in boys. In children with failure to thrive and fever of unknown origin, VUR should be suspected and urine culture should be obtained. VUR is present in up to 1.8% of children and in about 30–40% in those with febrile UTI [37, 38]. The pathogenesis of primary VUR is not well understood; it is proposed to be related to a failure in the

Fig. 13.13 Voiding cystourethrogram (VCUG) demonstrating bilateral vesicoureteral reflux (VUR), left greater than right



development of the vesicoureteral junction with a short submucosal ureteral tunnel. Secondary VUR is usually due to high bladder pressure and can be caused by bladder outlet obstruction, such as in posterior urethral valves in boys, neurogenic bladder, or lower urinary tract dysfunction.

Evaluation of children with febrile UTI is still controversial, and many different protocols have been proposed. Ultrasound is recommended in all children presenting with UTI to evaluate the presence of hydronephrosis, ureteral dilatation, bladder wall thickness, and high post-voiding residual, but the only way to diagnose VUR is by VCUG, in which the child is catheterized and contrast is instilled into the bladder. Fluoroscopy will assess for the reflux of contrast from the bladder into the ureter and kidney, and will classify the degree of the VUR, graded from I to V, depending on the degree of kidney dilatation and ureteral dilatation and tortuosity [39] (Fig. 13.14). Children with febrile UTI and VUR can also be assessed with a nuclear DMSA scan to evaluate the presence of renal scarring and to quantitate function.

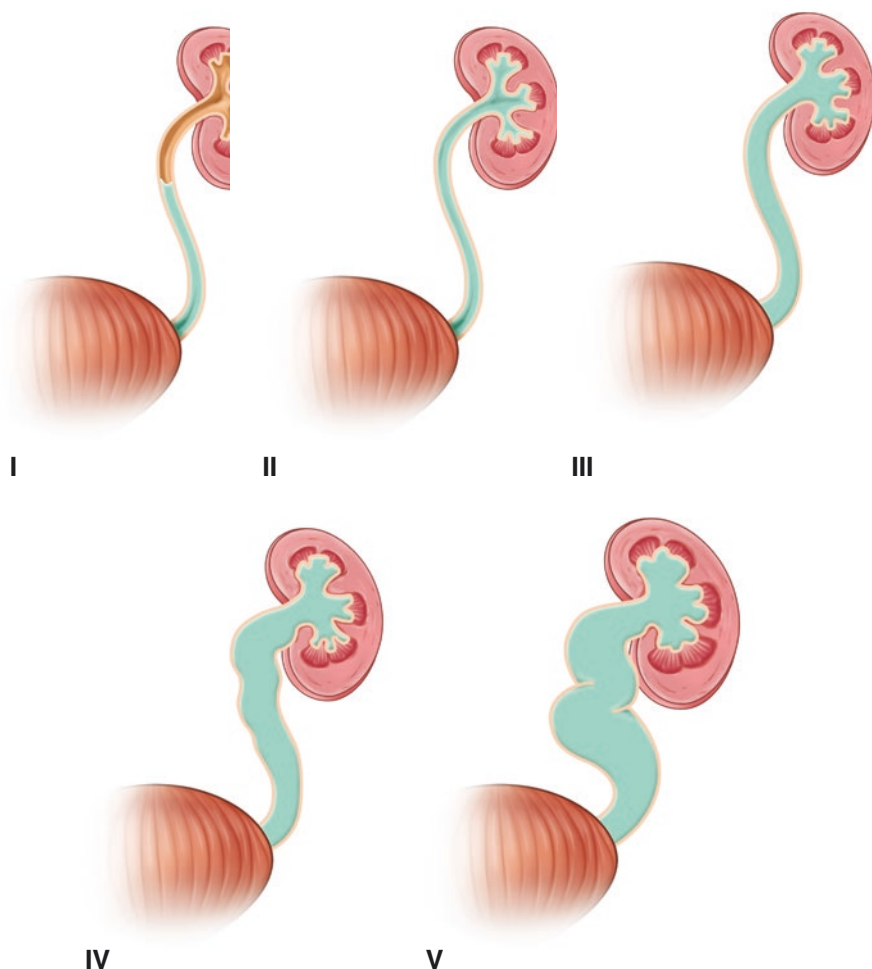


Fig. 13.14 Grading schema for vesicoureteral reflux

Most cases of VUR will resolve spontaneously as the child grows. The likelihood of resolution is associated with the grade of reflux, gender, age, voiding dysfunction, presence of renal scarring, and bladder volume measured on VCUG at the diagnosis of VUR [37]. To avoid recurrent UTIs, which increase the risk for new renal scar formation, the use of low-dose antibiotic prophylaxis has been proposed, but it remains controversial [40]. Antibiotic prophylaxis aims to maintain a sterile urinary tract and give time for spontaneous resolution of the VUR.

Surgical intervention is necessary in children who present with recurrent febrile UTIs, development of renal scars associated with infection, or renal compromise in a setting of VUR and high-pressure bladder. The goal of the surgical treatment is to create a longer tunnel between the bladder mucosa and muscularis propria, mimicking the physiological antireflux mechanism [41]. Minimally invasive approaches include an endoscopic subureteric injection of a bulking agent into the ureteral orifice [42]. As the grade of VUR increases, the success rate of endoscopic treatment decreases [42]. Open ureteral reimplantation is still the gold standard for the treatment of VUR, with the greatest success rates [41]. Laparoscopic and robotic-assisted laparoscopic procedures have grown in popularity and have been demonstrated to have good results.

Adrenals

The adrenal glands are bilateral yellow-orange structures that measure 3–5 cm transversely and weigh approximately 3–5 g. They are encased within the Gerota's fascia in the perinephric fat, but are anatomically and embryonically distinct from the kidneys.

Anatomy

The adrenal glands lie superior to the upper pole of the ipsilateral kidney, separated by a layer of connective tissue. The right adrenal gland is located superior to the left adrenal gland. Table 13.2 describes the anatomic relations of the adrenal gland to its adjacent organs.

Vasculature

The arterial blood supply of the adrenal gland is derived from three sources:

- Superior adrenal from the inferior phrenic artery. It is rarely a branch of the aorta, celiac axis, or intercostal arteries.
- Middle adrenal from the abdominal aorta
- Inferior adrenal from the ipsilateral renal artery

Table 13.2 Anatomic relations of the adrenal glands to adjacent organs

	Right	Left
<i>Shape</i>	Pyramid	Crescent
<i>Relation to kidney</i>	Cranial	Medial to upper pole
<i>Anterior</i>	<i>Lateral:</i> Liver <i>Medial:</i> Duodenum, inferior vena cava	<i>Superior:</i> Stomach <i>Inferior:</i> Tail of pancreas, splenic vessels
<i>Posterior</i>	<i>Superior:</i> Diaphragm <i>Inferior:</i> Kidney	<i>Medial:</i> Diaphragm <i>Lateral:</i> Kidney

The venous drainage varies by laterality. The right adrenal vein drains into the posterolateral IVC, whereas the left adrenal vein generally drains into the left renal vein. It can also sometimes drain into the left inferior phrenic vein.

Lymphatics

The adrenal lymphatics drain into the lumbar lymph nodes. The right adrenal lymphatics drain into the right paraaortic nodes anterior to the right crus of the diaphragm, right para-aortic nodes proximal to the junction of the left renal vein and vena cava, and the thoracic duct or posterior mediastinal nodes. The left adrenal lymphatics drain into the left lateral aortic nodes proximal to the celiac trunk and left renal vein, and through the diaphragm.

Nerves

The adrenal medulla is innervated by the celiac plexus and splanchnic nerves. The preganglionic sympathetic nerve fibers originate from the T10 to L1 spinal cord segments.

Embryology

The adrenal gland is composed of the cortex and the medulla. The adrenal cortex is derived from the intermediate mesoderm between the root of the dorsal mesentery medially and the mesonephros and undifferentiated gonad laterally. It is composed of three layers: the zona glomerulosa, which produces mineralocorticoids; the zona fasciculata, which produces glucocorticoids; and the zona reticularis, which produces sex steroids. The adrenal medulla is derived from the ectoderm and develops from migrating cells of the neural crest. It secretes catecholamines.

Congenital Anomalies of the Adrenal Glands

The adrenal gland may not develop. It can have an incomplete or absent cortex. It can be located ectopically, or it can be fused in the midline behind the aorta.

Bladder

Anatomy

The bladder is a round, hollow, muscular organ whose function is to store urine. In a normal adult, the bladder can store 300–500 mL of urine before the urge to urinate. In children up to age 12 years, bladder volume in milliliters can be estimated by the formula $(\text{age} + 2) \times 30$ [43]. The bladder is composed of three layers of tissue: the mucosa, the muscularis, and the serosa. The shape of the bladder changes to accommodate filling and emptying of urine.

The bladder is located below the peritoneal cavity, at the base of the pelvis. As it distends, the bladder can rise and can be palpated above the pubic symphysis. It is situated higher in infants and children, positioned more as an abdominal organ. Anteriorly, it borders the pubic symphysis and abdominal wall. The retropubic space is an extraperitoneal space between the bladder and the pubic symphysis, also known as the space of Retzius. Posteriorly, in females, the bladder lies in front of the uterus and the upper part of the vagina, separated by the vesicouterine pouch. In males, the bladder lies in front of the seminal vesicles and the rectum, separated by the rectovesical pouch. Superiorly, a layer of the parietal peritoneum and the peritoneal contents cover the bladder's dome. The remainder of the bladder is extraperitoneal. The obliterated urachus or median umbilical ligament connects the bladder dome to the umbilicus. Finally, inferiorly, in females, the bladder neck rests on the anterior vaginal wall, which is supported by the levator ani muscle. The trigone, the location of ureteral insertion, is in close proximity to the cervix, thus putting the ureters at risk during hysterectomy. In males, the bladder neck lies superior to the prostate, which is also supported by the levator ani muscle. The bladder neck leads inferiorly to the urethra.

The internal sphincter is located at the bladder neck and is a continuation of the detrusor muscle. It consists of smooth muscle and is innervated by the autonomic nervous system, providing involuntary control of micturition. In men, it lies proximal to the opening of the ejaculatory duct, which is in the prostate, and thus prevents retrograde ejaculation into the bladder.

The blood supply to the bladder runs primarily along the endopelvic fascia at the bladder base and urethra. The superior and inferior vesical arteries, which branch from the anterior trunk of the internal iliac artery, are the main arterial supply to the bladder. The bladder is also supplied by branches of the obturator and inferior gluteal arteries. The bladder is surrounded and supplied by a rich venous plexus that empties into the internal iliac or hypogastric veins. It can also empty into the veins of the hip bones, accounting for sites of bony metastases in bladder or prostate cancer. Most of the lymphatics drain into the external iliac lymph nodes, with some drainage into the obturator and internal iliac lymph nodes.

The bladder receives innervation from both the sympathetic and parasympathetic nervous system. The sympathetic preganglionic fibers arise from the T10 to L2 level and form the hypogastric plexus to innervate the trigone and bladder neck. The parasympathetic fibers arise from the S2 to S4 level and run in the pelvic splanchnic

nerves, synapsing on the bladder wall. The somatic nerves are carried by the parasympathetic pelvic splanchnic plexus and carry information to the S2 and S3 level. Pain fibers are conducted in the sympathetic nerves and are located in the presacral plexus, reaching up to the T6 level.

Embryology

Embryologically, the cloaca, composed of endoderm, is the terminal hindgut and is a common chamber into which the genitourinary and gastrointestinal tracts converge. During the 5th to 6th week of gestation, the cloaca partitions into the anterior urogenital sinus and the posterior anorectal canal. The mesonephric duct distal to the ureteric bud or the common excretory ducts fuses with the urogenital sinus and forms the primitive trigone. Other than the trigone, in males, the mesonephric duct forms the male reproductive system; in females, it mostly degenerates. The ureters separate from the mesonephric ducts and fuse into the urogenital sinus at the level of the trigone, forming the ureteral orifice. The ureteral orifice migrates cranially and laterally on the trigone. The urogenital sinus develops into the bladder. In males, it also forms the prostatic urethra, Cowper's glands, and the prostate. In females, it forms the urethra, lower vagina, Bartholin's glands, Skene's glands, and the hymen. The apex of the bladder tapers to become the urachus, which is continuous with the allantois. The urachus involutes and becomes a fibrous cord by the 12th week, forming the median umbilical ligament [44].

Congenital Abnormalities of the Urachus

The failure of the patent urachus to obliterate at any point will result in urachal anomalies. It can present as urine drainage from the umbilicus, granulomatous polyp, umbilical abscess, UTI, or abdominal pain. Sepsis may be present if an infection develops. Malignancy in adult life has been reported [45].

Patent Urachus

Patent urachus refers to an embryonic communication between the bladder and umbilicus; it occurs when the urachus does not involute (Fig. 13.15a). It is associated with intermittent to continuous drainage of urine from the umbilicus. Ultrasonography is currently the imaging study of choice and has been reported to have a sensitivity of 79–91% [46], though VCUG can be incorporated to confirm the communication. Surgery with total excision of the urachus is the treatment of choice if spontaneous closure does not occur [46, 47].

Urachal Cyst and Urachal Sinus

Lacunae of Luschka are small patent areas between the obliterated ends of the urachus. These are usually asymptomatic and are found incidentally or postmortem. If these lacunae enlarge; however, a urachal cyst, the persistence of a portion of the

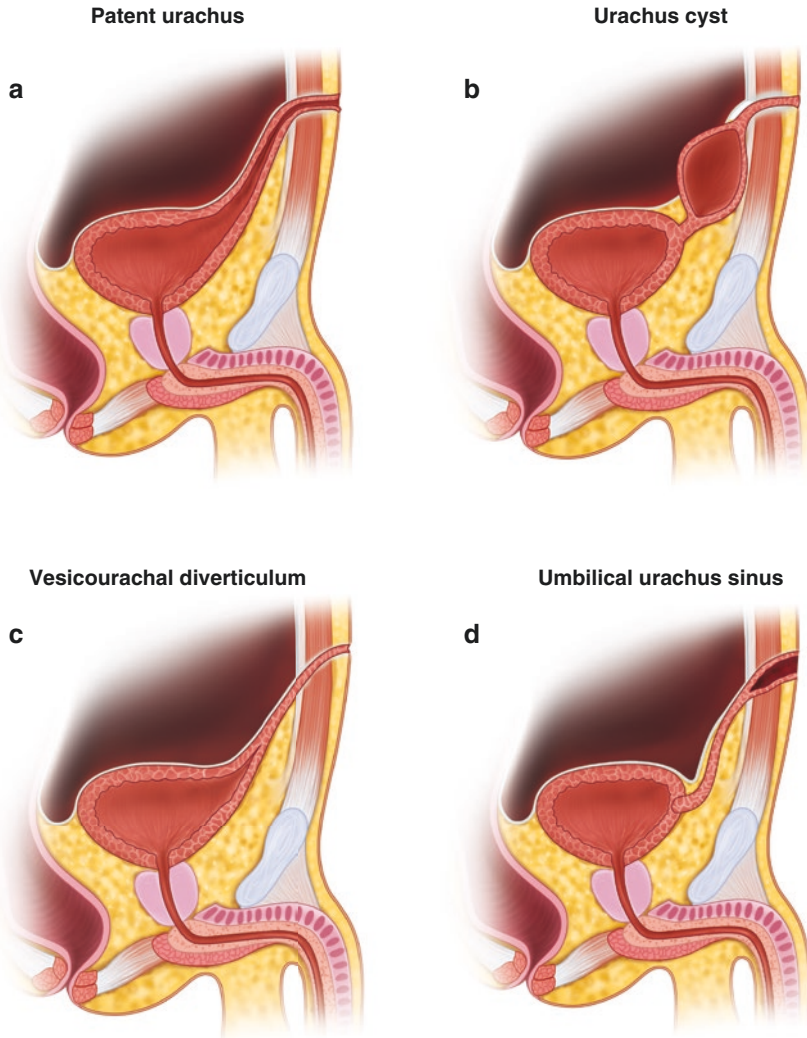


Fig. 13.15 Anomalies of the urachus. (a) Patent urachus. (b) Urachal cyst. (c) Vesicourachal diverticulum. (d) Umbilical urachal sinus

urachal canal containing squamous epithelial cells, can form (Fig. 13.15b). When the area that remains patent communicates with the bladder, it is termed a vesicourachal diverticulum (Fig. 13.15c), and when it communicates with the umbilicus but not the bladder, it is termed a *urachal sinus* (Fig. 13.15d).

Urachal cyst and sinus may present with umbilical drainage, periumbilical mass, or erythema of the inferior abdominal wall, and in more severe cases, with infection or sepsis [46–48]. As in the patent urachus, ultrasound is the imaging modality of choice, though CT scan and MRI can be utilized to confirm the diagnosis. In

symptomatic cases, drainage and antibiotics can be used initially, but surgical excision of the urachal remnant is definitive therapy [46–48].

Congenital Abnormalities of the Bladder

Bladder Exstrophy

The bladder exstrophy and epispadias complex is a congenital malformation characterized by a defect in the anterior inferior abdominal wall in which the bladder is open and exposed, in continuity with an anterior opening of the entire urethra and penis (Fig. 13.16). This is associated with a wide diastasis of the pubic symphysis. It is a rare condition, with an incidence of 1 in 10,000–50,000, affecting boys twice as often as girls [49]. It has been theorized to be due to maldevelopment of the cloacal membrane, preventing medial migration of the mesenchymal tissue and proper lower abdominal wall development, with persistent pubic diastasis [50]. It is associated with defects in the pelvic floor and pelvic bones, including widening of the pubic symphysis, malrotation of the pubic rami and innominate bones, and genital defects.

Prenatally, fetal ultrasound can demonstrate an absence of bladder filling, low positioning of the umbilicus, and abdominal mass [51]. After birth, a defect in the anterior inferior abdominal wall is observed, with the exposure of an open bladder. The penis and urethra are ventrally opened in all their extension. The pubic bones are separated and located on each side of the bladder. Bilateral inguinal hernias are commonly present [52]. Although the upper urinary tract is usually not affected, an abdominal ultrasound should be performed to exclude kidney malformations.

Fig. 13.16 Primary bladder exstrophy



Bladder exstrophy is one of the most challenging conditions for the pediatric urologist and should be treated in tertiary centers. After birth, the bladder should be covered with nonadherent plastic film to prevent adhesions to the diaper and inflammation (“cobblestoning”) of the bladder mucosa. The umbilical cord should be tied off with suture to prevent the umbilical clamp from irritating the bladder mucosa.

Treatment of bladder exstrophy is always surgical. It has been advocated that repair should be completed early in life, to facilitate the closure of the diastasis of the pubic symphysis, and performed by a multidisciplinary team [53, 54]. Complications are frequently seen, but specialized experience has led to improved bladder exstrophy surgical outcomes, such as urinary continence and erectile function [53–55].

Bladder Diverticulum

Bladder diverticula are herniations of the bladder mucosa due to a weakening in the bladder wall musculature. They can be congenital or acquired. Congenital bladder diverticula are located adjacent to the ureteral orifice in about 90% of the cases [56]; commonly known as Hutch diverticula, these are associated with vesicoureteral reflux (VUR) [57]. Acquired diverticulum occurs secondary to high pressure within the bladder, due to neurogenic bladder or bladder outlet obstruction from urethral stricture, benign prostatic hyperplasia, or posterior urethral valves (obstructing tissue in the prostatic urethra).

Most bladder diverticula are small and asymptomatic. The most common presentation in children is linked to infection, due to residual urine in the bladder [58]. Stones can form within the diverticula due to urinary stasis. Ultrasound and VCUG are the radiological tests of choice.

Surgical treatment is indicated when the diverticulum is symptomatic, especially in those at high risk for UTI. Some urologists advocate surgical intervention for diverticula greater than 3 cm in diameter [58]. In patients with acquired or secondary diverticula, treatment of the primary underlying condition should be addressed.

Bladder Septation or Duplication

In these rare conditions, the bladder is divided by a fibromuscular septum. The separation can be incomplete or complete and can be associated with other anomalies, including duplication of the urethra, genitalia, and hindgut.

The diagnosis is made by retrograde urethrogram, CT scan, or MRI. Symptoms of abdominal pain and UTI are the most common complaints. Treatment depends on the patient’s symptoms and other associated anomalies [59].

Megacystis

Fetal megacystis is a rare congenital disease characterized by a greatly dilated bladder. This finding suggests the presence of mechanical or functional bladder outlet obstruction, which can be partial or complete [60]. Ultrasonography will demonstrate an enlarged bladder from about 10–14 weeks of gestation, with a longitudinal bladder diameter greater than 8 cm [61].

In the majority of cases, megacystis is a consequence of posterior urethral valves, obstructing fibrous bands within the prostatic urethra [60]. A fetus with megacystis usually will present with oligohydramnios, which is associated with poor prognosis and a significant risk of perinatal mortality [62].

In utero intervention has been proposed to treat megacystis, but the severity of the disease will determine the perinatal survival [63].

Bladder Agenesis

The complete absence of the bladder is very rare; it occurs 30 times more frequently in females than in males [64]. It may be the result of atrophy of the urogenital sinus owing to a lack of distention with urine that is caused by failure of incorporation of the mesonephric ducts and ureters to the urogenital sinus.

In females, the ureters may empty into the Müllerian structures (uterus, vagina, or vestibule), allowing preservation of renal function, but in association with urinary incontinence [65]. In males, survival is possible only if the ureteral drainage is into the rectum or patent urachus [66].

Bladder agenesis is commonly associated with other urologic anomalies (renal dysplasia, anomalies of position and fusion, ectopic insertion of the ureters, or urethral agenesis) or with neurologic, vascular, orthopedic, or hindgut anomalies [64]. Diagnosis is usually due to associated anomalies, urinary incontinence, or UTI. In the majority of reported cases, MRI was the test of choice.

Bladder agenesis management depends on the relief of obstruction, when present, to preserve renal function. Ureteral implantation to a neobladder created from ileum or an external stoma are reliable options. Long-term prognosis is usually poor, however, because of the associated anomalies [67].

Prostate

Anatomy

The prostate is an exocrine gland located just below the bladder and surrounding the urethra. It produces about 30% of the semen. A normal prostate is about the size of a walnut (3 cm × 4 cm × 2 cm) and weighs 20–25 g. As men age, the prostate size increases.

Histologically, the prostate can be classified into four zones, shown on Table 13.3. Anatomically, it is classified into five lobes: the posterior, anterior, lateral (left and right), and median lobes. The median and lateral lobes are most prominent and visualized when performing a transurethral resection of the prostate. The posterior lobe is associated with the peripheral zone.

The base of the prostate sits inferior to the bladder; its apex is adjoined to the external sphincter and membranous urethra. Anteriorly, the prostate is fixed at the apex to the pubic bone by the puboprostatic ligaments. It is surrounded by extraperitoneal fat in the space of Retzius. Posteriorly, it is separated from the rectum and

Table 13.3 Zones of the prostate

Zone	Location	Pathology	% of Prostate
<i>Glandular</i>			
Peripheral	Posterior, palpable on digital rectal exam	70–80% prostate cancer	70% glandular tissue
Central	Surrounds the ejaculatory ducts from prostatic base to verumontanum	<5% prostate cancer; more aggressive	25% glandular tissue
Transition	Surrounds the urethra, separated from peripheral zone by concentric fibromuscular band (“surgical capsule”)	~20% prostate cancer Benign prostatic hyperplasia (region that enlarges as men age)	5% glandular tissue; increases with age
<i>Nonglandular</i>			
Anterior fibromuscular stroma	Anterior to glandular tissue, composed of fibrous tissue and muscle	–	5–30% of total prostate volume

seminal vesicles by Denonvilliers’ fascia and the pouch of Douglas. On each side, it is surrounded by the overlying endopelvic fascia and the pubococcygeus muscle of the levator ani. The superficial branch of the dorsal vein lies just outside the endopelvic fascia, and the dorsal vein complex runs deep to it. The neurovascular bundle runs posterolaterally in the prostatic fascia. The prostate surrounds the urethra as it runs from the bladder neck to the external sphincter. This denotes the prostatic urethra and is where the ejaculatory ducts insert into the urethra.

The prostate has a “false” and a “true” capsule. The “false” capsule, also known as the *surgical capsule*, refers to the layer of prostatic tissue between the transition zone and the peripheral zone. In simple prostatectomies and in transurethral resection of the prostate, the goal is to remove the enlarged adenoma to the level of the surgical capsule. The “true” or *anatomic* prostatic capsule is formed by collagen, elastin, and smooth muscle. The periprostatic venous plexus runs between the surgical and anatomic capsules. The true capsule is surrounded by visceral fascia, which also surrounds the bladder.

The prostatic artery is a branch of the inferior vesical artery. It has two main branches: the urethral and capsular branches. The urethral branches penetrate the junction between the prostate and the bladder posterolaterally at the 5 o’clock and 7 o’clock positions, and they travel to the bladder neck and urethra to supply the prostatic urethra. The capsular branch runs posterolateral to the prostate with the neurovascular bundle. It penetrates the prostate to supply the glandular tissue.

The venous drainage of the prostate runs in the periprostatic plexus between the surgical and anatomic prostatic capsules. It is composed of inferior vesical veins, which drain into the internal iliac vein. This internal iliac vein is connected to the vertebral vein plexus by Batson’s venous plexus and is hypothesized to be a route for bony metastases from prostate cancer. The lymphatic drainage of the prostate occurs primarily via the obturator and internal iliac lymph nodes.

The prostate is controlled by the cavernous nerve, which induces emission of semen. The prostate is flanked by two neurovascular bundles that travel through the floor of the pelvis to the penis; these bundles supply the corpora cavernosa and are

responsible for erections. Nerve-sparing procedures have been developed to try to preserve erectile function following prostatectomy.

Embryology

At approximately 10 weeks of gestation, under the influence of testosterone, the prostate starts to develop from the urogenital sinus. The prostatic urethra will evaginate to form at least five solid prostatic cords that develop lumina and acini. The smooth muscle and connective tissue are formed from the surrounding mesenchyme [68].

Congenital Abnormalities of the Prostate

Prostatic Agenesis

Agenesis of the prostate is extremely rare. It can be present in patients with 5-alpha reductase deficiency and testicular feminization (a mutation in the androgen receptor preventing reception of androgens/testosterone).

Prostatic Hypoplasia

Like other anomalies of the prostate, hypoplasia is also very rare. It can be present in patients with prune belly syndrome. It is associated with a dilated prostatic urethra.

Prostatic Cysts

Cysts of the prostate can have Müllerian or Wolffian duct origin. The differentiation between Müllerian cysts and prostatic utricle cysts can be confusing, and many describe both as being the same [69]. They arise from the posterior and bulbar urethra owing to an inappropriate secretion of testosterone [70]. These cysts, which are round and located in the midline, can vary widely in size [71]. Symptoms usually appear later in life, and patients are often asymptomatic. Symptoms, when present, include recurrent infections, epididymitis, irritative and obstructive voiding symptoms, hematuria, and urethral discharge. In the presence of large cysts, perineal pain and constipation may be present. Infertility and sexual dysfunction can be seen in adults [72]. The cysts can be visualized by ultrasound, CT, or MRI. Urethroscopy may be necessary to define the diagnosis. Treatment, in symptomatic cases, is the removal of the cyst by open, laparoscopic, or robotic-assisted techniques [73].

Seminal Vesicles and Vas Deferens

Anatomy

The seminal vesicles are located posterior to the bladder, prostate, and distal ureters. They join the ampulla of the vas deferens to form the ejaculatory ducts, which drain into the prostatic urethra at the level of the prostatic utricle (verumontanum). The

verumontanum is located at the angle of the prostatic urethra and is formed by a mound of the posterior wall called the *seminal colliculus*. The ejaculatory ducts open into the prostatic urethra lateral to the prostatic utricle. The seminal fluid produced by the seminal vesicles constitutes 50–80% of ejaculate.

The vas deferens is a continuation of the epididymis and runs through the inguinal canal and deep inguinal ring into the peritoneal cavity. It courses posteriorly along the lateral pelvis and then inferiorly behind the bladder. It crosses the distal ureters anteromedially to join the seminal vesicles and form the ejaculatory duct.

The blood supply for the seminal vesicles and vas deferens comes from the vesiculodeferential artery, which is a branch of the superior vesical artery. The venous drainage from the vas and seminal vesicle drain into the pelvic venous plexus. The lymphatic drainage of the seminal vesicle and vas deferens drains into the external and internal iliac nodes.

The seminal vesicle and vas deferens receive their innervation from the pelvic plexus, with contributions from the sympathetic hypogastric nerves.

Embryology

The seminal vesicle, vas deferens, ejaculatory duct, and epididymis develop from the mesonephric/Wolffian duct. After the ureter separates from the mesonephric duct, the seminal vesicles arise from the mesonephric duct in the 12th week. The mesonephric duct later becomes the vas deferens. The Müllerian duct (paramesonephric duct) regresses in response to the Müllerian inhibiting substance secreted by the Sertoli cells of the testicles to form the appendix testes, a small stalked appendage of the testicle; some theorize that the prostatic utricle also is a remnant of the Müllerian duct.

Congenital Abnormalities of the Seminal Vesicles and Vas Deferens

Seminal Vesicle Agenesis

Seminal vesicle agenesis can be unilateral or bilateral. Unilateral agenesis occurs if any insult happens at the time the ureteric bud arises from the mesonephric ducts, during the 7th week of gestation [74]; it is associated with ipsilateral renal agenesis in up to 79% of the cases [75]. Bilateral agenesis is associated with the cystic fibrosis gene [76], and patients usually have normal kidneys [74]. Association with vas deferens agenesis is common (80%). Patients with seminal vesical agenesis will present with low ejaculate volume and infertility. Patients who want to have children will need to have their sperm collected directly from the testis for assisted reproduction [77].

Hypoplasia of the Seminal Vesicle

As in seminal vesicle agenesis, seminal vesicle hypoplasia is associated with ipsilateral vas deferens agenesis, and patients may present with low ejaculate volume. Otherwise, they are often asymptomatic. Infertility also may occur in these patients [77].

Congenital Seminal Vesicle Cyst

An incomplete differentiation of the seminal vesicle duct may give rise to a seminal vesicle cyst [77]. As in the agenesis of the seminal vesicle, the cyst may be associated with renal agenesis in up to one-third of the cases [78]. Transrectal ultrasound is the best method to evaluate the presence and characteristics of the cyst. Most of the cysts are asymptomatic and require no treatment [78]. The most common symptom is infection, in which case surgical (open or laparoscopic) resection of the cyst would be indicated.

Congenital Absence of the Vas

Unilateral or bilateral absence of the vas may occur and refers to failure in development of the vas deferens. When bilateral, it is associated with cystic fibrosis; if unilateral, ipsilateral renal agenesis can be found.

Bilateral congenital agenesis of the vas deferens is responsible for 1–2% of cases of male infertility [79]. It is usually accompanied by agenesis of the other mesonephric structures, such as the seminal vesicle and epididymis. On physical examination, the testicles are normal but no vas deferens can be palpated. It is usually asymptomatic, and treatment is indicated for fertility reasons.

Unilateral absence of the vas deferens is less common and is usually detected during vasectomy. Infertility is not a common problem.

Ectopic Vas Deferens

Ectopic vas deferens is described as the high junction of the vas deferens to the ureter, forming a common mesonephric duct that inserts in the bladder or bladder neck [80]. It is usually associated with renal, genital, and rectal anomalies. The diagnosis of ectopic vas deferens should be suspected in children with imperforate anus and recurrent UTI [77] (Fig. 13.17).

Urethra

The urethra, the most distal segment of the urinary tract, consists of a muscular tube that starts at the bladder neck and opens to the exterior through the urethral meatus. Male and female urethras differ both embryologically and anatomically, so they will be described separately.

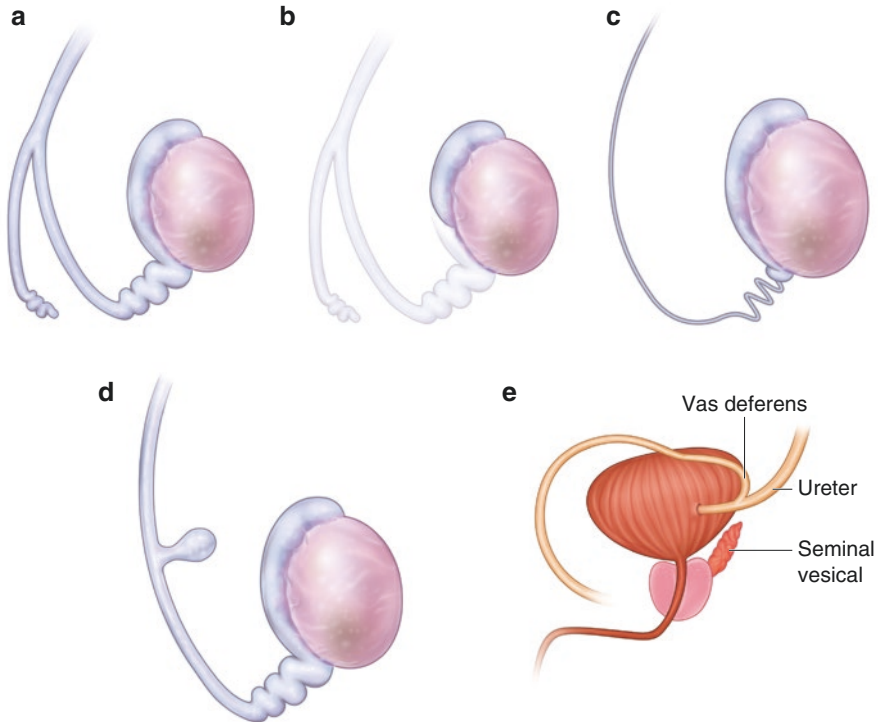


Fig. 13.17 Anomalies of the vas deferens: (a) Duplication. (b) Agenesis. (c) Aplasia. (d) Diverticulum. (e) Ectopic implantation into the ureter

Anatomy

Male Urethra

As the urogenital sinus divides, the pelvic portion forms the prostatic and membranous urethra, while the penile urethra derives from the phallic portion (urethral plate). The male urethra can be divided into the anterior and posterior urethra.

The posterior urethra is divided into two segments, the prostatic urethra and the membranous urethra. The *prostatic urethra* starts at the bladder neck and runs through the prostate to its apex. The prostatic utricle (verumontanum), where the ejaculatory ducts drain, opens at the inferior aspect. The *membranous urethra* spans the length from the prostatic apex to the perineal membrane and is surrounded by the muscular external urethral sphincter. The striated or external urethral sphincter lies posterior to the dorsal venous complex and is supported by the puboprostatic ligaments and the suspensory ligament of the penis. Its fixation to the ischial rami and inferior pubic rami makes the membranous urethra susceptible to disruption during a pelvic fracture.

The anterior urethra is divided into three portions: the bulbar, pendulous, and glanular urethras. It runs through the corpus spongiosum (supportive erectile tissue

surrounding the urethra, connecting to the glans) from the external sphincter to the external meatus. The *bulbar urethra* runs from the urogenital diaphragm to the base of the penis; within the corpus spongiosum, it lies between the split corpora cavernosa/erectile bodies. Bulbourethral or Cowper's glands originate around the striated urethral sphincter but empty into the bulbar urethra. The *pendulous* or *penile urethra*, also engulfed in the corpus spongiosum, represents the pendulous portion of the penis. The *glanular urethra* runs through the glans of the penis and the distal aspect, termed the *fossa navicularis*, and has a small dilatation just proximal to the external urethral orifice, the urethral meatus.

The blood supply to the urethra comes from the internal pudendal artery that forms the common penile artery, which branches as the dorsal and urethral arteries. The prostatic artery is supplied by the inferior vesical and middle rectal arteries. The venous drainage mirrors the arterial supply.

Female Urethra

The female urethra spans approximately 4 cm from the bladder neck to the vaginal vestibule. It is palpable in the anterior vaginal wall. Many small glands open into the urethra; when these glands become dilated, they can form outpouchings or urethral diverticula. The glands group together on either side of the urethra to form the Skene's glands and empty just lateral to the external urethral meatus, which is anterior to the vagina. The distal two-third of the female urethra are surrounded by the striated urethral sphincter. The pudendal and pelvic nerves provide somatic innervation to the striated urethral sphincter.

The female urethra is supplied by the interior pudendal, vaginal, and inferior vesical arteries and veins.

Embryology

Male Urethra

The male urethra is mainly derived from the urogenital sinus. The upper portion forms the bladder, the pelvic part forms the posterior (prostatic and membranous) urethra. The phallic part forms the anterior urethra. As the genital tubercle elongates to form the penile shaft and glans, a ventral groove on the genital tubercle, called the urethral groove, forms during the 6th week. As the urethral groove deepens, it forms the urethral plate, which extends into the glans penis. The urethral folds then fuse under the influence of dihydrotestosterone to form the penile urethra. The glanular urethra results from the ectoderm growing into and cannulating the distance between the glans to the urethral folds.

Female Urethra

The female urethra is also derived by the urogenital sinus. The entire urethra and upper portion of the vagina develop from the pelvic portion of the urogenital sinus. In the absence of dihydrotestosterone, the labioscrotal and urethral folds do not fuse across the midline, thus the lack of development of the penile urethra.

Congenital Abnormalities of the Urethra

Congenital Urethral Strictures

Urethral strictures can be congenital or acquired. Congenital urethral strictures are most common in the proximal bulbar urethra or the fossa navicularis; they are postulated to result from inadequate fusion of the anterior and posterior urethra. Acquired strictures result from inflammatory, ischemic, or traumatic processes that lead to scar formation and reduce the caliber of the urethral lumen.

The age of presentation generally reflects the severity of the stricture [81]. Patients will often present with lower urinary tract voiding symptoms such as difficulty voiding, weak stream, progression to urinary retention, urgency, and frequency, as well as painful ejaculation. Children may present with recurrent UTI, urinary incontinence, or failure to thrive. Irreversible renal injury can occur in severe cases. Urethral obstruction can present with hydronephrosis on antenatal ultrasound. Treatment depends on the severity of the lesion and symptoms. Diagnosis is based on retrograde urethrogram or cystoscopy. Urethral reconstruction with excision of the stenotic segment, urethral dilation, or direct visualizing internal urethrotomy, performed endoscopically, are the most common treatments.

Urethral Meatal Stenosis

Stenosis of the urethral meatus refers to a narrowing of the urethral opening. It is common in circumcised boys; it is presumed to be caused by irritation of the exposed meatus, which leads to its narrowing. Symptoms vary according to the severity of the stenosis and are those related to obstruction of the urinary flow, presenting with dysuria, hematuria, or other lower urinary tract symptoms. Though many patients with meatal stenosis are asymptomatic, patients will commonly present with a fine-caliber urinary stream and/or upward deviation of the urinary stream. Treatment, when required, is an incision of the ventral meatus (meatotomy or meatoplasty).

Posterior Urethral Valves

Posterior urethral valves (PUV) are membranes or folds of tissue derived from an anomalous insertion of Wolffian ducts into the cloaca (Type I) or an incomplete dissolution of the urogenital membrane (Type III) (Fig. 13.18). It is the most common cause of lower urinary tract obstruction in male infants, with an incidence of 1 in 8000–25,000 newborn boys [82]. It is life-threatening, associated with great prenatal and postnatal morbidity and mortality and the most common condition leading to end-stage renal disease in male children (25–40%) [83].

Classification: Type I Two membranous structures in the posterior urethra originating from the caudal end of the verumontanum and rising along the lateral margin of the urethra on each side, meeting at 12 o'clock. **Type III:** Circular diaphragm in the region of the caudal end of the verumontanum, with a central defect. Type II valves are no longer considered to exist [84].

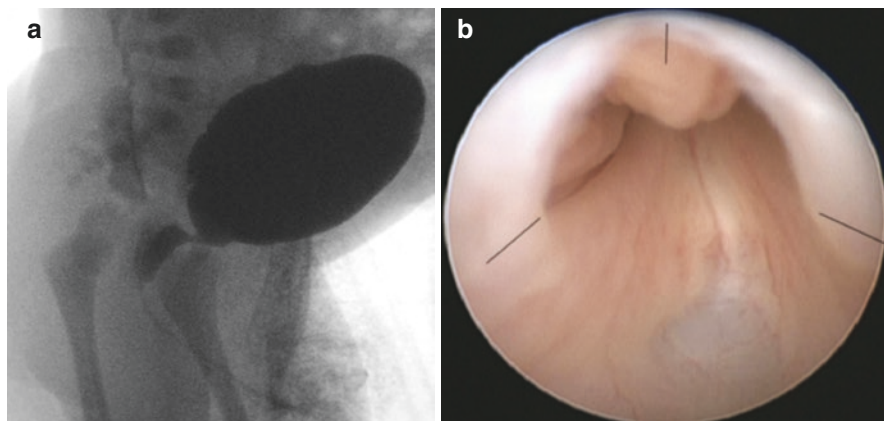


Fig. 13.18 Posterior urethral valves, Type 1 variant. (a) Voiding cystourethrogram confirming posterior urethral valves with urethral obstruction and associated dilatation of the posterior urethra. (b) Obstructing valve tissue

Fig. 13.19 Posterior urethral valve. The “keyhole sign” seen on antenatal ultrasound demonstrates dilatation of the bladder and of the posterior urethra



Valves can present in a spectrum of severity, depending on the degree of obstruction. Because obstruction starts early during fetal development, renal dysplasia is likely to occur in severe forms. The high pressure generated by the bladder in the attempt to empty will predispose to VUR and associated hydronephrosis. Urinary outlet obstruction and retention will reduce amniotic fluid (oligohydramnios), resulting in pulmonary hypoplasia and Potter sequence [85], characterized by low-set ears, wide-set eyes, micrognathia, limb contractures, and club foot.

With the increased use of obstetric ultrasound, most cases of PUV are diagnosed prenatally. The presence of a dilated bladder, distended posterior or prostatic urethra (“keyhole sign”) (Fig. 13.19), hydronephrosis, and associated oligohydramnios on prenatal ultrasound are signs of PUV. The future mother should be

counseled by a multidisciplinary team including an obstetrician, neonatologist, and pediatric urologist.

At birth, the neonate will present with delayed voiding or a weak stream. Distension of the bladder may be palpable in the suprapubic region, and palpable kidneys may be appreciated. If severe oligohydramnios was present, respiratory distress due to pulmonary hypoplasia can be found. Late presentation of boys with PUV is less common in industrialized nations, owing to prenatal imaging; when seen, they often present with weak stream, straining to void, urinary incontinence, and/or UTI. Associated hydronephrosis and renal compromise are common [86].

If PUV is suspected, initial management is based on bladder decompression with a catheter. Initial evaluation includes bladder and kidney ultrasound, VCUG, and serum levels of urea, creatinine, and electrolytes. Prompt evaluation with VCUG should be performed to confirm the diagnosis and allow prompt definitive intervention. Renal scintigraphy after 6–12 weeks of life can aid in evaluation of differential renal function and drainage.

Management of neonates with PUV is complex and requires an intensive care unit and a specialized team. Antenatal intervention has been proposed but remains controversial; it includes vesicoamniotic shunt [87], percutaneous fetal cystoscopy with valve ablation [88], or vesicostomy. Antenatal intervention should only be considered in the fetus with severe obstruction, identified early in pregnancy (second trimester) with associated oligohydramnios and poor renal function [86].

The first therapeutic measure in neonates is bladder drainage with a feeding tube. The catheter should be left in place until the neonate is stable, as these patients are at risk for respiratory problems, uremia, electrolyte imbalance, metabolic acidosis, and infection. When the patient is considered stable, endoscopic valve ablation is indicated (Fig. 13.20). In premature, small infants in whom the urethra is too small to accommodate endoscopic intervention, or in those whose renal function (serum creatinine >1.0 mg/dL) and hydronephrosis have not improved with catheter drainage, urinary diversion (ureterostomy or vesicostomy) should be considered [89].

After initial treatment, patients with PUV must be followed throughout their lives, as they are prone to develop voiding dysfunction due to the hypertrophied detrusor, later worsening of hydronephrosis, and compromised renal function. Many of these patients will progress to end-stage renal disease and require transplantation. Patients with high-pressure, poorly compliant bladders may require clean intermittent catheterization to empty their bladders. Voiding dysfunction and associated urinary incontinence can also be long-term problems. The goal of treatment is to maintain a low-pressure bladder and avoid progressive deterioration of renal function [89]. Monitoring should include urodynamic studies, serial kidney and bladder ultrasound, nuclear DMSA scan, as well as periodic monitoring of electrolytes and serum BUN and creatinine.

Anterior Urethral Valves

Anterior urethral valves are rare and can occur in any portion of the urethra. The condition is usually associated with urethral diverticulum. Symptoms vary according to the degree of obstruction, including recurrent UTI, difficulty with urination,

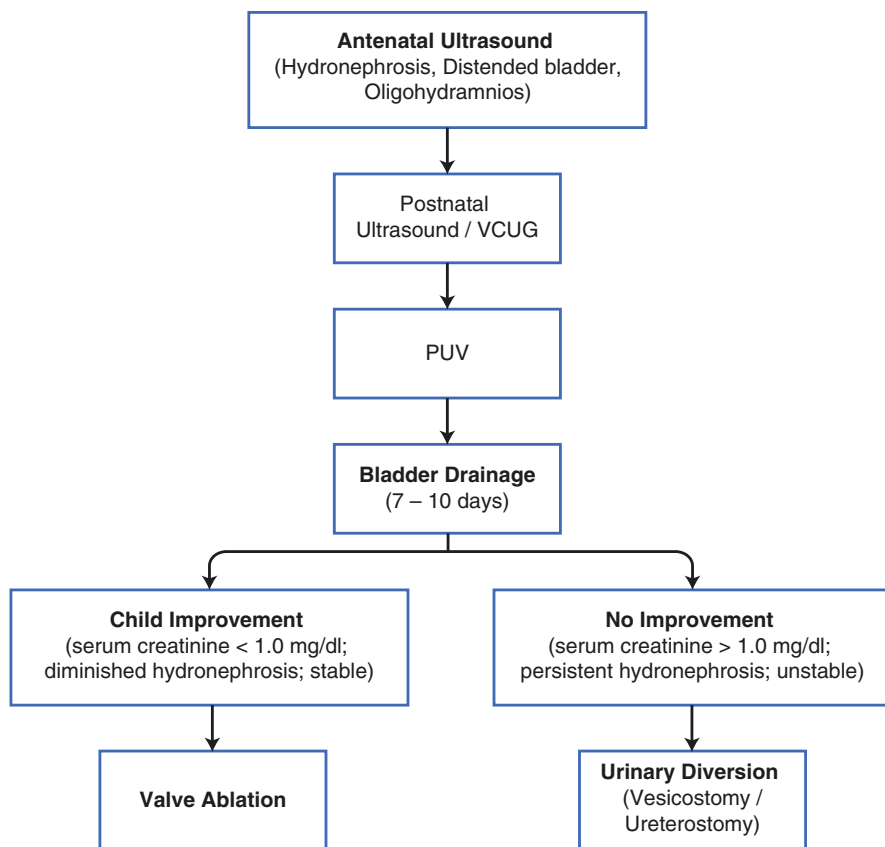


Fig. 13.20 Algorithm for management of posterior urethral valve (PUV). VCUG voiding cystourethrography

or even end-stage renal disease [90]. Treatment follows the same indication as in PUV. Endoscopic valve ablation is the procedure of choice, especially if the condition is not associated with a large diverticulum. In severe cases, urinary diversion can be performed prior to definitive treatment [91].

Urethral Diverticulum

Urethral diverticulum refers to an outpouching of the urethra. It is more common in females than in males, and accounts for up to 84% of periurethral masses in women [92]. It typically occurs in women after the second decade of life and can be caused by obstructed periurethral glands that rupture into the urethral lumen. Symptoms are nonspecific, and can present as postvoid dribbling, dysuria, dyspareunia, frequency, urgency, and hematuria. UTI is frequently present [93]. Because of the non-specificity of the symptoms, diagnosis is often delayed, on average up to 5 years [94]. Diagnosis is made with VCUG and/or MRI (Fig. 13.21). Treatment consists of resection of the diverticulum and urethral reconstruction.

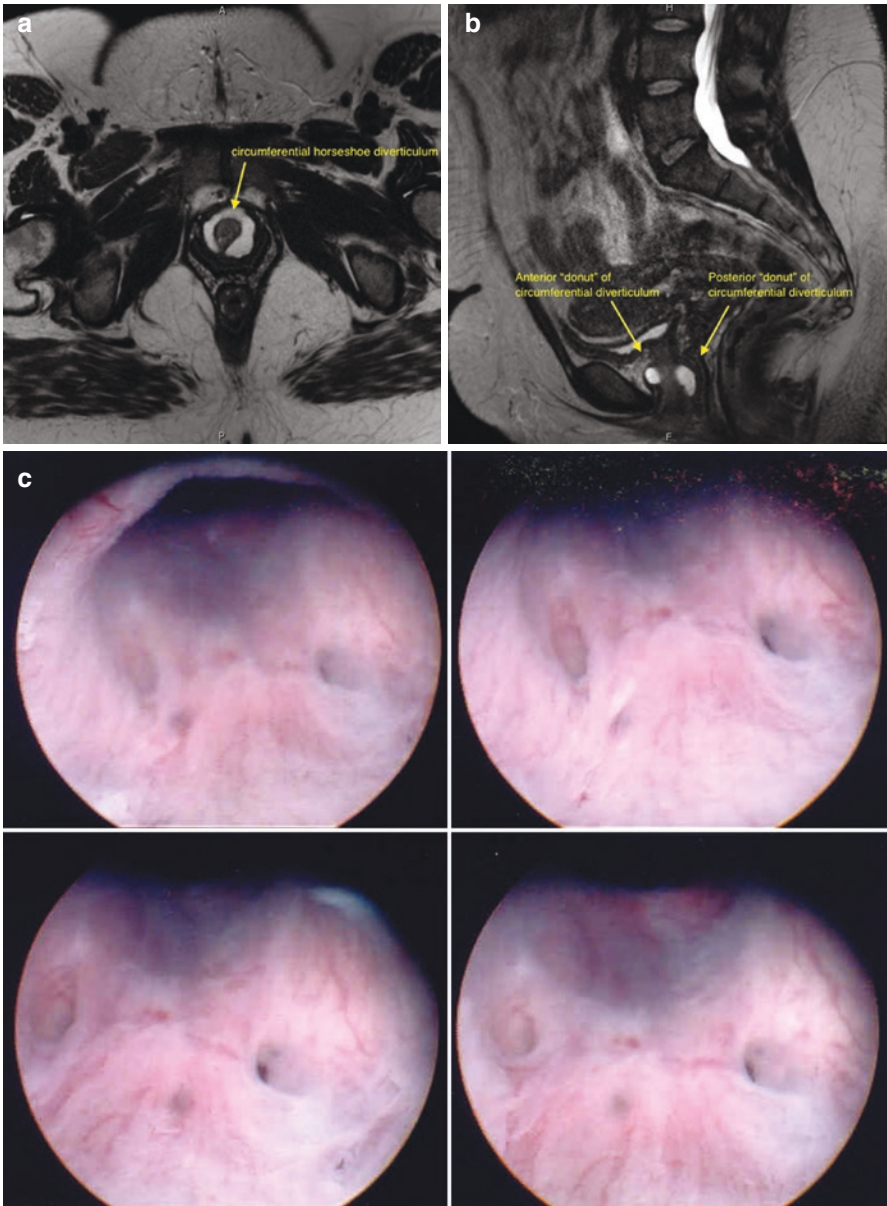


Fig. 13.21 Urethral diverticulum. (a) MRI demonstrating circumferential diverticulum in female urethra. (b) Endoscopic view of urethra and orifice to urethral diverticulum. (c, d) Bulge at anterior vaginal wall from urethral diverticulum (Tic)



Fig. 13.21 (continued)

In the male urethra, it can be related to anterior urethral valves, either with the valve causing obstruction and development of the diverticulum, or the diverticulum burrowing under the mucosa and causing obstruction, presenting as a flap valve [95]. There is a lack of the corpus spongiosum observed at the location of the diverticulum, and swelling of the ventral aspect of the penis can be seen (Fig. 13.22). It may be associated with UTI and urinary tract obstruction, with associated consequences. Diagnosis is made with VCUG, ultrasound, and/or urethroscopy. The best treatment option is diverticulum excision and urethral reconstruction [95].

Urethral Duplication

Duplication of the urethra is a rare congenital anomaly in which the urethra is duplicated in the sagittal plane (Fig. 13.23). This can be a complete duplication, tracking back to the bladder, or incomplete, arising from a more distal urethral location. The ventrally located urethra is usually the patent urethra. The dorsally positioned urethra may be blind-ending or associated with bladder exstrophy and epispadias. According to the classification by Effmann et al. [96], urethral duplication is divided into three types:

- Type 1 is an incomplete duplication (type 1A: distal incomplete duplication; type 1B: proximal incomplete duplication).
- Type 2 is a complete urethral duplication (type 2A: complete duplication with two meatuses; type 2B: only one meatus).
- Type 3 is urethral duplication as a component of complete or partial caudal duplication.

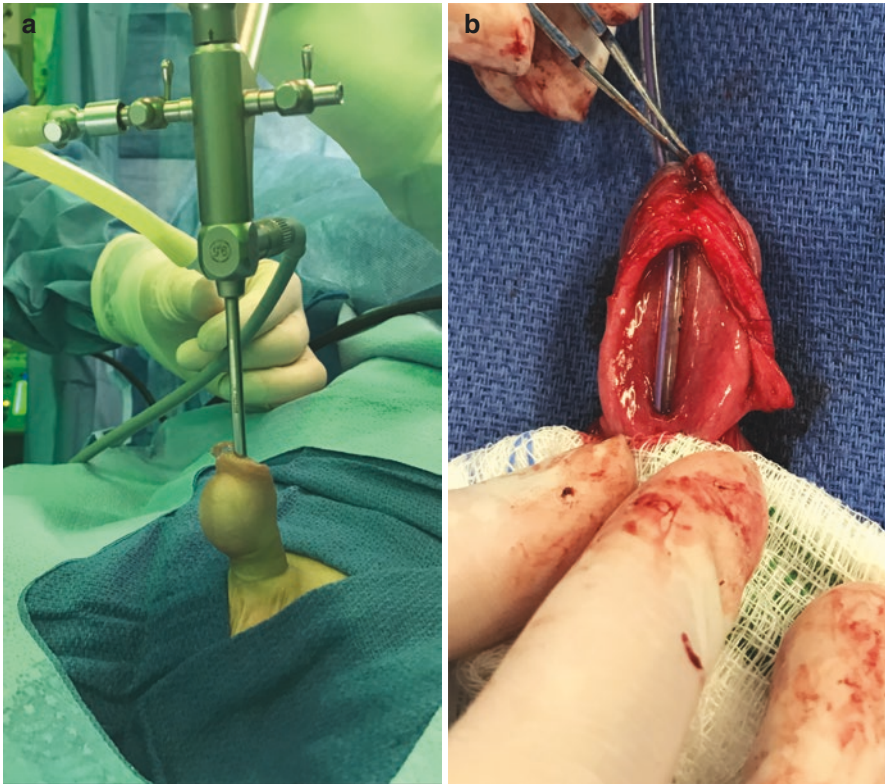


Fig. 13.22 Urethral diverticulum in a male patient. **(a)** Congenital urethral diverticulum in male patient, identified based on ballooning of ventral shaft with urination. **(b)** Diverticulectomy and urethroplasty performed to correct a urethral diverticulum

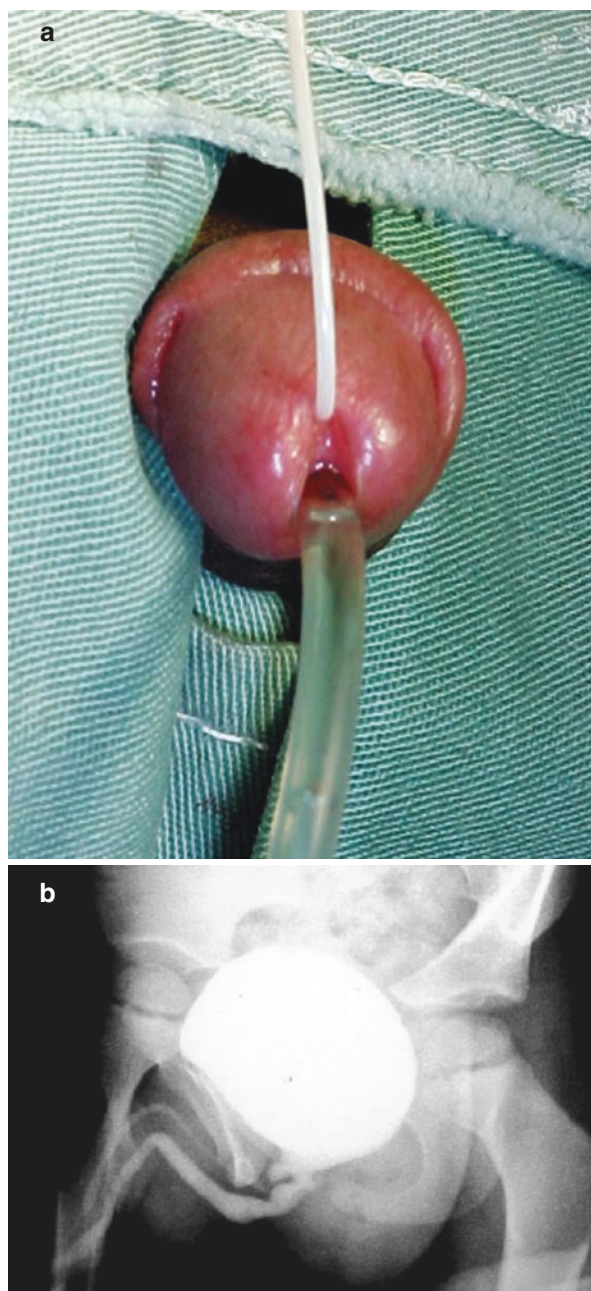
Patients can be asymptomatic, with only a small sinus close to the penopubic angle, but most present with urethral discharge, urinary incontinence, or UTI. Treatment in symptomatic cases is the resection of the accessory urethra. In complex cases, a more complex reconstruction may be indicated [97].

Male Penis

Anatomy

The penis is composed of three erectile bodies and the urethra. The three erectile bodies include the two-corpus cavernosa, which join beneath the pubis to form the majority of the penile body. The corpus cavernosa are separated by a septum that

Fig. 13.23 Duplicate urethra. **(a)** Duplicate urethra with catheter placed into the dorsal, smaller urethral lumen. **(b)** Voiding cystourethrogram (fluoroscopy) demonstrating normal-caliber ventral urethra and smaller, dorsally displaced urethra into a complete duplication



allows free communication between the two bodies and are enclosed by the tunica albuginea. Smooth muscle bundles surround the erectile bodies to form the endothelium-lined cavernous sinuses. The corpus spongiosum lies ventral to the corpus cavernosa and dilates distally to form the glans penis. The anterior urethra runs throughout the entire length of the corpus spongiosum.

The deep fascia or Buck's fascia surrounds the cavernosal bodies dorsally and splits to cover the spongiosum ventrally. Proximally at the perineum, it fuses with the tunica albuginea. Distally, it forms the corona at the base of the glans penis. The superficial fascia or dartos fascia is loosely attached to Buck's fascia on the penis. The dartos is also present in the scrotum and is contiguous with Scarpa's fascia in the abdomen and Colle's fascia in the perineum.

The arterial blood supply of the penile skin is different from the blood supply of the erectile bodies. The penile skin receives its blood supply from the external pudendal artery off of the femoral vessels, whereas the erectile bodies receive their blood supply from the internal pudendal artery, branching as the common penile artery. The common penile artery has three branches:

- The *bulbourethral artery* penetrates the perineum to supply the corpus spongiosum, the glans, and the urethra.
- The *cavernosal artery* supplies the cavernosal bodies. It gives off straight and helicine arteries. Erections are produced by dilation of the helicine arteries in conjunction with the sinusoidal smooth muscle relaxation.
- The *dorsal artery* travels just lateral to the deep dorsal vein and medial to the dorsal nerve on the underside of Buck's fascia. It gives off cavernous and circumferential branches to supply the spongiosum and urethra.

Penile arterial anatomy is highly variable. The cavernosal artery may be absent, or one might supply bilateral cavernosa. Accessory pudendal arteries may also supplement or replace the common penile artery branches.

The penis has three venous drainage systems:

- The *superficial system* drains the superficial penis and coalesces into the superficial dorsal vein, which drains into the left saphenous vein; sometimes it can also drain into the right saphenous vein.
- The *intermediate veins* include the deep dorsal and circumflex veins, which lie within and deep to Buck's fascia. They drain the erectile bodies and drain into the prostatic plexus.
- The *deep veins* include the crural and cavernosal veins, which drain into the internal pudendal vein.

The superficial inguinal lymph nodes drain the skin from the foreskin and penile shaft, and the deep inguinal lymph nodes drain the glans.

The penis receives innervation from the pudendal and cavernosal nerves. The pudendal nerves supply somatic motor and sensory penile innervation. The cavernous nerves supply parasympathetic innervation from S2 to S4 nerve fibers and induce erections.

Embryology

The formation of the external genitalia begins with the division of the cloacal folds, which develop on each side of the cloaca. They meet anteriorly to form the genital tubercle. The cloacal folds flanking the opening of the urogenital sinus become the urogenital folds; labioscrotal folds appear next to the urogenital folds. In males, the genital tubercle elongates to form the penile shaft and glans. A ventral groove on the genital tubercle, called the urethral groove, forms during the 6th week. The groove deepens to form the urethral plate, which extends into the glans penis. The urethra is tubularized as the lateral aspect of the urethral groove or urethral folds fuse to form the penile urethra. In females, the genital tubercle becomes the clitoris and the urogenital folds become the labia minora. The labioscrotal folds become the scrotum in males and the labia majora in females.

Congenital Anomalies of the Penis

Phimosis

Phimosis occurs when the foreskin is narrow and the prepuce cannot be retracted to exposes the glans (Fig. 13.24a). The inability to retract the prepuce is physiologic at birth, owing to adhesions between the glans and the prepuce. As the child grows, erections will stretch the phimotic narrowing. Epithelial debris (smegma) accumulates under the prepuce, gradually separating the foreskin from the glans, and the majority of boys will have their foreskin retractable by the age of 3 or 4 years [98]. Inflammatory or traumatic injury to the prepuce, occurring at any age, may result in pathologic phimosis due to scar formation or cicatrix of the opening of the foreskin, preventing retraction of the prepuce.

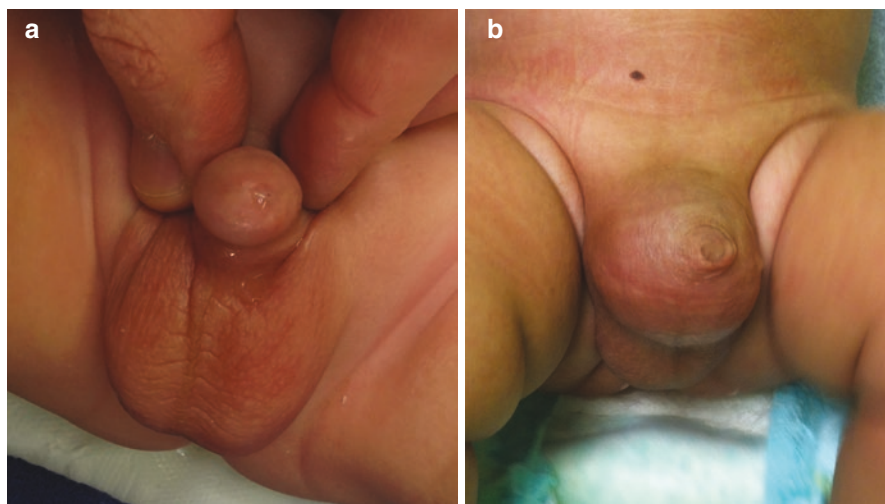


Fig. 13.24 Phimosis. (a) Congenital, physiologic phimosis. (b) Urine trapping and associated ballooning of the foreskin

Fig. 13.25 Paraphimosis. Uncircumcised boy with foreskin and phimotic band retracted proximal to the glans, causing constriction and distal penile edema



Phimosis can be associated with balanoposthitis, UTI, sexually transmitted diseases, and pain, as well as discomfort during erections and sexual intercourse. In tight phimosis, urine can become trapped in the foreskin, with associated ballooning (Fig. 13.24b). Persistent retraction of the foreskin with constriction of the distal penis can lead to swelling and inflammation, termed *paraphimosis* (Fig. 13.25). This condition is addressed by compressing the distal shaft skin, manipulating out the edema, and readvancing the foreskin over the glans.

Penile malignancy may occur in those with poor hygiene habits and phimosis, though overall it is rare. The presence of any of these complications is an indication for treatment of the phimosis, either with medical management using steroid cream or with circumcision, the surgical removal of the prepuce. Different types of steroid cream have been safely used to treat the phimotic ring, with a success rate of 67–95%, avoiding circumcision [98, 99].

The prevalence of neonatal circumcision has fluctuated over the years, being more common in specific cultures and geographic locations. It remains controversial, though more recently has gained support by the American Academy of Pediatrics [100, 101]. Circumcision is also widely performed for religious reasons, being a fundamental part of the Jewish and Muslim faiths.

Neonatal circumcision is usually performed under local anesthesia, using a clamp device (Gomco, Mogen, or Plastibell). Circumcision in older children is most often performed under anesthesia and performed with an incision technique at the inner and outer aspects of the preputial skin, excision of skin, and suture anastomosis, or using a plastic ring device [102].

Penile Torsion

Penile torsion is characterized by abnormal rotation of the penis (in some cases, only the glans). The rotation is more common to the left side, counterclockwise (Fig. 13.26) [103]. The degree of torsion varies from mild to severe (180°), but torsions greater than 90° are rare (0.7% of cases) [104].

Fig. 13.26 Penile torsion. Patient with counterclockwise penile torsion, $>45^\circ$



The cause of torsion is usually restricted to the skin and dartos. Although in most cases (torsion $<90^\circ$), surgical correction is not necessary, parents and patients will ask for it for cosmetic reasons. In those cases, degloving the penis and releasing all attachments from the skin to the inner layers and realigning the penis will resolve the problem [105]. More severe torsions ($>90^\circ$) will need more complex reconstruction [106, 107].

Buried Penis

Buried or concealed penis refers to a condition in which the penis is partially or completely hidden or trapped beneath the prepubic fat (Fig. 13.27). It is important to note that the hidden penis is normal in length, so this is a different condition from micropenis.

A concealed penis may represent one of several conditions:

- *Buried penis*, in which there is a lack of penile skin anchoring to deep fascia, and/or redundant suprapubic fat.
- *Webbed penis*, when there is a continuity of the penile and scrotal skin, not forming the penoscrotal angle.
- *Trapped penis*, when the penis is entrapped by the prepubic skin due to scar tissue [108].
- The so-called *congenital megaprepuce*, in which a prepuce sac is formed in consequence of a phimotic ring and ballooning of the foreskin [109] (Fig. 13.28).

Fig. 13.27 Buried or concealed penis. A normal penis (not seen) is concealed in a prominent suprapubic fat pad



Concern about a small penis is common, often leading to referral to a pediatric urologist. Symptoms of urinary retention, dilation of the prepuce (ballooning) during micturition, post-voiding dribbling, and infection may also be present [101]. Before recommending surgical treatment, the diagnosis of micropenis should be excluded and the patient/family should be reassured that the penis is of normal size. The main goal of the surgery is usually cosmetic. It consists of removal of prepubic fat, anchoring the Buck's fascia to the suprapubic tissue and/or prepucioplasty [110].

Penoscrotal Webbing

Penoscrotal webbing or “webbed penis” refers to fusion of the ventral penile skin to the scrotum. The penis is tethered to the scrotum in the midline, so the penoscrotal angle is obscured. The tethered scrotal skin will then be pulled distally with the penile skin during an erection, creating the impression of a “sail of skin” tethered to the ventral penile shaft (Fig. 13.29).

Frenulum Breve

Frenulum breve refers to a short or tight frenulum, which prevents the foreskin from being retracted completely. It can cause ventral curvature and pain with sexual activity. Treatment consists of division of the frenulum.

Microphallus

Microphallus or micropenis refers to an abnormally small penis—one that is at least 2.5 standard deviations below the mean for the age, based on the stretched penile



Fig. 13.28 (a) Concealed penis with phimosis. (b) Urine trapping and associated ballooning of the foreskin. (c) Congenital megaprepuce due to urine trapping and dilation of the inner preputial skin

length [111]. A careful evaluation should be performed prior to confirmation of the diagnosis, which can cause great psychological harm to the patient and his family.

The most common causes of micropenis are hypogonadotropic hypogonadism or hypergonadotropic hypogonadism, or it can be idiopathic. Cryptorchidism and small testes and scrotum can be present.

Treatment is focused in increasing penile size to improve body image. Exogenous testosterone (either topical or intramuscular) is the treatment of choice. If satisfactory size is not achieved, penile reconstruction or gender reassignment have been proposed, but outcomes are debatable [111].

Fig. 13.29 Penoscrotal fusion or “webbed penis”



Congenital Penile Curvature

Congenital penile curvature, or chordee, is most often associated with ventral or downward curvature of the penis, but it also can present as lateral curvature (Fig. 13.30). Isolated ventral curvature is not uncommon, although in most cases it is associated with hypospadias. The etiology of isolated ventral penile curvature can be related to skin tethering, fibrotic Buck's and dartos fascia, and corporeal disproportion [112]. A short congenital urethra is the cause of curvature in only about 7% of cases [112].

Children with suspected penile curvature should be evaluated by pressing the suprapubic fat, or sometimes by asking the parents to take a photo of the penis during erection. In cases of significant curvature, surgery is considered to prevent problems during sexual intercourse in the future. Reevaluation of the curvature with artificial erection is the first step of the treatment. Surgery consists of degloving the penis, release of all skin adhesions and the frenulum, excision of any fibrotic tissue, and, when needed, dorsal plication, and/or ventral grafts [104].

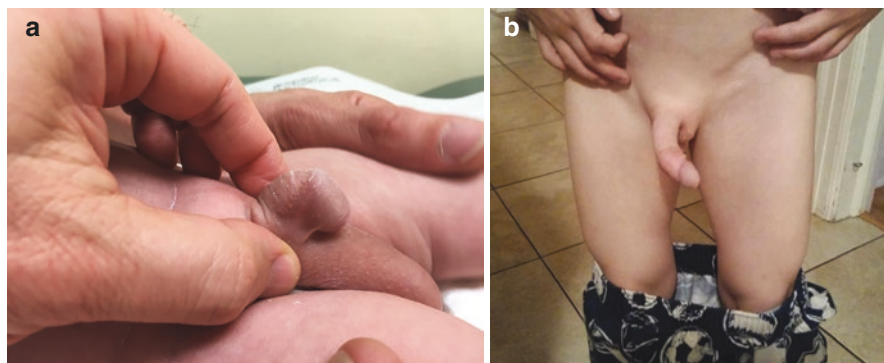


Fig. 13.30 Penile curvature. (a) Ventral curvature (chordee) and associated penoscrotal webbing. (b) Lateral penile curvature

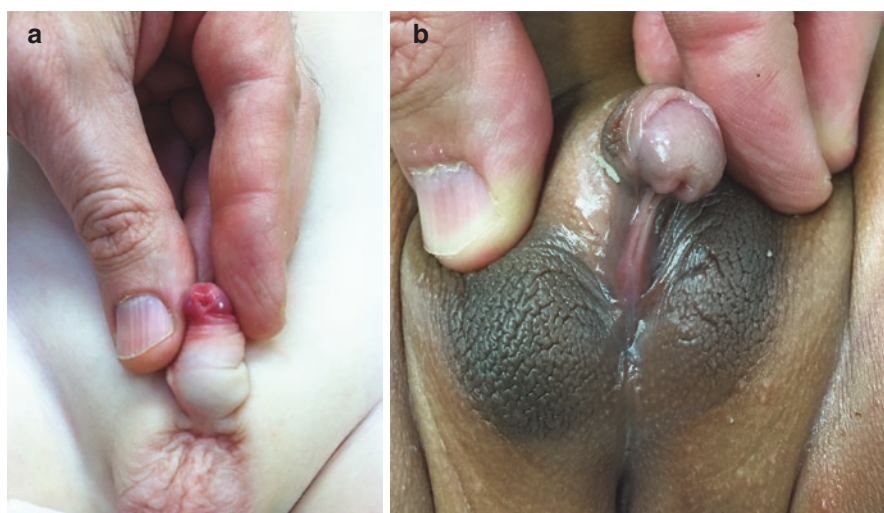


Fig. 13.31 Hypospadias. (a) Mild glanular hypospadias. (b) Proximal penoscrotal hypospadias

Hypospadias

Hypospadias is an arrest in penile development, with incomplete closure of the ventral aspect of the penis; it is characterized by an ectopically located urethral meatus on the ventral aspect of the penis. There is a spectrum of severity ranging from a mild form with a distal location of the meatus at the glans to severe, proximal hypospadias, with the urethral meatus located at the scrotum or perineum (Fig. 13.31). A preputial “dorsal hood” (due to an incomplete ventral closure of the foreskin) is present on the dorsal aspect of the penis. A ventral curvature is present in up to 33% of patients with more distal hypospadias [113] and in about 81% of the more severe,

proximal cases [114]. Hypospadias is a common anomaly, with an incidence varying among different regions; it ranges from 0.05% to 0.5% of boys worldwide [115].

Associated findings with hypospadias include cryptorchidism in 8–10% of cases and inguinal hernia in 9–15% [116]. When cryptorchidism is found in the presence of a proximal hypospadias, the diagnosis of disorder of sex development (DSD) should be considered and a karyotype and other genetic testing obtained (i.e., assessment of the androgen receptor). In more severe cases, an enlargement of the prostatic utricle may be present, which can lead to difficulty with urethral catheterization. Diagnosis of hypospadias is made during a clinical visit and on physical examination; imaging tests are usually not needed.

The goal of hypospadias correction is to achieve a good cosmetic appearance, straight penis, and normal function. Hypospadias surgery requires reconstruction of the penis, including urethroplasty with positioning of the urethral meatus on the tip of the glans, correction of the penile curvature, and reallocation of dorsal skin to correct ventral penile skin deficiency. Mid-shaft and distal hypospadias surgery is done in one stage, but severe, proximal hypospadias may require a staged procedure. The first stage aims to correct the ventral curvature and transfer skin or buccal mucosa to the ventral location to be used for subsequent urethroplasty. The second stage includes urethroplasty and glansplasty, bringing the urethral meatus to the orthotopic location. Many different techniques have been described, and the pediatric urologist should be able to choose the most appropriate technique for each case. Circumcision is performed in most hypospadias repairs, though foreskin reconstruction can be considered in repairs of mild, distal hypospadias.

The ideal age for hypospadias surgery is between 6 and 18 months [117, 118]. Optical magnification, fine instruments, and absorbable suture should be used to diminish tissue trauma and the risk of complications. The most common surgical complications of hypospadias repair include urethrocuteaneous fistula, urethral stricture, meatal stenosis, partial or complete wound dehiscence, persistent ventral curvature, and urethral diverticulum. Correction of surgical complications should be staged 6–9 months after initial repair, to allow complete healing with reduced scar tissue.

Epispadias

Epispadias is characterized by a dorsal positioning of the urethral meatus from the tip of the glans (Fig. 13.32). It is commonly associated with the bladder exstrophy complex. Epispadias without bladder exstrophy is extremely rare, occurring up to 1/11,700 males and 1/300,000 females [119]. In males, a dorsal curvature is seen, whereas a bifid clitoris is seen in females. The epispadiac penis is usually short. Many patients (35–85%) present with associated VUR [120]. Children with more severe epispadias, with a urethral defect as proximal as the bladder neck, will commonly experience urinary incontinence. These patients will also present with pubic diastasis.

Prior to treatment, evaluation of bladder capacity and VUR should be done.

Treatment consists of penile reconstruction, urethroplasty, plastic correction of the glans and prepuce, and correction of the dorsal curvature. If incontinence

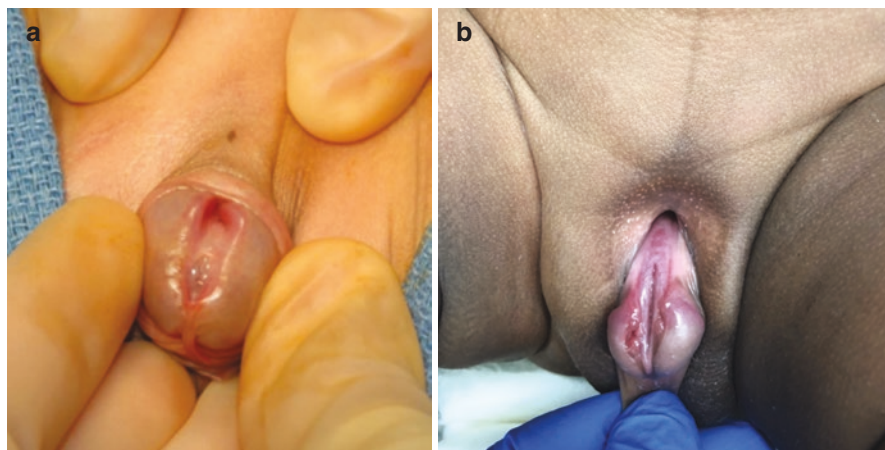


Fig. 13.32 Epispadias. (a) Glanular epispadias. (b) Penopubic epispadias

persists later in life, subsequent bladder neck reconstruction, often with associated ureteral reimplantation, is required to allow continence [120].

Penile Agenesis

Aphalia or penile agenesis is a very rare anomaly (affecting 1 in 30 million males) that is caused by failure of development of the genital tubercle. The phallus, including the erectile bodies, is completely absent, and the urethra opens along the perineum or goes to the rectum. It may be associated with renal aplasia or dysplasia and other caudal anomalies [121]. Gender reassignment has historically been applied to treat these patients, although more recently, better surgical techniques have allowed for neophalloplasty with acceptable results [122].

Penile Duplication

Diphallia or penile duplication is a very rare condition (1 in 5 or 6 million) caused by incomplete fusion of the genital tubercle. It is usually associated with other congenital abnormalities, including bladder exstrophy, cloacal exstrophy, duplicated bladder, hypospadias, and imperforate anus. Treatment consists of reconstruction of the penis, with or without excision of the smaller phallus.

Testicle/Scrotum

Anatomy

The scrotum, where the two testicles are located, is an extension of the abdominal wall inferior and posterior to the penis. The scrotum wall is composed of six layers, described in Table 13.4. The muscle layers of the scrotum serve as a thermoregulatory mechanism for the testis, contracting or relaxing depending on the outside temperature.

Table 13.4 Layers of the abdominal wall and scrotum

Abdominal wall	Scrotum
Skin	Skin
Scarpa's fascia	Dartos muscle
External oblique muscle	External spermatic fascia
Internal oblique muscle	Cremasteric muscle and fascia
Transversus abdominis muscle	–
Transversalis fascia	Internal spermatic fascia
Peritoneum	Tunica vaginalis

The right testicle lies lower than the left in approximately 85% of men. A fibrous capsule called the tunica albuginea covers the testis. The epididymis is located posterior to the testicle and connect the testicle to the vas deferens. The testicle and epididymis are surrounded by a serous membrane called the tunica vaginalis, which is an extension of the peritoneum.

The arterial supply to the testicles comes from three sources:

- The *testicular artery* or *internal spermatic or gonadal artery*, which arises from the aorta, just inferior to the superior mesenteric artery. It courses down the retroperitoneum, crosses anterior and lateral to the ureter, and enters the scrotum as part of the spermatic cord.
- The *cremasteric artery* arises from the inferior epigastric artery, which branches from the external iliac artery, and anastomoses with the testicular artery in the testis.
- The *artery to the vas deferens*, which is a branch of the inferior vesical artery that branches from the internal iliac artery.

The scrotum and the rest of the external genitalia receive their arterial blood supply from the internal pudendal artery, which is a branch of the internal iliac artery.

The venous drainage from the testicle traverses the pampiniform plexus in the spermatic cord, which ultimately coalesces into the gonadal vein. The right gonadal vein drains into the inferior vena cava, and the left gonadal vein drains into the left renal vein. Lymphatic fluid from the testes drains into the retroperitoneum. On the right, the primary drainage is to the interaortocaval nodes, followed by the precaval and preaortic nodes. On the left, the primary drainage is to the paraaortic and preaortic lymph nodes, followed by the interaortocaval lymph nodes. The scrotal lymphatic fluid drains into the inguinal lymph nodes.

Testicular innervation arises from the aortic and renal plexus, so renal pathology can lead to referred pain in the testicle. It also arises from the pelvic plexus. The scrotum and tunica vaginalis are innervated by the genital branch of the genitofemoral nerve.

Embryology

The genital ridge differentiates under the influence of the sex-determining region of the Y chromosome (the *SRY* gene) into the seminiferous tubules, Sertoli cells, and the Leydig cells. The tunica albuginea, which is a connective tissue layer,

compartmentalizes the testicle. The mesonephric or Wolffian ducts become the epididymis, vas deferens, seminal vesicles, and the ejaculatory ducts. The most cranial aspect becomes the vestigial appendix epididymis.

The testes migrate caudally from their location near the developing kidney at about 7–8 weeks of gestation. They are held by two ligamentous structures, the cranial suspensory ligament dorsally and what becomes the gubernaculum ventrally. By week 10–15, the testes have migrated from the abdomen to the internal inguinal ring. From month 3 to 7, the gubernaculum enlarges and the cranial suspensory ligament regresses. The gubernaculum enlarges and swells past the external inguinal ring and descends into the scrotum, creating an outpouching of the peritoneum called the processus vaginalis, through which the intra-abdominal testis exits the abdominal cavity into the scrotum. The scrotum is formed by the fusion of the labioscrotal folds. Once the testis migrates into the scrotum, the gubernaculum regresses and the processus vaginalis closes.

Congenital Abnormalities of the Testes and Scrotum

Cryptorchidism

Undescended testis or cryptorchidism is defined as the failure of the testis to descend into to the scrotum. It is one of the most common genital anomalies in boys, affecting 1–4% of full-term and up to 30–45% of preterm boys [123, 124]. Spontaneous testicular descent after birth may occur at about 60–90 days of life [125], and only about 0.8% of boys will still have undescended testis by the age of 6 months [126]. The likelihood that an undescended testis will migrate to the scrotum after 12 week of life is very low [127], so the child should be referred for further evaluation and treatment planning, as it is in the first 3–6 months of life that transformation of spermatogonia into the adult dark type occurs. In boys with cryptorchidism, Sertoli cell development is diminished, reducing this transformation [128]. Surgery for the undescended testicle, orchiopexy, is recommended between 6 and 18 months of life.

Testicular descent is divided into two stages, the abdominal and scrotal stages. In the abdominal stage, swelling and strengthening of the distal gubernaculum occurs. The scrotal stage is influenced by androgens, leading to an involution of the gubernaculum and its fibrous adherence to the inside of the scrotum [129]. Genetic inheritance has been demonstrated. Those with family history of undescended testis are 2.3–3.5 times more likely to present with cryptorchidism [130]. Exposure during pregnancy to diethylstilbestrol, some pesticides, or cigarette smoking, and problems such as preconception endometriosis and gestational diabetes have been correlated with an increased risk for undescended testicles [131].

Undescended testicles can be unilateral or bilateral and can vary in severity. In approximately 90% of cryptorchidic boys, the testes are palpable in the inguinal channel; about 10–20% are nonpalpable, in an intraabdominal location (Fig. 13.33) [129, 132]. The testes can be present anywhere along the path of descent, including the abdomen (as cranial as the kidney), along the inguinal canal, and in the upper part of the scrotum. The testis can also be ectopically located (outside the path of descent) in the perineum, thigh, or at the penile base (Fig. 13.34).

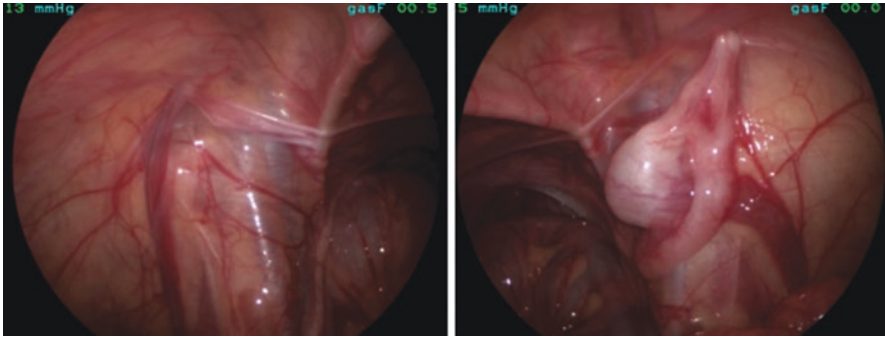


Fig. 13.33 Laparoscopic view of a right abdominal testicle

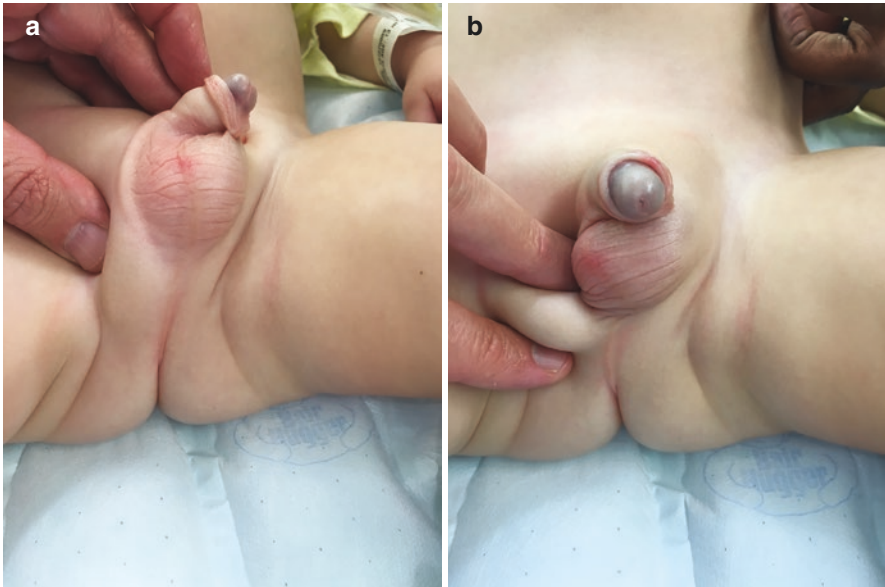


Fig. 13.34 Ectopic right testicle, (a) distal and (b) lateral to the scrotum

Undescended testes can be classified by the position where they are found during physical examination as nonpalpable, inguinal, suprascrotal, or high scrotal. Of nonpalpable testes, 50–60% may be present in the abdominal cavity (Fig. 13.33), but about 20% are absent owing to testicular agenesis or perinatal testicular torsion (Fig. 13.35), and 30% are atrophic [133].

Undescended testicles can be congenital or acquired, as a previously descended testis may ascend as the child grows, especially in retractile testis. The testis can also be retractile secondary to an active cremasteric reflex. A retractile testis is normal in size and can be easily manipulated back to the scrotum, where it should remain after manipulation, or it may reside spontaneously in the scrotum for some of the time [134]. A retractile testis cannot always be considered a normal variant,

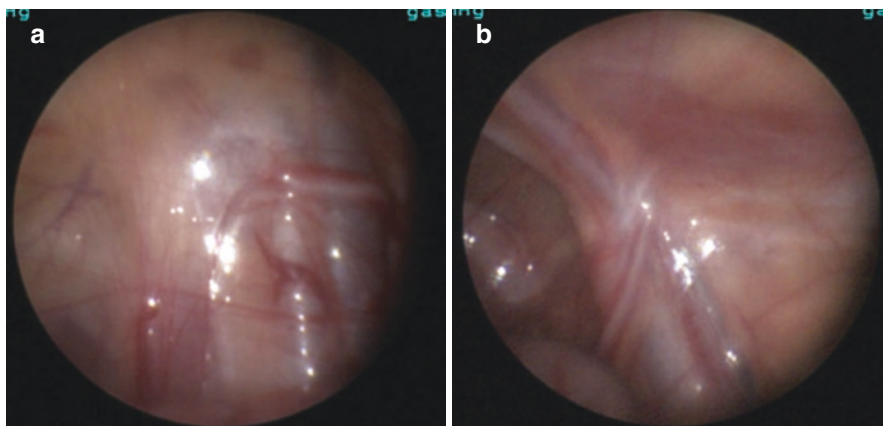


Fig. 13.35 (a, b) Laparoscopic view of left testicular agenesis from neonatal torsion with vas deferens entering into closed left internal ring and blind ending gonadal vessels ending just posterior to left internal ring. (b) Normal appearing vas deferens and gonadal vessels entering into closer right internal ring

as there is up to 32% risk of testicular ascent as the child grows, so these boys should be followed annually [135].

The most important tool for the diagnosis is a well-done clinical evaluation by an experienced professional. The exam should be performed in a quiet and warm room with the child relaxed. Once the testis is palpated, the diagnosis is obtained and no other testing is necessary. For nonpalpable testes, currently available imaging modalities are not sensitive enough to rule out or confirm an intra-abdominal testicle, so a diagnostic laparoscopy is essential [136].

The main concerns for boys with undescended testes are infertility and testicular tumor. Studies are contradictory in confirming whether unilateral cryptorchidism increases the risk of infertility [137–139], but bilateral cryptorchidism has been well shown to have a strong association with fertility compromise [138, 140]. In addition, studies have shown that a cryptorchidic boy has a 2.2–3.8 times higher than normal risk of developing testicular cancer [141], and about 11% of all testicular tumors are in men with a history of cryptorchidism [136]. This risk is also slightly increased in the contralateral normally descended testis [142]. There is also an increased risk of a congenital, indirect inguinal hernia with cryptorchidism, as the processus vaginalis fails to close, leaving a patent internal ring (Fig. 13.36).

Undescended testis should be treated in the first 6–18 months of life, to reduce the risk of harm to the testis and reduction in the number of germ cells [117, 128, 143]. Hormonal therapy with testosterone or gonadotropin-releasing hormone (GnRH) has poor results in the promotion of testicular descent. It has no place in the treatment of congenital cryptorchidism [136, 144], although it has been shown to increase the count of germ cells per tubule [145].

Surgical correction of an undescended testicle, an orchiopexy, is the treatment of choice. A palpable testis is managed with an inguinal incision to free the testicle of the cremasteric attachments and close the hernia sac/processus vaginalis. A separate scrotal incision is made to secure the testicle into a subdartos pouch. Some surgeons

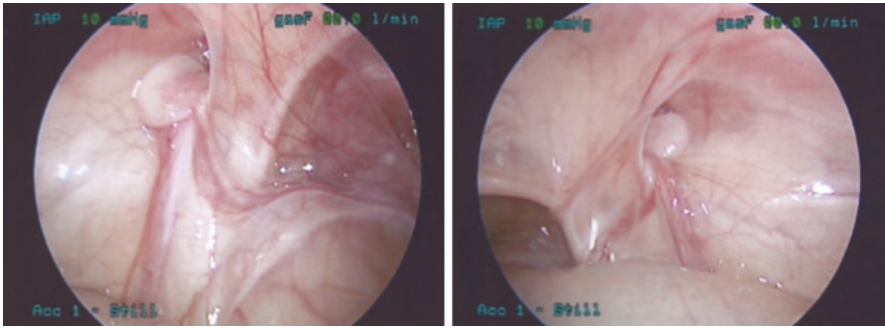


Fig. 13.36 (a, b) Laparoscopic view of a bilateral undescended testicles, just distal to the internal ring, in the inguinal canal, with associated patent processus vaginalis (a) left and (b) right. The patent processus vaginalis/internal ring has risk of development of an indirect inguinal hernia

advocate a single scrotal approach if the testicle can be manipulated into the distal, scrotal location. A nonpalpable testis is preferably managed with laparoscopy, during which three scenarios are possible:

- The testis may be found in the abdomen, as shown in Fig. 13.33.
- Blind ending testicular vessels due to agenesis may be found, “vanishing testis syndrome” (Fig. 13.35).
- The vas deferens and vessels may be found entering normally into the closed internal inguinal ring, demonstrating that the testis has descended beyond this location, into the inguinal canal. In this last scenario, open inguinal exploration is indicated to confirm the presence of a viable testicle or atrophy from neonatal testicular torsion.

Abnormalities of the Spermatic Cord

Abnormalities of the spermatic cord, which include hydrocele, cyst of the spermatic cord, and inguinal hernia, share the same etiological pathophysiology. During the descent of the testis into the scrotum, the testicle brings a patch of peritoneum, termed the processus vaginalis, that invaginates alongside the spermatic cord. This peritoneal canal should obliterate before the child is born (as happens in 95–98% of fetuses) [146]. When obliteration does not completely occur, an abnormality of the spermatic cord or tunica vaginalis is seen.

Hydrocele

Hydroceles can be categorized as communicating or noncommunicating. In communicating hydroceles, fluid travels from the peritoneal cavity into the scrotum through a patent processus vaginalis. Noncommunicating hydroceles represent fluid trapped within the tunica vaginalis beyond a closed patent processus vaginalis (Fig. 13.37). Noncommunicating hydroceles are common in infants, as some peritoneal fluid (which usually reabsorbs with time) may collect during the testicular descent. In older children, noncommunicating hydrocele can develop as a reaction

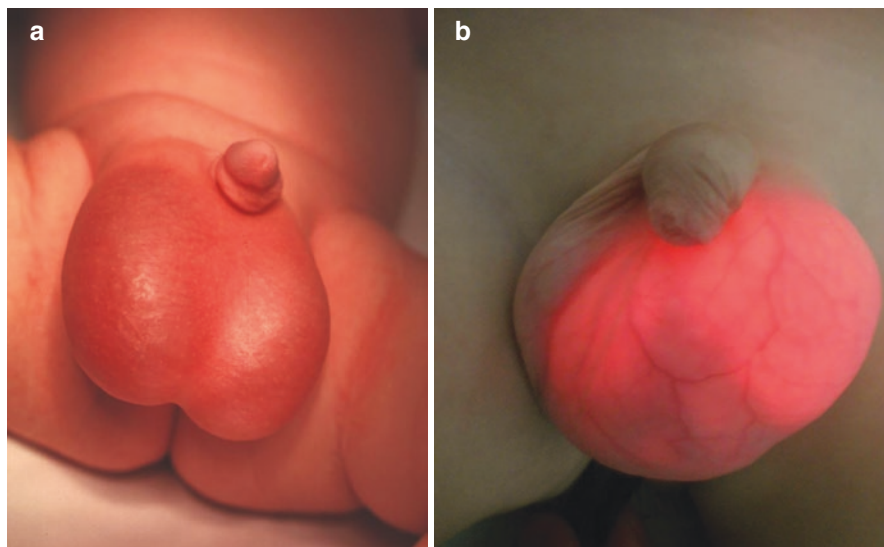


Fig. 13.37 Noncommunicating hydrocele. (a) Bilateral noncommunicating hydroceles in a male infant. (b) Transillumination of a left, noncommunicating hydrocele, confirming no hernia tracking into the scrotum

to infection, inflammation, trauma, or surgery. It represents an imbalance between how much inflammatory fluid is being produced versus how much is reabsorbed; surgical intervention is often required if the fluid is not reabsorbed soon after the inciting event has been resolved. In young children, hydroceles are commonly congenital, due to a failure of the processus vaginalis to obliterate, leaving a communication between the peritoneum and the scrotum, which allows fluid to collect between the layers of the tunica vaginalis or along the spermatic cord (Fig. 13.38a). A patent processus vaginalis is present in 0.7–4.7% of newborns, but it can also develop in settings of constipation or upper respiratory symptoms when the child is bearing down, opening what previously was thought to be a closed internal ring, the processus vaginalis.

The common complaint in children with communicating hydroceles is an intermittent, fluctuating, painless swelling of the scrotum that usually increases by the end of the day and is normal or decreased in the morning (Fig. 13.39). Physical examination will reveal a painless scrotal swelling or enlargement of the spermatic cord. Transillumination of the scrotum (Fig. 13.37b) will allow visualization of light passing through the skin and the fluid. Sometimes, ultrasound can help in defining the diagnosis, specifically excluding an inguinal hernia.

Spontaneous closure of the patent processus vaginalis and resolution of the hydrocele occurs in up to 83% of cases by the age of 18 months [147]. Therefore, most pediatric urologists and surgeons recommend hydrocele surgery after 2 years of age [148, 149]. Surgery to correct a communicating hydrocele is performed via an inguinal incision and includes ligation of the patent processus vaginalis and excision or eversion of the tunica vaginalis (Fig. 13.38b).

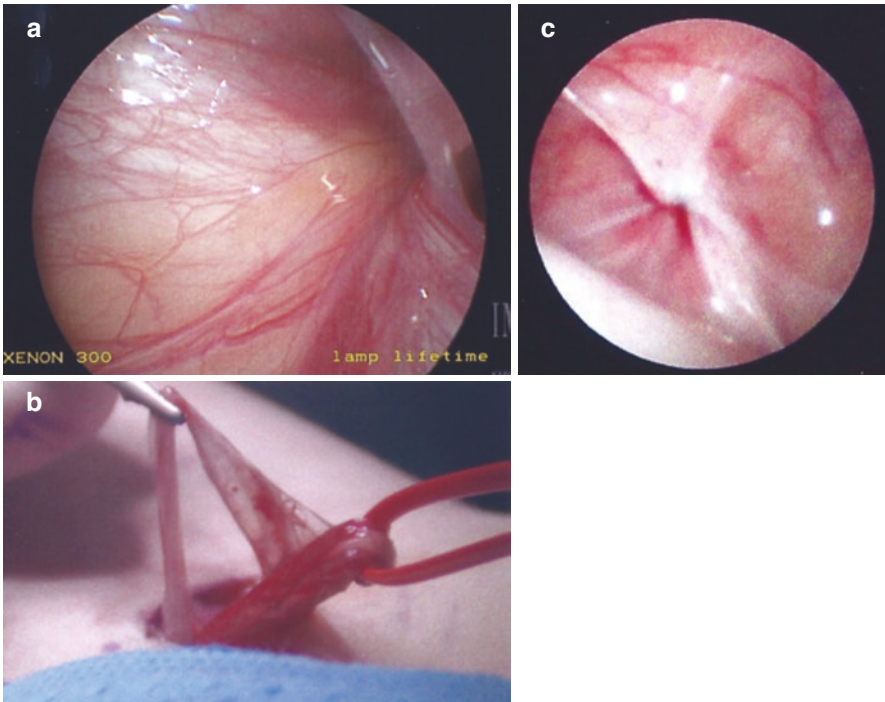


Fig. 13.38 Hydrocele repair. (a) Diagnostic laparoscopy confirming a patent processus vaginalis in a patient with a communicating hydrocele. (b) Hydrocele/hernia sac (processus vaginalis separated from cord structures) through an inguinal incision. (c) Laparoscopic view of closed internal ring after a communicating hydrocele/indirect inguinal hernia repair

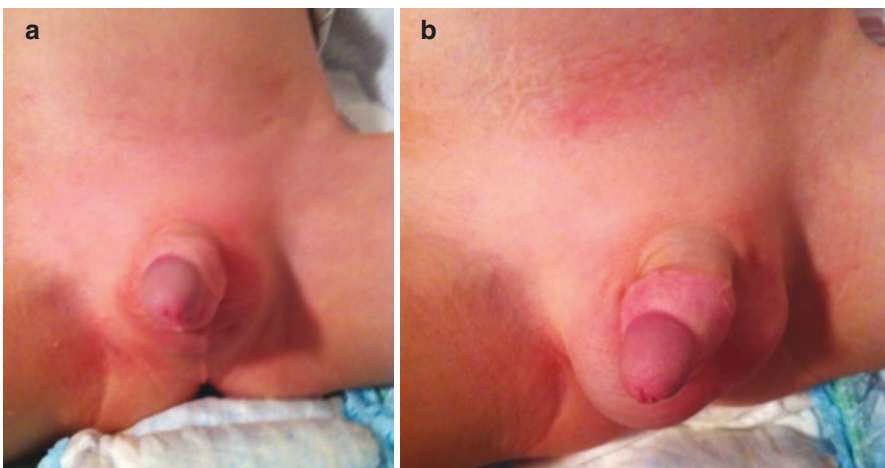


Fig. 13.39 (a, b) Right hydrocele, which increases when child is bearing down

Cyst of the Spermatic Cord

Cyst of the spermatic cord occurs when the distal portion of the processus vaginalis closes while the proximal portion is partially opened or closed, leaving a fluid collection in between, which can be either steady or intermittent.

Evaluation and treatment of cysts of the spermatic cord are similar to those described for hydroceles.

Inguinal Hernia

A partial or distal obliteration of the processus vaginalis can lead to an indirect inguinal hernia, allowing the descent of visceral contents into the inguinal canal—sometimes all the way to the scrotum, or to the labia in girls. It is one of the most common surgical problems in children, with an incidence of 1–5% in full-term infants and up to 30% in premature boys. It is 5–10 times more frequent in boys [150]. The only difference between an indirect inguinal hernia and a communicating hydrocele is what is travelling from the peritoneal cavity to the inguinal canal: visceral contents in the hernia versus peritoneal fluid in the hydrocele.

Patients will present with a sudden and intermittent swelling in the inguinal region associated with increased abdominal pressure (crying, straining to evacuate, or physical activity), when abdominal contents pass through the inguinal ring. Pain may or not be present, depending on incarceration of the visceral structure. Physical examination may be normal or may reveal a thickened spermatic cord. Sometimes, the “silk glove” sign can be found, which is the palpation of the layers of the patent processus vaginalis slipping over each other. In selected cases, ultrasound can help to confirm the diagnosis.

Inguinal hernia treatment in children is always surgical. Surgery should be performed shortly after diagnosis, to avoid incarceration [151], especially in neonates [152, 153]. The risk of surgical complications (testicular atrophy, recurrence, infection) is greater when an incarceration is present [154].

Varicocele in the Adolescent

Varicocele is the dilatation of the veins (varicose veins) of the pampiniform plexus, typically caused by incompetence of the valves in the gonadal veins draining the testicles, which allows venous backflow into the scrotum. It is more common on the left than the right because of the angle at which the left gonadal vein enters the left renal vein, which is also a higher insertion than that of the right gonadal vein into the vena cava. Varicocele is common in the adolescent, with an incidence ranging from 8% to 30% [155, 156].

Varicoceles are common, with an incidence of 15% in the male population; 15% of these cases are associated with fertility compromise, and varicocele causes 35–40% of infertility in men, being the most common cause [157]. As varicoceles are common in the general population, they represent the most common cause of infertility in men, 35–40%. Most adolescent varicoceles are asymptomatic and are detected during routine physical examination. Complaints of scrotal swelling and discomfort may be present. Physical examination should be performed with the patient in a standing position, at rest and performing a Valsalva maneuver. The

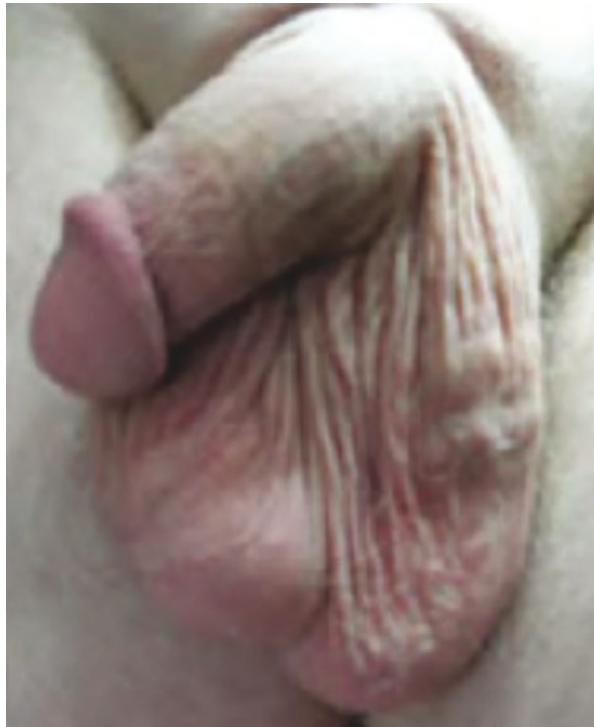
palpation of the spermatic cord will reveal engorgement of the spermatic veins in varying degrees that will allow grading of the varicocele:

- In Grade I, veins are palpable during Valsalva maneuver.
- In Grade II, engorged veins are palpable, but not visible, without the Valsalva maneuver.
- In Grade III, veins are visible through the skin with the patient standing [158] (Fig. 13.40).

The size of the testicle should be determined using either an orchidometer or by ultrasound. Ultrasound measurements are more accurate and can provide other information about the testis and the dilated veins [159].

Treatment of varicocele in the adolescent population is controversial. Semen analysis may not be readily available or sensitive in younger adolescents, impeding the verification of fertility. In affected patients, varicoceles can impede testicular growth. Most agree that a discrepancy in testicular volume differential greater than 20%, with compromised growth of the affected testicle, is an indication for surgery [160]. Grade III varicoceles are considered by some as another indication for treatment, though this remains controversial [160]. Some studies suggest that surgical intervention in young adults offers a moderate benefit in terms of preserving

Fig. 13.40 Left grade III varicocele



testicular function and future fertility [161]. Surgical treatment consists of ligation of the spermatic vein in the retroperitoneum [162] or the pampiniform plexus in the inguinal or subinguinal region [163]. The use of microsurgery techniques improves results and reduces morbidity [163]. Interventional radiologists can utilize an endovascular approach to embolize the gonadal veins.

Testicular Torsion

Testicular torsion is a urologic emergency and the most important cause of acute scrotum. It refers to rotation of the testis and spermatic cord causing obstruction to the blood supply to the testis, which can lead to ischemia and testicular loss. Torsion can be caused by a high insertion of the tunica vaginalis onto the testicle, termed a *bell clapper deformity*, which predisposes the testicle to twisting on the cord within the tunica vaginalis (intravaginal torsion) [164] (Fig. 13.41). In neonates or prenatally, the torsion is generally extravaginal or outside the tunica vaginalis, as the tunica vaginalis is not fixed in the scrotum; the testicle and tunica vaginalis twist on the spermatic cord, within the scrotum [165]. Infants are at risk of extravaginal torsion for the first 3–6 months of life.

Spermatic cord torsion can occur at any age from neonates to adulthood, but the peaks of highest incidence are in the perinatal period and puberty [166]. Torsion usually occurs one side at a time, though synchronous or asynchronous bilateral torsion is more common in neonates [167]. The presentation of neonatal torsion is usually painless scrotal swelling with or without inflammatory signs; because of the lack of symptoms, the salvage rate is very low (9%) [165]. In pubertal children, symptoms include acute pain, often associated with nausea and vomiting. This is accompanied by scrotal swelling and erythema, induration, and an abnormal, elevated, horizontal lie of the testicle within the scrotum. Approximately one-third of the patients will have a history of a prior similar episode [166]. Cremasteric reflex will be absent. Intermittent torsion may occur, in which the patient presents with repeated episodes of scrotal pain and swelling.

The first-line radiological test for evaluation of acute scrotum is color Doppler ultrasound to check for the presence of blood flow to the testis (*see* Fig. 13.41b); in many cases, it can predict the chances of testicular salvage [168].

Management of neonatal torsion is controversial; salvage rates are low, as the torsion event may have occurred in utero. One must balance the risks of anesthesia in the infant versus testicular loss and the potential for asynchronous torsion within the first 3–6 months of life. Surgery in bilateral neonatal torsion is always indicated, as failure to salvage the testicle will render the patient anorchic. Surgery is also always required in cases of adolescent intravaginal testicular torsion. In some instances, manual detorsion of the testis can be performed during physical examination, though surgery is still indicated even after successful detorsion. Given that the bell clapper deformity is an anatomic defect and thus is likely to be bilateral, intervention on both testicles is indicated [169]. If the testicle is viable after detorsion, orchiopexy is the treatment of choice, and orchiectomy should be reserved for those with a necrotic testis. Histological deleterious effects on spermatogenesis or loss of the testis may occur within a short time after the onset of symptoms, so surgery

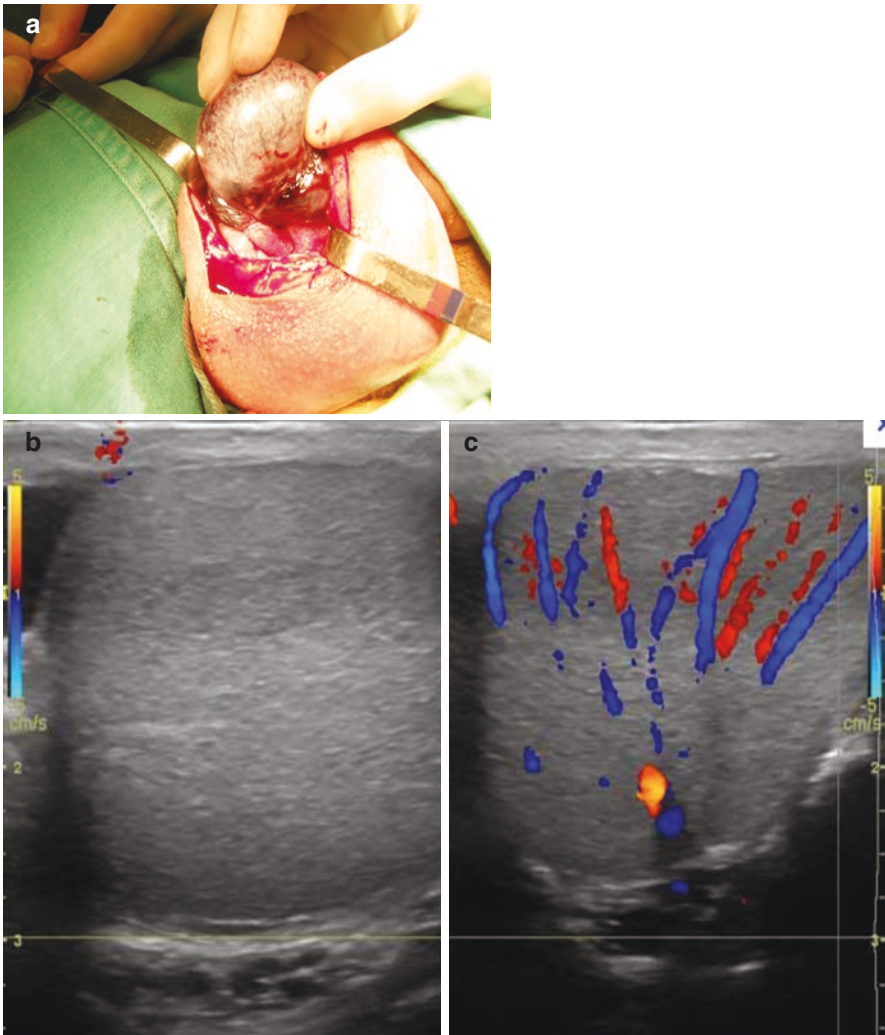


Fig. 13.41 Testicular torsion. Testicular torsion is intravaginal (within the tunica vaginalis) in adolescent patients and is related to the “bell clapper” deformity. (a) Ischemic testicle with torsion of the spermatic cord. (b) Doppler images confirming no blood flow to the right testicle (b), with normal flow to the left testicle (c)

should be performed as early as possible, with a window of 4–8 h depending on the number and tightness of rotations of the spermatic cord [170, 171]. The chances of saving the testis vary and depend on the time of surgical intervention related to the onset of symptoms. If surgery is done within to 6 h of the onset of symptoms, a salvage rate of 90–100% has been reported. The salvage rate decreases as the surgery is delayed, being around 50% if the delay is greater than 12 h, and less than 10% if greater than 24 h [171–173].

Differences of Sexual Development

Differences of sexual differentiation or development (DSD) are defined as the failure of normal development of the genitalia in which a miscorrelation of genotypic, phenotypic, and/or gonadal sex occurs [174, 175]. Genotypic sex is determined by the sexual chromosomes XX or XY (chromosomal sex) and the presence of the *SRY* gene (sex determining region), which initiates testicular development. Development of testis, under the influence of the *SRY* gene, occurs around the 6th week of gestation. The phenotypic sex will be determined based on endocrine/hormonal production and appropriate response of receptors to such hormones. According to the Consensus Statement on Management of Intersex Disorders, the new classification of DSD can be divided into 46,XY DSD, 46,XX DSD, Ovotesticular DSD, 4,6XX Testicular DSD, and 46,XY complete gonadal dysgenesis. It is estimated to be present in about 1 in 5000–6000 live births [176]. The external phenotypical appearance is often based on the presence of testosterone and the ability of the androgen receptor to interpret it. Internal reproductive Müllerian structures will regress if the testicles produce Müllerian Inhibiting Substance, but will persist if there is a mutation in the receptor required to interpret it.

Congenital Adrenal Hyperplasia

Congenital adrenal hyperplasia (CAH) comprises a group of autosomal recessive disorders characterized by deficiencies in the adrenal steroidogenesis pathway leading to impaired cortisol biosynthesis. This can lead to compromise in the production of cortisol and aldosterone production, with shunting to overproduction of androgen/testosterone. Three common enzymatic deficiencies are associated with female virilization, with 21-hydroxylase deficiency (21-OHD) due to a mutation in the 21-hydroxylase gene (*CYP21A2*) being the most common cause of classic CAH [177].

In cases of CAH, chromosomal sex can be either 46,XX for females or 46,XY for males, though the virilized phenotype is more pronounced in affected female patients. In girls with CAH, genitalia appearance can be categorized based on the Prader scale, which measures the degree of virilization of the clitoris, ranging from minimal clitoromegaly to a phallic, penile structure (Fig. 13.42). Ovaries are usually small but in the normal position. Müllerian structures persist, and the Wolffian ducts regress despite excessive prenatal androgen exposure. A persistent urogenital sinus can be observed in virilized girls, with an incomplete separation of the urethra and vagina resulting in a single perineal orifice and urogenital sinus (Fig. 13.43). In affected males, apart from hyperpigmentation and increased musculature (“little Hercules”), genitalia will be normal [177, 178].

Besides genital alterations, classic CAH can present as a salt-losing variant, which is a neonatal emergency. In this form, there is a deficiency of both aldosterone and cortisol, and the neonate can present in adrenal crisis, with severe dehydration and vomiting, followed by hypoglycemia, hyperkalemia, hyponatremia, and



Fig. 13.42 (a–d) Clitoromegaly in patients with congenital adrenal hyperplasia

hypotension in the first weeks after birth. In many countries, screening for CAH is done routinely in the neonate period by dosing 17-hydroxyprogesterone.

In older children and adults, signs of virilization are the major symptoms leading to investigation and diagnosis. Children may present with premature development of pubic hair (before 8 years of age), greater than normal growth, enlargement of the



Fig. 13.43 Congenital adrenal hyperplasia (CAH) can cause (a) clitoromegaly and (b) a common urogenital sinus. (c) A retrograde genitogram demonstrates filling of the urethra and vagina, which come together distally to a single introital orifice

phallus in boys, and clitoromegaly in girls. Adult women may have hirsutism, irregular menses, anovulation, and infertility.

Treatment for classic CAH consists initially of glucocorticoid and mineralocorticoid hormone replacement. In moments of greater stress, stress-dose steroids are necessary. A great concern in women with CAH is genital reconstruction, sexuality, and sex assignment. Genitoplasty may require urogenital sinus mobilization, separating the vagina from the urethra, clitoroplasty, and labial reconstruction [179].

Gender assignment can generate controversy; 46,XX CAH patients, according to 2006 consensus [175], should be raised as females because sexual and reproductive functions are preserved [180].

Müllerian Duct Disorders

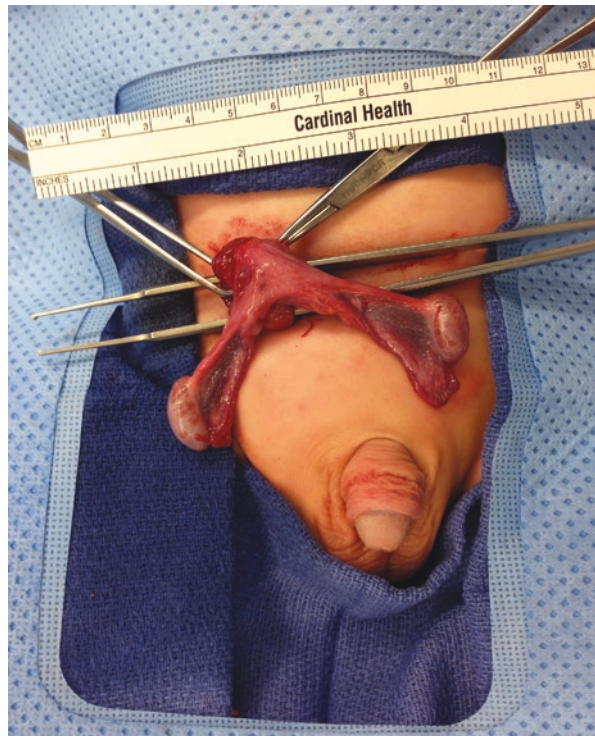
The Müllerian (paramesonephric) ducts are embryological structures that differentiate to form the upper two thirds of the vagina, uterus, and fallopian tubes in females. In males, under the influence of Müllerian Inhibiting Substance (produced by Sertoli cells of the testicle), the Müllerian structures regress, and testosterone promotes the differentiation of the Wolffian (mesonephric) ducts into the epididymis, seminal vesicles, and vas deferens.

Persistent Müllerian Ducts

In rare occasions, a failure of the Müllerian structures to regress will occur in normal external phenotype males (46,XY) if the testicles cannot produce Müllerian Inhibiting Substance or if there is a mutation in the receptor that interprets it. In this case, the Müllerian structures persist, with maintenance of a uterus and fallopian tubes, termed *hernia ureteri inguinale*. In such cases, the testicle will often be undescended because of tethering of the fallopian tubes (Fig. 13.44). This condition can be sporadic, or there may be autosomal recessive inheritance.

These patients may present with undescended, abdominal testis, located in a position analogous to ovaries [181], with inguinal hernia containing testis, uterus, and fallopian tubes, with a contralateral normal testis, or both testes may be in the same hernia sac [182]. Preoperative diagnosis is difficult; the condition should be suspected in patients presenting bilateral undescended testes or unilateral

Fig. 13.44 Persistent Müllerian structures identified during inguinal hernia repair; testicles, fallopian tubes, and uterus were delivered through a right inguinal incision



undescended testis with contralateral inguinal hernia. The gonads should be biopsied and treatment definition postponed to a second stage, after better evaluation and discussion with the family [181].

Mayer-Rokitansky-Küster-Hauser (MRKH) Syndrome

The MRKH syndrome is a rare syndrome occurring in about 1 of 4000–5000 females [183]. It is characterized by a partial or complete aplasia of the Müllerian structures (upper vagina, uterus, and fallopian tubes) due to their failure to develop in 46,XX female patients. Other malformations such as kidney abnormalities (pelvic kidney or renal agenesis) may be present.

Patients with MRKH syndrome will have normal 46,XX karyotype and normal ovaries, with normal external genitalia and normal hormonal function [184]. Because internal reproductive organs are compromised, the patient can present with an imperforate hymen and obstructed vagina canal, and at puberty can present based on primary amenorrhea and cyclic pelvic pain [184]. Women with MRKH syndrome have difficulties during sexual intercourse due to a shortened vagina, and are infertile. Physical examination will reveal an atrophic or absent vagina (Fig. 13.45a) and no palpable uterus. Ultrasound is an effective method for confirming the diagnosis, but MRI is the imaging method of choice [185].

Conservative management with vaginal dilation is an option, though many patients will be managed surgically with creation of a neovagina. Surgical options available include skin or buccal free grafts or sigmoid or ileal pedicle grafts.

Partial and Complete Androgen Insensitivity

Androgen insensitivity syndromes are the most common disorders of sexual development. Androgen receptors can be partially or completely insensitive to

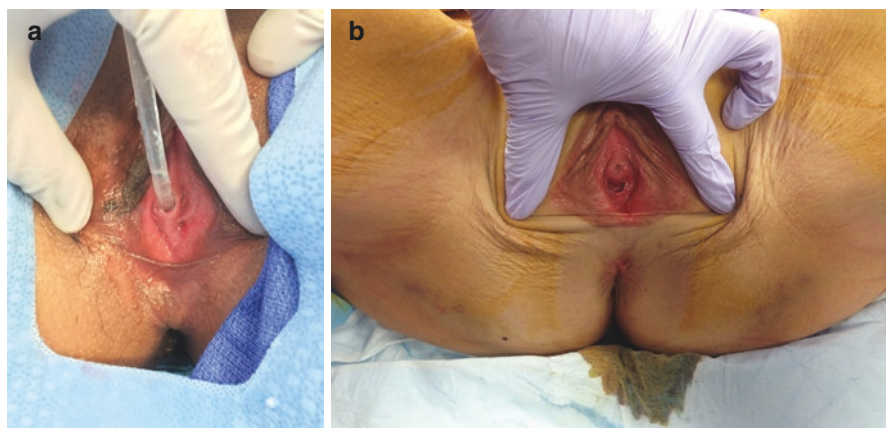


Fig. 13.45 Superficial, blind-ending vagina in a patient with (a) Mayer-Rokitansky-Küster-Hauser (MRKH) syndrome and in (b) 46,XY complete androgen insensitivity syndrome

androgen stimuli; the classification of partial or complete androgen insensitivity depends on the degree of the receptors' resistance to androgens [186].

Management of these patients requires an individualized multidisciplinary approach throughout their whole life, involving a pediatric urologist, pediatrician, pediatric endocrinologist, gynecologist, psychologist, and social worker.

Complete Androgen Insensitivity Syndrome

Complete androgen insensitivity syndrome (CAIS) is characterized by a complete failure of development of male genitalia in a 46,XY patient, who will present with a female external phenotype and abdominal testicles (Fig. 13.45b). Testosterone production by the testis is normal, though the body cannot interpret testosterone owing to a mutation in the androgen receptor. There is thus no virilization of the external genitalia. Müllerian structures regress owing to production of Müllerian Inhibiting Substance produced by the abdominal testicles. Patients with CAIS are raised as female, as they have external female genitalia and cannot be treated with testosterone to induce virilization. Diagnosis can be made prenatally when external genitalia do not match genetic testing on the fetus, but historically, diagnosis has most commonly been made during puberty because of the absence of menarche. In some cases, an inguinal hernia in infancy will lead to the diagnosis, when a testicle is discovered in the hernia sac [187] (Fig. 13.46). Pubic and axillary hair is sparse; breast development occurs as excessive androgen is aromatized into estrogen [186].

Because the great majority of these patients are raised as a woman, the hypoplastic vagina will need to be dilated, which is usually effective, or it can be reconstructed (neovagina) in order to allow sexual intercourse. Testes are often removed to prevent the potential for gonadal tumors, though management is becoming more controversial. Gonadectomy prior to puberty is discouraged, as the excess

Fig. 13.46 46,XY disorder of sex development (DSD), complete androgen insensitivity. Testicles are undescended and can be identified at time of hernia repair. Historically, testicles will be removed after puberty because of the potential for the development of testicular cancer



testosterone will be converted to estrogen, allowing for the development of secondary female sexual characteristics at puberty. Most patients with CAIS will not have psychosexual problems and will assimilate the female identity and behavior similar to that of other women [187].

Partial Androgen Insensitivity Syndrome

Patients with partial androgen insensitivity syndrome (PAIS) may present with a wide variety of genital development, with a spectrum ranging from proximal hypospadias and micropenis to female-appearing genitalia. Palpable testes may be present in a bifid scrotum, though often there is associated cryptorchidism.

Because of the ambiguous aspect of the genitalia, diagnosis is usually made early in life, and questions regarding sex assignment and early treatment should be addressed. Most PAIS patients are raised as males (80%) [188]. In these patients, hypospadias, scrotal reconstruction, and orchiopexy should be done early in life. Androgen supplementation may be necessary during and after puberty in some patients, though response may depend on the degree of resistance of the androgen receptor [187]. Some children may require aromatase inhibitors, as excess testosterone can be converted to estrogen, causing gynecomastia.

References

1. Hains DS, Bates CM, Ingraham S, Schwaderer AL. Management and etiology of the unilateral multicystic dysplastic kidney: a review. *Pediatr Nephrol.* 2009;24:233–41.
2. Calaway AC, Whittam B, Szymanski KM, Misseri R, Kaefer M, Rink RC, et al. Multicystic dysplastic kidney: is an initial voiding cystourethrogram necessary? *Can J Urol.* 2014;21:7510–4.
3. Chang A, Sivananthan D, Nataraja RM, Johnstone L, Webb N, Lopez PJ. Evidence-based treatment of multicystic dysplastic kidney: a systematic review. *J Pediatr Urol.* 2018;14:510–9.
4. Bergmann C. Genetics of autosomal recessive polycystic kidney disease and its differential diagnoses. *Front Pediatr.* 2017;5:221.
5. Davda S, Vohra A. Adult duplex kidneys: an important differential diagnosis in patients with abdominal cysts. *JRSM Short Rep.* 2013;4:13.
6. Doery AJ, Ang E, Ditchfield MR. Duplex kidney: not just a drooping lily. *J Med Imaging Radiat Oncol.* 2015;59:149–53.
7. Didier RA, Chow JS, Kwatra NS, Retik AB, Lebowitz RL. The duplicated collecting system of the urinary tract: embryology, imaging appearances and clinical considerations. *Pediatr Radiol.* 2017;47:1526–38.
8. Taghavi K, Kirkpatrick J, Mirjalili SA. The horseshoe kidney: surgical anatomy and embryology. *J Pediatr Urol.* 2016;12:275–80.
9. Pawar AS, Thongprayoon C, Cheungpasitporn W, Sakhujia A, Mao MA, Erickson SB. Incidence and characteristics of kidney stones in patients with horseshoe kidney: a systematic review and meta-analysis. *Urol Ann.* 2018;10:87–93.
10. Segura JW, Kelalis PP, Burke EC. Horseshoe kidney in children. *J Urol.* 1972;108:333–6.
11. Cascio S, Sweeney B, Granata C, Piaggio G, Jasonni V, Puri P. Vesicoureteral reflux and ureteropelvic junction obstruction in children with horseshoe kidney: treatment and outcome. *J Urol.* 2002;167:2566–8.
12. Baggenstoss AH. Congenital anomalies of the kidney. *Med Clin North Am.* 1951;1:987–1004.

13. Srinivas MR, Adarsh KM, Jeelson R, Ashwini C, Nagaraj BR. Congenital anatomic variants of the kidney and ureter: a pictorial essay. *Jpn J Radiol.* 2016;34:181–93.
14. Potter EL. Bilateral renal agenesis. *J Pediatr.* 1946;29:68–76.
15. Woolf AS, Hillman KA. Unilateral renal agenesis and the congenital solitary functioning kidney: developmental, genetic and clinical perspectives. *BJU Int.* 2007;99:17–21.
16. Wasilewska A, Zoch-Zwierz W, Jadeszko I, Porowski T, Biernacka A, Niewiarowska A, et al. Assessment of serum cystatin C in children with congenital solitary kidney. *Pediatr Nephrol.* 2006;21:688–93.
17. Dursun H, Bayazit AK, Cengiz N, Seydaoglu G, Buyukcelik M, Soran M, et al. Ambulatory blood pressure monitoring and renal functions in children with a solitary kidney. *Pediatr Nephrol.* 2007;22:559–64.
18. Eid S, Iwanaga J, Loukas M, Oskouian RJ, Tubbs RS. Pelvic kidney: a review of the literature. *Cureus.* 2018;10:e2775.
19. Mesrobian HG, Mirza SP. Hydronephrosis: a view from the inside. *Pediatr Clin N Am.* 2012;59:839–51.
20. Chen F. Genetic and developmental basis for urinary tract obstruction. *Pediatr Nephrol.* 2009;24:1621–32.
21. Nguyen HT, Herndon CD, Cooper C, Gatti J, Kirsch A, Kokorowski P, et al. The Society for Fetal Urology consensus statement on the evaluation and management of antenatal hydronephrosis. *J Pediatr Urol.* 2010;6:212–31.
22. Riccabona M, Avni FE, Blickman JG, Dacher JN, Darge K, Lobo ML, et al. Imaging recommendations in paediatric urology. Minutes of the ESPR urology task force session on childhood obstructive uropathy, high-grade fetal hydronephrosis, childhood haematuria, and urolithiasis in childhood. ESPR Annual Congress, Edinburgh, UK, June 2008. *Pediatr Radiol.* 2009;39:891–8.
23. Weitz M, Portz S, Laube GF, Meerpohl JJ, Bassler D. Surgery versus non-surgical management for unilateral ureteric-pelvic junction obstruction in newborns and infants less than two years of age. *Cochrane Database Syst Rev.* 2016;7:CD010716.
24. Mackie GG, Stephens FD. Duplex kidneys: a correlation of renal dysplasia with position of the ureteric orifice. *Birth Defects Orig Artic Ser.* 1977;13:313–21.
25. Fernbach SK, Feinstein KA, Spencer K, Lindstrom CA. Ureteral duplication and its complications. *Radiographics.* 1997;17:109–27.
26. Perimenis P, Gyftopoulos K, Athanasopoulos A, Pastromas V, Barbalias G. Retrocaval ureter and associated abnormalities. *Int Urol Nephrol.* 2002;33:19–22.
27. Tamhankar AS, Savalia AJ, Sawant AS, Pawar PW, Kasat GV, Patil SR. Transperitoneal laparoscopic repair of retrocaval ureter: sur experience and review of literature. *Urol Ann.* 2017;9:324–9.
28. Tyrirtzis SI, Wiklund NP. Ureteral strictures revisited...trying to see the light at the end of the tunnel: a comprehensive review. *J Endourol.* 2015;29:124–36.
29. Hellstrom M, Hjalmas K, Jacobsson B, Jodal U, Oden A. Normal ureteral diameter in infancy and childhood. *Acta Radiol Diagn (Stockh).* 1985;26:433–9.
30. Farrugia MK, Hitchcock R, Radford A, Burki T, Robb A, Murphy F, et al. British Association of Paediatric Urologists consensus statement on the management of the primary obstructive megaureter. *J Pediatr Urol.* 2014;10:26–33.
31. Hodges SJ, Werle D, McLorie G, Atala A. Megaureter. *Sci World J.* 2010;10:603–12.
32. Report of working party to establish an international nomenclature for the large ureter. *Birth Defects Orig Artic Ser.* 1977;13(5):3–8.
33. Hanna MK, Jeffs RD, Sturgess JM, Barkin M. Ureteral structure and ultrastructure. Part III. The congenitally dilated ureter (megaureter). *J Urol.* 1977;117:24–7.
34. Vlad M, Ionescu N, Ispas AT, Ungureanu E, Stoica C. Morphological study of congenital megaureter. *Romanian J Morphol Embryol.* 2007;48:381–90.
35. Garne E, Loane M, Wellesley D, Barisic I, Eurocat Working Group. Congenital hydronephrosis: prenatal diagnosis and epidemiology in Europe. *J Pediatr Urol.* 2009;5:47–52.

36. Baskin LS, Zderic SA, Snyder HM, Duckett JW. Primary dilated megaureter: long-term followup. *J Urol*. 1994;152:618–21.
37. Arlen AM, Cooper CS. Controversies in the management of vesicoureteral reflux. *Curr Urol Rep*. 2015;16:64.
38. Lebowitz RL. The detection and characterization of vesicoureteral reflux in the child. *J Urol*. 1992;148:1640–2.
39. Lebowitz RL, Olbing H, Parkkulainen KV, Smellie JM, Tamminen-Mobius TE. International system of radiographic grading of vesicoureteric reflux. International Reflux Study in Children. *Pediatr Radiol*. 1985;15:105–9.
40. de Bessa J Jr, de Carvalho Mrad FC, Mendes EF, Bessa MC, Paschoalin VP, Tiraboschi RB, et al. Antibiotic prophylaxis for prevention of febrile urinary tract infections in children with vesicoureteral reflux: a meta-analysis of randomized, controlled trials comparing dilated to nondilated vesicoureteral reflux. *J Urol*. 2015;193:1772–7.
41. Hajiyev P, Burgu B. Contemporary management of vesicoureteral reflux. *Eur Urol Focus*. 2017;3:181–8.
42. Routh JC, Inman BA, Reinberg Y. Dextranomer/hyaluronic acid for pediatric vesicoureteral reflux: systematic review. *Pediatrics*. 2010;125:1010–9.
43. Austin PF, Bauer SB, Bower W, Chase J, Franco I, Hoebeke P, et al. The standardization of terminology of lower urinary tract function in children and adolescents: update report from the standardization committee of the International Children's Continence Society. *Neurourol Urodyn*. 2016;35:471–81.
44. Razvi S, Murphy R, Shlasko E, Cunningham-Rundles C. Delayed separation of the umbilical cord attributable to urachal anomalies. *Pediatrics*. 2001;108:493–4.
45. Nakanishi K, Kawai T, Suzuki M, Torikata C. Prognostic factors in urachal adenocarcinoma. A study in 41 specimens of DNA status, proliferating cell-nuclear antigen immunostaining, and argyrophilic nucleolar-organizer region counts. *Hum Pathol*. 1996;27:240–7.
46. Stopak JK, Azarow KS, Abdessalam SF, Raynor SC, Perry DA, Cusick RA. Trends in surgical management of urachal anomalies. *J Pediatr Surg*. 2015;50:1334–7.
47. Yapo BR, Gerges B, Holland AJ. Investigation and management of suspected urachal anomalies in children. *Pediatr Surg Int*. 2008;24:589–92.
48. Mesrobian HG, Zacharias A, Balcom AH, Cohen RD. Ten years of experience with isolated urachal anomalies in children. *J Urol*. 1997;158:1316–8.
49. Arlen AM, Smith EA. Disorders of the bladder and cloacal anomaly. *Clin Perinatol*. 2014;41:695–707.
50. Kumar SKV, Mammen A, Varma KK. Pathogenesis of bladder exstrophy: a new hypothesis. *J Pediatr Urol*. 2015;11:314–8.
51. Gearhart JP, Ben-Chaim J, Jeffs RD, Sanders RC. Criteria for the prenatal diagnosis of classic bladder exstrophy. *Obstet Gynecol*. 1995;85:961–4.
52. Connolly JA, Peppas DS, Jeffs RD, Gearhart JP. Prevalence and repair of inguinal hernias in children with bladder exstrophy. *J Urol*. 1995;154:1900–1.
53. Phillips TM, Gearhart JP. Primary closure of bladder exstrophy. *BJU Int*. 2009;104:1308–22.
54. Grady RW, Mitchell ME. Complete primary repair of exstrophy. Surgical technique. *Urol Clin North Am*. 2000;27:569–78, xi.
55. Dickson AP. The management of bladder exstrophy: the Manchester experience. *J Pediatr Surg*. 2014;49:244–50.
56. Tokunaka S, Koyanagi T, Matsuno T, Gotoh T, Tsuji I. Paraureteral diverticula: clinical experience with 17 cases with associated renal dysmorphism. *J Urol*. 1980;124:791–6.
57. Hutch JA. Vesico-ureteral reflux in the paraplegic: cause and correction. *J Urol*. 1952;68:457–69.
58. Silay MS, Koh CJ. Management of the bladder and calyceal diverticulum: options in the age of minimally invasive surgery. *Urol Clin North Am*. 2015;42:77–87.
59. Pirincci N, Gecit I, Gunes M, Tanik S, Ceylan K. Complete duplication of the bladder and urethra in the coronal plane: case report with review of the literature. *Urol Int*. 2013;90:118–20.

60. Taghavi K, Sharpe C, Stringer MD. Fetal megacystis: a systematic review. *J Pediatr Urol.* 2017;13:7–15.
61. Sebire NJ, Von Kaisenberg C, Rubio C, Snijders RJ, Nicolaides KH. Fetal megacystis at 10–14 weeks of gestation. *Ultrasound Obstet Gynecol.* 1996;8:387–90.
62. Lee J, Kimber C, Shekleton P, Cheng W. Prognostic factors of severe foetal megacystis. *ANZ J Surg.* 2011;81:552–5.
63. Smith-Harrison LI, Hougen HY, Timberlake MD, Corbett ST. Current applications of in utero intervention for lower urinary tract obstruction. *J Pediatr Urol.* 2015;11:341–7.
64. Nazer II, Alhashmi G, Sharief SN, Hefni NA, Ibrahim A, El-Desoky SM, et al. A case of urinary bladder agenesis and bilateral ectopic ureters: a case report. *BMC Urol.* 2018;18:83.
65. Aragona F, Glazel GP, Zaramella P, Zorzi C, Talenti E, Perale R, et al. Agenesis of the bladder: a case report and review of the literature. *Urol Radiol.* 1988;10:207–9.
66. Patkowski D, Apoznanski W, Szydelko T, Jaworski W, Smigiel R. Bladder agenesis in a male neonate. *J Pediatr Surg.* 2008;43(11):e1–3.
67. Rezaie MA, Mansourian E, Delui HR, Amirmajidi NM. Bladder and urethral agenesis: a report of two cases. *Urology.* 2010;76:60–1.
68. Mong A, Bellah R. Imaging the pediatric prostate. *Radiol Clin N Am.* 2006;44:749–56, ix.
69. Kato H, Komiyama I, Maejima T, Nishizawa O. Histopathological study of the müllerian duct remnant: clarification of disease categories and terminology. *J Urol.* 2002;167:133–6.
70. Shima H, Yabumoto H, Okamoto E, Orestano L, Ikoma F. Testicular function in patients with hypospadias associated with enlarged prostatic utricle. *Br J Urol.* 1992;69:192–5.
71. McDougall EM, Clayman RV, Bowles WT. Laparoscopic excision of müllerian duct remnant. *J Urol.* 1994;152:482–4.
72. Ritchey ML, Benson RC Jr, Kramer SA, Kelalis PP. Management of müllerian duct remnants in the male patient. *J Urol.* 1988;140:795–9.
73. Lima M, Aquino A, Domini M, Ruggeri G, Libri M, Cimador M, et al. Laparoscopic removal of müllerian duct remnants in boys. *J Urol.* 2004;171:364–8.
74. Kim B, Kawashima A, Ryu JA, Takahashi N, Hartman RP, King BF Jr. Imaging of the seminal vesicle and vas deferens. *Radiographics.* 2009;29:1105–21.
75. Arora SS, Breiman RS, Webb EM, Westphalen AC, Yeh BM, Coakley FV. CT and MRI of congenital anomalies of the seminal vesicles. *AJR Am J Roentgenol.* 2007;189:130–5.
76. Anguiano A, Oates RD, Amos JA, Dean M, Gerrard B, Stewart C, et al. Congenital bilateral absence of the vas deferens. A primarily genital form of cystic fibrosis. *JAMA.* 1992;267:1794–7.
77. Vohra S, Morgentaler A. Congenital anomalies of the vas deferens, epididymis, and seminal vesicles. *Urology.* 1997;49:313–21.
78. Heaney JA, Pfister RC, Meares EM Jr. Giant cyst of the seminal vesicle with renal agenesis. *AJR Am J Roentgenol.* 1987;149:139–40.
79. Jequier AM, Ansell ID, Bullimore NJ. Congenital absence of the vasa deferentia presenting with infertility. *J Androl.* 1985;6:15–9.
80. Schwarz R, Stephens FD. The persisting mesonephric duct: high junction of vas deferens and ureter. *J Urol.* 1978;120:592–6.
81. Narborough GC, Elliott S, Minford JE. Congenital stricture of the urethra. *Clin Radiol.* 1990;42:402–4.
82. Casale AJ. Early ureteral surgery for posterior urethral valves. *Urol Clin North Am.* 1990;17:361–72.
83. Bhadoo D, Bajpai M, Panda SS. Posterior urethral valve: prognostic factors and renal outcome. *J Indian Assoc Pediatr Surg.* 2014;19:133–7.
84. Young HH, Frontz WA, Baldwin JC. Congenital obstruction of the posterior urethra. *J Urol.* 3: 289–365, 1919. *J Urol.* 2002;167:265–7; discussion 268.
85. Christianson C, Huff D, McPherson E. Limb deformations in oligohydramnios sequence: effects of gestational age and duration of oligohydramnios. *Am J Med Genet.* 1999;86:430–3.
86. Nasir AA, Ameh EA, Abdur-Rahman LO, Adeniran JO, Abraham MK. Posterior urethral valve. *World J Pediatr.* 2011;7:205–16.

87. Debska M, Kretowicz P, Oledzka A, Gastol P, Dangel J, Swiatkowska-Freund M, et al. Early vesico-amniotic shunting -- does it change the prognosis in fetal lower urinary tract obstruction diagnosed in the first trimester? *Ginekol Pol.* 2017;88:486–91.
88. Martinez JM, Masoller N, Devlieger R, Passchyn E, Gomez O, Rodo J, et al. Laser ablation of posterior urethral valves by fetal cystoscopy. *Fetal Diagn Ther.* 2015;37:267–73.
89. Lopez Pereira P, Martinez Urrutia MJ, Jaureguizar E. Initial and long-term management of posterior urethral valves. *World J Urol.* 2004;22:418–24.
90. Routh JC, McGee SM, Ashley RA, Reinberg Y, Vandersteen DR. Predicting renal outcomes in children with anterior urethral valves: a systematic review. *J Urol.* 2010;184:1615–9.
91. McLellan DL, Gaston MV, Diamond DA, Lebowitz RL, Mandell J, Atala A, et al. Anterior urethral valves and diverticula in children: a result of ruptured Cowper's duct cyst? *BJU Int.* 2004;94:375–8.
92. Blaivas JG, Flisser AJ, Bleustein CB, Panagopoulos G. Periurethral masses: etiology and diagnosis in a large series of women. *Obstet Gynecol.* 2004;103:842–7.
93. Itani M, Kielar A, Menias CO, Dighe MK, Surabhi V, Prasad SR, et al. MRI of female urethra and periurethral pathologies. *Int Urogynecol J.* 2016;27:195–204.
94. Romanzi LJ, Groutz A, Blaivas JG. Urethral diverticulum in women: diverse presentations resulting in diagnostic delay and mismanagement. *J Urol.* 2000;164:428–33.
95. Gupta DK, Srinivas M. Congenital anterior urethral diverticulum in children. *Pediatr Surg Int.* 2000;16:565–8.
96. Effmann EL, Lebowitz RL, Colodny AH. Duplication of the urethra. *Radiology.* 1976;119:179–85.
97. Onofre LS, Gomes AL, Leao JQ, Leao FG, Cruz TM, Carnevale J. Urethral duplication--a wide spectrum of anomalies. *J Pediatr Urol.* 2013;9(6 Pt B):1064–71.
98. Hayashi Y, Kojima Y, Mizuno K, Kohri K. Prepuce: phimosis, paraphimosis, and circumcision. *ScientificWorldJournal.* 2011;11:289–301.
99. Pileggi FO, Martinelli CE Jr, Tazima MF, Daneluzzi JC, Vicente YA. Is suppression of hypothalamic-pituitary-adrenal axis significant during clinical treatment of phimosis? *J Urol.* 2010;183:2327–31.
100. Circumcision policy statement. American Academy of Pediatrics. Task Force on Circumcision. *Pediatrics.* 1999;103:686–93.
101. Chan IH, Wong KK. Common urological problems in children: prepuce, phimosis, and buried penis. *Hong Kong Med J.* 2016;22:263–9.
102. Bastos Netto JM, de Araujo JG Jr, de Almeida Noronha MF, Passos BR, de Bessa J Jr, Figueiredo AA. Prospective randomized trial comparing dissection with Plastibell(R) circumcision. *J Pediatr Urol.* 2010;6:572–7.
103. Hsieh JT, Wong WY, Chen J, Chang HJ, Liu SP. Congenital isolated penile torsion in adults: untwist with plication. *Urology.* 2002;59:438–40.
104. Montag S, Palmer LS. Abnormalities of penile curvature: chordee and penile torsion. *ScientificWorldJournal.* 2011;11:1470–8.
105. Bar-Yosef Y, Binyamini J, Matzkin H, Ben-Chaim J. Degloving and realignment--simple repair of isolated penile torsion. *Urology.* 2007;69:369–71.
106. Bauer R, Kogan BA. Modern technique for penile torsion repair. *J Urol.* 2009;182:286–90; discussion 290–1.
107. Bhat A, Bhat MP, Saxena G. Correction of penile torsion by mobilization of urethral plate and urethra. *J Pediatr Urol.* 2009;5:451–7.
108. Maizels M, Zaontz M, Donovan J, Bushnick PN, Firlit CF. Surgical correction of the buried penis: description of a classification system and a technique to correct the disorder. *J Urol.* 1986;136:268–71.
109. O'Brien A, Shapiro AM, Frank JD. Phimosis or congenital megaprepuce? *Br J Urol.* 1994;73:719–20.
110. Liu X, He DW, Hua Y, Zhang DY, Wei GH. Congenital completely buried penis in boys: anatomical basis and surgical technique. *BJU Int.* 2013;112:271–5.
111. Wiygul J, Palmer LS. Micropenis. *ScientificWorldJournal.* 2011;11:1462–9.

112. Donnahoo KK, Cain MP, Pope JC, Casale AJ, Keating MA, Adams MC, et al. Etiology, management and surgical complications of congenital chordee without hypospadias. *J Urol*. 1998;160:1120–2.
113. Tugtepe H, Thomas DT, Kandirici A, Yener S, Dagli T. Should we routinely test for chordee in patients with distal hypospadias? *Eur J Pediatr Surg*. 2015;25:195–8.
114. Snodgrass W, Prieto J. Straightening ventral curvature while preserving the urethral plate in proximal hypospadias repair. *J Urol*. 2009;182:1720–5.
115. Springer A, van den Heijkant M, Baumann S. Worldwide prevalence of hypospadias. *J Pediatr Urol*. 2016;12:152.e1–7.
116. Kraft KH, Shukla AR, Canning DA. Hypospadias. *Urol Clin North Am*. 2010;37:167–81.
117. Timing of elective surgery on the genitalia of male children with particular reference to the risks, benefits, and psychological effects of surgery and anesthesia. *American Academy of Pediatrics. Pediatrics*. 1996;97:590–4.
118. Riedmiller H, Androulakakis P, Beurton D, Kocvara R, Gerharz E. European Association of Urology. EAU guidelines on paediatric urology. *Eur Urol*. 2001;40:589–99.
119. Grady RW, Mitchell ME. Management of epispadias. *Urol Clin North Am*. 2002;29:349–60, vi.
120. Frimberger D. Diagnosis and management of epispadias. *Semin Pediatr Surg*. 2011;20:85–90.
121. Evans JA, Erdile LB, Greenberg CR, Chudley AE. Agenesis of the penis: patterns of associated malformations. *Am J Med Genet*. 1999;84:47–55.
122. De Castro R, Merlini E, Rigamonti W, Macedo A Jr. Phalloplasty and urethroplasty in children with penile agenesis: preliminary report. *J Urol*. 2007;177:1112–6; discussion 1117.
123. Chung E, Brock GB. Cryptorchidism and its impact on male fertility: a state of art review of current literature. *Can Urol Assoc J*. 2011;5:210–4.
124. Hutson JM, Southwell BR, Li R, Lie G, Ismail K, Harisis G, et al. The regulation of testicular descent and the effects of cryptorchidism. *Endocr Rev*. 2013;34:725–52.
125. Ashley RA, Barthold JS, Kolon TF. Cryptorchidism: pathogenesis, diagnosis, treatment and prognosis. *Urol Clin North Am*. 2010;37:183–93.
126. Berkowitz GS, Lapinski RH, Dolgin SE, Gazella JG, Bodian CA, Holzman IR. Prevalence and natural history of cryptorchidism. *Pediatrics*. 1993;92:44–9.
127. Hutson JM, Thorup J. Evaluation and management of the infant with cryptorchidism. *Curr Opin Pediatr*. 2015;27:520–4.
128. Cortes D, Clasen-Linde E, Hutson JM, Li R, Thorup J. The Sertoli cell hormones inhibin-B and anti Mullerian hormone have different patterns of secretion in prepubertal cryptorchid boys. *J Pediatr Surg*. 2016;51:475–80.
129. Vikraman J, Hutson JM, Li R, Thorup J. The undescended testis: clinical management and scientific advances. *Semin Pediatr Surg*. 2016;25:241–8.
130. Schnack TH, Zdravkovic S, Myrup C, Westergaard T, Wohlfahrt J, Melbye M. Familial aggregation of cryptorchidism--a nationwide cohort study. *Am J Epidemiol*. 2008;167:1453–7.
131. Holland AJ, Nassar N, Schneuer FJ. Undescended testes: an update. *Curr Opin Pediatr*. 2016;28:388–94.
132. Kanemoto K, Hayashi Y, Kojima Y, Maruyama T, Ito M, Kohri K. Accuracy of ultrasonography and magnetic resonance imaging in the diagnosis of non-palpable testis. *Int J Urol*. 2005;12:668–72.
133. Pirgon O, Dundar BN. Vanishing testes: a literature review. *J Clin Res Pediatr Endocrinol*. 2012;4:116–20.
134. Komarowska MD, Hermanowicz A, Debek W. Putting the pieces together: cryptorchidism - do we know everything? *J Pediatr Endocrinol Metab*. 2015;28:1247–56.
135. Agarwal PK, Diaz M, Elder JS. Retractable testis--is it really a normal variant? *J Urol*. 2006;175:1496–9.
136. Braga LH, Lorenzo AJ, Romao RLP. Canadian Urological Association-Pediatric Urologists of Canada (CUA-PUC) guideline for the diagnosis, management, and followup of cryptorchidism. *Can Urol Assoc J*. 2017;11:E251–60.
137. van Brakel J, Kranse R, de Muinck Keizer-Schrama SM, Hendriks AE, de Jong FH, Bangma CH, et al. Fertility potential in men with a history of congenital undescended testes: a long-term follow-up study. *Andrology*. 2013;1:100–8.

138. Lee PA. Fertility after cryptorchidism: epidemiology and other outcome studies. *Urology*. 2005;66:427–31.
139. Miller KD, Coughlin MT, Lee PA. Fertility after unilateral cryptorchidism. Paternity, time to conception, pretreatment testicular location and size, hormone and sperm parameters. *Horm Res*. 2001;55:249–53.
140. Virtanen HE, Toppari J. Cryptorchidism and fertility. *Endocrinol Metab Clin N Am*. 2015;44:751–60.
141. Lip SZ, Murchison LE, Cullis PS, Govan L, Carachi R. A meta-analysis of the risk of boys with isolated cryptorchidism developing testicular cancer in later life. *Arch Dis Child*. 2013;98:20–6.
142. Akre O, Pettersson A, Richiardi L. Risk of contralateral testicular cancer among men with unilaterally undescended testis: a meta analysis. *Int J Cancer*. 2009;124:687–9.
143. Kolon TF, Herndon CD, Baker LA, Baskin LS, Baxter CG, Cheng EY, et al. Evaluation and treatment of cryptorchidism: AUA guideline. *J Urol*. 2014;192:337–45.
144. Ritzén EM, Bergh A, Bjerknes R, Christiansen P, Cortes D, Haugen SE, et al. Nordic consensus on treatment of undescended testes. *Acta Paediatr*. 2007;96:638–43.
145. Chua ME, Mendoza JS, Gaston MJ, Luna SL Jr, Morales ML Jr. Hormonal therapy using gonadotropin releasing hormone for improvement of fertility index among children with cryptorchidism: a meta-analysis and systematic review. *J Pediatr Surg*. 2014;49:1659–67.
146. Skandalakis JE, Colborn GL, Androulakis JA, Skandalakis LJ, Pemberton LB. Embryologic and anatomic basis of inguinal herniorrhaphy. *Surg Clin North Am*. 1993;73:799–836.
147. Hall NJ, Ron O, Eaton S, Pierro A. Surgery for hydrocele in children--an avoidable excess? *J Pediatr Surg*. 2011;46:2401–5.
148. Lau ST, Lee YH, Caty MG. Current management of hernias and hydroceles. *Semin Pediatr Surg*. 2007;16:50–7.
149. Clarke S. Pediatric inguinal hernia and hydrocele: an evidence-based review in the era of minimal access surgery. *J Laparoendosc Adv Surg Tech A*. 2010;20:305–9.
150. Brandt ML. Pediatric hernias. *Surg Clin North Am*. 2008;88:27–43, vii–viii.
151. Stylianos S, Jacir NN, Harris BH. Incarceration of inguinal hernia in infants prior to elective repair. *J Pediatr Surg*. 1993;28:582–3.
152. Vaos G, Gardikis S, Kambouri K, Sigalas I, Kourakis G, Petoussis G. Optimal timing for repair of an inguinal hernia in premature infants. *Pediatr Surg Int*. 2010;26:379–85.
153. Antonoff MB, Kreykes NS, Saltzman DA, Acton RD. American Academy of Pediatrics Section on Surgery hernia survey revisited. *J Pediatr Surg*. 2005;40:1009–14.
154. Lee SL, Gleason JM, Sydorak RM. A critical review of premature infants with inguinal hernias: optimal timing of repair, incarceration risk, and postoperative apnea. *J Pediatr Surg*. 2011;46:217–20.
155. Zampieri N, Zuin V, Corroppo M, Chironi C, Cervellione RM, Camoglio FS. Varicocele and adolescents: semen quality after 2 different laparoscopic procedures. *J Androl*. 2007;28:727–33.
156. Kumanov P, Robeva RN, Tomova A. Adolescent varicocele: who is at risk? *Pediatrics*. 2008;121:e53–7.
157. Fretz PC, Sandlow JJ. Varicocele: current concepts in pathophysiology, diagnosis, and treatment. *Urol Clin North Am*. 2002;29:921–37.
158. Stahl P, Schlegel PN. Standardization and documentation of varicocele evaluation. *Curr Opin Urol*. 2011;21:500–5.
159. Chiba K, Ramasamy R, Lamb DJ, Lipschutz LI. The varicocele: diagnostic dilemmas, therapeutic challenges and future perspectives. *Asian J Androl*. 2016;18:276–81.
160. Locke JA, Noparast M, Afshar K. Treatment of varicocele in children and adolescents: a systematic review and meta-analysis of randomized controlled trials. *J Pediatr Urol*. 2017;13:437–45.
161. Nork JJ, Berger JH, Crain DS, Christman MS. Youth varicocele and varicocele treatment: a meta-analysis of semen outcomes. *Fertil Steril*. 2014;102:381–7.e6.
162. Barroso U Jr, Andrade DM, Novaes H, Netto JM, Andrade J. Surgical treatment of varicocele in children with open and laparoscopic Palomo technique: a systematic review of the literature. *J Urol*. 2009;181:2724–8.

163. Al-Kandari AM, Shabaan H, Ibrahim HM, Elshebiny YH, Shokeir AA. Comparison of outcomes of different varicocelectomy techniques: open inguinal, laparoscopic, and subinguinal microscopic varicocelectomy: a randomized clinical trial. *Urology*. 2007;69:417–20.
164. Witherington R, Jarrell TS. Torsion of the spermatic cord in adults. *J Urol*. 1990;143:62–3.
165. Nandi B, Murphy FL. Neonatal testicular torsion: a systematic literature review. *Pediatr Surg Int*. 2011;27:1037–40.
166. Nistal M, Paniagua R, Gonzalez-Peramato P, Reyes-Mugica M. Perspectives in pediatric pathology, Chapter 19. Testicular torsion, testicular appendix torsion, and other forms of testicular infarction. *Pediatr Dev Pathol*. 2016;19:345–59.
167. Bagci S, Bachour H, Woelfle JF, Mueller A, Bartmann P, Franz AR. Bilateral perinatal testicular torsion in an infant: a rare neonatal emergency. *Pediatr Int*. 2010;52:e227–8.
168. DaJusta DG, Granberg CF, Villanueva C, Baker LA. Contemporary review of testicular torsion: new concepts, emerging technologies and potential therapeutics. *J Pediatr Urol*. 2013;9:723–30.
169. Favorito LA, Cavalcante AG, Costa WS. Anatomic aspects of epididymis and tunica vaginalis in patients with testicular torsion. *Int Braz J Urol*. 2004;30:420–4.
170. Bartsch G, Frank S, Marberger H, Mikuz G. Testicular torsion: late results with special regard to fertility and endocrine function. *J Urol*. 1980;124:375–8.
171. Sharp VJ, Kieran K, Arlen AM. Testicular torsion: diagnosis, evaluation, and management. *Am Fam Physician*. 2013;88:835–40.
172. Kapoor S. Testicular torsion: a race against time. *Int J Clin Pract*. 2008;62:821–7.
173. Makela E, Lahdes-Vasama T, Rajakorpi H, Wikstrom S. A 19-year review of paediatric patients with acute scrotum. *Scand J Surg*. 2007;96:62–6.
174. Hughes IA, Houk C, Ahmed SF, Lee PA, Lawson Wilkins Pediatric Endocrine Society/ European Society for Paediatric Endocrinology Consensus Group. Consensus statement on management of intersex disorders. *J Pediatr Urol*. 2006;2:148–62.
175. Lee PA, Houk CP, Ahmed SF, Hughes IA, International Consensus Conference on Intersex organized by the Lawson Wilkins Pediatric Endocrine Society and the European Society for Paediatric Endocrinology. Consensus statement on management of intersex disorders. International Consensus Conference on Intersex. *Pediatrics*. 2006;118:e488–500.
176. Rawal AY, Austin PF. Concepts and updates in the evaluation and diagnosis of common disorders of sexual development. *Curr Urol Rep*. 2015;16(12):83.
177. Witchel SF. Congenital adrenal hyperplasia. *J Pediatr Adolesc Gynecol*. 2017;30:520–34.
178. Nermoen I, Husebye ES, Myhre AG, Lovas K. Classic congenital adrenal hyperplasia. *Tidsskr Nor Laegeforen*. 2017;137:540–3.
179. Jesus VM, Buriti F, Lessa R, Toralles MB, Oliveira LB, Barroso U Jr. Total urogenital sinus mobilization for ambiguous genitalia. *J Pediatr Surg*. 2018;53:808–12.
180. Furtado PS, Moraes F, Lago R, Barros LO, Toralles MB, Barroso U Jr. Gender dysphoria associated with disorders of sex development. *Nat Rev Urol*. 2012;9:620–7.
181. Agrawal AS, Kataria R. Persistent mullerian duct syndrome (PMDS): a rare anomaly the general surgeon must know about. *Indian J Surg*. 2015;77:217–21.
182. Manjunath BG, Shenoy VG, Raj P. Persistent mullerian duct syndrome: how to deal with the mullerian duct remnants - a review. *Indian J Surg*. 2010;72:16–9.
183. Evans TN, Poland ML, Boving RL. Vaginal malformations. *Am J Obstet Gynecol*. 1981;141:910–20.
184. Patnaik SS, Brazile B, Dandolu V, Ryan PL, Liao J. Mayer-Rokitansky-Kuster-Hauser (MRKH) syndrome: a historical perspective. *Gene*. 2015;555:33–40.
185. Bombard DS 2nd, Mousa SA. Mayer-Rokitansky-Kuster-Hauser syndrome: complications, diagnosis and possible treatment options: a review. *Gynecol Endocrinol*. 2014;30:618–23.
186. Tadokoro-Cuccaro R, Hughes IA. Androgen insensitivity syndrome. *Curr Opin Endocrinol Diabetes Obes*. 2014;21:499–503.
187. Hughes IA, Davies JD, Bunch TI, Pasterski V, Mastroyannopoulou K, MacDougall J. Androgen insensitivity syndrome. *Lancet*. 2012;380:1419–28.
188. Ahmed SF, Khwaja O, Hughes IA. The role of a clinical score in the assessment of ambiguous genitalia. *BJU Int*. 2000;85:120–4.



Samuel Kim and Deepak Narayan

Introduction

Duodenal fossae are thought to develop from malrotation of the mid-gut and abnormal peritoneal adhesions and formation of vascular folds during embryogenesis [1, 2]. These fossae can become the sites of internal hernias, sometimes necessitating surgical intervention. This chapter describes seven types of duodenal fossae: the fossa of Landzert, the fossa of Waldeyer, the superior duodenal fossa, the inferior duodenal fossa, the duodenojejunal fossa, the right retroduodenal fossa, and the left retroduodenal fossa.

The Fossa of Landzert and the Fossa of Waldeyer

The fossa of Landzert, or the left paraduodenal fossa, occurs in approximately 2% of cadaver dissections [3]. It is caused by the raising up of a peritoneal fold by the inferior mesenteric vein as it runs along the lateral side of fossa and then above it [4]. It lies to the left of the fourth (ascending) segment of the duodenum, bound by the inferior mesenteric vein anteriorly and parietal peritoneum posteriorly (Fig. 14.1). The aorta lies to the right of the fossa, and the left kidney lies to the left of the fossa. Its orifice, which opens to the right, extends posteriorly and downward toward the left [4]. It is important to note that the inferior mesenteric vein and ascending branch of the left colic artery lie near the fossa opening in the anterior

S. Kim (✉) · D. Narayan (Deceased)
Section of Plastic and Reconstructive Surgery, Yale New Haven Hospital,
New Haven, CT, USA

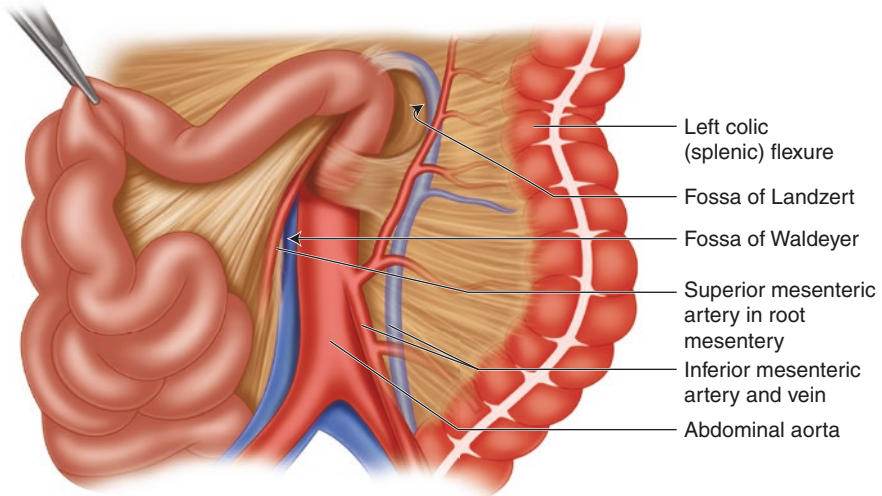


Fig. 14.1 Fossa of Landzert and Waldeyer. Depicted is the paraduodenal fossa of Landzert (arrow pointing to fossa entrance). Note the inferior mesenteric vein (IMV) running downward along the anterior edge of the fossa. Also depicted is the Fossa of Waldeyer (arrow pointing to fossa entrance). Note the superior mesenteric artery and small intestine mesentery running anterior to the fossa edge

wall and must be considered during surgical correction of a left paraduodenal hernia [5].

The fossa of Waldeyer, also called the right paraduodenal fossa and the mesentericoparietal fossa, occurs in approximately 1% of cadaver dissections [3]. It lies inferior to the third segment (transverse) of the duodenum, within the first part of the jejunum mesentery. The superior mesenteric artery (or ileocolic artery) is positioned anteriorly and the lumbar vertebrae, posteriorly (Fig. 14.1). Its orifice opens to the left and leads to the right and downward [2, 4].

The fossae of Landzert and Waldeyer are significant because most paraduodenal hernias occur through these fossae (Fig. 14.2). While internal abdominal hernias are a relatively rare cause of intestinal obstructions (0.2–0.9%) [6], up to 53% of all internal hernias are paraduodenal hernias [7, 8]. Approximately 75% of paraduodenal hernias occur through the fossa of Landzert, and 25% occur through the fossa of Waldeyer [9].

The Superior and Inferior Duodenal/Paraduodenal Fossae

The superior duodenal fossa occurs in approximately 50% of cadaver dissections [10]. It lies to the left of the fourth (ascending) segment of the duodenum just below the ligament of Treitz and anterior to the second lumbar vertebra (Fig. 14.3). It is bound anteriorly by a peritoneal fold and posteriorly by the parietal peritoneum. The inferior mesenteric vein courses along the left side of the fossa. The superior duodenal fossa opens downward, and its blind extremity is directed upward, usually 1–2 cm deep [2].

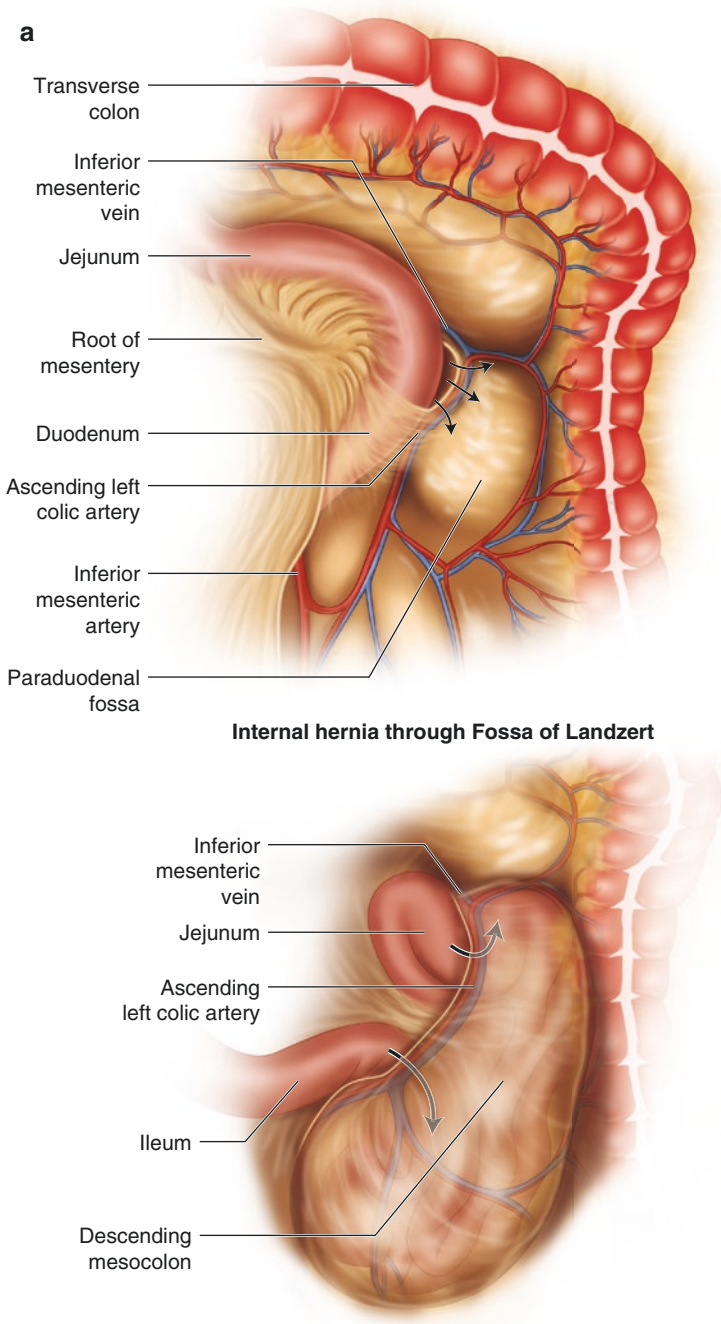


Fig. 14.2 Internal hernias through the Fossa of Landzert (a) and Waldeyer (b)

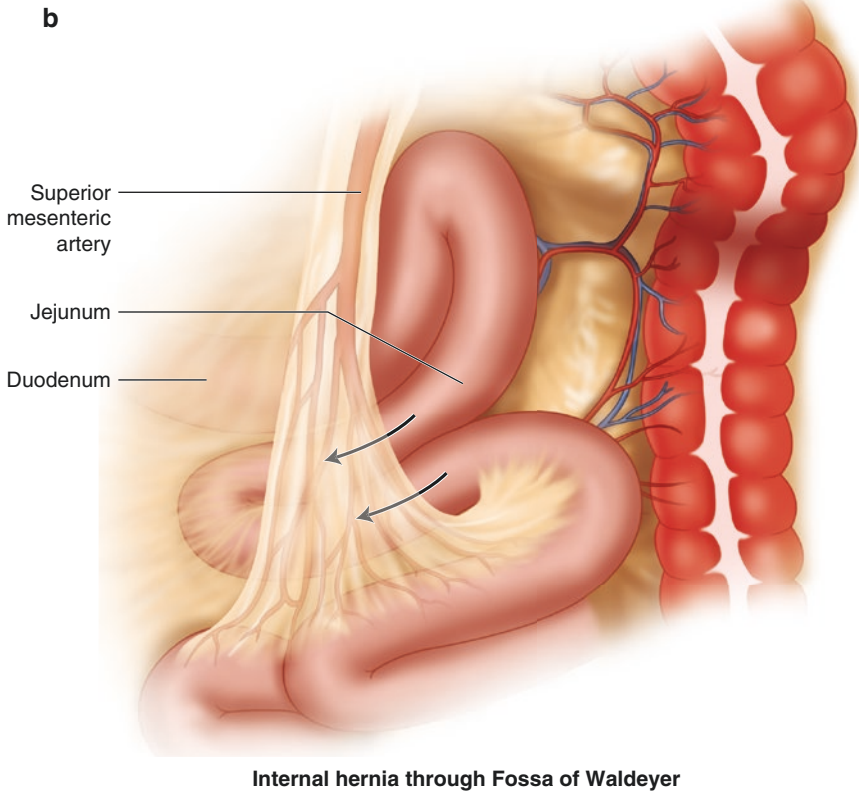
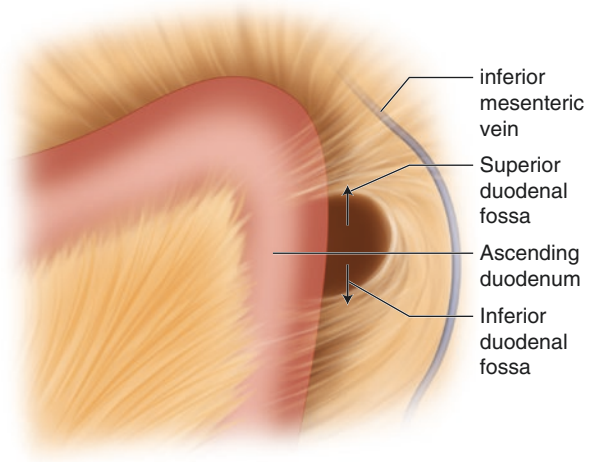


Fig. 14.2 (continued)

Fig. 14.3 Superior and inferior duodenal fossae. Note the common opening from fusion of the surrounding peritoneal folds



The inferior duodenal fossa occurs in approximately 70% of cadaver dissections [10]. It lies to the left of the fourth (ascending) segment of the duodenum, anterior to the third lumbar vertebra, just below the location of the superior duodenal fossa (Fig. 14.5). Like the superior duodenal fossa, the inferior duodenal fossa is also bound by a peritoneal fold and parietal peritoneum. The inferior duodenal fossa opens upward, and its blind extremity is directed downward to a variable depth of up to 5 cm [2].

The superior and inferior duodenal fossae coexist 75% of the time. Occasionally, they can share a common opening from fusion of the surrounding peritoneal folds at the orifices (Fig. 14.3) [2, 11].

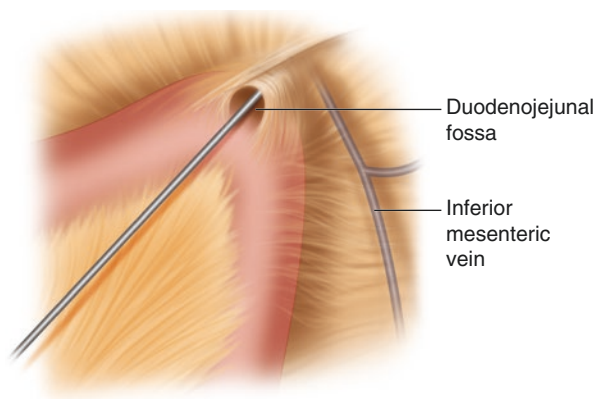
Duodenojejunal Fossa

The duodenojejunal fossa can be seen at the duodenojejunal angle by pulling the transverse colon upward and the jejunum downward (Fig. 14.4). The fossa is actually buried in the root of the transverse colon, where it fuses with the peritoneal investment of the duodenojejunal angle [2]. The cavity opens upward and to the left, with a depth of up to 3.5 cm [11]. The duodenojejunal fossa can be found in 15–20% of cadaver dissections [10].

Right and Left Retroduodenal Fossae

The retroduodenal fossae result when the mesoduodenum fails to fuse with the posterior parietal peritoneum. The right retroduodenal fossa lies behind the second (descending) segment of the duodenum, between the head of the pancreas anteriorly and the inferior vena cava posteriorly (Fig. 14.5). The fossa is bordered superiorly and inferiorly by the superior and inferior genu, avascular folds that anchor the duodenum [1]. The left retroduodenal fossa lies behind the

Fig. 14.4 Duodenojejunal fossa. An instrument is directed into the opening of the duodenojejunal fossa



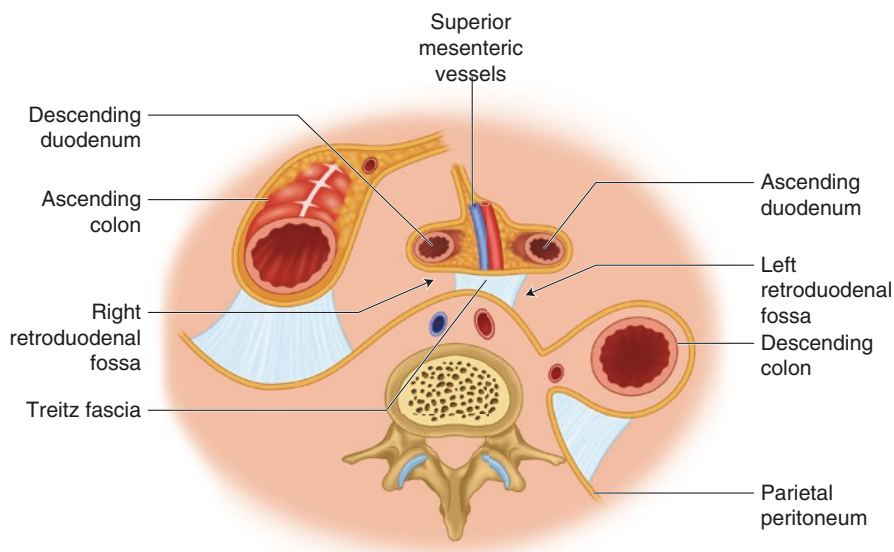


Fig. 14.5 Left and right retroduodenal fossa. Note the opening of the left retroduodenal fossa behind the fourth (ascending) portion of the duodenum

fourth (ascending) segment of the duodenum, bounded superiorly by the superior duodenal fold and inferiorly by the inferior duodenal fold (Fig. 14.5) [1].

References

1. Peltier J, Gars DL, Page C, Yzet T, Laude M. The duodenal fossae: anatomic study and clinical correlations. *Surg Radiol Anat.* 2005;27:303–7.
2. Desjardins AU. Left paraduodenal hernia. *Ann Surg.* 1918;67:195–201.
3. Parsons PB. Paraduodenal hernias. *Am J Roentgenol Radium Ther Nucl Med.* 1953;69:563–89.
4. Meyers MA, Charnsangavej C, Oliphant M. Internal abdominal hernias. In: Meyers MA, Charnsangavej C, Oliphant M, editors. *Meyers' dynamic radiology of the abdomen.* New York: Springer; 2011. p. 381–409.
5. Tireli M. Left paraduodenal hernia. *Br J Surg.* 1982;69:114.
6. Isabel L, Birrell S, Patkin M. Paraduodenal hernia. *Aust N Z J Surg.* 1995;65:64–6.
7. Takeyama N, Gokan T, Ohgiya Y, Satoh S, Hashizume T, Hataya K, et al. CT of internal hernias 1. *Radiographics.* 2005;25:997–1015.
8. Khan MA, Lo AY, Vande Maele DM. Paraduodenal hernia. *Am Surg.* 1998;64:1218–22.
9. Jones TW. Paraduodenal hernia and hernias of the foramen of Winslow. In: Nyhus IM, Harkins HN, editors. *Hernia.* Philadelphia: JB Lippincott; 1964. p. 577–601.
10. Moynihan BG. The Arris and Gale lectures on the anatomy and surgery of the peritoneal fossae: delivered at the Royal College of Surgeons of England. *Br Med J.* 1899;1(1992):522–5.
11. Tambe SV, Rana KK, Kakar A, Aggarwal S, Aggarwal A, Kakar S, et al. Clinical importance of duodenal recesses with special reference to internal hernias. *Arch Med Sci.* 2017;13:148–56.



Amberly Reynolds, Brittany Bozzell, Sarah Alturkustani,
and Rajuno Ettarh

Osteoporosis

Overview

- A. Osteoporosis arises when bone mass drops to a critical level, below which fracture risk is substantially higher. This usually occurs when there is an imbalance between bone formation and resorption [1].
- B. Types/causes: Primary osteoporosis is either classified as type I (postmenopausal), which is related to the onset of menopause, or type II (senile), which is related to aging [2]. Trabecular (spongy, cancellous) bone appears to be more prone to type I osteoporosis, whereas type II equally affects trabecular and cortical (compact) bones (Fig. 15.1). Subsequently, trabecular bone is at a higher risk of osteoporotic fractures such as vertebral body, distal radius, and intertrochanteric hip fractures [3].
- C. Osteoporosis can also be secondary to long-term corticosteroid use or endocrinopathy.

A. Reynolds · S. Alturkustani
Tulane University School of Medicine, New Orleans, LA, USA

B. Bozzell
Louisiana State University Health Sciences Center, School of Allied Health Professions,
Shreveport, LA, USA

R. Ettarh (✉)
Department of Medical Education/Anatomy, California University of Science and Medicine,
Colton, CA, USA
e-mail: EttarhR@cusm.org

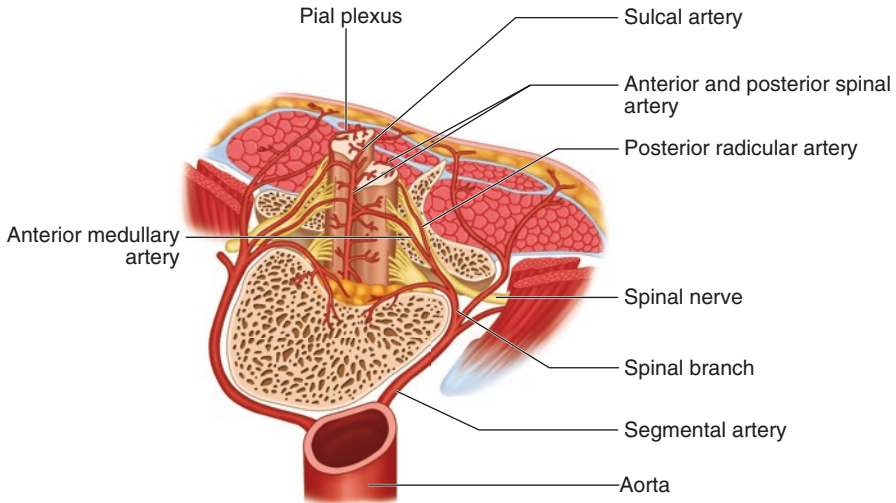


Fig. 15.1 Section through vertebra showing trabecular/cancellous matrix. The matrix is abnormally affected in osteoporosis. The perforating arteries of the spinal cord and their origins are also shown. Note the back muscles and the pial arterial plexus connecting the main longitudinal trunks of the cord laterally

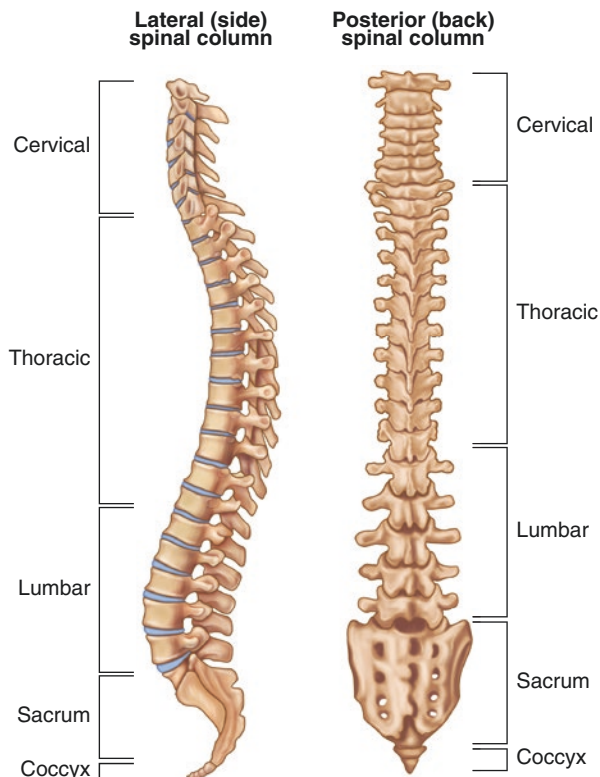
Vertebral Fractures (VFs)

- A. Most common types of osteoporotic fractures can remain undetected by patients or physicians. These fractures represent a strong factor for other subsequent osteoporotic fractures and they affect a large portion of the elderly population [2].
- B. Mechanism of VFs: Normally, the compressive loads to each of the vertebrae are evenly distributed along the anterior aspect of vertebral bodies. However, with the diminished bone mineral density, the underlying bone tissues fail to withstand these concentrated anterior forces and eventually collapse. This is commonly seen in the thoracic spine (Fig. 15.2), as there is some degree of pre-existing kyphosis [4].
- C. Complications of VFs: In addition to back pain and dysfunction, VFs may cause severe spinal deformities, compromised pulmonary function [5–7], early satiety, gastric distress, and impaired gait [8].

Surgical Intervention

Percutaneous vertebroplasty (VP) and kyphoplasty (KP) are methods of injecting polymethylmethacrylate (PMMA) percutaneously into fractured osteoporotic vertebral bodies with the aim of immediate stabilization and pain relief. PMMA is injected at low viscosity directly into the cancellous bone in the VP technique [9]. KP differs from VP in that a contrast-filled inflatable balloon is inserted into the

Fig. 15.2 Normal vertebral column. In scoliosis, the vertebral column is abnormally curved laterally when viewed anteriorly or posteriorly. In kyphosis, there is a pronounced posterior curvature in the thoracic section of the vertebral column



vertebral body, allowing a degree of fracture reduction and leaving a cavity behind after withdrawal, which is filled with high-viscosity PMMA [10].

Postoperative Care

- Patients can be mobilized 2 hours after the surgery.
- If the patient already has a thoracolumbar orthosis, it is recommended to continue wearing it for 1–2 weeks postoperatively.
- An adequate treatment for osteoporotic patients needs to be established to prevent further fractures [11].

Lumbar Disc Herniation (LDH)

Overview

- A. Lumbar discs can prolapse secondary to longstanding poor posture, or extensive load on the lumbar vertebrae. The central portion of the intervertebral disc (nucleus pulposus) may be displaced in response to increased pressure or torque

on the lumbar spine [12]. Consequently, the nerve roots become compressed, causing nerve pain, numbness, and sharp pain around the lower back and ischium. In some cases, symptoms can be severe enough to disrupt a patient’s everyday activities (Figs. 15.3 and 15.4).

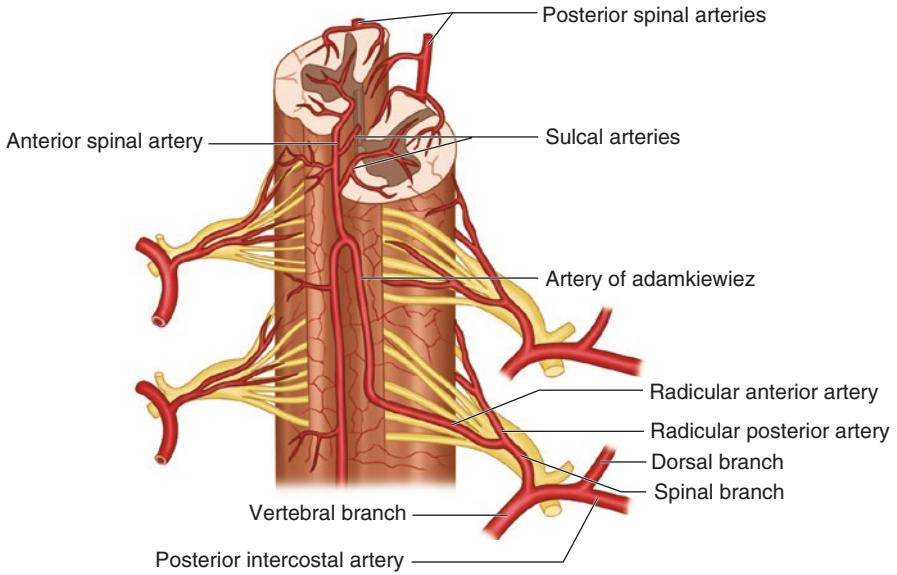


Fig. 15.3 The main arterial supply to the spinal cord. The spinal nerve roots intermingle with the vessels. Note the anastomosis of the anterior spinal artery with the two vertebral arteries. Also shown are the medullary feeder arteries branching off the segmental poster intercostal arteries

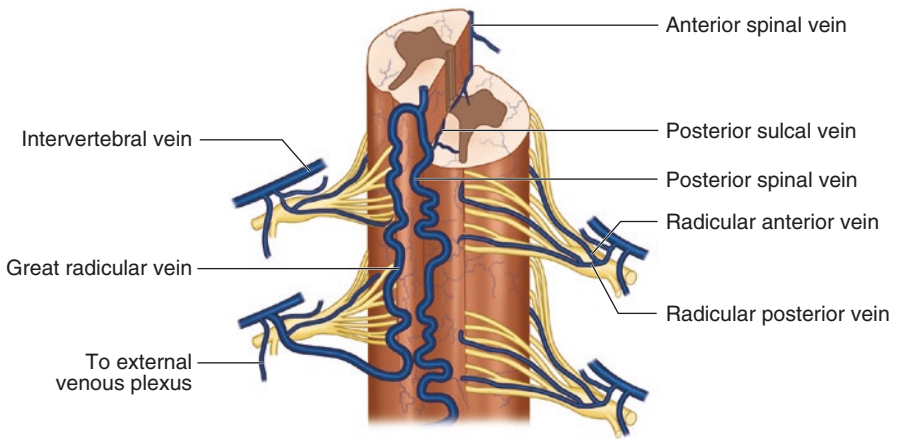


Fig. 15.4 Veins draining the spinal cord. The spinal nerve roots emerge from the anterior and posterior parts of the spinal cord

- B. Types: Based on the degree of involvement of annulus fibrosus, LDH is classified into contained and non-contained. In the contained type, the outermost layer of annulus fibrosus is intact, keeping the nucleus pulposus away from the epidural tissue. In the non-contained type, by contrast, the herniated nucleus pulposus is in direct contact with the epidural tissue.
- C. Complications of LDH: Seven percent of patients suffer from cauda equina syndrome, which may paralyze the lower body and cause lifelong bowel and urinary incontinence [13]. Furthermore, the patient may suffer some psychological issues due to pain and disability, including depression and low self-esteem [9].

Surgical Intervention

The term “microsurgical discectomy” describes the removal of herniated parts of lumbar intervertebral discs through a posterior approach with the help of a surgical microscope and microsurgical instruments. For herniated lumbar discs that are medial, paramedian (between midline and medial border of the pedicle), or intraforaminal (between medial and lateral border of the pedicle), the pathology is approached through a paramedian incision. The dorsolumbar fascia is incised and the muscles are retracted without dissecting their insertions (see Fig. 15.1). Ligamentum flavum is opened laterally and the nerve root is exposed and mobilized. The herniated part of the lumbar disc is removed and the rest of the nucleus pulposus can be removed from the intervertebral space in order to decrease the rate of recurrent herniations [11].

Postoperative Care

- The patient can be mobilized 6 hours after the surgery.
- Isometric exercises should be performed from the first postoperative day and on.
- It is advised to minimize postoperative physical therapy in the first 2–3 weeks following the operation.
- Patients are instructed to mobilize and carry out all activities that do not worsen symptoms.
- Postoperative hospitalization ranges between 1 and 8 days, depending on each individual case [11].

Lumbar Stenosis (LSS)

Overview

- A. LSS is characterized by narrowing of the lumbar spinal canal caused by degenerative changes. It is usually accompanied by instability in one or more lumbar segments [14], causing impingement of nerve roots along their path, either inside the dural sac or the dural sleeve (see Figs. 15.3 and 15.4).

- B. Types/causes: Based on etiology, LSS can be classified as primary or acquired [15]. LSS most commonly results from degenerative changes such as facet joint degeneration, hypertrophic ligamenta flava, degenerative spondylolisthesis, lumbar intervertebral disc protrusion, or a combination of these conditions [7]. Another classification was established based on the anatomical location of the narrowing: central spinal stenosis versus lateral recess stenosis.
- C. Symptoms/complications: These are quite variable, ranging from absolute absence of symptoms to severely disabling neurogenic claudication (spinal claudication) [16]. This is the cardinal symptom of LSS, characterized by diffuse buttock and leg pain, paresthesia, and cramping of one or both lower extremities induced by walking and relieved by sitting or forward bending [17]. Back pain is the most common presenting symptom, accounting for 95% of all cases. Urinary incontinence and uncontrolled defecation have also been reported, accounting for 33% and 12% of all cases, respectively [13].

Surgical Intervention

In recent years, a new surgical approach, microdecompression, has replaced open laminectomy, which was often combined with two other surgeries: medial facetectomy and foraminotomy. Microdecompression is less invasive yet equally effective [18, 19]. The procedure can be either unilateral or bilateral. Unlike a decompressive laminectomy, the spinous process and the supra and interspinous ligaments are left intact when performing a microdecompression [19].

Bilateral microdecompression means resection of the bone from the inferior aspect of the cranial lamina, and, occasionally, from the superior aspect of the subjacent lamina. Resection of the medial aspect of the facet joint is performed to alleviate the lateral recess. Flavectomy is performed to expose the spinal canal. The same procedure is then repeated on the contralateral side. When performing a unilateral microdecompression for bilateral decompression, the spinous process is undercut in addition to the ipsilateral decompression. By angling the microscopic view and occasionally tilting the operating table following ipsilateral decompression, removal of the contralateral ligamentum flavum and resection of the medial aspects of the contralateral facet joints are possible [19].

Postoperative Care

- Patients are preferably discharged the next morning.
- Drains must be removed before discharge.
- Ambulation is encouraged on the day of surgery, and return to work within a week, depending on the occupation.
- Physical conditioning is recommended both pre- and postoperatively, specifically, underwater exercises [11].

Scoliosis

Overview

- A. Scoliosis is usually defined as a curve on a standing radiograph of the spine measuring at least 10 degrees [20, 21].
- B. Types/causes: Scoliosis can be classified as congenital, idiopathic, and neuromuscular syndrome related. The first two types are due to a primary problem related to the spine itself. In congenital scoliosis, the vertebrae undergo malformation that eventually disrupts the normal spinal alignment (see Fig. 15.2). Idiopathic scoliosis develops spontaneously and the main cause remains unclear, although several studies have shown a familial occurrence, denoting an underlying genetic etiology [22]. Neuromuscular scoliosis is considered secondary to a more systemic disorder, such as cerebral palsy, Duchenne muscular dystrophy, and paralysis. In this type, the spine deviates laterally toward the functioning muscles and away from the weaker ones.
- C. Symptoms/complications: Pain and pulmonary dysfunction are the two most common complications experienced by patients of all three types. In cases of idiopathic scoliosis where the thoracic curvature exceeds 70 degrees, pulmonary function is impeded. However, curves less than 90 degrees may be asymptomatic [23–25]. More serious pulmonary complications can be caused by congenital scoliosis due to the decreased height of trunk and severe curvatures forming during early infancy. Combined with the multiple rib abnormalities, lung development will be hindered causing pulmonary dysfunction [26, 27]. Patients with neuromuscular scoliosis also suffer pulmonary dysfunction, but it remains unclear whether it is secondary to respiratory muscle weakness or spinal deformity [28]. Pain can occur in all forms of scoliosis, but the incidence compared to general population is not known. Particularly, neuromuscular scoliosis can result in pain due to unequal pressure placed on the skin secondary to muscle weakness.

Surgical Interventions

Video-assisted thoracic surgery (VATS), also known as thoracoscopy, is a technique in which small incisions are made in the chest wall through which a video camera and small instruments are placed allowing for access, visualization, and manipulation of structures within the chest including the anterior spine. It can be performed with an anterior spinal release and fusion (VATS-RF), or with an anterior spinal fusion and instrumentation (VATS-ASFI). VATS for spinal deformities offers benefits over the traditional thoracotomy including smaller incisions and thus less postoperative pain and pulmonary dysfunction [11].

Postoperative Care

The postoperative care of VATS-ASFI is very similar to that of posterior spinal fusion and instrumentation (PSFI) because they are usually performed together.

- Suction drainage is performed using the chest tube. Chest tube discontinuation depends on several factors: the number of levels released anteriorly, the adequacy of pleural closure, and the amount of chest tube drainage after the surgery.
- As soon as the chest tube is removed, the patient can move out of bed on that day and start walking activities the next day.
- Aggressive pulmonary toilet is required to prevent atelectasis.
- When the single-rod instrumentation is used, the patient can be measured for a brace on the second postoperative day, and be fitted with it on the third or fourth day. Prior to receiving the brace, however, the patient should already be moving out of bed and ambulating.
- Depending on the patient's conditions, he or she can be discharged anywhere from the second to the fifth postoperative day [11].

References

1. Riggs BL, Melton LJ. The prevention and treatment of osteoporosis. *N Engl J Med.* 1992;327:620–7.
2. Aebi M, Gunzburg R, Szpalski M. *The aging spine.* New York: Springer; 2005.
3. Riggs BL, Melton LJ. Evidence for two distinct syndrome of involuntional osteoporosis. *Am J Med.* 1983;309:899–901.
4. Ismail AA, Cooper C, Felsenberg D, Varlow J, Kanis JA, Silman AJ, et al. Number and type of vertebral deformities: epidemiological characteristics and relation to back pain and height loss. *European Vertebral Osteoporosis Study Group. Osteoporosis Int.* 1999;9:206–13.
5. Leech JA, Dulberg C, Kellie S, Pattee L, Gay J. Relationship of lung function to severity of osteoporosis in women. *Am Rev Respir Dis.* 1990;141:68–71.
6. Schlaich C, Minne HW, Bruckner T, Wagner G, Gebest HJ, Grunze M, et al. Reduced pulmonary function in patients with spinal osteoporotic fractures. *Osteoporos Int.* 1998;8:261–7.
7. Amundsen T, Weber H, Lilleås F, Nordal HJ, Abdelnoor M, Magnaes B. Lumbar spinal stenosis: clinical and radiologic features. *Spine (Phila Pa 1976).* 1995;20:1178–86.
8. Gold DT. The clinical impact of vertebral fractures: quality of life in women with osteoporosis. *Bone.* 1996;18:S185–9.
9. Garfin SR, Hansen AY, Reiley MA. Kyphoplasty and vertebroplasty for the treatment of painful osteoporotic compression fractures. *Spine.* 2001;26:1511–5.
10. Heini PF, Wlchli B, Berlemann U. Percutaneous transpedicular vertebroplasty with PMMA: operative technique and early results. *Eur Spine J.* 2000;9:445–50.
11. Mayer HM. *Minimally invasive spine surgery: a surgical manual.* Berlin: Springer; 2011.
12. Biderman A, Borkan J, Hermoni D, Reis S. Talking about the pain: a patient-centered study of low back pain in primary care. *Soc Sci Med.* 1995;40:977–88.
13. Hsin-Ni Chen, Yun-Fang Tsai. A predictive model for disability in patients with lumbar disc herniation. *J Orthop Sci.* 2013;18:220–9.
14. Egli D, Hausmann O, Schmid M, Boos N, Dietz V, Curt A. Lumbar spinal stenosis: assessment of cauda equina involvement by electrophysiological recordings. *J Neurol.* 2007;254:741–50.

15. Postacchini F. Management of lumbar spinal stenosis. Instructional course lecture. *J Bone Joint Surg*. 1996;78-B:154–64.
16. Arbit E, Pannullo S. Lumbar stenosis: a clinical review. *Clin Orthop Relat Res*. 2001;384:137–43.
17. Porter RW. Spinal stenosis and neurogenic claudication. *Spine (Phila Pa 1976)*. 1996;21:2046–52.
18. Smith ZA, Fessler RG. Paradigm changes in spine surgery: evolution of minimally invasive techniques. *Nat Rev Neurol*. 2012;8:443–50.
19. Thome C, Zevgaridis D, Leheta O, Bazner H, Pockler-Schoniger C, Wohrle J, et al. Outcome after less-invasive decompression of lumbar spinal stenosis: a randomized comparison of unilateral laminotomy, bilateral laminotomy, and laminectomy. *J Neurosurg Spine*. 2005;3:129–41.
20. Binstadt DH, Lonstein JE, Winter RB. Radiographic evaluation of the scoliotic patient. *Minn Med*. 1978;61(8):474–8.
21. Cobb JR. Scoliosis; quo vadis. *J Bone Joint Surg Am*. 1958;40-A(3):507–10.
22. Kouwenhoven JW, Castelein RM. The pathogenesis of adolescent idiopathic scoliosis: review of the literature. *Spine (Phila Pa 1976)*. 2008;33(26):2898–908.
23. Barrios C, Pérez-Encinas C, Maruenda JI, Laguña M. Significant ventilatory functional restriction in adolescents with mild or moderate scoliosis during maximal exercise tolerance test. *Spine (Phila Pa 1976)*. 2005;30(14):1610–5.
24. Smyth RJ, Chapman KR, Wright TA, Crawford JS, Rebeck AS. Pulmonary function in adolescents with mild idiopathic scoliosis. *Thorax*. 1984;39(12):901–4.
25. Weber B, Smith JP, Briscoe WA, Friedman SA, King TK. Pulmonary function in asymptomatic adolescents with idiopathic scoliosis. *Am Rev Respir Dis*. 1975;111(4):389–97.
26. Ramírez N, Cornier AS, Campbell RM Jr, Carlo S, Arroyo S, Romeu J. Natural history of thoracic insufficiency syndrome: a spondylothoracic dysplasia perspective. *J Bone Joint Surg Am*. 2007;89(12):2663–75.
27. Campbell RM Jr, Smith MD, Mayes TC, Mangos JA, Willey-Courand DB, Kose N, et al. The characteristics of thoracic insufficiency syndrome associated with fused ribs and congenital scoliosis. *J Bone Joint Surg Am*. 2003;85-A(3):399–408.
28. Finder JD, Birnkrant D, Carl J, Farber HJ, Gozal D, Iannaccone ST, et al. Respiratory care of the patient with Duchenne muscular dystrophy: ATS consensus statement. *Am J Respir Crit Care Med*. 2004;170(4):456–65.



Neuraxial and Peripheral Nerve Block Placement in Patients with Anatomical Anomalies

16

Donna-Ann Thomas, Sible Antony, David Sum,
and Abbas Asgerally

Introduction

Anatomical variations have proven in the past to make the placement of neuraxial anesthesia and peripheral nerve blocks technically challenging and sometimes unsuccessful with the use of anatomical landmarks with or without nerve stimulation for placement. Patients with skeletal changes such as scoliosis and kyphosis require technical expertise and adaptability for successful placement of neuraxial analgesia. Multiple cadaver studies have shown these anatomical variations, which with the use of sonography, have increased the proceduralist success rate in the placement of neuraxial and peripheral nerve blocks. In this chapter, we discuss common anatomical anomalies, which should be considered when placing these blocks.

Anomalies in Neuraxial Anesthesia

Neuraxial anesthesia is a term that refers to all types of blocks that involve applying local anesthetic such as spinal analgesia around the nerves in the central nervous system, and local anesthetics such as epidural and caudal anesthesia in the epidural space. Traditionally, the success and safety of placement are dependent on

D.-A. Thomas (✉)

Department of Anesthesiology, Division of Pain Medicine, Yale School of Medicine,
New Haven, CT, USA

e-mail: donna-ann.thomas@yale.edu

S. Antony

Department of Anesthesiology, Yale University School of Medicine, New Haven, CT, USA

D. Sum

Town Square Anesthesia, Huntley, IL, USA

A. Asgerally

Serendib Pain Care LLC, Vancouver, WA, USA

anatomical landmarks along the spine. This section will first focus on normal anatomical landmarks and then discuss some of the anomalies encountered within practice.

Anatomical Landmarks

The normal vertebral column consists of 7 cervical, 12 thoracic, 5 lumbar vertebrae followed by the sacrum and coccyx. Each vertebra contains the pedicle, transverse process, superior and inferior articular processes, and spinous process. An intervertebral disk separates each vertebral body from the other. There are four synovial joints associated with each vertebra: two superior and two inferior articular processes, which allow for articulation with the other vertebrae. The landmarks that determine the boundaries of the spinal canal are important to visualize as your spinal/epidural needle enters the skin. The anterior boundary is the vertebral body. The lateral boundary is the transverse process. The posterior boundary is the spinous process and laminae. The angle of the transverse and spinal process is different within the cervical, thoracic, and lumbar regions. This angle often impacts how steep a provider will orient the needle while performing an epidural/spinal. The spinous process helps define midline position. The spinous processes are more horizontal within the cervical and lumbar regions. This angle then becomes more caudad within the thoracic region, particularly T4–T9. The interlaminar spaces also become small in size as you move up the vertebral column (Fig. 16.1).

The vertebral column is also supported by several ligaments. As a provider enters the needle into a patient's back, the provider should be able to identify these structures through tactile feel: skin, subcutaneous tissue and fat, the supraspinous ligament, the interspinous ligament, the ligamentum flavum, epidural space, and dura. After the ligamentum flavum, the epidural space is encountered. The approximate

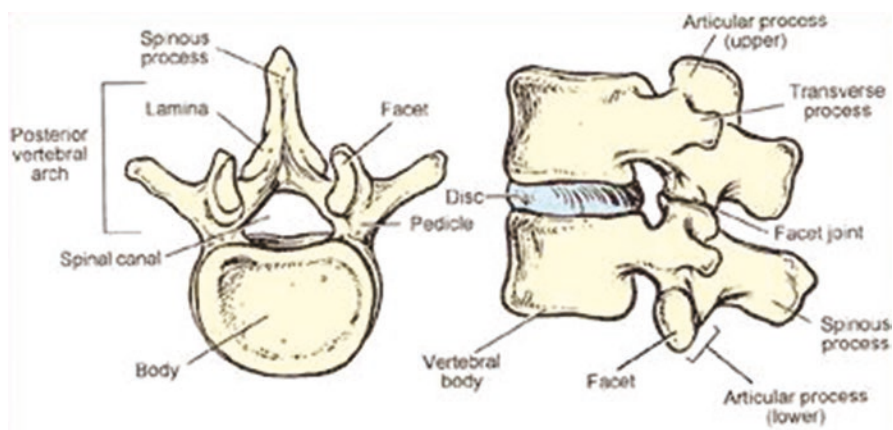


Fig. 16.1 Vertebral anatomy is used to identify landmarks while performing neuraxial anesthesia [1]

distance from the skin to epidural space varies depending on a thin/obese patient but on average is 4–6 cm [2]. The epidural space extends from the foramen magnum at the base of the skull to the sacral hiatus. This space often contains fat, lymphatics, and veins that form a plexus called Batson's plexus. These are the veins that become engorged during pregnancy.

Anomalies

Spread of local anesthetic in neuraxial anesthesia is determined by the physical characteristics of the solution, gravity, and the configuration of the vertebral column. One of most common anatomical anomalies encountered during placement of neuraxial anesthesia involves curvature of the vertebral column. Providers may have a difficult time determining midline and bony landmarks in patients with obesity, kyphosis, or scoliosis.

Prior teaching thought of the epidural space as one continuous space, but it is now thought that there are septations within this space formed by epidural fat. These septations can create longitudinal or transverse barriers to the flow path for local anesthetics leading to a unilateral, patchy, or partial epidural block [3]. Previous surgeries within the vertebral column can lead to adhesions, which may also interfere with spread of local anesthetic.

Some patients with connective tissue disorders (Marfan's disease, Ehlers-Danlos syndrome, neurofibromatosis, ankylosing spondylitis) may have an enlargement of their dura called dural ectasia, which can affect neuraxial anesthesia placement. These dural ectasias are most common in the lumbosacral region and may lead to an increase in volume of cerebrospinal fluid (CSF) in the lumbar theca [4]. This increase in volume is thought to restrict the spread of intrathecal local anesthetics. Neuraxial anesthesia may also be difficult to perform in this patient population due to a high degree of scoliosis/kyphosis.

Imaging During Placement of Neuraxial Anesthesia

Due to the advances in imaging technology, many of these anatomical anomalies can be overcome, and the success rate of neuraxial blocks has improved. Two approaches can be used with ultrasound to identify landmarks. The longitudinal (parasagittal) or transverse (axial) views can be used to identify landmarks such as the spinous process, articular process, ligamentum flavum, anterior/posterior dural matter, and vertebral bodies (Figs. 16.2 and 16.3).

Using imaging to aid in placement of neuraxial anesthesia can allow for visualization of the interlaminar space, optimization of needle insertion angle, and provide a more accurate estimation of depth to the epidural/intrathecal space from the skin. This technique increases a provider's first attempt success rate in patients with anatomical variations.

Fig. 16.2 The following image is a transverse scan at the L2–3 interspinous space. The transverse process (TP) and facet joints are visible in this view. PLL posterior longitudinal ligament [5]

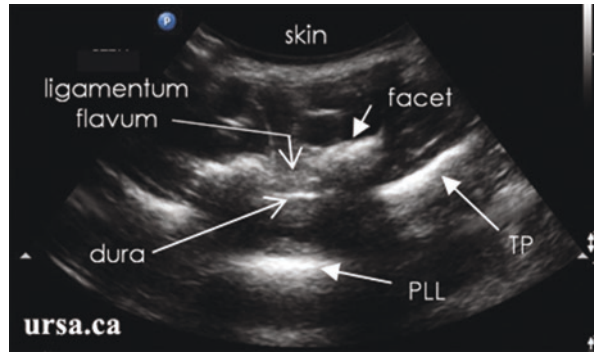
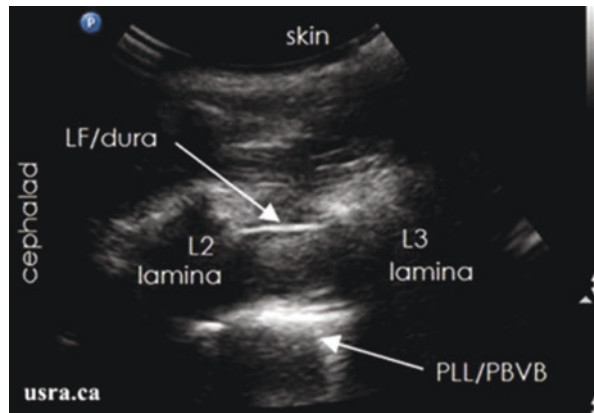


Fig. 16.3 Longitudinal paramedian scan at L2–3 interlaminar space [5]



Upper Extremity

The upper extremity is innervated by the brachial plexus, which is formed by the ventral rami of the C5–T1 spinal nerves. These nerves pass through the cervicoaxillary canal to reach the axilla and continue down the arm to the hand, providing sensory and motor innervations to the different regions. The plexus is divided into roots, trunks, divisions, cords, and finally branches. The five roots of these nerves, emerging from C5, C6, C7, C8, and T1, merge to form three trunks, the superior, middle, and inferior, which in turn divide into anterior and posterior divisions that then regroup into three cords. The cords, which are named according to their position in respect to the axillary artery (posterior, lateral, and medial), finally form the terminal branches along with collaterals given off along the way [6, 7].

When performing regional anesthesia for the upper extremity, blocks can be performed to target the different segments of the brachial plexus depending on which portion of the upper extremity needs to be targeted for a sensory or motor block. The muscles are innervated in a proximal-to-distal fashion so that the higher cervical segments innervate proximal muscles, while the more distal muscles are innervated by the lower segments (C8–T1). The main blocks performed to target the brachial

plexus include approaches via the interscalene, supraclavicular, infraclavicular, and axillary blocks. Additionally, wrist or digit blocks can be performed to target terminal branches. Performing these blocks requires a thorough understanding of normal anatomy. Anomalies, however, always exist.

The three trunks emerge between the anterior and medial scalene muscles in the neck, while the roots of the plexus are located deep to the prevertebral fascia. The trunks divide into the anterior and posterior division behind the clavicle and travel down to the axilla, where they combine to form the cords. Past this point the terminal branches continue down the arm as individual nerves. Having this general distribution in normal anatomy, blocks are performed to target the different regions of the plexus. The interscalene brachial plexus block is useful for shoulder, elbow and arm surgery, but classically is not recommended for the hand since it has potential to spare the inferior trunk with decreased blockade of C8 and T1 roots. The supraclavicular approach allows local anesthetic to reach the distal trunks and origins of the divisions, the point where the brachial plexus is at its smallest surface area. This block will allow for adequate blockade of entire plexus. The infraclavicular brachial plexus block targets the cords that lie deep to the pectoralis muscles and inferior to the coracoid process. This block can spare the proximal medial portion of the arm and shoulder. Once the cords pass into the axilla, they result in the terminal branches: primarily the median, ulnar, radial and musculocutaneous nerves. The arrangement of these nerves around the axillary artery allows for regional blocks targeting these individual nerves to be performed [6, 7].

Many anatomic variations in the brachial plexus actually exist. Much of this data is from cadaveric dissections. In 1918, Kerr had published the 29 forms of brachial plexus dissected from 175 cadavers. More recently, other authors have described even more forms [8]. Current technology using ultrasound has also allowed these variations to be more easily recognized (Fig. 16.4a–c). It has been speculated that up to 53.5% of plexuses studied in cadavers have an anatomic variation from the classic description [9].

A frequent anomaly noted in interscalene region is the C5 or C6 nerve root passing either anterior to or through the anterior scalene muscle bypassing the interscalene groove that could cause sparing of these nerves during this approach for the block. About 25% of cadaver dissections described by Natis et al. include such an abnormal superior trunk [10]. The same anomaly was noted by ultrasonography in volunteers as published by Kessler et al. [11]. Other variations include plexuses that may be more cephalad or caudad than expected. Roots that do not form into trunks or an accessory phrenic nerve that arises directly from the brachial plexus can confound the block when a peripheral nerve block is used [11, 12].

The supraclavicular brachial plexus block is most concerning given the proximity of the needle to the dome of the lung, increasing the risk of a pneumothorax (Fig. 16.5). However, this risk is decreased dramatically with the use of real-time ultrasound. This approach still allows for maximal blockade of all the nerves. The infraclavicular approach to brachial plexus block allows for a decreased risk of pneumothorax; however, it also reduces the ability of blocking the entire plexus with a single injection. At the level of the coracoid process, the terminal branches

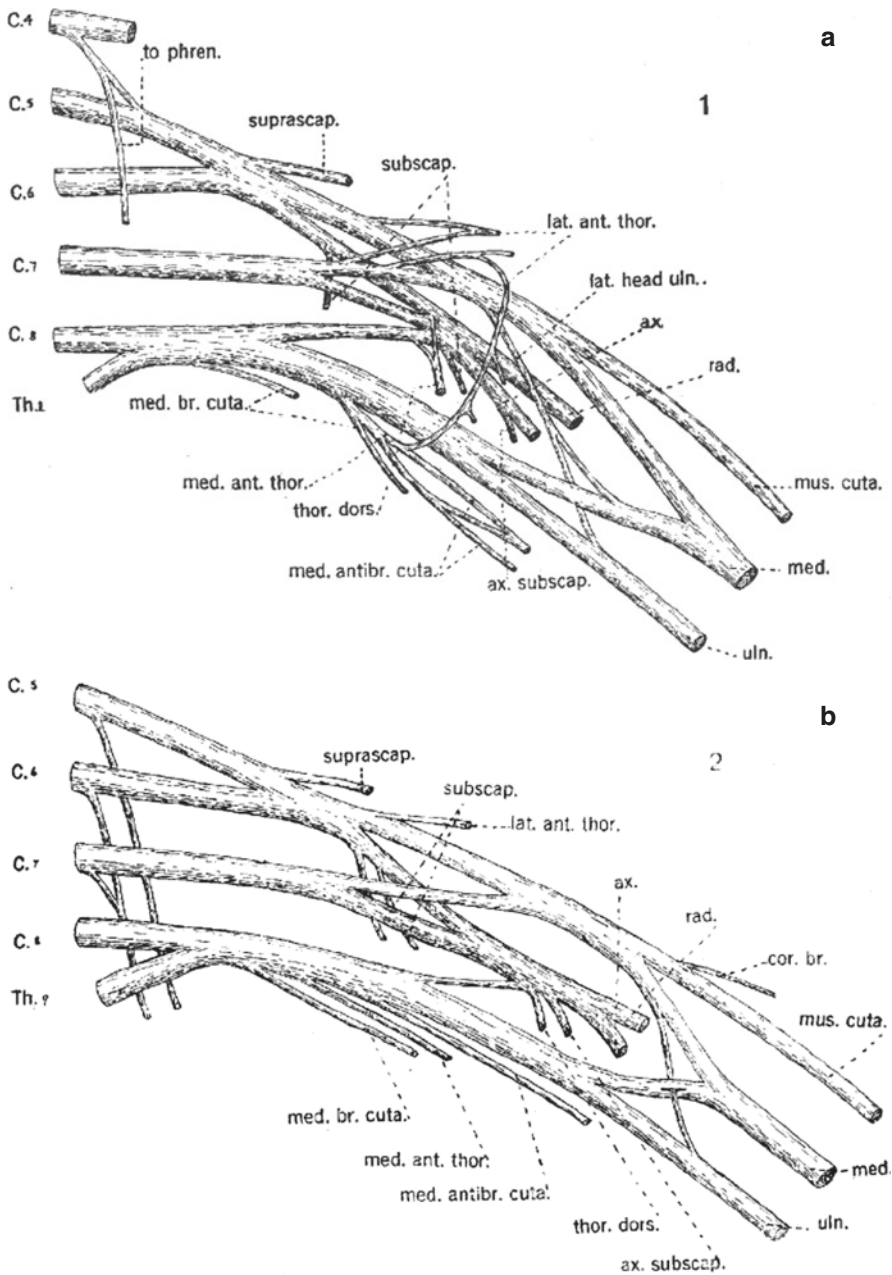


Fig. 16.4 (a-c) Anatomical illustration of three common variation of the brachial plexus

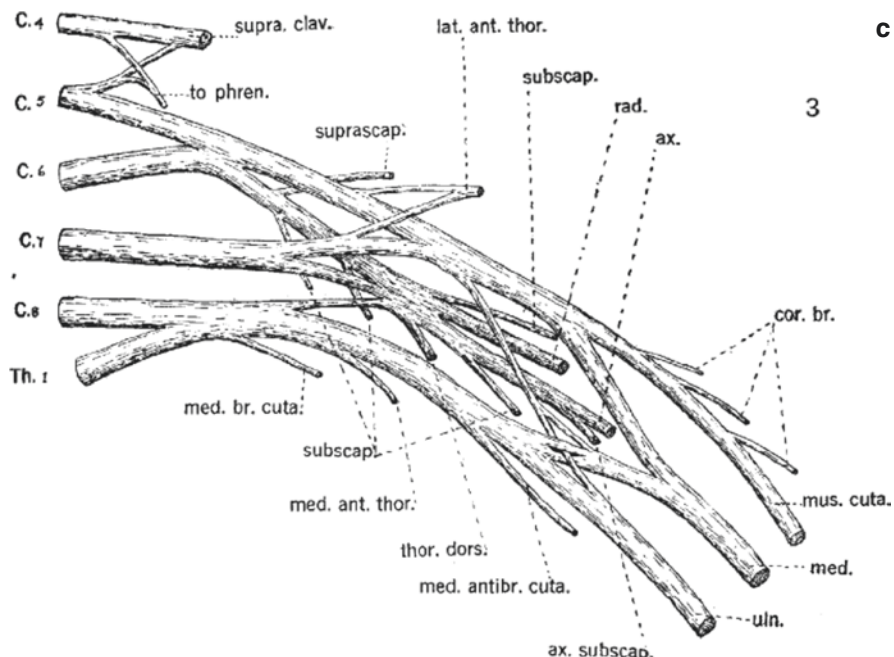
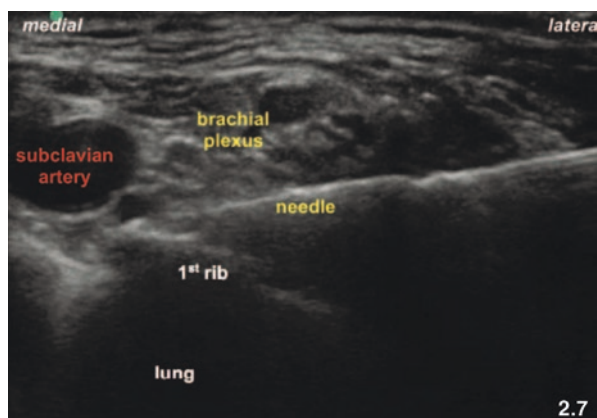


Fig. 16.4 (continued)

Fig. 16.5 Ultrasound-guided supraclavicular brachial plexus block showing needle position



start to divert away from the cords. For instance, the musculocutaneous and axillary nerve may be more difficult to block at this level. As the cadaver studies have indicated, the brachial plexus contains many variations in the formation of trunks and cords. Variations include the absence of the inferior trunk, no discrete posterior cord, and missing T1 contribution to the posterior cord [13]. Additionally, anomalies in the vasculature can also lead to increased risk of intravascular injection. Once again, real-time ultrasound helps to reduce these risks [14].

In the axilla, the nerve blocks are dependent on position in relation to the axillary artery. Common teaching is that the median nerve is lateral to the artery, ulnar nerve anteromedial, while the radial nerve lies posterior to the artery. Retzl et al. reported how in 69 volunteers ultrasound showed variations in this conventional positioning in about 50% of the subjects [15]. Additionally, vascular anomalies that can confound the axillary brachial plexus block are also common, and the use of ultrasound is once more helpful in this regard.

Lower Extremity

In contrast to the relative compactness of the brachial plexus in the upper extremity, nerves supplying the lower extremity are widely spaced from one another as they enter the thigh. To help determine which peripheral nerve block (PNB) to use for analgesia or anesthesia in the lower extremity, it is important to appreciate the innervation of the affected region and requirements of the surgical procedure. The lumbar plexus is comprised of the ventral rami of L1–4 with occasional contribution from T12. This plexus gives rise to the ilioinguinal, genitofemoral, and three major nerves of the lower limb: obturator (L2–4), femoral (L2–4), and lateral femoral cutaneous (L1–3) nerves (Fig. 16.6). Motor and sensory innervation to the anterior thigh and sensory innervation to the medial leg are provided by these nerves. The remainder of the lower extremity is innervated by nerves originating from the sacral plexus, which arises from L4–5 and S1–4. For example, the posterior thigh and the entire area distal to the knee, with the exception of medial aspect, receive innervation from the tibial and peroneal portions of the sciatic nerve.

One of the most common lower extremity PNBs to be performed is that on the femoral nerve. Innervation to the major hip flexors and knee extensors, and much of the sensation to the hip and thigh, is provided by this nerve. The majority of the skin of the medial leg and ankle joint is innervated by the saphenous nerve, which is the most medial branch of the femoral nerve. A femoral nerve block is often used as part of a postoperative analgesia plan for thigh and knee procedures, as this solitary block is insufficient to provide surgical anesthesia. However, it can be combined with a sciatic block to provide complete anesthesia below the knee [16]. The femoral nerve block was traditionally approached just at or slightly distal to the inguinal ligament. An alternative technique gaining more popularity is the adductor canal block, where the femoral nerve is approached more distally near the mid-thigh since by this point, the nerve has already given off much of the innervation to the quadriceps muscles (Fig. 16.7). Sparing this major muscle group, which is responsible for stabilizing the knee during weight-bearing, makes possible earlier postoperative ambulation and rehabilitation [17]. Femoral nerve blocks have a relatively low rate of complications, although injury to the femoral vessels is possible.

Another major PNB in the lower extremity is the sciatic nerve block. The nerve can be blocked at several locations along its course down the posterior aspect of the lower extremity. For knee procedures, blockade of the sciatic nerve can occur in the gluteal region via classic posterior or anterior approaches. Due to the deep position

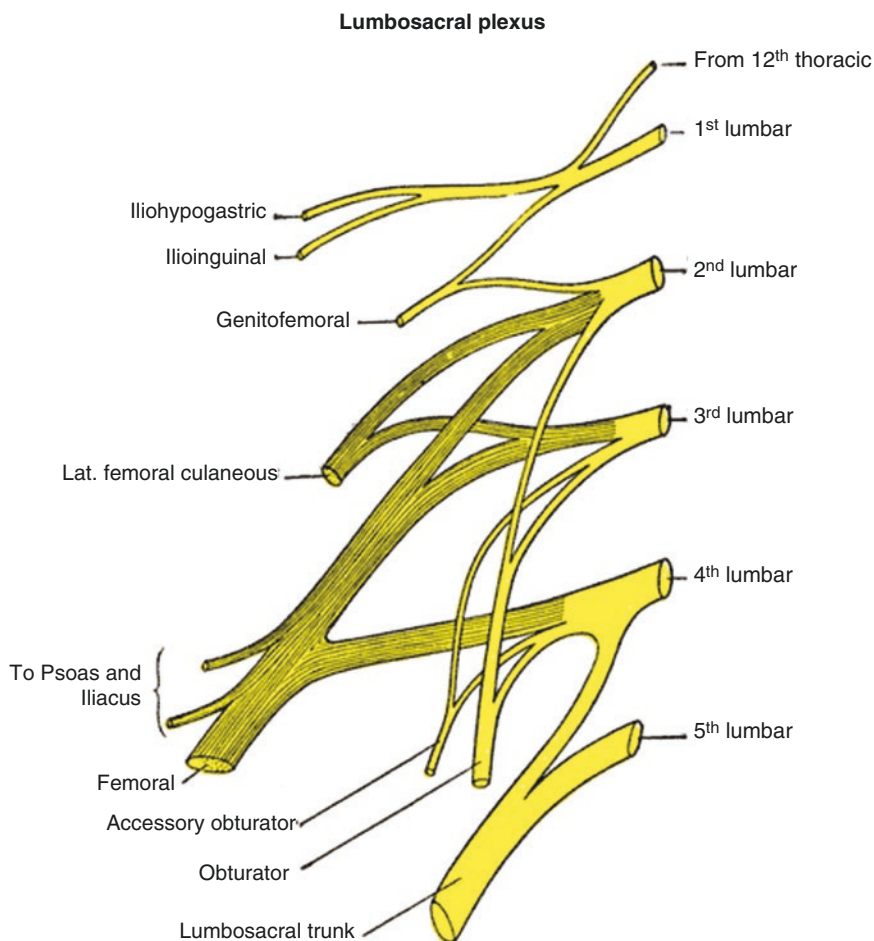


Fig. 16.6 Anatomy of the lumbar plexus

of the nerve at this position, vascular puncture resulting in hematoma formation is a risk to be aware of [18]. The popliteal approach to the sciatic nerve block offers excellent coverage for ankle and foot procedures while still sparing most of the hamstring innervation. The major risk to this approach is once again vascular injury due to the proximity of the popliteal vessels.

For procedures to be done on the foot or toes, an ankle block can be performed at the level of the malleolus to block all five nerves innervating the foot. Sensation to the foot is supplied by saphenous nerve anteromedially, while four terminal branches of the sciatic nerve system (deep peroneal, superficial peroneal, posterior tibial, and sural nerves) supply the remainder of the foot. While a complete ankle block necessitates a series of five blocks, these can be streamlined to minimize the number of separate needle insertions. Ankle blocks carry a low risk of complications, as long as excessive local anesthetic volumes and the use of vasoconstrictors are minimized.

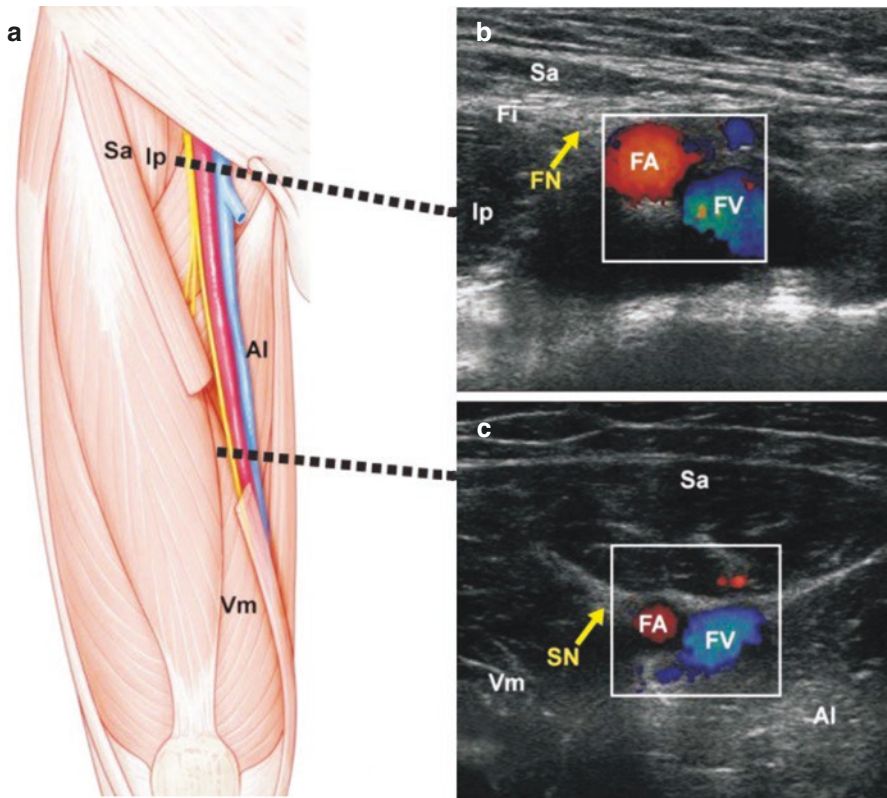


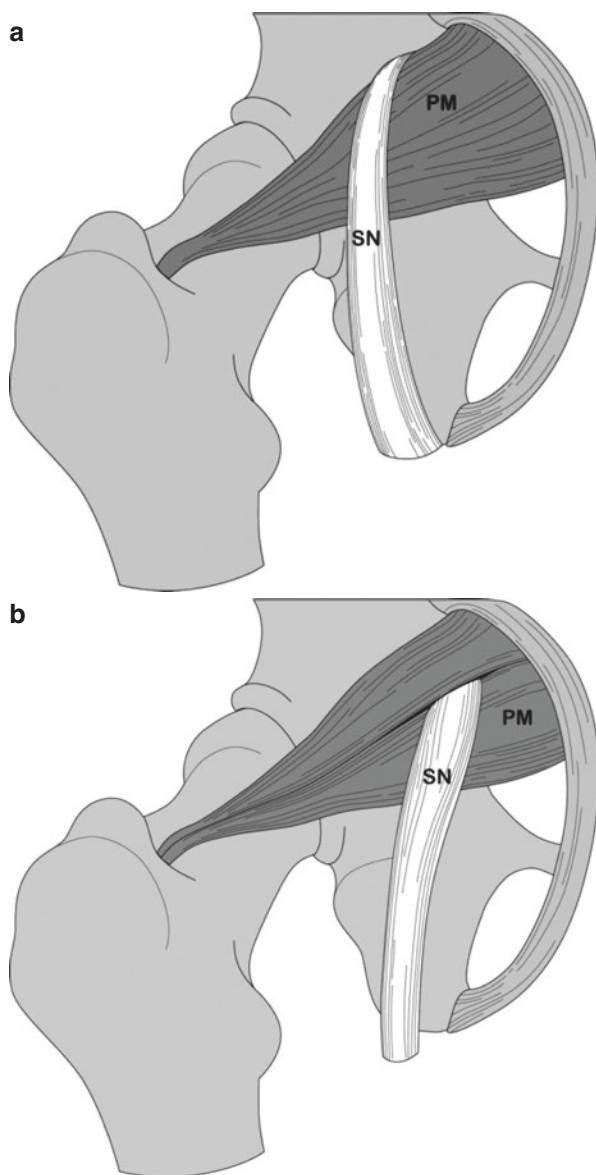
Fig. 16.7 Anatomical landmarks for the adductor canal block. Artistic anatomical drawing of the femoral nerve, vein and artery (a) with an ultrasound correlation showing the classic femoral nerve block approach (b) and the adductor canal approach (c)

In addition to the more distal lower extremity PNBs discussed previously, a posterior lumbar plexus or psoas compartment block can be done to accommodate procedures on the hip, anterior thigh, and knee. This block will cover regions innervated by the femoral, lateral femoral cutaneous, and obturator nerves. In conjunction with a gluteal sciatic nerve block, total anesthesia to the lower limb can be attained. Owing to the lumbar plexus being close to multiple sensitive structures, however, this deep block is technically difficult to perform and carries one of the highest complication rates of the various PNBs. Retroperitoneal hematomas, epidural or spinal anesthetic spread, intravenous injection, and renal or ureteral injury are some examples of adverse events reported during placement of this block [19].

Similar to the brachial plexus, various anatomic variations may be present in patients undergoing lower extremity nerve blocks. The data is primarily from studies of cadavers, with contributions from case reports of patients noted to have anatomic anomalies during block placement. One meta-analysis, for instance, looked at the relative position of the sciatic nerve in the gluteal region compared to position

of the piriformis muscle. In pooling data from over 6000 cadavers from 18 studies, 16.2% of dissected specimens had a sciatic nerve that exited above or through the piriformis muscle, whereas the nerve typically exits below the muscle [20] (Fig. 16.8). Following the sciatic nerve more distally, it typically bifurcates into the tibial and common peroneal nerves at the apex of the popliteal fossa [21]. In a study of 25 cadavers, 12% of the limbs examined exhibited anatomic variations with sciatic bifurcation occurring anywhere between the sacral plexus and popliteal space

Fig. 16.8 (a, b) Sciatic nerve exiting above and through the piriformis muscle; typically, the nerve exists below the muscle. Beaton and Anson type “F.” *PM* piriformis muscle, *SN* sciatic nerve [20]



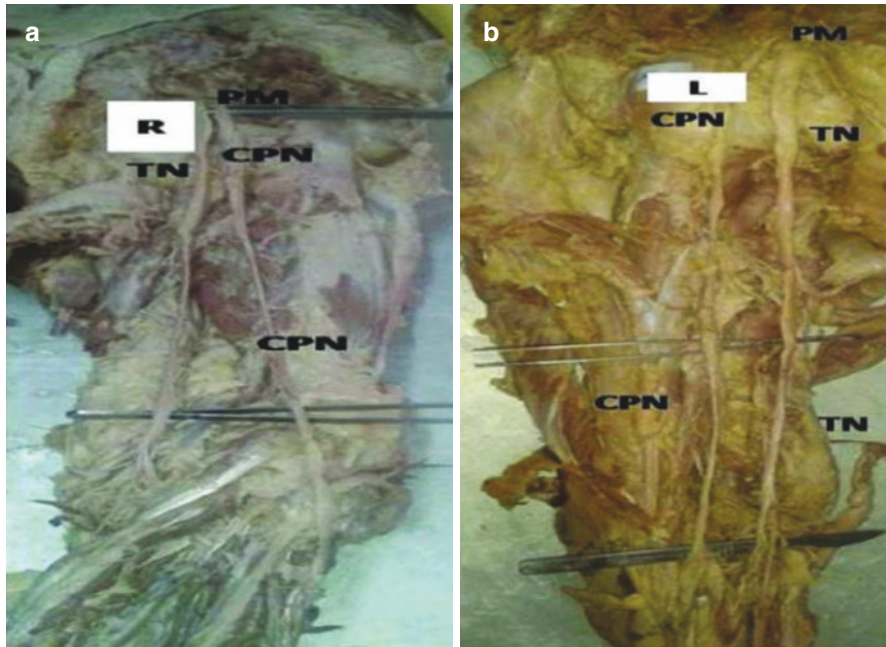


Fig. 16.9 (a, b) Cadaver dissection of the sciatic nerve showing a higher division of the sciatic nerve [22]

[22] (Fig. 16.9). Another study of 19 cadavers found anatomic variations of the femoral nerve in up to 35% of limbs examined. These variations primarily involved nerve bifurcation into two or three segments separated by fibers of the psoas major and even proximal branching above the inguinal ligament [23].

Current PNB placement techniques utilizing ultrasound visualization along with nerve stimulators allow aberrant anatomy to be identified during block placement and accommodations to be made during the procedure. As illustrated by the prior examples, clear understanding of sonoanatomy and anatomic function is essential for successful and safe placement of PNBs, particularly when patients with anatomic anomalies are encountered.

References

1. Spoonamore MJ. Spine anatomy, 2015. <http://www.uscspine.com/spine-health-education/spinal-anatomy.cfm>. Accessed 12 Feb 2017.
2. Deschner B, Allen M, de Leon O. Epidural blockade. In: Hadzic A, editor. Textbook of regional anesthesia and acute pain management. New York: McGraw-Hill; 2007.
3. Fettes PD, Jansson JR, Wildsmith JA. Failed spinal anaesthesia: mechanisms, management, and prevention. *Br J Anaesth.* 2009;102(6):739–48.

4. Lacassie HJ, Millar S, Leithe LG, Muir HA, Montaña R, Poblete A, et al. Dural ectasia: a likely cause of inadequate spinal anaesthesia in two parturients with Marfan's syndrome. *Br J Anaesth*. 2005;94(4):500–4.
5. Ultrasound of Regional Anesthesia: Neuraxial Blocks. 2008. <http://www.usra.ca/regional-anesthesia/specific-blocks/upper-limb/suprablok.php>.
6. Delaunay L. Anatomy of brachial plexus. In: Chelly JE, editor. *Peripheral nerve blocks: a color atlas*. 2nd ed. Philadelphia: Lippincott, Williams, and Wilkins; 2004.
7. Orebaugh SL, Williams BA. Brachial plexus anatomy: normal and variant. *Sci World J*. 2009;9:300–12.
8. Kerr AT. The brachial plexus of nerves in man, the variations in its formation and branches. *Am J Anat*. 1918;23(2):285–395.
9. Bonnel F. Microscopic anatomy of the adult human brachial plexus: an anatomical and histological basis for microsurgery. *Microsurgery*. 1984;5(3):107–17.
10. Natsis K, Totlis T, Tsikaras P, Anastasopoulos N, Skandalakis P, Koebeke J. Variations of the course of the upper trunk of the brachial plexus and their clinical significance for the thoracic outlet syndrome: a study on 93 cadavers. *Am Surg*. 2006;72(2):188–92.
11. Kessler J, Gray AT. Sonography of scalene muscle anomalies for brachial plexus block. *Reg Anesth Pain Med*. 2007;32(2):172–3.
12. Loukas M, Kinsella CR Jr, Louis RG Jr, Gandhi S, Curry B. Surgical anatomy of the accessory phrenic nerve. *Ann Thorac Surg*. 2006;82(5):1870–5.
13. Pandey S, Shukla V. Anatomical variations of the cords of brachial plexus and the median nerve. *Clin Anat*. 2007;20(2):150–6.
14. Koscielniak-Nielsen ZJ. Ultrasound-guided peripheral nerve blocks: what are the benefits? *Acta Anaesthesiol Scand*. 2008;52(6):727–37.
15. Retzl G, Kapral S, Greher M, Mauritz W. Ultrasonographic findings of the axillary part of the brachial plexus. *Anesth Analg*. 2001;92(5):1271–5.
16. Tran DQ, Clemente A, Finlayson RJ. A review of approaches and techniques for lower extremity nerve blocks. *Can J Anaesth*. 2007;54(11):922–34.
17. Chen J, Lesser JB, Hadzic A, Reiss W, Resta-Flarer F. Adductor canal block can result in motor block of the quadriceps muscle. *Reg Anesth Pain Med*. 2014;39(2):170–1.
18. Ota J, Sakura S, Hara K, Saito Y, et al. Ultrasound-guided anterior approach to sciatic nerve block: a comparison with the posterior approach. *Anesth Analg*. 2009;108(2):660–5.
19. Amiri HR, Zamani MM, Safari S. Lumbar plexus block for management of hip surgeries. *Anesth Pain Med*. 2014;4(3):e19407.
20. Smoll NR. Variations of the piriformis and sciatic nerve with clinical consequence: a review. *Clin Anat*. 2010;23(1):8–17.
21. Vloka JD, Hadzić A, April E, Thys DM. The division of the sciatic nerve in the popliteal fossa: anatomical implications for popliteal nerve blockade. *Anesth Analg*. 2001;92(1):215–7.
22. Adibatti M, Sangeetha V. Study on variant anatomy of sciatic nerve. *J Clin Diagn Res*. 2014;8(8):AC07–9.
23. Anloague PA, Huijbregts P. Anatomical variations of the lumbar plexus: a descriptive anatomy study with proposed clinical implications. *J Man Manip Ther*. 2009;17(4):e107–14.

Part IV

Upper and Lower Extremities



Upper Extremity Variations

17

Samuel Kim, Xiaolu Xu, James E. Clune,
and Deepak Narayan

Nerves

Median Nerve

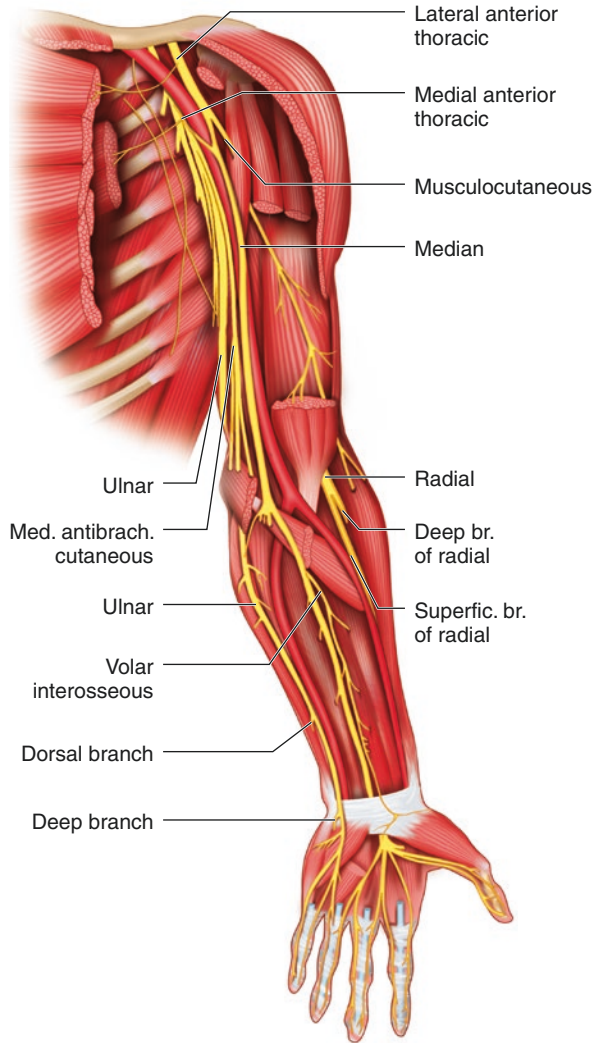
Normal Course

The median nerve originates from the lateral (C5–7) and medial cords (C8, T1) of the brachial plexus (Fig. 17.1). The median nerve enters the arm lateral to the brachial artery, crosses anterior to the artery near the insertion of the coracobrachialis, and descends medial to the artery until reaching the cubital fossa. In the fossa, the nerve situates in between the bicipital aponeurosis and brachialis. The median nerve enters the forearm between the two heads of the pronator teres, crosses lateral to the ulnar artery, and passes posterior to a tendinous bridge between the humeroulnar and radial heads of the flexor digitorum superficialis before descending the forearm along the flexor digitorum superficialis and anterior to the flexor digitorum profundus. It emerges from behind the lateral edge of the flexor digitorum superficialis 5 cm proximal to the flexor retinaculum, and lies superficially between the flexor digitorum superficialis and flexor carpi radialis tendons. The median nerve enters the hand deep to the flexor retinaculum and innervates the thenar muscles and the

S. Kim (✉) · J. E. Clune · D. Narayan (Deceased)
Section of Plastic and Reconstructive Surgery, Yale New Haven Hospital,
New Haven, CT, USA

X. Xu
Yale School of Medicine, New Haven, CT, USA

Fig. 17.1 The course of the median nerve from the brachial plexus to the hand



two radial lumbricals via its motor branches, and innervates the palmar aspect of the first, second, and third fingers and the radial half of the fourth finger via its sensory cutaneous branches [1].

Variations and Pathology

Carpal tunnel syndrome (CTS), a common pathology affecting the median nerve, is often treated by surgical decompression. Awareness of the variations of the median nerve near the carpal tunnel is important when treating CTS. One particular branch to be cognizant of during carpal tunnel surgery is the thenar branch or recurrent motor branch. This branch normally divides from the median nerve radially at the

distal margin of the transverse carpal ligament. However, the thenar branch has also been found to pierce through the transverse carpal ligament or leave the median nerve within the carpal tunnel under the transverse carpal ligament (Fig. 17.2) [2]. The thenar branch has even been found to divide from the median nerve ulnarly.

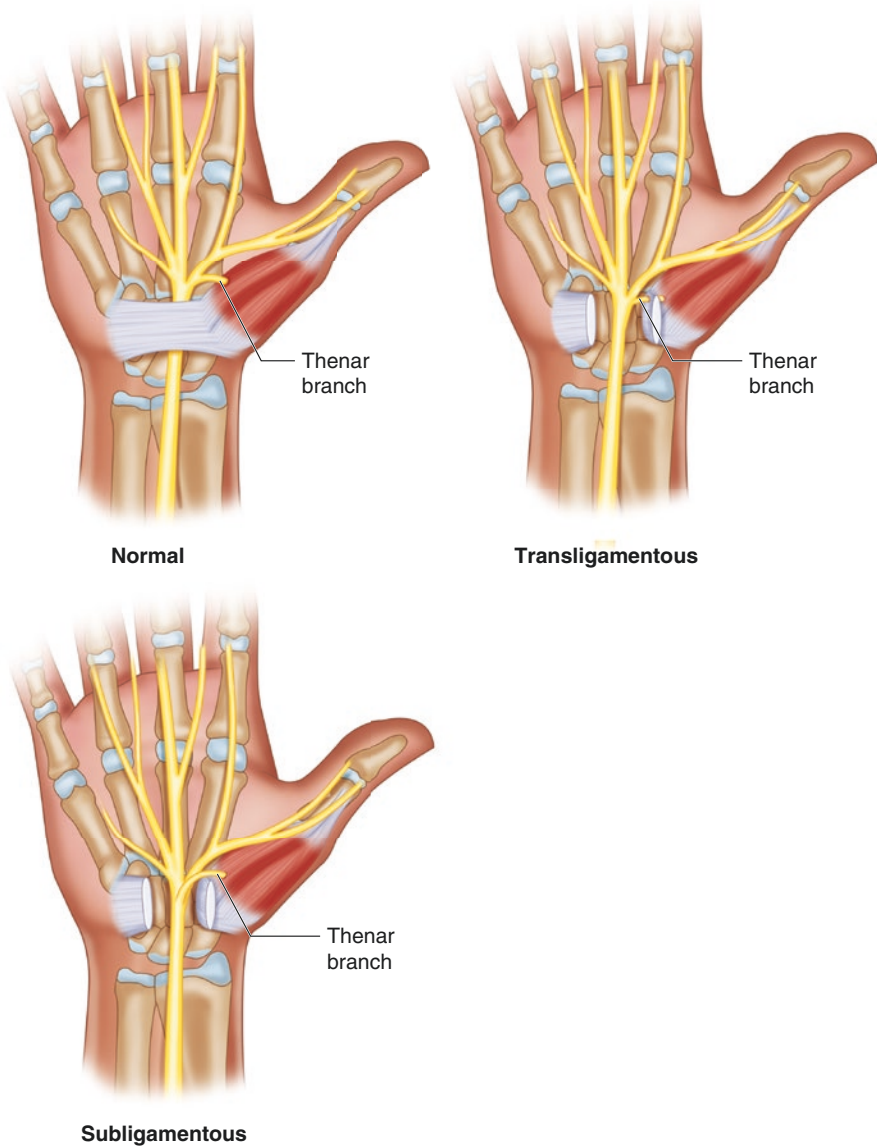


Fig. 17.2 The thenar branch normally leaves the median nerve distal to the transverse carpal ligament. However, the thenar branch can pierce through the transverse carpal ligament (transligamentous) or leave the median nerve under the transverse carpal ligament (subligamentous) [2]

Lanz [2] organized these variations of the thenar branch into one group and additionally described three other groups of median nerve variations at the wrist including accessory branches at the distal carpal tunnel, a high division of the median nerve (sometimes in association with a median artery), and accessory branches proximal to the carpal tunnel [2–10].

Variations of the median nerve may also exist more proximally. A rare variation of the median nerve supplying the anterior compartment of the arm in the absence of a musculocutaneous nerve bilaterally has been reported [11–13]. Variation of a distal union of the lateral and medial cords and piercing of the coracobrachialis by the proximal lateral cord instead of the musculocutaneous nerve has also been reported. Due to the possible use of a coracobrachialis flap in postmastectomy reconstruction, it is important to be aware of this variation [14].

Multiple communicating branches may pass from the median nerve (and sometimes the anterior interosseous nerve) to the ulnar nerve called Martin-Gruber anastomoses (Fig. 17.3). Martin-Gruber anastomoses are present in about 17% of the global population. These branches arise from the median nerve proximally and pass medially between the flexor digitorum superficialis and the flexor digitorum profundus, deep to the ulnar artery, and join the ulnar nerve. This results in median nerve innervation of a variable number of intrinsic muscles of the hand, and presumably explains cases of functional “ulnar intrinsics” muscles despite ulnar nerve transection, and functional “median intrinsics” muscles despite median nerve transection [15]. Rarely, the reverse may occur, where communicating branches from the ulnar nerve pass to the median nerve, usually in the distal forearm near the carpal tunnel. This is termed a Marinacci communication (Fig. 17.3). Hand surgeons should be aware of these communications between the median and ulnar nerve, which can mask upper extremity nerve lesions [1, 14, 15].

Palmar Cutaneous Branch of the Median Nerve

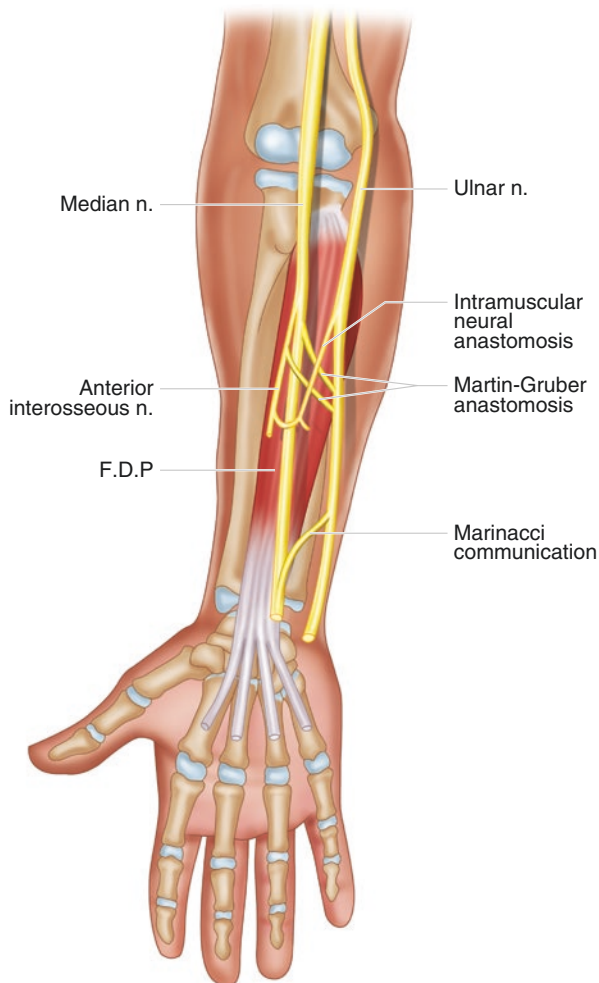
Normal Course

The palmar cutaneous nerve (PCN) branches off the radial aspect of the median nerve at an average of 4–5 cm proximal to the wrist flexion crease (Fig. 17.4) [16, 17]. It runs in a small tunnel of sheath ulnar to the flexor carpi radialis and deep to the antebrachial fascia between the flexor carpi radialis (FCR) and palmaris longus (PL). It then pierces and emerges from the antebrachial fascia, where it runs superficial to the flexor retinaculum and divides into medial and lateral branches. The lateral branches supply the thenar skin and connect with the lateral cutaneous nerve of the forearm. Medial branches supply the central palmar skin and connect with the palmar cutaneous branch of the ulnar nerve.

Variations and Pathology

A few variations of the PCN should be noted because surgeons frequently operate near the PCN, and injury to the PCN can result in complex regional pain syndrome at a rate of 3–10% [16, 18]. Takeoff of the PCN from the ulnar side of the median

Fig. 17.3 Martin-Gruber anastomoses and Marinacci communications. Martin-Gruber anastomoses are communicating branches that pass from the median nerve or anterior interosseous nerve to the ulnar nerve. Marinacci communications are the reverse, where communicating branches from the ulnar nerve pass to the median nerve



nerve is seen in about 15% of patients, and in these cases, the PCN tends to position closer to (mean distance of 0.3 cm) or crossover to the ulnar side of the palmaris longus (PL). Therefore, care should be taken to draw longitudinal incisions at 1 cm ulnar to the PL during its harvest to avoid damaging the PCN [19]. In other cases, the PCN is noted to either insert into or pass through PL tendon 1–1.5 cm proximal to its insertion into the aponeurosis. Transecting the PL at a more proximal position (at least 2 cm from the aponeurotic insertion) is recommended to avoid PCN damage [17, 20].

The PCN may sometimes crossover or enter the FCR sheath and course along its radial aspect. It is important to recognize this variant in cases of volar plating for distal radius fracture, because the PCN variant will be at risk for injury during the FCR radial dissection [16].

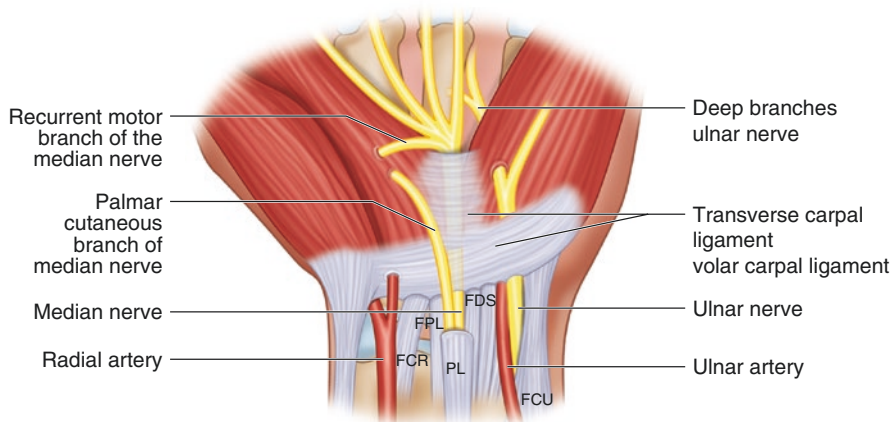


Fig. 17.4 Palmar cutaneous nerve. The palmar cutaneous nerve branches off the radial aspect of the median nerve 4–5 cm proximal to the wrist flexion crease

Taleisnik et al. demonstrated that the PCN can have a trans-retinaculum course, which is at risk for injury in the longitudinal division of the ligament during carpal tunnel releases. He recommended a curved longitudinal incision on the ulnar side of the axis of the ring finger [20]. However, Hobbs et al. suggested that Taleisnik's incision may jeopardize the palmar branch of the ulnar nerve and recommended, instead, a skin incision 1 cm ulnar to the axis of the third metacarpal, in the axis of the ring finger [21]. They also noted that in 8% of hands a communication exists between the superficial radial nerve and the PCN that should be considered in surgeries requiring radial palmar wrist incisions (e.g., volar wrist ganglion cyst) [22].

Anterior Interosseous Nerve (AIN)

Normal Course

The anterior interosseous nerve (AIN) arises from the median nerve posteriorly between the two heads of pronator teres about 5 cm distal to the medial epicondyle. This motor branch of the median nerve supplies the anterior compartment of the forearm, classically innervating the flexor pollicis longus (FPL), the pronator quadratus (PQ), and the radial half of the flexor digitorum profundus (FDP) (Fig. 17.5).

Variation and Pathology

Anterior interosseous nerve syndrome (AINS) or Kiloh-Nevin syndrome is a rare entrapment syndrome of the AIN that affects the motor function of the FPL, the PQ, and the radial half of FDP (i.e., second and third digit). The compression is usually caused by the fibrous bands from the deep heads of the pronator teres to the brachialis fascia, but compression from other fibrous bands can also occur. The AIN and ulnar nerve can variably innervate the radial and ulnar FDPs. In one study of 50

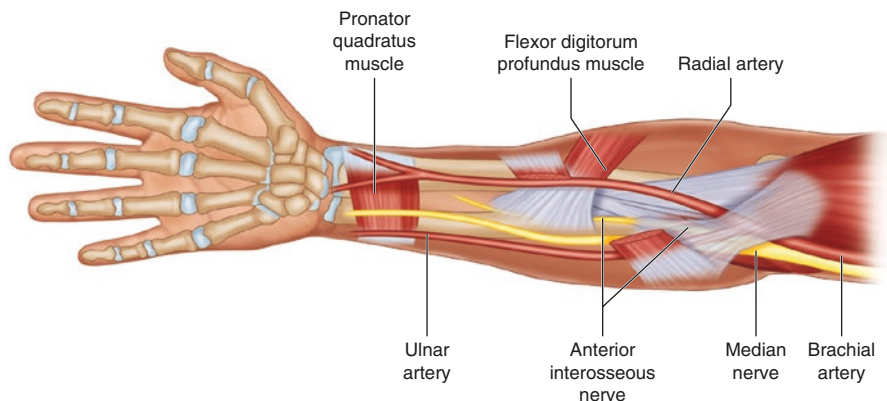


Fig. 17.5 Course of the anterior interosseous nerve

hands, 50% of hands had AIN innervation to all FDPs, with the ulnar nerve providing dual innervation to the FDP of the third-fifth digits. The second most common finding (34%) was dual innervation to the third and fourth FDPs [23]. Clinically, these variations manifest as variable symptoms in AINS: the second digit is consistently affected, whereas the third digit and the PQ are occasionally spared depending on the innervation pattern [24, 25]. The presence of Martin-Gruber anastomoses (see above) in the setting of AINS can also lead to palsy of the intrinsic muscles of the hand (normally innervated by the ulnar nerve).

Ulnar Nerve

Normal Course

The ulnar nerve carries fibers from the C8 and T1 nerve roots as it originates from the medial cord of the brachial plexus (occasionally also from the C7 nerve root of the lateral cord) (Fig. 17.6). The ulnar nerve descends along the posteromedial aspect of the humerus. It lies posterior and posteromedial to the intermuscular septum and brachial artery, respectively, and anterior to the medial head of the triceps brachii muscle. As the ulnar nerve descends in the upper arm, the arcade of Struthers, a band of fascia attached to the intermuscular septum, covers the ulnar nerve about 8 cm proximal to the medial epicondyle of the humerus. The ulnar nerve descends posterior to the medial epicondyle of the humerus and medial to the olecranon of the ulna before entering the cubital tunnel. The cubital tunnel is defined by the medial epicondyle, the olecranon, and a fascial layer extending from the flexor carpi ulnaris muscle and the arcuate ligament of Osborne.

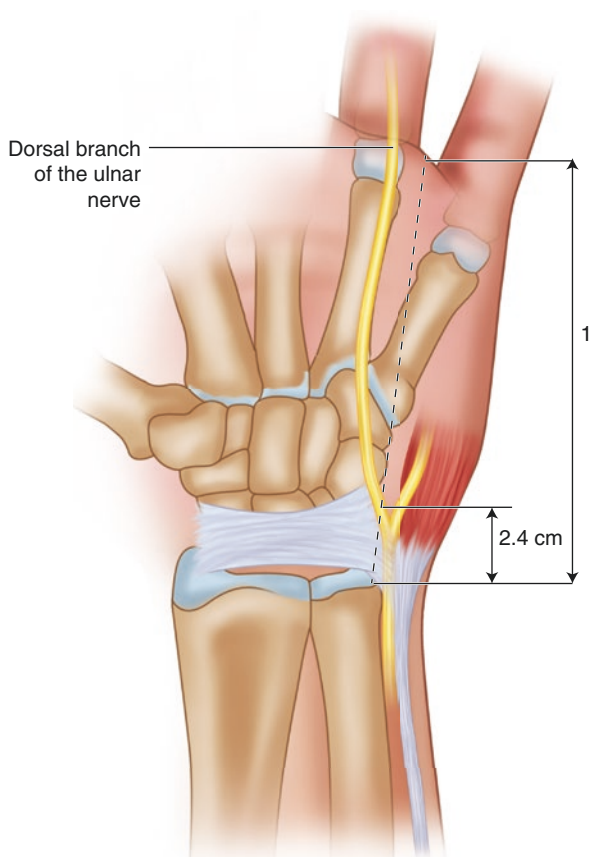
After exiting the cubital tunnel, the ulnar nerve enters the anterior compartment of the forearm between the ulnar and humeral heads and under the aponeurosis of the flexor carpi ulnaris muscle. The ulnar nerve then courses along the ulna with the ulnar artery, deep to the flexor carpi ulnaris muscle. It gives off three branches in the

Variations and Pathology

A few variations occur near the elbow that are important for the surgeon to be aware of, particularly when managing ulnar nerve pathology such as in cubital tunnel syndrome. The ulnar nerve can pass in front of the medial epicondyle of the humerus instead of passing posterior to it. The ulnar nerve may also send a variable number of sensory branches to the elbow joint capsule at various distances from the elbow [26, 27]. Several studies found that the motor branch from the ulnar nerve providing innervation to the flexor carpi ulnaris originated anywhere from 40 mm proximal to 73 mm distal to the medial epicondyle [28, 29]. Although not normally a branch of the ulnar nerve, the medial antebrachial cutaneous nerve also can send a variable number of superficial branches to the elbow region [30]. One report described that the medial antebrachial cutaneous nerve originated from the ulnar nerve in the region of the elbow [31]. These branches are all susceptible to iatrogenic injury when surgically managing compression of the ulnar nerve not only in the cubital tunnel, but also in any pathology involving the elbow region.

The dorsal branch of the ulnar nerve follows a fairly consistent course on the dorsum of the wrist and hand by crossing a line drawn between the ulnar styloid and the fourth web space, on average 2.4 cm distal to the ulnar styloid (Fig. 17.7) [32].

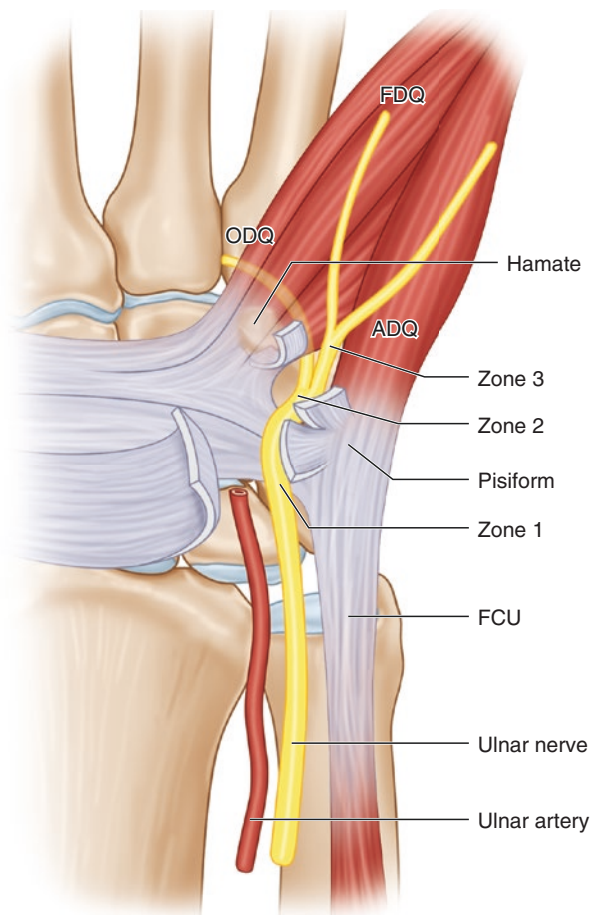
Fig. 17.7 Dorsal branch of the ulnar nerve. The dorsal branch of the ulnar nerve normally travels along the dorsum of the hand crossing radially over a line drawn between the ulnar styloid and the fourth web space 2.4 cm distal to the ulnar styloid [32]



However, aberrant branches that cross the wrist immediately distal to the ulnar styloid or ulnar head to innervate the radial side of the hand have been reported. Standard portals for wrist arthroscopy involve placement of the 6-radial portal within the proximal fifth of a line drawn between the ulnar styloid and fourth web space to avoid damage to the dorsal branch of the ulnar nerve. However, extreme care must still be taken as variations described above have been shown to cross this standard area of portal placement [32].

Ulnar tunnel syndrome, or Guyon's canal syndrome, occurs due to compression of the ulnar nerve within Guyon's canal. The location of the compression within Guyon's canal is categorized by three zones: zone I, the bifurcation; zone II, along the deep branch; and zone III, along the superficial branch (Fig. 17.8). Compressions at zone I, zone II, and zone III typically produce motor and sensory deficits, exclusively motor deficits, and exclusively sensory deficits, respectively. However, division patterns of the ulnar nerve within Guyon's canal are variable, with several different patterns described. Lindsey and Watumull described a trifurcated nerve

Fig. 17.8 Guyon's canal compression zones. Compression of the ulnar nerve within Guyon's canal can occur in one of three zones: the bifurcation (zone I), along the deep branch (zone II), or along the superficial branch (zone III)



pattern resulting in a motor branch and two sensory branches within Guyon's canal [33]. Murata et al. categorized these variations into five types (Fig. 17.9) [34]. Interestingly, several instances of communications between the distal branches were found among the different types. Varying symptoms are described depending on the level of compression.

Although not a variation of the ulnar nerve itself, the contents of Guyon's canal may differ, which are thought to contribute to compression of the ulnar nerve. An accessory abductor digiti minimi or accessory flexor digiti minimi traveling in Guyon's canal and a fibrous arch between the hook of hamate and the pisiform have both been described as common occurrences and possible contributors to ulnar nerve entrapment [35].

Sensory innervation to the hand varies significantly. The medial proper palmar digital nerve of the fifth finger has been described as originating from the dorsal branch of the ulnar nerve and traveling outside of Guyon's canal before reaching the palmar medial fifth finger [36–40]. The ulnar nerve can provide sensory innervation to more than the typical 1.5 digits of the hand both palmarly and dorsally, and innervation of the dorsal first phalanx has even been reported [36, 41, 42]. In these specific situations, compression of the ulnar nerve can result in sensory symptoms different from those in the ring and little finger.

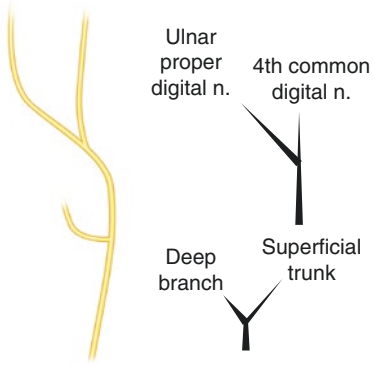
First illustrated by Berrettini in 1741, communications exist between the common digital nerves of the ulnar and median nerves. These are called Berrettini anastomoses (Fig. 17.10a) [43]. The incidence of Berrettini anastomoses is thought to be over 80%, which would technically make them a normal structure rather than an anatomic variant. Damage to these anastomoses resulting in sensory deficits has been described during surgeries such as carpal tunnel release [44]. Therefore, care must be taken to avoid damaging these neural communications.

Riche and Cannieu first described a neural connection between the deep branches of the ulnar nerve and the recurrent branch of the median nerve at the thenar eminence, which was later termed the Riche-Cannieu anastomosis (RCA) [45]. This anastomosis has been reported in up to 83.3% of cases (Fig. 17.10b) [45, 46]. The ulnar nerve can innervate any number of the thenar muscles and intrinsic hand muscles normally innervated by the median nerve through this neural connection, and should be kept in mind in the presence of atypical muscle deficits in carpal tunnel syndrome or ulnar nerve compression at Guyon's canal or more proximally [47–51].

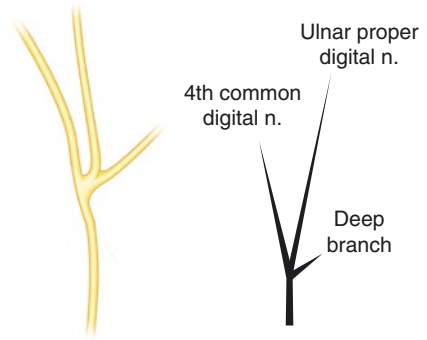
Radial Nerve

Normal Course

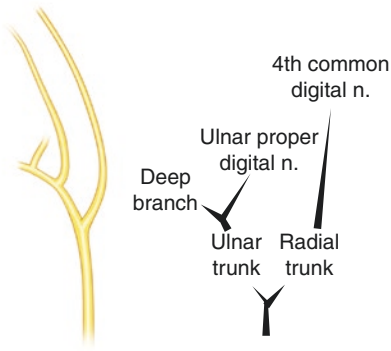
The radial nerve originates from the posterior cord of the brachial plexus and carries fibers from the C5–T1 nerve roots (Fig. 17.11). It splits from the axillary nerve just proximal to the quadrangular space and travels posterior to the axillary and brachial arteries and anterior to the long head of the triceps brachii muscle through the triangular interval. The radial nerve then proceeds posterolaterally in conjunction with the brachial artery deep to the long head and lateral head of the triceps brachii and



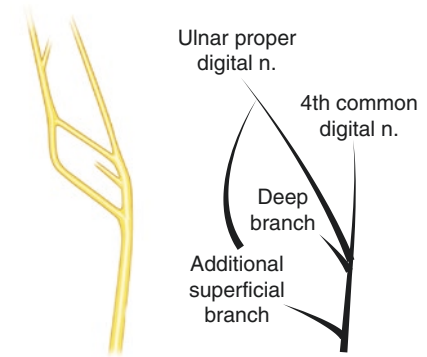
Type 1



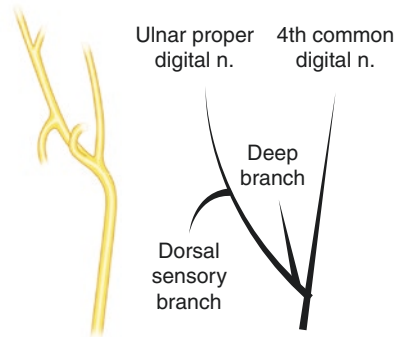
Type 2



Type 3



Type 4



Type 5

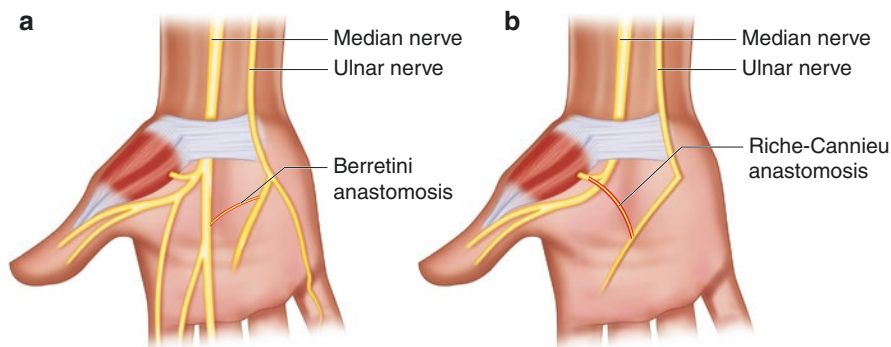


Fig. 17.10 Berrettini and Riche-Cannieu anastomoses. **(a)** Berrettini anastomoses are communications between the common digital nerves of the ulnar and median nerves. **(b)** Riche-Cannieu anastomoses are communications between the deep branches of the ulnar nerve and the recurrent branch of the median nerve

superficial to the medial head of the triceps brachii along the spiral groove (or radial sulcus). Innervation of the triceps brachii occurs along this course. Emerging from the spiral groove on the lateral side of the humerus, the nerve then pierces the lateral intermuscular septum, entering the anterior compartment of the upper arm approximately 10 cm proximal to the lateral epicondyle of the humerus. It then courses between the brachialis and brachioradialis muscles, sending branches to the brachialis muscle and the brachioradialis muscle. The radial nerve passes anterior to the lateral epicondyle as it enters into the forearm, branching into superficial (sensory) and deep branches (posterior interosseous nerve).

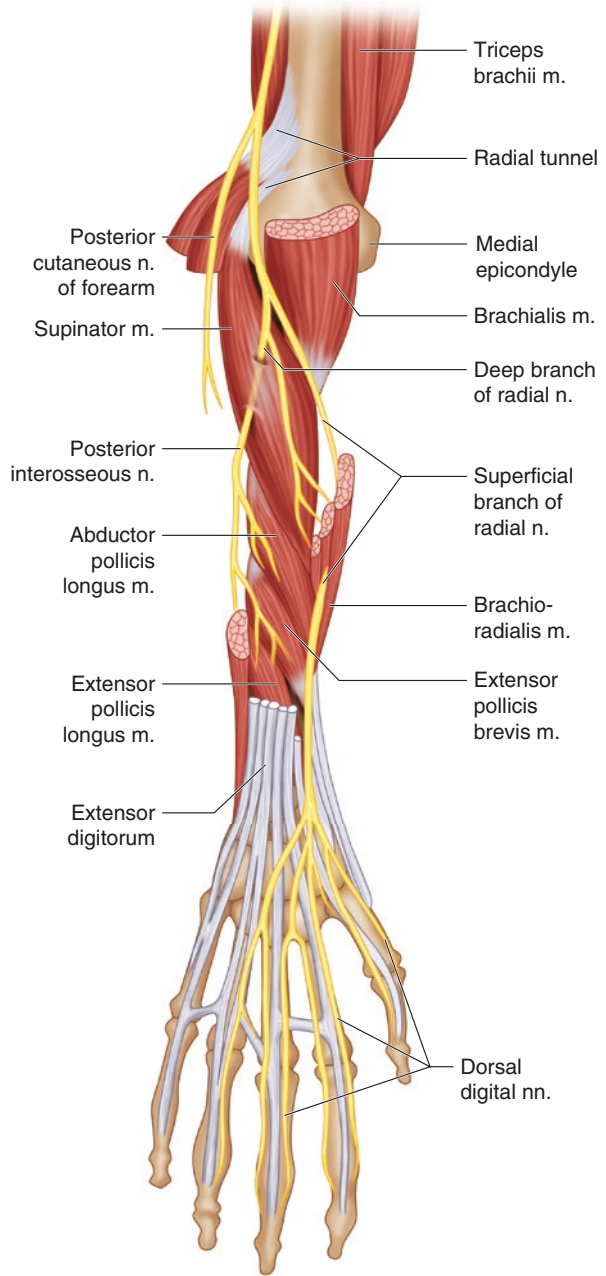
Variations and Pathology

Although the musculocutaneous nerve primarily innervates the brachialis [52], the radial nerve sends between one and three accessory branches to the brachialis muscle in up to 86% of cases [53, 54]. The radial nerve can also send one, two, and three branches to the brachioradialis muscle 46.5%, 40%, and 14% of the time, respectively, according to a study by Latev and Dalley [55]. Care should be taken to avoid cutting these nerves during tendon-transfer procedures using the brachioradialis. Atypical signs and symptoms can occur in injuries to the proximal radial nerve in variations where it communicates with the ulnar nerve and when it provides motor innervation to the extensor carpi radialis brevis, which is normally provided by the deep branch of the radial nerve further distally. This is known to occur in up to 20% of cases [56].

←

Fig. 17.9 Types of ulnar nerve branching within Guyon's canal. In type I, the ulnar nerve bifurcates into the deep branch and the superficial trunk (normal). In type II, the ulnar nerve trifurcates into the deep branch, the common digital nerve of the ring finger, and the proper digital nerve. In type III, the ulnar nerve bifurcates into radial and ulnar trunks. In type IV, an additional superficial branch divides from the ulnar nerve proximally. In type V, the dorsal branch of the ulnar nerve communicates with the proper digital nerve [34]

Fig. 17.11 Course of the radial nerve from the brachial plexus to the hand

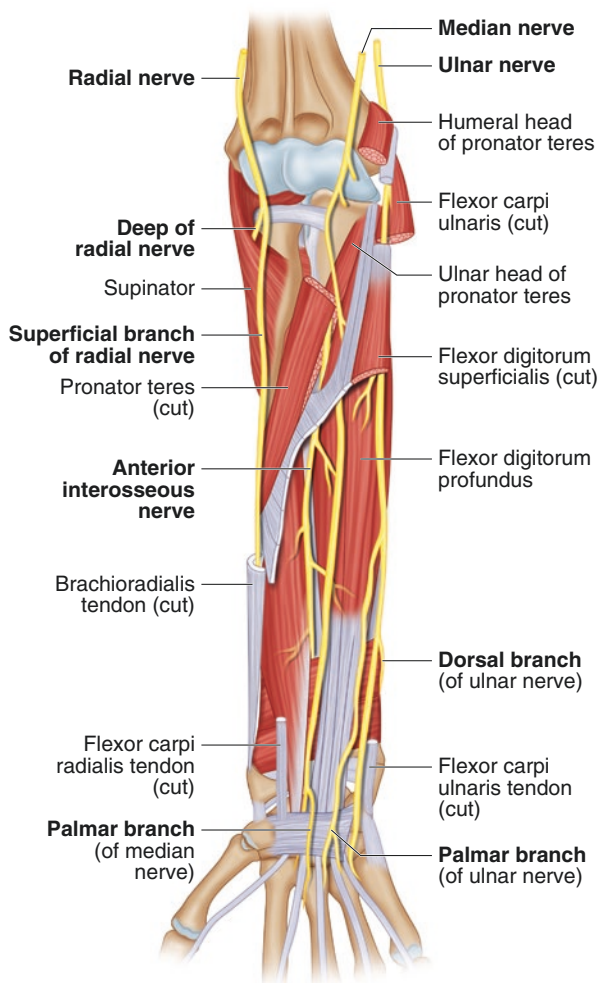


Superficial Branch of the Radial Nerve

Normal Course

The superficial branch of the radial nerve, or the radial sensory nerve (RSN), descends in the forearm underneath the brachioradialis (Fig. 17.12). In the middle-to-distal forearm, it passes between the tendons of the brachioradialis and the extensor carpi radialis longus by passing through the fascia that binds the two tendons to enter into the subcutaneous tissue of the posterior forearm. From there it divides into lateral and medial branches that go on to give sensory innervation to the dorsal aspect of the thumb and index finger and the dorsoradial aspect of the middle finger.

Fig. 17.12 Course of the superficial branch of the radial nerve



Variations and Pathology

Variations of the RSN have been found as it travels from underneath the brachioradialis to reach the subcutaneous tissue. Abrams et al. discovered cases where the RSN pierced the brachioradialis tendon itself as it traveled superficially, and this variation is thought to be present in 3–10% of individuals [57]. Other variations include one in which the RSN pierces a fused brachioradialis and extensor carpi radialis longus tendon [58], and another in which the RSN emerges from the fascia between a split brachioradialis tendon [59]. These variations may all predispose to compression neuropathy, otherwise known as Wartenberg's syndrome, and may be encountered during surgical correction of this pathology.

Compression neuropathy of the radial sensory nerve produces paresthesia, pain, or numbness along with its typical distribution. Variations in the RSN can also produce more atypical signs and symptoms that can confuse the clinical picture. The RSN commonly gives varying degrees of sensory innervation to the ulnar dorsum of the hand, which can lead to a mistaken diagnosis of ulnar nerve pathology for actual RSN or radial nerve pathology [60–65]. The RSN can provide motor innervation to the extensor carpi radialis brevis in up to 32% of individuals, which is normally provided by the posterior interosseous nerve. The RSN also occasionally provides motor innervation to the brachioradialis, which is normally innervated by the radial nerve more proximally [53].

Appleton first described a case where the RSN was completely absent and the lateral antebrachial cutaneous nerve (LACN) and ulnar nerve provided sensory innervation to the typical RSN territory. Other subsequent studies have found similar findings [66–68]. While this variation is rare, communication between the LACN and the RSN is more common, with one study finding the overlap between these two nerves in as many as 75% of individuals [69]. These variations can lead to errors in the diagnosis of injuries to the RSN.

Deep Branch of the Radial Nerve

Normal Course

The deep branch of the radial nerve passes under the arcade of Fröhse, a fibrous arch formed from the superior part of the superficial layer of the supinator, and proceeds between the two heads of the supinator. It winds around the lateral head of the radius between the two planes of the supinator to reach the posterior forearm, after which it is known as the posterior interosseous nerve (PIN) of the forearm (Fig. 17.13). It passes over the abductor pollicis longus muscle origin and then descends along the posterior interosseous membrane, providing motor innervation to the muscles of the posterior compartment of the forearm. The PIN enters the wrist on the radial side of the fourth extensor compartment, providing sensory fibers to the dorsal wrist capsule.

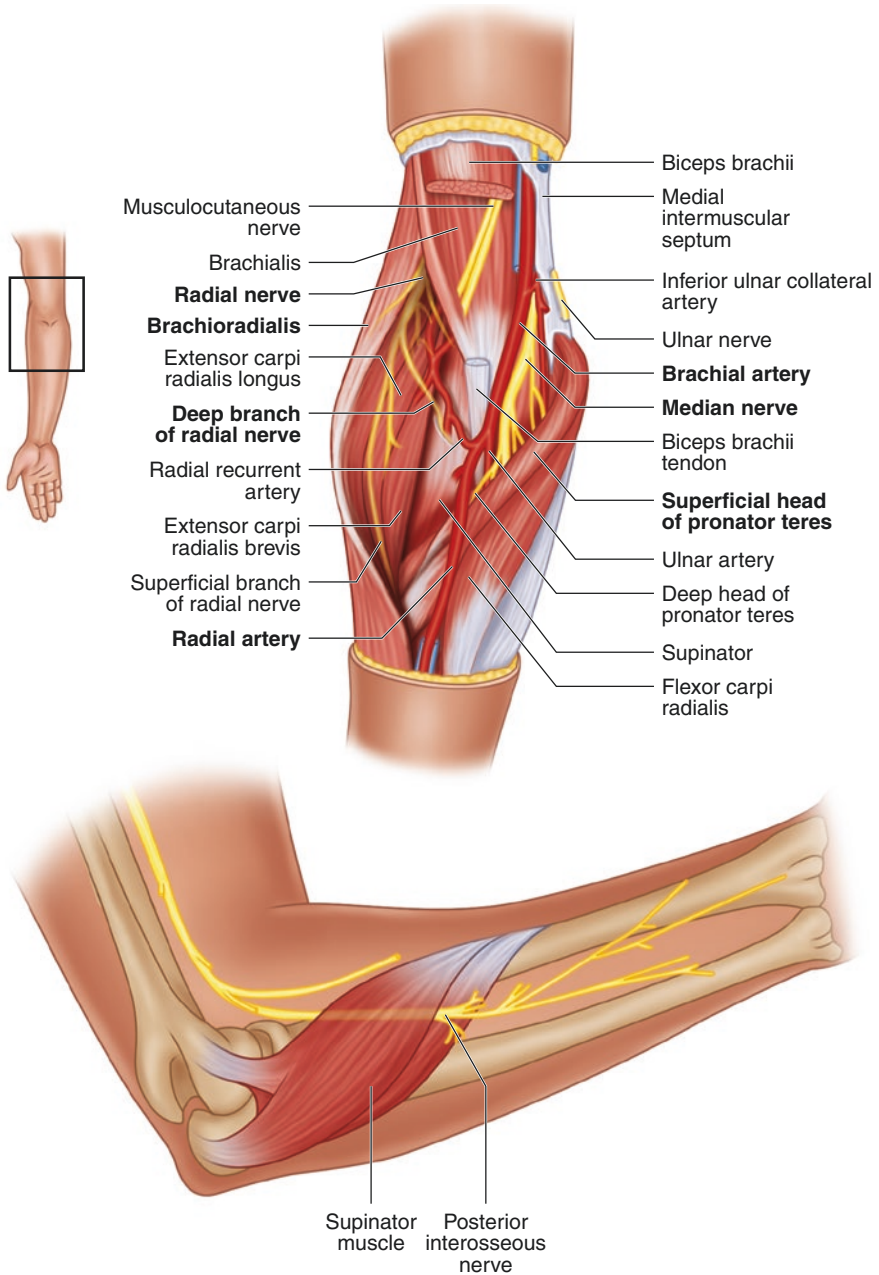


Fig. 17.13 Course of the deep branch of the radial nerve (posterior interosseous nerve). The deep branch of the radial nerve is called the posterior interosseous nerve when it emerges from between the two heads of the supinator to reach the posterior forearm

Variations and Pathology

The typical order of innervation to the muscles of the forearm (proximal to distal) by the deep branch of the radial nerve/posterior interosseous nerve is as follows: extensor carpi radialis brevis (ECRB), supinator, extensor digitorum (ED), extensor carpi ulnaris (ECU), extensor digiti minimi (EDM), abductor pollicis longus (APL), and extensor indicis (EI). This order of innervation can vary. Innervation by multiple branches (e.g., supinator) and variable innervation by different branches (radial, superficial sensory, or posterior interosseous nerve innervation to the ECRB) have also been reported. Awareness of the normal and variable innervation patterns is helpful when treating pathologies like radial tunnel syndrome and posterior interosseous nerve compression syndrome [70].

The course of the PIN itself can vary. Though normally it passes between the two planes of the supinator muscle, it has been reported to pass superficial or deep to the supinator muscle instead. The terminal branch of the PIN has also been occasionally found on the ulnar side of the fourth extensor compartment, which surgeons should be aware of when harvesting the PIN as a nerve graft [71].

Muscles and Tendons

Anterior Compartment

Superficial Muscles

The superficial muscles of the anterior compartment of the forearm include the flexor carpi ulnaris, flexor carpi radialis, palmaris longus, and the pronator teres (Fig. 17.14).

Flexor Carpi Ulnaris

The flexor carpi ulnaris (FCU) has two heads, with the humeral head originating proximally from the medial epicondyle of the humerus and the ulnar head from the medial border of the olecranon and posterior border of ulna, and inserting onto the base of fifth metacarpal bone, the hook of hamate, and pisiform. The FCU functions to flex and adduct the wrist joint.

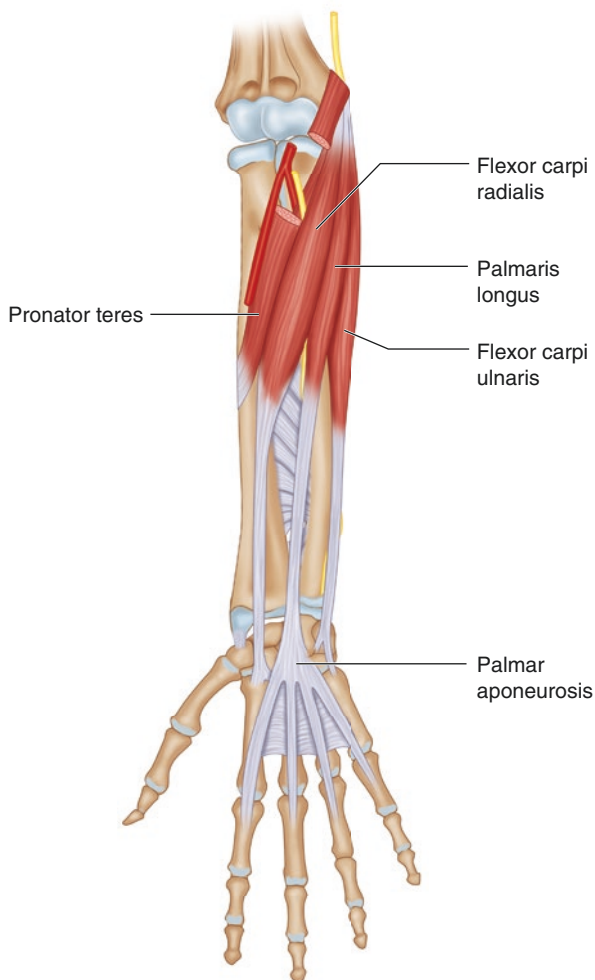
Flexor Carpi Radialis

flexor carpi radialis (FCR) originates proximally from the common flexor tendon attached to the medial epicondyle of the humerus, and inserts onto the base of second and third metacarpals, with a small slip to the trapezial tuberosity. It functions to flex and abduct at the wrist joint.

Variations

FCR is often harvested for the reconstruction of forearm and hand defects. Although rare, FCR agenesis has been reported in the literature and should be kept in mind when planning to harvest this muscle for reconstruction [72, 73].

Fig. 17.14 Superficial muscles of the anterior compartment of the forearm. The superficial muscles of the anterior compartment include the flexor carpi ulnaris, flexor carpi radialis, palmaris longus, and pronator teres



Palmaris Longus

The palmaris longus (PL) originates from the common flexor tendon on the medial epicondyle of the humerus and inserts onto the palmar aponeurosis. The PL functions as a weak flexor of the wrist and elbow.

Variations

The PL is commonly used as a tendon graft donor because its function is redundant and its absence has no functional or aesthetic consequence. It is important to note that the PL is one of the most variable muscles in the human body. The PL is absent in 11.8% of the United States population, but absent in only 2.9% of Asian and 4.5% of African American populations. Additionally, the absence of the PL is more likely in females and in the left upper extremity [74]. In the absence of the PL, the FCU

can take over by sending fibers to and strengthening the palmar aponeurosis. A reverse PL is a rare anatomic anomaly. It is essentially the opposite of a normal PL: the tendon originates proximally and the muscle belly inserts onto the palmar aponeurosis distally [75, 76]. This reversed muscle belly can also divide into multiple muscle slips, inserting onto the flexor retinaculum, the flexor carpi radialis, and the palmar carpal ligament [77]. A reversed PL can hypertrophy due to overuse, causing effort-related distal median nerve compression, or less commonly, Guyon's syndrome [78, 79]. Both duplication and bifurcation of the PL either at the level of the muscle belly or at the tendon has also been documented. Finally, both the origin and the insertion of the PL can vary. The PL can arise from the antebrachial fascia, bicipital aponeurosis, FCR, FCU, or FDS. The PL can insert onto the antebrachial fascia, fascia of the thenar eminence, carpal bones, expansion of the FCU insertion over the wrist, FDS, FDP, or FCR [76, 80]. Surgeons need to be aware of these variations of the PL when planning to harvest the PL as a tendon graft (Fig. 17.15).

Pronator Teres

The pronator teres (PT) consists of two heads: the humeral head and the ulnar head. The humeral head arises from the common flexor tendon attached to the medial epicondyle of the humerus, and the ulnar head arises from the coronoid process of the ulna. The PT inserts distally onto the lateral surface of the middle-third radius.

Variations

The origin of the PT can extend proximally to Struthers' ligament, a tendinous arch between the medial epicondyle and the supracondylar process of the humerus. This variation along with the presence of Struthers' ligament can entrap the median nerve, causing pronator teres syndrome. Symptoms include pain, weakness, and paresthesia. Ischemic pain and embolization of the hand and fingers may result if the brachial artery becomes entrapped between the elbow joint and Struthers' ligament [81].

Intermediate Muscle

The intermediate muscle of the anterior compartment of the forearm includes the flexor digitorum superficialis (FDS). The FDS is sometimes considered part of the superficial layer of the anterior compartment of the forearm.

Flexor Digitorum Superficialis

The flexor digitorum superficialis (FDS) consists of two heads: the humeral head and the radial head. The humeral head arises from the common flexor tendon attached to the medial epicondyle of the humerus and the coronoid process of the ulna, and the radial head arises from the diaphysis of the radius. The four FDS tendons travel through the carpal tunnel and insert onto the volar base of the middle phalanges of the second to fifth digits. The FDS functions to flex the digits at the proximal interphalangeal joint (Fig. 17.16).

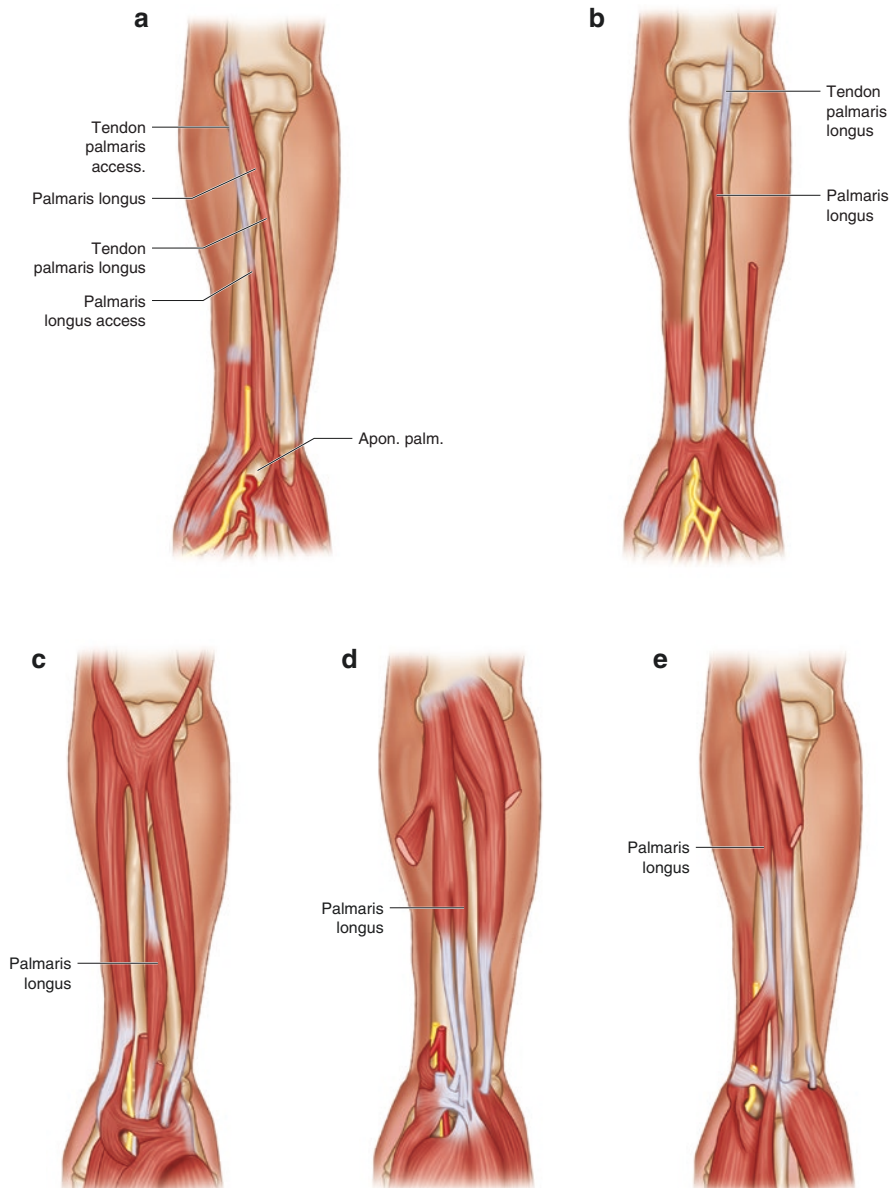


Fig. 17.15 Variations of the palmaris longus. Palmaris longus variations can include (a) a palmaris longus duplication; (b) a palmaris longus with a distal muscle belly (reverse palmaris longus); (c) a palmaris longus with a central muscle belly; (d) a bifid palmaris longus; and (e) a palmaris longus with a divided tendon [76]

Fig. 17.16 Flexor digitorum superficialis



Variations

FDS insertions are variable in the literature. Bernardes and Cassell both reported cases where the PL tendon replaced the FDS tendon insertion at the base of the middle phalanx of the fourth digit [82]. The FDS instead gave digastric medial head tendons to the second and fifth digits, and a lateral head tendon to the third digit [80]. The FDS tendon to the fifth digit is found to be absent in 18.5% of the patients [83]. The FDS tendons have also been reported to form muscle bellies distal to the flexor retinaculum, causing symptomatic “pseudotumors” in the palm. These were treated through debulking or transection [84–87]. Another case reported an FDS tendon penetrating the median nerve 4 cm proximal to the wrist crease, which caused numbness and tingling in the median nerve distribution [88]. Many different variations of the FDS have been described in the literature. Elliot et al. categorized these anomalies into five types: (1) FDS tendon to FDS tendon attachment, (2) FDS tendon to flexor retinaculum attachment, (3) FDS tendon with a digastric muscle, (4) FDS muscle belly extension distally, and (5) FDS anomalies in the forearm [87] (Fig. 17.17).

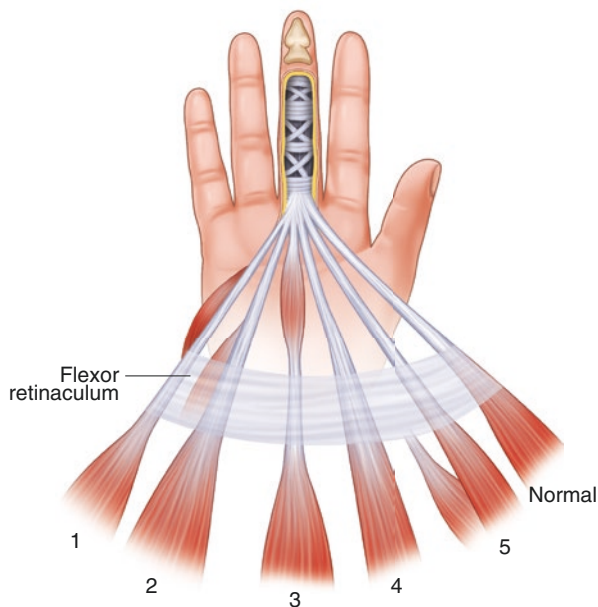


Fig. 17.17 Variations of the flexor digitorum superficialis (FDS). FDS variations can be categorized into five types. Type I: An anomalous muscle can arise on the FDS tendon and reinsert back onto the FDS tendon more distally. Type II: An anomalous muscle can arise from the flexor retinaculum and insert onto the FDS tendon more distally. Type III: A digastric muscle can be found in the FDS tendon in the palm. Type IV: The FDS muscle belly can extend distally as far as into the carpal tunnel. Type V: Other anomalies of the FDS can occur proximally in the forearm [87]

Deep Muscles

The deep muscles of the anterior compartment of the forearm include the flexor digitorum profundus, flexor pollicis longus, and the pronator quadratus (Fig. 17.18).

Flexor Digitorum Profundus

The flexor digitorum profundus (FDP) originates proximally on the upper anterior surface of the ulna and interosseous membrane. The FDP divides into four tendons, which travel through the carpal tunnel and insert onto the volar surface of the distal second through fifth phalanges. It functions to flex the distal interphalangeal, proximal interphalangeal, and wrist joints.

Variations

Rarely, the FDP tendons to the fourth and fifth fingers share a common tendon that bifurcates at the mid-palmar level. This common FDP tendon has a configuration that shifts more loads to the fifth finger, which is therefore at risk for spontaneous rupture when flexing against increased resistance [89, 90]. Another variation is the presence of an accessory head of the FDP, called Gantzer's muscle, which most commonly arises from the deep portion of the flexor digitorum superficialis muscle and courses distally to insert onto the FDP (14–25%). Gantzer's muscle can also

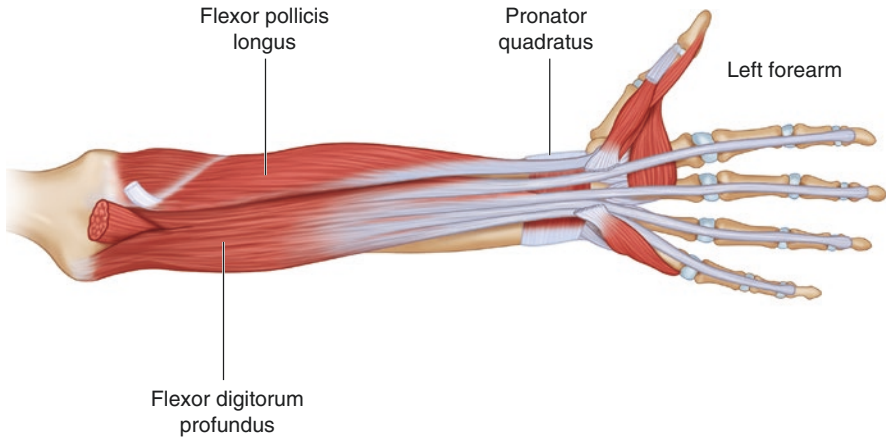
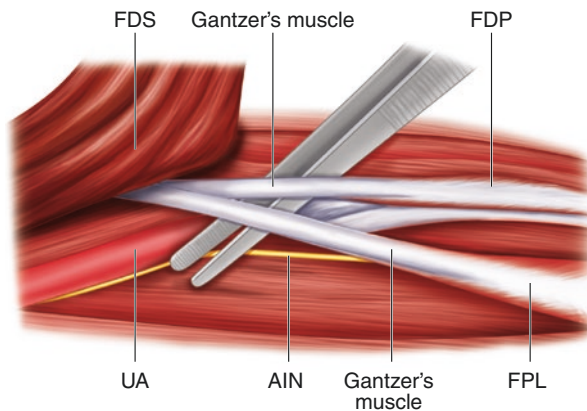


Fig. 17.18 Deep muscles of the anterior compartment of the forearm. The deep muscles of the anterior compartment include the flexor digitorum profundus, the flexor pollicis longus, and the pronator quadratus

Fig. 17.19 Gantzer's muscle. Gantzer's muscle is a term used for both an accessory head of the flexor digitorum profundus and an accessory head of the flexor pollicis longus. They can occur separately or together



differentially insert onto the flexor pollicis longus. Because this accessory head lies between the median nerve anteriorly and AIN posteriorly, it has been reported to cause AINS or restricted movement of the FDP [91, 92] (Fig. 17.19).

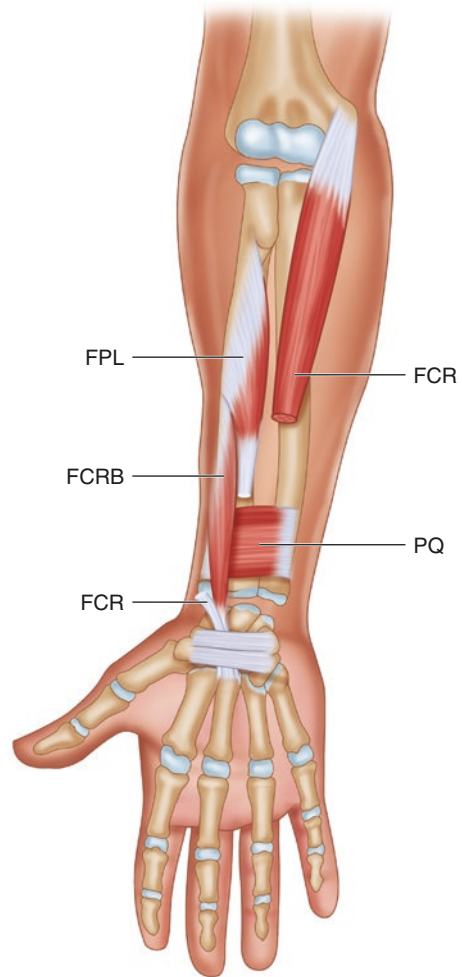
Flexor Pollicis Longus

The flexor pollicis longus (FPL) originates proximally on the anterior surface of the radius and interosseous membrane, travels through the carpal tunnel, and inserts onto the volar surface of the first distal phalanx. It functions to flex the first interphalangeal joint.

Variations

An accessory head of the FPL (also called Gantzer's muscle) most commonly arises from the deep portion of the flexor superficialis muscle and courses distally to insert onto the FPL in 14–25% of the global population (Fig. 17.20). Like Gantzer's

Fig. 17.20 Flexor carpi radialis brevis (FCRB). The FCRB originates from the lower third of the radius and inserts variably onto the second through fourth metacarpals or radial carpal bones



muscle inserting onto the FDP, this accessory head can also cause AINS because of its relative position [91, 92].

Pronator Quadratus

The pronator quadratus (PQ) originates proximally on the anterior surface of the distal quarter of the ulna and inserts onto the anterior surface of the distal quarter of the radius. It functions to pronate the forearm.

Anomalous Muscles

Flexor Carpi Radialis Brevis

Flexor carpi radialis brevis (FCRB) is a rare anomalous muscle of the flexor compartment, occurring in approximately 2.6–7.5% of the global population. It

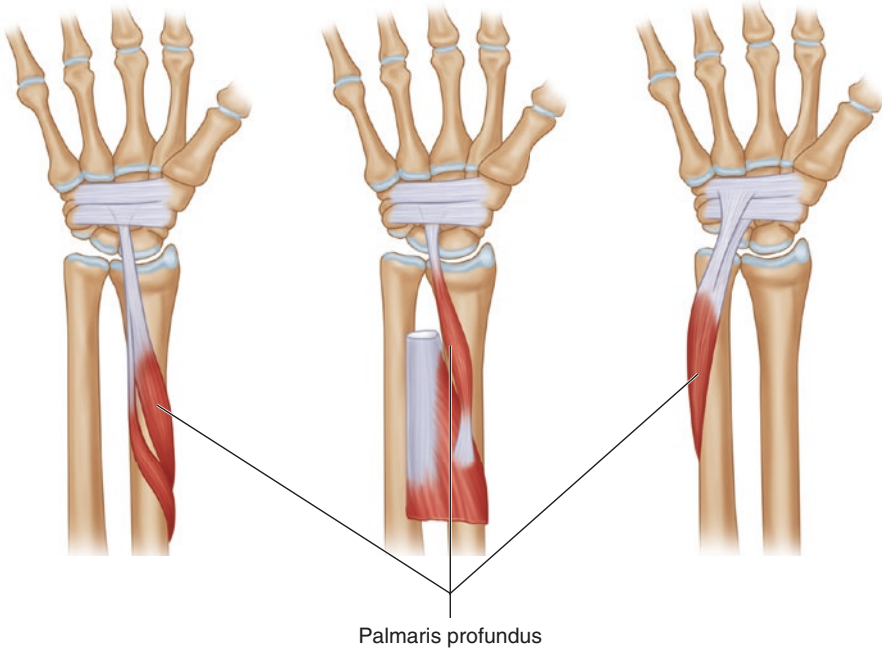


Fig. 17.21 Palmaris profundus. The palmaris profundus is a duplicated palmaris longus that inserts onto the palmar aponeurosis. The palmaris profundus can originate from the proximal radius, from the FDS, or from the ulna [96]

originates from the lower third of the radius between the origin of the flexor pollicis longus (FPL) and insertion of the PQ, runs inside the FCR sheath parallel to the FCR, and inserts variably onto the second through fourth metacarpals or radial side carpal bones [93, 94] (Fig. 17.20).

Palmaris Profundus

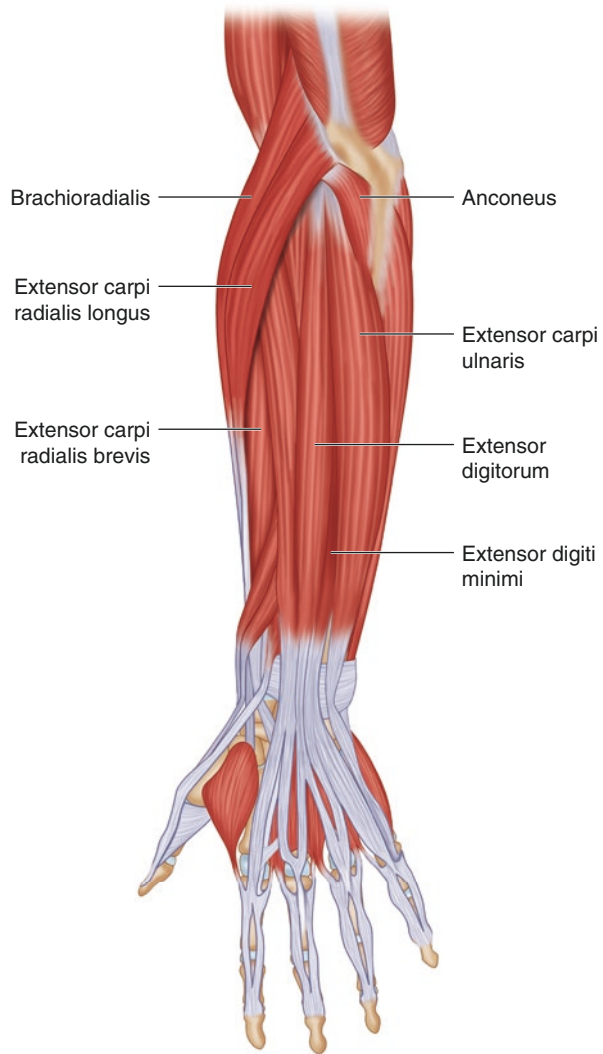
The palmaris profundus is a duplicated PL reported to coexist with or replace the PL. It has an incidence of 0.8% in 1600 extremities studied by Reimann et al. [76]. Whereas an accessory PL shares an origin with the PL, the palmaris profundus has a different origin than the PL, and it inserts into a palmar aponeurosis or its miniature duplicate (a duplicate palmar aponeurosis that passes dorsal to the normal palmar aponeurosis) (Fig. 17.21). The palmaris profundus has the potential to cause carpal tunnel syndrome by compressing on the median nerve that is not released with conventional surgery, but requires detachment of the duplicated tendon [6, 95, 96].

Posterior Compartment

Superficial Muscles

The superficial muscles of the posterior compartment of the forearm include the anconeus, brachioradialis, extensor carpi radialis longus, extensor carpi radialis

Fig. 17.22 Superficial muscles of the posterior compartment of the forearm. The superior muscles of the posterior compartment include the anconeus, brachioradialis, extensor carpi radialis longus, extensor carpi radialis brevis, extensor digitorum communis, extensor digiti minimi, and extensor carpi ulnaris



brevis, extensor digitorum communis, extensor digiti minimi, and the extensor carpi ulnaris (Fig. 17.22).

Anconeus

The anconeus originates proximally from the lateral epicondyle of the humerus and inserts onto the posterior and lateral olecranon of the ulna. The anconeus functions to assist the triceps brachii in extending the elbow and is considered by some to be a continuation of the triceps brachii.

Brachioradialis

The brachioradialis originates proximally on the proximal aspect of the lateral supracondylar ridge of the humerus and lateral intermuscular septum. It inserts on the distal radius, just proximal to the styloid process. Although it is part of the posterior compartment, the brachioradialis actually functions to flex the forearm at the elbow.

Extensor Carpi Radialis Longus

The extensor carpi radialis longus (ECRL) originates proximally from the distal aspect of the lateral supracondylar ridge of the humerus and lateral intermuscular septum. It inserts on the dorsal base of the second metacarpal. The ECRL functions to extend and abduct the wrist.

Extensor Carpi Radialis Brevis

The extensor carpi radialis brevis (ECRB) originates proximally from the lateral epicondyle of the humerus. It inserts on the dorsal base of the third metacarpal. The ECRB primarily functions to extend and abduct the wrist.

Extensor Digitorum Communis

The extensor digitorum communis (EDC) originates proximally from the lateral epicondyle of the humerus. It separates into four tendons in the distal forearm where they travel into the hand to pass over each MCP joint. Each tendon separates into three bands after the MCP joint. The central band inserts on the dorsal base of the middle phalanx and the two lateral bands continue distally to rejoin and insert on the dorsal base of the distal phalanx. The EDC primarily functions to extend the wrist, MCP, and PIP joints.

Variations

Numerous variations of the EDC to each of the second through fifth fingers have been described in the literature. The index finger most commonly receives one EDC tendon but has been rarely described receiving two tendons [97]. Both the long finger and ring finger commonly receive one, two, or three tendons from the EDC. Each finger has even been described as receiving four EDC tendons [97, 98]. The EDC tendon contribution to the small finger is usually as a single tendon or absent [97]. The single tendon contribution to the small finger has been described as coming from one common tendon that bifurcates to insert on the ring and little fingers, one independent tendon that inserts onto the little finger, and an intertendinous connection that extends to the small finger from the EDC to the ring finger (Fig. 17.23) [99].

Extensor Digiti Minimi

The extensor digiti minimi (EDM) originates proximally from the lateral epicondyle of the humerus. It inserts on the dorsal base of fifth proximal phalanx joined with the EDC tendon to the small finger when present. The EDM functions to extend the MCP and PIP joints of the small finger.

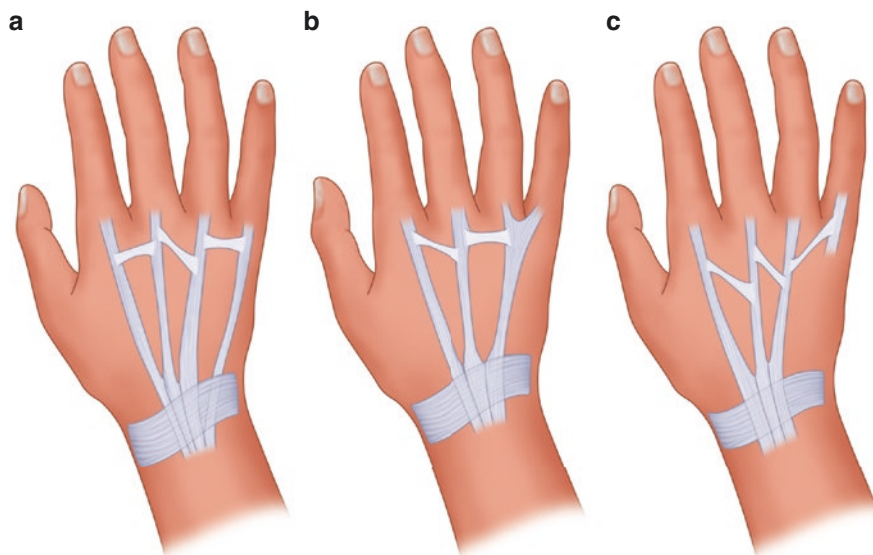


Fig. 17.23 Extensor digitorum communis (EDC) variations to the small finger. (a) A single EDC to the small finger; (b) a single EDC bifurcates and inserts onto the ring and the small finger; (c) an intertendinous connection extends to the small finger from the EDC to the ring finger [99]

Variations

The EDM commonly has multiple tendon slips that insert variably onto the ring and little finger. In a meta-analysis of the reported number of EDM tendons by Yammine, 11.5% had one EDM tendon, 77.6% had two EDM tendons, 7% had three EDM tendons, and 0.6% had four EDM tendons [100]. The variability of the EDM and its insertions has been suggested as a contributing factor to the development of tenosynovitis around the EDM. It is important to note that the EDM tendon is frequently used for tendon transfer procedures, particularly to correct abduction deformities of the little finger. EDM tendon transfer in the absence of an EDC tendon to the small finger may result in the loss of small finger extension [101].

Extensor Carpi Ulnaris

The extensor carpi ulnaris (ECU) originates proximally from the lateral epicondyle of the humerus. It inserts on the dorsal base of the fifth metacarpal. The ECU functions to extend and adduct the wrist.

Variations

An accessory tendinous slip has been described arising from the ECU in up to 34% of upper limbs studied [102]. This accessory tendinous slip can insert onto the base, midsection, or head of the fifth metacarpal [102]. Tenosynovitis of this accessory slip has been described as the cause of wrist pain and dysfunction [102, 103].

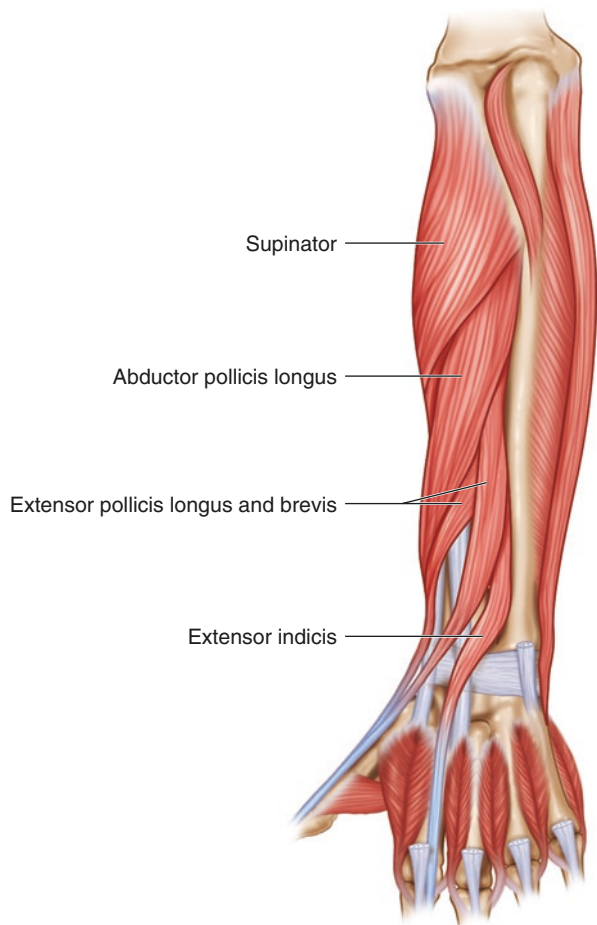
Deep Muscles

The deep muscles of the posterior compartment of the forearm include the supinator, abductor pollicis longus, extensor pollicis longus, extensor pollicis brevis, and extensor indicis proprius (Fig. 17.24).

Supinator

The supinator consists of two muscle planes. The superficial plane originates from the lateral epicondyle and the radial collateral and annular ligaments. The deep plane originates from the supinator crest and fossa of the ulna. The supinator inserts on the lateral, anterior, and posterior surfaces of the proximal third of the radius. As its name suggests, the supinator functions to supinate the arm.

Fig. 17.24 Deep muscles of the posterior compartment of the forearm. The deep muscles of the posterior compartment include the supinator, abductor pollicis longus, extensor pollicis longus, extensor pollicis brevis, and extensor indicis proprius



Abductor Pollicis Longus

The abductor pollicis longus (APL) originates from the interosseous membrane and adjacent posterior surfaces of the radius and ulna in the mid forearm. It inserts onto the radial, dorsal base of the first metacarpal. The APL functions to abduct the thumb at the CMC joint. Along with the extensor pollicis brevis (EPB), it forms the radial border of the anatomical snuffbox.

Variations

The APL has multiple accessory tendons in the majority of cases, with or without accessory muscle bellies, and has even been described with seven accessory tendons [104, 105]. In a cadaver study of the APL by Kuthanan and Chareonwat, 11% of all APLs had one tendon, 63% had two tendons, and 26% had three tendons [106]. These accessory tendons of the APL are thought to contribute to the development of De Quervain syndrome. Intersection syndrome is caused by the confining nature of the area where the APL and EPB intersect over the ECRL and ECRB in the forearm. The presence of accessory tendons can add additional risk to the development of this syndrome [107–109].

While the classic insertion of the APL tendon is onto the base of the first metacarpal, the APL tendon more commonly inserts onto the trapezium, thenar muscle, and thenar muscle fascia. These variations have been reported as the cause of trapeziometacarpal joint laxity and subluxation [107, 110].

Extensor Pollicis Longus

The extensor pollicis longus (EPL) originates from the posterior surface of the ulna and interosseous membrane in the mid forearm and inserts onto the dorsal base of the distal phalanx of the thumb. The EPL functions to extend the thumb at the MCP and IP joints. It forms the ulnar border of the anatomical snuffbox.

Variations

Duplication of the EPL, with or without a separate muscle belly, can rarely occur. Both the EPL and its duplicate have been described coursing through the third dorsal compartment, in other dorsal compartments (e.g., first, fourth), or separately through different dorsal compartments [111–115]. When an additional tendon is present, both tendons can rejoin in the hand to have a single insertion onto the distal phalanx or have separate and anomalous insertions. The anomalous course of the EPL and a duplicate EPL can contribute to the development of tenosynovitis and wrist pain [115, 116].

Extensor Pollicis Brevis

The extensor pollicis brevis (EPB) originates from the posterior surface of the radius and interosseous membrane in the mid forearm. It inserts onto the dorsal base of the proximal phalanx of the thumb. The EPB functions to extend and abduct the thumb at the MCP joint. Along with the APL, it forms the radial border of the anatomical snuffbox.

Variations

The EPB is absent in up to 7% of cadaver dissections in a UK study [117]. When present, it can be fused to a variable extent to the APL [117]. In addition to its typical insertion onto the proximal phalanx, the EPB has been commonly described inserting onto the distal phalanx, both the distal and proximal phalanx, and uniting with the EPL as a single insertion [118]. The EPB is thought to play a more minor role in thumb function, and is therefore used as a donor in a number of different hand procedures [118]. Knowledge of these EPB variations may help in surgical planning as well as in the identification of the EPB during surgery.

Extensor Indicis Proprius

The extensor indicis proprius (EIP) originates from the posterior surface of the ulna and interosseous membrane in the distal forearm, medial and distal to the origin of the EPL. It runs to the ulnar side to the EDC-index tendon at the metacarpal head, and inserts on to the extensor hood of the index finger. The EIP functions to extend the index finger, allowing it to move independently of the other digits.

Variations

The EIP can lie palmar or radial to the EDC-index tendon over the metacarpal head [97, 119]. The EIP tendon has important uses as a graft and can be confused for EDC-index tendon in cases of tendon transfers and transplants. The EIP can also have two or even three tendon slips, which insert variably onto the thumb, index, or long fingers (Fig. 17.25) [97, 99, 119].

Anomalous Muscles

Extensor Pollicis et Indicis

This anomalous muscle has been described arising from the ulna between a normal EIP and EPL and splitting into two slips before inserting into the extensor hood of both the thumb and index finger or to either digit alone (Fig. 17.26) [120–122]. Its incidence has been variably reported in less than 1% and up to 5% [123–125].

Extensor Digitorum Brevis Manus

The extensor digitorum brevis manus (EDBM) is an anomalous muscle that appears in about 4% of the global population [126]. It can originate from the dorsal wrist joint capsule, the distal end of the radius, the dorsal metacarpal surface, or from the dorsal radiocarpal ligament [126]. The EDBM travels within the fourth dorsal wrist compartment and usually inserts onto the extensor hood of the index or middle finger, but has also been described inserting onto the ring finger, little finger, or multiple fingers (i.e., multiple tendons) [127]. The EDBM shares a close relationship with the EIP when found together, and is thought to compensate for the EIP in its absence (Fig. 17.27) [128]. Surgeons should be aware of such cases particularly when the EDBM is the only independent index finger extensor. The EDBM has been implicated as a cause of chronic dorsal wrist pain and can be easily mistaken for a ganglion, synovial condition, or benign tumor [129].

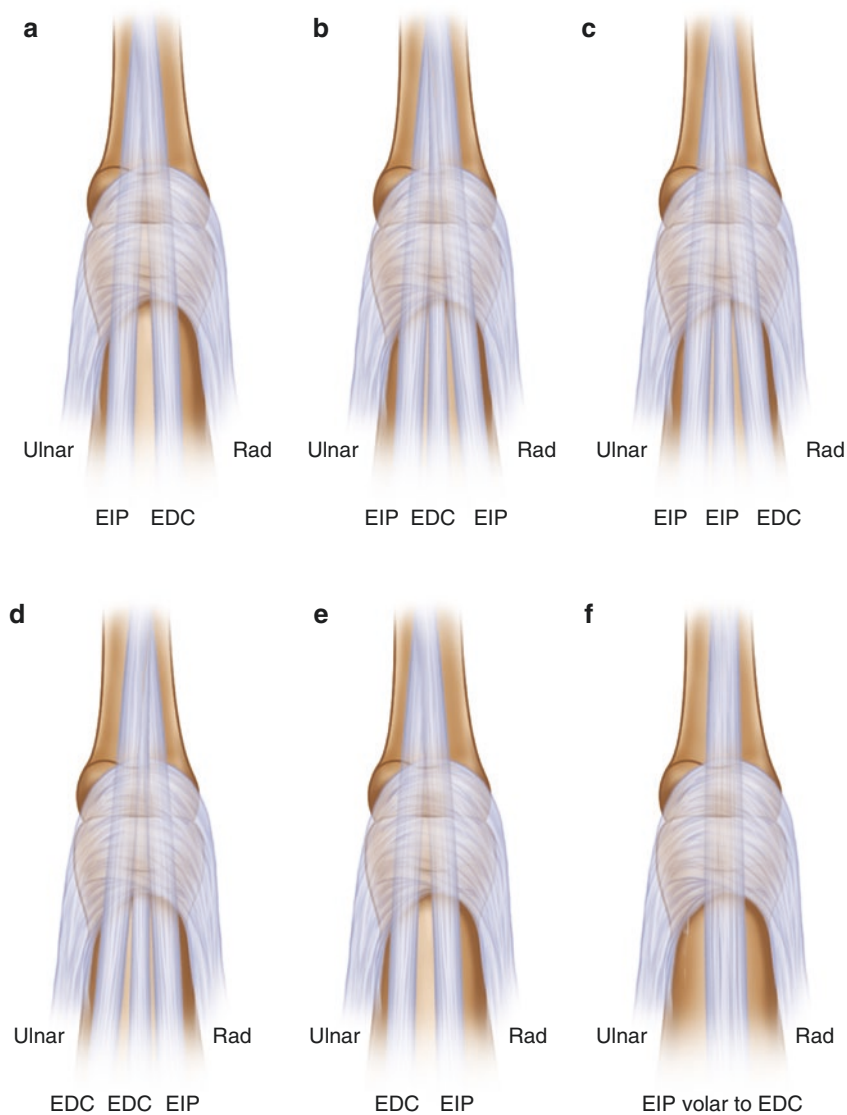


Fig. 17.25 Extensor indicis proprius (EIP) variations. (a) EIP lies ulnar to the EDC; (b) EDC flanked by two EIP tendons; (c) two EIP tendons lie ulnar to the EDC; (d) EIP lies ulnar to two EDC tendons; (e) EIP lies radial to the EDC; (f) EIP lies volar to the EDC [119]

Extensor Medii Proprius

The extensor medii proprius (EMP) is another anomalous muscle with a reported incidence of up to 10%. The EMP originates in the distal ulna just distal and ulnar to the EIP (Fig. 17.28). It has been described inserting onto the dorsal hood of the

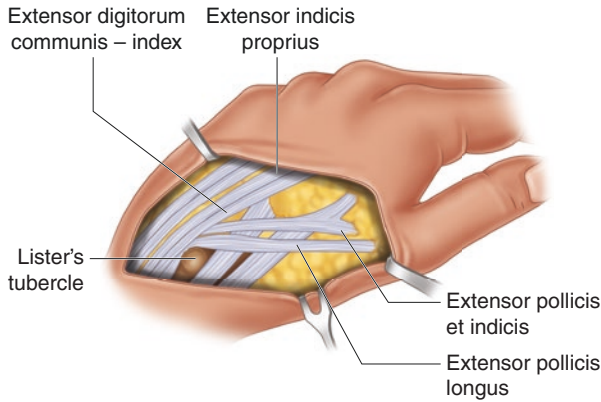


Fig. 17.26 Extensor pollicis et indicis. The extensor pollicis et indicis arises between the extensor indicis proprius and extensor pollicis longus and splits to insert onto both the thumb and index finger or to either digit alone [120]

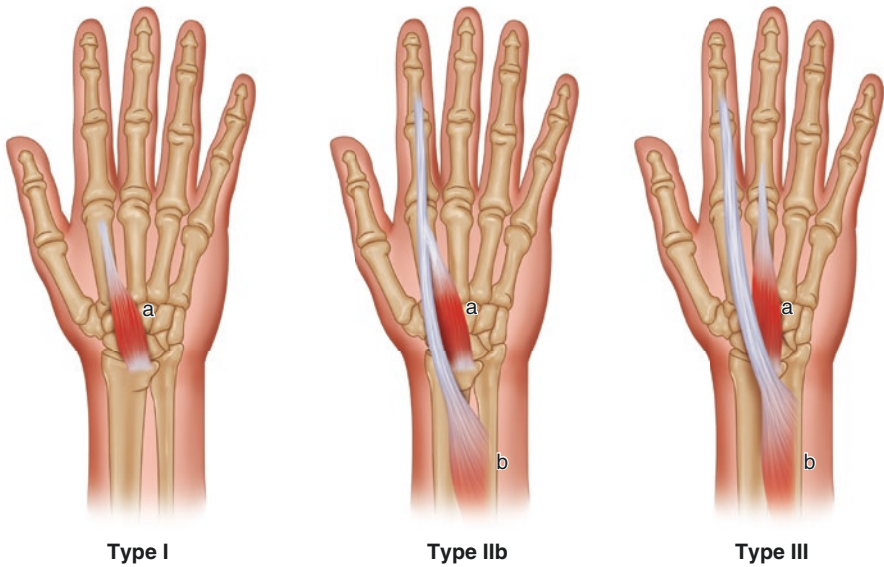
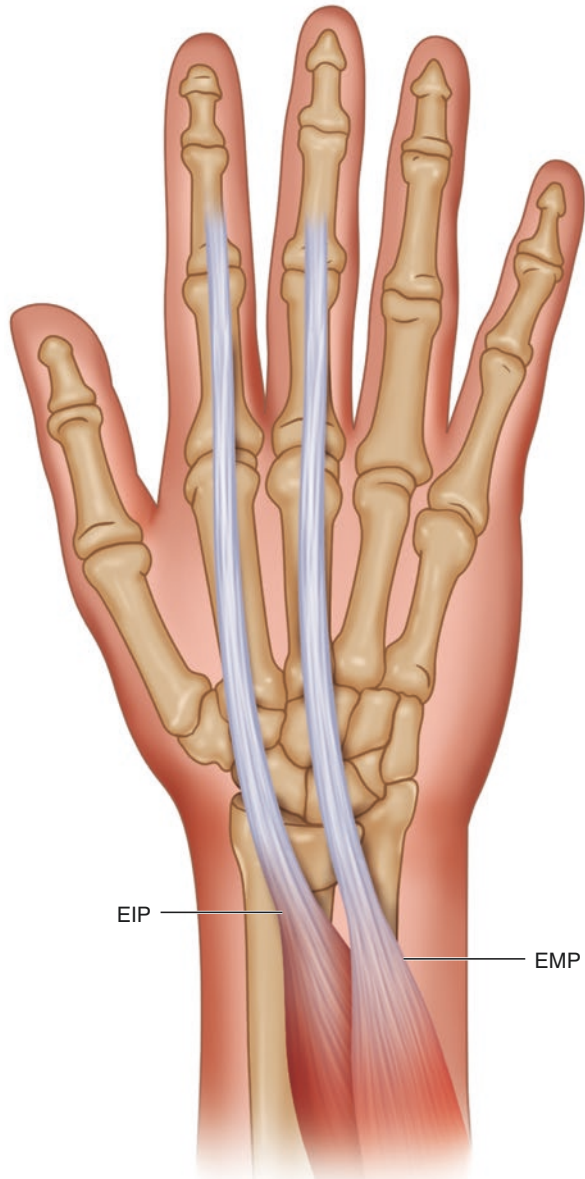


Fig. 17.27 Extensor digitorum brevis manus (EDBM). The EDBM can be classified into three types. Type I: The EDBM can insert onto the dorsal hood of the index finger in the absence of an extensor indicis proprius (EIP). Type II: Both the EIP and EDBM can insert onto the index finger. Type III: The EDBM can insert onto the long finger while the EIP inserts onto the index finger. (Adapted from Ogura et al. [128])

Fig. 17.28 Extensor medii proprius. The extensor medii proprius originates in the distal ulna and has been described inserting variably onto the dorsal hood of the long finger ulnar to the EDC tendon or onto the intertendinous fascia proximal to the third metacarpophalangeal joint



long finger ulnar to the EDC tendon or onto the intertendinous fascia proximal to the third metacarpophalangeal joint. The EMP lies palmar to the EDC and can be missed, particularly when it inserts proximally to the MCP joint [130].

Carpal Bones

Normal Anatomy

The wrist, or carpus, is a complex association of bones that includes the distal radius and ulna, the eight carpal bones, and the proximal metacarpals (Fig. 17.29). The eight carpal bones are grouped into two rows. The proximal row articulates with the distal radius and ulna and consists of the scaphoid, lunate, triquetrum, and pisiform. The distal row articulates with the bases of the metacarpals and consists of the trapezium, trapezoid, capitate, and hamate. The concave, palmar side of the carpus forms the carpal tunnel.

Variations

Carpal Bipartition and Fusion/Coalition

Carpal bipartitions, or divided carpals, are very rare anatomic variants. The bipartite scaphoid is the best known of the carpal bipartitions and has a prevalence of 0.13% in a study of 743 radiographs by O’Rahilly [131]. An absence of trauma and radiographic signs (e.g., absence of degenerative changes, smooth and regular edges, symmetry) can help to distinguish these bipartitions from carpal fractures.

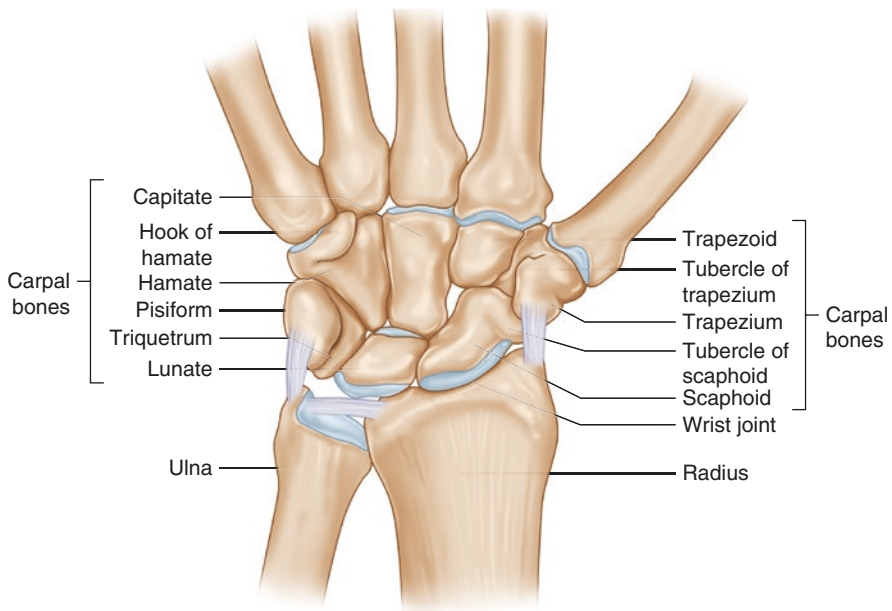


Fig. 17.29 Carpal bones. The carpal bones include the scaphoid, lunate, triquetrum, and pisiform of the proximal row, and the trapezium, trapezoid, capitate, and hamate of the distal row

Carpal fusions have a prevalence of roughly 0.1% in the general US population and are more commonly found in females and African Americans [131, 132]. While almost every possible combination has been described, the most common are a fusion between the lunate and triquetrum (lunotriquetral), which represents almost 90% of all carpal fusions [133]. Some patients with a lunotriquetral fusion may have a widened scapholunate joint space on radiographs. However, this is a normal variant without decreased joint stability [134].

Accessory Ossicles

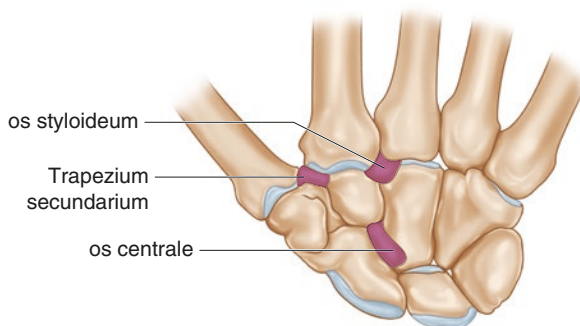
Accessory ossicles, or secondary ossification centers, are normal variants of which over 20 have been described [131, 135]. They are largely congenital in origin and their prevalence is thought to range anywhere from 0.4% to 1.6% [131, 136]. Of these accessory ossicles, the more common ones include the lunula, the os styloideum, the triangulare, the epilunate, the trapezium secundarium, and the os hamuli (Fig. 17.30) [135]. It is important not to mistake these accessory ossicles for fractures or loose bodies.

The os styloideum (carpal boss) is located over the dorsum of the base of the second or third metacarpal and is sometimes fused with the metacarpal base over which it lies. The os styloideum is important because it can undergo osteoarthritic changes or affect an overlying ganglion, limiting wrist motion and causing wrist pain [137, 138].

Lunate Variation

The lunate can be categorized anatomically into two types. The type I lunate has a single facet that articulates with the midcarpal joint. The type II lunate has an additional medial facet that articulates with the hamate (Fig. 17.31). The prevalence of the type II lunate ranges from 65.5% to 73% [139]. Viegas, in a cadaveric dissection of 165 wrists, found that about 44% of type II lunates demonstrated significant cartilage erosion at the proximal pole of the hamate, while only 0–2% of type I lunates exhibited such pathology [140]. Since this erosion is not easily identifiable on radiographs, type II lunates may be a cause of unidentified ulnar-sided wrist pain.

Fig. 17.30 Accessory ossicles. Examples of accessory ossicles shown here are the os styloideum, trapezium secundarium, and os centrale



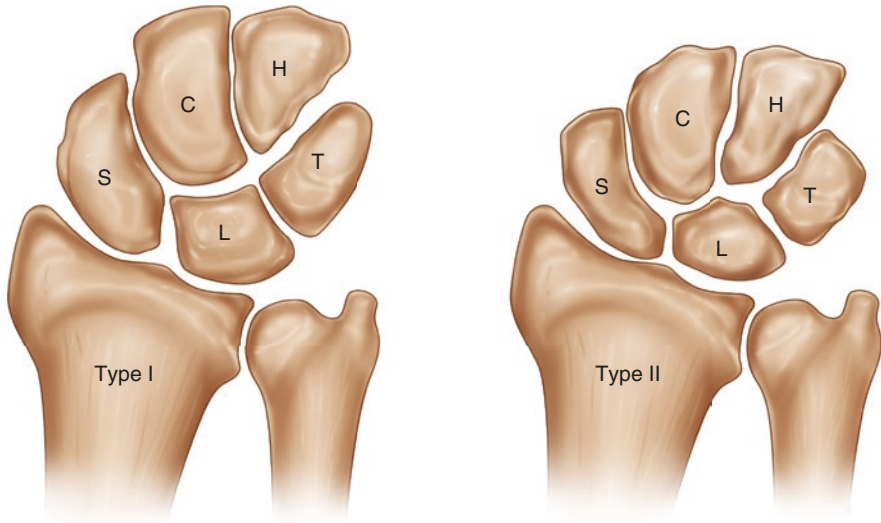


Fig. 17.31 Lunate types. (a) A type I lunette has a single facet articulating with the midcarpal joint. (b) A type II additionally has a medial facet articulating with the hamate

References

1. Standring S. Gray's anatomy: the anatomical basis of clinical practice. 40th ed. Spain: Churchill-Livingstone; 2008.
2. Lanz U. Anatomical variations of the median nerve in the carpal tunnel. *J Hand Surg Am.* 1977;2(1):44–53.
3. Mitchell R, Chesney A, Seal S, McKnight L, Thoma A. Anatomical variations of the carpal tunnel structures. *Can J Plast Surg.* 2009;17(3):e3–7.
4. Amadio PC. Bifid median nerve with a double compartment within the transverse carpal canal. *J Hand Surg Am.* 1987;12(3):366–8.
5. Fernandez-Garcia S, Pi-Folguera J, Estallo-Matino F. Bifid median nerve compression due to a musculotendinous anomaly of FDS to the middle finger. *J Hand Surg Br.* 1994;19(5):616–7.
6. Jones DP. Bilateral palmaris profundus in association with bifid median nerve as a cause of failed carpal tunnel release. *J Hand Surg Am.* 2006;31(5):741–3.
7. Schultz RJ, Endler PM, Huddleston HD. Anomalous median nerve and an anomalous muscle belly of the first lumbrical associated with carpal-tunnel syndrome. *J Bone Joint Surg Am.* 1973;55(8):1744–6.
8. Szabo RM, Pettey J. Bilateral median nerve bifurcation with an accessory compartment within the carpal tunnel. *J Hand Surg Br.* 1994;19(1):22–3.
9. Takami H, Takahashi S, Ando M. Bipartite median nerve with a double compartment within the transverse carpal canal. *Arch Orthop Trauma Surg.* 2001;121(4):230–1.
10. Beris AE, Lykissas MG, Kontogeorgakos VA, Vekris MD, Korompilias AV. Anatomic variations of the median nerve in carpal tunnel release. *Clin Anat.* 2008;21(6):514–8.
11. Bhanu PS, Sankar KD. Bilateral absence of musculocutaneous nerve with unusual branching pattern of lateral cord and median nerve of brachial plexus. *Anat Cell Biol.* 2012;45(3):207–10.
12. Sarkar A, Saha A. Bilateral absence of musculocutaneous nerve: a case report. *J Clin Diagn Res.* 2014;8(9):AD06–7.

13. Nakatani T, Tanaka S, Mizukami S. Absence of the musculocutaneous nerve with innervation of coracobrachialis, biceps brachii, brachialis and the lateral border of the forearm by branches from the lateral cord of the brachial plexus. *J Anat.* 1997;191(Pt 3):459–60.
14. Butz JJ, Shiwochan DG, Brown KC, Prasad AM, Murlimanju BV, Viswanath S. Bilateral variations of brachial plexus involving the median nerve and lateral cord: an anatomical case study with clinical implications. *Australas Med J.* 2014;7(5):227–31.
15. Leibovic SJ, Hastings H 2nd. Martin-Gruber revisited. *J Hand Surg Am.* 1992;17(1):47–53.
16. Jones C, Beredjikian P, Matzon JL, Kim N, Lutsky K. Incidence of an anomalous course of the palmar cutaneous branch of the median nerve during volar plate fixation of distal radius fractures. *J Hand Surg Am.* 2016;41(8):841–4.
17. Dowdy PA, Richards RS, McFarlane RM. The palmar cutaneous branch of the median nerve and the palmaris longus tendon: a cadaveric study. *J Hand Surg Am.* 1994;19(2):199–202.
18. McCann PA, Clarke D, Amirfeyz R, Bhatia R. The cadaveric anatomy of the distal radius: implications for the use of volar plates. *Ann R Coll Surg Engl.* 2012;94(2):116–20.
19. Cheung JW, Shyu JF, Teng CC, Chen TH, Su CH, Shyr YM, et al. The anatomical variations of the palmar cutaneous branch of the median nerve in Chinese adults. *J Chin Med Assoc.* 2004;67(1):27–31.
20. Taleisnik J. The palmar cutaneous branch of the median nerve and the approach to the carpal tunnel. An anatomical study. *J Bone Joint Surg Am.* 1973;55(6):1212–7.
21. Hobbs RA, Magnussen PA, Tonkin MA. Palmar cutaneous branch of the median nerve. *J Hand Surg Am.* 1990;15(1):38–43.
22. Engber WD, Gmeiner JG. Palmar cutaneous branch of the ulnar nerve. *J Hand Surg Am.* 1980;5(1):26–9.
23. Oh CS, Won HS, Lee KS, Chung IH, Kim SM. Anatomic variation of the innervation of the flexor digitorum profundus muscle and its clinical implications. *Muscle Nerve.* 2009;39(4):498–502.
24. Hill NA, Howard FM, Huffer BR. The incomplete anterior interosseous nerve syndrome. *J Hand Surg Am.* 1985;10(1):4–16.
25. Wertsch JJ. AAEM case report #25: anterior interosseous nerve syndrome. *Muscle Nerve.* 1992;15(9):977–83.
26. Mazurek MT, Shin AY. Upper extremity peripheral nerve anatomy: current concepts and applications. *Clin Orthop Relat Res.* 2001;383:7–20.
27. Khoo D, Carmichael SW, Spinner RJ. Ulnar nerve anatomy and compression. *Orthop Clin North Am.* 1996;27(2):317–38.
28. Sunderland S, Hughes ES. Metrical and non-metrical features of the muscular branches of the ulnar nerve. *J Comp Neurol.* 1946;85:113–25.
29. Gonzalez MH, Lotfi P, Bendre A, Mandelbroyt Y, Lieska N. The ulnar nerve at the elbow and its local branching: an anatomic study. *J Hand Surg Br.* 2001;26(2):142–4.
30. Lowe JB 3rd, Maggi SP, Mackinnon SE. The position of crossing branches of the medial antebrachial cutaneous nerve during cubital tunnel surgery in humans. *Plast Reconstr Surg.* 2004;114(3):692–6.
31. Chow JC, Papachristos AA, Ojeda A. An aberrant anatomic variation along the course of the ulnar nerve above the elbow with coexistent cubital tunnel syndrome. *Clin Anat.* 2006;19(7):661–4.
32. Tindall A, Patel M, Frost A, Parkin I, Shetty A, Compson J. The anatomy of the dorsal cutaneous branch of the ulnar nerve – a safe zone for positioning of the 6R portal in wrist arthroscopy. *J Hand Surg Br.* 2006;31(2):203–5.
33. Lindsey JT, Watumull D. Anatomic study of the ulnar nerve and related vascular anatomy at Guyon's canal: a practical classification system. *J Hand Surg Am.* 1996;21(4):626–33.
34. Murata K, Tamai M, Gupta A. Anatomic study of variations of hypothenar muscles and arborization patterns of the ulnar nerve in the hand. *J Hand Surg Am.* 2004;29(3):500–9.
35. Bozkurt MC, Tağil SM, Ozçakar L, Ersoy M, Tekdemir I. Anatomical variations as potential risk factors for ulnar tunnel syndrome: a cadaveric study. *Clin Anat.* 2005;18(4):274–80.
36. Kaplan EB. Variation of the ulnar nerve at the wrist. *Bull Hosp Joint Dis.* 1963;24:85–8.

37. Bozkurt MC, Cezayirli E, Tagil SM. An unusual termination of the ulnar nerve in the palm. *Ann Anat.* 2002;184(3):271–3.
38. Windisch G. Unusual vascularization and nerve supply of the fifth finger. *Ann Anat.* 2006;188(2):171–5.
39. McCarthy RE, Nalebuff EA. Anomalous volar branch of the dorsal cutaneous ulnar nerve: a case report. *J Hand Surg Am.* 1980;5(1):19–20.
40. Konig PS, Hage JJ, Bloem JJ, Prose LP. Variations of the ulnar nerve and ulnar artery in Guyon's canal: a cadaveric study. *J Hand Surg Am.* 1994;19(4):617–22.
41. Bozkurt MC, Tagil SM, Ersoy M, Tekdemir I. Muscle variations and abnormal branching and course of the ulnar nerve in the forearm and hand. *Clin Anat.* 2004;17(1):64–6.
42. Martin CH, Seiler JG 3rd, Lesesne JS. The cutaneous innervation of the palm: an anatomic study of the ulnar and median nerves. *J Hand Surg Am.* 1996;21(4):634–8.
43. Dogan NU, Uysal II, Seker M. The communications between the ulnar and median nerves in upper limb. *Neuroanatomy.* 2009;8(1):15–9.
44. May JW Jr, Rosen H. Division of the sensory ramus communicans between the ulnar and median nerves: a complication following carpal tunnel release. A case report. *J Bone Joint Surg Am.* 1981;63(5):836–8.
45. Kimura I, Ayyar DR, Lippmann SM. Electrophysiological verification of the ulnar to median nerve communications in the hand and forearm. *Tohoku J Exp Med.* 1983;141(3):269–74.
46. Harness D, Sekeles E. The double anastomotic innervation of thenar muscles. *J Anat.* 1971;109(Pt 3):461–6.
47. Kim BJ, Date ES, Lee SH, Lau EW, Park MK. Unilateral all ulnar hand including sensory without forearm communication. *Am J Phys Med Rehabil.* 2004;83(7):569–73.
48. Ganes T. Complete ulnar innervation of the thenar muscles combined with normal sensory fibres in a subject with no peripheral nerve lesion. *Electromyogr Clin Neurophysiol.* 1992;32(10–11):559–63.
49. Dumitru D, Walsh NE, Weber CF. Electrophysiologic study of the Riche-Cannieu anomaly. *Electromyogr Clin Neurophysiol.* 1988;28(1):27–31.
50. Gutmann L. AAEM minimonograph #2: important anomalous innervations of the extremities. *Muscle Nerve.* 1993;16(4):339–47.
51. Refaiean M, King JC, Dumitru D, Cuetter AC. Carpal tunnel syndrome and the Riche-Cannieu anastomosis: electrophysiologic findings. *Electromyogr Clin Neurophysiol.* 2001;41(6):377–82.
52. Moore KL, Dalley AF, Agur AM. Clinically oriented anatomy. 7th ed. Baltimore: Lippincott Williams & Wilkins; 2014.
53. Mackinnon SE, Novak CB. Compression neuropathies. In: Wolfe SW, Pederson WC, Hotchkiss RN, Kozin SH, Cohen MS, editors. *Green's operative hand surgery.* Philadelphia: Elsevier Churchill Livingstone; 2011. p. 977–1014.
54. Mahakkanukrauh P, Somsarp V. Dual innervation of the brachialis muscle. *Clin Anat.* 2002;15(3):206–9.
55. Latev MD, Dalley AF 2nd. Nerve supply of the brachioradialis muscle: surgically relevant variations of the extramuscular branches of the radial nerve. *Clin Anat.* 2005;18(7):488–92.
56. Khullar M, Kalsey G, Laxmi V, Khullar S. Variations in the nerve supply to the extensor carpi radialis brevis. *J Clin Diagn Res.* 2012;6(1):13–6.
57. Abrams RA, Brown RA, Botte MJ. The superficial branch of the radial nerve: an anatomic study with surgical implications. *J Hand Surg Am.* 1992;17(6):1037–41.
58. Linell EA. The distribution of nerves in the upper limb, with reference to variabilities and their clinical significance. *J Anat.* 1921;55(Pt 2–3):79–112.
59. Ehrlich W, Dellon AL, Mackinnon SE. Classical article: cheiralgia paresthetica (entrapment of the radial nerve). A translation in condensed form of Robert Wartenberg's original article published in 1932. *J Hand Surg Am.* 1986;11(2):196–9.
60. Auerbach DM, Collins ED, Kunkle KL, Monsanto EH. The radial sensory nerve. An anatomic study. *Clin Orthop Relat Res.* 1994;308:241–9.

61. Bas H, Kleinert JM. Anatomic variations in sensory innervation of the hand and digits. *J Hand Surg Am.* 1999;24(6):1171–84.
62. Peterson AR, Giuliani MJ, McHugh M, Shipe CC. Variations in dorsomedial hand innervation. Electrodiagnostic implications. *Arch Neurol.* 1992;49(8):870–3.
63. McCluskey LF. Anomalous superficial radial sensory innervation of the ulnar dorsum of the hand: a cause of “paradoxical” preservation of ulnar sensory function. *Muscle Nerve.* 1996;19(7):923–5.
64. Kuruvilla A, Laaksonen S, Falck B. Anomalous superficial radial nerve: a patient with probable autosomal dominant inheritance of the anomaly. *Muscle Nerve.* 2002;26(5):716–9.
65. Leis AA, Wells KJ. Radial nerve cutaneous innervation to the ulnar dorsum of the hand. *Clin Neurophysiol.* 2008;119(3):662–6.
66. Appleton AB. A case of abnormal distribution of the n. Musculo-cutaneus, with complete absence of the ramus cutaneus n. radialis. *J Anat Physiol.* 1911;46(Pt 1):89–94.
67. Huanmanop T, Agthong S, Luengchawapong K, Sasiwongpakdee T, Burapasomboon P, Chentanez V. Anatomic characteristics and surgical implications of the superficial radial nerve. *J Med Assoc Thai.* 2007;90(7):1423–9.
68. Stopford JS. The variation in distribution of the cutaneous nerves of the hand and digits. *J Anat.* 1918;53(Pt 1):14–25.
69. Mackinnon SE, Dellon AL. The overlap pattern of the lateral antebrachial cutaneous nerve and the superficial branch of the radial nerve. *J Hand Surg Am.* 1985;10(4):522–6.
70. Branovacki G, Hanson M, Cash R, Gonzalez M. The innervation pattern of the radial nerve at the elbow and in the forearm. *J Hand Surg Br.* 1998;23(2):167–9.
71. Missankov AA, Sehgal AK, Mennen U. Variations of the posterior interosseous nerve. *J Hand Surg Br.* 2000;25(3):281–2.
72. Innocenti M, Tani M, Carulli C, Ghezzi S, Raspanti A, Menichini G. Radial forearm flap plus flexor carpi radialis tendon in Achilles tendon reconstruction: surgical technique, functional results, and gait analysis. *Microsurgery.* 2015;35(8):608–14.
73. Rumball KM, Tonkin MA. Absence of flexor carpi radialis. *J Hand Surg Br.* 1996;21(6):778.
74. Ioannis D, Anastasios K, Konstantinos N, Lazaros K, Georgios N. Palmaris longus muscle’s prevalence in different nations and interesting anatomical variations: review of the literature. *J Clin Med Res.* 2015;7(11):825–30.
75. Murabit A, Gnarra M, Mohamed A. Reversed palmaris longus muscle: anatomical variant – case report and literature review. *Can J Plast Surg.* 2013;21(1):55–6.
76. Reimann AF, Daseler EH, Anson BJ, Beaton LE. The palmaris longus muscle and tendon. A study of 1600 extremities. *Anat Rec.* 1944;89(4):495–505.
77. Acikel C, Ulkur E, Karagoz H, Celikoz B. Effort-related compression of median and ulnar nerves as a result of reversed three-headed and hypertrophied palmaris longus muscle with extension of Guyon’s canal. *Scand J Plast Reconstr Surg Hand Surg.* 2007;41(1):45–7.
78. Bencteux P, Simonet J, el Ayoubi L, Renard M, Attignon I, Dacher JN, et al. Symptomatic palmaris longus muscle variation with MRI and surgical correlation: report of a single case. *Surg Radiol Anat.* 2001;23(4):273–5.
79. Depuydt KH, Schuurman AH, Kon M. Reversed palmaris longus muscle causing effort-related median nerve compression. *J Hand Surg Br.* 1998;23(1):117–9.
80. Bernardes A, Melo C, Pinheiro S. A combined variation of palmaris longus and flexor digitorum superficialis: case report and review of literature. *Morphologie.* 2016;100(331):245–9.
81. Jelev L, Georgiev GP. Unusual high-origin of the pronator teres muscle from a Struthers’ ligament coexisting with a variation of the musculocutaneous nerve. *Romanian J Morphol Embryol.* 2009;50(3):497–9.
82. Cassell MD, Bergman RA. Palmaris longus muscle substituting for the ring finger slip of flexor digitorum superficialis. *Anat Anz.* 1990;171(3):201–4.
83. Guler F, Kose O, Turan A, Baz AB, Akalin S. The prevalence of functional absence of flexor digitorum superficialis to the little finger: a study in a Turkish population. *J Plast Surg Hand Surg.* 2013;47(3):224–7.

84. Coenen L, Biltjes I. Pseudotumor of the palm due to an anomalous flexor digitorum superficialis muscle belly. *J Hand Surg Am.* 1991;16(6):1046–51.
85. Sanger JR, Krasniak CL, Matloub HS, Yousif NJ, Kneeland JB. Diagnosis of an anomalous superficialis muscle in the palm by magnetic resonance imaging. *J Hand Surg Am.* 1991;16(1):98–101.
86. Still JM Jr, Kleinert HE. Anomalous muscles and nerve entrapment in the wrist and hand. *Plast Reconstr Surg.* 1973;52(4):394–400.
87. Elliot D, Khandwala AR, Kulkarni M. Anomalies of the flexor digitorum superficialis muscle. *J Hand Surg Br.* 1999;24(5):570–4.
88. Skie M, Ciocanel D. Anomaly of flexor digitorum superficialis penetrating through the median nerve: case report. *J Hand Surg Am.* 2010;25(1):27–9.
89. Davis C, Armstrong J. Spontaneous flexor tendon rupture in the palm: the role of a variation of tendon anatomy. *J Hand Surg Am.* 2003;28(1):149–52.
90. Masaki F, Isao T, Aya Y, Ryuuji I, Yohjiroh M. Spontaneous flexor tendon rupture of the flexor digitorum profundus secondary to an anatomic variant. *J Hand Surg Am.* 2007;32(8):1195–9.
91. Jones M, Abrahams PH, Sañudo JR, Campillo M. Incidence and morphology of accessory heads of flexor pollicis longus and flexor digitorum profundus (Gantzer's muscles). *J Anat.* 1997;191(Pt 3):451–5.
92. Pai MM, Nayak SR, Krishnamurthy A, Vadgaonkar R, Prabhu LV, Ranade AV, et al. The accessory heads of flexor pollicis longus and flexor digitorum profundus: incidence and morphology. *Clin Anat.* 2008;21(3):252–8.
93. Lee YM, Song SW, Sur YJ, Ahn CY. Flexor carpi radialis brevis: an unusual anomalous muscle of the wrist. *Clin Orthop Surg.* 2014;6(3):361–4.
94. Mantovani G, Lino W Jr, Fukushima WY, Cho AB, Aita MA. Anomalous presentation of flexor carpi radialis brevis: a report of six cases. *J Hand Surg Eur Vol.* 2010;35(3):234–5.
95. Mathew AJ, Sukumaran TT, Joseph S. Versatile but temperamental: a morphological study of palmaris longus in the cadaver. *J Clin Diagn Res.* 2015;9(2):AC01–3.
96. Pirola E, Hébert-Blouin MN, Amador N, Amrami KK, Spinner RJ. Palmaris profundus: one name, several subtypes, and a shared potential for nerve compression. *Clin Anat.* 2009;22(6):643–8.
97. von Schroeder HP, Botte MJ. Anatomy of the extensor tendons of the fingers: variations and multiplicity. *J Hand Surg Am.* 1995;20(1):27–34.
98. Zilber S, Oberlin C. Anatomical variations of the extensor tendons to the fingers over the dorsum of the hand: a study of 50 hands and a review of the literature. *Plast Reconstr Surg.* 2004;113(1):214–21.
99. el-Badawi MG, Butt MM, al-Zuhair AG, Fadel RA. Extensor tendons of the fingers: arrangement and variations—II. *Clin Anat.* 1995;8(6):391–8.
100. Yamine K. The prevalence of the extensor digiti minimi tendon of the hand and its variants in humans: a systematic review and meta-analysis. *Anat Sci Int.* 2015;90(1):40–6.
101. Hirai Y, Yoshida K, Yamanaka K, Inoue A, Yamaki K, Yoshizuka M. An anatomic study of the extensor tendons of the human hand. *J Hand Surg Am.* 2001;26(6):1009–15.
102. Nakashima T. An accessory extensor digiti minimi arising from extensor carpi ulnaris. *J Anat.* 1993;182(Pt 1):109–12.
103. Barfred T, Adamsen S. Duplication of the extensor carpi ulnaris tendon. *J Hand Surg Am.* 1986;11(3):423–5.
104. Baba MA. The accessory tendon of the abductor pollicis longus muscle. *Anat Rec.* 1954;119(4):541–7.
105. Shiraishi N, Matsumura G. Anatomical variations of the extensor pollicis brevis tendon and abductor pollicis longus tendon—relation to tenosynovectomy. *Okajimas Folia Anat Jpn.* 2005;82(1):25–9.
106. Kulthanan T, Chareonwat B. Variations in abductor pollicis longus and extensor pollicis brevis tendons in the Quervain syndrome: a surgical and anatomical study. *Scand J Plast Reconstr Surg Hand Surg.* 2007;41(1):36–8.

107. Fabrizio PA, Clemente FR. A variation in the organization of abductor pollicis longus. *Clin Anat.* 1996;9(6):371–5.
108. Stein AH Jr. Variations of the tendons of insertion of the abductor pollicis longus and the extensor pollicis brevis. *Anat Rec.* 1951;110(1):49–55.
109. Allison DM. Pathologic anatomy of the forearm: intersection syndrome. *J Hand Surg Am.* 1986;11(6):913–4.
110. Martinez R, Omer GE Jr. Bilateral subluxation of the base of the thumb secondary to an unusual abductor pollicis longus insertion: a case report. *J Hand Surg.* 1985;10(3):396–9.
111. Bryce TH. Myology. In: Quain's elements of anatomy, vol. 4, part II. London: Longmans, Green, and Co; 1923. p. 153–5.
112. Chiu DT. Supernumerary extensor tendon to the thumb: a report on a rare anatomic variation. *Plast Reconstr Surg.* 1981;68(6):937–9.
113. Cohen BE, Haber JL. Supernumerary extensor tendon to the thumb: a case report. *Ann Plast Surg.* 1996;36(1):105–7.
114. De Greef I, De Smet L. Accessory extensor pollicis longus: a case report. *Eur J Plast Surg.* 2006;28(8):532–3.
115. Rubin G, Wolovelsky A, Rinott M, Rozen N. Anomalous course of the extensor pollicis longus: clinical relevance. *Ann Plast Surg.* 2011;67(5):489–92.
116. Beatty JD, Remedios D, McCullough CJ. An accessory extensor tendon of the thumb as a cause of dorsal wrist pain. *J Hand Surg Br.* 2000;25(1):110–1.
117. Dawson S, Barton N. Anatomical variations of the extensor pollicis brevis. *J Hand Surg Br.* 1986;11(3):378–81.
118. Kulshreshtha R, Patel S, Arya AP, Hall S, Compson JP. Variations of the extensor pollicis brevis tendon and its insertion: a study of 44 cadaveric hands. *J Hand Surg Eur Vol.* 2007;32(5):550–3.
119. Gonzalez MH, Weinzeig N, Kay T, Grindel S. Anatomy of the extensor tendons to the index finger. *J Hand Surg Am.* 1996;21(6):988–91.
120. Culver JE Jr. Extensor pollicis and indicis communis tendon: a rare anatomic variation revisited. *J Hand Surg Am.* 1980;5(6):548–9.
121. Kaplan EB, Nathan P. Accessory extensor pollicis longus. *Bull Hosp Joint Dis.* 1969;30(2):203–7.
122. Macalister A. Additional observations on muscular anomalies in human anatomy (third series) with a catalogue of the principal muscular variations hitherto published. *Trans R Ir Acad Sci.* 1875;25:1–34.
123. Cauldwell EW, Anson BJ, Wright RR. The extensor indicis proprius muscle—a study of 263 consecutive specimens. *Q Bull Northwest Univ Med Sch.* 1943;17(4):267–79.
124. Wood J. On some variations in human myology. *Proc R Soc Lond.* 1863;13:299–303.
125. Wagenseil F. Untersuchungen über die muskulatur der chinesen. *Z Morphol Anthropol.* 1936;36(H. 1):39–150.
126. Yamine K. The prevalence of extensor digitorum brevis manus and its variants in humans: a systematic review and meta-analysis. *Surg Radiol Anat.* 2015;37(1):3–9.
127. Rodriguez-Niedenführ M, Vázquez T, Golanó P, Parkin I, Sañudo JR. Extensor digitorum brevis manus: anatomical, radiological and clinical relevance. A review. *Clin Anat.* 2002;15(4):286–92.
128. Ogura T, Inoue H, Tanabe G. Anatomic and clinical studies of the extensor digitorum brevis manus. *J Hand Surg Am.* 1987;12(1):100–7.
129. Nakano M, Watanabe Y, Masutani M. A case of extensor digitorum brevis manus. *Dermatol Online J.* 2003;9(5):21.
130. Klena JC, Riehl JT, Beck JD. Anomalous extensor tendons to the long finger: a cadaveric study of incidence. *J Hand Surg Am.* 2012;37(5):938–41.
131. O'Rahilly R. A survey of carpal and tarsal anomalies. *J Bone Joint Surg Am.* 1953;35–A(3):626–42.
132. Pfirrmann CW, Zanetti M. Variants, pitfalls and asymptomatic findings in wrist and hand imaging. *Eur J Radiol.* 2005;56(3):286–95.

133. Delaney TJ, Eswar S. Carpal coalitions. *J Hand Surg Am.* 1992;17(1):28–31.
134. Metz VM, Schimmerl SM, Gilula LA, Viegas SF, Saffar P. Wide scapholunate joint space in lunotriquetral coalition: a normal variant? *Radiology.* 1993;188(2):557–9.
135. Timins ME. Osseous anatomic variants of the wrist: findings on MR imaging. *AJR Am J Roentgenol.* 1999;173(2):339–44.
136. Bogart FB. Variations of the bones of the wrist. *Am J Roentgenol.* 1932;28:638–46.
137. Conway WF, Destouet JM, Gilula LA, Bellinghausen HW, Weeks PM. The carpal boss: an overview of radiographic evaluation. *Radiology.* 1985;156(1):29–31.
138. Resnick D. *Bone and joint imaging.* Philadelphia: Saunders; 1989. p. 1073.
139. Viegas SF. Advances in the skeletal anatomy of the wrist. *Hand Clin.* 2001;17(1):1–11.
140. Viegas SF, Wagner K, Patterson R, Peterson P. Medial (hamate) facet of the lunate. *J Hand Surg Am.* 1990;15(4):564–71.



Anatomical Anomalies of the Foot and Ankle

18

Beau Vesely, Melissa Gulosh, Gabriel V. Gambardella,
and Peter A. Blume

An anomaly is something that is structurally unusual or irregular, and many anatomical anomalies have been identified in the foot and ankle. Some anomalous structures are identified incidentally upon evaluation or radiographic analysis and are generally not pathologic. Instances certainly exist, however, where an anomaly may be the source of pain, deformity, or altered function. It is beneficial for the foot and ankle specialist, and general practitioner, to have an understanding of the most common anomalies associated with the foot and ankle in order to direct treatment. Furthermore, a surgeon specializing in treating disease of the foot and ankle should be aware of anomalous structures to optimize surgical outcomes and prevent unforeseen postoperative complications. These structures can be musculoskeletal, vascular, or neurological. This chapter aims to discuss many of the commonly seen anatomical anomalies of the foot and ankle. Some rare anomalies are also discussed.

Musculoskeletal Anomalies of the Foot and Ankle

The majority of chief complaints encountered by the foot and ankle specialist precede musculoskeletal diagnoses. Signs and symptoms may include pain, weakness, altered function, and deformity. Upon evaluation, in general, an anomalous structure may not be grossly identified, aside from those presenting

B. Vesely
Krohn Clinic, Black River Falls, WI, USA

M. Gulosh
Novant Health UVA Culpeper Medical Center, Culpeper, VA, USA

G. V. Gambardella
Bloomfield Foot Specialists, Bloomfield, CT, USA

P. A. Blume (✉)
Department of Podiatry, Diabetes Center, Yale School of Medicine, New Haven, CT, USA

with obvious deformities, such as syndactyly or polydactyly. More often, when these structures are the source of symptoms, they are noted on radiographs or advanced imaging.

The skeletal structure of the foot is a complex configuration consisting of the following categories of bones: tarsals (7), metatarsals (5), and phalanges (14). Each foot typically contains 26 of the 206 bones in the body, without taking into account anomalous structures. There are numerous anatomic variants that exist, including sesamoids and accessory ossicles, coalitions, and congenital deformities. There are also 17 muscular structures isolated to the foot, while many tendons insert to bones of the foot that originate in the leg. Various insertions and extra muscles may be pathologic.

Common Accessory and Sesamoid Bones of the Foot

Sesamoid bones form developmentally within tendons from their own ossification center, functioning to reduce friction of the tendon in which they are partially or completely embedded, and allow for efficient gliding or serve as a pulley mechanism [1]. Accessory bones are supernumerary or extra bones, that may form due to anomalies in ossification or fusion failure of a secondary ossification center [2]. Some of the accessory and sesamoid bones are fairly common, while others are quite rare. There are more sesamoid and accessory bones in the foot than anywhere else in the body [3].

The two most constant sesamoid bones of the foot are the medial (tibial) and lateral (fibular) sesamoids. They are found in nearly 100% of individuals [4, 5] and are located within the tendons of the flexor hallucis brevis at the level of the first metatarsophalangeal joint. Variants do occur within these sesamoids themselves. A bipartite sesamoid (sesamoid bone presenting as two separate identifiable bones) can be observed radiographically (Fig. 18.1). This observation was demonstrated in 2.7% of nearly 1000 feet, but has been reported to occur in as many as 33.5% of feet [1, 6]. When a patient presents with plantar forefoot pain, a bipartite sesamoid must be distinguished from a fracture or avascular necrosis, and obtaining a thorough history from the patient can aid in the diagnosis. Obtaining bilateral radiographs also may help in making this distinction [7]. Occasionally, a radiograph may reveal an interphalangeal sesamoid of the hallux. This sesamoid lies within the tendon of the flexor hallucis longus. It has been demonstrated in 2–13% of feet [1]. A painful callus on the plantar region of the hallux may be indicative of this sesamoid, and excision may be warranted to obtain symptom relief. Extreme care must be taken when sesamoid excision is performed to avoid excessive removal of tendinous tissue. Overzealous excision can cause weakness, and possible rupture, of the tendon, which can result deformity.

Sesamoids are rarely found at the second through fifth metatarsals, and are typically asymptomatic. They are located at the level of the metatarsophalangeal joints within the tendons of the flexor digitorum brevis (FDB), and are usually incidental findings noted on X-ray.

Fig. 18.1 Incidental finding of a bipartite tibial sesamoid is present. Note the regular contour of the sesamoid. Irregularity of the contour, in addition to positive clinical examination findings, could possibly indicate fracture



The more common accessory bones of the foot include the os tibiale externum, os perineum, os trigonum, os intermetatarsium, and os vesalianum. Literature has reported the presence of these accessory bones in 10–23% of the population [3, 5].

The os tibiale externum, also referred to as an accessory navicular, is located within the substance of the posterior tibial tendon (PTT) as it inserts into the navicular bone (Fig. 18.2). The posterior tibial tendon plays a crucial role in dynamic stabilization of the medial longitudinal arch and in resisting internal tibial torsion. Symptomatic accessory navicular can be associated with pain, tendon dysfunction, and progressive pes planus deformity [8]. The os tibiale externum has been reported to occur in 4–21% of the population [2, 5].

The os peroneum is embedded within the tendon of peroneus longus (PL), just proximal to the tendon's course in the peroneal groove of the cuboid bone. It is best visualized on a medial-oblique radiograph. This anatomic variant can produce lateral foot pain or os peroneum syndrome, and can be mistaken for a fracture. Its presence has been reported in 4.7–9% of individuals [1, 2, 9, 10].

The os trigonum is closely associated with the lateral tubercle of the posterior process of the talus. It occurs when a secondary ossification center of the lateral tubercle fails to fuse with the primary talus. This secondary center of ossification is typically visible on radiographs in girls between the ages of 8 and 10 years, and in

Fig. 18.2 DP view of the foot revealing an accessory navicular with close proximity to the navicular tuberosity



boys between the ages of 11 and 13. It typically fuses in the same year that it becomes radiographically visible [11, 12]. When fusion fails, a fibrocartilaginous synchondrosis forms with the body of the talus. Os trigonum syndrome can present as posterior ankle pain or impingement. Dancers, particularly those involved in ballet and point, are at risk for developing posterior ankle pain, which may be exacerbated with this ossicle. As the flexor hallucis longus (FHL) tendon courses through the posterior process of the talus it can become inflamed (tenosynovitis) or entrapped, causing pain. This skeletal anomaly is one of the largest and most common accessory bones in the foot, with an estimated occurrence in 2–25% of individuals [1, 5, 13, 14].

The os intermetatarsium is a small accessory ossicle located adjacent to the medial cuneiform and the base of the first and second metatarsals. Because of its location, it can occasionally be mistaken for a Lisfranc fracture in the setting of trauma [15]. It is one of the more commonly occurring skeletal anomalies found in 0.2–10% of individuals [1, 5, 9].

The os vesalianum is found proximal to a well-developed tuberosity of the base of the fifth metatarsal [9]. Its importance clinically is in the differentiation between an accessory ossicle and an avulsion fracture at the base of the fifth metatarsal. The os vesalianum is rarely seen, and has been reported in only 0.1–1% of feet [1, 13, 16].

Uncommon Accessory and Sesamoid Bones of the Foot and Ankle

The os sustentaculi is a rare, small ossicle located near the posterior aspect of the sustentaculum tali of the talus. This failed secondary center of ossification forms a fibrocartilaginous synchondrosis with the talus. Similar to an os trigonum, it can cause pathology with force or trauma when the connection is disrupted, and can be confused with a fracture in the setting of trauma. It is present in from 0.3% to 0.4% of feet [5].

The os calcaneus secundarium is an accessory ossicle of the anterior facet of the calcaneus. It has been reported in 0.6–7% of the population [9, 17]. It is located dorsally between the proximal aspect of the cuboid and navicular and the head and neck of the talus [17]. It can be difficult to differentiate this from an avulsion fracture of the anterior process of the calcaneus in inversion and plantar flexion ankle injuries.

The os supranaviculare, os supratolare, and os talotibiale are rare accessory bones located at the dorsal aspect of the talus that can be misdiagnosed as an avulsion fractures with plantar flexion injuries of the ankle. There is a reported prevalence of 0.2–3.5% [1, 5, 18].

The os subtibiale and os subfibulare are rare accessory bones located near the distal aspect of the tibial and fibular malleoli, respectively. They occur when a secondary center ossification fails to fuse with the distal aspect of the tibia or fibula, and can be misdiagnosed as avulsion fractures in the setting of ankle trauma [19–22]. The os subtibiale and os subfibulare have been reported to occur between 0.9% and 2.1% of patients, respectively.

Brachymetatarsia

Brachymetatarsia is a rare congenital deformity of one or more metatarsals in that it is greater than 5 mm shorter than is adjacent metatarsal (Fig. 18.3) [23]. This skeletal deformity can be cosmetically displeasing as well as painful, and occurs with greater frequency in females (female-to-male ratio of 25:1) [24, 25]. Between 44% and 72% of cases reported are bilateral and most often involve the fourth metatarsal [26]. Studies have demonstrated incidence of this structural anomaly in a wide range of individuals, from one out of 625 people to one out of 4686 [25, 26]. Surgical correction can be achieved by osteotomies with bone grafting or corticotomy with distraction osteogenesis, both of which aim to lengthen the affected metatarsal [23] and normalize the appearance of the foot and metatarsal parabola.

Coalitions in the Foot and Ankle

Coalition refers to the union or connection between two or more bones that is not normally present. The union may be osseous (synostosis), fibrous, or cartilaginous (synchondrosis) [27]. Impaired segmentation of mesenchymal cells in the formation

Fig. 18.3 A shortened fourth metatarsal is evident, the most commonly affected metatarsal in brachymetatarsia



of osseous structures has been credited with the congenital malformation [28]. However, coalitions may also be the result of trauma. The most common coalition in the foot is found at the distal interphalangeal joint of the fifth toe. It can occur in up to 50% in individuals of European descent and in 73% those of Japanese descent [29]. This coalition is usually not symptomatic, and therefore may not require treatment.

Tarsal coalitions in the foot are fairly uncommon abnormalities, but are often underdiagnosed and can be the cause of a painful rigid pes planovalgus deformity. The majority of tarsal coalitions involved are the fibrocartilaginous or osseous bar between the calcaneus and navicular [30]. Also common are coalitions within the articular facets of the talocalcaneal joint, with the middle articulation being the most common (Fig. 18.4) [30]. In a retrospective study of 27,483 foot and ankle MRIs, tarsal coalitions were identified in 0.6% of the population studied. Of the coalitions evaluated, 77.2% were located between the calcaneal and navicular bones, and the remaining cases were located within the subtalar joint [31]. These abnormalities can be treated conservatively with appropriate orthotics, physical therapy, non-steroidal anti-inflammatory medications, physical therapy, and corticosteroid injections. However, for those who do not respond well to conservative treatment, surgery to resection the coalition or arthrodesis may be necessary.

Fig. 18.4 CT scan of the ankle revealing a synostosis (osseous union) of the talocalcaneal joint. A middle facet coalition is present



Accessory Musculotendinous Structures of the Foot and Ankle

Accessory muscles in the ankle are relatively common. The four most common are peroneus quartus (PQ), accessory flexor digitorum longus (aFDL), accessory soleus (aS), and peroneocalcaneus internus (PCI). The PQ, aFDL, and aS, when present, are found on the medial aspect of the ankle and may contribute to neurological symptoms of tarsal tunnel syndrome (TTS). Treatment of TTS caused by anomalous muscles may include resection of the anomalous muscle, release of the tarsal tunnel, and external neurolysis of the tibial nerve [32]. MRI is very useful to visualize abnormal soft tissue lesions in and around the tarsal tunnel, as reported by Buschmann [33].

Peroneus quartus is typically located in the lateral compartment of the leg, accompanying the peroneus longus and peroneus brevis (PB) tendons. The PQ may also be referred to as peroneus accessorius and peroneus calcaneus externus. The function of the PQ is ankle eversion and subtalar joint stabilization. Presence of the PQ is usually asymptomatic, but can cause crowding in the fibular malleolar sulcus, resulting in pain. Chaney and colleagues report that the muscle is present in about 3% of the population [34]. Other studies, however, have reported that its presence ranges from 6.6% to 27% [35, 36]. Presence of the tendon may contribute to lateral

ankle stenosis (“retromalleolar conflict”) or laxity of the superior peroneal retinaculum (SPR), predisposing tearing of the PB tendon [34]. Surgical intervention may require tendon resection, or use of PQ to repair the SPR [33]. One should consider absorbable suture to temporarily anastomose the PB and PL, as literature has shown adhesions and impingement can occur after resection, causing pain and need for revision surgery [37].

The aFDL is variable in both origin and location of the musculotendinous unit in relation to the FHL. Position of its tendon with respect to the neurovascular bundle in the tarsal tunnel may result in tarsal tunnel syndrome. A patient may be asymptomatic if the tendon passes deep to the neurovascular bundle; however, if the tendon crosses superficially, it can compress the tibial nerve [38]. Boutin et al. found the aFDL to be the second-most common accessory muscle in the lower leg (2–8%) [32]. Variations in the origin include from the FHL, soleus muscle, flexor retinaculum, tibia, or fibula. It typically courses posterior to FDL and the neurovascular bundle, through tibial tunnel as a fleshy structure, and often inserts into quadratus plantae (QP) muscle. This is usually asymptomatic.

Harvesting the aFDL in place of the FHL or FDL for tendon transfers is a surgical consideration when the anomaly is known to be present [39]. The aFDL is also a risk factor for developing FHL tenosynovitis and, because of its variability and mostly asymptomatic nature, it may not be noticed on MRI. Endoscopy is safe tool for diagnosis of the condition, and curative treatment is afforded by excision of the aFDL muscle [40].

The aS muscle normally originates from the upper third of tibial and fibular shafts. In about 16% of persons, an accessory muscle can originate adjacent to the tibia, fibula, or anterior portion of the soleus muscle [32]. The muscle inserts on either the superior or medial surface of calcaneus. The aS muscle can cause entrapment syndrome and can appear as a soft tissue swelling or mass, which can induce pain with exercise (closed compartment ischemia) [41]. An MRI can determine its presence and affect choice of surgery for patients with soft tissue defects in the leg. Surgical considerations include fasciotomy and excision. Kinoshita and colleagues [41] treated 49 feet for tarsal tunnel syndrome, and noted 8 feet with an accessory muscle as the cause for nerve impingement; 6 with an accessory flexor digitorum longus muscle, and one with an accessory soleus. Patients underwent tibial nerve decompression and accessory muscle excision. They reported patients achieved symptom resolution at an average of 4.1 months with no functional deficit.

Peroneocalcaneus internus muscle is a rare anomaly located in the posterior calf and typically originates on the medial aspect of distal fibula, extends into tarsal tunnel and inserts into small tubercle on the calcaneus, distal to sustentaculum tali [32]. It may displace the FHL muscle medially and indirectly compress the medial neurovascular bundle.

Peroneus tertius is a deflection of extensor tendons and described by Hallisy as an evolutionary selection allowing eversion of the foot [42]. It has been reported to be as large as an individual bundle of extensor digitorum longus (EDL) or as small as an aponeurotic branch from EDL and present in greater than 90% of feet. There are variable insertions, but typically the tendon inserts on the dorsal base of fifth

metatarsal base. Absence of peroneus tertius has been reported in 10.5% of lower extremities and an interesting study hypothesized the absence of peroneus tertius to be a predisposing factor for ankle ligament disabilities [34]. Although no significant weakness difference has been demonstrated with or without the peroneus tertius, it is plausible to use the peroneus tertius for reconstruction and augmentation of the anatomical structures around the talocrural articulation [34].

Deformities

Clubfoot

Talipes equinovarus is one of the most common congenital abnormalities, occurring in about 1–2 cases per 1000 live births. The prenatal diagnosis can be made from the 12th week via vaginal ultrasound or from third trimester abdominal ultrasound. Diagnosis before birth ranges from 0.43% to 59.8% of cases. Patients diagnosed prenatally are afforded earlier and less invasive postnatal treatment than those diagnosed after birth.

Prenatal diagnosis allows initiation of treatment soon after birth and the seeking of genetic counseling if desired [43]. Treatment should be deferred to a surgeon who specializes in clubfoot correction. Serial casting of the foot may correct the deformity in some patients, while others may require a more complex approach, with surgical release of ligaments and lengthening of tendons. Radiographic evaluation of newborn feet is difficult as there is incomplete ossification of the tarsal bones. The talus is often deformed, small, and eccentrically located [44].

Trisomy 21:—Sandal Gap

Down syndrome is one of the most common of all genetic malformation syndromes, with an estimated occurrence of one per 600–800 births. Podiatric characteristics found in Down syndrome include syndactyly 1% (1% normal karyotype), brachydactyly 2.5%, and sandal gap 9.5% (7% normal karyotype). Cardinal features in the newborn include hypotonia, poor Moro reflex, hyperextensibility of joints, excess skin on the posterior neck, slanted palpebral fissures, and a flat facial profile. Of patients with this syndrome, 49.5% have been shown to have one of the following features, which heighten suspicion of the diagnosis: simian crease, sandal gap, epicanthic folds, hypotonia, upslanting palpebral fissures, and/or protruding tongue [45].

Amniotic Band Syndrome

Congenital constriction syndrome occurs in approximately one per 15,000 births. Bands of fetal membrane may intertwine and entrap fetal tissues leading to constriction, fusion, and/or necrosis of distal extremities. Treatment may require plastic

surgery techniques to release skin tensions, amputation, and desyndactylization, and may require multiple stages. Of children with congenital constriction band syndrome, 27–31% also have incidence of clubfoot deformity, likely explained by a band in the supramalleolar area or more proximal bands. Fibrous bands may be removed or unwound, which untethers the digits from each other [46].

Amniotic band syndrome is a complex collection of asymmetric congenital anomalies. Distal ring constrictions, intrauterine amputations, and acrosyndactyly are the most common findings in distal extremities. On average, three extremity parts are affected. Early amniotic rupture leads to formation of mesodermal fibrous strands that entangle limbs and appendages. Nearly all cases reach final form prior to birth, with tissue necrosis healing in utero. The incidence is 1 in 1200–5000 births, and 60% demonstrate an abnormal gestation history [46].

According to the literature, no two cases are alike. Classification systems exist depending on constriction severity, presence of lymphedema, and intrauterine amputation.

Shallow grooves or bands require no operative treatment unless they interfere with circulation or lymphatic drainage. Deep constrictive bands require immediate surgical release to prevent risk of gangrene or auto-amputation with surgical excision of the fibrous band and any necrotic tissue, with skin-plasty as the most common procedure. Two-staged procedures are recommended to avoid devascularization to the distal segment, with only half of the band released at a time. It is uncommon for underlying bones to be affected [47].

Hypoplasia of Lower Extremity/Fibular Hemimelia

Congenital aplasia of the fibula is often associated with a ball and socket ankle joint, anteromedial bowing and shortening of the tibia, tarsal coalition, and absent lateral rays of the foot. Partial or complete absence of the fibula is the most common abnormality of the long bones and may be part of a genetically determined syndrome [48]. Seven to twenty per million living births and a 2:1 male-to-female predilection have been reported. Expression is variable, from mild-to-severe deformity with associated anomalies of the foot. Shortening of the limb is the most common sign and is typically unilateral.

The goal of treatment is to allow maximal function by achieving adequate lower extremity alignment, length, and stability [49].

Tibial Hemimelia

Congenital absence of the tibia, which is rare, is typically associated with additional congenital abnormalities. The associated foot anomalies include tibial ray deficiencies or tarsal coalitions. Common treatment is amputation of the limb or foot. Limb preservation is dependent on knee stability, expected limb shortening, and ability to successfully reconstruct the foot deformity [50].

Sirenomelia

Sirenomelia is also known as mermaid syndrome, and is the most severe form of caudal recession syndrome. It is found in 0.98–4.2 per 100,000 live births with a 3:1 male-to-female predilection. Eight to fifteen percent of cases occur in twins. Characteristics include single midline lower limb, sacral and pelvic bone anomalies, absent external genitalia, imperforated anus, and renal dysgenesis or agenesis. There are seven classifiable types of sirenomelia, which are distinguished by the number of femur, tibia, and metatarsal bones. The etiology is unclear, but the two main hypotheses are abnormal origination of umbilical artery vessel and/or defective blastogenesis [51].

Syndactyly and Polydactyly

Syndactyly and polydactyly refer to the congenital unification of toes and the acquisition of an extra toe, or toes, respectively. They can occur alone, or be part of a genetic syndrome such as Down syndrome or Apert's syndrome. Regarding syndactyly, the conjoined toes may not become symptomatic; a patient may, however, decide to have his or her toes desyndactylized for aesthetic purposes. If the deformity affects the first and second toes, and the syndactylization is complete, the individual will have difficulty wearing sandals. Desyndactylization and skin grafting of the defect are the surgery of choice for these individuals.

When a patient demonstrates a polydactyly, finding comfortable footwear may be problematic. Preoperative X-rays must be taken for operative planning to determine the most "normal" anatomy of the foot, as amputation of the extra digit(s) will hopefully render a foot that appears to be normal.

Peripheral Nerve Anomalies of the Foot and Ankle

Anomalous innervation in the peripheral nervous system is not uncommon and should be regarded as normal variant.

The accessory deep peroneal nerve (aDPN) is the most common anomaly/variant of the peroneal nerve to innervate the extensor digitorum muscle [52]. It has been found to branch off the distal part of the superficial peroneal nerve, traverse the lateral compartment along the posterior border of peroneal brevis muscle, pass behind the lateral malleolus near sural nerve to reach dorsum of foot [53–55]. When present, stimulation of the fibular head excites the entire muscle, but volar ankle stimulation does not [53]. There has been documentation of complete absence of DPN motor branch to EDB and total innervation by aDPN [56].

Diagnostic studies include the electromyography studies, nerve conduction velocities, and electroneurography. It is important to be aware of this variant because during the performance of EMG testing, unrecognized anomalous innervation can alter results and data interpretation [57].

The aDPN has been found in 18–25% of studied legs [54, 55, 58] and bilateral existence in 44–57% of legs [54]. Entrapment of this accessory nerve can be caused by excess adiposity, a soft tissue mass, or exertional compartment syndrome [56]. With symptoms of pain and numbness to areas of known distribution it is imperative to perform tinel's and valleix's tapping to include this entrapment neuropathy as a potential differential diagnosis [59].

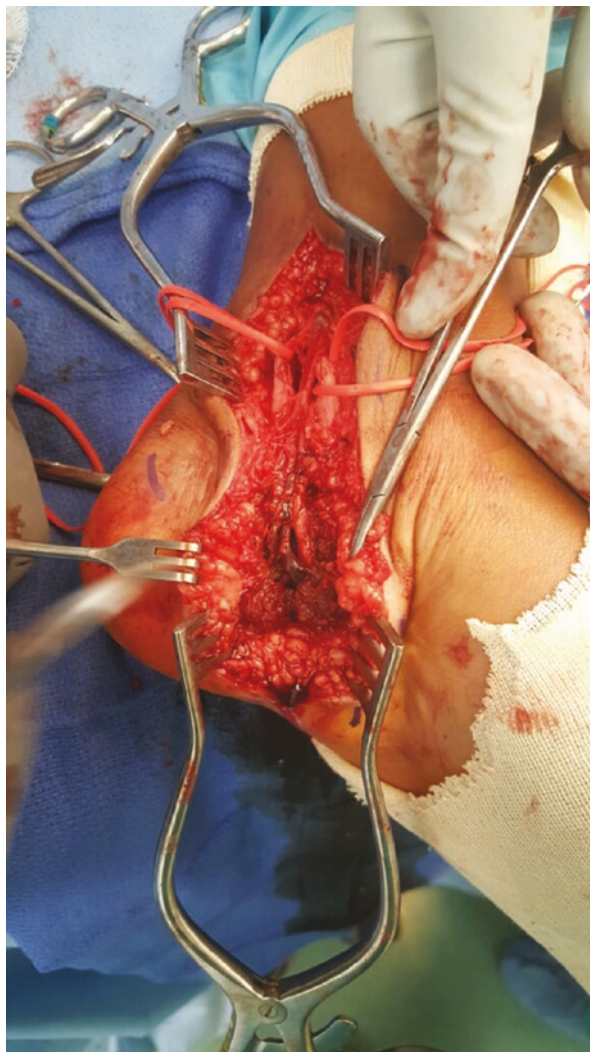
The superficial peroneal nerve (SPN) has great anatomic variability with differences among emergence from fascia, the height of bifurcation, its course about the lower leg and foot, the branching pattern and its distribution area. In 63.3–96.7% of cases, the SPN penetrates the crural fascia as a single trunk and divides after its emergence. Most emerge 10.5–12.5 cm proximal from the tip of the lateral malleolus, with ranges of 9.1–12.5 cm [60]. Duscher et al. found that the nerve became more superficial within the muscle compartment until it penetrates the crural fascia about 4–5 cm above the ankle joint [61].

The anomalous portion is a high penetration point, 14–15 cm above the lateral malleolar tip [62]. Awareness of possible presence of an accessory SPN or emergence is important in surgical dissection for ankle fractures and ankle arthroscopy. Complications from arthroscopy range from 0.9% to 17%. Thirty-three to fifty percent of the occurrences involve injury to the cutaneous nerves, primarily the SPN or one of its branches. It is recommended that the anterolateral portal should be placed as close to fibula as possible [63]. Transillumination may aid in identifying the nerve prior to making the anterolateral portal incision. The medial and intermediate dorsal cutaneous nerves, off the SPN, also have variable branching points and awareness of the high variability of the nerve location must be respected during surgery.

When performing surgery to the lateral midfoot, rearfoot, and ankle, the sural nerve remains at risk for iatrogenic injury. The sural nerve trunk is typically located approximately 14 mm posterior and 14 mm inferior to tip of the malleolus, superficial, and slightly inferior to peroneal tendons; however, 41% were found to be crossing peroneal longus, or crossed more proximally, coursing superior to the tendon [64]. Considerable variations of the sural nerve have been identified in the rearfoot, with bifurcations or trifurcations in 91% of specimens. It is important to be aware of the anastomotic branch which can be found traversing medially toward the sinus tarsi, superficial to EDB and within 1.5 cm on the anterior process of the calcaneus [64]. In this region, the nerve can easily be injured during incisions or dissection. The nerve is at risk for iatrogenic injury with incision and dissection during surgeries such as peroneal tendon repair and subtalar joint arthrodesis.

In general, the tibial nerve division occurs within 2 cm of the tip of the medial malleolus. A complete anesthetic block of the tibial nerve with injections over the upper limit of this area is unsuccessful in about 20% of cases. A complete anesthetic block 8 cm above the upper limit has been successful in 96% of cases. When drawing a line between the tip of the medial malleolus and the posterosuperior tip of the calcaneal tuberosity, the tibial nerve has been shown to bifurcate into the medial and lateral plantar nerve 82.2% of the time. The bifurcation of the tibial nerve was more proximal in 26.7% of cases [65]. Dellon and colleagues found that the nerve bifurcated 5

Fig. 18.5 Intraoperative picture of the tibial nerve taken during a tarsal tunnel release and decompression neuroplasty of the tibial nerve. Patient had symptoms of paresthesias and neurogenic heel pain, mimicking symptoms of plantar fasciitis. In this picture, note the proximal bifurcation of the tibial nerve. The medial and lateral plantar nerves have been isolated



cm proximal to the medial malleolar tip in 1 out of 31 cases [66]. Proximal bifurcation of the tibial nerve may predispose a patient to TTS (Fig. 18.5) [67].

The saphenous nerve is a cutaneous branch of the femoral nerve and becomes cutaneous on the medial side of the knee, and follows the greater saphenous vein to the medial malleolus. Duscher et al. found a close relationship with the vein, which poses increased risk of injury during vein stripping or during harvest for bypass surgery [61]. This nerve was also found to have increased incidence of injury during minimally invasive plating techniques of the medial malleolus. Marsland and colleagues found the saphenous nerve to be the most variable of all the nerves evaluated. They found that it has a broad distribution at the ankle joint, with variable numbers of branches and termination points, predisposing it to injury during surgery [68].

Vascular Anomalies of the Foot and Ankle

Anomalies of the pedal vasculature, although rare, can be clinically and surgically relevant. The arterial supply of the foot and ankle is comprised of three source arteries, all of which arise from the popliteal artery.

The popliteal artery divides into its terminal branches, the anterior and posterior tibial arteries, at the inferior border of the popliteus muscle. In a study of 553 limbs by Calisir et al., the usual branching pattern of a true anterior tibial artery and tibio-peroneal trunk was found in 87% of limbs. Variations of this branching pattern were found in 13% of the population, with the most common variant represented as a true trifurcation of the posterior, anterior, and peroneal arteries, which was found in 4.2% of lower extremities [69]. These three arteries descend through the compartments of the leg to supply to distal lower extremity.

At the level of the ankle joint, the anterior tibial artery (ATA) becomes more superficial and is crossed anteriorly by the tendon of extensor hallucis longus. It can be palpated as the dorsalis pedis artery (DPA) inferior to the superior extensor retinaculum. In a study by Vazquez et al., the anterior tibial artery continued as the DPA in 95.7% of 287 cases between the EHL and the first (medial) tendon of EDL; however, three variants were found. In 2% of the limbs studied, the ATA was deep to the EDL and peroneus tertius in a more lateral position. The peroneal artery replaced the DPA on the dorsum of the foot in 1.33% of the population in this study, but this variation has been reported as high as 12% [70, 71]. At the level of the talonavicular joint, Rimchala and Chuckpaiwong found that the DPA can be found, on average, 23.75 and 22.81 mm, in male and females, respectively, from the most medial cortex of the navicular tuberosity in a study of 132 feet [72]. Understanding the possible location of this artery is imperative to avoid a vascular injury in surgeries such as talo-navicular arthrodesis, total ankle replacement, and ankle arthrodesis using an anterior approach.

Branches of the DPA include the arcuate artery as well as its two terminal branches, the first dorsal metatarsal and deep plantar arteries. The arcuate artery, in the majority of cases, is created from the DPA, but can be a branch of lateral tarsal artery (10–30%), or can be completely absent in up to 33% of feet [73]. The arcuate artery joins the second, third, and fourth metatarsal arteries in 50% of feet [74]. The first dorsal metatarsal artery, typically a terminal branch of the DPA, was found to be the case in 90.6% of a study of 32 feet [75, 76]. May and colleagues found an absence of connection between the DPA and first dorsal metatarsal artery in 18% of cases [77].

Approximately 5 cm superior to the lateral malleolus, the peroneal artery perforates the interosseous membrane anteriorly as the perforating branch of the peroneal artery. The artery is at risk of injury during open ankle fracture reduction and surgeries necessitating a distal fibulectomy/fibulotomy. In approximately 1% of cases, this artery can be absent and is replaced by the anterior tibial artery [70]. Conversely, Yamada et al. found that the DPA can arise from the peroneal artery in 6.7% of the population studied [73].

The posterior tibial artery (PTA), a terminal branch of the popliteal artery, begins at the lower border of the popliteus muscle between the tibia and fibula. It descends obliquely through the posterior compartment of the leg, deep to the soleus muscle. At the ankle it is located posterior to the medial malleolus lying medial to the tibial nerve deep to flexor retinaculum. It divides in its terminal branches, the medial and lateral plantar arteries, anywhere between the proximal part of the medial malleolus and before entering the foot, deep to the abductor hallucis muscle. The lateral plantar artery, usually larger than its medial counterpart, travels laterally of from the porta pedis, giving off osseous and muscular branches in the lateral column of the foot. The medial terminal branch proceeds medially and becomes the deep plantar arch between the third and fourth muscle layers. The arch is completed on the medial aspect from the deep plantar branch of the DPA. In a study of the feet of 100 cadavers, the main component of the deep plantar arch was formed from the first proximal perforating artery in 82% of cases [78], but the deep branch of the lateral plantar artery can be the dominant artery in as high as 38% of cases [79].

Rarely, vascular anomalies can cause pathology in the foot and ankle. Arteriovenous malformations infrequently present in the lower extremity as soft tissue masses and almost always have systemic manifestations from genetic disease, but have been reported in the literature [80]. More commonly venous aneurysms or varicose veins can present as tarsal tunnel syndrome [81]. Linscheid reported that in 13 of 34 patients who presented with tarsal tunnel syndrome, varicose veins were responsible for their symptoms [82]. Excision of the varicose vein and decompression neuroplasty may be required as treatment.

References

1. Coskun N, Yuksel M, Cevener M, Arican RY, Ozdemir H, Bircan O, et al. Incidence of accessory ossicles and sesamoid bones in the feet: a radiographic study of the Turkish subject. *Surg Radiol Anat.* 2009;31:19–24.
2. Miller TT. Painful accessory bones of the foot. *Semin Musculoskelet Radiol.* 2002;6(2):153–61.
3. Vasiljević V, Marković L, Vasić-Vilić J, Mihajlović D, Nikolić B, Milosević S. Accessory bones of the feet—radiological analysis of frequency. *Vojnosanit Pregl.* 2010;67(6):469–72.
4. Longo UG, Marinozzi A, Petrillo S, Spiezia F, Maffulli N, Denaro V. Prevalence of accessory ossicles and sesamoid bone in hallux valgus. *J Am Podiatr Med Assoc.* 2013;103(3):208–12.
5. Kelikian AS, editor. *Osteology*. In: Sarrafian's: anatomy of the foot and ankle. 3rd ed. Philadelphia: Lippincott Williams and Wilkins; 2011. p. 89–112.
6. Karasick D, Schweitzer ME. Disorders of the hallux sesamoid complex: MR features. *Skelet Radiol.* 1998;27:411–8.
7. Potter HG, Pavlov H, Abrahams TG. The hallux sesamoids revisited. *Skelet Radiol.* 1992;21:437–44.
8. Sullivan JA, Miller WA. The relationship of the accessory navicular to the development of the flat foot. *Clin Orthop Relat Res.* 1979;144:233–7.
9. Mellado JM, Ramos A, Salvadó E, Camins A, Danús M, Saurí A. Accessory ossicles and sesamoid bones of the ankle and foot: imaging findings, clinical significance and differential diagnosis. *Eur Radiol.* 2003;13:164–77.

10. Sobel M, Pavlov H, Geppert MJ, Thompson FM, DiCarlo EF, Davis WH. Painful os peroneum syndrome: a spectrum of conditions responsible for plantar lateral foot pain. *Foot Ankle Int.* 1994;15:112–24.
11. Lawson JP. Symptomatic radiographic variants in extremities. *Radiology.* 1985;159(3):625–31.
12. Nault ML, Kocher MS, Micheli LJ. Os trigonum syndrome. *J Am Acad Orthop Surg.* 2014;22(9):545–53.
13. Tsuruta T, Shiokawa Y, Kato A, Matsumoto T, Yamazoe Y, Oike T, et al. Radiological study of accessory skeletal elements in the foot and ankle. *Nihon Seikeigeka Gakkai Zasshi.* 1981;55(4):357–70.
14. Lawson JP. International Skeletal Society Lecture in honor of Howard D. Dorfman. Clinically significant radiologic anatomic variants of the skeleton. *AJR Am J Roentgenol.* 1994;163(2):249–55.
15. Karasick D. Fractures and dislocations of the foot. *Semin Roentgenol.* 1994;29(2):152–75.
16. Boya H, Ozcan O, Tandoğan R, Günel I, Araç S. Os vesalianum pedis. *J Am Podiatr Med Assoc.* 2005;95(6):583–5.
17. Bulut MD, Yavuz A, Bora A, Gökalp MA, Özkaçmaz S, Batur A. Three-dimensional CT findings of os calcaneus secundarius mimicking a fracture. *Case Rep Radiol.* 2014;2014:537062.
18. Nwawka OK, Hayashi D, Diaz LE, Goud AR, Arndt WF 3rd, Roemer FW, et al. Sesamoids and accessory ossicles of the foot: anatomical variability and related pathology. *Insights Imaging.* 2013;4(5):581–93.
19. Berg EE. The symptomatic os subfibulare: avulsion fracture of the fibula associated with recurrent instability of the ankle. *J Bone Joint Surg Am.* 1991;73(8):1251–4.
20. Ogden JA, Lee J. Accessory ossification patterns and injuries of the malleoli. *J Pediatr Orthop.* 1990;10(3):306–16.
21. Li X, Shi L, Liu T, Wang L. Progress in the clinical imaging research of bone diseases on ankle and foot sesamoid bones and accessory ossicles. *Intractable Rare Dis Res.* 2012;1(3):122–8.
22. Coughlin MJ. Sesamoid and accessory bones of the foot. In: Coughlin MJ, Mann RA, Saltzman CL, editors. *Surgery of the foot and ankle.* 8th ed. Philadelphia: Mosby; 2007.
23. Bartolomei FJ. Surgical correction of brachymetatarsia. *J Am Podiatr Med Assoc.* 1990;80(2):76–82.
24. Munuera Martínez PV, Lafuente Sotillos G, Domínguez Maldonado G, Salcini Macías JL, Martínez Camuña L. Morphofunctional study of brachymetatarsia of the fourth metatarsal. *J Am Podiatr Med Assoc.* 2004;94(4):347–52.
25. Urano Y, Kobayashi A. Bone-lengthening for shortness of the fourth toe. *J Bone Joint Surg Am.* 1978;60(1):91–3.
26. Jones MD, Pinegar DM, Rincker SA. Callus distraction versus single-stage lengthening with bone graft for treatment of brachymetatarsia: a systematic review. *J Foot Ankle Surg.* 2015;54(5):927–31.
27. Lawrence DA, Rolen MF, Haims AH, Zayour Z, Moukaddam HA. Tarsal coalitions: radiographic, CT, and MR imaging findings. *HSS J.* 2014;10(2):153–66.
28. Flynn JF, Wukich DK, Conti SF, Hasselman CT, Hogan MV, Kline AJ. Subtalar coalitions in the adult. *Foot Ankle Clin.* 2015;20(2):283–91.
29. Sammarco GJ, Hockenbury RT. Fracture of an interphalangeal coalition: a report of two cases. *Foot Ankle Int.* 2000;21(8):690–2.
30. Murphy JS, Mubarak SJ. Talocalcaneal Coalitions. *Foot Ankle Clin.* 2015;20(4):681–91.
31. Nalaboff KM, Schweitzer ME. MRI of tarsal coalition. *Bull NYU Hosp Jt Dis.* 2008;66(1):14–21.
32. Boutin RD. Muscle disorders. In: Resnick D, editor. *Diagnosis of bone and joint disorders.* 4th ed. Philadelphia: Saunders; 2002.
33. Buschmann WR, Cheung Y, Jahss MH. Magnetic resonance imaging of anomalous leg muscles: accessory soleus, peroneus quartus, and the flexor digitorum longus accessories. *Foot Ankle.* 1991;12:109–16.
34. Chaney DM, Lee MS, Khan MA, Krueger WA, Mandracchia VJ, Yoho RM. Study of ten anatomical variants of the foot and ankle. *J Am Podiatr Med Assoc.* 1996;86(11):532–7.

35. Sobel M, Levy ME, Bohne WH. Congenital variations of the peroneus quartus muscle: anatomic study. *Foot Ankle*. 1990;11(2):81–9.
36. Athavale SA, Swathi, Vangara SV. Anatomy of the superior peroneal tunnel. *J Bone Joint Surg Am*. 2011;93(6):564–71.
37. Chinzei N, Kanzaki N, Takakura Y, Takakura Y, Toda A, Fujishiro T, et al. Surgical management of the peroneus quartus muscle for bilateral ankle pain. *J Am Podiatr Med Assoc*. 2015;105(1):85–91.
38. Kurtoglu Z, Uluutku MH, Can MA, Onderoglu S. An accessory flexor digitorum longus muscle with high division of the tibial nerve. *Surg Radiol Anat*. 2001;23(1):61–3.
39. Holzmann M, Al mudallal N, Rohleck K, Singh R, Lee S, Fredieu J. Identification of the flexor digitorum accessories longus muscle with unique distal attachments. *Foot (Edinb)*. 2009;19(4):224–6.
40. Ogut T, Ayhan E. Hindfoot endoscopy for accessory flexor digitorum longus and flexor hallucis longus tenosynovitis. *Foot Ankle Surg*. 2011;17(1):e7–9.
41. Kinoshita M, Okuda R, Morikawa J, Abe M. Tarsal tunnel syndrome associated with an accessory muscle. *Foot Ankle Int*. 2003;24(2):132–6.
42. Hallisy JE. The muscular variation in the human foot: a quantitative study. *Am J Anat*. 1930;45:411–42.
43. Rosselli P, Nossa S, Huerfano E, Betancur G, Guzmán Y, Castellanos C, et al. Prenatal ultrasound diagnosis of congenital talipes equinovarus in Bogota between 2003 and 2012. *Iowa Orthop J*. 2015;35:156–9.
44. Suda R, Suda AJ, Grill F. Sonographic classification of idiopathic clubfoot according to severity. *J Pediatr Orthop*. 2006;15(2):134–40.
45. Devlin L, Morrison P. Accuracy of the clinical diagnosis of Down Syndrome. *Ulster Med J*. 2004;73(1):4–12.
46. Light TR, Ogden JA. Congenital constriction band syndrome. Pathophysiology and treatment. *Yale J Biol Med*. 1993;66(3):143–55.
47. Walter JH Jr, Goss LR, Lazzara AT. Amniotic band syndrome. *J Foot Ankle Surg*. 1998;37(4):325–33.
48. Maffulli N, Fixsen JA. Fibular hypoplasia with absent lateral rays of the foot. *J Bone Joint Surg Br*. 1991;73(6):1002–4.
49. Marcovici T, Sabau I, Simesdrea I, Tepeneu P, Marginean O, Daescu C, et al. Postaxial hypoplasia of the lower extremity in children—case report. *Jurnalul Pediatriei*. 2009;12(47–48):36–9.
50. Shahcheraghi GH, Javid M. Functional assessment in tibial hemimelia (can we also save the foot in reconstruction?). *J Pediatr Orthop*. 2016;36(6):572–81.
51. Nokeangtong K, Kaewchai S, Visrutaratna P, Khuwuthyakorn V. Sirenomelia type VI (symplus apus) in one of dizygotic twins at Chiang Mai University Hospital. *BMJ Case Rep*. 2015;2015:pil: bcr2014208501. <https://doi.org/10.1136/bcr-2014-208501>.
52. Ubogu EE. Complete innervation of extensor digitorum brevis by accessory peroneal nerve. *Neuromuscul Disord*. 2005;15(8):562–4.
53. Van Dijk JG, Van der Hoeven BJ. Compound muscle action potential cartography of an accessory peroneal nerve. *Muscle Nerve*. 1998;21(10):1331–3.
54. Lambert EH. The accessory deep peroneal nerve. A common variation in innervation of the EDB. *Neurology*. 1969;19(2):1169–76.
55. Neundörfer B, Seiberth R. The accessory deep peroneal nerve. *J Neurol*. 1975;209(2):125–9.
56. Murad H, Neal P, Katiirji B. Total innervation of the extensor digitorum brevis by the accessory deep peroneal nerve. *Eur J Neurol*. 1999;6(3):371–3.
57. Budak F, Gönenç Z. Innervation anomalies in upper and lower extremities (an electrophysiological study). *Electromyogr Clin Neurophysiol*. 1999;39(4):231–4.
58. Stamboulis E. Accessory deep peroneal nerve. *Electromyogr Clin Neurophysiol*. 1987;27:289–92.
59. Kayal R, Katiirji B. Atypical deep peroneal neuropathy in the setting of an accessory deep peroneal nerve. *Muscle Nerve*. 2009;40(2):313–5.

60. Southerland JT, editor. Tarsal tunnel syndrome. In: McGlamry's comprehensive textbook of foot and ankle surgery. 4th ed. Philadelphia: Lippincott Williams & Wilkins; 2013. p. 934–49.
61. Duscher D, Wenny R, Entenfellner J, Weninger P, Hirtler L. Cutaneous innervation of the ankle: an anatomic study showing danger zones for ankle surgery. *Clin Anat*. 2014;27(4):653–8.
62. Paraskevas GK, Natsis K, Tzika M, Ioannidis O. Potential entrapment of an accessory superficial peroneal sensory nerve at the lateral malleolus: a cadaveric case report and review of literature. *J Foot Ankle Surg*. 2014;53(1):92–5.
63. Blair JM, Botte MJ. Surgical anatomy of the superficial peroneal nerve in the foot and ankle. *Clin Orthop Relat Res*. 1994;305:229–38.
64. Lawrence SJ, Botte MJ. The sural nerve in the foot and ankle: an anatomic study with clinical and surgical implications. *Foot Ankle Int*. 1994;15(9):490–4.
65. Kim DI, Kim YS, Han SH. Topography of human ankle joint: focused on posterior tibial artery and tibial nerve. Neurovascular structure in human ankle. *Anat Cell Biol*. 2015;48(2):130–7.
66. Dellon AL, McKinnon SE. Tibial nerve branching in the tarsal tunnel. *Arch Neurol*. 1984;41(6):645–6.
67. Havel PE, Ebraheim NA, Clark SE, Jackson WT, DiDio L. Tibial nerve branching in the tarsal tunnel. *Foot Ankle*. 1988;9(3):117–9.
68. Marsland D, Dray A, Little NJ, Solan MC. The saphenous nerve in foot and ankle surgery: its variable anatomy and relevance. *Foot Ankle Surg*. 2013;19(2):76–9.
69. Calisir C, Simsek S, Tepe M. Variations in the popliteal artery branching in 342 patients studied with peripheral CT angiography using 64-MDCT. *Jpn J Radiol*. 2015;33(1):13–20.
70. Vazquez T, Rodríguez-Niedenfuhr M, Parkin I, Viejo F, Sanudo J. Anatomic study of blood supply of the dorsum of the foot and ankle. *Arthroscopy*. 2006;22(3):287–90.
71. Bailleul JP, Olivez PR, Mestdagh H, Vilette B, Depreux R. Anatomie descriptive et topographique de l'artère dorsale du pied. *Bull Assoc Anat (Nancy)*. 1984;68(200):15–25.
72. Rimchala C, Chuckpaiwong B. Relationship of the dorsalis pedis artery to the tarsal navicular. *J Foot Ankle Surg*. 2015;54(1):66–8.
73. Yamada T, Gloviczki P, Bower TC, Naessens JM, Carmichael SW. Variations of the arterial anatomy of the foot. *Am J Surg*. 1993;166(2):130–5.
74. Singh BN, Burmeister W, Machado K, Rodriguez L, Santos-Dookie A. Variations of the origin of the arcuate artery. *J Am Podiatr Med Assoc*. 2013;103(3):181–4.
75. Lee JH, Dauber W. Anatomic study of the dorsalis pedis-first dorsal metatarsal artery. *Ann Plast Surg*. 1997;38(1):50–5.
76. Lefebvre D, Jaeger JF, Roux P, Hammoudi S, Bastide G. Interosseous dorsal artery of the first intermetatarsal space: anatomic variations and value in functional vascular studies. *J Mal Vasc*. 1989;14(1):39–41.
77. May JW Jr, Chait LA, Cohen BE, O'Brien BM. Free neurovascular flap from the first web of the foot in hand reconstruction. *J Hand Surg Am*. 1977;2(5):387–93.
78. Hamada N, Ikuta Y, Ikeda A. Arteriographic study of the arterial supply of the foot in one hundred cadaver feet. *Acta Anat (Basel)*. 1994;151(13):198–206.
79. Ozer MA, Govsa F, Bilge O. Anatomic study of the deep plantar arch. *Clin Anat*. 2005;18(6):434–42.
80. Kunze B, Kluba T, Ernemann U, Miller S. Arteriovenous malformation: an unusual reason for foot pain in children. *Foot Ankle Online J*. 2009;2(12):1. <https://doi.org/10.3827/foaj.2009.0212.0001>.
81. Ayad M, Whisenhunt A, Hong E, Heller J, Salvatore D, Abai B, et al. Posterior tibial vein aneurysm presenting as tarsal tunnel syndrome. *Vascular*. 2015;23(3):322–6.
82. Linscheid RL, Burton RC, Fredericks EJ. Tarsal-tunnel syndrome. *South Med J*. 1970;63(11):1313–23.



Upper and Lower Extremity Vascular Variations

19

Xiaolu Xu, Samuel Kim, James E. Clune,
and Deepak Narayan

Vascular variations in the upper and lower extremities are common entities. Generally speaking, most common are variations in depth, number of vessels, size, takeoff point, branching patterns, persistence of embryonic remnant, and failure of development. These apply to both upper and lower extremities, arteries, and veins. Clinically, these variations can affect surgical planning, such as designing flaps based on certain blood supplies and drainage patterns.

Arteries in the Arm and Forearm

Normal Course (Fig. 19.1)

Brachial Artery

The brachial artery is the major continuation of the axillary artery. It begins at the distal and inferior border of the tendon of the teres major, continues superficially on the ventral surface of the arm, and ends about a centimeter distal to the elbow joint in the cubital fossa under the cover of the bicipital aponeurosis. It then divides into

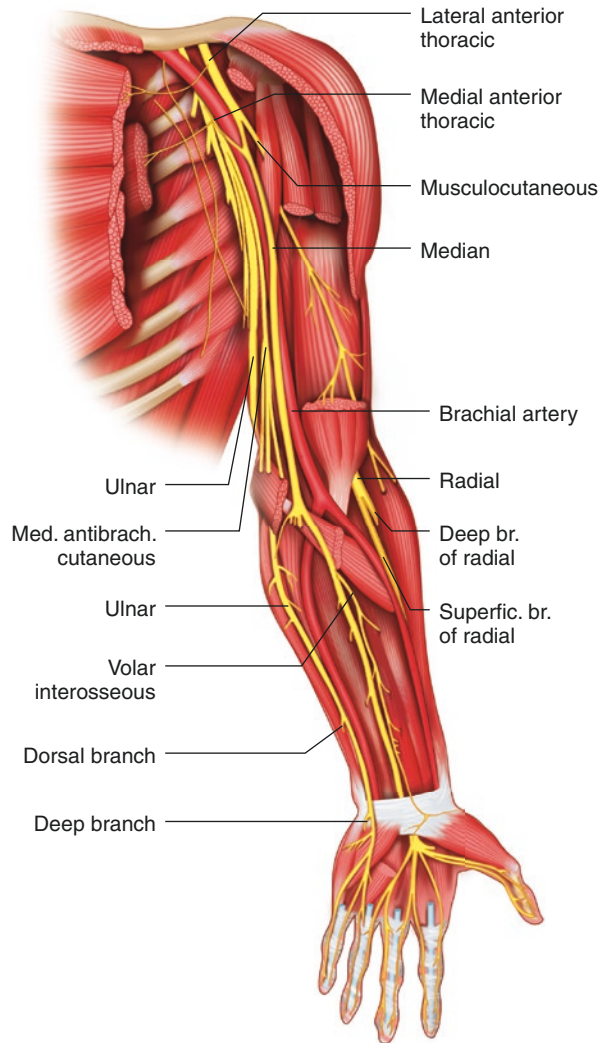
X. Xu (✉)

Yale School of Medicine, New Haven, CT, USA

S. Kim · J. E. Clune · D. Narayan (Deceased)

Section of Plastic and Reconstructive Surgery, Yale New Haven Hospital,
New Haven, CT, USA

Fig. 19.1 Normal anatomy of upper extremity vasculature [2]



the radial and ulnar arteries. Proximally, the median nerve lies immediately lateral to the brachial artery. Distally, the median nerve crosses in front of the brachial artery to its medial aspect, and lies medial to it in the cubital fossa. The brachial artery gives out the profunda brachii artery, a nutrient artery of the humerus. Additionally, it gives off the superior ulnar collateral artery, middle ulnar collateral artery, inferior ulnar collateral artery, and muscular branches [1, 2].

Radial Artery

The radial artery is the more direct continuation of the brachial artery, despite its smaller caliber compared to the ulnar artery. It starts 1 cm distal to the flexion crease of the elbow and descends along the radial side of the forearm accompanied by a

pair of interconnected *venae comitantes*. The artery lies medial to the radial shaft proximally and anterior to it distally. The radial artery runs superficially, covered by the muscle belly of the brachioradialis proximally, but only by skin and fasciae distally. The superficial radial nerve lies lateral to the middle third of the radial artery, whose multiple branches supply the nerve throughout its length. The radial artery gives out the radial recurrent artery, cutaneous branches, and muscular branches [2].

Ulnar Artery

The ulnar artery is the larger terminal branch of the brachial artery. Like the radial artery, it normally starts 1 cm distal to the flexion crease of the elbow. Proximally, it courses superficial to the brachialis and deep to all the forearm flexor muscles, except the deep flexors. When it reaches the medial forearm midway between the elbow and wrist, the ulnar artery becomes superficial distally, covered only by skin and fasciae. It enters the hand superficial to the flexor retinaculum and lateral to the pisiform. It is accompanied by the ulnar nerve and the *venae comitantes*. The ulnar artery gives out the common interosseous artery, anterior interosseous artery, posterior interosseous artery, posterior interosseous recurrent artery, cutaneous branches, and muscular branches [2].

Variations and Pathology

Superficial Brachial Artery (SBA)

The SBA (3.6–9.6%) is a variant of the brachial artery that courses in front of, rather than behind, the median nerve. It adopts its superficial course usually below the median nerve roots, but it can also occur above the roots [3]. Instead of crossing the median nerve posteriorly, the SBA may cross it anteriorly. The SBA also gives off a small branch deep to the median nerve to provide collateral supply to the biceps brachii.

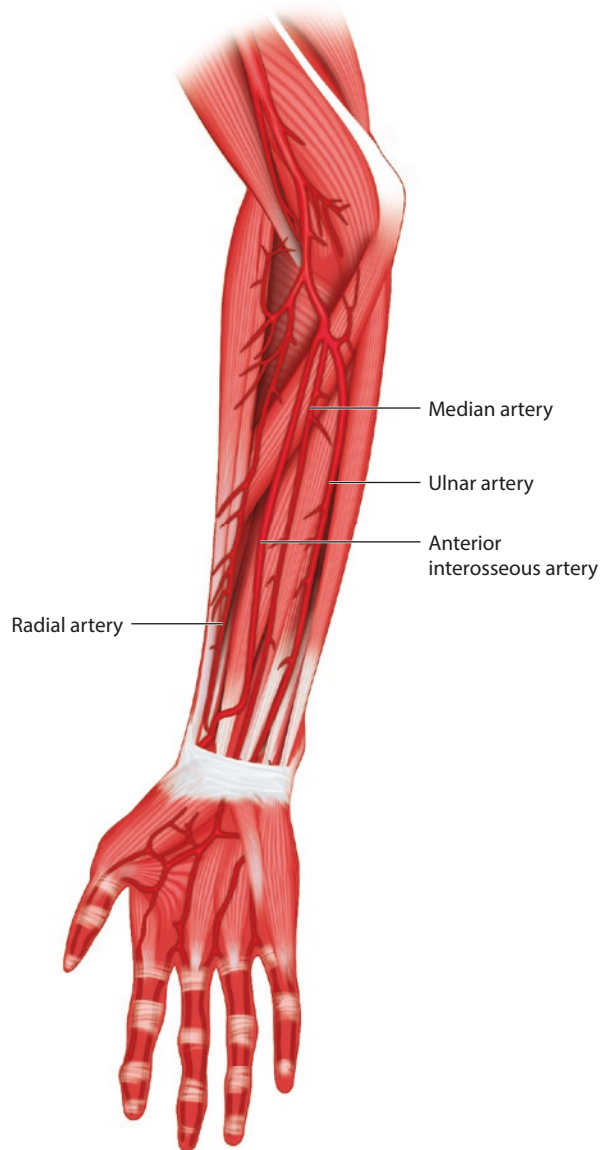
SBA injury can occur if its superficial course is mistaken for the basilic vein during cannulation or venipuncture [4, 5]. Because of the proximity of the proximal brachial artery to the terminal branches of the brachial plexus, an appreciation of the neurovascular relationship is necessary to avoid nerve injuries. The brachial artery or its large branches can be used for end-to-end anastomosis in microvascular reconstruction. Therefore, awareness of its course is necessary for locating and avoiding injury to this important vessel [6]. A case of insertion of a birth control implant into the brachial artery which caused perfuse bleeding and brachial artery occlusion has been reported. Therefore, physicians other than surgeons should also be aware of this variation [7].

Accessory Brachial Artery (ABA)

The brachial artery can bifurcate at the lower border of the teres major and reunite at the cubital fossa. This extra anomalous artery (0.26–11.4%) was first described as the ABA by McCormack in 1953 [8]. It is sometimes referred to as the superficial

brachial artery while the normal course brachial artery is referred to as the deep brachial artery. It courses superficially and medially to the brachial artery and in front of the median nerve. It rejoins the brachial artery in or proximal to the cubital fossa [9, 10] (Fig 19.2b). ABA injury can occur if its superficial course is mistaken for the basilic vein during cannulation or venipuncture [4, 5]. Because of its superficial course and accessory nature, the vessel can provide large size pedicles for raising flaps in reconstructive surgeries [11].

Fig. 19.2 Median artery. A persistent median artery takes off from anterior interosseous artery, and directly supplies palmar arch or common digital arteries [28]



Brachioradial Artery (BRA)

The BRA (11.1%) is a radial artery with a high origin. The origins include the axillary artery (2.48%) or anywhere along the brachial artery (8.62%) proximal to its normal bifurcation. It runs superficial to the median nerve along the arm and passes either anterior or posterior to the bicipital aponeurosis. It may anastomose with the normal (deep) brachial artery at the cubital fossa. The radial recurrent artery (RRA) can arise from the BRA (46%), deep brachial artery (34%), or the anastomosis between them (20%) [10].

If the origin of the BRA is in the axillary artery, the course of the BRA is likely to cross that of the median nerve in the cubital fossa, making the median nerve immediately deep to the BRA. This poses a risk of median nerve injury in the event of an aggressive dissection. The surgeon should be alerted to this configuration by the absence of bifurcation at the cubital fossa [12].

Superficial Brachioradial Artery (SBRA)

The SBRA (1.25–5.9%) is a high-origin radial artery coursing over the brachioradialis muscle or the tendons that define the snuffbox. It coexists with a brachial artery that branches into ulnar and interosseous arteries or occasionally radial and ulnar arteries. In the latter case, it has been described by Kadanoff and Balkansky as a duplicate radial artery [10, 13, 14].

Occasionally, the distal portion of the SBRA can be hypoplastic and make cannulation difficult [14]. Also, existence of a superficial radial artery implies the absence of a normal radial pulse at the wrist level [15].

Superficial Brachioulnar Artery (SBUA)

The SBUA (2.7%) is a high-origin ulnar artery that courses over the forearm flexor muscles. It coexists with a brachial or superficial brachial artery that branches into a radial artery and common interosseous trunk, or occasionally, radial and ulnar arteries. In this latter case, the SBUA is also considered a duplicate ulnar artery. It may also coexist with a median artery, which is considered a normal feature. The SBUA originates more frequently in the proximal third of the brachial artery than anywhere else. It runs superficial to the median nerve and deep to the brachial fascia, but occasionally courses subcutaneously above the fascia. Most often, it runs posterior to the bicipital aponeurosis [10]. The superficial ulnar artery tends to have a marked abnormal distal course. It passes superficial to the pronator teres and flexor carpi radialis, is occasionally serpentine toward the wrist, and enters the hand either lateral to flexor carpi ulnaris tendon or partially covered by it [12].

Because of the popularity of radial forearm flaps in reconstruction, ensuring the integrity of the ulnar artery is necessary to avoid devascularization of the hand. Anomalous ulnar arteries are vulnerable to injury. For instance, the superficial ulnar artery is more susceptible to injuries such as accidental venipuncture or crush injury than the normal ulnar artery, especially if only covered by a skin graft post-reconstruction. It is advisable to consider an alternative reconstruction or replace the anomalous ulnar artery under or within a flexor muscle due to this vulnerability [12, 16, 17]. In addition, when raising an ulnar artery free flap by circumferential incision, injury can

occur to a superficial ulnar artery running underneath the skin paddle and lead to devascularization of the entire hand. The superficial ulnar artery gives several good-sized fasciocutaneous branches in the forearm. A fasciocutaneous flap, similar to a radial forearm flap, can be raised safely on this anomalous vessel [18, 19].

Brachioulnar Artery (BUA)

The BUA (0.52%) is a high origin ulnar artery with a normal course. It is very rare [10].

Superficial Brachioulnoradial Artery (SBURA)

The SBURA (0.14–1.3%) is a superficial brachial artery that branches at the elbow level into radial and ulnar arteries which course over the superficial forearm flexors. It coexists with a normal brachial artery that continues as the common interosseous trunk. It is found to originate in the brachial or axillary arteries, with the former being more frequent. Anastomosis has been found between the normal brachial artery and the radial artery from SBURA [20]. The radial and ulnar recurrent arteries arise from the interosseous trunk [10].

Brachiointerosseous Artery (BIA)

The BIA (0.26%) is a high-origin interosseous artery coexisting with a brachial artery that branches into radial and ulnar arteries. Its origin has been reported to take place proximal to median nerve roots. It is very rare [21].

Superficial Brachiomedian Artery (SBMA)

The SBMA (0.5–1%) is a high-origin median artery that courses over the superficial flexor muscles. It coexists with a normal brachial artery with a normal branching pattern. It arises from either the axillary or brachial arteries. It joins the median nerve in the distal third of the forearm and enters the palm through the carpal tunnel as a normal median artery [10].

Superficial Radial Artery (SRA)

The SRA (0.74%) is a rare radial artery that has a normal radial artery origin but crosses over the tendons that define the anatomic snuffbox. Its superficial course can be adopted at any level, with the distal superficial course being most frequent [8]. It can give off an anomalous median artery that crosses with the median nerve in the carpal tunnel [10]. A clinically important variant of the SRA is the superficial dorsal antebrachial artery (see below).

Radial Artery Distal Takeoff

Distal takeoff was reported in a couple of reconstructive cases where the origin of the radial artery was found to be deep to pronator teres. In the event of raising a radial forearm flap, a radial artery with distal takeoff provides no proximal fasciocutaneous perforator, therefore making it impossible to raise a proximal skin paddle. Due to its deep positioning to the pronator teres, dissection of the radial artery becomes more challenging and requires division of the pronator teres [12, 22].

Superficial Dorsal Antebrachial Artery (SDAA)

The SDAA (3.8%) is a division of the radial artery at the distal fourth of the forearm. This aberrant artery courses laterally and superficial to the tendon of the dorsal long muscles of the thumb. After entering the first interspace, it gives a strong contribution to the thumb and continues on as the deep palmar arch [8, 12]. It is associated with either an absent or hypoplastic radial artery [23]. In the event of raising a radial forearm flap, the SDAA can result in a false positive Allen's test preoperatively. If it is not recognized intraoperatively, this poses a risk of thumb ischemia. Surgeons should palpate the entire forearm and cubital fossa for the presence of this superficial artery [12, 23, 24].

Radial Artery Agenesis

Radial artery agenesis (<0.03%) is extremely rare. In these cases, its territory is supplied by anterior interosseous artery or the median artery [13, 25].

Duplication of the Ulnar Artery

Real duplication includes the presence of an SBUA as discussed above. Partial duplication also occurs. In these cases, the SBUA reaches the palm as its usual course, but the normal ulnar artery sends out a recurrent ulnar artery and a common interosseous trunk. The normal ulnar artery ends as the rudimentary small muscular branches supplying the forearm flexors [10].

Ulnar Artery Agenesis

Ulnar artery agenesis is extremely rare (<0.015%) [10]. One case was reported where the territory normally supplied by the ulnar artery was instead supplied by the radial and interosseous arteries [26]. A few encounters of bilateral ulnar artery hypoplasia have been reported while raising forearm flaps [12, 27].

Median Artery

The median artery (1.5–50%) is a frequent anatomical variation of the upper limb as a persistent embryonic remnant. Two patterns of median artery exist: (1) a palmar pattern (20%), where the median artery is large, long, and reaches the palm and (2) an antebrachial pattern (76%), where the artery is slender, short, and terminates before the wrist. Both patterns have variable origins. The palmar pattern most frequently originates from the caudal angle between the ulnar artery and its common interosseous trunk (Fig. 19.2). The antebrachial pattern most often originates from anterior interosseous artery. The palmar pattern terminates at the first, second, or both common digital arteries, or joins the superficial palmar arch [8, 10, 28].

The median artery may cause carpal tunnel syndrome because it courses along with the median nerve as it passes under the flexor retinaculum [29]. Rarely, a thrombosed median artery can also cause carpal tunnel syndrome and recurrent digital ischemia [30, 31]. The median artery may also perforate the median nerve, which may be a cause of pronator teres syndrome [32–34]. In raising a radial flap, a persistent median artery is occasionally the dominant vessel supplying the radial territory while the radial artery is vestigial. In these cases, the median artery can be used as a medial artery forearm flap if handled properly and creatively [35, 36].

Radial Collateral Artery (RCA)

The RCA normally arises from the profunda brachii artery. Origin from the posterior humeral circumflex artery has been reported, and it is associated with bilateral agenesis of the profunda brachii artery (6.7%) [37, 38]. Because the RCA and its several septocutaneous perforators supply the vascular territory of the lateral arm flap, surgeons need to beware of this variation while dissecting the vessels for transfer [39].

Radial Recurrent Artery (RRA)

The RRA normally arises from the radial artery just distal to the brachial artery bifurcation. The RRA can sometimes arise from the high-origin radial artery or the brachial artery. In other cases, the RRA can arise from the ulnar artery. Because the RRA is sometimes used as the anastomotic vessel at the recipient site during a radial forearm flap reconstruction, surgeons need to beware of these variations [6, 40].

Posterior Interosseous Artery (PIA)

The PIA usually branches from the common interosseous artery (CIA), a branch from the ulnar artery in the proximal third of the forearm. It perforates the skin on the dorsal aspect of the forearm and anastomoses both proximally and distally with the anterior interosseous artery (AIA), another branch of the CIA. Because of its proximal and distal anastomosis with the AIA, PIA territory can be raised as a flap with ligation of the proximal end and supply from the recurrent flow from the AIA to cover hand defects. Surgeons should be aware of the occasional high origin of the PIA from the ulnar artery as well as trauma or anatomical variation that affects the presence or patency of the distal anastomosis. Should defects in the distal pedicle exist, the PIA flap can be raised as a free flap [41–43].

Arteries in the Hand

Normal Course

Superficial Palmar Arch (SPA)

The SPA is an anastomosis between the ulnar and radial arteries, fed mainly by the ulnar artery. The ulnar artery enters the palm with the ulnar nerve anterior to the flexor retinaculum and lateral to the pisiform. It forms a complete arch when it anastomoses with the superficial palmar branch of the radial artery (Fig. 19.3) [2].

Deep Palmar Arch (DPA)

The DPA is formed by the passage of the deep branch of the radial artery from dorsal to deep palmarly through the two heads of the first dorsal interosseous muscle before curving along the base of the metacarpal bones and anastomosing with one or both deep palmar branches of the ulnar artery (Fig. 19.4) [2, 44].

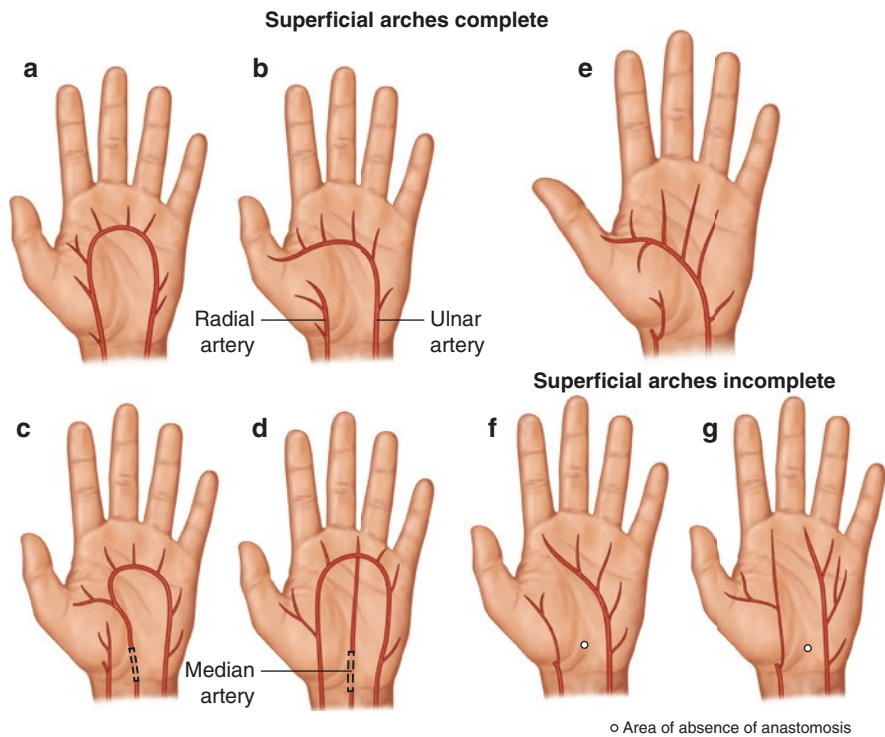


Fig. 19.3 Superficial palmar arch patterns: (a–e) complete superficial arches; (f–g) incomplete superficial arches [44]

Variations and Pathology

Superficial Palmar Arch (SPA)

The SPA is categorized by Coleman and Anson into a complete arch and incomplete arch [45]. They further subcategorized a complete SPA into five types according to arterial patterns of anastomosing vessels. They also subcategorized an incomplete SPA into two types [44, 45].

Complete SPA (See Fig. 19.3a–e)

The complete SPA (79%) is defined as an SPA with anastomosis between its contributing vessels [45]. It is further subcategorized into five subtypes (Table 19.1) [44–46].

Incomplete SPA (See Fig. 19.3f, g)

The incomplete SPA (17%) is defined as a superficial palmar arch without anastomosis between contributing vessels or an ulnar artery failing to reach the thumb–first dorsal web space. The incomplete SPA is subcategorized into four subtypes (Table 19.2).

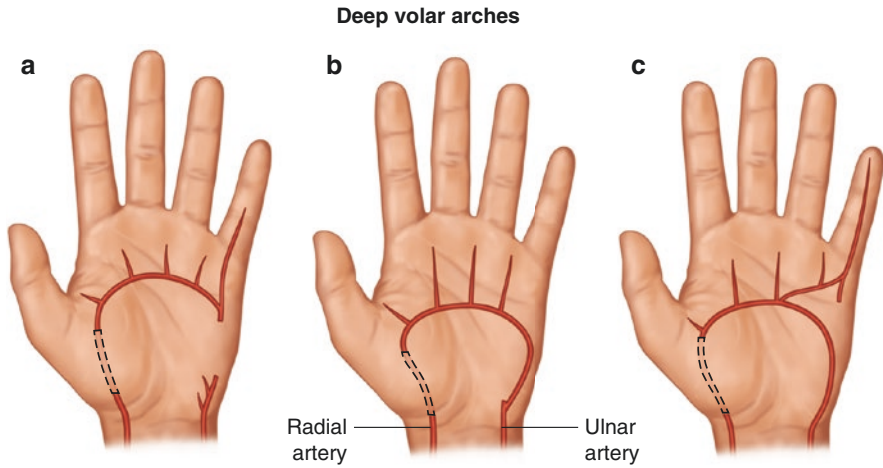


Fig. 19.4 Deep palmar arch patterns [44]

Table 19.1 Complete superficial palmar arch patterns

Complete SPA patterns	Anatomical courses
Type A (40%)	This is the “textbook” anastomosis that occurs between the superficial palmar branch of the radial artery and the continuation of the ulnar artery.
Type B (32%)	The SPA is formed completely by the ulnar artery with formation of the common digital vessels extending into the thumb-index web.
Type C (2.68%)	This SPA is formed by anastomosis between ulnar and median arteries without contribution from the radial artery.
Type D (0.81%)	This SPA is formed by anastomosis among the radial, median, and ulnar arteries.
Type E (1.22%)	This SPA is formed by anastomosis between a large-sized branch from the deep palmar arch and the ulnar artery.

Pathology

In the event of using an ulnar artery-based flap for orofacial reconstruction, surgeons need to beware of the anastomotic pattern of the SPA. In ulnar-only complete SPA (type B) and incomplete SPA types, ligation of the ulnar artery will cause whole or partial hand ischemia.

Deep Palmar Arch (DPA) (See Fig. 19.4a–c)

The DPA is always complete but can be divided into three categories depending on the pattern of the anastomosis (Table 19.3) [44].

Table 19.2 Incomplete superficial palmar arch patterns

Incomplete SPA patterns	Anatomical courses
Type A (3%):	This SPA is formed by the superficial palmar branch of the radial artery and the ulnar artery without anastomosis.
Type B (8.84%):	This SPA is formed solely by the ulnar artery without supply to the thumb or index finger.
Type C (2.7%):	This SPA is contributed by the superficial branch of the median artery and the ulnar artery without anastomosis.
Type D (0.08%):	This SPA is formed by the superficial vessels of the radial artery, the median artery, and the ulnar artery without anastomosis.

Table 19.3 Deep palmar arch patterns

DPA patterns	Anatomical courses
Type A (44.4%):	The anastomosis occurs between the deep palmar branch of the radial artery and the inferior deep branch of the ulnar artery.
Type B (33.4%):	The anastomosis occurs between the deep palmar branch of the radial artery and the superior deep branch of the ulnar artery.
Type C (20%):	The anastomosis occurs between both deep branches of the ulnar artery and the deep palmar branch of the radial artery.

Veins in the Arm, Forearm, and Hand

Normal Course

Deep Veins

In the forearm, venae comitantes run along with the radial and ulnar arteries and unite to form the paired brachial veins near the elbow. Distally, the radial veins receive the deep dorsal veins of the hand. The ulnar veins drain the deep palmar venous arch and connect with superficial veins near the wrist. The venae comitantes of the anterior and posterior interosseous arteries also contribute to the ulnar veins near the elbow. The ulnar vein is also connected via a large branch to the median cubital vein, a branch of the cephalic vein. Proximally, the brachial veins accompany the brachial artery as venae comitantes. They join to form the axillary vein near the lower border of the subscapularis. The medial branch often joins the basilic vein before it becomes the axillary vein.

Cephalic Vein (CV)

The CV usually forms over the anatomical snuffbox from the radial end of the dorsal venous plexus and receives veins from both aspects of the forearm. Distal to the

elbow, the median cubital vein from the CV reaches the basilic vein and is joined by a branch from the deep veins. The cephalic vein continues to ascend in front of the elbow superficial to a groove between the brachioradialis and biceps and ascends lateral to the biceps and between the pectoralis major and deltoid before emptying into the axillary vein [44].

Basilic Vein (BV)

The BV starts medially in the dorsal venous network of the hand, ascends postero-medially in the forearm, and is joined by the median cubital vein at the elbow. It continues to ascend superficial to and between the biceps and pronator teres and is crossed by filaments of the medial cutaneous nerve of the forearm. It then joins the brachial veins to form the axillary vein [2].

Median Vein (MV)

The MV of the forearm drains the superficial palmar venous plexus and ascends to join either the basilic or median cubital vein or divides distal to the elbow to join both veins [15].

Variations and Pathology

Variation in Superficial Veins

A high frequency of upper limb superficial venous variability occurs at the level of the cubital fossa. Regarding the interconnection between the basilic and cephalic veins, in the most frequent “textbook” arrangement (70%) the basilic and cephalic veins are connected by the median cubital vein (branch of the cephalic vein). The second most frequent arrangement (27.5%) is when the basilic and cephalic veins are joined by the median basilic and median cephalic veins, respectively, from a bifurcating ascending median vein which forms an M-pattern. The least common arrangement (3.3%) is when the basilic and cephalic veins are not cross-connected in the cubital fossa region (Fig. 19.5).

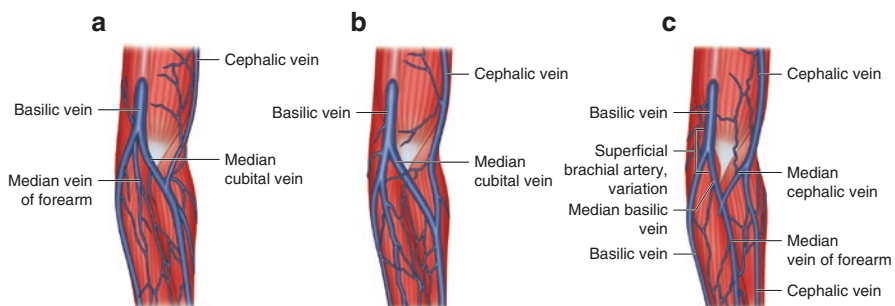


Fig. 19.5 Variations of the upper extremity venous patterns [2]

Agenesis of the cephalic vein is exceedingly rare, occurring in less than 1% of the population. An accessory cephalic vein occurs in about 15% of cadavers studied. It presents as a short vein that arises either in the dorsal forearm plexus or on the ulnar side of the dorsal venous network of the hand. It joins the cephalic vein distal to the cubital fossa.

The median vein most commonly (45%) empties into the median cubital vein from the cephalic vein, but in 35% of cases it empties directly into the basilic vein. Rarely (4.2%), there is an accessory median cubital vein that runs proximal and parallel to the median cubital vein [2, 47–49].

Pathology

The superficial veins are most frequently used for intravenous access and drug delivery, and are also used in microsurgery. Because of its large caliber, a cephalic vein is commonly used as a recipient vein for drainage of a flap. It can also be harvested distally and pedicled proximally to provide microvascular drainage in the chest or trunk. In patients with end-stage kidney disease, an arteriovenous fistula is often created for dialysis access. It is therefore important for surgeons to be aware of the venous variations in the upper extremities when creating these fistulas.

Arteries in the Lower Limbs

Femoral Artery (FA)

Normal Course

The FA begins at the level of inguinal ligament. It is the direct continuation of the external iliac artery, entering the thigh behind the inguinal ligament, midway between the anterior superior iliac spine and the pubic symphysis. It then branches off to form the profunda femoris artery. The FA continues as the superficial femoral artery (SFA) to descend along the anteromedial aspect of the thigh in the femoral triangle, entering and passing through the adductor hiatus, where it becomes the popliteal artery. The FA gives off the superficial circumflex iliac artery, the superficial epigastric artery, the superficial external pudendal artery, the deep external pudendal artery, the profunda femoris artery, and the descending genicular artery.

Variations and Pathology

The duplicated superficial femoral artery (DSFA) is a rare vascular anomaly that most commonly arises in the proximal or mid-segment of the SFA. The SFA bifurcates to form the DSFA, which then converges near the adductor hiatus to continue its normal course as a single SFA. No significant clinical symptoms have been observed in these patients, but knowledge of the DSFA is helpful for avoiding misinterpretation of vascular imaging and optimizing endovascular access [50].

The persistent sciatic artery (PSA) is a rare embryonic remnant of the lower limb. Its presence is associated with an incomplete or absent SFA. The PSA branches off the internal iliac artery and passes through the greater sciatic foramen. It then

courses along the adductor magnus and joins the popliteal artery at the popliteal fossa (Fig. 19.6). The PSA tends to be enlarged and tortuous in its course. Clinically, the PSA is prone to aneurysm formation, claudication, and ischemia from early atherosclerosis. It may, however, be used for revascularization in cases of a diseased FA [51, 52]. Cowie's sign, a combination of diminished or absent femoral pulse with a palpable popliteal pulse, is pathognomonic for a PSA.

Profunda Femoris Artery (PFA)

Normal Course

The PFA branches off laterally from the CFA about 3.5 cm below the inguinal ligament and descends behind the CFA toward the medial aspect of the femur. As it travels distally, the PFA passes between the pectineus and adductor longus, the adductor longus and adductor brevis, and eventually, the adductor longus and adductor magnus, before piercing the adductor magnus. It anastomoses with the upper muscular branches of the popliteal artery. Proximally, it gives off lateral and medial circumflex arteries, and distally, the perforating and muscular branches. There are generally four perforators from the PFA: the first three are branches which arise from the PFA proximal, anterior, and distal to adductor brevis, and perforate the adductor magnus along its femoral attachment to reach the flexor aspect of the thigh. The terminal PFA becomes the fourth perforator.

Variations and Pathology

Rajani et al. found that the PFA arises most commonly from the posterolateral and lateral aspects (71.21%) of the FA, whereas a posterior and posteromedial origin occurs in 24.24% of cases [53]. DeLong et al. and Haddock et al. found that almost all their patients (98.9–100%) had adequate PFA perforators with an average number of 3.3–5 perforators. These perforators were evenly distributed between medial (near the adductor magnus) and lateral (near the biceps femoris and vastus lateralis) halves of the thigh, 5.0 cm distal to the gluteal fold [54, 55].

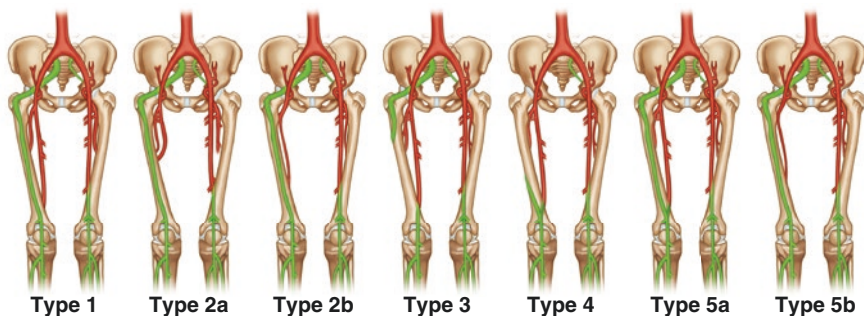


Fig. 19.6 Lower extremity variations: different patterns of persistent sciatic artery (green: PSA, red: SFA) [51]

The perforators are classified into septocutaneous (48.3–65%) and musculocutaneous (35–51.7%) perforators. The perforators occasionally (18.2–37.5%) branch off the common femoral trunk together with the PFA [55, 56]. These perforators serve as the vascular basis for the profunda artery perforator (PAP) flap. Surgeons are encouraged to use preoperative imaging modalities to optimally plan the perforator harvest.

Medial Femoral Circumflex Artery (MFCA)

Normal Course

The MFCA arises from the FA or the posteromedial aspect of the PFA. It curves medially around the femur between the pectineus and psoas major, followed by the obturator externus and adductor brevis. It divides into the transverse and ascending branches at the upper border of the adductor magnus. The transverse branch runs deep between the adductor longus and magnus and anastomoses with the inferior gluteal, the lateral circumflex, and the first perforating artery of the PFA. This anastomosis is known as the *cruciate anastomosis*. The ascending branch reaches the trochanteric fossa and anastomoses with the gluteal and the lateral circumflex of the FA [6].

Variations and Pathology

The MFCA most commonly arises from either the PFA (12–85.7%) or the FA (11–78%) [57]. In rare cases, it can arise from SFA (2.5–6.7%) or the LFCA (0.6–15%). The transverse branch has its origin from the MFCA (46–100%) or directly from the PFA (0–45%) [58–60]. Because the transverse branch and its cutaneous perforators form the dominant vascular supply to the gracilis flap, surgeons need to beware of these variations when planning operations.

Lateral Femoral Circumflex Artery (LFCA)

Normal Course

The LFCA branches off at the root of the PFA, courses laterally, and divides into the ascending, transverse, and descending branches. The ascending branch reaches the lateral aspect of the hip joint and anastomoses with the superior gluteal and deep circumflex iliac arteries supplying the greater trochanter. It also anastomoses with the MFCA to form a ring to supply the femoral neck and head. The transverse branch winds around the femur immediately distal to the greater trochanter and participates in the cruciate anastomosis. The descending branch, arising from either the FA or the PFA, descends along and supplies the anterior border of vastus lateralis. It terminates near the knee joint by branching into septocutaneous and musculocutaneous perforators. The descending branch and its septocutaneous perforators are the vascular basis for the anterolateral thigh (ALT) flap [61].

Variations and Pathology

The descending branch of the LFCA and its perforators are highly variable. A systemic review by Lakhiani et al. found that the descending branch can originate from the PFA (6.25–13%) and the FA (1–6%) [62]. The perforators may arise from the descending branch (57–100%), the transverse branch (4–35%), or the ascending branch (2.6–14.5%). The perforators exist as two types [61, 63]. The septocutaneous perforators (37.8%) course between the rectus femoris and vastus lateralis. The musculocutaneous perforators (81.9%) penetrate the vastus lateralis. In rare cases (5.4%), the perforators were absent. Of all the perforators, the septocutaneous perforators have been shown to range from 18.1% to 40.8%, whereas the musculocutaneous perforators usually dominate (60–80%). Because of the difficulty in dissecting musculocutaneous perforators, the agenesis of septocutaneous perforators limits the use of ALT flaps. In rare cases of descending perforator agenesis, the tensor fasciae lata supplied by the ascending branch or the anteromedial thigh flap can be harvested [64–66].

Descending Genicular Artery (DGA)

Normal Course

The DGA is a distal branch arising from the FA just proximal to the adductor hiatus. It travels distally in vastus medialis to the medial aspect of the knee. Distally, it anastomoses with the medial superior genicular artery. The DGA gives off a saphenous branch and muscular branches. The saphenous branch arises close to the DGA origin and travels to the medial knee alongside the saphenous nerve to supply the skin of the proximomedial leg. Distally, it anastomoses with the medial inferior genicular artery. The muscular branches supply the adductor magnus and vastus medialis. It also gives off articular branches that anastomose with the arteries around the knee joint. The DGA and its branches form the main pedicle of the medial femoral condyle flap commonly used for bony reconstruction [67].

Variations and Pathology

Three types of DGA branching patterns have been proposed by Dubois et al. [68]. In type I (20%), all three branches (articular, muscular, and saphenous) arise from the DGA. In type II (30%), one of the branches arises proximally from the FA. In type III (10%), all three branches arise separately from the FA (Fig. 19.7). Clinically, because the medial femoral condyle flap is usually harvested in combination with a cutaneous or muscular paddle, the variable branching may affect harvesting of the latter. A type I pattern does not affect flap dissection, whereas a type II pattern can affect the chimeric flap because branches to the skin or muscle paddle can arise at different points from the bony flap. A type III pattern also affects the chimeric flap because the pedicle would be too short [69].

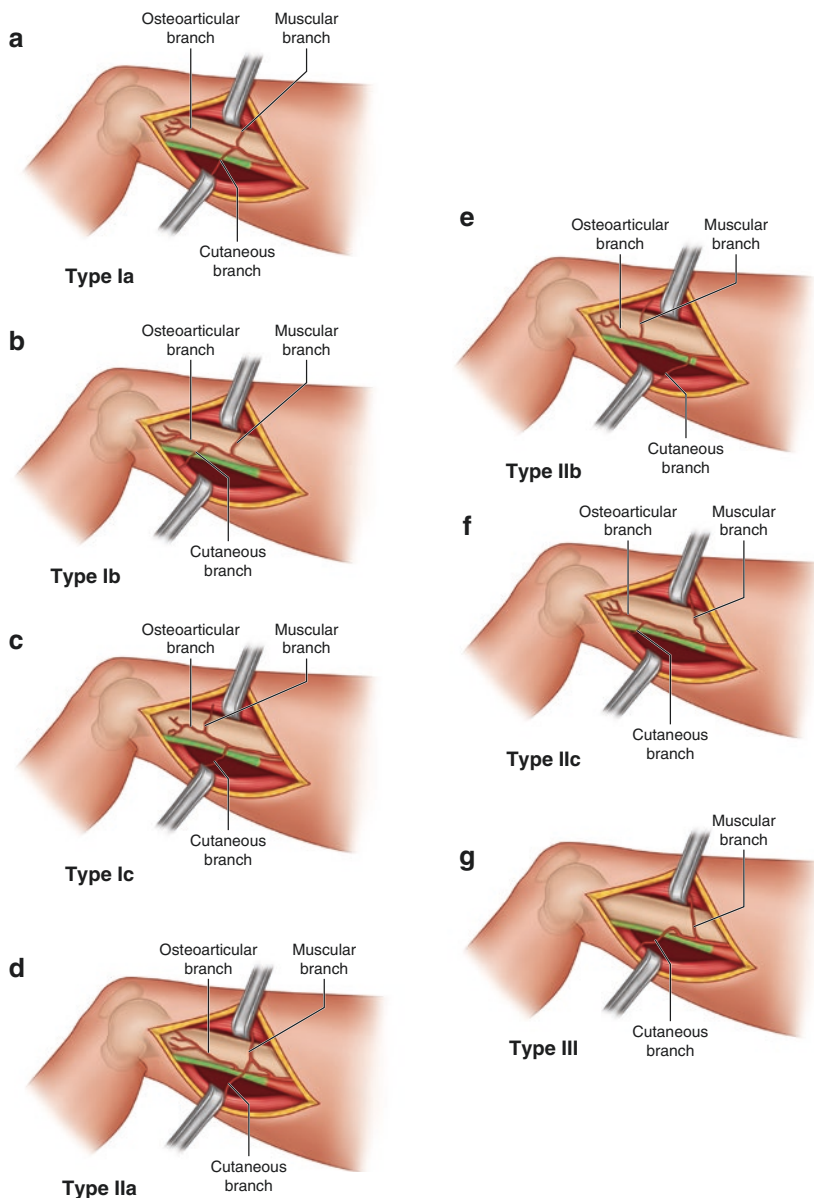


Fig. 19.7 Lower extremity variations: branching patterns of descending genicular artery: (T. Ziegler) **(a)** Dubois Ia: The DGA divides into three terminal branches (19%). **(b)** Dubois Ib: The MB occurs first and leaves behind a saphenoarticular trunk (14%). **(c)** Dubois Ic: The SB occurs first and leaves behind a musculoarticular trunk (30%). **(d)** Dubois IIa: The AB originates separately from the SFA, and the DGA divides only into the SB and MB (5%). **(e)** Dubois IIb: The SB originates separately from the SFA and the DGA divides only into the MB and AB (15%). **(f)** Dubois IIc: The MB originates separately from the SFA, and the DGA divides only into the AB and SB (15%). **(g)** Dubois III: The SB, AB, and MB arise separately from the SFA (2%) [69]

Popliteal Artery (PLA)

Normal Course

The PLA is the direct continuation of the femoral artery after it passes through the adductor hiatus. It courses through the popliteal fossa and branches into the anterior tibial artery (ATA) and the tibioperoneal trunk (TPT) at the level of lower border of the popliteus muscle. The TPT then further bifurcates into the posterior tibial artery (PTA) and the peroneal artery (PA). The PLA also gives out the sural artery, the medial superior genicular artery, the lateral superior genicular artery, the middle genicular artery, the lateral inferior genicular artery, the medial inferior genicular artery, and the muscular branches.

Anterior Tibial Artery (ATA)

Normal Course

The ATA is the continuation of the popliteal artery that begins at the lower border of the popliteus muscle posterior to the tibia. It passes between the tibia and fibula through an aperture above the upper border of the interosseous membrane, staying deep to the anterior compartment. It then descends along the anterior surface of the interosseous membrane, between the tibialis anterior and the extensor digitorum longus muscles. It ends by coursing anterior to the ankle joint in the inferior aspect of the leg and emerges superficially to become the dorsalis pedis.

Posterior Tibial Artery (PTA)

Normal Course

The PTA is the larger continuation of the popliteal artery that begins at the lower border of the popliteus muscle posterior to the tibia. It descends obliquely toward the tibial side behind the tibia on the deep muscle of the leg. In the lower part of its course, it lies midway between the medial malleolus and the medial process of the calcaneal tuberosity. It then divides into the medial and lateral plantar arteries. The PTA also gives out the peroneal artery proximally. The PTA gives off many perforators to the anteromedial and posterior aspects of the leg.

Peroneal Artery (PRA)

Normal Course

The PRA arises from the proximal posterior tibial (also known as the tibial-fibular trunk) 2.5 cm distal to the inferior border of the popliteus muscle. It then passes obliquely toward and descends along the medial aspect of the fibula in a fibrous canal between the tibialis posterior and the flexor hallucis longus. It anastomoses with branches of the dorsalis pedis of the foot. The PRA and its perforators provide the vascular basis for the fibular flap and the peroneal perforator flap, respectively.

Variations and Pathology

The PLA branching variations have been well studied. According to the Kim-Lippert's classification system [70, 71], three major types and a few subtypes of branching patterns exist (Fig. 19.8).

Type I is defined as PLA branching at the lower border of the popliteus muscle. The most common type (89.2%) is the "normal" branching pattern described above. Very rarely, the PLA trifurcates (1.5%) into the ATA, PTA, and PRA. Also, rarely, the PLA can first divide into the PTA and anterior TPT (0.4%), which then divides into the ATA and PRA. *Type II* is defined as the high division of the PLA at the level of or proximal to the knee joint. A high origin of the ATA, the PTA or the PRA is very rare (about 1%).

Type III is the most clinically relevant, defined as hypoplastic or aplastic branching with altered distal supply, including a hypoplastic or aplastic PTA (3.3%), ATA (1.5%), or both (peroneal arteria magna) (0.4%) [72]. When the type III variation occurs, the PRA usually partially or completely overtakes the blood supply to form the dorsalis pedis and plantar arch [2, 73]. In peroneal arteria magna, the PRA becomes the sole arterial supply to the foot. It is therefore a contraindication to a fibular free flap harvest, a procedure that devascularizes the PRA and relies on collateral perfusion from the PTA and ATA, which would lead to leg and foot ischemia [74, 75]. In other cases, peripheral vascular disease may also occlude an anatomically normal tibial artery, leading to an acquired peroneal arteria magna. Clinically, a modified Allen's test in the leg cannot reliably detect the dominant blood supply in the leg [76–78]. As a result, careful preoperative planning with

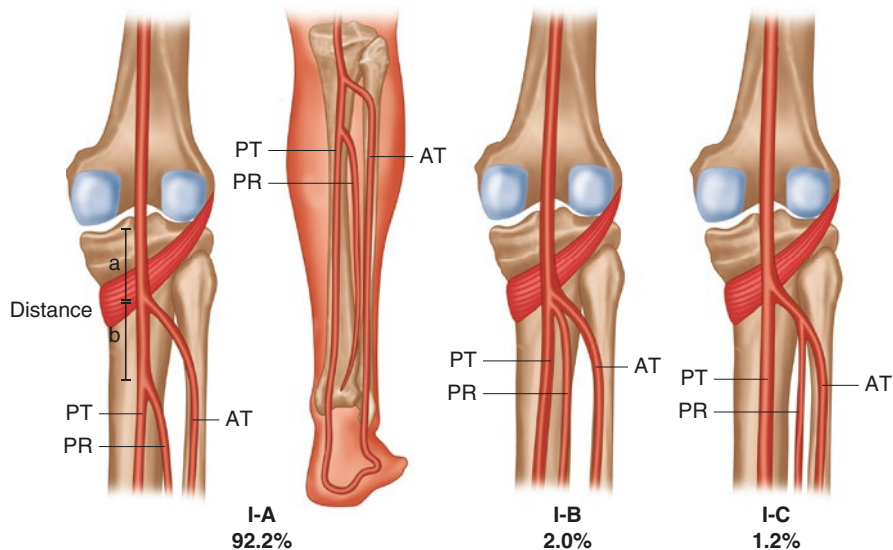


Fig. 19.8 Lower extremity variations. Branching patterns of popliteal-tibial-peroneal arteries: (a) normal branching pattern; (b) trifurcation; (c) posterior tibial artery branches first, and anterior tibial and peroneal arteries branch from a common trunk [70]

magnetic-resonance arteriography, angiography, or ankle-arm index screening is necessary for harvesting fibula free flap [79]. *Type IV* is exceedingly rare, defined as a hypoplastic (0.14%) or aplastic (0.07) PR.

Medial Plantar Artery (MPA)

Normal Course

The MPA is the smaller terminal branch of the PTA that passes along the medial side of the foot between abductor hallucis and flexor digitorum brevis. It ends by reaching the medial border of the hallux and anastomoses with a branch of the first plantar metatarsal artery. It gives off a deep branch to the plantar metatarsal arteries and a superficial branch to the medial aspect of the first toe at the level of the talonavicular joint. The MPA provides the vascular basis for the medial plantar flap and the deep branch to the abductor hallucis muscle flap [80–82].

Variations and Pathology

The MPA branches have substantial variability. Three branching patterns have been identified: the MPA divides into a predominant superficial branch and a small deep branch (54%); the MPA continues as a single large superficial vessel without a deep branch (38%); the MPA divides into a large deep branch to the big toe and a small superficial branch (8%) (Fig. 19.9) [82–84]. On raising the adductor hallucis flap, the main trunk of MPA will be interrupted without collateral perfusion to the medial plantar region in the latter two patterns. Surgeons need to be aware of these variations when raising flaps based on the MPA territory.

Lateral Plantar Artery (LPA)

Normal Course

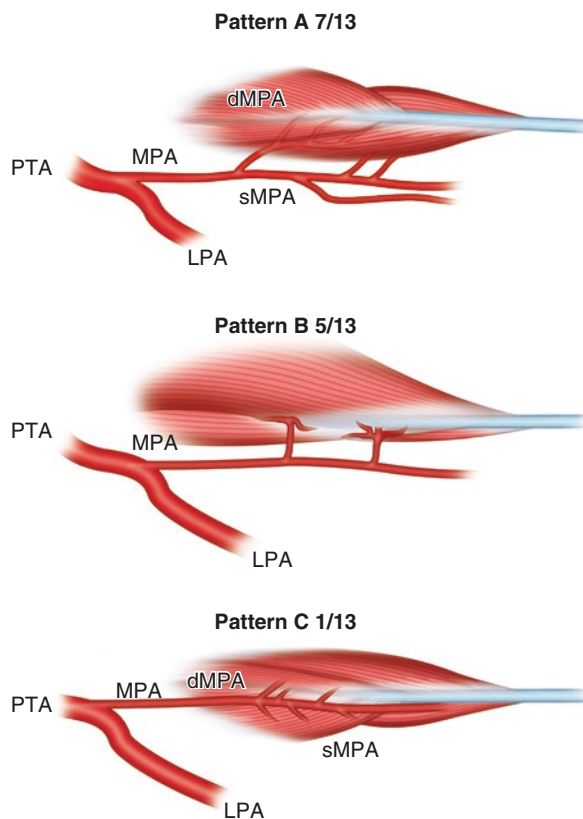
The LPA is the larger terminal branch of the PTA that passes distally and laterally to the fifth metatarsal base before turning medially and anastomosing with the dorsalis pedis between the first and second metatarsal bases to form the plantar arch. It then continues distally and ends at the fifth metatarsal base.

Dorsalis Pedi Artery (DPA)

Normal Course

The DPA is the continuation of the ATA. It starts at the anterior and medial one-third of the ankle joint. It courses toward the first intermetatarsal space superficial to the first dorsal interosseous muscle before turning toward the sole and contributing to the plantar arch. It gives off the lateral and medial tarsal arteries, the arcuate artery, the first dorsal metatarsal artery, and the cutaneous branches.

Fig. 19.9 Lower extremity variations: medial plantar artery [82]. PTA posterior tibial artery, LPA lateral plantar artery, MPA medial plantar artery, sMPA superficial medial plantar artery, dMPA deep medial plantar artery



Variations and Pathology

Depending on the PLA branching pattern (see above), the DPA can arise from the ATA or the PRA. The course of the DPA is also variable. Instead of coursing medially, the DPA, in rare cases (1.9–4%), deviates laterally from the midline before coursing toward the first intermetatarsal space. In other cases (6%), the arcuate branch is absent. Also, rarely (2%), in the absence of the ATA, the PRA courses laterally to form the lateral tarsal branch instead of the DPA. The dorsum of the foot is supplied by a large LPA [85].

Plantar Arch (PAA)

Normal Course

The PAA is a deeply situated anastomosis between the DPA and the LPA. It extends from the fifth metatarsal base laterally and curves toward the proximal end of the first interosseous space. It gives off three perforating branches, four plantar metatarsal branches, and a number of branches to supply the skin, the fasciae, and the muscles of the sole.

Variations and Pathology

The anastomosing arteries to the PAA vary depending on the branching pattern of the PLA (see above). In cases of tibial artery agenesis, the PAA is formed between the remaining tibial artery and the PRA. In cases of peroneal arteria magna, the PAA is formed solely by the PRA. The PRA divides proximally to send off the DPA and the MPA, which together form the PAA [72, 86]. Depending on the calibers of the terminal vessels supplying the PAA, there are the DPA-dominant type (48%), the LPA-dominant type (38%), and the balanced type (14%) [83, 87, 88]. Arterial bypass in ischemic foot disease and foot tissue transfer to the hand are common clinical procedures in which these anatomic variations of the PAA may affect the surgical plan.

First Dorsal Metatarsal Artery (FDMA)

Normal Course

The FDMA is a branch that arises from the DPA. It courses distally on top of the first dorsal interosseous muscle (FDIM) and sends out two dorsal digital arteries around the level of the metatarsophalangeal joint to supply the skin of the great and second toes. The FDMA then courses distally in the first intermetatarsal space and anastomoses with the first plantar metatarsal artery.

Variations and Pathology

The FDMA can originate from the DPA (85–90.6%), the plantar arch via the lateral plantar artery (9.4–10.88%), or both (10%). The courses are variable and classified according to Gilbert's system [89]. *Type I* (57%) is the normal course, defined as the FDMA running on the FDIM. *Type II* (32.9%) is defined as the FDMA passing under the tibial lateral head of the FDIM and emerging from the distal end of the first and second metatarsal bones. *Type III* (8.2%) is defined as agenesis of the FDMA. An intramuscular type (18.8%) is defined as the FDMA partially or completely embedded in the FDIM [90–92]. Clinically, the FDMA-based free tissue transfers, including the great toe transplant, are commonly performed procedures that can be affected by these variations.

Veins in the Lower Limbs

Femoral Vein (FV)

Normal Course

The FV is the direct continuation of the popliteal vein proximally at the adductor hiatus. It ascends posterolateral to the FA in the distal adductor canal, posteromedial to the FA behind the femoral triangle, and becomes the external iliac vein behind the inguinal ligament. The FV receives muscular tributaries, which are the profunda femoris vein, the long saphenous vein, and the lateral and medial circumflex femoral veins.

Popliteal Vein (PLV)

Normal Course

The PLV is formed by the union of the venae comitantes of the anterior and posterior tibial veins at the distal border of the popliteus muscle. It ascends through the popliteal fossa and passes through the adductor hiatus to become the femoral vein.

Variations and Pathology

The FV and PV are termed together the femoropopliteal vein (FPV). There are a few types of variations shown using ultrasonographic studies [93]:

- Agenesis (0.7%) of the FPV in the presence of a persistent sciatic vein.
- Partial duplication or multiplication with a complex network of the FPV (20–42%).
- Malpositioning medial to the popliteal artery (6.5%), anterior rotation (1%), and posterior rotation (0.4%).

Due to the FPV being a common site for deep venous thrombosis (DVT), it is important for ultrasonographers to acknowledge these common variations when assessing lower extremity DVT.

Persistent Sciatic Vein (PSV)

Normal Course

The PSV is a rare developmental remnant. It can exist as an isolated entity or in association with Klippel-Trenaunay syndrome (KTS). The PSV arises distally from the PLV or from the union of small tributaries in the upper thigh. It passes through the sciatic notch and ends in the internal iliac venous system, the deep femoral venous system, or an embryonic subcutaneous venous network. Clinically, patients with PSV have a high incidence (25%) of pulmonary embolism and a high incidence (28.6%) of severe anorectal bleeding. In rare cases, it has also been reported to attach to the popliteal sciatic nerve. Anesthetists should therefore be aware of this variation when performing popliteal sciatic nerve block [94–96].

Great Saphenous Vein (GSV)

Normal Course

The GSV is a continuation of the medial marginal vein of the foot distally and joins the FV proximally near the inguinal ligament. It ascends anterior to the medial malleolus, posteriorly toward the medial tibial and femoral condyles, and along the medial aspect of the thigh. It then passes through the saphenous hiatus in the middle of the fascia lata of the thigh and joins the FV inferolateral to the pubic tubercle. The GSV receives a large number of tributaries. In the leg, it receives the short

saphenous vein and deep veins. Just distal to the knee, it receives three large tributaries from the anterior leg, the medial malleolar region, and the calf. In the thigh, the GSV receives the large posteromedial vein, the anterolateral vein, and the peringuinal veins.

Variations and Pathology

The posterior accessory great saphenous vein (PAGSV, 27–70% of patients with varicose disease) is an anomalous vein that begins behind the medial malleolus, ascends parallel to the GSV, and joins the GSV just distal to the knee [97, 98].

Short Saphenous Vein (SSV)

Normal Course

The SSV, a continuation of the lateral marginal vein, begins posterior to the lateral malleolus and ascends laterally to the calcaneal tendon. It courses toward the midline of the calf, deep to the deep fascia before emerging from it proximally and terminating in the PLV. It receives the deep veins on the dorsal foot while sending communicating branches proximally and medially to join the GSV. The termination is variable.

Variations and Pathology

The course of the SSV varies. Occasionally, the SSV pierces the adductor magnus muscle during its ascending course and can be compressed by this muscle, forming varicosities [99]. The SSV has variable terminations classified according to the locations of the saphenopopliteal junction (Fig. 19.10):

- Low junction, defined as the junction occurring more than 2 cm below the popliteal skin crease.
- Typical junction, defined as the junction occurring less than 2 cm below or up to 7 cm above the crease.
- High junction, defined as the junction occurring higher than 7 cm above the crease.
- Very high junction, defined as the junction occurring 12 cm above the crease. In this case, the extension above 12 cm is termed the *Giacomini vein*, which is present in 15–90% of the cases.

The extension can terminate in the GSV or the deep sural muscular veins, or it can bifurcate (35–90%) with one branch joining the GSV and the other joining the PLV or deep posterior femoral veins [2, 100, 101]. Clinically, these anatomical variations may contribute to venous stasis of the leg and lead to varicosities. It may affect the planning of a coronary bypass with an SSV graft. It may also cause sural nerve entrapment in certain cases [95].

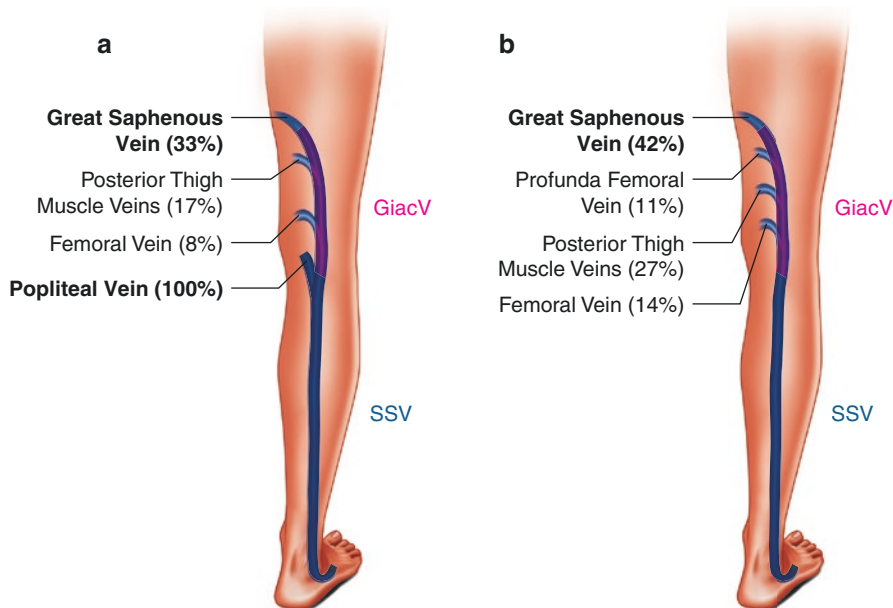


Fig. 19.10 Lower extremity variations: extension of short saphenous vein – Giacomini vein: (a) normal SSV-popliteal junction; (b) high SSV termination [100]

Posterior Tibial Veins (PTVs)

Normal Course

The PTVs accompany and follow the course of the PTA. They receive tributaries from the venous plexus in the soleus as well as connections from the superficial veins and the fibular veins.

Anterior Tibial Veins (ATVs)

Normal Course

The ATVs are the proximal continuations of the venae comitantes of the DPA. They unite with the PTVs to form the PLV at the distal border of popliteus.

Variations and Pathology

The tibial veins can have a proximal extension beyond the distal border of the popliteus before forming the PLV. In an ultrasonography study, 83% of the subjects were found to have an extension of the tibial vein by an average of 2.2 cm [93].

Peroneal Veins (PRVs)

Normal Course

The PRVs accompany and follow the course of the PRA and receive from the soleus and superficial veins.

Deep Plantar Venous Arch (DPVA)

Normal Course

The DPVA situates alongside the PAA, anastomoses with the dorsal digital veins, and receives tributaries from the plantar digital veins. It sends out the medial and lateral plantar veins running along the corresponding arteries. It communicates with the GSV and the SSV to form the PTV.

Dorsal Venous Arch (DVA)

Normal Course

The DVA situates on the dorsal aspect of the foot. It is formed by the union of the medial and lateral marginal veins. The DVA communicates with the GSV and SSV via the medial and lateral marginal veins. It also communicates with the dorsal and plantar digital veins via the dorsal metatarsal veins.

References

1. Moore KL, Agur AMR, Dalley AF. *Essential clinical anatomy*. 4th ed. Baltimore: Lippincott Williams & Wilkins; 2011. p. xxviii, 703.
2. Standring S, Gray H. *Gray's anatomy: the anatomical basis of clinical practice*. 40th ed. Edinburgh: Churchill Livingstone/Elsevier; 2008. p. xxiv, 1551.
3. Fuss FK, Matula CW, Tschabitscher M. The superficial brachial artery. *Anat Anz*. 1985;160(4):285–94.
4. Hazlett JW. The superficial ulnar artery with reference to accidental intra-arterial injection. *Can Med Assoc J*. 1949;61(3):289–93.
5. Karlsson S, Niechajev IA. Arterial anatomy of the upper extremity. *Acta Radiol Diagn (Stockh)*. 1982;23(2):115–21.
6. Wei F-C, Mardini S. *Flaps and reconstructive surgery*. Amsterdam: Elsevier; 2016. p. 636, online resource.
7. Mourtialon P, Tixier H, Loffroy R, Maillart JC, Calmelet P, Dellinger P, et al. Vascular complication after insertion of a subcutaneous contraceptive implant. *Acta Obstet Gynecol Scand*. 2008;87(11):1256–8.
8. McCormack LJ, Cauldwell EW, Anson BJ. Brachial and antebrachial arterial patterns; a study of 750 extremities. *Surg Gynecol Obstet*. 1953;96(1):43–54.
9. Chakravarthi KK, Siddaraju KS, Venumadhav N, Sharma A, Kumar N. Anatomical variations of brachial artery – its morphology, embryogenesis and clinical implications. *J Clin Diagn Res*. 2014;8(12):AC17–20.

10. Rodriguez-Niedenfuhr M, Vázquez T, Nearn L, Ferreira B, Parkin I, Sañudo JR. Variations of the arterial pattern in the upper limb revisited: a morphological and statistical study, with a review of the literature. *J Anat.* 2001;199(Pt 5):547–66.
11. Gupta R, Aggarwal A, Gupta T, Kaur H, Gaba S, Sahni D. Superficial upper limb vasculature and its surgical implications. *Indian J Plast Surg.* 2016;49(2):258–60.
12. Funk GF, Valentino J, McCulloch TM, Graham SM, Hoffman HT. Anomalies of forearm vascular anatomy encountered during elevation of the radial forearm flap. *Head Neck.* 1995;17(4):284–92.
13. Kadanoff D, Balkansky G. 2 cases with rare variations of arteries of the upper extremities. *Anat Anz.* 1966;118(4):289–96.
14. Calisir C, Baylam Geleri D, Celik L. Superficial brachioradial artery: multidetector-row computed tomography angiography findings in one case. *Diagn Interv Imaging.* 2015;96(4):401–3.
15. Diz JC, Ares X, Tarrazo AM, Alvarez J, Meañes ER. Bilateral superficial radial artery at the wrist. *Acta Anaesthesiol Scand.* 1998;42(8):1020.
16. Thoma A, Young JE. The superficial ulnar artery “trap” and the free forearm flap. *Ann Plast Surg.* 1992;28(4):370–2.
17. Fatah MF, Nancarrow JD, Murray DS. Raising the radial artery forearm flap: the superficial ulnar artery “trap”. *Br J Plast Surg.* 1985;38(3):394–5.
18. Devansh MS. Superficial ulnar artery flap. *Plast Reconstr Surg.* 1996;97(2):420–6.
19. Ramani CV, Kundagulwar GK, Prabha YS, Dushyanth J. Anomalous superficial ulnar artery based flap. *Indian J Plast Surg.* 2014;47(1):124–6.
20. Pabst R, Lippert H. Bilateral occurrence of a. brachialis superficialis, a. ulnaris superficialis and a. mediana. *Anat Anz.* 1968;123(2):223–6.
21. Nakatani T, Tanaka S, Mizukami S. Superficial brachial artery continuing as the common interosseous artery. *J Anat.* 1997;191(Pt 1):155–7.
22. Small JO, Millar R. The radial artery forearm flap: an anomaly of the radial artery. *Br J Plast Surg.* 1985;38(4):501–3.
23. Morris LG, Rowe NM, Delacure MD. Superficial dorsal artery of the forearm: case report and review of the literature. *Ann Plast Surg.* 2005;55(5):538–41.
24. Heden P, Gylbert L. Anomaly of the radial artery encountered during elevation of the radial forearm flap. *J Reconstr Microsurg.* 1990;6(2):139–41.
25. Poteat WL. Report of a rare human variation: absence of the radial artery. *Anat Rec.* 1986;214(1):89–95.
26. Nunoo-Mensah J. An unexpected complication after harvesting of the radial artery for coronary artery bypass grafting. *Ann Thorac Surg.* 1998;66(3):929–31.
27. Ro HS, Roh SG, Shin JY, Lee NH, Yang KM. Unusual anatomic variations associated with bilateral ulnar artery hypoplasia. *J Craniofac Surg.* 2016;27(3):749–50.
28. Rodríguez-Niedenfuhr M, Sañudo JR, Vázquez T, Nearn L, Logan B, Parkin I. Median artery revisited. *J Anat.* 1999;195(Pt 1):57–63.
29. Chalmers J. Unusual causes of peripheral nerve compression. *Hand.* 1978;10(2):168–75.
30. Beran SJ, Friedman RM, Kassir M. Recurrent digital ischemia due to thrombosis of the persistent median artery. *Plast Reconstr Surg.* 1997;99(4):1169–71.
31. Levy M, Pauker M. Carpal tunnel syndrome due to thrombosed persisting median artery. A case report. *Hand.* 1978;10(1):65–8.
32. Gainor BJ, Jeffries JT. Pronator syndrome associated with a persistent median artery. A case report. *J Bone Joint Surg Am.* 1987;69(2):303–4.
33. Proudman TW, Menz PJ. An anomaly of the median artery associated with the anterior interosseous nerve syndrome. *J Hand Surg Br.* 1992;17(5):507–9.
34. Jones NF, Ming NL. Persistent median artery as a cause of pronator syndrome. *J Hand Surg Am.* 1988;13(5):728–32.
35. Acarturk TO, Tuncer U, Aydogan LB, Dalay AC. Median artery arising from the radial artery: its significance during harvest of a radial forearm free flap. *J Plast Reconstr Aesthet Surg.* 2008;61(10):e5–8.
36. Davidson JS, Pichora DR. Median artery forearm flap. *Ann Plast Surg.* 2009;62(6):627–9.

37. Naveen K, Jyothsna P, Nayak SB, Mohandas RKG, Swamy RS, Deepthinath R, et al. Variant origin of an arterial trunk from axillary artery continuing as profunda brachii artery—a unique arterial variation in the axilla and its clinical implications. *Ethiop J Health Sci.* 2014;24(1):93–6.
38. Sun R, Ding Y, Sun C, Li X, Wang J, Li L, et al. Color Doppler sonographic and cadaveric study of the arterial vascularity of the lateral upper arm flap. *J Ultrasound Med.* 2016;35(4):767–74.
39. Katsaros J, Schusterman M, Beppu M, Banis JC Jr, Acland RD. The lateral upper arm flap: anatomy and clinical applications. *Ann Plast Surg.* 1984;12(6):489–500.
40. Hamahata A, Nakazawa H, Takeuchi M, Sakurai H. Usefulness of radial recurrent artery in transplant of radial forearm flap: an anatomical and clinical study. *J Reconstr Microsurg.* 2012;28(3):195–8.
41. Chen HC, Cheng MH, Schneeberger AG, Cheng TJ, Wei FC, Tang YB. Posterior interosseous flap and its variations for coverage of hand wounds. *J Trauma.* 1998;45(3):570–4.
42. Pauchot J, Lepage D, Leclerc G, Flamans B, Obert L, Tropet Y. Posterior interosseous free flap because of absence of posterior interosseous pedicle. A report of an individualised salvage procedure and of an exceptional anatomical variation. Review of the literature. *Ann Chir Plast Esthet.* 2010;55(1):56–60.
43. Zancolli EA, Angrigiani C. Posterior interosseous island forearm flap. *J Hand Surg Br.* 1988;13(2):130–5.
44. Gellman H, Botte MJ, Shankwiler J, Gelberman RH. Arterial patterns of the deep and superficial palmar arches. *Clin Orthop Relat Res.* 2001;383:41–6.
45. Coleman SS, Anson BJ. Arterial patterns in the hand based upon a study of 650 specimens. *Surg Gynecol Obstet.* 1961;113:409–24.
46. Joshi SB, Vatsalaswamy P, Bahetee BH. Variation in formation of superficial palmar arches with clinical implications. *J Clin Diagn Res.* 2014;8(4):AC06–9.
47. Charles CM. On the arrangement of the superficial veins of the cubital fossa in American white and American negro males. *Anat Rec.* 1932;54:9–14.
48. Okamoto K. A study of the superficial veins in the superior extremity of live Japanese. *Anat Rec.* 1922;23:323–31.
49. Vucinic N, Eric M, Macanovic M. Patterns of superficial veins of the middle upper extremity in Caucasian population. *J Vasc Access.* 2016;17(1):87–92.
50. Hapugoda S, Hsu CC-T, Kwan GNC, Watkins TW, Rophael JA. Duplication of the superficial femoral artery: comprehensive review of imaging literature and insight into embryology. *Acta Radiol Open.* 2016;5(7):2058460116659098.
51. van Hooft IM, Zeebregts CJ, van Sterkenburg SMM, de Vries WR, Reijnen MMPJ. The persistent sciatic artery. *Eur J Vasc Endovasc Surg.* 2009;37(5):585–91.
52. Tsilimparis N, Khare A, Riesenmann PJ, Reeves JG. Persistent left sciatic artery eliminated need for revascularization in a 13-year-old with pseudoaneurysm of the superficial femoral artery. *Vasc Endovasc Surg.* 2013;47(3):250–3.
53. Rajani SJ, Ravat MK, Rajani JK, Bhedi AN. Cadaveric study of profunda femoris artery with some unique variations. *J Clin Diagn Res.* 2015;9(5):AC01–3.
54. DeLong MR, Hughes DB, Bond JE, Thomas SM, Boll DT, Zenn MR. A detailed evaluation of the anatomical variations of the profunda artery perforator flap using computed tomographic angiograms. *Plast Reconstr Surg.* 2014;134(2):186e–92e.
55. Haddock NT, Greaney P, Otterburn D, Levine S, Allen RJ. Predicting perforator location on preoperative imaging for the profunda artery perforator flap. *Microsurgery.* 2012;32(7):507–11.
56. Ahmadzadeh R, Bergeron L, Tang M, Geddes CR, Morris SF. The posterior thigh perforator flap or profunda femoris artery perforator flap. *Plast Reconstr Surg.* 2007;119(1):194–200; discussion 201–2.
57. Al-Talalwah W. The medial circumflex femoral artery origin variability and its radiological and surgical intervention significance. *Springerplus.* 2015;4:149.

58. Macchi V, Vigato E, Porzionato A, Tiengo C, Stecco C, Parenti A, et al. The gracilis muscle and its use in clinical reconstruction: an anatomical, embryological, and radiological study. *Clin Anat*. 2008;21(7):696–704.
59. Coquerel-Beghin D, Milliez PY, Auquit-Auckbur I, Lemierre G, Duparc F. The gracilis musculocutaneous flap: vascular supply of the muscle and skin components. *Surg Radiol Anat*. 2006;28(6):588–95.
60. Giordano PA, Abbes M, Pequignot JP. Gracilis blood supply: anatomical and clinical re-evaluation. *Br J Plast Surg*. 1990;43(3):266–72.
61. Song YG, Chen GZ, Song YL. The free thigh flap: a new free flap concept based on the septocutaneous artery. *Br J Plast Surg*. 1984;37(2):149–59.
62. Lakhiani C, Lee MR, Saint-Cyr M. Vascular anatomy of the anterolateral thigh flap: a systematic review. *Plast Reconstr Surg*. 2012;130(6):1254–68.
63. Kimata Y, Uchiyama K, Ebihara S, Nakatsuka T, Harii K. Anatomic variations and technical problems of the anterolateral thigh flap: a report of 74 cases. *Plast Reconstr Surg*. 1998;102(5):1517–23.
64. Xu DC, Zhong SZ, Kong JM, Wang GY, Liu MZ, Luo LS, et al. Applied anatomy of the anterolateral femoral flap. *Plast Reconstr Surg*. 1988;82(2):305–10.
65. Zhou G, Qiao Q, Chen GY, Ling YC, Swift R. Clinical experience and surgical anatomy of 32 free anterolateral thigh flap transplantations. *Br J Plast Surg*. 1991;44(2):91–6.
66. Pribaz JJ, Orgill DP, Epstein MD, Sampson CE, Hergrueter CA. Anterolateral thigh free flap. *Ann Plast Surg*. 1995;34(6):585–92.
67. Bakri K, Shin AY, Moran SL. The vascularized medial femoral corticoperiosteal flap for reconstruction of bony defects within the upper and lower extremities. *Semin Plast Surg*. 2008;22(3):228–33.
68. Dubois G, Lopez R, Puwanarajah P, Noyelles L, Lauwers F. The corticoperiosteal medial femoral supracondylar flap: anatomical study for clinical evaluation in mandibular osteoradionecrosis. *Surg Radiol Anat*. 2010;32(10):971–7.
69. Garcia-Pumarino R, Franco JM. Anatomical variability of descending genicular artery. *Ann Plast Surg*. 2014;73(5):607–11.
70. Kim D, Orron DE, Skillman JJ. Surgical significance of popliteal arterial variants. A unified angiographic classification. *Ann Surg*. 1989;210(6):776–81.
71. Lippert H, Pabst R. Arterial variations in man: classification and frequency. München: J.F. Bergmann; 1985. p. 121.
72. Abou-Foul AK, Borumandi F. Anatomical variants of lower limb vasculature and implications for free fibula flap: systematic review and critical analysis. *Microsurgery*. 2016;36(2):165–72.
73. Zwass A, Abdelwahab IF. A case report of anomalous branching of the popliteal artery. *Angiology*. 1986;37(2):132–5.
74. Astarci P, Siciliano S, Verhelst R, Lacroix V, Noirhomme P, Rubay J, et al. Intra-operative acute leg ischaemia after free fibula flap harvest for mandible reconstruction. *Acta Chir Belg*. 2006;106(4):423–6.
75. Rosson GD, Singh NK. Devascularizing complications of free fibula harvest: peronea arteria magna. *J Reconstr Microsurg*. 2005;21(8):533–8.
76. Blackwell KE. Donor site evaluation for fibula free flap transfer. *Am J Otolaryngol*. 1998;19(2):89–95.
77. Carroll WR, Esclamado R. Preoperative vascular imaging for the fibular osteocutaneous flap. *Arch Otolaryngol Head Neck Surg*. 1996;122(7):708–12.
78. Sandhu GS, Rezaee RP, Wright K, Jesberger JA, Griswold MA, Gulani V. Time-resolved and bolus-chase MR angiography of the leg: branching pattern analysis and identification of septocutaneous perforators. *AJR Am J Roentgenol*. 2010;195(4):858–64.
79. Futran ND, Stack BC Jr, Zachariah AP. Ankle-arm index as a screening examination for fibula free tissue transfer. *Ann Otol Rhinol Laryngol*. 1999;108(8):777–80.
80. Harrison DH, Morgan BD. The instep island flap to resurface plantar defects. *Br J Plast Surg*. 1981;34(3):315–8.

81. Shanahan RE, Gingrass RP. Medial plantar sensory flap for coverage of heel defects. *Plast Reconstr Surg.* 1979;64(3):295–8.
82. Macchi V, Tiengo C, Porzionato A, Stecco C, Parenti A, Mazzoleni F, et al. Correlation between the course of the medial plantar artery and the morphology of the abductor hallucis muscle. *Clin Anat.* 2005;18(8):580–8.
83. Adachi B. *Arteriensystem der Japaner.* Kyoto: Verlag der Keiserlich-Japanischen Universität zu Kyoto; 1928.
84. Rodriguez-Vegas M. Medialis pedis flap in the reconstruction of palmar skin defects of the digits: clarifying the anatomy of the medial plantar artery. *Ann Plast Surg.* 2014;72(5):542–52.
85. Kim JW, Choi YJ, Lee HJ, Yi KH, Kim HJ, Hu KS. Anatomic study of the dorsalis pedis artery, first metatarsal artery, and second metatarsal bone for mandibular reconstruction. *J Oral Maxillofac Surg.* 2015;73(8):1627–36.
86. Lutz BS, Siemers F, Shen ZL, Machens HG, Wippermann B, Berger A. Free flap to the arteria peronea magna for lower limb salvage. *Plast Reconstr Surg.* 2000;105(2):684–7.
87. Kalicharan A, Rennie C, Pillay P, Haffajee MR. The anatomy of the plantar arterial arch. *Int J Morphol.* 2015;33(1):36–42.
88. Ozer MA, Govsa F, Bilge O. Anatomic study of the deep plantar arch. *Clin Anat.* 2005;18(6):434–42.
89. Gilbert A. Composite tissue transfers from the foot: anatomic basis and surgical technique. In: Daniller A, Strauch B, editors. *Symposium on microsurgery.* St. Louis: Mosby; 1976.
90. Gabrielli C, Olave E. Origins of the dorsal metatarsal arteries in humans. *Scand J Plast Reconstr Surg Hand Surg.* 2002;36(4):221–5.
91. Hou Z, Zou J, Wang Z, Zhong S. Anatomical classification of the first dorsal metatarsal artery and its clinical application. *Plast Reconstr Surg.* 2013;132(6):1028e–39e.
92. Lee JH, Dauber W. Anatomic study of the dorsalis pedis–first dorsal metatarsal artery. *Ann Plast Surg.* 1997;38(1):50–5.
93. Park EA, Chung JW, Lee W, Yin YH, Ha J, Kim SJ, et al. Three-dimensional evaluation of the anatomic variations of the femoral vein and popliteal vein in relation to the accompanying artery by using CT venography. *Korean J Radiol.* 2011;12(3):327–40.
94. Cherry KJ, Gloviczki P, Stanson AW. Persistent sciatic vein: diagnosis and treatment of a rare condition. *J Vasc Surg.* 1996;23(3):490–7.
95. Hamilton HE, Darke SG. Persistent sciatic vein - unusual cause of reflux from the popliteal fossa and sural nerve damage. *Eur J Vasc Endovasc Surg.* 1999;17(6):539–41.
96. Srisuwan T, Arworn S, Rerkasem K. Case series of isolated primary persistent sciatic vein. *Int J Low Extrem Wounds.* 2013;12(3):219–22.
97. Bhatt D. *Cardiovascular intervention: a companion to Braunwald's heart disease.* Philadelphia: Elsevier; 2015.
98. Yuce I, Oguzkurt L, Eren S, Levent A, Kantarci M, Yalcin A, et al. Assessment of posterior accessory great saphenous vein of the leg using ultrasonography: a preliminary study. *Surg Radiol Anat.* 2016;38(1):123–6.
99. Shetty P, D'Souza MR, Nayak SB. An unusual course and termination of Small saphenous vein: a case report. *J Clin Diagn Res.* 2016;10(3):AD01–2.
100. Delis KT, Knaggs AL, Khodabakhsh P. Prevalence, anatomic patterns, valvular competence, and clinical significance of the Giacomini vein. *J Vasc Surg.* 2004;40(6):1174–83.
101. Prakash, Kumari J, Nishanth Reddy N, Kalyani Rao P, Preethi Ramya T, Singh G. A review of literature along with a cadaveric study of the prevalence of the Giacomini vein (the thigh extension of the small saphenous vein) in the Indian population. *Romanian J Morphol Embryol.* 2008;49(4):537–9.

Part V

Vascular Access and Anesthesia



Vascular Access and Anesthesia for Patients with Cardiac Anatomic Anomalies

20

Nat Dumrongmongcolgul, Robert J. Searles,
Michael D. Casimir, and Qingbing Zhu

Introduction

Congenital heart disease (CHD) encompasses a range of both structural and conduction abnormalities. The annual incidence of CHD is about 1% of births per year in the United States (approximately 40,000) [1]. Of these roughly 40,000 cases, about 7000 are considered critical congenital heart conditions, such as coarctation of the aorta, large septal defects, Ebstein's anomaly, tetralogy of Fallot (TOF), patent ductus arteriosus (PDA), aortic stenosis, transposition of the great vessels (TGV), aortopulmonary shunts, Eisenmenger's anomaly, and rhythm disturbances such as Wolff-Parkinson-White (WPW) syndrome. The advents of earlier detection and advances in surgical procedures have made it possible for many of these patients to survive to adulthood; in fact, approximately 68% reach 18 years of age [2]. With such a growing population of adults with CHD, the need for anesthesia practitioners to manage this population is more pertinent than ever.

N. Dumrongmongcolgul

Department of Anesthesia, Guam Regional Medical City, Dededo, GU, USA

R. J. Searles

Department of Anesthesiology, Spartanburg Regional Medical Center, Spartanburg, SC, USA

M. D. Casimir

Department of Anesthesiology, NYU Winthrop Hospital, Mineola, NY, USA

Q. Zhu (✉)

Department of Anesthesiology, Yale University School of Medicine, New Haven, CT, USA

e-mail: qingbing.zhu@yale.edu

Pathophysiology

CHD usually consists of a specific cardiovascular anatomic abnormality, with different degrees of left and right heart flow shunt through the defect or the obstruction. If these abnormalities are not corrected, heart failure will be the final pathway, ending in death. Atrial septal defect (ASD), ventricular septal defect (VSD), and PDA can be simple defects between the left and right circulations. But they also can be shunts for anatomic obstructions, temporarily extending life by delaying heart failure and death. Cardiac surgeries are partial or final treatments to correct the obstructions and shunts. With the continual advancements in the management of patients with CHD, it is becoming more common to see adults with previously corrected or optimized conditions presenting for noncardiac surgery. Understanding the pathophysiology of each CHD and the manifestations produced by both pre- and postcorrective surgeries are fundamental for the provision of safe and effective anesthetic care for this patient population.

Cardiac Shunt

Under normal circumstances, blood flow through the heart can be described as unidirectional, with two contiguous circuits: through the right heart to the pulmonary circuit and through the left heart to the systemic circuit. A shunt occurs when the blood returning from one circuit bypasses the other circuit and recirculates through the same circuit. The normal venous blood returns from the systemic circulation into the inferior and the superior vena cavae, which bring the deoxygenated blood into the right atrium (RA). The blood then passes the tricuspid valve (TV) into the right ventricle (RV), from which it goes through the pulmonary valve (PV) into the pulmonary circulation. In the pulmonary circuit, the lungs oxygenate the blood. It then returns to the left atrium (LA) via pulmonary veins and passes through the mitral valve (MV) into the left ventricle (LV). From the left ventricle, the oxygenated blood travels out to the aorta via the aortic valve (AV) and goes into the systemic circulation.

Under normal conditions, the right-sided deoxygenated blood is separated from the left-sided oxygenated blood by intra-atrial and intraventricular septa. If there is an aberrant connection between the right and left heart, then a shunt exists. In any septal defect, the chamber with the higher pressure determines the direction of blood flow through the septal defect.

Shunts are also described as *physiologic* or *anatomic*. Physiologic shunts are present when the blood is recirculated within the same system and never passes to the other system, as seen in TGV. Anatomic shunts exist when there is a communication between the two systems. When examining a shunt, one needs to discuss total blood flow and effective blood flow. Effective blood flow is the volume of blood that is transferred from one circuit to the other. Total blood flow is equal to the sum of the effective blood flow and the amount of recirculated or shunted blood. Many congenital defects dictate that we minimize the volume of shunted blood in order to

improve systemic oxygen saturation and blood flow, but others like TGV demand increased shunting in order to maintain systemic oxygen saturation that is compatible with life. Aortic saturation, a way to measure the effect of the shunt on systemic oxygen saturation, can be calculated by the following formula:

$$\text{Systemic oxygen saturation} = \frac{\left[\begin{array}{l} (\text{Systemic venous saturation} \times \text{Recirculated blood flow}) + \\ (\text{Pulmonary venous saturation} \times \text{Effective blood flow}) \end{array} \right]}{\div \text{Total systemic blood flow}}$$

Quantification of Shunts

Quantification of a shunt can be calculated by this equation, comparing pulmonary flow (Qp) and systemic flow (Qs):

$$Qp / Qs = (\text{SatAO} - \text{SatMX}) / (\text{SatPV} - \text{SatPA})$$

where, SatAO—aortic blood oxygen saturation; SatMX—systemic mixed venous blood oxygen saturation; SatPV—pulmonary vein blood oxygen saturation; SatPA—pulmonary artery blood oxygen saturation.

Typically, the systemic and the pulmonary blood flow are equal, so the equation is equal to 1, but when blood flow is greater in the pulmonary circuit (as in a left-to-right shunt) the result is greater than 1. A left-to-right shunt can be approximately quantified as *small* if the equation equals 1.5 or less, *moderate* if it is greater than 1.5–2.0, and *large* if it equals to or more than 2.0.

Shunts can be further divided into *simple* and *complex* forms. Simple shunts are determined by the size of the defect between the two circulations. Complex shunts are not only determined by the defect size but also depend on cardiac anatomic obstructions. For a simple shunt, the larger the defect, the more the shunt is affected by the balance between systemic vascular resistance and pulmonary vascular resistance. Also, the larger the orifice or the pressure gradient is, the greater is the influence that pharmacologic and mechanical intervention will have on the direction and amount of shunted blood. Thus, the balance between pulmonary vascular resistance and systemic vascular resistance allows the provider to direct the amount of blood passing through the shunt [3].

Examples of primary left-to-right shunts are ASD, VSD, and PDA. These defects cause an increase in pulmonary artery pressure secondary to chronic right-heart volume overload, and they lead to chronically increased pulmonary vascular resistance. Elevated right-heart and pulmonary vascular pressures eventually lead to pulmonary hypertension and right-heart hypertrophy. Subsequent to these, there can be a reversal of flow through the defect, which creates a right-to-left shunt that causes the deoxygenated blood to bypass the pulmonary circuit and go into the systemic circuit, resulting in cyanosis of the patient. This end stage of an initial left-to-right shunt is known as Eisenmenger's syndrome.

Table 20.1 Conditions changing pulmonary vascular resistance (PVR)

PVR increased by	PVR decreased by
Hypoxia	Good oxygenation
Hypercapnia	Hypocapnia
Acidosis	Alkalosis
High peak airway pressure	Anemia
Polycythemia	Vasodilators
Vasoconstrictors	Fentanyl
Hypothermia	Nitric oxide
Insufficient anesthesia	Milrinone
Partial paralysis	Prostacyclin
Atelectasis	

Examples of primary right-to-left shunts (cyanotic congenital heart defects) are TOF, hypoplastic left heart syndrome (HLHS), pulmonary valve atresia, and tricuspid valve atresia [3, 4].

Other Mechanical and Dynamic Obstruction

Congenital anatomic abnormalities may cause mechanical and dynamic obstruction. Mechanical subvalvular, valvular, supravalvular, or great vessel obstruction can cause the failure of the left, right, or both ventricles. Dynamic obstruction may be seen in TOF, severe septal deviation secondary to failure of one ventricle, or idiopathic hypertrophic subaortic stenosis (IHSS). Increased heart rate, decreased preload, decreased systemic vascular resistance (SVR), and increased ventricular contractility may enhance dynamic obstruction.

Changes in pulmonary vascular resistance (PVR) can be the result of a number of conditions or medications, as listed in Table 20.1.

If PVR is too high, it may further worsen the mechanical obstruction such as pulmonary valve stenosis, or it may further worsen the dynamic obstruction such as severe septal deviation secondary to failure of the right ventricle.

Anesthetic Perioperative Management

The preoperative evaluation of patients with CHD or patients with previous operations for CHD should involve a multidisciplinary team that includes anesthesiologists, cardiologists, and surgeons. The risk is increased in those with poor functional class, pulmonary hypertension, congestive heart failure, and cyanosis.

Prior to any surgical intervention, one should understand the specific CHD, its location, its severity, and the patient's history of cardiac surgery or residual defects. A thorough cardiac assessment of the defect, the direction of flow in the defect, the pressures in each chamber and in the great vessels, and of overall cardiac function should be conducted prior to any intervention.

History

History taking should focus on the cardiac lesion, alterations in physiology, functional capacity, previous surgery, any residual defects, and other congenital anomalies. Poor functional capacity may manifest as poor weight gain, dyspnea on feeding, or delay of growth. Medications should be reviewed in detail, including antiplatelet agents, anticoagulants, ACE inhibitors, and diuretics.

Physical Examination

Physical examination also provides valuable information. Patients with severe right-to-left shunt may exhibit signs of heart failure such as hypoxia, tachypnea, edema, or hepatosplenomegaly [5]. One should also assess the pulse and the blood pressure in all four extremities for any irregularities. Left upper-extremity blood pressure may differ from lower-extremity pressure in certain situations such as coarctation of the aorta, and previous interventions may make arterial and venous access more difficult or even unattainable.

Laboratory Tests and Imaging

Complete blood count and coagulation studies should always be requested. Polycythemia secondary to chronic hypoxia can lead to hyperviscosity syndrome [6]. For patients on diuretic therapy, electrolytes should be checked. Chest radiography is useful for the evaluation of pulmonary vasculature. Echocardiography provides information about anatomy, function, and direction of flow. Cardiac catheterization provides information regarding pressure, shunt, and anatomy. Cardiac MRI has many advantages, such as the creation of a digital image of the heart and major vessels. It can demonstrate functional information, shunts, and defects.

Monitoring

As with providing anesthesia for any surgery, before selecting the most appropriate technique for anesthesia and monitoring, all the patient's coexisting conditions must be comprehensively reviewed. Well-planned vascular access and hemodynamic monitoring are essential when preparing for surgical intervention in a patient with a history of CHD. In order to influence hemodynamic variables and oxygenation during the procedure, special access and monitoring must be achieved, and in some cases (as in TGV), these must be done bilaterally. The use of two oxygen probes should be applied to ensure accuracy during critical times of the procedure.

With standard noninvasive monitoring, the ECG should be reviewed frequently; prolonged PR interval and right bundle branch block are common findings in this

patient group. Additionally, transesophageal echocardiography (TEE) should be used to monitor the direction and magnitude of the shunt on color flow mode; agitated saline also may be used to demonstrate the jet. Further, TEE can be used to verify closure of the defect and assess cardiac function throughout the surgical case.

Vascular Access

Vascular access should include one or two large-bore peripheral intravenous (LBPIV) lines, double- or triple-lumen central venous pressure (CVP) lines, and arterial catheterization (A-line) [7]. An infrared vein finder and ultrasound may help with the insertion of a peripheral IV line in a patient with difficult venous insertion (Figs. 20.1, 20.2, and 20.3). Ultrasound always helps to identify the insertion of the CVP line or pulmonary artery catheter (PAC). Special care must be taken to ensure that air bubbles are removed from IV tubing and stopcocks to reduce the risk of air embolism and stroke. This risk is greater in a patient with the right-to-left shunt, but a patient with the left-to-right shunt may have shunt reversal during certain phases of the cardiac cycle, surgical manipulation, or coughing (in an awake patient). Meticulous de-airing of lines is recommended. Air filters should be applied to all IV lines. For newborn infants, umbilical arterial and venous catheters can be used for

Fig. 20.1 Ultrasound is used to guide needle insertion into the right internal jugular vein (RIJ)



Fig. 20.2 Ultrasound identifies guidewire in the RIJ with the probe head parallel to the vein

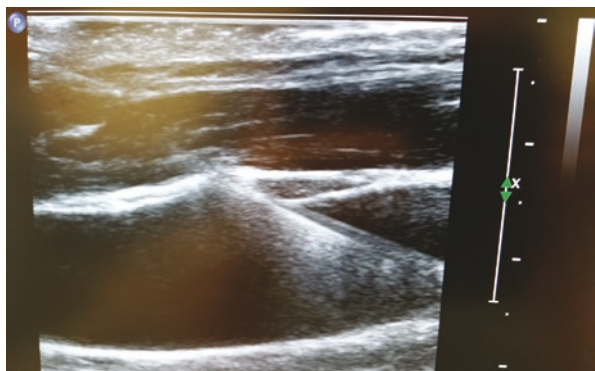
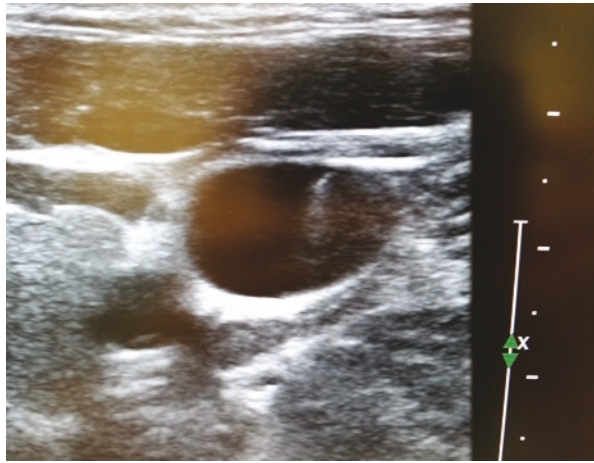


Fig. 20.3 Ultrasound identifies guidewire in the RIJ with the probe head perpendicular to the vein and internal carotid artery



intraoperative and postoperative monitoring. It is necessary to have blood prepared for transfusion, and an infusion fluid warmer should be available.

Intraoperative Considerations

Inhalational induction has a very minimal effect on a patient with left-to-right shunt. The patient can still have decreased gas exchange due to pulmonary congestion. Halothane depresses cardiac contractility more than isoflurane and sevoflurane [8]. At concentrations less than 1.5 MAC, isoflurane and sevoflurane do not alter the ratio of pulmonary to systemic blood flow [9]. Because of these benefits and less irritation, sevoflurane has become a popular choice for induction. Nitrous oxide should be avoided for maintenance, owing to the expansion of microbubbles. Nitrous oxide increases PVR in adults but does not appear to affect infants [10]. The right-to-left shunt will prolong inhalation induction significantly, because the shunting pulmonary blood dilutes the anesthetic agent in the systemic blood [11].

Intravenous induction is prolonged in a patient with left-to-right shunting because the recirculation of blood in the lungs results in a reduced concentration of drugs in the brain tissue. Right-to-left shunt, on the other hand, increases the speed of intravenous induction, as the blood bypasses the lungs and goes directly to the systemic circulation without pulmonary uptake.

Propofol has been used in patients with CHD in many settings. It decreases SVR, resulting in decreased blood pressure. The net result is an increase in right-to-left shunt, which may lead to oxygen desaturation, as well as shunt reversal. It does not affect PVR or mean pulmonary artery pressure [12].

Ketamine has sympathomimetic effects that cause increased heart rate, blood pressure, SVR, pulmonary blood flow, and cardiac output. These effects make ketamine a popular choice for induction. Adverse effects include emergence reactions, vomiting, and increased intracranial pressure [13, 14].

Opioids serve an important role in balanced anesthesia. Opioids blunt stress responses from airway manipulation and provide excellent hemodynamic stability with minimal change in heart rate and blood pressure. Fentanyl decreases PVR.

Subacute Endocarditis Prophylaxis

Antibiotic prophylaxis is recommended for patients undergoing dental procedures who have the following conditions: prosthetic cardiac valve, previous endocarditis, unrepaired cyanotic CHD (including those with palliative shunts and conduits), complete repair of CHD with prosthetic material or device (during the first 6 months after the procedure), repaired CHD with a residual defect, and cardiac transplantation recipients. Antibiotic prophylaxis is no longer recommended for patients undergoing genitourinary procedures [15]. Table 20.2 lists the recommended antibiotics for subacute endocarditis prophylaxis. The recommended regimen is a single dose of 30–60 minutes before the procedure begins.

Noncardiac Surgery in Patients with CHD

The mortality of children with CHD undergoing major surgery is 16%, compared with 3% for minor surgery [16]. Heart failure, pulmonary hypertension, cardiac arrhythmias, and cyanosis put the patient at higher risk. The risk for intraoperative cardiac arrest can be up to 10% in a patient with heart failure symptoms [17].

Table 20.2 Antibiotic recommendations for subacute endocarditis prophylaxis

Situation	Agent	Regimen (single dose 30–60 min before procedure)	
		Adults	Children
Oral	Amoxicillin	2 g	50 mg/kg
Unable to take oral medication	Ampicillin <i>or</i>	2 g IM or IV	50 mg/kg IM or IV
	Cefazolin or ceftriaxone	1 g IM or IV	50 mg/kg IM or IV
Allergic to penicillins or ampicillin—oral	Cephalexin ^{a, b} <i>or</i>	2 g	50 mg/kg
	Clindamycin <i>or</i>	600 mg	20 mg/kg
	Azithromycin or clarithromycin	500 mg	15 mg/kg
Allergic to penicillins or ampicillin and unable to take oral medication	Cefazolin or ceftriaxone ^b	1 g IM or IV	50 mg/kg IM or IV
	<i>or</i> clindamycin	600 mg IM or IV	20 mg/kg IM or IV

From Wilson et al. [15]; with permission
IM intramuscular, *IV* intravenous

^aOr other first- or second-generation oral cephalosporin in equivalent adult or pediatric dosage

^bCephalosporins should not be used in an individual with a history of anaphylaxis, angioedema, or urticaria with penicillins or ampicillin

Heart failure can be caused by volume overload, which can occur with residual shunts or incompetent valves, or by pressure overload, which is due to outflow tract obstruction.

The presence of pulmonary hypertension (PHT) is a clear predictor of perioperative morbidity. Patients with PHT have reduced pulmonary vascular compliance, so respiratory tract infections are poorly tolerated. Chronic cyanosis leads to polycythemia. Dehydration should be avoided because of an increased risk of hyperviscosity syndrome and cerebral vein thrombosis [17].

Regional Anesthesia for Noncardiac Surgery

Regional anesthesia can be safely used for patients with CHD. Spinal anesthesia is increasingly used as an anesthetic method for infants undergoing procedures below the T10 dermatome. The hemodynamic changes in infants with CHD undergoing spinal anesthesia are not different from the changes in healthy infants [18]. Spinal anesthesia with 1 mg/kg of bupivacaine or tetracaine can be used safely for hernia repair in infants with CHD [19].

Eisenmenger's syndrome is very challenging for anesthesia. The key is to maintain a balance between SVR and PVR. General anesthesia has been recommended for these patients over regional anesthesia because relative sympathectomy during regional anesthesia may decrease SVR and do not promote left-to-right shunting. Slow titration of epidural anesthesia is necessary to avoid abrupt sympathectomy. Patients may require vasopressors to help in maintaining SVR during the procedure. Nevertheless, mortality is more a result of disease and the surgical procedure, rather than of the type of anesthesia [20].

Anesthesia Management and Vascular Access for Specific Congenital Conditions

Ventricular Septal Defect (VSD)

Ventricular septal defect (Fig. 20.4), the most common type of CHD, is classified into four types: perimembranous (the most frequent), inlet, trabecular, and infundibular. Shunting depends on the PVR/SVR and the diameter of the defect. Complications may include RV failure, heart block, or persistent left-to-right shunt.

Vascular access: Large-bore peripheral IV (LBPIV), central venous pressure (CVP) line, an arterial line (A-line), transesophageal echocardiography (TEE).

Atrial Septal Defect (ASD)

Atrial septal defect (Fig. 20.5) is seen more often in females than in males. It can be divided into three types: secundum defect (the most common type), which includes

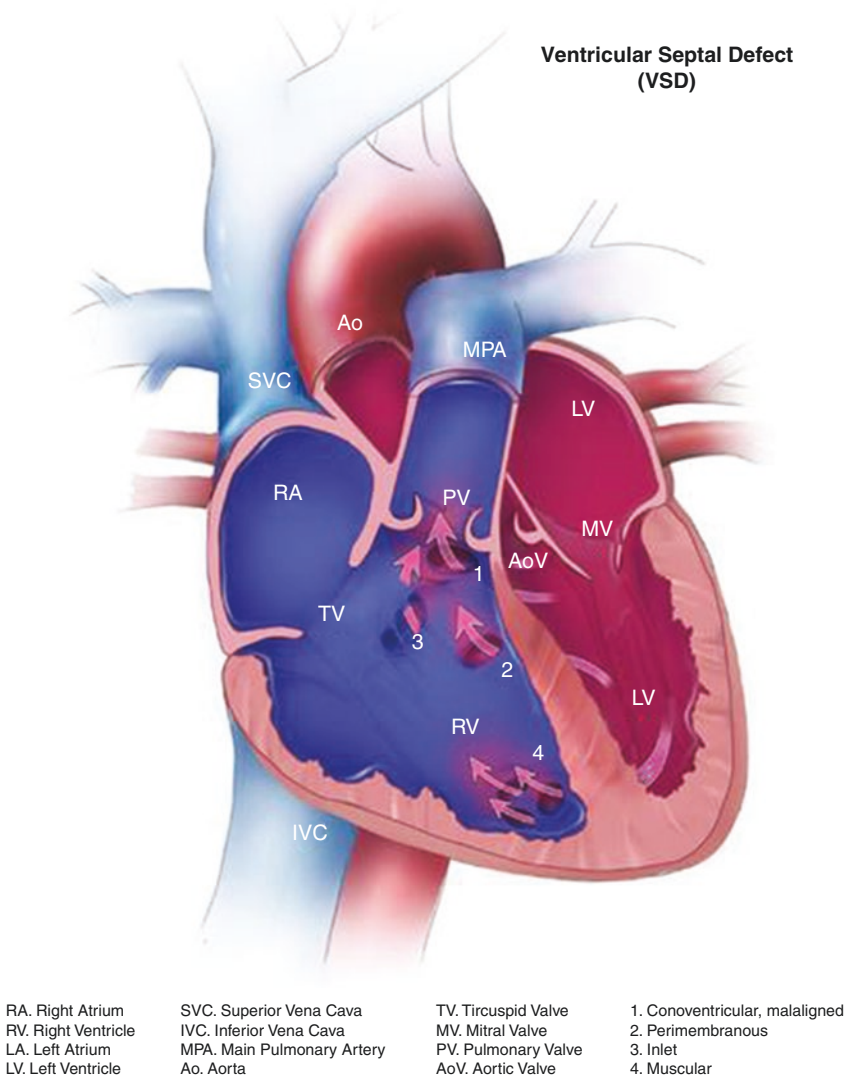


Fig. 20.4 Ventricular septal defect (VSD). (Courtesy of the Centers for Disease Control and Prevention and the National Center on Birth Defects and Developmental Disabilities. <https://www.cdc.gov/ncbddd/heartdefects/ventricularseptaldefect.html>)

patent foramen ovale (PFO); primum defect; and venosus defect. Congestive heart failure, pulmonary hypertension, and atrial arrhythmia may show up in late adult life, if ASD does not close spontaneously and its diameter is greater than 8 mm. Shunt direction depends on the ratio of PVR/SVR. The risk of paradoxical embolization and the cerebrovascular accident should be considered. Subacute

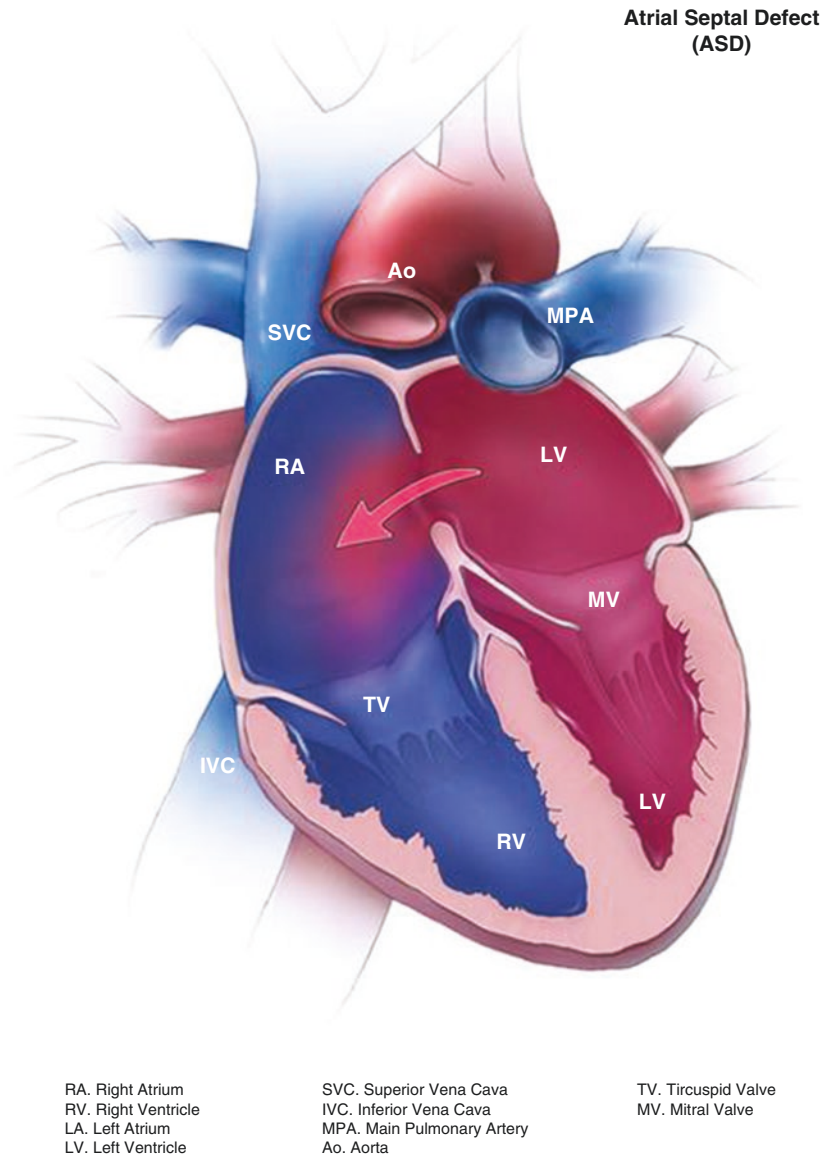


Fig. 20.5 Atrial septal defect (ASD). (Courtesy of the Centers for Disease Control and Prevention and the National Center on Birth Defects and Developmental Disabilities. <https://www.cdc.gov/ncbddd/heartdefects/atrialseptaldefect.html>)

bacterial endocarditis (SBE) prophylaxis is not necessary for a simple ASD, but it should be used for ASD with mitral valve prolapse (MVP) or mitral regurgitation. Complications may include atrial dysrhythmias, heart block, and valve regurgitation.

Vascular access: LBPIV, CVP, A-line, TEE.

Atrioventricular Septal Defect (AVSD)

Atrioventricular septal defect (Fig. 20.6), also called *atrioventricular canal* defect, is an inferior primum ASD, an inlet VSD, and the defect of the atrioventricular valves. It is commonly seen in Down syndrome, TOF, transposition of the great vessels (TGV), and asplenic patients. Blood flows between all four chambers, depending on the PVR/SVR and the pressure of the chambers. Air bubbles in IV lines should be avoided. Complications include right ventricular failure, worsening of mitral regurgitation (MR) and tricuspid regurgitation (TR), and atrioventricular conduction abnormality.

Vascular access: LBPIV, CVP, A-line, TEE.

Patent Ductus Arteriosus (PDA)

Patent ductus arteriosus (Fig. 20.7) typically arises from the aorta distal to the left subclavian artery and connects to the pulmonary artery. PDA usually closes within 12 hours after birth and forms the ligamentum arteriosus by 3 weeks. Persistent shunting of a PDA is more often seen in females. The direction and amount of the PDA flow depend on the PVR/SVR. PDA may cause pulmonary hypertension, endocarditis, paradoxical emboli, cyanosis, and heart failure. The surgical approach to the closure of the PDA risks to damage (to) the phrenic and the left recurrent laryngeal nerves, so they should be reassessed after surgery [21].

Vascular access: LBPIV, CVP, A-line. Blood pressure and pulse oximetry should be checked in both upper and lower extremities to monitor for accidental aortic ligation.

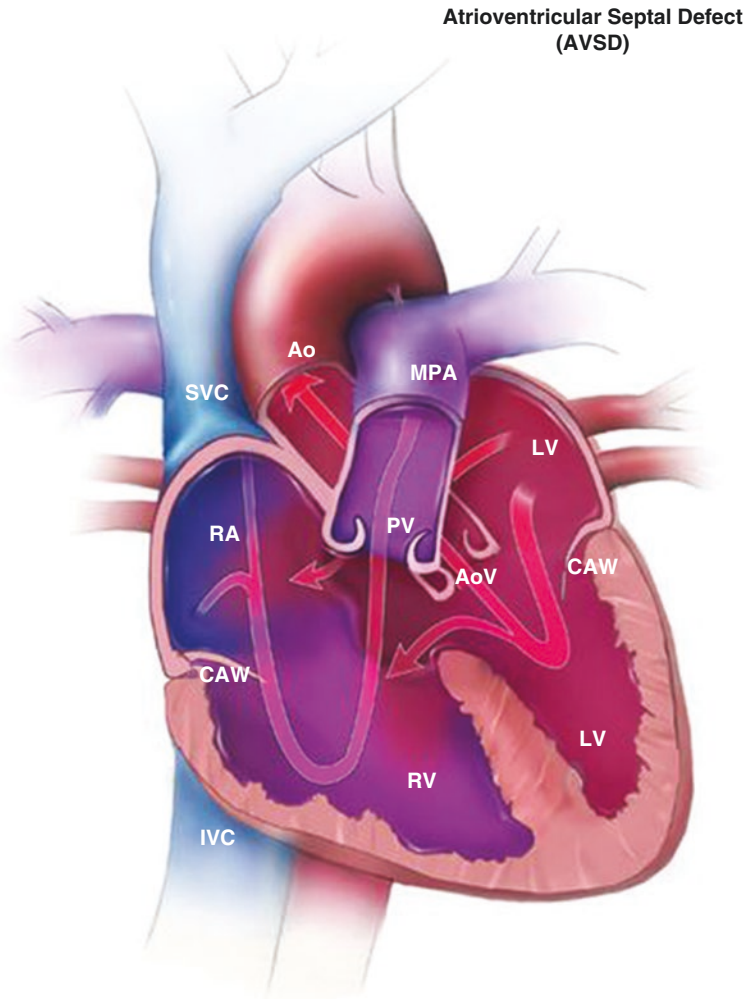
Congenital Pulmonary Stenosis

Congenital pulmonary stenosis (Fig. 20.8) is a mechanical obstruction to blood flow from the right ventricle to the pulmonary arteries. This obstruction can be infundibular, valvular, or in the pulmonary arterial branch. It will cause RV hypertrophy, ischemia, and failure.

Vascular access: LBPIV, CVP, A-line, possible pulmonary artery catheter (PAC), TEE.

Coarctation of the Aorta

Congenital narrowing of the upper descending aorta typically occurs at the junction of the ductus arteriosus, distal to the left subclavian artery (Fig. 20.9). In neonates, stenosis is usually preductal and aortic flow is ductus-dependent, resulting in cyanosis due to right-to-left shunting when the PVR/SVR ratio increases. With the closure



RA. Right Atrium
RV. Right Ventricle
LA. Left Atrium
LV. Left Ventricle

SVC. Superior Vena Cava
IVC. Inferior Vena Cava
MPA. Main Pulmonary Artery
Ao. Aorta

CAW. Common Atrioventricular Valve
PV. Pulmonary Valve
AoV. Aortic Valve

Fig. 20.6 Atrioventricular septal defect (AVSD). (Courtesy of the Centers for Disease Control and Prevention and the National Center on Birth Defects and Developmental Disabilities. <https://www.cdc.gov/ncbddd/heartdefects/avsd.html>)

of the ductus arteriosus, LV afterload will increase acutely, and a coexisting ASD or VSD can result in significant left-to-right shunting. During the procedure, myocardial depression or significant changes of SVR should be avoided, as an increase of SVR can further reduce LV cardiac output [22].

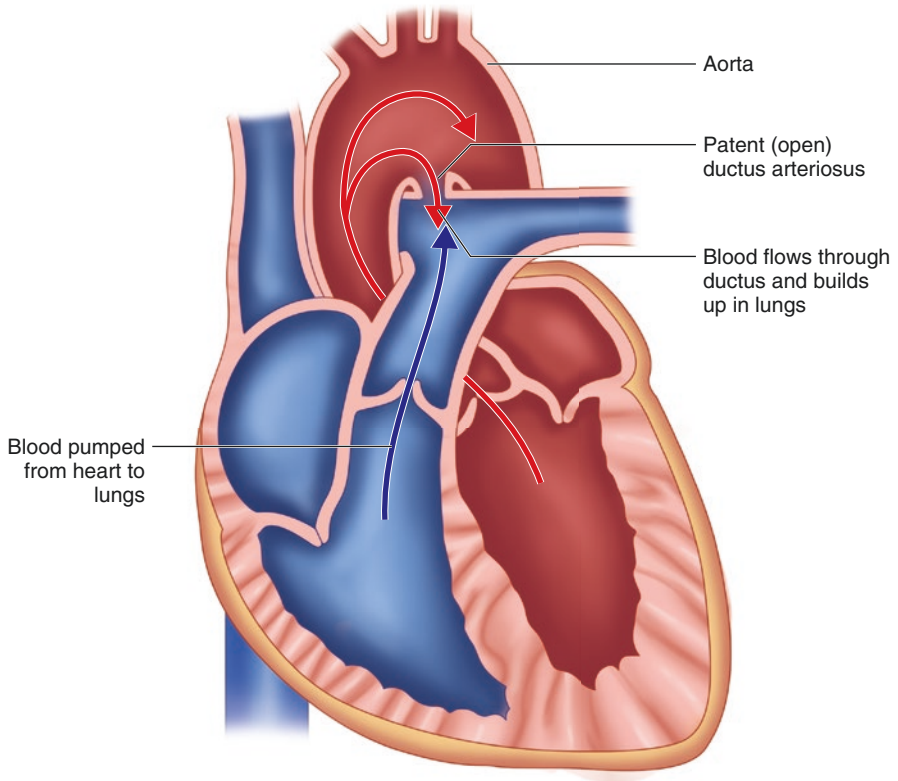


Fig. 20.7 Patent ductus arteriosus (PDA) lies between the distal aortic arch and the pulmonary artery

Vascular access: LBPIV, CVP, A-line, and TEE. Right radial A-line placement allows for blood pressure monitoring during occlusion of the aortic arch [23]. The IV and A-line should not be placed in the left upper extremity, because the surgery may interfere with the left subclavian artery and vein. It is necessary to monitor blood pressure above and below the level of coarctation. Upper- and lower-extremity cuff pressures should be compared.

Congenital Aortic Stenosis

Congenital aortic stenosis, which can be classified as subvalvular, valvular, or supravalvular, usually causes obstruction of the LV outflow. The most common form is a congenital bicuspid aortic valve (Fig. 20.10). In this condition, the aortic valve does not fully open, or it tends to degenerate and causes mechanical obstruction and pressure overload in the LV, limiting cardiac output. Anesthetic management should be directed toward maintenance of LV function, maintenance of

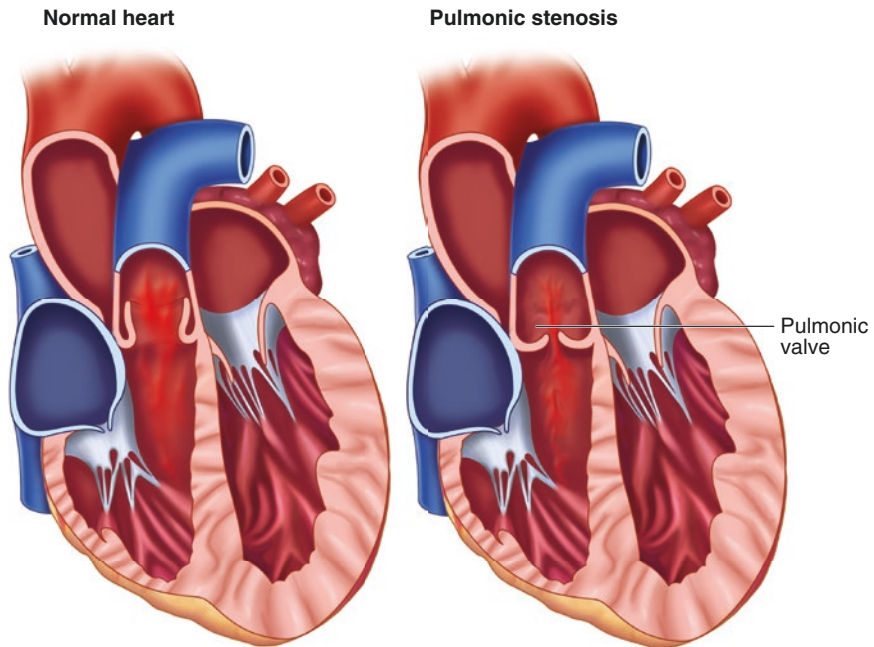


Fig. 20.8 *Left*, normal opening of the pulmonary valve. *Right*, a narrow opening in congenital pulmonary stenosis

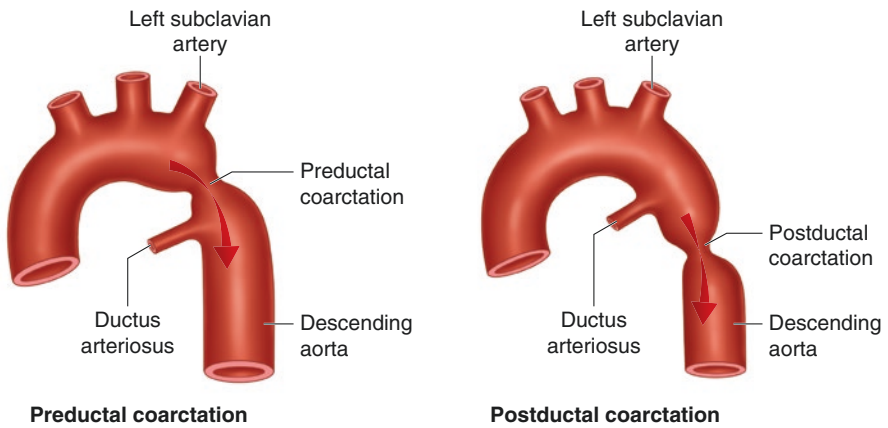
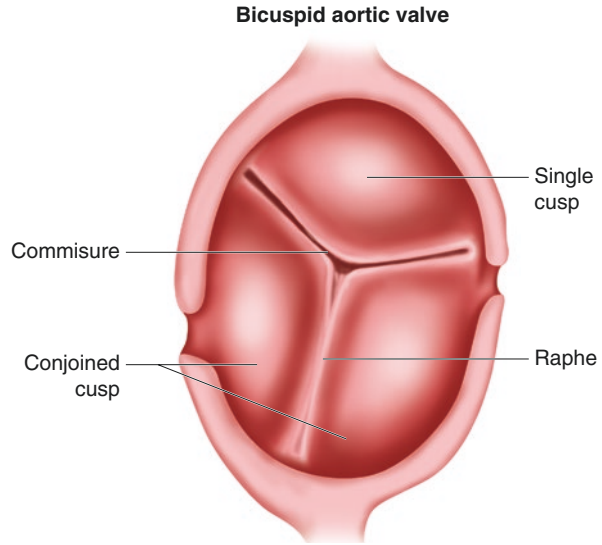


Fig. 20.9 Coarctation of the aorta. *Left*, preductal coarctation is narrowing of the descending aorta before the ductus arteriosus. *Right*, postductal coarctation is narrowing of the descending aorta after the ductus arteriosus

afterload for coronary perfusion, and maintenance of a suitable preload, heart rate, and sinus rhythm.

Vascular access: LBPIV, CVP, A-line, possible PAC, TEE.

Fig. 20.10 Bicuspid aortic valve forms by fusion of the lower two cusps, with a raphe in the connection



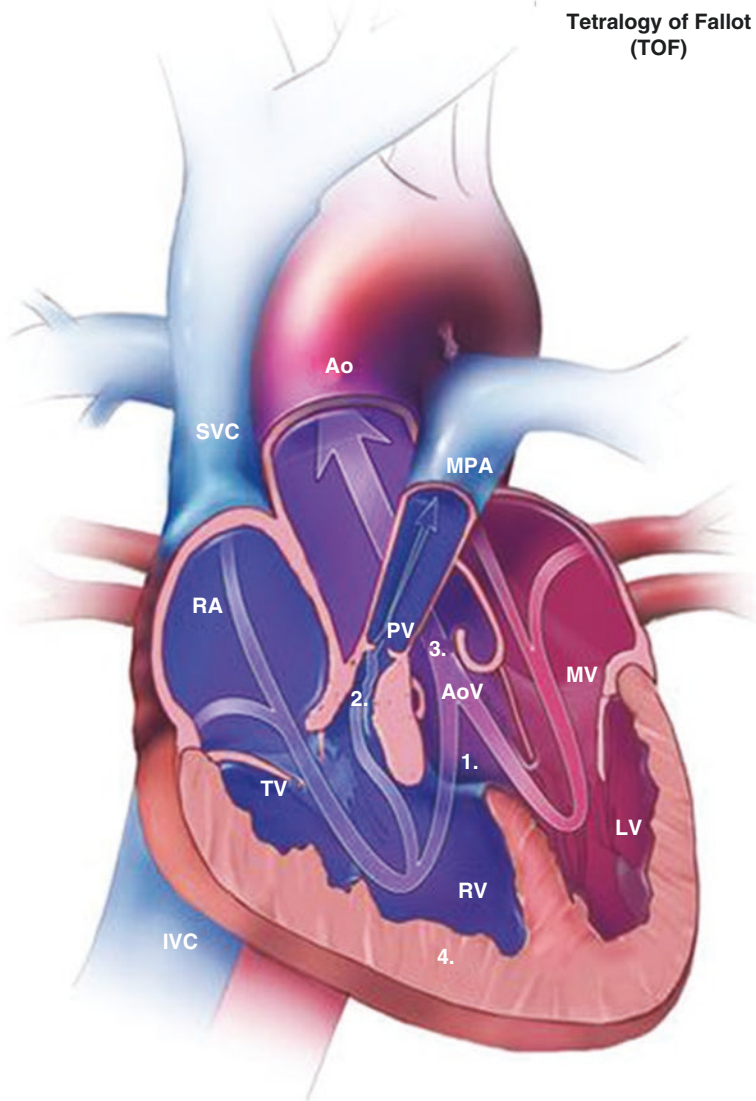
Tetralogy of Fallot (TOF)

Tetralogy of Fallot (Fig. 20.11) has four components: overriding aorta, VSD, pulmonary artery (PA) stenosis, and RV hypertrophy. TOF is the most common form of cyanotic CHD. The severity of the disease depends upon the obstruction of the RV outflow tract or the PA stenosis. Significant right-to-left shunting may result in cyanosis. Appropriate measures should be taken to avoid air bubbles in IV tubing and stopcocks. Pulmonary blood flow and shunt depend on PVR/SVR. After cardiopulmonary bypass, special attention must be directed toward RV afterload reduction, and placement of a PA catheter may be helpful [24]. Inotropic agents may also be necessary to support RV function. Heart block is common and may require a permanent pacemaker.

Vascular access: LBPIV, CVP, A-line, possible PAC, TEE.

Transposition of the Great Vessels (TGV)

In the form of CHD called dextro-transposition (D-TGV), there are two independent circulation systems, as the LV and LA connect to the pulmonary artery (PA) and pulmonary vein (PV), and the RV and RA connect to the aorta and systemic vein (Fig. 20.12). Connections between the two circulations in the atrium, ventricle, or ductus arteriosus make the survival of the baby possible. Multiple surgeries in early life can allow the patient to survive to adulthood before the PVR falls and the left ventricle becomes weak. A Mustard procedure or Senning procedure is performed to direct systemic venous blood return to the LV and the pulmonary venous blood return to the RV. The Jatene operation exchanges the aorta back to the LV and



RA. Right Atrium
RV. Right Ventricle
LA. Left Atrium
LV. Left Ventricle

SVC. Superior Vena Cava
IVC. Inferior Vena Cava
MPA. Main Pulmonary Artery
Ao. Aorta

TV. Tircuspid Valve
MV. Mitral Valve
PV. Pulmonary Valve
AoV. Aortic Valve

Fig. 20.11 Tetralogy of Fallot (TOF). (Courtesy of the Centers for Disease Control and Prevention and the National Center on Birth Defects and Developmental Disabilities. <https://www.cdc.gov/ncbddd/heartdefects/tetralogyoffallot.html>)

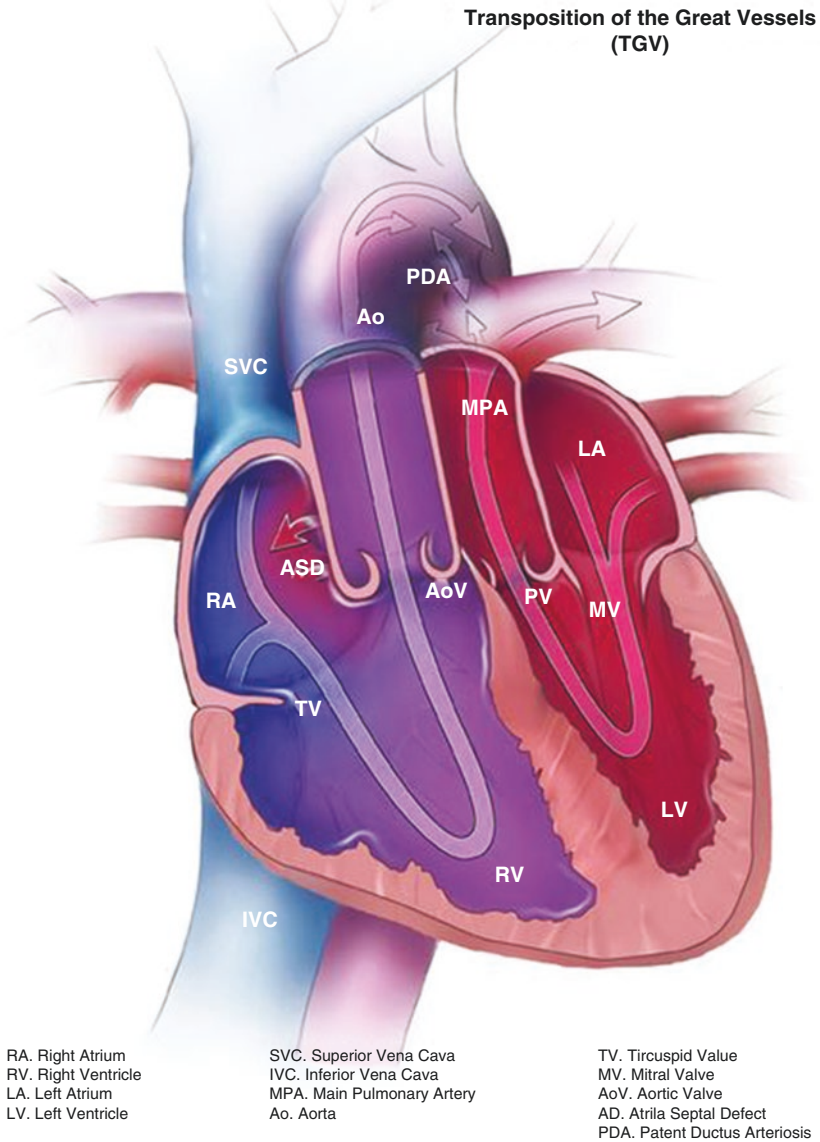


Fig. 20.12 Dextro-transposition of the great vessels (d-TGV). (Courtesy of the Centers for Disease Control and Prevention and the National Center on Birth Defects and Developmental Disabilities. <https://www.cdc.gov/ncbddd/heartdefects/d-tga.html>)

the PA forward to the RV outflow tract. At the same time, the coronary ostia are reimplemented in the proximal real aorta. The Rastelli procedure is used for TGV with VSD and subpulmonic stenosis; it patches the VSD to guide the LV blood flow to

the aorta while connecting the RV to the PA with a valved external conduit. The goal in anesthesia is to prevent myocardial ischemia, balance the PVR/SVR, check for baffle leaks or obstruction, and treat dysrhythmia.

In the form of levo-transposition (L-TGV), blood from the venae cavae drains into the RA and then through the mitral valve into the LV, which ejects the blood into the PA and to the pulmonary circulation. At the same time, saturated blood from the PV drains into the LA and then through the tricuspid valve into the RV, which ejects the saturated blood into the aorta, to the systemic circulation. L-TGV may be asymptomatic until RV failure occurs by 45 years of age. Other complications may include complete heart block, VSD, pulmonary stenosis, and increased risk of endocarditis.

Vascular access: LBPIV, CVP, A-line, TEE.

Truncus Arteriosus

In truncus arteriosus (Fig. 20.13), a single artery gives rise to the coronary artery, aorta, and pulmonary artery, with possible VSD. The mixing of systemic and pulmonary flow may happen at the level of the VSD or the truncus artery. Pulmonary flow depends on the PVR/SVR. Surgery is done by repairing the VSD and separating the PA from the truncus, with a valved conduit connected to the RV. Both aortic and pulmonary valves can become stenotic with growth, and severe regurgitation may present in later life.

Vascular access: LBPIV, CVP, A-line, TEE.

Tricuspid Atresia

In tricuspid atresia (Fig. 20.14), blood from the RA cannot go through the tricuspid valve to the RV; it usually bypasses through a PFO or ASD to the LA, then back to the RV through a VSD, or it goes to the PA through a PDA to the pulmonary circuit.

Several surgeries are used to increase the flow of the PA. The classic Blalock-Taussig shunt anastomoses the right subclavian artery directly with the right PA, whereas the modified Blalock-Taussig shunt connects the two with a tube graft. A Glenn shunt connects the superior vena cava (SVC) to the right PA. The Fontan procedure anastomoses an isolated RA to the PA; the procedure is completed later by connecting the two ends of the SVC to the right PA. A fenestrated Fontan procedure is completed by connecting the end of the inferior vena cava (IVC) with a Gore-Tex tube graft to the right PA, channeled through the RA and SVC. A fenestration is placed in the midportion of the Gore-Tex baffle, creating a small right-to-left shunt to the LA. Pulmonary blood flow is totally dependent on having the CVP higher than the LA pressure and PVR.

Therefore large-bore IVs or central venous access should be obtained before induction. CVP should be carefully monitored. Residual right-to-left shunt at the atrial level may still cause some cyanosis. PVR should be carefully controlled to the low side to avoid too much right-to-left shunt.

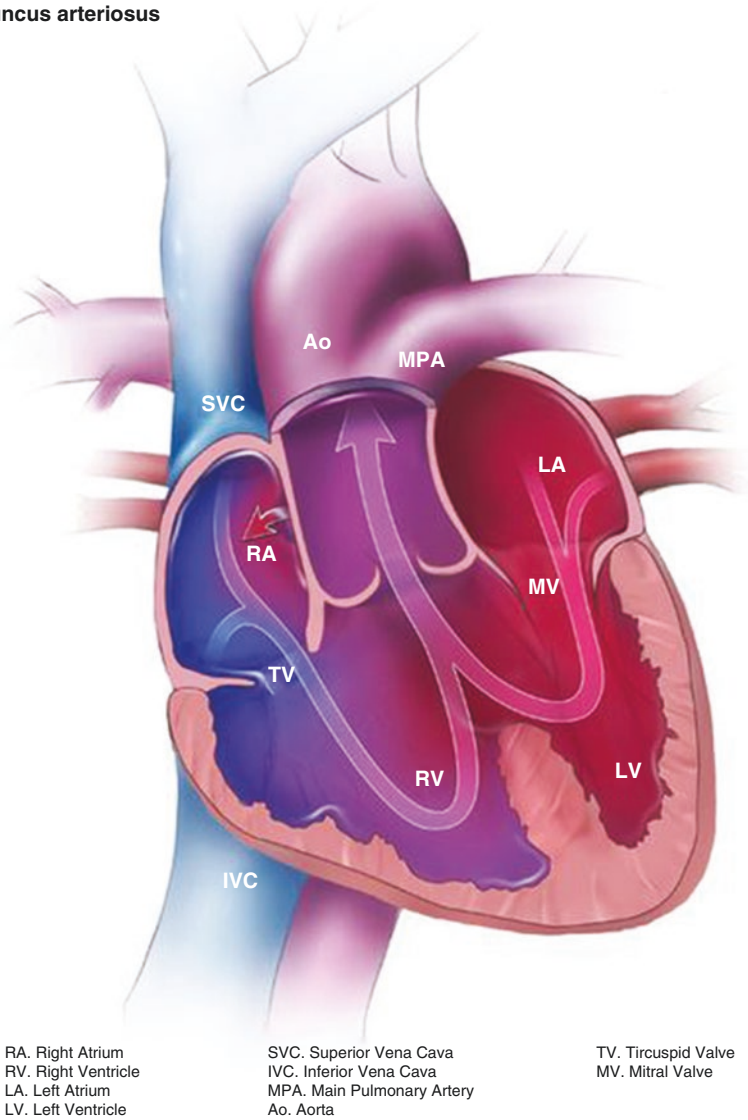
Truncus arteriosus

Fig. 20.13 Truncus arteriosus. (Courtesy of the Centers for Disease Control and Prevention and the National Center on Birth Defects and Developmental Disabilities. <https://www.cdc.gov/ncbddd/heartdefects/truncusarteriosus.html>)

Vascular access: Pre-induction LBPIV, CVP, and A-line. After induction, TEE may be used to facilitate surgery.

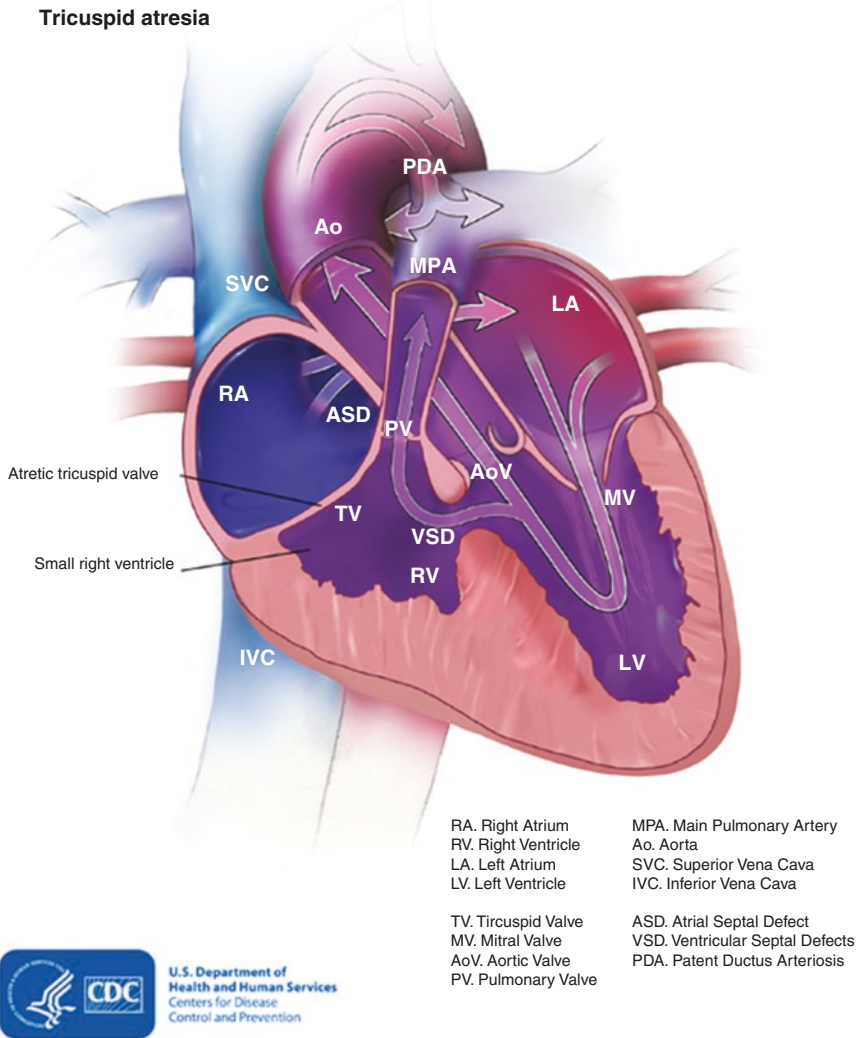


Fig. 20.14 Tricuspid atresia. (Courtesy of the Centers for Disease Control and Prevention and the National Center on Birth Defects and Developmental Disabilities. <https://www.cdc.gov/ncbddd/heartdefects/tricuspid-atresia.html>)

Double-Outlet Right Ventricle (DORV)

In this congenital anomaly (Fig. 20.15), both of the great arteries (aorta and pulmonary artery) arise, at least in part, from the right ventricle. Maintenance of oxygenated blood is made possible by a coexisting VSD. During surgery, it may be

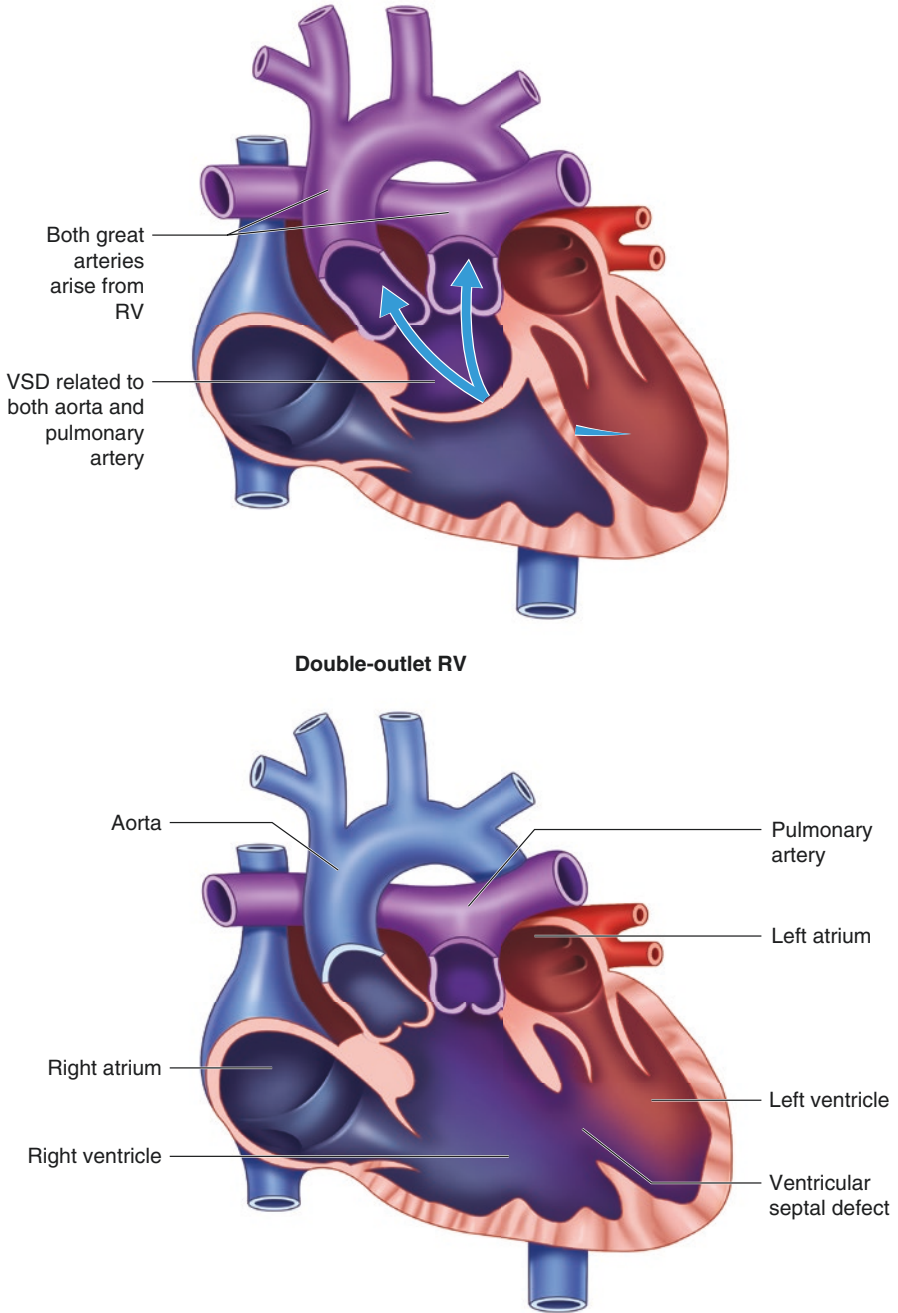


Fig. 20.15 Double-outlet right ventricle (DORV). Ao aorta, LA left atrium, LV left ventricle, PA pulmonary artery, RA right atrium, RV right ventricle, VSD ventricular septal defect

necessary to adjust the concentration of oxygen, to manipulate the PVR/SVR, and to use nitric oxide to maintain 75–85% oxygen saturation and suitable pulmonary blood flow [21].

Vascular access: LBPIV, CVP, A-line, TEE.

Hypoplastic Left Heart Syndrome (HLHS)

The hypoplastic left heart is a congenital anomaly in which the left ventricle is severely underdeveloped (Fig. 20.16). It is commonly associated with malformation of the aorta, with stenotic or completely closed aortic and mitral valves. In HLHS, the right ventricle supplies blood to both the pulmonary circuit and the systemic circuit. In order to be compatible with life, oxygenated blood in the LA is shunted to the RA via an ASD. From there, oxygenated blood and deoxygenated blood mix, enter the RV, and then flow out the pulmonary artery. A large PDA allows the RV to provide oxygenated blood to the aorta distal to the hypoplastic arch. Oxygenation and perfusion of the body critically depend on the balance of PVR/SVR. Myocardial ischemia and heart failure are also frequently seen in HLHS [21].

Vascular access: LBPIV, CVP, A-line monitoring \pm bilateral upper extremity, and TEE. Arterial data from the right upper extremity may display different pressure from that in the left upper extremity.

Eisenmenger's Syndrome

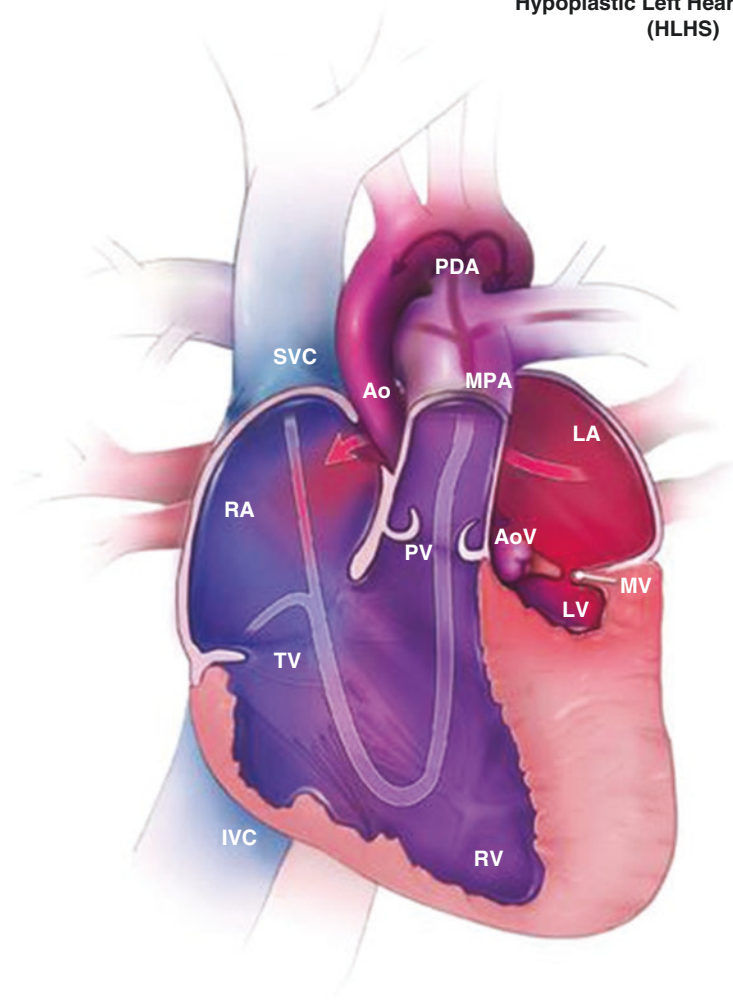
Eisenmenger's syndrome (Fig. 20.17) usually is the end stage of other CHD with blood shunted from right to left. SVR must be maintained higher than PVR in order to minimize the right-to-left deoxygenated blood flow. Further, sudden decreases in SVR may cause the decrease of diastolic filling of the LV, secondary to the RV bulging into the LV. In this situation, myocardial ischemia may result from the decreased cardiac output.

Vascular access: LBPIV, CVP, A-line, and TEE. Invasive arterial blood pressure monitoring should be obtained in the preinduction period, because hypotension commonly seen during induction must be treated promptly. During the procedure, TEE should be used to monitor the defect and verify its closure. If it is decided that a pulmonary artery catheter is to be deployed, extra care should be taken to avoid inadvertently crossing from the right heart to the left heart through the defect [25].

Dextrocardia

Dextrocardia is a rare congenital condition in which the apex of the heart points toward the right (dextro) instead of the left (Fig. 20.18). ECG leads must be placed in a mirror image of the typical pattern. Dextrocardia itself does not present any life-threatening issues, but occasionally it can be associated with other congenital

Hypoplastic Left Heart Syndrome (HLHS)



RA. Right Atrium
RV. Right Ventricle
LA. Left Atrium
LV. Left Ventricle

SVC. Superior Vena Cava
IVC. Inferior Vena Cava
MPA. Main Pulmonary Artery
Ao. Aorta
PDA. Patent Ductus Arteriosus

TV. Tricuspid Valve
MV. Mitral Valve
PV. Pulmonary Valve
AoV. Aortic Valve

Fig. 20.16 Hypoplastic left heart syndrome (HLHS). (Courtesy of the Centers for Disease Control and Prevention and the National Center on Birth Defects and Developmental Disabilities. <https://www.cdc.gov/ncbddd/heartdefects/hlhs.html>)

anomalies. Dextrocardia with situs inversus is just like a mirror image of the normal thoracic and abdominal structures. Occasionally, it may be associated with asplenia or polysplenia.

Vascular access: LBPIV, possible CVP, A-line, TEE in complicated surgery.

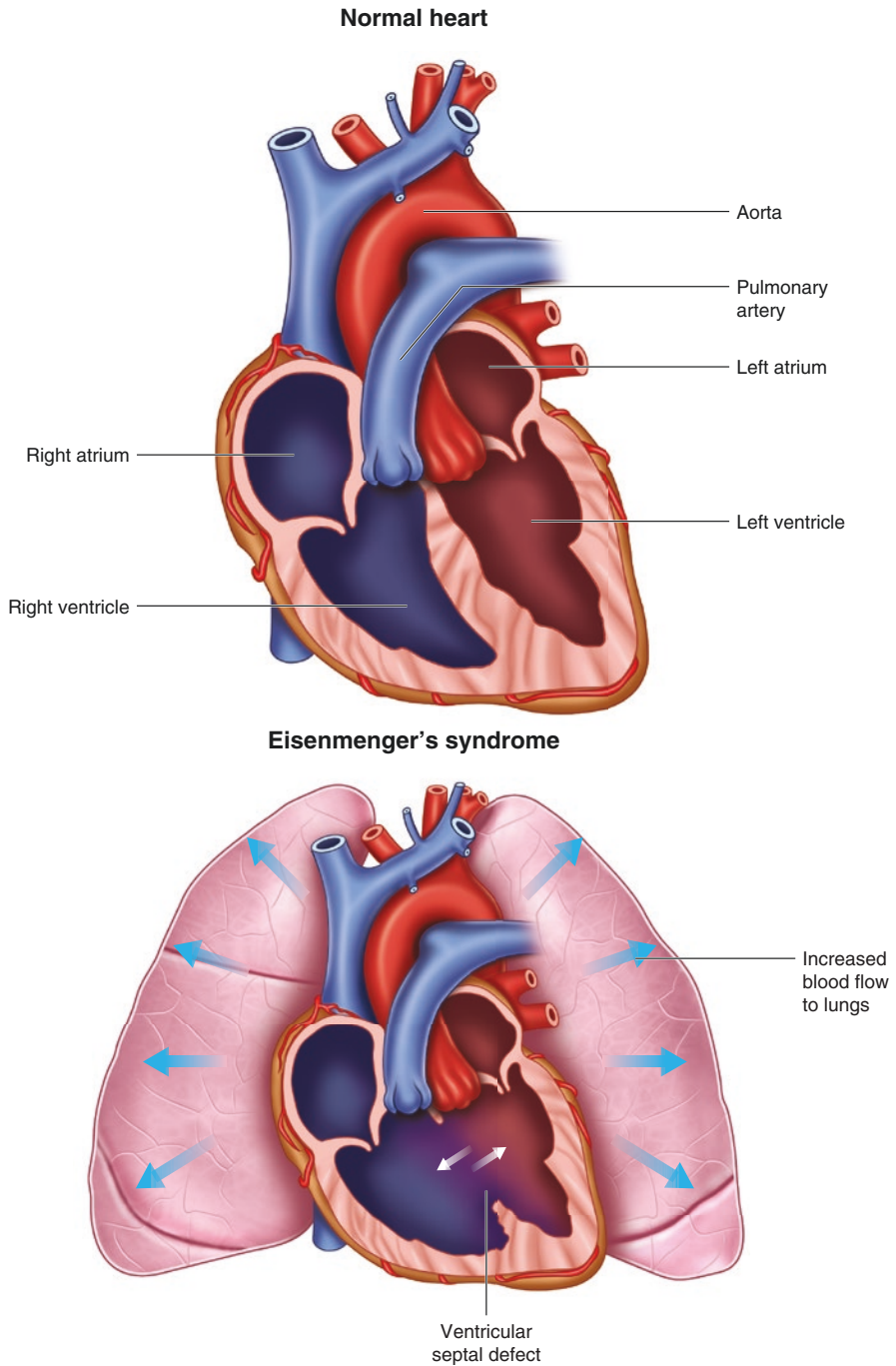


Fig. 20.17 Eisenmenger's syndrome. *Top*, a normal heart. *Bottom*, Eisenmenger's syndrome, with blood flowing freely between the right and left ventricles

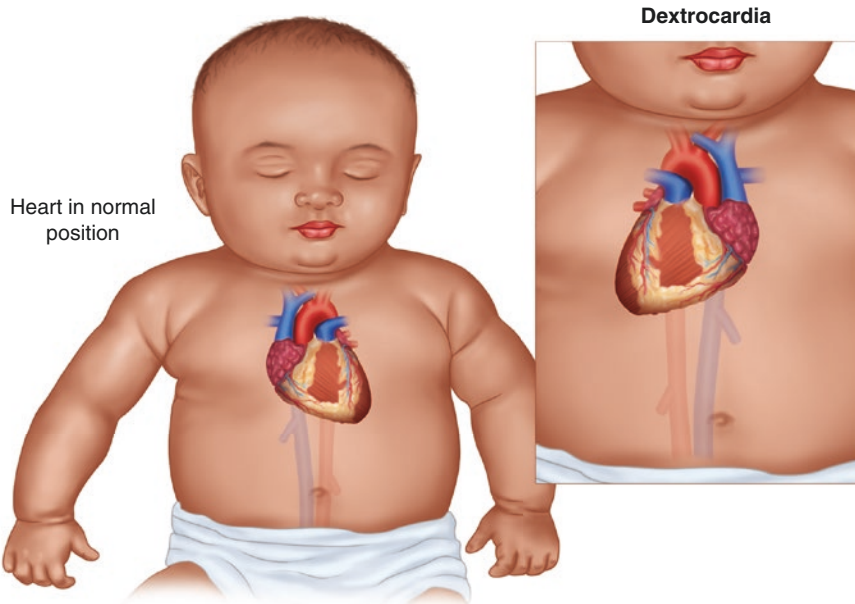


Fig. 20.18 Dextrocardia. The normal heart (*left*) is the mirror image of dextrocardia (*right*)

Interrupted Aortic Arch

In this very rare congenital heart disease, the aorta is not completely developed. The most common is type B, which involves disruption between the left common carotid and left subclavian arteries. This condition is considered a neonatal emergency. An untreated patient usually dies within 10 days [26]. Type A involves disruption just beyond the left subclavian artery. Type C involves disruption between the innominate artery and the left common carotid artery. Aortic arch surgery requires a period of circulatory arrest and deep hypothermia.

Vascular access: LBPIV, CVP, and A-line. It is recommended to avoid left central venous access because the surgeon may need to manipulate the innominate vein for surgical exposure. Bilateral arterial lines are often placed, as the right axillary artery may be used for cerebral perfusion cannulation [27].

Pulmonary Artery Aneurysm and Idiopathic Dilatation of the Pulmonary Trunk

Idiopathic dilatation of the pulmonary trunk is a rare vascular abnormality. In most cases, pulmonary artery aneurysm occurs with other conditions, such as congenital heart disease, hypertension, vasculitis, or connective tissue disease. Patients may present with symptoms of dyspnea, chest pain, cough, or hemoptysis, but most are asymptomatic. Idiopathic pulmonary artery aneurysm is a diagnosis established by the exclusion of other diseases that may cause pulmonary artery aneurysm [28].

Abrupt increases in blood pressure will increase tension on the vessel wall and may lead to aneurysmal rupture [29].

Vascular access: LBPIV, CVP, A-line.

Total Anomalous Pulmonary Venous Return (TAPVR)

TAPVR is an uncommon cyanotic heart disease. Oxygenated blood returns to the RA instead of the LA (Fig. 20.19). It is incompatible with life unless there is a right-to-left shunt, such as PFO or ASD. The pulmonary vein may connect to the SVC, IVC, coronary sinus, RA, or the portal venous system. Right heart dilatation resulting from volume overload may subsequently progress to heart failure and pulmonary hypertension [30]. Managing PVR and supporting ventricular function are key for anesthesia. The surgeon will usually place a pulmonary artery catheter in the field.

Vascular access: LBPIV, CVP, A-line, possible PAC, TEE.

Partial Anomalous Pulmonary Venous Return

Partial anomalous pulmonary venous return is a congenital cardiac abnormality characterized by the connection of some of the pulmonary veins to the right atrium, SVC, or IVC. The patient may be asymptomatic during childhood, but if left untreated, pulmonary hypertension may develop later in life [31].

Vascular access: LBPIV, CVP, A-line, TEE.

Pulmonary Atresia

Pulmonary atresia is an uncommon condition that affects 1–3% of patients with CHD. The valve orifice fails to develop and may form a dome-like structure. Venous return is shunted from right to left ventricle through a PFO, or an ASD, or a VSD, or a PDA (Fig. 20.20). The presence of a PDA allows some blood flow to the pulmonary vascular bed then returns to the left atrium. Anesthesia management will focus on the adjustment of the PVR/SVR.

Vascular access: LBPIV, CVP, A-line.

Ebstein's Anomaly

Ebstein's anomaly is characterized by apical displacement of the septal and posterior leaflets of the tricuspid valve. Displacement of the tricuspid valve causes “atrialization” of the right ventricle (Fig. 20.21). It is commonly associated with ASD and an accessory pathway, which predisposes the patient to develop arrhythmias. Avoidance of increased PVR/SVR and arrhythmia are key for anesthesia [32].

Vascular access: LBPIV, CVP, A-line, TEE.

Total anomalous pulmonary venous return

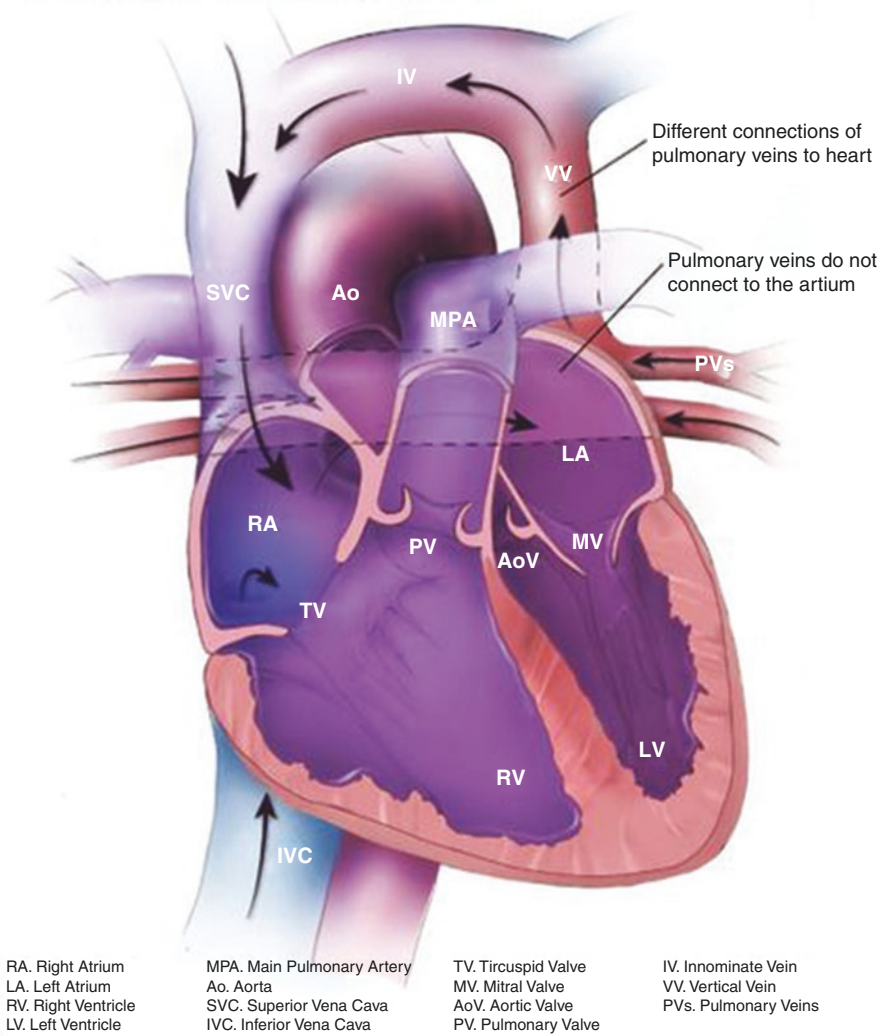


Fig. 20.19 Total anomalous pulmonary venous return (TAPVR). (Courtesy of the Centers for Disease Control and Prevention and the National Center on Birth Defects and Developmental Disabilities. <https://www.cdc.gov/ncbddd/heartdefects/tapvr.html>)

Bland-White-Garland Syndrome

Bland-White-Garland syndrome is a very rare disease characterized by the origin of the left coronary artery from the pulmonary trunk. Coronary steal into the pulmonary trunk leads to extensive myocardial ischemia. Without surgical repair, most

Pulmonary atresia with intact ventricular septum

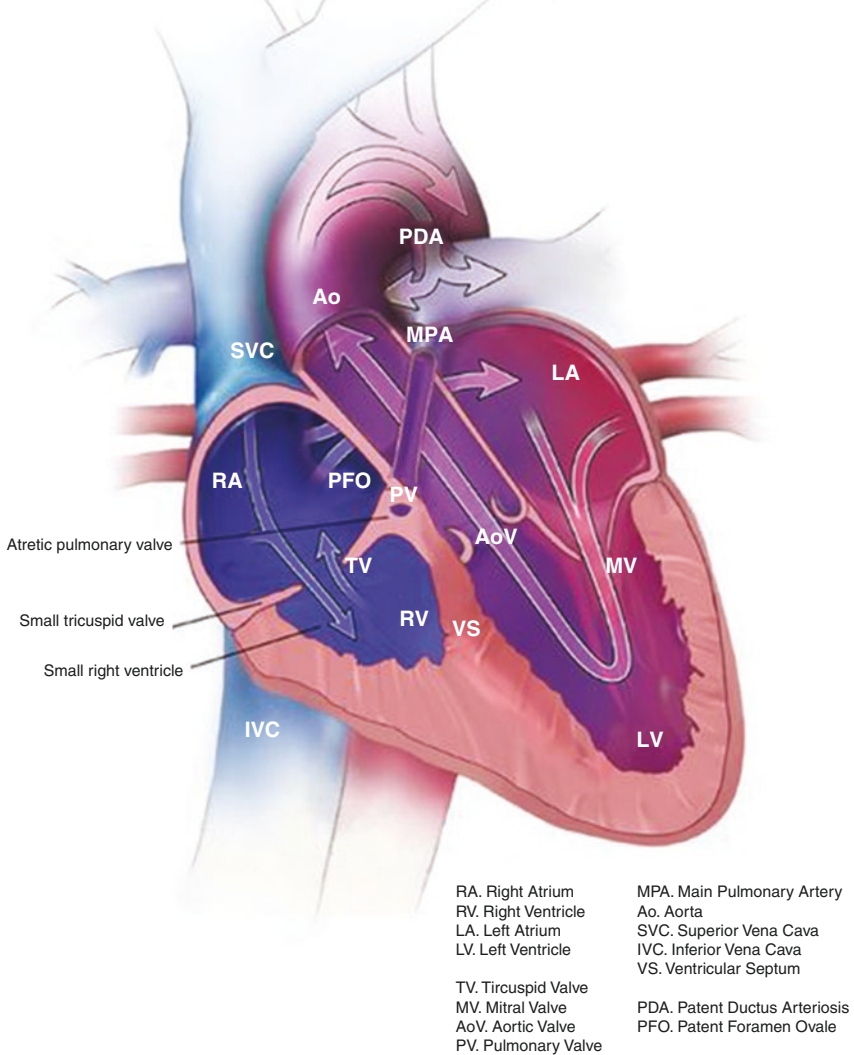


Fig. 20.20 Pulmonary atresia, in this case with an intact ventricular septum. (Courtesy of the Centers for Disease Control and Prevention and the National Center on Birth Defects and Developmental Disabilities. <https://www.cdc.gov/ncbddd/heartdefects/pulmonaryatresia.html>)

patients die within the first month of life [33]. Anesthetic goals are directed toward maintaining preload, avoiding a decrease in PVR, maintaining contractility, maintaining low SVR, and avoiding tachycardia.

Vascular access: LBPIV, CVP, A-line [34].

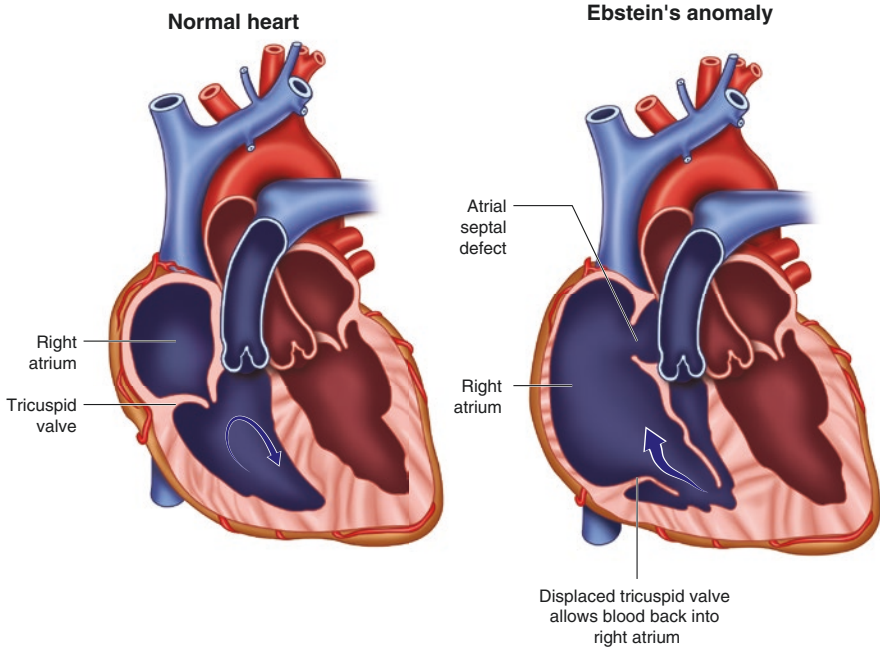


Fig. 20.21 Ebstein's anomaly. *Left*, a normal heart. *Right*, apical displacement of the tricuspid valve, with atrialization of the right ventricle, plus an atrial septal defect

Cor Triatriatum

Cor triatriatum is a rare congenital heart condition in which the left or right atrium is subdivided by a membrane, resulting in three atrial chambers. Coexisting cardiac anomalies include ASD, mitral regurgitation, or pulmonary stenosis or atresia. The patient may be asymptomatic if the blood flow from the proximal to the distal chamber is adequate, but most patients will not survive without surgical correction [35].

Vascular access: LBPIV, CVP, A-line. The insertion of a PA catheter may be difficult [36].

Double-Outlet Left Ventricle

Double-outlet left ventricle is a cardiac malformation in which both the aorta and the pulmonary artery originate from the left ventricle. This condition is often associated with VSD, pulmonic stenosis, PDA, and tricuspid atresia. The most common form is atrial situs solitus with atrioventricular concordance. Treatment involves VSD closure and biventricular repair of the left ventricle. Pulmonary root translocation is another alternative [37]. Anesthesia may need to control PVR/SVR and provide ventricular support.

Vascular access: LBPIV, CVP, A-line, TEE.

Pulmonary Hypertension

Pulmonary arterial hypertension is characterized by mean pulmonary artery pressure >25 mmHg with pulmonary capillary wedge pressure <15 mmHg [38]. Primary pulmonary hypertension is a diagnosis of exclusion, after eliminating causes of secondary pulmonary hypertension. The trademark of primary pulmonary hypertension is an increase of PVR, which may result in RV failure, syncope, and death. Lung and heart-lung transplantation may be the ultimate treatment.

Whereas mild pulmonary hypertension may have no significant effect on anesthetic management, severe pulmonary hypertension or an acute exacerbation of moderate pulmonary hypertension can result in acute right heart failure and cardiogenic shock. It is important to avoid exacerbating factors, including hypoxemia, hypercarbia, acidosis, hypothermia, hypervolemia, and increased intrathoracic pressure [39, 40]. It is also important to consider the effects of anesthetic drugs on the pulmonary circulation. Selective pulmonary vasodilators, such as adenosine, prostacyclin, and nitric oxide, can be used to optimize RV function.

Vascular access: LBPIV, A-line, possible CVP, PAC, TEE [41, 42].

Bicuspid Aortic Valve

In this common congenital condition, two-valve leaflets fuse during development, resulting in a bicuspid rather than tricuspid configuration (*see* Fig. 20.10). This condition occurs in 1–2% of the general population and is twice as common in males [43]. In many cases, a bicuspid aortic valve will have no effect on the patient's health, but calcification later in life may result in severe aortic stenosis, requiring replacement of the aortic valve. There is also an association with the development of ascending aortic aneurysms [44].

In patients who develop severe aortic stenosis, anesthetic management should be directed toward maintenance of LV function, maintenance of afterload for coronary perfusion, and maintenance of a suitable preload, heart rate, and sinus rhythm.

Vascular access: LBPIV, CVP, A-line, possible PAC, TEE [45].

Quadricuspid Aortic Valve

The quadricuspid aortic valve is characterized by the presence of four valvular cusps. It is an extremely rare condition, occurring in approximately 1 in 6000 patients undergoing aortic valve surgery [46]. The most common complication is aortic regurgitation due to incomplete closure of the four cusps during systole [47]. Other associated complications include left ventricular hypertrophy and bundle branch blocks. It is important to control the heart rate.

Vascular access: LBPIV, CVP, A-line, possible PAC, TEE.

Anesthesia Management and Vascular Access in Other Heart Conditions

The following conditions may be seen in the normal heart or in the presence of congenital heart defects, familial tendencies, various infections, and environmental factors.

Behçet Disease

Behçet disease is an immune-mediated vasculitis that affects the small vessels; it most commonly presents with mucous membrane ulceration and ocular problems, but the disease can affect the cardiovascular system. Constrictive pericarditis is a frequent manifestation, and chronic aortic regurgitation resulting from aortic root disease has also been observed [48]. Anesthetic management of patients with constrictive pericarditis is focused on the patient's hemodynamic profile.

Vascular access: LBPIV, CVP, A-line.

Infectious Aneurysm (Mycotic Aneurysm)

The term *mycotic aneurysm* may be used to describe any infected aneurysm, but most often refers to an aneurysm that occurs when bacteria originating from the heart (e.g., infective endocarditis) result in arterial wall infection and subsequent dilatation [49]. This medical condition is associated with serious morbidity and mortality. Antibiotic therapy and aggressive surgical debridement are the main treatment strategies. In severe cases, vascular reconstruction is needed [50].

Patients undergoing repair of mycotic aneurysms by means of in situ replacement or extra-anatomic reconstruction require invasive blood pressure monitoring with an arterial line, as well as central venous access for monitoring of intravascular volume status and administration of fluids and blood products. In aortic reconstructions, patients may require cardiopulmonary bypass, and when the aneurysm involves the aortic arch, a deep hypothermic circulatory arrest may be necessary.

Vascular access: LBPIV, CVP, A-line, possible PAC, TEE.

Rasmussen Aneurysm

This exceedingly rare condition describes a pulmonary or bronchial artery aneurysm, which was traditionally related to pulmonary tuberculosis but can also occur with other destructive lung lesions [51]. Patients typically present with hemoptysis, and the diagnosis is made by CT angiography [52]. Therapeutic embolization is the mainstay of treatment. A ruptured aneurysm is a catastrophic situation with high mortality. One-lung ventilation and cardiopulmonary bypass may be required for the repair of a ruptured aneurysm.

Vascular access: LBPIV, A-line, possible CVP.

Intravascular Pulmonary Metastases

Several common cancer types (e.g., liver, kidney, stomach, breast) are known to embolize to the pulmonary arterial system [53]. Patients may be asymptomatic or may present with nonspecific respiratory symptoms so that misdiagnosis of thromboembolic disease is common. Surgical resection of pulmonary metastases may be performed if patients meet certain criteria, including the ability to tolerate the surgical procedure [54].

Vascular access: LBPIV, A-line, possible CVP.

Takayasu Arteritis

Takayasu arteritis is a granulomatous vasculitis affecting larger vessels, particularly the aorta and its major branches and the pulmonary arteries. It is characterized by vascular narrowing and fibrosis of the intimal layer, and is 8–9 times more common in women than in men. Takayasu arteritis can present with weakened or absent pulses in the upper extremities, and for this reason it is often referred to as the “pulseless disease” [55]. Granulomatous inflammation can lead to arterial stenosis, thrombosis, and aneurysm formation. Treatment commonly involves steroids, but for patients who do not respond to this therapy, large-vessel reconstructive surgery (including bypass grafting) may be required to achieve tissue reperfusion [55]. Surgical procedures involving the aortic arch are likely to require a hypothermic circulatory arrest.

Vascular access: LBPIV, CVP, A-line.

Rheumatic Heart Disease

Rheumatic heart disease is due to an autoimmune reaction to group A beta-hemolytic Streptococci that results in valvular damage through the processes of repeated inflammation with fibrinous repair [56]. Scarring of valve leaflets can result in valvular stenosis or regurgitation, and ultimately leads to heart failure. In the acute phase, rheumatic heart disease often produces pancarditis, endocarditis, myocarditis, and pericarditis [57]. Any valve may be affected, but the mitral valve is most commonly involved (65–70%), followed by the aortic valve (25%) [56]. Severe valve insufficiency in acute rheumatic heart disease can cause heart failure and death [57]. Up to 40% of patients with rheumatic heart disease have chronic manifestations with progressive valvular deformity, particularly of the mitral valve [57]. Valve involvement may lead to atrial thrombus formation and predispose the patient to atrial fibrillation [58]. Patients may ultimately require valve replacement.

Vascular access: LBPIV, CVP, A-line, possible PAC, TEE.

Kawasaki Disease

Kawasaki disease is an autoimmune vasculitis involving predominantly the medium-sized blood vessels [58]. Cardiac complications of Kawasaki disease are significant; it is the main cause of acquired heart disease in children in the United States [58]. Coronary artery aneurysms occur in up to 25% of untreated children, and death can occur secondary to myocardial infarction from thrombus formation or aneurysmal rupture [58]. Mitral and tricuspid valvular insufficiencies are commonly seen in the acute phase. Most valvular lesions resolve after the acute phase ends, but some lesions may persist and worsen [59]. Late-onset aortic or mitral insufficiency may also occur, and some patients require valve replacement.

Vascular access: LBPIV, CVP, A-line, possible PAC, TEE.

Idiopathic Dilated Cardiomyopathy

Idiopathic dilated cardiomyopathy is a primary myocardial disease with unknown etiology, which involves a ventricular or biventricular dilatation with impaired contractility. Anesthetic management of these patients can be challenging, owing to the associated progressive heart failure [60]. The goals of anesthetic management are avoidance of myocardial depression, the elevation of ventricular afterload, hypotension, and volume overload [61].

Vascular access: LBPIV, possible CVP, A-line, TEE.

Infective Endocarditis

Infective endocarditis is characterized by inflammation of the inner tissues of the heart, including the valves, typically due to bacterial pathogens. The organism attaches to the valvular surface and forms a vegetation, which impairs valvular function [62]. Damaged valves with associated turbulent flow predispose to the development of infective endocarditis. There are two different presentations: subacute (typically due to Streptococci of low virulence and associated with a mild clinical course) and acute (typically due to *Staphylococcus aureus* and associated with a fulminant clinical course). The mainstay of treatment is intravenous antibiotic therapy [62]. Patients with significant valvular lesions leading to heart failure will require surgical debridement of the infected material and may need valve replacement [63].

Vascular access: LBPIV, CVP, A-line, possible PAC, TEE.

References

1. Hoffman JL, Kaplan S. The incidence of congenital heart disease. J Am Coll Cardiol. 2002;39:1890–900.

2. Oster ME, Lee KA, Honein MA, Riehle-Colarusso T, Shin M, Correa A. Temporal trends in survival among infants with critical congenital heart defects. *Pediatrics*. 2013;131:e1502–8.
3. Schure AY, DiNardo JA. Cardiac physiology and pharmacology. In: Coté CJ, Lerman J, editors. *Practice of anesthesia for infants and children*. 5th ed. Philadelphia: Elsevier Saunders; 2013. p. 354–85.
4. Cardiac defects with a right to left shunt (cyanotic). *Cardiac Health*. 2009. <https://www.cardiachealth.org/professionals/cardiac-anatomy/cardiac-defects-with-a-right-to-left-shunt-cyanotic>. Accessed 06 Nov 2019.
5. Menghraj SJ. Anaesthetic considerations in children with congenital heart disease undergoing non-cardiac surgery. *Indian J Anaesth*. 2012;56:491–5.
6. DeFilippis AP, Law K, Curtin S, Eckman JR. Blood is thicker than water: the management of hyperviscosity in adults with cyanotic heart disease. *Cardiol Rev*. 2007;15:31–4.
7. DiNardo JA, Zvara DA. Congenital heart disease. In: *Anesthesia for cardiac surgery*. 3rd ed. Malden: Blackwell; 2008. p. 167–251.
8. Rivenes SM, Lewin MB, Stayer SA, Bent ST, Schoenig HM, McKenzie ED, et al. Cardiovascular effects of sevoflurane, isoflurane, halothane, and fentanyl-midazolam in children with congenital heart disease: an echocardiographic study of myocardial contractility and hemodynamics. *Anesthesiology*. 2001;94:223–9.
9. Laird TH, Stayer SA, Rivenes SM, Lewin MB, McKenzie ED, Fraser CD, Andropoulos DB. Pulmonary-to-systemic blood flow ratio effects of sevoflurane, isoflurane, halothane, and fentanyl/midazolam with 100% oxygen in children with congenital heart disease. *Anesth Analg*. 2002;95:1200–6.
10. Hickey PR, Hansen DD, Strafford M, Thompson JE, Jonas RE, Mayer JE. Pulmonary and systemic hemodynamic effects of nitrous oxide in infants with normal and elevated pulmonary vascular resistance. *Anesthesiology*. 1986;65:374–8.
11. Huntington JH, Malviya S, Voepel-Lewis T, Lloyd TR, Massey KD. The effect of a right-to-left intracardiac shunt on the rate of rise of arterial and end-tidal halothane in children. *Anesth Analg*. 1999;88:759–62.
12. Oklu E, Bulutcu FS, Yalcin Y, Ozbek U, Cakali E, Bayindir O. Which anesthetic agent alters the hemodynamic status during pediatric catheterization? Comparison of propofol versus ketamine. *J Cardiothorac Vasc Anesth*. 2003;17:686–90.
13. Kurdi MS, Theerth KA, Deva RS. Ketamine: current applications in anesthesia, pain, and critical care. *Anesth Essays Res*. 2014;8:283–90.
14. White MC. Approach to managing children with heart disease for noncardiac surgery. *Paediatr Anaesth*. 2011;21:522–9.
15. Wilson W, Taubert KA, Gewitz M, Lockhart PB, Baddour LM, Levison M, et al. Prevention of infective endocarditis: guidelines from the American Heart Association: a guideline from the American Heart Association Rheumatic Fever, Endocarditis, and Kawasaki Disease Committee, Council on Cardiovascular Disease in the Young, and the Council on Clinical Cardiology, Council on Cardiovascular Surgery and Anesthesia, and the Quality of Care and Outcomes Research Interdisciplinary Working Group. *Circulation*. 2007;116:1736–54.
16. Hennein HA, Mendeloff EN, Cillely RE, Bove EL, Coran AG. Predictors of postoperative outcome after general surgical procedures in patients with congenital heart disease. *J Pediatr Surg*. 1994;29:866–70.
17. Murphy TW, Smith JH, Ranger MR, Haynes SR. General anesthesia for children with severe heart failure. *Pediatr Cardiol*. 2011;32:139–44.
18. Kachko L, Birk E, Simhi E, Tzeitlin E, Freud E, Katz J. Spinal anesthesia for noncardiac surgery in infants with congenital heart diseases. *Paediatr Anaesth*. 2012;22:647–53.
19. Shenkman Z, Johnson VM, Zurakowski D, Arnon S, Sethna NF. Hemodynamic changes during spinal anesthesia in premature infants with congenital heart disease undergoing inguinal hernia correction. *Paediatr Anaesth*. 2012;22:865–70.
20. Martin JT, Tautz TJ, Antognini JF. Safety of regional anesthesia in Eisenmenger’s syndrome. *Reg Anesth Pain Med*. 2002;27:509–13.

21. Jaffe RA, Samuels SI. Anesthesiologist's manual of surgical procedures. 3rd ed. Philadelphia: Lippincott William & Wilkins; 2003.
22. Kouchoukos NT, Blackstone EG, Doty DB, et al. Coarctation of the aorta and interrupted aortic arch. In: Kouchoukos NT, Karp RB, Blackstone EH, Doty DB, Hanley FL, editors. *Kirklin/Barratt-Boyes cardiac surgery*. 3rd ed. Philadelphia: Churchill Livingstone; 2003. p. 1315–76.
23. Spaeth JP, Loepke AW. Anesthesia for left-sided obstructive lesions. In: Andropoulos DB, Stayer SA, Russel LA, Mossad EB, editors. *Anesthesia for congenital heart disease*. Chichester: Blackwell Publishing; 2010. p. 398–418.
24. Reitz BA, Yuh DD, editors. *Congenital cardiac surgery*. New York: McGraw-Hill; 2002.
25. Lanigan MJ, Chaney MA, Tissot C, Beghetti M, Dimopoulos K. CASE 10—2014 Eisenmenger syndrome: close the hole? *J Cardiothorac Vasc Anesth*. 2014;28:1146–53.
26. Reardon MJ, Hallman GL, Cooley DA. Interrupted aortic arch: brief review and summary of an eighteen-year experience. *Tex Heart Inst J*. 1984;11:250–9.
27. Gargiulo G, Oppido G, Angeli E, Pace Napoleone C. Neonatal aortic arch surgery. *Multimed Man Cardiothorac Surg*. 2007;2007(723):mmcts.2006.002345.
28. Orman G, Guvenc TS, Balci B, Duymus M, Sevingil T. Idiopathic pulmonary artery aneurysm. *Ann Thorac Surg*. 2013;95:e33–4.
29. Bartter T, Irwin RS, Nash G. Aneurysms of the pulmonary arteries. *Chest*. 1988;94:1065–75.
30. Khanna S, Choudhury M, Kiran U. Total anomalous pulmonary venous connection: post operative problems and management. *Indian J Anaesth*. 2009;53:71–4.
31. Sears EH, Aliotta JM, Klinger JR. Partial anomalous pulmonary venous return presenting with adult-onset pulmonary hypertension. *Pulm Circ*. 2012;2:250–5.
32. Sinha PK, Kumar B, Varma PK. Anesthetic management for surgical repair of Ebstein's anomaly along with coexistent Wolff-Parkinson-White syndrome in a patient with severe mitral stenosis. *Ann Card Anaesth*. 2010;13:154–8.
33. Szmigielska A, Roszkowska-Blaim M, Golabek-Dylewska M, Tomik A, Brzewski M, Werner B. Bland-White-Garland syndrome – a rare and serious cause of failure to thrive. *Am J Case Rep*. 2013;14:370–2.
34. Gupta K, Gupta M, Mehrotra M, Prasad J. Anaesthesia for repair of anomalous origin of left coronary artery from pulmonary artery. *Indian J Anaesth*. 2015;59:136–7.
35. Sabade S, Vagrati A, Patil S, Kalligudd P, Dhulked V, Dixit MD, et al. Anaesthetic management of a child with “cor-triatrium” and multiple ventricular septal defects – a rare congenital anomaly. *Indian J Anaesth*. 2010;54:242–5.
36. Bisinov EA, Dieter RS, Ballantyne F 3rd, Wolff MR, Stein JH. Echocardiographic diagnosis and catheter treatment of hypotension caused by cor-triatrium dexter. *J Am Soc Echocardiogr*. 2003;16:897–8.
37. Menon SC, Hagler DJ. Double-outlet left ventricle: diagnosis and management. *Curr Treat Options Cardiovasc Med*. 2008;10:448–52.
38. Farber H, Loscalzo J. Pulmonary arterial hypertension. *N Engl J Med*. 2004;351:1655–65.
39. Subramaniam K, Yared JP. Management of pulmonary hypertension in the operating room. *Semin Cardiothorac Vasc Anesth*. 2007;11:119–36.
40. Gille J, Seyfarth HJ, Gerlach S, Malcharek M, Czeslick E, Sablotzki A. Perioperative anesthesiological management of patients with pulmonary hypertension. *Anesthesiol Res Pract*. 2012;2012:356982.
41. Hofer CK, Senn A, Weibel L, Zollinger A. Assessment of stroke volume variation for prediction of fluid responsiveness using the modified FloTrac and PiCCOplus system. *Crit Care*. 2008;12:R82.
42. Fischer LG, Van Aken H, Bürkle H. Management of pulmonary hypertension: physiological and pharmacological considerations for anesthesiologists. *Anesth Analg*. 2003;96:1603–16.
43. Tzemos N, Therrien J, Yip J, Thanassoulis G, Tremblay S, Jamorski MT, et al. Outcomes in adults with bicuspid aortic valves. *JAMA*. 2008;300:1317–25.
44. Nishimura RA. Cardiology patient pages. Aortic valve disease. *Circulation*. 2002;106:770–2.
45. Hines RL, Marschall KE. *Stoelting's anesthesia and co-existing disease*. 5th ed. Philadelphia: Churchill Livingstone; 2008.

46. Godefroid O, Colles P, Vercauteren S, Louagie Y, Marchandise B. Quadricuspid aortic valve: a rare etiology of aortic regurgitation. *Eur J Echocardiogr.* 2006;7:168–70.
47. Tutarel O. The quadricuspid aortic valve: a comprehensive review. *J Heart Valve Dis.* 2004;13:534–7.
48. Hatemi G, Seyahi E, Fresko I, Hamuryudan V. Behçet's syndrome: a critical digest of the recent literature. *Clin Exp Rheumatol.* 2012;30:S80–9.
49. Bisdas T, Teebken OE. Mycotic or infected aneurysm? Time to change the term. *Eur J Vasc Endovasc Surg.* 2011;41:570; author reply 570–1.
50. Müller BT, Wegener OR, Grabitz K, Pillny M, Thomas L, Sandmann W. Mycotic aneurysms of the thoracic and abdominal aorta and iliac arteries: experience with anatomic and extra-anatomic repair in 33 cases. *J Vasc Surg.* 2001;33:106–13.
51. van den Heuvel MM, van Rensburg JJ. Images in clinical medicine. Rasmussen's aneurysm. *N Engl J Med.* 2006;355:e17.
52. Karmakar S, Nath A, Neyaz Z, Lal H, Phadke RV. Bronchial artery aneurysm due to pulmonary tuberculosis: detection with multidetector computed tomographic angiography. *J Clin Imaging Sci.* 2011;1:26.
53. Ting PT, Burrowes PW, Gray RR. Intravascular pulmonary metastases from sarcoma: appearance on computed tomography in 3 cases. *Can Assoc Radiol J.* 2005;56:214–8.
54. Todd TR. The surgical treatment of pulmonary metastases. *Chest.* 1997;112:287S–90S.
55. Weyand CM, Goronzy JJ. Medium- and large-vessel vasculitis. *N Engl J Med.* 2003;349:160–9.
56. Marijon E, Mirabel M, Celermajer DS, Jouven X. Rheumatic heart disease. *Lancet.* 2012;379:953–64.
57. Guilherme L, Ramasawmy R, Kalil J. Rheumatic fever and rheumatic heart disease: genetics and pathogenesis. *Scand J Immunol.* 2007;66:199–207.
58. Wang CL, Wu YT, Liu CA, Kuo HC, Yang KD. Kawasaki disease: infection, immunity and genetics. *Pediatr Infect Dis J.* 2005;24:998–1004.
59. Kato H, Sugimura T, Akagi T, Sato N, Hashino K, Maeno Y, et al. Long-term consequences of Kawasaki disease. A 10- to 21-year follow-up study of 594 patients. *Circulation.* 1996;94:1379–85.
60. Kaur H, Khetarpal R, Aggarwal S. Dilated cardiomyopathy: an anaesthetic challenge. *J Clin Diagn Res.* 2013;7:1174–6.
61. Popescu WM, Malik A. Heart failure and cardiomyopathy. In: Hines RL, Marschall KE, editors. *Anaesthesia and co-existing disease.* 7th ed. Philadelphia: Elsevier; 2017. p. 63–76.
62. Heiro M, Helenius H, Mäkilä S, Hohenthal U, Savunen T, Engblom E, et al. Infective endocarditis in a Finnish teaching hospital: a study on 326 episodes treated during 1980–2004. *Heart.* 2006;92:1457–62.
63. Bonow RO, Carabello BA, Chatterjee K, de Leon AC Jr, Faxon DP, Freed MD, et al. American College of Cardiology/American Heart Association Task Force on Practice Guidelines. 2008 focused update incorporated into the ACC/AHA 2006 guidelines for the management of patients with valvular heart disease: a report of the American College of Cardiology/American Heart Association Task Force on Practice Guidelines (Writing Committee to revise the 1998 guidelines for the management of patients with valvular heart disease). Endorsed by the Society of Cardiovascular Anesthesiologists, Society for Cardiovascular Angiography and Interventions, and Society of Thoracic Surgeons. *J Am Coll Cardiol.* 2008;52:e1–142.

Index

A

- Abdominal testicle, 320
- Abdominal wall and scrotum, 318
- Abductor pollicis longus (APL), 405
- Aberrant right subclavian artery, 137
- Abnormalities of the spermatic cord, 322
- Accessory bones
 - common, of foot, 420, 422
 - uncommon, of foot and ankle, 423
- Accessory brachial artery (ABA), 439, 440
- Accessory deep peroneal nerve (aDPN), 429, 430
- Accessory flexor digitorum longus (aFDL), 426
- Accessory musculotendinous structures, 425–427
- Accessory navicular with close proximity to the navicular tuberosity, 422
- Accessory nerve (CN XI), 28
- Accessory ossicles, 411
- Achalasia, 147
- Achondroplasia, 116
- Acquired spinal disorders anatomy
 - lumbar disc herniation, 351, 353
 - complications, 353
 - postoperative care, 353
 - surgical intervention, 353
 - types, 353
 - lumbar stenosis, 353
 - postoperative care, 354
 - surgical intervention, 354
 - symptoms/complications, 354
 - types/causes, 354
 - osteoporosis, 349
 - postoperative care, 351
 - primary, 349
 - surgical intervention, 350
 - vertebral fractures, 350
 - scoliosis
 - definition of, 355
 - postoperative care, 356
 - surgical interventions, 355
 - symptoms/complications, 355
 - types/causes, 355
- Acute mesenteric ischemia, 166
- Adrenals
 - anatomy, 286
 - lymphatics, 287
 - nerves, 287
 - vasculature, 286
 - congenital anomalies, 287
 - embryology, 287
- Agensis and hypoplasia of pancreas, 245
- Airway management
 - for additional congenital syndromes, 73
 - congenital airway anomalies, 59–61
 - Apert's syndrome, 68
 - Beckwith-Weidemann syndrome, 65
 - cleft lip and palate, 62, 63
 - Crouzon's syndrome, 68
 - Goldenhar syndrome, 68
 - juvenile rheumatoid arthritis, 64
 - Klippel-Feil syndrome, 70
 - laryngeal clefts, 72, 73
 - laryngeal webs, 71, 72
 - laryngotracheomalacia, 61, 62
 - mucopolysaccharidoses, 64
 - obstructive sleep apnea, 68, 69
 - Pierre-Robin syndrome, 66
 - pyriform aperture stenosis, 72
 - subglottic stenosis, 70, 71
 - Treacher Collins syndrome, 66
 - trisomy 21, 65
 - definition of, 57
 - difficult airway, 59
 - endotracheal tube size selection and depth insertion, 61
 - general principles of, 74

- Airway management (*cont.*)
 endotracheal tube, 76
 LMA, 75, 76
 pre-oxygenation, 76
 mallampati classification, 74
 normal airway anatomy, 57–59
 pediatric vs. adult airway, 59
 pre-operative assessment, 73, 74
 tracheal intubation, 74
- Amniotic band syndrome, 427, 428
- Anatomic abnormalities, 112
- Anatomical anomalies
 anatomical landmarks, 360, 361
 burn injuries, 42 (*see* Microstomia)
 connective tissue disorders, 361
 coronoid process hyperplasia, 38
 dural ectasia, 361
 lower extremity, 366–370
 Marfan syndrome, 47, 48
 management of, 48
 oral-facial manifestations of, 48
 masticatory muscle tendon-aponeurosis
 hyperplasia, 39, 40
 management, 40
 oral-facial manifestations of, 40
 neuraxial anesthesia, 359, 361
 placement of, 361
 obesity, 46
 management of, 47
 oral-facial manifestations of, 46
 oral submucous fibrosis, 38
 management, 39
 oral-facial manifestations of, 39
 Rett syndrome, 48, 50
 management of, 50, 51
 oral-facial manifestations of, 50
 scleroderma
 localized, 40
 management in operating room, 42
 oral-facial manifestations of, 41
 systemic, 40
 subcutaneous emphysema, 43
 clinical signs, 43
 etiologies of, 44
 management of, 44
 occurrence of, 44
 symptoms of, 44
 temporomandibular joint, 35
 ankylosis, 37, 38
 closed lock management, 36, 37
 tori
 management of, 51–53
 oral-facial manifestations of, 51
 upper extremity, 362, 363, 365, 366
- Anatomical anomalies of foot and ankle
 deformities
 amniotic band syndrome, 427, 428
 clubfoot, 427
 hypoplasia of lower extremity/fibular
 hemimelia, 428
 sirenomelia, 429
 syndactyly and polydactyly, 429
 tibial hemimelia, 428
 trisomy 21, 427
 musculoskeletal anomalies of the foot and
 ankle (*see* Musculoskeletal
 anomalies of the foot and ankle)
 peripheral nerve anomalies, 429–431
 vascular anomalies, 432, 433
- Anconeus, 401
- Angiotensin-converting enzyme (ACE)
 inhibitors, 258
- Ankylosis, 37
- Annular pancreas, 175, 194, 242–244
- Anomalies of the urachus, 290
- Anomalies of the vas deferens, 298
- Anomalous left pulmonary artery (LPA), 139
- Anomalous muscles
 EDBM, 406
 EMP, 407
 extensor pollicis et indicis, 406
 flexor carpi radialis brevis, 399
 palmaris profundus, 400
- Anomalous origin of LPA from RPA, 140
- Anomalous origin of the pulmonary artery,
 138, 140
- Anomalous pancreaticobiliary junction
 (APBJ), 246, 247
- Anomalous right pulmonary artery (RPA),
 138, 139
- Anterior compartment
 anomalous muscle, 399, 400
 deep muscle, 397–399
 intermediate muscle, 394, 396
 superficial muscles, 392–394
- Anterior infrahyoid muscles, 22
- Anterior interosseous artery (AIA), 444
- Anterior interosseous nerve (AIN), 380, 381
 normal course, 380
 variation and pathology, 380
- Anterior mandibular space, 58
- Anterior scalene muscle, 26
- Anterior superior iliac spine (ASIS), 145
- Anterior tibial artery (ATA), 432, 454
 normal course, 454
- Anterior tibial veins (ATVs), 461
- Anterior urethra, 298
- Anterior urethral valves, 302, 303

- Anteromedial thigh flap, 452
 Aortic arches, 125
 Aortic saturation, 471
 Aortic stenosis, 114, 115
 Apert's syndrome, 68, 429
 Aphalia, 317
 Aplasia cutis congenital and epidermolysis
 bullosa, 187
 Aponeurosis, 5
 Arachnoid mater, 6
 Arch anatomical variants
 cervical aortic arch, 133
 coarctation of the aorta, 129–131
 double aortic arch, 126, 127
 ductus diverticulum, 133, 135
 hypoplastic ascending aorta, 129
 interrupted aortic arch, 131, 133
 patent ductus arteriosus, 133
 right-sided aortic arch, 127, 128
 Arnold's nerve, 99
 Arteria lusoria, 86
 Arterial supply to the spinal cord, 352
 Artery to the vas deferens, 318
 Atrial septal defect (ASD), 470, 477, 479
 Atrialization, 495
 Atrioventricular septal defect (AVSD),
 480, 481
 Auerbach's plexus, 150
 Autosomal dominant PKD (ADPKD), 270
 Autosomal recessive PKD (ARPKD), 270
- B**
- Bare area, 207
 Barrett's esophagus, 150
 Basilic vein (BV), 448
 Beckwith-Wiedemann syndrome, 65, 246
 Behçet disease, 500
 Berretini anastomoses, 385
 Berretini and Riche-Cannieu anastomoses, 387
 Biconcave articular disc, 35
 Bicuspid aortic valve, 484, 499
 Bifurcation, 430, 431
 Bilateral inguinal hernias, 291
 Bilateral microdecompression, 354
 Bilateral renal agenesis, 274
 Bilateral vesicoureteral reflux (VUR), 284
 Biliary anatomy
 choledochal cysts
 anatomy and classification, 230, 231
 management, 231, 232
 gallbladder, anatomy of, 221, 223, 225
 intrahepatic biliary anatomy, 225, 227, 228
 portal triad and pringle maneuver, 228, 230
 Bipartite tibial sesamoid, 421
 Bismuth–Corlette classification of choledochal
 cysts, 231
 Bladder
 anatomy, 288
 congenital abnormalities
 bladder agenesis, 293
 bladder diverticulum, 292
 bladder exstrophy, 291, 292
 bladder septation/duplication, 292
 megacystis, 292, 293
 embryology, 289
 urachus, congenital abnormalities
 patent urachus, 289
 urachal cyst and urachal sinus,
 289, 290
 Bladder agenesis, 293
 Bladder diverticulum, 292
 Bladder exstrophy, 291, 292
 Bladder septation or duplication, 292
 Bland-White-Garland syndrome, 496
 Blood supply
 brain, 8
 esophagus, 148
 face, 11
 gallbladder, 171, 172
 kidneys, 254–256
 large intestine, 165, 166
 lymphatics, 257
 pancreas, 175, 238, 239
 rectum, 169
 small intestine, 161
 stomach, 157
 ureters, 261
 urinary bladder, 263
 Bochdalek's foramen, 275
 Bovine arch, 135, 136
 Bowman's capsule, 253, 258
 Bowman's space, 258
 Brachial artery, 437
 Brachial plexus, 30
 Brachiointerosseous artery (BIA), 442
 Brachioradial artery (BRA), 441
 Brachioradialis, 402
 Brachioulnar artery (BUA), 442
 Brachymetatarsia, 423, 424
 Brain
 blood supply, 8
 brainstem, 8
 cerebellum, 8
 cerebrum, 7
 diencephalon, 8
 ventricular system, 8
 Brainstem, 8

- Branch vessel variants
 aberrant right subclavian artery, 137
 anomalous origin of the pulmonary artery, 138, 140
 bovine arch, 135
 common brachiocephalic trunk, 138
 thyroidea ima artery, 137
- Branchial cleft cyst, 108
- Branchial complex, variations and pathology, 106–108
- Brunner's glands, 162
- Bruxism, 50
- Buck's fascia, 308
- Bulbar urethra, 299
- Bulbourethral artery, 308
- Bulbourethral/cowper's glands, 299
- Buried/concealed penis, 311, 312
- Buried penis, 311
- Burn injuries, 42
- C**
- Calcitonin gene-related peptide (CGRP), 239
- Cantlie's line, 219
- Carbohydrates, 163
- Cardiac anatomic anomalies
 anesthesia management and vascular access
 atrial septal defect, 477
 atrioventricular septal defect, 480
 Behçet disease, 500
 bicuspid aortic valve, 499
 bland-white-garland syndrome, 496
 coarctation of the aorta, 480, 482
 congenital aortic stenosis, 482, 483
 congenital pulmonary stenosis, 480
 cor triatriatum, 498
 dextrocardia, 491
 DORV, 489
 double-outlet left ventricle, 498
 Ebstein's anomaly, 495
 Eisenmenger's syndrome, 491
 HLHS, 491
 idiopathic dilatation of the pulmonary trunk, 494
 idiopathic dilated cardiomyopathy, 502
 infectious aneurysm (mycotic aneurysm), 500
 infective endocarditis, 502
 interrupted aortic arch, 494
 intravascular pulmonary metastases, 501
 Kawasaki disease, 502
 partial anomalous pulmonary venous return, 495
 patent ductus arteriosus, 480
 pulmonary arterial hypertension, 499
 pulmonary artery aneurysm, 494
 pulmonary atresia, 495
 quadricuspid aortic valve, 499
 rasmussen aneurysm, 500
 rheumatic heart disease, 501
 Takayasu arteritis, 501
 TAPVR, 495
 tetralogy of Fallot, 484
 transposition of the great vessels, 484, 487
 tricuspid atresia, 487
 truncus arteriosus, 487
 ventricular septal defect, 477
- anesthetic perioperative management
 history, 473
 intraoperative considerations, 475, 476
 laboratory tests and imaging, 473
 monitoring, 473, 474
 physical examination, 473
 subacute endocarditis prophylaxis, 476
 vascular access, 474, 475
- noncardiac surgery in patients with CHD, 476
 regional anesthesia for, 477
- pathophysiology, 470
 cardiac shunt, 470
 mechanical and dynamic obstruction, 472
 quantification of shunts, 471, 472
- Cardiac shunt, 470
- Carotid artery
 normal course, 81, 82
 variations and pathologies, 82, 83
- Carotid endarterectomies (CEA), 94
- Carpal bipartitions, 410, 411
- Carpal bones
 normal anatomy, 410
 variation
 accessory ossicles, 411
 carpal bipartitions and fusion/coalition, 410, 411
 lunate variation, 411
- Carpal tunnel syndrome (CTS), 376, 443
- Caudal recession syndrome, 429
- Caudate lobe, 210, 225
- Cave of Retzius, 262
- Cavernosal artery, 308
- Central venous pressure (CVP), 477
- Cephalic vein (CV), 447

- Cerebellum, 8
 Cerebral palsy (CP), 120, 121
 Cerebrum, 7
 Cervical aortic arch, 133, 135
 Cholecystectomy, 225
 Cholecystokinin (CCK), 157, 173
 Choledochal cysts
 anatomy and classification, 230, 231
 management, 231, 232
 Chordee, 314
 Choroid plexus, 10
 Chwalla's membrane, 278
 Chylothorax, 103
 Circular pharyngeal muscles, 24, 25
 Classic mammalian feature, 104
 Cleft lip and palate, 62, 63
 Clitoromegaly, 330, 331
 Clubfoot, 427
 Coalition, 423–425
 Coarctation of the aorta, 129–131, 480,
 482, 483
 Common brachiocephalic trunk, 138, 139
 Common carotid artery (CCA), 81, 82
 Common congenital syndromes, regional
 anesthesia
 achondroplasia, 116
 aortic stenosis, 114, 115
 cerebral palsy, 120, 121
 EDS, 118
 noonan syndrome, 113, 114
 obesity, 116
 scoliosis, 118–120
 trisomy 18, 121
 trisomy 21, 117
 turner syndrome, 111–113
 Common hepatic artery, 239
 Common interosseous artery (CIA), 444
 Communicating hydroceles, 323
 Complete androgen insensitivity syndrome
 (CAIS), 334
 Complete ankylosis, 38
 Complete SPA, 445
 Complete superficial palmar arch patterns, 446
 Complete ureteral duplication with
 hydroureteronephrosis, 281
 Compression neuropathy of the radial sensory
 nerve, 390
 Concealed penis with phimosis, 313
 Congenital absence of Vas, 297
 Congenital adrenal hyperplasia
 (CAH), 329–331
 Congenital airway anomalies, 59–61
 Apert's syndrome, 68
 Beckwith-Wiedemann syndrome, 65
 cleft lip and palate, 62, 63
 Crouzon's syndrome, 68
 Goldenhar syndrome, 68
 juvenile rheumatoid arthritis, 64
 Klippel–Feil syndrome, 70
 laryngeal clefts, 72, 73
 laryngeal webs, 71, 72
 laryngotracheomalacia, 61, 62
 mucopolysaccharidoses, 64
 obstructive sleep apnea (OSA), 68, 69
 Pierre–Robin syndrome, 66
 pyriform aperture stenosis, 72
 subglottic stenosis, 70, 71
 Treacher–Collins syndrome, 66
 trisomy 21, 65
 Congenital aortic stenosis, 482, 483
 Congenital constriction syndrome, 427
 Congenital esophageal stenosis, 180, 181
 Congenital heart disease (CHD), 469, 470
 noncardiac surgery in patients
 with, 476
 regional anesthesia for, 477
 pathophysiology, 470
 Congenital megaprepuce, 311
 Congenital microgastria, 186
 Congenital nasal pyriform aperture stenosis
 (CNPAS), 72
 Congenital pancreatic cyst, 246
 Congenital penile curvature, 314
 Congenital pulmonary stenosis, 480
 Congenital seminal vesicle cyst, 297
 Congenital urethral strictures, 300
 Connective tissue disorders, 361
 Continuous positive airway pressure, 69
 Cor triatriatum, 498
 Coronoid impingement syndrome, *see*
 Coronoid process hyperplasia
 Coronoid process hyperplasia, 38
 Cortical collecting tubes, 259
 Couinaud's segments, 212
 Cranial nerve VII, *see* Facial nerve
 Cranial nerves, 9–10
 Cremasteric artery, 318
 Cricothyroid muscle, 24
 Crossed fused renal ectopia, 271, 273
 Crossed renal ectopia anomalies, 274
 Crouzon's syndrome, 68
 Cruciate anastomosis, 451
 Cryptorchidism, 319–322
 Ctrioventricular canal defect, 480
 Cutaneous sensation, 10
 Cyst of the spermatic cord, 325
 Cystic artery, 171
 Cystic veins, 172

D

- Deep branch of the radial nerve, 391
 - normal course, 390
 - variations and pathology, 392
 - Deep muscle
 - abductor pollicis longus, 405
 - EIP, 406
 - EPB, 405, 406
 - EPL, 405
 - flexor digitorum profundus, 397
 - flexor pollicis longus, 398
 - pronator quadratus, 399
 - supinator, 404
 - Deep palmar arch (DPA), 444, 446, 447
 - Deep plantar venous arch (DPVA), 462
 - Deep veins, 308, 447
 - Deep venous thrombosis (DVT), 459
 - Descending genicular artery (DGA), 453
 - normal course, 452
 - variations and pathology, 452
 - Dextrocardia, 491, 494
 - Dextro-transposition (D-TGV), 484
 - Dextro-transposition of the great vessels (d-TGV), 486
 - Diaphragm, 152
 - Diencephalon, 8
 - Dietl's crisis, 277
 - Differentiation or development (DSD)
 - congenital adrenal hyperplasia, 329–331
 - definition, 329
 - Müllerian (paramesonephric) ducts, 332
 - MRKH syndrome, 333
 - persistent Müllerian ducts, 332
 - partial and complete androgen insensitivity, 333
 - complete androgen insensitivity syndrome (CAIS), 334
 - partial androgen insensitivity syndrome, 335
 - Difficult airway, 59
 - Difficult mask ventilation (DMV), 76
 - Digastric muscle, 21
 - normal course, 105
 - variations and pathology, 105
 - Diphallia, 317
 - Disc kidney (doughnut, shield, pancake kidney), 274
 - Disorder of sex development (DSD), 316, 334
 - Divided carpals, 410
 - Dorsal artery, 308
 - Dorsal branch of the ulnar nerve, 383
 - Dorsal venous arch (DVA), 462
 - Dorsalis pedis artery (DPA), 432, 456, 457
 - Double aortic arch, 126
 - Double-outlet left ventricle, 498
 - Double-outlet right ventricle, 489, 490
 - Down syndrome, *see* Trisomy 21
 - Duct of wirsung, 238
 - Ductal anatomy, 238
 - Ductal variants, 246, 247
 - Ductus diverticulum, 133, 135, 136
 - Duodenal atresia and stenosis, 190, 192, 194
 - Duodenal blood supply, 161
 - Duodenal fossae
 - duodenojejunal fossa, 347
 - fossa of Landzert, 343, 344
 - fossa of Waldeyer, 343, 344
 - right and left retroduodenal fossae, 347, 348
 - superior and inferior duodenal/paraduodenal fossae, 344, 347
 - Duodenal web, 193
 - Duodeno-duodenostomy, 193, 194
 - Duodenojejunal fossa, 347
 - Duodenum
 - annular pancreas, 194
 - duodenal atresia and stenosis, 190, 192, 194
 - jejuno-ileal atresia, 195, 196
 - preduodenal portal vein, 194
 - rotational abnormalities, 189, 190
 - Duplicate urethra, 307
 - Duplicated superficial femoral artery (DSFA), 449
 - Duplication of ulnar artery, 443
 - Duplications cyst, 182, 183
 - Dura mater, 6
 - Dural ectasia, 361
 - Dural venous sinuses, 6
- E**
- Eastric muscularis externa, 158
 - Ebstein's anomaly, 495, 498
 - Ectopic pancreas, 243–245
 - Ectopic right testicle, distal, 320
 - Ectopic ureters, 278
 - Ectopic vas deferens, 297
 - Edwards syndrome, *see* Trisomy 18
 - Extensor digitorum longus (EDL), 426
 - Ehlers–Danlos syndrome (EDS), 118
 - Eisenmenger's syndrome, 471, 477, 491, 493
 - Endoscopic retrograde
 - cholangiopancreatography (ERCP), 241
 - Endotracheal tube (ETT), 61, 76
 - Epispadias, 316, 317

- Esophageal atresia (EA), *see*
Tracheoesophageal fistula (TEF)
- Esophageal cardiac glands, 150
- Esophageal cysts, 182
- Esophageal stenosis, 180
- Esophageal webs and rings, 181, 182
- Esophagus, 146
 - blood supply, 148
 - congenital esophageal stenosis, 180, 181
 - duplications cyst, 182, 183
 - embryological development, 147
 - esophageal wall, 147
 - esophageal webs and rings, 181, 182
 - histology, 149, 150
 - innervation, 148
 - lymphatic drainage, 148
 - physiology, 151
 - tracheoesophageal fistula, 183–186
- Extensor carpi radialis brevis (ECRB), 402
- Extensor carpi radialis longus (ECRL), 402
- Extensor carpi ulnaris (ECU), 403
- Extensor digiti minimi (EDM), 402, 403
- Extensor digitorum brevis manus (EDBM), 406, 408
- Extensor digitorum communis (EDC), 402, 403
- Extensor indicis proprius (EIP), 406, 407
- Extensor medii proprius (EMP), 407, 409
- Extensor pollicis brevis (EPB), 405, 406
- Extensor pollicis et indicis, 406, 408
- Extensor pollicis longus (EPL), 405
- External branch of the superior laryngeal nerve (EBSLN), 97
- External carotid artery (ECA), 81–83
- F**
- Face
 - blood supply, 11
 - cutaneous sensation, 10
 - muscles, 11
 - parotid gland, 11
- Facial artery
 - normal anatomy, 88
 - variations, 88, 89
- Facial nerve
 - normal course, 98
 - variations and pathologies, 98, 99
- Factor XI deficiency, 114
- Fascial layers, 15, 16
- Fats, 163
- Female pelvis, 261
- Female urethra, 264
 - anatomy, 299
 - embryology, 299
- Femoral artery (FA)
 - normal course, 449
 - variations and pathology, 449, 450
- Femoral vein (FV), 458
- Femoropopliteal vein (FPV), 459
- Fentanyl, 476
- Fetal hydronephrosis, 277
- Fibrocartilaginous synchondrosis, 422
- First branchial cleft, 108
- First dorsal interosseous muscle (FDIM), 458
- First dorsal metatarsal artery (FDMA), 458
- Flavectomy, 354
- Flexor carpi radialis (FCR), 392
- Flexor carpi radialis brevis (FCRB), 399
- Flexor carpi ulnaris (FCU), 392
- Flexor digitorum brevis (FDB), 420
- Flexor digitorum profundus (FDP), 397
- Flexor digitorum superficialis (FDS), 394, 396, 397
- Flexor hallucis longus (FHL) tendon, 422
- Flexor pollicis longus (FPL), 398, 400
- Foregut structures, 149
- Fossa navicularis, 299
- Fossa of Landzert, 343, 344
- Fossa of Waldeyer, 343, 344, 346
- Frenulum breve*, 312
- Frontal lobe, 7
- Fusion/coalition, 410, 411
- G**
- Galactose, 163
- Gallbladder anatomy, 221, 223, 225
- Gantzer's muscle, 398
- Gastric atresia, 186, 187
- Gastroesophageal (GE) junction, 155
- Gastrointestinal system, anatomy of
 - abdominal cavity
 - abdominal structures, 153, 154
 - inguinal canal, 154, 155
 - muscle layers, 151–153
 - esophagus, 146
 - achalasia, 147
 - blood supply, 148
 - embryology, 147, 148
 - esophageal wall, 147
 - histology, 149, 150
 - innervation, 148
 - lymphatic, 148
 - musculature, 147
 - physiology, 151
 - tracheoesophageal fistulas (TEs), 147
 - gallbladder, 170

- Gastrointestinal system, anatomy of (*cont.*)
- blood supply, 171, 172
 - embryology, 171
 - histology, 172
 - innervation, 171
 - lymphatic, 172
 - physiology, 172, 173
 - structure, 170
 - large intestine, 163
 - blood supply, 165, 166
 - embryology, 164
 - Hirschsprung's disease, 165
 - histology, 167
 - innervation, 165
 - lymphatic, 166
 - omphalocele, 164
 - physiology, 167, 168
 - structure, 164
 - pancreas, 173
 - blood supply, 175
 - embryology, 174, 175
 - histology, 176
 - innervation, 175
 - lymphatic channels, 176
 - physiology, 176, 177
 - structure, 173, 174
 - rectum, 168
 - blood supply, 169
 - embryology, 169
 - histology, 170
 - innervation, 169
 - lymphatics, 170
 - physiology, 170
 - structure, 168
 - small intestine
 - blood supply, 161
 - embryology, 160
 - histology, 162
 - innervation, 160
 - lymphatic vessels, 161, 162
 - physiology, 162, 163
 - structure, 158, 159
 - stomach
 - blood supply, 157
 - embryology, 156
 - hepatogastric ligament, 155
 - histology, 158
 - innervation, 156, 157
 - lymphatic drainage, 157
 - structure, 155
 - surface anatomy, 145, 146
- Gastrointestinal tract, anomalies of
- duodenum
 - annular pancreas, 194
 - duodenal atresia and stenosis, 190, 192, 194
 - jejuno-ileal atresia, 195, 196
 - preduodenal portal vein, 194
 - rotational abnormalities, 189, 190
 - esophagus
 - congenital esophageal stenosis, 180, 181
 - duplications cyst, 182, 183
 - esophageal Webs and Rings, 181, 182
 - tracheoesophageal fistula, 183–186
 - omphalomesenteric duct, 196
 - Meckel's diverticulum, 196–199
 - umbilical band, 200, 201
 - umbilical enteric fistula, 200
 - umbilical polyps, 200
 - stomach
 - gastric atresia, 186, 187
 - hourglass stomach, 189
 - microgastria, 186
 - pyloric stenosis, 188
- Geniohyoid, 20
- Genitoplasty, 331
- Genitourinary system, anatomy of, 251
- kidneys
 - blood supply, 254–256
 - embryology, 254
 - histology and physiology, 257–259
 - innervation, 254
 - lymphatics, 257
 - structure, 252–254
 - lymphatics and bloodstream, 251
 - ureters, 259
 - blood supply, 261
 - innervation, 260
 - lymphatics, 261
 - structure, 260
 - urethra
 - clinical, 264
 - female, 264
 - male, 263
 - urination, 264
 - urinary bladder, 261–263
- Ghrelin, 157
- Glanular urethra, 299
- Glucagon, 177
- Glucose, 163
- Goldenhar syndrome, 68
- Gonadotropin-releasing hormone (GnRH), 321
- Grave's disease, 96
- Great saphenous vein (GSV), 459, 460
- Greater sac, 154
- Guyon's canal compression zones, 384
- Guyon's canal syndrome, 384

H

Head anatomy
 brain
 blood supply, 8
 brainstem, 8
 cerebellum, 8
 cerebrum, 7
 diencephalon, 8
 ventricular system, 8
 face
 blood supply, 11
 cutaneous sensation, 10
 muscles, 11
 parotid gland, 11
 meninges, 5
 arachnoid mater, 6
 dura mater, 6
 pia mater, 6, 7
 oral cavity
 palate, 11
 submandibular and sublingual
 glands, 13
 tongue, 12
 scalp, 5
 skull, 3, 4
 Hemifacial macrosomia, *see* Goldenhar
 syndrome
 Hemihepatectomy, 212
 Hemorrhage, 89
 Henle's loop, 254, 258
 Hepatic anatomy
 hepatocyte, 205–207
 liver segments, 210, 211
 nomenclature, 212
 surface anatomy, 207, 208
 Hepatic arterial supply, 216
 Hepatic vein anatomy, 217, 219, 220
 Hepatic veins and fissures, 220
 Hepatobiliary anatomy, 205
 Hepatobiliary disease, 205
 Hepatocyte, 205–207
 Hernia ureteri inguinale, 332
 Heterotaxia syndromes (HS), 190
 Heterotopic pancreas, *see* Ectopic
 pancreas
 Hilum, 252
 Hirschsprung's disease, 165
 Horner's syndrome, 101
 Horseshoe kidney, 271, 272
 Hourglass stomach, 189
 Human gastrointestinal tract, 159
 Hydroceles, 322–324
 Hydronephrosis, 271
 Hyoglossus muscle, 21, 22

Hypertrophic cardiomyopathy, 113
 Hypertrophic pyloric stenosis
 (HPS), 188
 Hypoglossal nerve (cranial nerve XII), 29
 normal course, 93
 variations and pathologies, 93, 94
 Hypoplasia, 129
 lower extremity/fibular hemimelia, 428
 of seminal vesicle, 297
 Hypoplastic ascending aorta, 129
 Hypoplastic left heart syndrome (HLHS), 472,
 491, 492
 Hypospadias, 315, 316
 Hypothalamus, 8
 Hypothyroidism, 111
 Hysterectomy, 288

I

Iatrogenic injury of the vagus nerve, 99
 Iatrogenic SE, 44
 Idiopathic dilatation of the pulmonary
 trunk, 494
 Idiopathic dilated cardiomyopathy, 502
 Incomplete SPA, 445
 Incomplete superficial palmar arch
 patterns, 447
 Infantile hypertrophic pyloric stenosis, 155
 Infectious aneurysm (mycotic aneurysm), 500
 Infective endocarditis, 502
 Inferior ectopia, 271
 Inferior pharyngeal constrictor muscle, 25
 Infraclavicular brachial plexus block, 363
 Inguinal canal, 154, 155
 Inguinal hernia, 325
 Innominate artery
 normal course, 83
 variations and pathology, 83, 85
 Intermediate muscle, 394, 396
 Intermediate veins, 308
 Internal carotid artery (ICA), 81, 83
 Internal jugular vein (IJV), 93
 Internal mesenteric artery (IMA), 169
 Internal oblique muscle, 152
 Internal sphincter, 288
 Interrupted aortic arch (IAA),
 131–133, 494
 Interscalene brachial plexus
 block, 363
 Intrahepatic biliary anatomy, 225–228
 Intrahepatic biliary ductal system, 225
 Intravascular pulmonary metastases, 501
 Intravenous induction, 475
 Ischemic preconditioning, 230

J

Jejunal vasculature, 159
 Jejuno-ileal atresia, 195, 196
 Juvenile rheumatoid arthritis, 64
 Juxtaglomerular apparatus (JG), 259

K

Kawasaki disease, 502
 Ketamine, 475
 Kidney abnormalities, 111
 Kidneys, 251, 253, 255

- in abdominal cavity, 252
- abnormalities, 111
- anatomic relations to adjacent organs, 268
- anatomy, 267, 268
- blood supply, 254–256
- congenital anomalies
 - anomalies of number, 274
 - fusion anomalies, 271, 274
 - multicystic dysplastic kidney, 269, 270
 - polycystic kidney disease, 270
 - renal duplication, 270, 271
 - renal ectopia, 275
 - rotation anomalies, 274
- embryology, 254, 269
- histology and physiology, 257–259
- innervation, 254
- lymphatics, 257
- structure, 252–254

Kiloh-Nevin syndrome, 380
 Kimura technique, 193
 King-Denborough syndrome, 114
 Kinking, 83
 Klippel–Feil syndrome, 70
 Klippel–Trenaunay syndrome (KTS), 459
 Kyphoplasty (KP), 350

L

Large-bore peripheral intravenous (LBPIV), 474, 477
 Large esophageal duplication, 182
 Laryngeal clefts, 72, 73
 Laryngeal mask airways (LMAs), 64, 69, 75, 76
 Laryngeal muscles, 24
 Laryngeal webs, 71, 72
 Laryngotracheomalacia, 61, 62
 Lateral antebrachial cutaneous nerve (LACN), 390
 Lateral femoral circumflex artery (LFCA)

- normal course, 451
- variations and pathology, 452

 Lateral plantar artery (LPA), 456
 Left colic flexure, 165
 Left grade III varicocele, 326

Left hepatic duct, 227
 Left medial duct, 227
 Left paraduodenal fossa, 343
 Left retroduodenal fossa, 348
 Left upper quadrant (LUQ), 159
 Left ventricular hypertrophy, 114–115
 Levator scapulae muscles, 17
 Levo-transposition (L-TGV), 487
 Liver masses, 232
 Localized scleroderma, 40
 Longitudinal pharyngeal muscles, 25
 Longus colli muscle, 26
 Loose connective tissue, 5
 Love handles, 146
 Lower extremity, 366–370
 L-shaped kidney (tandem kidney), 274
 Lumbar disc herniation (LDH)

- complications, 353
- postoperative care, 353
- surgical intervention, 353
- types, 353

 Lumbar stenosis (LSS), 353

- postoperative care, 354
- surgical intervention, 354
- symptoms/complications, 354
- types/causes, 354

 Lump kidney (cake kidney), 274
 Lunate types, 412
 Lunate variation, 411
 Lymphatics, thoracic duct

- normal anatomy, 101, 102
- variations and anomalies, 101–104

M

Magnetic resonance cholangiopancreatography (MRCP), 241, 243
 Male penis

- anatomy, 306, 308
- congenital anomalies
 - buried/concealed penis, 311, 312
 - congenital penile curvature, 314
 - epispadias, 316, 317
 - Frenulum breve*, 312
 - hypospadias, 315, 316
 - microphallus/micropenis, 312, 313
 - penile agenesis, 317
 - penile duplication, 317
 - penile torsion, 310, 311
 - penoscrotal webbing, 312
 - phimosis, 309, 310
- embryology, 309

 Male urethra, 263

- anatomy, 298, 299
- embryology, 299

 Malignant hyperthermia (MH), 114

- Mallampati classification system, 74, 75
 Mallory-Azan staining, 176
 Malrotation and midgut volvulus, 189, 190
 Mandibular hypoplasia and anteriorly displaced tongue, 58, 66
 Mandibulo-facial Dysostosis, *see* Treacher Collins syndrome
 Marfan syndrome (MFS), 47–49
 management of, 48
 oral-facial manifestations of, 48
 Marinacci communication, 378, 379
 Martin-Gruber anastomoses, 379
 Masticatory muscle tendon-aponeurosis hyperplasia (MMAH), 39, 40
 Mayer-Rokitansky-Küster-Hauser (MRKH) syndrome, 333
 Mechanical and dynamic obstruction, 472
 Meckel's diverticulum (MD), 196–199
 Medial femoral circumflex artery (MFCA)
 normal course, 451
 variations and pathology, 451
 Medial plantar artery (MPA), 456, 457
 Median artery, 440, 443
 Median nerve, 376, 377
 normal course, 375
 palmar cutaneous branch
 normal course, 378
 variations and pathology, 378–380
 variations and pathology, 376, 378
 Median vein (MV), 448
 Megacolon, 165
 Megacystis, 292, 293
 Megaureter, 283, 284
 Meissner's plexus, 150
 Membranous urethra, 298
 Meninges, 5
 arachnoid mater, 6
 dura mater, 6
 pia mater, 6, 7
 Mental prominence, 51
 Mermaid syndrome, *see* Sirenomelia
 Meyer-Cotton grading system for subglottic stenosis, 71
 Microdecompression, 354
 Microgastria, 186
 Micrognathia, 66
 Micropenis, 312
 Microphallus/micropenis, 312, 313
 Microstomia, 42
 management of, 43
 manifestations of, 42
 Microsurgical dissection, 353
 Micturition, 264
 Middle (medius) scalene muscle, 26
 Middle pharyngeal constrictor muscle, 25
 Mild pulmonary hypertension, 499
 Mild right hydronephrosis, 277
 Morrison's pouch, 154
 Mucopolysaccharidoses, 64
 Müllerian (paramesonephric) ducts, 332
 MRKH syndrome, 333
 persistent Müllerian ducts, 332
 Müllerian inhibiting substance, 329
 Multicystic dysplastic kidney (MCDK), 269, 270
 Multidetector row computed tomography (MDCT), 103
 Muscle sparing approach, 184
 Muscles, face, 11
 Muscles of mastication, 12, 34
 Muscularis externa, 150
 Muscularis mucosae, 149
 Musculoskeletal anomalies of foot and ankle
 accessory musculotendinous structures, 425–427
 brachymetatarsia, 423
 coalition, 423, 424
 common accessory and sesamoid bones of the foot, 420, 422
 uncommon accessory and sesamoid bones of the foot and ankle, 423
 Mycotic aneurysm, 500
 Mylohyoid muscle, 21
 Myocardial ischemia, 491
- N**
- Neck anatomy, 14
 bones and cartilages, 17, 18
 fascial layers, 15, 16
 musculature, 18
 anterior infrahyoid muscles, 22
 beneath the mandible, 20–24
 circular pharyngeal muscles, 24, 25
 digastric muscle, 21
 floor of oral cavity, 20–24
 geniohyoid, 20
 hyoglossus muscle, 21, 22
 laryngeal muscle, 24
 longitudinal pharyngeal muscles, 25
 mylohyoid muscle, 21
 omohyoid muscle, 22
 prevertebral muscles, 25, 26
 sternocleidomastoid muscle, 18, 19
 sternothyroid muscle, 22
 stylohyoid muscle, 21
 subclavius muscle, 20
 suprahyoid muscles, 20–24
 thyrohyoid muscle, 22
 platysma, 14, 15
 Neonatal circumcision, 310
 Neonatal torsion, 327

Nerves

- facial nerve
 - normal course, 98
 - variations and pathologies, 98, 99
 - hypoglossal nerve (cranial nerve XII)
 - normal course, 93
 - variations and pathologies, 93, 94
 - phrenic nerve
 - normal anatomy, 100
 - variations and anomalies, 101
 - recurrent laryngeal nerve
 - normal course, 94, 95
 - variations and pathologies, 95, 96
 - superior laryngeal nerve
 - normal course, 97
 - variations and pathologies, 97, 98
 - vagus nerve
 - normal course, 99
 - variations and pathology, 99, 100
- Neuraxial and peripheral nerve blocks, 359
 Neuraxial anesthesia, 115, 359, 361
 Neurocranium, 3, 4
 Neuromuscular scoliosis, 355
 Neurovasculature, 27–31
 Non-communicating hydroceles, 322, 323
 Non-invasive ventilation, 62
 Nonrecurrent laryngeal nerve, 96
 Noonan syndrome, 113, 114
 Normal aortic arch, 124
 Normal vertebral column, 351

O

- Obesity, 46, 116
 - management of, 47
 - oral-facial manifestations of, 46
- Obstructive sleep apnea (OSA), 68–70
 Occipital lobe, 8
 Oculo-auriculo-vertebral syndrome, *see*
 Goldenhar syndrome
 Omohyoid muscle, 22
 Omphalocele, 164
 Omphalomesenteric duct (OMD), 196
 - Meckel's diverticulum, 196–199
 - umbilical band, 200, 201
 - umbilical enteric fistula, 200
 - umbilical polyps, 200
- Omphalomesenteric remnants, 196
 Opioids, 476
 Oral cancer, 39
 Oral cavity
 - palate, 11
 - submandibular and sublingual glands, 13
 - tongue, 12

- Oral submucous fibrosis (OSF), 38
 - management, 39
 - oral-facial manifestations of, 39
- Oral-facial manifestations
 - of Marfan syndrome, 48
 - of obesity, 46
 - of oral submucous fibrosis, 39
 - with Rett syndrome, 50
 - of scleroderma, 41
 - of Tori, 51
- Os intermetatarsium, 422
 Os peroneum, 421
 Os styloideum (carpal boss), 411
 Os subfibulare, 423
 Os subtibiale, 423
 Osteochondromas, 38
 Osteomas, 38
 Osteoporosis, 349
 - primary, 349
 - vertebral fractures, 350
- Os tibiale externum, 421
 Os trigonum, 421
 Os vesalianum, 422

P

- Palatal torus, 52
 Palate, 11, 13
 Palatopharyngeus muscle, 25
 Palmar cutaneous nerve (PCN)
 - normal course, 378
 - variations and pathology, 378–380
- Palmaris longus (PL), 379, 393–395
 Palmaris profundus, 400
 Pancreas, 235
 - anatomy
 - blood supply, 238, 239
 - ductal anatomy, 238
 - innervation, 239
 - lymphatic drainage, 239
 - spatial orientation, 237
 - annular pancreas, 244
 - autonomic nerve supply, 242
 - congenital anomalies and normal variants
 - of pancreas and pancreatic duct
 - agenesis and hypoplasia of pancreas, 245
 - annular pancreas, 242, 243
 - ductal variants, 246, 247
 - ectopic pancreas, 243–245
 - pancreas divisum, 240, 242
 - pancreatic cysts, 246
 - ectopic pancreas, 245
 - embryologic development, 235, 236

- In vivo* orientation of, 237
- normal pancreatic ductal configuration, 238
- pancreas divisum, 243
- pancreatic arterial supply, 240
- pancreatic hypoplasia, 245
- pancreatic lymph drainage, 241
- Pancreas divisum, 175, 240, 242, 243
- Pancreatic cysts, 246
- Pancreatic exocrine secretions, 176
- Pancreatic hypoplasia, 245
- Pancreaticobiliary system, 174
- Pandora's box, 104
- Paracolic gutters (recesses), 154
- Paraduodenal hernias, 345
- Paralytatics, 63
- Paraphimosis, 310
- Parasympathetic fibers, 264
- Parasympathetic innervation, 156
- Parasympathetic stimulation of the small intestine, 161
- Parietal lobe, 8
- Parotid gland, 11
- Partial and complete androgen insensitivity, 333, 334
- Partial androgen insensitivity syndrome (PAIS), 335
- Partial anomalous pulmonary venous return, 495
- Patent ductus arteriosus (PDA), 133, 134, 480, 482
- Patent processus vaginalis, 323
- Patent urachus, 289
- Pediatric vs. adult airway, 59
- Pendulous/penile urethra, 299
- Penile agenesis, 317
- Penile arterial anatomy, 308
- Penile curvature, 315
- Penile duplication, 317
- Penile torsion, 310, 311
- Penoscrotal fusion, 314
- Penoscrotal webbing, 312
- Pentoxifylline, 34
- Percutaneous vertebroplasty (VP), 350
- Peripheral nerve anomalies of the foot and ankle, 429–431
- Peripheral nerve block (PNB), 366
- Peristalsis, 151
- Peroneal artery (PRA)
 - normal course, 454
 - variations and pathology, 455, 456
- Peroneal veins (PRVs), 462
- Peroneocalcaneus internus muscle, 426
- Peroneus brevis (PB) tendons, 425
- Peroneus tertius, 426
- Persistent fetal branches, 83
- Persistent Müllerian ducts, 332
- Persistent primitive hypoglossal, 83
- Persistent sciatic artery (PSA), 449, 450, 459
- Phimosis, 309, 310
- Phrenic nerve
 - normal anatomy, 100
 - variations and anomalies, 101
- Physical therapy, 34, 40, 43
- Physiology, 158
- Pia mater, 6, 7
- Pierre-Robin syndrome, 66, 67
- Plantar Arch (PAA), 457, 458
- Platysma, 14, 15
- PNB placement, 366, 368, 370
- Podocytes, 258
- Polycystic disease, 246
- Polycystic kidney disease (PKD), 270
- Polymethylmethacrylate (PMMA), 350
- Polysplenia syndrome, 245
- Popliteal artery (PLA), 454
- Popliteal vein (FV), 459
- Popliteal-tibial-peroneal arteries, 455
- Portal triad and pringle maneuver, 228, 230
- Portal vein, 220–222
- Portal vein embolization (PVE), 232
- Portal vein/hepatic vein relationship, 216
- Postductal type, 131
- Posterior abdominal wall muscles, 153
- Posterior accessory great saphenous vein (PAGSV), 460
- Posterior compartment
 - anomalous muscles, 406, 407
 - deep muscles, 404–406
 - superficial muscles, 400–403
- Posterior interosseous artery (PIA), 444
- Posterior interosseous nerve (PIN), 390
- Posterior interosseous nerve compression syndrome, 392
- Posterior scalene muscle, 26
- Posterior spinal fusion and instrumentation (PSFI), 356
- Posterior tibial artery (PTA), 433, 454
- Posterior tibial tendon (PTT), 421
- Posterior tibial veins (PTVs), 461
- Posterior urethral valve (PUV), 300–303
- Posterior urethral valves, type 1 variant, 301
- Postoperative nausea and vomiting (PONV), 116
- Postsynaptic parasympathetic neurons, 14
- Potter's syndrome, 274
- Preductal type, 130
- Preduodenal portal vein, 194
- Pre-oxygenation, 76

- Prevertebral muscles, 25, 26
 Primary bladder exstrophy, 291
 Primary obstructive megaureter, 283
 Primary osteoporosis, 349
 Pringle maneuver, 229
 Proatlantal intersegmental arteries, 83
 Profunda artery perforator (PAP) flap, 451
 Profunda femoris artery (PFA)
 normal course, 450
 variations and pathology, 450, 451
 Pronator quadratus (PQ), 399
 Pronator teres (PT), 394
 Propofol, 475
 Prostaglandin E1 (PGE1), 133
 Prostate
 anatomy, 293–295
 congenital abnormalities
 prostatic agenesis, 295
 prostatic cysts, 295
 prostatic hypoplasia, 295
 embryology, 295
 Prostatic agenesis, 295
 Prostatic cysts, 295
 Prostatic hypoplasia, 295
 Prostatic urethra, 298
 Proteins, 163
 Proximal posterior tibial, 454
 Pulmonary arterial hypertension, 499
 Pulmonary artery aneurysm, 494
 Pulmonary artery catheter (PAC), 474, 480
 Pulmonary atresia, 495, 497
 Pulmonary hypertension (PHT), 477
 Pulmonary vascular resistance (PVR), 472
 Pyloric stenosis, 188
 Pyriform aperture stenosis, 72
 normal course, 389
 variations and pathology, 390
 Radial recurrent artery (RRA), 444
 Radial sensory nerve (RSN), 389
 Radial tunnel syndrome, 392
 Radiation therapy-induced trismus, 34
 Rasmussen aneurysm, 500
 Rectosphincteric reflex, 170
 Rectus abdominis muscle, 152
 Rectus capitis anterior muscle, 26
 Rectus capitis lateralis muscle, 26
 Recurrent digital ischemia, 443
 Recurrent laryngeal nerve (RLN)
 normal course, 94, 95
 variations and pathologies, 95, 96
 Regional and neuraxial anesthesia, 120
 Regional anesthesia, 362
 achondroplasia, 116
 aortic stenosis, 114, 115
 cerebral palsy, 120, 121
 EDS, 118
 Noonan syndrome, 113, 114
 obesity, 116
 scoliosis, 118–120
 Trisomy 18, 121
 Trisomy 21, 117
 Turner syndrome, 111–113
 Regional anesthesia for noncardiac surgery,
 CHD, 477
 Renal agenesis, 274
 Renal arteries and veins, 257
 Renal blood flow (RBF), 258
 Renal blood supply and drainage, 268
 Renal crossed fused anomalies, 273
 Renal duplication, 270, 271
 Renal ectopia, 275
 Renal malrotation, 274
 Renal parenchyma, 267
 Restricted mouth opening (RMO), 33
 Retrocaval ureter, 283
 Retromalleolar conflict, 426
 Retroperitoneal hematomas, 368
 Rett syndrome (RTS), 48, 50
 management of, 50, 51
 oral-facial manifestations of, 50
 Rheumatic heart disease, 501
 Rib notching in coarctation of the aorta, 131
 Riche-Cannieu anastomosis (RCA), 385
 Right and left retroduodenal fossae, 347, 348
 Right anterior biliary duct, 228
 Right hepatic vein (RHV), 219
 Right internal jugular vein (RIJ), 474
 Right lower quadrant (RLQ), 159
 Right paraduodenal fossa, 344
- Q**
 Quadricuspid aortic valve, 499
 Quantification of shunts, 471, 472
- R**
 Radial artery, 438
 Radial artery agenesis, 443
 Radial artery distal takeoff, 442
 Radial collateral artery (RCA), 444
 Radial forearm flaps, 441
 Radial nerve, 388
 deep branch of
 normal course, 390
 variations and pathology, 392
 normal course, 385
 superficial branch of

- Right posterior duct, 228
- Right-sided aortic arch, 127, 128
- Right-sided aortic arch with aberrant left subclavian artery, 127, 128
- Right-sided aortic arch with a retropharyngeal component, 128
- Right-sided aortic arch without a retropharyngeal component, 128
- Root canal therapy, 35, 48
- Rotational abnormalities, 189, 190
- Rugae, 158

- S**
- Sandal gap, 427
- Scalp, anatomy of, 5
- Scleroderma, 40, 41
 - localized, 40
 - management, 41, 42
 - oral-facial manifestations of, 41
 - systemic, 40
- Scoliosis, 112, 119, 120
 - definition of, 355
 - postoperative care, 356
 - surgical interventions, 355
 - symptoms/complications, 355
 - types/causes, 355
- Second branchial cleft cyst, 107
- Secondary ossification centers, 411
- Sectionectomy, 212
- Sedation, 48
- Segment nomenclature, 213
- Segmentectomies, 212
- Selective pulmonary vasodilators, 499
- Seminal colliculus, 296
- Seminal vesicle agenesis, 296
- Seminal vesicles and vas deferens
 - anatomy, 295, 296
 - congenital abnormalities
 - congenital absence of the vas, 297
 - congenital seminal vesicle cyst, 297
 - ectopic vas deferens, 297
 - hypoplasia of the seminal vesicle, 297
 - seminal vesicle agenesis, 296
 - embryology, 296
- Senning procedure, 484
- Sensory (afferent) fibers, 161
- Serosa, 150
- Sesamoid bones
 - common, of foot, 420, 422
 - uncommon, of foot and ankle, 423
- Short saphenous vein (SSV), 460
- Short saphenous vein–Giacomini vein, 461
- Sigmoid or S-shaped kidney, 271
- Sirenomelia, 429
- Skull, anatomy of, 3, 4
- Sniffing position, 59
- Soft tissue
 - branchial complex, 106–108
 - digastric muscle
 - normal course, 105
 - variations and pathology, 105
 - sternocleidomastoid muscle
 - normal anatomy, 104
 - variations and pathology, 104, 105
 - thyroglossal duct, 106, 107
- Somatostatin, 177
- Space of Retzius, 288
- Sternocleidomastoid muscle (SCM), 18, 19
 - normal anatomy, 104
 - variations and pathology, 104, 105
- Sternothyroid muscle, 22
- Stomach
 - anatomy, 156
 - blood supply, 157
 - embryology, 156
 - gastric atresia, 186, 187
 - histology, 158
 - hourglass stomach, 189
 - innervation, 156
 - lymphatic drainage, 157
 - microgastria, 186
 - physiology, 158
 - pyloric Stenosis, 188
 - structure, 155
- Striated or external urethral sphincter, 298
- Stylohyoid muscle, 21
- Subacute bacterial endocarditis (SBE), 478–479
- Subacute endocarditis prophylaxis, 476
- Subclavian artery, 86
 - normal course, 85
 - variations and pathology, 85, 86
- Subclavius muscle, 20
- Subcutaneous emphysema (SE), 43
 - clinical signs, 43
 - etiologies of, 44
 - management of, 44
 - occurrence of, 44
 - symptoms of, 44
- Subglottic area, 70
- Subglottic stenosis, 70, 71
- Submandibular and sublingual glands, 13
- Submucosa, 149
- Subpulmonic stenosis, 486
- Superficial brachial artery (SBA), 439
- Superficial brachiomedian artery (SBMA), 442
- Superficial brachioradial artery (SBRA), 441

- Superficial brachioulnar artery (SBUA), 441, 442
 Superficial brachioulnoradial artery (SBURA), 442
 Superficial branch of the radial nerve, 389
 normal course, 389
 variations and pathology, 390
 Superficial dorsal antebrachial artery (SDAA), 443
 Superficial muscles, 23, 392, 393, 400, 401
 anconeus, 401
 brachioradialis, 402
 extensor carpi radialis brevis, 402
 extensor carpi radialis longus, 402
 extensor carpi ulnaris, 403
 extensor digiti minimi, 402, 403
 extensor digitorum communis, 402
 flexor carpi radialis, 392
 flexor carpi ulnaris, 392
 palmaris longus, 393, 394
 pronator teres, 394
 Superficial nerves, 27–31
 Superficial palmar arch (SPA), 444, 445
 Superficial peroneal nerve (SPN), 430
 Superficial radial artery (SRA), 442
 Superficial system, 308
 Superior and inferior duodenal/paraduodenal fossae, 344, 347
 Superior duodenal fossa, 347
 Superior ectopic kidney, 274
 Superior laryngeal nerve (SLN)
 normal course, 97
 variations and pathologies, 97, 98
 Superior mesenteric artery (SMA), 161, 217
 Superior peroneal retinaculum (SPR), 426
 Superior pharyngeal constrictor muscle, 24
 Supernumerary kidneys, 275
 Supinator, 404
 Supraclavicular brachial plexus block, 363
 Supraglottoplasty, 62
 Sural nerve trunk, 430
 Surgical capsule, 294
 Sympathetic and parasympathetic nervous systems, 169
 Syndactyly and polydactyly, 429
 Systemic arterial anatomy, 218
 Systemic arterial supply, 215–217
 Systemic scleroderma, 40
- T**
- Takayasu arteritis, 501
 Taleisnik's incision, 380
 Talipes equinovarus, 427
 Tarsal coalitions, 424
 Temporal lobe, 8
 Temporomandibular joint (TMJ), 35–37, 58
 ankyloses, 38
 ankylosis, 37
 closed lock management, 36, 37
 Testicle/acrotum
 anatomy, 317, 318
 congenital abnormalities
 abnormalities of the spermatic cord, 322
 cryptorchidism, 319–322
 cyst of the spermatic cord, 325
 hydroceles, 322, 323
 inguinal hernia, 325
 testicular torsion, 327, 328
 varicocele in the adolescent, 325–327
 embryology, 318, 319
 Testicular agenesis from neonatal torsion, 321
 Testicular artery/internal spermatic or gonadal artery, 318
 Testicular descent, 319
 Testicular torsion, 327, 328
 Tetralogy of Fallot (TOF), 484, 485
 Thalamus, 8
 Third branchial cleft, 108
 Thoracic aorta and its variants, 123
 aortic arch, embryology of, 124, 125
 arch anatomical variants, 125
 cervical aortic arch, 133
 coarctation of the aorta, 129–131
 double aortic arch, 126, 127
 ductus diverticulum, 133, 135
 hypoplastic ascending aorta, 129
 interrupted aortic arch, 131, 133
 patent ductus arteriosus, 133
 right-sided aortic arch, 127, 128
 branch vessel variants
 aberrant right subclavian artery, 137
 anomalous origin of the pulmonary artery, 138, 140
 bovine arch, 135
 common brachiocephalic trunk, 138
 thyroidea ima artery, 137
 Thoracic duct
 normal anatomy, 101, 102
 variations and anomalies, 101–104
 Thoracoscopy, 355
 Thyroglossal duct, 106, 107
 Thyrohyoid muscle, 22
 Thyroidea ima artery, 89, 90, 137, 138
 Tibial hemimelia, 428
 Tibial nerve, 430, 431
 Tibial-fibular trunk, 454

- Tibioperoneal trunk (TPT), 454
 Todani classification, 231
 Tongue, 12, 13
 Tori, 51, 53
 management of, 51–53
 oral-facial manifestations of, 51
 Torus mandibularis, 51
 Torus palatinus, 51
 Total anomalous pulmonary venous return (TAPVR), 495, 496
 Trabecular bone, 349
 Trabecular/cancellous matrix, 350
 Tracheal intubation, 74
 Tracheoesophageal fistula, 184
 Tracheoesophageal fistula (TEF), 147, 148, 183–186
 Transesophageal echocardiography (TEE), 474, 477
 Transposition of the great vessels, 484, 487
 Transversus abdominis muscle, 152
 Trapped penis, 311
 Traumatic hematomas, 37
 Treacher-Collins syndrome, 66, 67
 Treatment-resistant epilepsy (TRE), 99
 Triangle of Calot, 225
 Tricuspid atresia, 487, 489
 Trissectionectomy, 212
 Trismus
 definition of, 33
 head and neck radiotherapy, caused by, 34
 infectious origins of, 35
 management of post-radiotherapy, 34
 source of, 34
 Trisomy 18, 121, 122
 Trisomy 21, 65, 117, 427
 Truncus arteriosus, 487, 488
 Tunica vaginalis, 318
 Turner syndrome, 111
 Type I choledochal cysts, 230
 Type II choledochal cysts, 230
 Type III choledochal cysts, 230
 Type IV choledochal cysts, 230
 Type V cysts, 231
- U**
 Ulnar artery, 439
 agenesis, 443
 duplication of, 443
 Ulnar nerve, 382, 383, 387
 normal course, 381, 382
 variation and pathology, 383, 385
 Ulnar tunnel syndrome, 384
 Umbilical band, 200, 201
 Umbilical enteric fistula, 200
 Umbilical hernia, 160
 Umbilical polyps, 200
 Uncinate process, 237
 Uncuffed endotracheal tube size, 61
 Uncuffed tubes, 60
 Undescended testicle, 320, 322
 Undescended testis, 319
 Unilateral agenesis, 274
 Unilateral ureteropelvic junction obstruction (UPJO), 277, 278
 Upper airway obstruction, 60
 Upper and lower extremity vascular variations
 arteries in arm and forearm
 accessory brachial artery, 439, 440
 brachial artery, 437
 brachiointerosseous artery, 442
 brachioradial artery, 441
 BUA, 442
 duplication of ulnar artery, 443
 median artery, 443
 PIA, 444
 radial artery, 438, 443
 radial artery distal takeoff, 442
 RCA, 444
 RRA, 444
 SBMA, 442
 SBRA, 441
 SBUA, 441, 442
 SBURA, 442
 SRA, 442
 superficial brachial artery, 439
 superficial dorsal antebrachial artery, 443
 ulnar artery, 439, 443
 arteries in hand
 complete SPA, 445
 DPA, 444, 446
 incomplete SPA, 445
 pathology, 446
 SPA, 444, 445
 arteries in lower limbs
 ATA, 454
 DGA, 452
 DPA, 456, 457
 FDMA, 458
 femoral artery, 449, 450
 LFCA, 451, 452
 LPA, 456
 MFCS, 451
 MPA, 456
 PFA, 450, 451
 plantar arch, 457, 458
 popliteal artery, 454

- Upper and lower extremity vascular variations (*cont.*)
- PRA, 454–456
 - PTA, 454
 - veins in arm, forearm, and hand
 - basilic vein, 448
 - cephalic vein, 447
 - deep veins, 447
 - median vein, 448
 - pathology, 449
 - variation in superficial veins, 448, 449
 - veins in the lower limbs
 - ATV, 461
 - dorsal venous arch, 462
 - DPVA, 462
 - femoral vein, 458
 - GSV, 459, 460
 - peroneal veins, 462
 - persistent sciatic vein, 459
 - popliteal vein, 459
 - PTV, 461
 - SSV, 460
- Upper extremity, 362, 363, 365, 366
- carpal bones
 - accessory ossicles, 411
 - carpal bipartitions and fusion/coalition, 410, 411
 - lunate variation, 411
 - normal anatomy, 410
 - muscles and tendons
 - anterior compartment, 392–394, 396–400
 - posterior compartment, 400–407
 - nerves
 - anterior interosseous nerve, 380
 - deep branch of the radial nerve, 390, 392
 - median, 375, 376, 378
 - palmar cutaneous branch of the median nerve, 378–380
 - radial nerve, 385, 387
 - superficial branch of the radial nerve, 389, 390
 - ulnar nerve, 381–383, 385
 - venous patterns, 448
- Upper pole hydroureteronephrosis, 282
- Urachal cyst and urachal sinus, 289, 290
- Urachus, congenital abnormalities
- patent urachus, 289
 - urachal cyst and urachal sinus, 289, 290
- Ureteral caliber, 283
- Ureteral duplication, 278, 280
- Ureteral peristalsis, 276
- Ureteral stenosis, 283
- Ureteric anatomy, 276
- Ureterocele, 278, 279, 281, 282
- Ureters, 259, 260
- anatomy, 275, 276
 - blood supply, 261
 - congenital anomalies
 - ectopic ureters, 278
 - megaureter, 283, 284
 - retrocaval ureter, 283
 - UPJO, 277, 278
 - ureteral duplication, 278, 280
 - ureteral stenosis, 283
 - ureterocele, 278, 279, 281
 - vesicoureteral reflux, 284–286
 - embryology, 276
 - innervation, 260
 - lymphatics, 261
 - structure, 260
- Urethra
- clinical, 264
 - congenital abnormalities
 - anterior urethral valves, 302, 303
 - congenital urethral strictures, 300
 - posterior urethral valves, 300–302
 - urethral diverticulum, 303, 305
 - urethral duplication, 305, 306
 - urethral meatal stenosis, 300
 - female, 264
 - anatomy, 299
 - embryology, 299
 - male, 263
 - anatomy, 298, 299
 - embryology, 299
 - urination, 264
- Urethral diverticulum, 303–306
- Urethral duplication, 305, 306
- Urethral meatal stenosis, 300
- Urinary bladder, 261–263
- Urinary outlet obstruction, 301
- Urination, 264
- Urologic anomalies and surgical implication, *see* Kidneys
- V**
- Vagus and thoracic splanchnic nerves, 239
- Vagus nerve, 146
- normal course, 99
 - variations and pathology, 99, 100
- Vagus nerve (CN X), 29, 148, 156
- Vagus nerve stimulation (VNS) therapy, 99
- Valsalva maneuver, 326
- Variation in superficial veins, 448, 449
- Varicocele in the adolescent, 325–327

- Vascular access, 474, 475, 498
ASD, 479
AVSD, 480
Behçet disease, 500
bicuspid aortic valve, 499
Bland-White-Garland syndrome, 497
Congenital aortic stenosis, 483
congenital pulmonary stenosis, 480
Dextrocardia, 492
Double-outlet right ventricle, 491
Ebstein's anomaly, 495
Eisenmenger's syndrome, 491
hypoplastic left heart syndrome, 491
infective endocarditis, 502
interrupted aortic arch, 494
intravascular pulmonary metastases, 501
Kawasaki disease, 502
mycotic aneurysm, 500
partial anomalous pulmonary venous
return, 495
patent ductus arteriosus, 480
pulmonary artery aneurysm and idiopathic
dilatation of the pulmonary
trunk, 495
pulmonary atresia, 495
quadricuspid aortic valve, 499
Rasmussen aneurysm, 500
rheumatic heart disease, 501
Takayasu arteritis, 501
tetralogy of Fallot (TOF), 484
total anomalous pulmonary venous
return, 495
transposition of the great vessels, 487
tricuspid atresia, 488
truncus arteriosus, 487
VSD, 477
- Vascular and biliary anatomy, 215
hepatic vein anatomy, 217, 219, 220
portal vein, 220–222
systemic arterial supply, 215–217
- Vascular anomalies of the foot and ankle,
432, 433
- Vasculature of the neck, 30
- Veins draining the spinal cord, 352
- Ventricular septal defect (VSD), 470, 477, 478
- Ventricular system, 8
- Venulae rectae, 255
- Vertebral arterial system, 84
- Vertebral arteries
normal course, 87
variations and pathology, 87, 88
- Vertebral column, 360
- Vertebral column integrity, 58
- Vertebral fractures (VF), 350
- Vesicoureteral reflux (VUR), 279,
284–286, 292
- Video-assisted thoracic surgery (VATS), 355
- Viscerocranium, 4
- Vocal cord paralysis, 100
- Voiding cystourethrography (VCUG), 279,
284, 286
- Von Hippel-Landau disease, 246
- W**
- Webbed penis, 311, 312, 314
- Weigert-Meyer law, 278
- Wind-sock deformity, 192
- Wolffian duct, 254